

Northumbria Research Link

Citation: Risdonne, Valentina (2022) Materials and techniques for coating of the nineteenth-century plaster casts. A scientific and archival investigation of the Victoria & Albert museum cast collection. Doctoral thesis, Northumbria University.

This version was downloaded from Northumbria Research Link:
<http://nrl.northumbria.ac.uk/id/eprint/49513/>

Northumbria University has developed Northumbria Research Link (NRL) to enable users to access the University's research output. Copyright © and moral rights for items on NRL are retained by the individual author(s) and/or other copyright owners. Single copies of full items can be reproduced, displayed or performed, and given to third parties in any format or medium for personal research or study, educational, or not-for-profit purposes without prior permission or charge, provided the authors, title and full bibliographic details are given, as well as a hyperlink and/or URL to the original metadata page. The content must not be changed in any way. Full items must not be sold commercially in any format or medium without formal permission of the copyright holder. The full policy is available online: <http://nrl.northumbria.ac.uk/policies.html>

**MATERIALS AND TECHNIQUES
FOR COATING OF THE
NINETEENTH-CENTURY
PLASTER CASTS.
A SCIENTIFIC AND ARCHIVAL
INVESTIGATION OF THE
VICTORIA & ALBERT MUSEUM
CAST COLLECTION.**

V RISDONNE

PhD

Volume 1 of 2

2022

**MATERIALS AND TECHNIQUES
FOR COATING OF THE
NINETEENTH-CENTURY
PLASTER CASTS.
A SCIENTIFIC AND ARCHIVAL
INVESTIGATION OF THE
VICTORIA & ALBERT MUSEUM
CAST COLLECTION.**

VALENTINA RISDONNE

A thesis submitted in partial fulfilment of the requirements of
the University of Northumbria at Newcastle for the degree of
Doctor of Philosophy

Research undertaken in the Faculty of Arts, Design & Social
Sciences and in collaboration with the Victoria & Albert
Museum

Volume 1 of 2

January 2022

This thesis presents the first interdisciplinary and multi-analytical study of the historical coatings of nineteenth-century plaster casts of the Victoria and Albert Museum (V&A) collection. The findings presented herein are anticipated to support the decision-making for the care, preservation and conservation of these objects.

Seventeen historical manuals and fourteen patents were reviewed to understand the nineteenth-century practice for coating plaster casts. More than eighty organic and inorganic materials were mentioned in over a hundred recipes retrieved in the literature. When specified, the purpose of the application of the coating was to ensure a desired appearance and/or improve the durability of the object by hardening and waterproofing the surfaces.

A selection of twelve nineteenth-century casts produced in different European workshops was analysed. A multi-analytical approach was designed to observe the stratigraphy – by Visible Light Reflectance (VLR) and Ultra-Violet fluorescence (UVf) Optical Microscopy (OM) - and characterise the inorganic - by Scanning Electron Microscopy-Energy - dispersive X-ray spectroscopy (SEM-EDS) and X-Ray Diffraction (XRD) - and organic components – by Fourier-Transform Infrared spectroscopy (FT-IR), Gas Chromatography/Mass Spectrometry (GC/MS) and pyrolysis-GC/MS. A complex layer system and evidence of coatings' diffusion into the bulk were consistently identified. The bulk was made of calcium sulfate dihydrate ($\text{CaSO}_4 \cdot 2\text{H}_2\text{O}$) and mineral carbonate and clay inclusions. In most of the analysed casts, the coating contained aluminium, silicon and an organic medium that was either aged diterpenic or shellac resin.

To study the changes on coated plaster surfaces upon ageing, reconstructions made of gypsum plaster coated with linseed oil, shellac, barite (BaSO_4) and beeswax were made, based on the analysis and the literature review. The reconstructions were aged using selected conditions of temperature, humidity and light. The aged samples were soiled and cleaned using a novel cleaning method. The effects of ageing were evaluated with visible and UVf photographs, SEM, High-Resolution 3-Dimensional (HR 3D) surface measurements, glossimetry, colourimetry and FT-IR. Linseed oil and shellac penetrated the pores, barite chemically modified the surface by interacting with the calcium sulfate, whereas beeswax formed a film on the plaster surface. Polyolefin-supported polyacrylamide ultra-thin hydrogel films were tested for the removal of soil from the reconstructions and proved effective, in particular on the film-forming coatings.

*To those who persist
to those who inspired me
and to the women with thirsty minds and feisty hearts*

VOLUME 1

Abstract	III
List of contents	VII
List of tables and figures	XIII
List of accompanying material and publications	XXXIX
List of Abbreviations	XLI
Preface	XLIII
Acknowledgements	XLV
Author's declaration	XLVII
Chapter 1. Background and context	1
1.1. Introduction	3
1.1.1. A world of reproductions	4
1.1.2. Authenticity, value and function	7
1.1.3. Plaster workshops and <i>Formatori</i>	11
1.2. The V&A Cast Courts and the collection	13
1.3. Making plaster casts	19
1.3.1. The coatings	21
1.4. Research and conservation	25
1.5. Research rationale	30
1.5.1. Gap in knowledge	30
1.5.2. Research questions	31
1.5.3. Aim	31
1.5.4. Objectives	31
1.6. Thesis Outline	33
Chapter 2. Defining a methodology	35
2.1. Introduction	37
2.2. The literature research	41
2.2.1. The archives	41
2.2.2. Historical technical literature and patents	46

2.3. Scientific investigation of the V&A casts	50
2.3.1. The objects	50
2.3.2. The analysis	53
2.4. Surface reconstructions and cleaning trials	61
2.4.1. Accelerated ageing	62
2.4.2. Artificial soiling	69
2.4.3. Cleaning trials	70
2.4.4. Assessing ageing and cleaning	72
2.5. Conclusion	75
Chapter 3. Historical materials and techniques for plaster casting	77
3.1. Materials, properties, and techniques	79
3.1.1. Gypsum and plaster	79
3.1.1.1. Lime plaster	80
3.1.1.2. Natural gypsum	80
3.1.1.3. Gypsum plaster	82
3.1.2. Before casting	83
3.1.3. Plaster casting	88
3.1.4. Separating agents	90
3.2. Finishing and coating	92
3.3. Conclusion	111
Chapter 4. Characterization of the V&A casts	113
4.1. Introduction	115
4.2. Experimental Method	116
4.2.1. Sampling	116
4.2.2. Instrumentation	117
4.2.2.1. Photographic equipment	117
4.2.2.2. Microscopies	118
4.2.2.3. X-Ray Diffractometry (XRD)	118
4.2.2.4. Fourier Transformed-InfraRed Spectroscopy (FT-IR)	119
4.2.2.5. pyrolysis- Gas Chromatography/Mass Spectrometry (py-GC/MS)	120
4.2.3. Sample processing	121
4.2.3.1. Processing for stratigraphy observation and analysis	121
4.2.3.2. Processing for GC/MS and py-GC/MS	122
4.2.4. Database formation	126
4.3. Results and discussion	127
4.3.1. Dust	129

4.3.2. Plaster bulk	131
4.3.3. Coatings and interface with the substrate	140
4.3.4. Areas of retouching or repair	154
4.4. Similarities and differences within the groups	157
4.5. Conclusion	159
Chapter 5. Surface reconstructions. Part 1: ageing	161
5.1. Introduction	163
5.1.1. Linseed oil	163
5.1.2. Shellac	165
5.1.3. Barite	166
5.1.4. Beeswax	167
5.2. Experimental method	168
5.2.1. Coated plaster surface reconstructions	168
5.2.1.1. Plaster substrates	168
5.2.1.2. Coatings	169
5.2.1.3. Accelerated ageing equipment and parameters	170
5.2.1.4. Artificial soiling	171
5.2.1.5. The build-up of the stratigraphy	172
5.2.2. Evaluation	174
5.2.2.1. Gravimetry	174
5.2.2.2. Visual examination	175
5.2.2.3. Visible (vis) and Ultraviolet fluorescence (UVf) reflectance	176
5.2.2.4. Scanning Electron Microscopy (SEM)	176
5.2.2.5. Colourimetry	176
5.2.2.6. Glossimetry	178
5.2.2.7. High Resolution (HR) 3D surface measurements	178
5.2.2.8. Fourier-transform infrared spectroscopy (FT-IR)	179
5.2.3. Database formation	179
5.3. Results and discussion	180
5.3.1. Gravimetry	180
5.3.2. Visual examination, Visible (vis) reflectance and Ultraviolet fluorescence (UVf) imaging	182
5.3.3. Topographical and morphological studies	187
5.3.4. Colour, gloss, and roughness measurements	198
5.3.4.1. Control plaster plates (uncoated and beeswax)	201
5.3.4.2. Plaster plates coated with linseed oil	204
5.3.4.3. Plaster plates coated with shellac	206

5.3.4.4. Soiled plaster surface plates with barite	209
5.3.5. Fourier-transform infrared spectroscopy (FT-IR)	212
5.3.5.1. Unsoiled and uncoated plaster plates	213
5.3.5.2. Soiled uncoated plaster plates	214
5.3.5.3. Plaster plates coated with cold-pressed linseed oil	215
5.3.5.4. Plaster plates coated with boiled linseed oil	218
5.3.5.5. Plaster plates coated with shellac	221
5.3.5.6. Soiled plaster surface plates with barite	224
5.3.5.7. Plaster plates coated with beeswax	224
5.4. Considerations on accelerated ageing	226
5.5. Conclusion	228
Chapter 6. Surface reconstructions. Part 2: cleaning	231
6.1. Introduction	233
6.1.1. Cleaning plaster casts	234
6.1.2. Polyolefin-Supported Hydrogels	237
6.2. Experimental method	239
6.2.1. Cleaning method	239
6.2.1.1. pH and conductivity measurements	239
6.2.1.2. The solutions	239
6.2.1.3. Cleaning tests	240
6.2.2. Evaluation of the cleaning efficacy	242
6.2.3. Database formation	242
6.3. Results and discussion	243
6.3.1. pH, conductivity and preliminary tests	244
6.3.2. Visual examination, visible (Vis) reflectance and ultraviolet fluorescence (UVf) imaging	247
6.3.3. Topographical and morphological studies	257
6.3.4. Colour, gloss, and roughness measurements	267
6.3.5. Fourier-transform infrared spectroscopy (FT-IR)	279
6.3.6. Summary of results	280
6.4. Conclusion	281
Chapter 7. Conclusions	283
7.1. The research questions	285
7.2. Historical materials and their purposes	287
7.3. Original and modern materials	289
7.4. Towards the assessment of deterioration of plaster casts coatings	290
7.5. Designing preservation and conservation	292

7.6. The database and future perspectives	293
List of References	297
About the author	323

Appendices and ***Glossary*** can be found in **VOLUME 2**.

LIST OF TABLES AND FIGURES

TABLES

VOLUME 1

Table 2.1	List of manuals and historical books reviewed for this study.	47
Table 2.2	Description of the patents reviewed for this study.	49
Table 2.3	Average values recorded by five sensors located in Galleries 46, 46A and 46B.	64
Table 3.1	Summary of gypsum properties.	81
Table 3.2	Separating agents as found in the historical literature.	91
Table 3.3	Summary of recipes as found in the historical literature.	95
Table 3.4	List of recipes used to achieve the desired appearance onto a plaster cast surface.	103
Table 3.5	Summary of the materials encountered in the historical sources reviewed for this study and their intended purpose.	108
Table 4.1	Sample numbers as related to the Museum number, divided by group.	117
Table 4.2	Summary of methods used for GC/MS samples preparation and equipment settings.	125
Table 4.3	ATR/FT-IR peaks identified in the spectra acquired in the dust sample (REPRO.1873-380_1).	129
Table 4.4	FT-IR peaks identified in the spectra acquired from the gypsum plaster reference (A) , the polyester casting resin reference (B) and plaster bulk of the objects (C) (REPRO.1873-380_2) shown in Figure 4.10.	136
Table 4.5	GC/MS markers used to characterise the organic component.	139
Table 4.6	P/S and A/P ratios calculated in the samples analysed by (py-)GC/MS. Relevant samples processing and analytical details are described in Sections 4.2.2 and 4.2.3.	144
Table 4.7	Summary of FT-IR peaks characteristic of the organic materials identified by GC/MS, according to literature*.	147
Table 4.8	Summary of features observed in the samples analysed. Samples codes described in Table 4.1.	153

Table 4.9	Summary of features observed in the samples taken from areas of repair. Samples codes described in Table 4.1.	156
Table 4.11	Summary of findings divided by group. Objects' Museum accession numbers shown in Table 4.1.	158
Table 5.1	Quantities and times for the preparation of the plaster plates.	169
Table 5.2	Scheme of the plates (P), including coatings and ageing.	173
Table 5.3	Steps and time intervals (Δt) of the surface reconstructions making and ageing.	174
Table 5.4	Colour changes according to CIE formulae ΔE_{00} and Yellow Index (YI_{313}) [SCI] before/after ageing.	199
Table 5.5	Summary of measurements acquired from the control sections d (unsoiled - US) and a (soiled - S) of the unaged (P1, 5 and 9) and aged (P3, 7 and 11) plates at t_{37} (plates description in Table 5.2).	202
Table 5.6	Summary of measurements acquired from the control sections d (unsoiled - US) and a (soiled - S) of the unaged (P2, 6 and 10) and aged (P4, 8 and 12) plates at t_{37} (plates description in Table 5.2).	204
Table 5.7	Summary of measurements acquired from the sections e and f (unsoiled - US) and b and c (soiled - S) coated with cold-pressed (b and e) and boiled linseed oil (c and f) of the unaged (P1) and aged (P3) plates at t_{37} (plates description in Table 5.2).	206
Table 5.8	Summary of measurements acquired from the sections e and f (unsoiled - US) and b and c (soiled - S) coated with shellac6% (b and e) and shellac18% (c and f) of the unaged (P5) and aged (P7) plates at t_{37} (plates description in Table 5.2).	208
Table 5.9	Summary of measurements acquired from the sections e and f (unsoiled - US) and b and c (soiled - S) coated with barite20° (b and e) and barite60° (c and f) of the unaged (P9) and aged (P11) plates at t_{37} (plates description in Table 5.2).	210
Table 5.10	Summary of measurements acquired from the unsoiled, unaged (P2, 6 and 10) and aged (P4, 8 and 12), plates at t_{37} (plates description in Table 5.2). P2 and 4 are coated with linseed oil and beeswax, P6 and 8 with shellac and P10 and P12 with barite.	211
Table 5.11	Summary of measurements acquired from the soiled, unaged (P2, 6 and 10) and aged (P4, 8 and 12), plates at t_{37} (plates description in Table 5.2). P2 and 4 are coated with linseed oil and beeswax, P6 and 8 with shellac and P10 and P12 with barite.	211
Table 5.12	ATR/FT-IR bands and relevant assignments of the spectra acquired from the plaster substrate at t_{12} .	212
Table 5.13	FT-IR bands and relevant assignments of the spectra acquired from unsoiled areas (d of P1, 3, 5, 7, 9 and 11) and soiled areas (a of P1, 3, 5, 7, 9 and 11) at t_{37} .	215

Table 5.14	FT-IR bands and relevant assignments of the spectra acquired from unsoiled (unaged P1e and aged P3e) and soiled (unaged P1b and aged P3b) areas of the plaster surface coated with cold-pressed linseed oil (1-1) at t_{37} .	218
Table 5.15	FT-IR bands and relevant assignments of the spectra acquired from unsoiled (unaged P1f and aged P3f) and soiled (unaged P1c and aged P3c) areas of the plaster surface coated with boiled linseed oil (1-2) at t_{37} .	220
Table 5.16	FT-IR bands and relevant assignments of the spectra acquired from unsoiled (unaged P5e and aged P7e) and soiled (unaged P5b and aged P7b) areas of the plaster surface coated with shellac6% (2-1) at t_{37} .	222
Table 5.17	FT-IR bands and relevant assignments of the spectra acquired from unsoiled (unaged P5f and aged P7f) and soiled (unaged P5c and aged P7c) areas of the plaster surface coated with shellac18% (2-2) at t_{37} .	224
Table 5.18	FT-IR bands and relevant assignments of the spectra acquired from unsoiled (unaged P9e,f and aged P11e,f) and soiled (unaged P9b,c and aged P11b,7c) areas of the plaster surface coated with barite20° (3-1) and barite60° (3-2) at t_{37} .	225
Table 6.1	The solutions prepared for the tests.	240
Table 6.2	pH* and conductivity** (σ) measurements of the surfaces of the plates.	246
Table 6.3	Preliminary tested solutions according to the pH and conductivity of the soiled surface.	247
Table 6.4	Summary of measurements acquired from the uncoated plaster surfaces a (S) of the unaged (P1, 5 and 9) and aged (P3, 7 and 11) plates after cleaning.	276
Table 6.5	Summary of measurements acquired from the plaster surfaces coated with linseed oil, sections b (1-1) and c (1-2), unaged (P1) and aged (P3), after cleaning.	276
Table 6.6	Summary of measurements acquired from the plaster surfaces coated with shellac, sections b (2-1) and c (2-2), unaged (P5) and aged (P7), after cleaning.	277
Table 6.7	Summary of measurements acquired from the plaster surfaces coated with barite, sections b (1-1) and c (1-2), unaged (P9) and aged (P11), after cleaning.	277
Table 6.8	Summary of measurements acquired from the plaster surfaces coated with beeswax (4) a (S) of the unaged (P2, 6 and 10) and aged (P4, 8 and 12) after cleaning.	278
Table 6.9	Summary of measurements acquired from the plaster surfaces coated with coatings (1, 2 or 3) and beeswax (4) a (S) of the unaged (P2, 6 and 10) and aged (P4, 8 and 12) after cleaning.	278
Table 6.10	Summary of observations on the effectiveness of the polyolefin-supported hydrogels (PE-PAM) in combination with the solutions described in Section 6.2.1.2 (pages 239-40) for the removal of soiling from the different mock-up coated plaster surfaces.	280

VOLUME 2

Table A9.1	XRD peaks (2θ , °) of the plaster casts analysed for this study.	431
------------	--	-----

FIGURES**VOLUME 1**

Chapter 1 Frontpage	Drawing of the Cast Courts, Room 46a, The West Court, about 1873, England. Museum no. D.564-1905. © Victoria and Albert Museum, London/as specified by the rights holder. Source: Collection Management System.	1
Figure 1.1	Ann Macbeth and another woman in a Glasgow School of Art drawing and painting class, both holding palettes, with plaster casts in the background, c. 1912. Glasgow School of Art Archives. Source: The Glasgow School of Art. Archives and Collection. (2020).	6
Figure 1.2	V&A's 2014 publicity campaign. Photographer: James Medcraft. © Victoria and Albert Museum, London/as specified by the rights holder. Source: Inspiring Beautiful Free Shoot (2014).	14
Figure 1.3	South Kensington Museum, North Court, south-west corner, showing the cast of Trajan's Column (REPRO.1864-128), 1868. Stereoscopic albumen print. Photographer: Davis Burton, No. 3 in the London Series. © Victoria and Albert Museum, London/as specified by the rights holder. Source: V&A's Collection Management System.	16
Figure 1.4	Painted plaster cast (REPRO.1903-25) of a green sandstone cross (Muiredach's High Cross) purchased from the Dublin Museum in 1903 for £32 10s. © Victoria and Albert Museum, London/as specified by the rights holder. Source: V&A's Collection Management System.	18
Figure 1.5	Plaster casts of a lead Statuette figure of a seated girl (A.2-1946) made in the Sculpture Conservation Studio at the V&A to illustrate that plasters can carry many different finishes. © Victoria and Albert Museum, London/as specified by the rights holder.	22
Figure 1.6	Plaster cast and reconstruction of the Peplos Kore in the Cambridge Museum of Classical Archaeology. The original (ca 530 BC) now stands in the Acropolis Museum in Athens. © Cambridge Museum of Classical Archaeology.	23

Figure 1.7	Plaster cast of a Putto (CMS number REPRO.1888-519). The plaster is finished to resemble bronze. © Victoria and Albert Museum, London/as specified by the rights holder. Source: V&A's Collection Management System.	24
Chapter 2 Frontpage	The Studio of Bartolomeo Cavaceppi. © German Archaeological Institute. Source: Cavaceppi, B. (1798) Frontispiece to Raccolta d'antiche statue, busti, teste cognite ed altre sculture antiche scelte restaurate da Bartolomeo Cavaceppi scultore romano. vol. 1 Rome, Generoso Salomoni.	35
Figure 2.1	Two letters from the Archive of the Museo dell'Arte Classica (Museo dei Gessi) at the University of Sapienza, Rome (Italy). The two letters were written by Enrico Cantoni (c. 1859-1923) to Professor Emanuel Löwy (1857-1938) on the 1st of July (A) and 13th of July (B) 1914.	42
Figure 2.2	(A) V&A's object number 1665-1926. Photograph, the font in the Cathedral of Hildesheim, Germany, gelatine silver print, late nineteenth to the early twentieth century. Photographic record: 2016JA0650. © Victoria and Albert Museum, London/as specified by the rights holder. Source: V&A's Collection Management System. (B) Description of the object on the V&A' Register of Acquisition, 28th of February 1874. From the Archive of the Sculpture Department at the Victoria and Albert Museum, London.	44
Figure 2.3	Image taken from 'The Times' (21 November 1908) showing a drawing of the New Building of the Victoria and Albert Museum	45
Figure 2.4	V&A casts of the Küsthardt Group. Dimensions are available in Appendix 5. © Victoria and Albert Museum, London/as specified by the rights holder. Source: V&A's Collection Management System.	51
Figure 2.5	V&A casts of the Notre-Dame Group. Dimensions are available in Appendix 5. © Victoria and Albert Museum, London/as specified by the rights holder. Source: V&A's Collection Management System.	52
Figure 2.6	V&A casts of the Franchi Group. Dimensions are available in Appendix 5. © Victoria and Albert Museum, London/as specified by the rights holder. Source: V&A's Collection Management System.	52
Figure 2.7	(A) A closer look at the surface of V&A's object number REPRO.A.1916-3152 shows marks due to the use of tools during manufacturing. (B) A closer look at V&A's object number REPRO.1874-29 shows the stamp of the workshop where the cast was manufactured. © Victoria and Albert Museum, London/as specified by the rights holder.	55
Figure 2.8	Observing details of the V&A plaster cast of the Pisano Pulpit (REPRO.1864-83) (A) with the aid of UV illumination allowed to identify areas that have characteristic fluorescence (B) . © Victoria and Albert Museum, London/as specified by the rights holder.	56
Figure 2.9	The Weston Cast Court at the V&A. The massive skylight windows are the major source of light. © Victoria and Albert Museum, London/as specified by the rights holder.	67

Figure 2.10	Global Horizontal Irradiation map for the UK. © 2019 The World Bank, Source: Global Solar Atlas 2.0, Solar resource data: Solargis.	69
Chapter 3 Frontpage	Mould ready for assembling. Plate 2. Source: Wager, V. H. (1963) Plaster casting: for the student sculptor. London. Alec Tiranti.	77
Figure 3.1	Detail of a plaster cast of a relief on the outside of Notre-Dame Cathedral in Paris, in the V&A collection (REPRO.1890-80). Uneven distribution of the plaster during the casting process could cause the formation of air pockets as can be seen in the picture (yellow circle). © Victoria and Albert Museum, London/as specified by the rights holder.	84
Figure 3.2	X-ray photography of the V&A's plaster cast of Michelangelo's Tondo Taddei (REPRO.1902-98) showed that the cast was reinforced with metal rods (A) . Side views of the object show that the presence of the rods created cracks (B) and rust stains (C) . Images courtesy of Victor Borges. © Victoria and Albert Museum, London/as specified by the rights holder.	87
Figure 3.3	Detail of a plaster cast of a relief on the outside of Notre-Dame Cathedral in Paris, in the V&A collection (REPRO.A.1916-3153). A closer look allowed to identify marks and scratches due to the use of tools. © Victoria and Albert Museum, London/as specified by the rights holder.	93
Figure 3.4	Simplified drawing representing the possible interactions of the coating with the porous plaster surface. The material applied onto the surface can penetrate the pores without forming a film (A) , penetrate the pores and form a film on the surface (B) or form a film without penetrating the surface (C) .	99
Figure 3.5	(A) Plaster cast from one of the shields on the Royal Albert Hall (REPRO.1901-16). White plaster cast. (B) A plaster cast of an Effigy of Isabella of Angouleme (REPRO.A.1938-4). Painted plaster cast. © Victoria and Albert Museum, London/as specified by the rights holder. Source: V&A's Collection Management System.	101
Figure 3.6	(A) A plaster cast of the lid of a casket (REPRO.1873-235). The plaster is finished to resemble ivory. (B) A plaster cast of a font (REPRO.1877-1). The plaster is finished to resemble gold. (C) A plaster cast of a Lectern (REPRO.1872-65). The plaster is finished to resemble brass. (D) A plaster cast of a wooden statue of St Stephen (REPRO.1906-3). The plaster is finished to resemble painted wood. (E) A plaster cast of Donatello's David (REPRO.1885-197). The plaster is finished to resemble bronze. © Victoria and Albert Museum, London/as specified by the rights holder. Source: V&A's Collection Management System.	102
Chapter 4 Frontpage	Samples mounted in resin on Scanning Electron Microscope supports.	113
Figure 4.1	The image summarises the steps performed to cast the samples in polyester resin. The sample was observed under the stereomicroscope (A) , positioned in the hole half-filled with dry resin (B) and covered with casting resin until filling the whole cube-shaped hole (C) .	121

Figure 4.2	Proposed mechanism of methylation of carboxylic acids with TMAH.	123
Figure 4.3	Proposed mechanism of methylation with 3-(Trifluoromethyl)phenyltrimethylammonium Hydroxide (A → C).	124
Figure 4.4	VLR OM (A) and BSE (B) images and outline of the layers (C) . Sample 4 taken from REPRO.1864-57 (D) (Raising of Lazarus, object dimensions 122.0X117.0 cm) clearly shows the substrate (plaster bulk, layer 0) and the coating (layer 2). Layer 1 is the interface, where the coating has penetrated the plaster bulk (yellow under VLR and denser in the BSE image).	127
Figure 4.5	In sample REPRO.1890-80_2 no differences in the elemental distribution were observed but the top layer appears denser. VLR (A) , UVf (B) and BSE (C) images. The sample was taken from REPRO.1890-80 (D) (Assumption of the Virgin, object dimensions 152.5X160.0 cm).	128
Figure 4.6	Sample 1 was taken from REPRO.1873-380 (Tombstone of the Presbyter Bruno, object dimensions 218.5X77.0 cm) (A) . Fibres of different colours are visible in the micrograph (B) taken with the FT-IR microscope. ATR/FT-IR analysis of the dust (C) shows the presence of several contributions including sulfates, carbonates and organic material. Assignment of significant peaks can be seen in Table 4.3.	130
Figure 4.7	Sample 2 was adhered with Ag paint and coated with Pt (A) and analysed in SEM high-vacuum mode, which allowed to observe the tabular mineral structure of gypsum plaster (B) . The structure can be also seen in the cross-sections analysed in SEM low-vacuum mode (REPRO-1873-380_4) (C) . The samples were taken from REPRO.1873-380 (Tombstone of the Presbyter Bruno, object dimensions 218.5X77.0 cm) (D) .	132
Figure 4.8	EDS spectrum of sample REPRO-1873-380_2 shows that the plaster bulk is made of calcium sulfate (Ca, S and O) and contains Si, Al, Na and Mg.	133
Figure 4.9	Sample REPRO.1890-80_1: BSE image (A) shows the tabular mineral structure of the calcium sulfate and the EDS mapping indicates that the sample largely consisted of calcium sulfate (Ca, S, O) and several other inclusions (Al, Mg, Si, Sr). C and O are also present due to the environment and to the casting polyester resin. The sample was taken from REPRO.1890-80 (Assumption of the Virgin, object dimensions 152.5X160.0 cm) (B) .	134
Figure 4.10	FT-IR spectra acquired in ATR mode (gypsum plaster reference) (A) , and in DR of polyester casting resin reference (B) and plaster bulk of the objects (C) (REPRO.1873-380_2).	135
Figure 4.11	FT-IR reference spectra of gypsum (IMP00024 Gypsum, from chalk sample, Kremer, 5815, GCI, tran) (A) , calcite (IMP00108 Calcite, source unknown, PMA, tran) (B) and silica (IMP00322 Quartz, silica, Forbes: Howe&French, 187, SCC, tran) (C) from the IRUG database (Price et al., 2009).	137

Figure 4.12	py-GC chromatograms of three samples: sample from the plaster bulk only (A-B) (REPRO.1873-380_2) and another sample (C) (REPRO.1873-561_6) showing markers of diterpenic resin and FAs; a sample (D) (REPRO.1890-81_4) showing shellac resin markers. (A) : 0-40 min and (B-D) : 16-28 min. Labels' assignments are described in Table 4.5.	138
Figure 4.13	EI-MS of methyl azelate (A) (1) , methyl palmitate (P) (2) and methyl stearate (S) (3) . The list of peaks can be seen in Table 4.5.	139
Figure 4.14	Example of Si-Al and diterpenic resin coating (REPRO.1873-380_11). VLR (A) and UVf (B) OM images, BSE image (D) and EDS mapping showing Al and Si. The sample was taken from REPRO.1873-380 (Tombstone of the Presbyter Bruno, object dimensions 218.5X77.0 cm) (C) .	140
Figure 4.15	Examples of Si-Al-Sr and diterpenic resin coating. REPRO.1864-57_2 (A) , REPRO.A.1916-3152_3 (B) and REPRO.A.1916-3152_4 (C) BSE image and EDS mapping showing Al, Si and Sr. The samples were taken from REPRO.1864-57 (Christ at Bethany, object dimensions 135.0X112.0 cm) (D) and REPRO.A.1916-3152 (Death of the Virgin, object dimensions 90.0X86.0 cm) (E) .	141
Figure 4.16	Example of Si-Al and shellac coating (REPRO.1874-45_2). BSE image (A) and EDS mapping of Al and Si are shown. The sample was taken from REPRO.1874-45 (Christ, St. Godehard and St. Epiphanius, object dimensions 107.0X213.5 cm) (B) .	142
Figure 4.17	Examples of FT-IR reference spectra of kaolin (IMP00109 Kaolin pigment, hydrous, Eglehard, ASP 600, PMA, tran) (A) , sandarac (INR00056 Sandarac AF Suter GCI tran) (B) , copal (INR00011 Copal Sarmi from Agathis alba Roy. Trop. Inst, CIA) (C) and shellac (INR00008 Shellac Lacifer lacca SAM M Jahan Ethno41 GCI tra) (D) from the IRUG database (Price et al., 2009).	146
Figure 4.18	Diffuse Reflectance (DR) FT-IR spectrum acquired from a sample in which diterpenic resin was confirmed by py-GC/MS (REPRO.A.1916-3152_3) (A) and reference spectra of gypsum (B) , polyester resin (C) and copal (D) shown in Figures 4.11 and 4.17.	147
Figure 4.19	Diffuse Reflectance (DR) FT-IR spectrum acquired from a sample in which shellac was confirmed by py-GC/MS (REPRO.1890-81_4) (A) and reference spectra of gypsum (B) , polyester resin (C) and shellac (D) shown in Figures 4.11 and 4.17.	148
Figure 4.20	EI MS of methyl 7-Oxodehydroabietic acid (5) and methyl dehydroabietate (6) . A list of peaks can be seen in Table 4.5.	149
Figure 4.21	REPRO.1864-57_3 UVf image (A) showing a white fluorescing coating and a layer fluorescing pink-orange, which is consistent with shellac. The samples were taken from REPRO.1864-57 (Christ at Bethany, object dimensions 135.0X112.0 cm) (B) .	150
Figure 4.22	Sample 1 from REPRO.1874-29 (Brass font, object dimensions 183.0x990.0 cm) (A) shows a Cu and shellac coating. VLR (B) and UVf (C) OM, BSE (D) images and EDS mapping showing Al, Cu, Mg and Si.	150

Figure 4.23	El-MS of jalaric acid (8), shelloic acid (9), shellolic acid (10) and aleuritic acid (11). The list of peaks can be seen in Table 4.5.	151
Figure 4.24	El-MS of phthalic anhydride (12) and dimethyl phthalate (13). The list of peaks can be seen in Table 4.5.	152
Figure 4.25	Sample 6 taken from REPRO.1874-29 (Brass font, object dimensions 183.0x990.0 cm) (D). VLR (A) and UVf (B) OM and BSE (C) images. EDS mapping showing C, O, Al, Si, Cl, S, Ca, Ti, Fe, Cu, Zn, Ba and Pb.	154
Figure 4.26	REPRO.1873-380_4. VLR OM (A) and BSE (C) images. EDS mapping showing Si, Al, Fe and Ti. The sample was taken from REPRO.1873-380 (Tombstone of the Presbyter Bruno, object dimensions 218.5X77.0 cm) (B).	155
Chapter 5 Frontpage	Coated plaster surface reconstructions in the Merca Scientific MGF8401 Excell Humidity cabinet MER 180 SCN/RH.	161
Figure 5.1	Plaster was added to the water in the traditional 'island' method (A) until a creamy consistency was achieved (B).	168
Figure 5.2	The bottom halves of the plaster plates were protected with Melinex [®] sheets (A) while the top half was airbrushed with the artificial soiling solution (B).	171
Figure 5.3	The scheme of the sectors on the plates is shown on the left. The sectors were named from a to f. S= soiled, US= unsoiled. On the right is shown an example: on P1, P1b is the sector coated with (1-1) and soiled (S).	172
Figure 5.4	Plots of the gravimetry data of the twelve plaster plates (P1-12), for the whole experiment from t_0 to t_{38} (A), corrected and normalised as described in Section 5.2.2.1. The initial drying time from t_0 to t_6 is shown in (B) and after coating application from t_{19} and t_{38} (C). t_{20} marks the application of the linseed oil (1), shellac (2) and barite (3) coatings, t_{28} the beginning of the accelerated ageing and t_{32} the application of the beeswax coating (4) P2, 4, 6, 8, 10 and 12. For details and t_z labels refer to Table 5.3 on page 174.	181
Figure 5.5	Vis and UVf images of the unaged (UA) sections P1e and P1b and the aged (A) sections P3e and P3b of the cold-pressed linseed oil coating (1-1) at t_{37} . Each square is 1x1 cm. Cold-pressed linseed oil after accelerated ageing showed discolouration for the soiled (S) sections under visible illumination and the bright light-blue fluorescence almost disappeared. The aged and soiled area (b) has an increased porosity.	184
Figure 5.6	Vis and UVf images of the unaged (UA) sections P1f and P1c and the aged (A) sections P3f and P3c of the boiled linseed oil coating (1-2) at t_{37} . Each square is 1x1 cm. Boiled linseed oil appears slightly discoloured after accelerated ageing under visible illumination, but the bright light-blue fluorescence colour under UV remains unchanged upon ageing. The arrows indicate areas where the coating was not absorbed by the substrate.	184

Figure 5.7	Vis and UVf images of the unaged (UA) sections P5e and P5b and the aged (A) sections P7e and P7b of the shellac6% coating (2-1) at t_{37} . Each square is 1x1 cm. Shellac6% is slightly discoloured under visible light and the light-blue fluorescence dulled, after ageing. The aged and soiled area (b) shows increased porosity, probably due to the complete drying of the surface.	185
Figure 5.8	Vis and UVf images of the unaged (UA) sections P5f and P5c and the aged (A) sections P7f and P7c of the shellac18% coating (2-2) at t_{37} . Each square is 1x1 cm. Shellac18% is slightly discoloured under visible light and the light-blue fluorescence dulled, after ageing. In the soiled area (c), the arrows in the image show that the soiling mixture has not adhered uniformly, suggesting that the shellac coating has been absorbed unevenly by the plaster.	185
Figure 5.9	Vis and UVf images of the unaged (UA) sections P9e and P9b and the aged (A) sections P11e and P11b of the barite20° coating (3-1) at t_{37} . Each square is 1x1 cm. Under visible light, barite20° appears to be slightly whitened after accelerated ageing, and the UV fluorescence was not particularly intense.	186
Figure 5.10	Vis and UVf images of the unaged (UA) sections P9f and P9c and the aged (A) sections P11f and P11c of the barite60° coating (3-2) at t_{37} . Each square is 1x1 cm. Under visible light, barite60° appears to be slightly whitened after accelerated ageing, and the UV fluorescence was not particularly intense.	186
Figure 5.11	Vis and UVf images (1x1 cm) of sections P2d (plaster and beeswax, US, UA), P2a (plaster and beeswax, S, UA), P4d (plaster and beeswax, US, A) and P4a (plaster and beeswax, S, A) at t_{37} . Each square is 1x1 cm. The arrows point the brush marks highlighted by the presence of the soiling mixture. Upon ageing, the colour of the soiled section slightly faded, and the brush marks are less noticeable (P4a).	187
Figure 5.12	BSE (SEM MAG: 300x) (left) and FT-IR microscope survey (1x1 mm) (right) micrographs of control unaged (top) sections P1d (US) and P1a (S), and aged (bottom) sections P3d (US) and P3a (S) at t_{37} . Only an increased presence of 'voids' (or 'pores') after ageing is observed (P1 vs. P3).	189
Figure 5.13	HR 3D images (5.3x5.3 mm) of sections P1d (only plaster, US, UA), P1a (only plaster, S, UA), P3d (only plaster, US, A) and P3a (only plaster, S, A) at t_{37} . An increased presence of 'voids' (or 'pores') after ageing is observed (P1 vs. P3), possibly due to further drying of the surface.	190
Figure 5.14	BSE (SEM MAG: 300x) (left) and micrographs (1x1 mm) (right) images of unaged (top) sections P1e (US) and P1b (S), and aged (bottom) sections P3e (US) and P3b (S) coated with cold-pressed linseed oil at t_{37} . The discolouration from a darker to a lighter tone after ageing can be seen in the micrograph. The 'tabular' structure of gypsum plaster is visible in the BSE images despite the coats.	191

Figure 5.15	BSE (SEM MAG: 300x) (left) and micrographs (1x1 mm) (right) of unaged (top) sections P1f (US) and P1c (S), and aged (bottom) sections P3f (US) and P3c (S) coated with boiled linseed oil at t_{37} . The discolouration from a darker to a lighter tone after ageing can be seen in the micrograph. The 'tabular' structure of gypsum plaster is visible in the BSE images despite the coats.	191
Figure 5.16	HR 3D images of sections e (US) and b (S), on P1 (UA) and P3 (A), coated with cold-pressed linseed oil at t_{37} . No significant differences can be observed in the HR 3D images, supporting the assumption that the cold-pressed linseed oil penetrated the plaster.	192
Figure 5.17	HR 3D images of sections f (US) and c (S), on P1 (UA) and P3 (A), coated with boiled linseed oil at t_{37} . No significant differences can be observed in the HR 3D images, supporting the assumption that the boiled linseed oil penetrated the plaster.	192
Figure 5.18	BSE (SEM MAG: 300x) (left) and micrographs (1x1 mm) (right) of unaged (top) sections P5e (US) and P5b (S), and aged (bottom) sections P7e (US) and P7b (S) coated with shellac6% at t_{37} . The discolouration from a darker to a lighter tone after ageing can be seen in the micrograph. The 'tabular' structure of gypsum plaster can be seen in the BSE images (see <i>Section 3.1.1</i>).	193
Figure 5.19	BSE (SEM MAG: 300x) (left) and micrographs (1x1 mm) (right) of unaged (top) sections P5f (US) and P5c (S), and aged (bottom) sections P7f (US) and P7c (S) coated with shellac18% at t_{37} . The discolouration from a darker to a lighter tone after ageing can be seen in the micrograph. The 'tabular' structure of gypsum plaster can be seen in the BSE images (see <i>Section 3.1.1</i>).	193
Figure 5.20	HR 3D images of sections e (US) and b (S), on P5 (UA) and P7 (A), coated with shellac6% at t_{37} . No significant differences can be observed in the HR 3D images, but the soiled section appears somehow more even.	194
Figure 5.21	HR 3D images of sections f (US) and c (S), on P5 (UA) and P7 (A), coated with shellac18% at t_{37} . No significant differences can be observed in the HR 3D images, but the soiled section appears somehow more even.	194
Figure 5.22	BSE (SEM MAG: 300x) (left) and micrographs (1x1 mm) (right) of unaged (top) sections P9e (US) and P9b (S), and aged (bottom) sections P11e (US) and P11b (S) coated with barite20° at t_{37} . In the BSE images, the structure of the mineral barite solution appears brighter (barium, Ba, has a higher atomic number than that of calcium, Ca, and for this reason, the BSE image is brighter), and the needle-like structure, similar to the 'tabular' structure of gypsum plaster (Aquilano et al., 2016; Cox et al., 1974) is tighter and finer. No obvious changes in this structure can be observed in the BSE image upon ageing.	195

Figure 5.23	BSE (SEM MAG: 300x) (left) and micrographs (1x1 mm) (right) of unaged (top) sections P9f (US) and P9c (S), and aged (bottom) sections P11f (US) and P11c (S) coated with barite60° at t ₃₇ . In the BSE images, the structure of the mineral barite solution appears brighter (barium, Ba, has a higher atomic number than that of calcium, Ca, and for this reason, the BSE image is brighter), and the needle-like structure, similar to the 'tabular' structure of gypsum plaster (Aquilano et al., 2016; Cox et al., 1974) is tighter and finer. No obvious changes in this structure can be observed in the BSE image upon ageing.	195
Figure 5.24	HR 3D images of sections e (US) and b (S), on P9 (UA) and P11 (A), coated with Barite20° at t ₃₇ . The surfaces, apart from the presence of pores in the soiled sections, appear uniform throughout their area and consistent before and after ageing (P9 to P11 of the relevant area).	196
Figure 5.25	HR 3D images of sections f (US) and c (S), on P9 (UA) and P11 (A), coated with barite60° at t ₃₇ . The surfaces, apart from the presence of pores in the soiled sections, appear uniform throughout their area and consistent before and after ageing (P9 to P11 of the relevant area).	196
Figure 5.26	BSE (SEM MAG: 300x) (left) and micrographs (1x1 mm) (right) of unaged sections P2d (plaster and beeswax, US, UA) and P2a (plaster and beeswax, S, UA) and aged sections P4d (plaster and beeswax, US, A) and P4a (plaster and beeswax, S, A) at t ₃₇ . The gypsum plaster structure cannot be seen after the application of beeswax and the surfaces show a coherent and smooth surface with an orange-peel like appearance.	197
Figure 5.27	HR 3D images (5.3x5.3 mm) of plaster-beeswax control sections P2d (US, UA), P2a (S, UA), P4d (US, A) and P2a (S, A) at t ₃₇ . Brush marks are visible in the HR 3D images (black arrows) and upon ageing the marks are not as visible.	197
Figure 5.28	Colour changes before/after ageing according to CIE formula ΔE_{00} ($\pm 0.4\%$) [SCI]. The most significant changes can be seen in the areas coated with linseed oil, unsoiled (US) and soiled (S) and soiled shellac18% (2-2) and barite60° (3-2). The rest of the sections show changes under or close to the smallest noticeable difference.	199
Figure 5.29	Yellow Index (YI ₃₁₃) [SCI] of the unsoiled (i) and soiled (ii) sections. The changes in YI are overall small before (UA)/after (A) ageing, indicating a small decrease in the yellow component. In a few exceptional cases (e.g., boiled linseed oil+beeswax) the YI increases after ageing.	200
Figure 5.30	Reflectance (%) ($\pm 0.05\%$) [SCI] of the d (unsoiled - US) (i) and a (soiled - S) (ii) plaster control sections of P1, 5 and 9 (unaged - UA) and P3, 7 and 11 (aged - A) at t ₃₇ showing that the surfaces are darker after the application of the soiling.	201
Figure 5.31	L* (± 0.05) measurements of the d (unsoiled - US) and a (soiled - S) control sections of P1, 5 and 9 (unaged - UA) and P3, 7 and 11 (aged - A) at t ₃₇ . L* is relatively constant across the US control sections, UA and A, and varies in the S areas.	202

Figure 5.32	Reflectance (%) (± 0.05 %) of the d (unsoiled - US) (i) and a (soiled - S) (ii) plaster-beeswax (4) control sections of P2, 6 and 10 (unaged - UA) and P4, 8 and 12 (aged - A) at t_{37} showing that the R% of the surfaces is consistent in the UA and A areas. The surfaces are darker after the application of the soiling.	203
Figure 5.33	L^* (± 0.05) measurements of the d (unsoiled - US) and a (soiled - S) sections of P2, 6 and 10 (unaged - UA) and P4, 8 and 12 (aged - A) at t_{37} . L^* is relatively constant across the US control sections, UA and A, and varies in the S areas.	203
Figure 5.34	Reflectance (%) (± 0.05 %) of unsoiled – US, and soiled - S sections, on P1 (UA) and P3 (A), coated with cold-pressed linseed oil (1-1) (i) and boiled linseed oil (1-2) (ii) at t_{37} and relevant surfaces (iii and iv) with an additional layer of beeswax (4) on P2 (unaged - UA) and P4 (aged - A). All the US sections are whiter than the relevant S areas, UA and A. Only the area where beeswax was applied on top of boiled linseed oil shows significant changes in R%, with the US aged area becoming darker than the relevant unaged one.	205
Figure 5.35	b^* (± 0.01) measurements of unsoiled – US, and soiled - S sections, on P1 (unaged - UA) and P3 (aged - A), coated with cold-pressed linseed oil (1-1) (i) and boiled linseed oil (1-2) (ii) at t_{37} and relevant surfaces with an additional layer of beeswax (4) on P2 (UA) and P4 (A). In all the section the b^* value is reduced after ageing. Only in the coating boiled linseed oil-beeswax and increase of the yellow component can be seen.	205
Figure 5.36	Reflectance (%) (± 0.05 %) unsoiled – US, and soiled - S sections, on P5 (unaged - UA) and P7 (aged - A), coated with shellac6% (2-1) (i) and shellac18% (2-2) (ii) at t_{37} and relevant surfaces (iii and iv) with an additional layer of beeswax (4) on P6 (UA) and P8 (A). All the US sections are whiter than the relevant S areas, UA and A.	207
Figure 5.37	a^* (± 0.001) (i and iii) and b^* (± 0.01) (ii and iv) measurements of unsoiled – US, and soiled - S sections, on P5 (unaged - UA) and P7 (aged - A), coated with shellac6% (2-1) and shellac18% (2-2) at t_{37} and relevant surfaces with an additional layer of beeswax (4) on P6 (UA) and P8 (A). a^* and b^* decrease in all the sections after ageing.	208
Figure 5.38	Reflectance (%) (± 0.05 %) unsoiled – US, and soiled - S sections, on P9 (unaged - UA) and P11 (aged - A), coated with barite20° (3-1) (i) and barite60° (2-2) (ii) at t_{37} and relevant surfaces (iii and iv) with an additional layer of beeswax (4) on P10 (UA) and P12 (A). The surfaces did not relevantly change after ageing and the most significant changes in R% can be seen between the US and S areas.	209
Figure 5.39	L^* measurements of unsoiled – US, and soiled - S sections, on P9 (unaged - UA) and P11 (aged - A), coated with barite20° (3-1) (i) and barite60° (3-2) (ii) at t_{37} and relevant surfaces with an additional layer of beeswax (4) on P10 (UA) and P12 (A). The L^* values are consistent with and without the beeswax coating..	210

Figure 5.40	ATR/FT-IR spectra acquired from all the plaster plates at t_{12} . The peaks positions are summarised in Table 5.12.	212
Figure 5.41	Diffuse Reflectance (DR) FT-IR spectra acquired from areas of the unsoiled and unaged plaster surfaces coated with cold-pressed linseed oil P1e (1-1), light blue spectra, and with boiled linseed oil P1f (1-2), purple spectra, at t_{37} .	219
Chapter 6 Frontpage	Agarose gel used to measure pH and conductivity of the coated plaster surface reconstructions.	231
Figure 6.1	The disk made of agarose (A) was cut into plugs (B) to measure the pH and conductivity of the surfaces (C).	239
Figure 6.2	Preliminary tests to choose the solution were undertaken with the aid of a swab (A) and small cuts (0.5x0.5 cm) of the PE (B). For example, in P3c (C), it can be seen the areas where the pH and conductivity (σ) measurements were taken, the areas where sol B was used with a cotton swab, with PAM _{15-E3} and PAM ₁₅ . The test area (2x2 cm) was cleaned with sol B and PAM ₁₅ .	241
Figure 6.3	Photographs (2x2 cm) taken under Vis and UV illumination of the uncoated gypsum plaster surfaces (areas P1a and P3a). The labels on the photographs indicate the type of illumination and if the image was acquired from unaged (UA) or aged (A) plates, before (S) or after (AC) cleaning with PE-PAM-TEA solution pH 8.5 (Sol B). The relevant unsoiled (US) sections P1d and P3d are also shown.	249
Figure 6.4	Photographs (2x2 cm) taken under Vis and UV illumination of the uncoated gypsum plaster surfaces (P5a and P7a). The labels on the photographs indicate the type of illumination and if the image was acquired from unaged (UA) or aged (A) plates, before (S) or after (AC) cleaning with PE-PAM-HCl solution pH6 (Sol D). The relevant unsoiled (US) sections P5d and P7d are also shown.	249
Figure 6.5	Photographs (2x2 cm) taken under Vis and UV illumination of the uncoated gypsum plaster surfaces (P9a and P11a). The labels on the photographs indicate the type of illumination and if the image was acquired from unaged (UA) or aged (A) plates, before (S) or after (AC) cleaning with PE-PAM-TEA solution pH 8 (Sol A). The relevant unsoiled (US) sections P9d and P11d are also shown.	250
Figure 6.6	Photographs (2x2 cm) taken under Vis and UV illumination of the gypsum plaster surfaces coated with cold-pressed linseed oil (1-1) (P1b and P3b). The labels on the photographs indicate the type of illumination and if the image was acquired from unaged (UA) or aged (A) plates, before (S) or after (AC) cleaning with PE-PAM-EDTA solution pH 8.5 (Sol H). The relevant unsoiled (US) sections P1e and P3e are also shown.	250
Figure 6.7	Photographs (2x2 cm) taken under Vis and UV illumination of the gypsum plaster surfaces coated with boiled linseed oil (1-2) (P1c and P3c). The labels on the photographs indicate the type of illumination and if the image was acquired from unaged (UA) or aged (A) plates, before (S) or after (AC) cleaning with PE-PAM-TEA solution pH8.5 (Sol B). The relevant unsoiled (US) sections P1f and P3f are also shown..	251

Figure 6.8	Photographs (2x2 cm) taken under Vis and UV illumination of the gypsum plaster surfaces coated with shellac6% (2-1) (P5b and P7b). The labels on the photographs indicate the type of illumination and if the image was acquired from unaged (UA) or aged (A) plates, before (S) or after (AC) cleaning with PE-PAM-HCl solution pH 6 (Sol D). The relevant unsoiled (US) sections P5e and P7e are also shown.	251
Figure 6.9	Photographs (2x2 cm) taken under Vis and UV illumination of the gypsum plaster surfaces coated with shellac18% (2-2) (P5c and P7c). The labels on the photographs indicate the type of illumination and if the image was acquired from unaged (UA) or aged (A) plates, before (S) or after (AC) cleaning with PE-PAM-HCl solution pH 6 (Sol D). The relevant unsoiled (US) sections P5f and P7f are also shown.	252
Figure 6.10	Photographs (2x2 cm) taken under Vis and UV illumination of the gypsum plaster surfaces coated with barite20° (3-1) (P9b and P11b). The labels on the photographs indicate the type of illumination and if the image was acquired from unaged (UA) or aged (A) plates, before (S) or after (AC) cleaning with PE-PAM-TEA solution pH 8 (Sol A) (for the UA area) and PE-PAM-EDTA solution pH 8.5 (Sol H) (for the A area). The relevant unsoiled (US) sections P9e and P11e are also shown.	252
Figure 6.11	Photographs (2x2 cm) taken under Vis and UV illumination of the gypsum plaster surfaces coated with barite60° (3-2) (P9c and P11c). The labels on the photographs indicate the type of illumination and if the image was acquired from unaged (UA) or aged (A) plates, before (S) or after (AC) cleaning with PE-PAM-EDTA solution pH 8.5 (Sol H). The relevant unsoiled (US) sections P9f and P11f are also shown.	253
Figure 6.12	Photographs (2x2 cm) taken under Vis and UV illumination of the gypsum plaster surfaces coated with beeswax (4) (P2a and P4a). The labels on the photographs indicate the type of illumination and if the image was acquired from unaged (UA) or aged (A) plates, before (S) or after (AC) cleaning with PE-PAM-IMS solution (Sol I). The relevant unsoiled (US) sections P2d and P4d are also shown.	253
Figure 6.13	Photographs (2x2 cm) taken under Vis and UV illumination of the gypsum plaster surfaces coated with cold-pressed linseed oil (1-2) and beeswax (4) (P2b and P4b). The labels on the photographs indicate the type of illumination and if the image was acquired from unaged (UA) or aged (A) plates, before (S) or after (AC) cleaning with PE-PAM-IMS solution (Sol I). The relevant unsoiled (US) sections P2e and P4e are also shown.	254
Figure 6.14	Photographs (2x2 cm) taken under Vis and UV illumination of the gypsum plaster surfaces coated with boiled linseed oil (2-2) and beeswax (4) (P2c and P4c). The labels on the photographs indicate the type of illumination and if the image was acquired from unaged (UA) or aged (A) plates, before (S) or after (AC) cleaning with PE-PAM-IMS solution (Sol I). The relevant unsoiled (US) sections P2f and P4f are also shown.	254

Figure 6.15	Photographs (2x2 cm) taken under Vis and UV illumination of the gypsum plaster surfaces coated with shellac6% (2-1) and beeswax (4) (P6b and P8b). The labels on the photographs indicate the type of illumination and if the image was acquired from unaged (UA) or aged (A) plates, before (S) or after (AC) cleaning with PE-PAM-IMS solution (Sol I). The relevant unsoiled (US) sections P6e and P8e are also shown.	255
Figure 6.16	Photographs (2x2 cm) taken under Vis and UV illumination of the gypsum plaster surfaces coated with shellac18% (3-2) and beeswax (4) (P6c and P8c). The labels on the photographs indicate the type of illumination and if the image was acquired from unaged (UA) or aged (A) plates, before (S) or after (AC) cleaning with PE-PAM-IMS solution (Sol I). The relevant unsoiled (US) sections P6f and P8f are also shown.	255
Figure 6.17	Photographs (2x2 cm) taken under Vis and UV illumination of the gypsum plaster surfaces coated with barite20° (3-1) and beeswax (4) (P10b and P12b). The labels on the photographs indicate the type of illumination and if the image was acquired from unaged (UA) or aged (A) plates, before (S) or after (AC) cleaning with PE-PAM-IMS solution (Sol I). The relevant unsoiled (US) sections P10e and P12e are also shown.	256
Figure 6.18	Photographs (2x2 cm) taken under Vis and UV illumination of the gypsum plaster surfaces coated with barite60° (3-2) and beeswax (4) (P10c and P12c). The labels on the photographs indicate the type of illumination and if the image was acquired from unaged (UA) or aged (A) plates, before (S) or after (AC) cleaning with PE-PAM-IMS solution (Sol I). The relevant unsoiled (US) sections P10f and P12f are also shown.	256
Figure 6.19	From left to right: BSE images (SEM MAG: 300x), FT-IR survey micrographs (1x1 mm) and the HR 3D images (5.3x5.3 mm) of the uncoated gypsum plaster surfaces (P1a and P3a) before (S) and after (AC) cleaning with PE-PAM-TEA solution pH8.5 (Sol B). A reduction of the quantity of the black particles of soil can be seen after cleaning in all the images. The 3D images highlight the removal of the soiling, but also some unevenness of the surface after cleaning. The smoothing of the surface can be seen in the BSE images after cleaning.	258
Figure 6.20	From left to right: BSE images (SEM MAG: 300x), FT-IR survey micrographs (1x1 mm) and the HR 3D images (5.3x5.3 mm) of the uncoated gypsum plaster surfaces (P5a and P7a) before (S) and after (AC) cleaning with PE-PAM-TEA solution pH 8 (Sol A). A reduction of the quantity of the black particles of soil can be seen after cleaning in all the images. The smoothing of the surface can be seen in the BSE images after cleaning.	259
Figure 6.21	From left to right: BSE images (SEM MAG: 300x), FT-IR survey micrographs (1x1 mm) and the HR 3D images (5.3x5.3 mm) of the uncoated gypsum plaster surfaces (P9a and P11a) before (S) and after (AC) cleaning with PE-PAM-HCl solution pH 6 (Sol D). A reduction of the quantity of the black particles of soil can be seen after cleaning in all the images. The smoothing of the surface can be seen in the BSE images after cleaning.	260

Figure 6.22	<p>From left to right: BSE images (SEM MAG: 300x), FT-IR survey micrographs (1x1 mm) and the HR 3D images (5.3x5.3 mm) of the plaster surfaces coated with cold-pressed linseed oil (1-1) (P1b and P3b) before (S) and after (AC) cleaning with PE-PAM-EDTA solution pH 8.5 (Sol H). A reduction of the quantity of the black particles of soil can be seen after cleaning in all the images. The 3D images highlight the removal of the soiling, but also some unevenness of the surface after cleaning. The smoothing of the surface can be seen in the BSE images after cleaning.</p>	261
Figure 6.23	<p>From left to right: BSE images (SEM MAG: 300x), FT-IR survey micrographs (1x1 mm) and the HR 3D images (5.3x5.3 mm) of the plaster surfaces coated with boiled linseed oil (1-2) (P1c and P3c) before (S) and after (AC) cleaning with PE-PAM-TEA solution pH 8.5 (Sol B). A reduction of the quantity of the black particles of soil is observed, but the cleaning of the boiled linseed oil was less effective than the cleaning of the cold-pressed linseed oil and some soiling can still be seen in the images. The 3D images highlight some unevenness of the surface after cleaning and the smoothing effect is less pronounced.</p>	262
Figure 6.24	<p>From left to right: BSE images (SEM MAG: 300x), FT-IR survey micrographs (1x1 mm) and the HR 3D images (5.3x5.3 mm) of the plaster surfaces coated with shellac6% (2-1) (P5b and P7b) before (S) and after (AC) cleaning with PE-PAM-HCl solution pH 6 (Sol D). A reduction of the quantity of the black particles of soil can be seen after cleaning in all the images. The cleaning was less effective in the unaged areas, as can be observed in the images of the P5b, where soiling particles can still be seen. The smoothing effect shown in the previous images was less pronounced for the areas coated with shellac, possibly because of a harder and drier surface.</p>	263
Figure 6.25	<p>From left to right: BSE images (SEM MAG: 300x), FT-IR survey micrographs (1x1 mm) and the HR 3D images (5.3x5.3 mm) of the plaster surfaces coated with shellac18% (2-2) (P5c and P7c) before (S) and after (AC) cleaning with PE-PAM- HCl solution pH 6 Sol D. A reduction of the quantity of the black particles of soil can be seen after cleaning in all the images. A reduction of the quantity of the black particles of soil can be seen after cleaning in all the images. The cleaning was less effective in the aged areas, as can be observed in the images of the P7c, where soiling particles can still be seen. The smoothing effect shown in the previous images was less pronounced for the areas coated with shellac, possibly because of a harder and drier surface.</p>	264
Figure 6.26	<p>From left to right: BSE images (SEM MAG: 300x), FT-IR survey micrographs (1x1 mm) and the HR 3D images (5.3x5.3 mm) of the plaster surfaces coated with barite20° (3-1) (P9b and P11b) before (S) and after (AC) cleaning with PE-PAM-TEA solution pH 8 (Sol A) and -EDTA solution pH 8.5 (Sol H). A reduction of the quantity of the black particles of soil can be seen after cleaning in all the images, and overall very few changes were observed in the texture of the surface.</p>	265

Figure 6.27	From left to right: BSE images (SEM MAG: 300x), FT-IR survey micrographs (1x1 mm) and the HR 3D images (5.3x5.3 mm) of the plaster surfaces coated with barite ^{60°} (3-2) (P9c and P11c) before (S) and after (AC) cleaning with PE-PAM-EDTA solution (Sol H). A reduction of the quantity of the black particles of soil can be seen after cleaning in all the images, and overall very few changes were observed in the texture of the surface.	266
Figure 6.28	From left to right: BSE images (SEM MAG: 300x), FT-IR survey micrographs (1x1 mm) and the HR 3D images (5.3x5.3 mm) of the plaster surfaces coated with beeswax (4) (P2a and P4a) before (S) and after (AC) cleaning with PE-PAM-IMS solution (Sol I). The soil mixture seemed to have been almost entirely removed from both the unaged and aged areas. The soil that was not removed was mostly located in the pores (see for example black arrow in micrograph of area P4a after cleaning). Overall, the cleaning appeared more homogeneous and effective in the aged areas.	267
Figure 6.29	Colour changes before(S)/after(AC) cleaning according to CIE formula ΔE_{00} ($\pm 0.4\%$) [SCI]. The colour change after cleaning is visible in most of the sections. Only in a few areas (P6c, P8c, P9b, P10a, P10b, P11b, P12c) the cleaning did not cause a change higher than the smallest visible difference.	269
Figure 6.30	Colour differences between the unsoiled (US) areas and the soiled areas after cleaning (AC) according to CIE formula ΔE_{00} ($\pm 0.4\%$) [SCI]. Despite changes in colour after cleaning were observed, as shown in Figure 6.35, the difference in colour between the unsoiled and cleaned areas is noticeable. This is also due to other factors, such as continued ageing and the wetting of the surfaces.	270
Figure 6.31	Figure 6.38. Yellow Index (YI_{313}) [SCI] of the unsoiled (US) and soiled sections before (S) and after cleaning (AC). All the soiled sections show a higher YI than the unsoiled relevant section. In most of the sections a decrease of yellowness in the soiled areas before(S)/after(AC) cleaning can be seen. In a few areas (P1c, P2a, P5c, P6a, P6b, P6c, P8c, P10a, P10b, P10c, P12c) an increase of yellowness in observed after cleaning. This can be due to the yellowing of the surface due to ageing, after an initial bleaching highlighted in Section 5.3.	271
Figure 6.32	Gloss _{85°} of the sections US (grey), S (dark grey) and AC (blue) showed that a significant increase of gloss is achieved after cleaning. The AC values can be seen in Tables 6.4 to 6.9, the US and S in Tables 5.5 to 5.11. Plot (i) shows Gloss _{85°} of the uncoated plaster sections, (ii) of the sections coated with linseed oil, shellac and barite and (iii) and (iv) the respectively relevant sections also coated with beeswax.	272
Figure 6.33	R_a of the sections US (grey), S (dark grey) and AC (green) showed that overall, the surfaces were smoothed after cleaning (AC). In a few cases (e.g., P12a and P6b) an increase of roughness is seen, and it can be due to the local porosity. The AC values can be seen in Tables 6.4 to 6.9, the US and S in Tables 5.5 to 5.11. Plot (i) shows R_a of the uncoated plaster sections, (ii) of the sections coated with linseed oil, shellac and barite and (iii) and (iv) the respectively relevant sections also coated with beeswax.	272

Figure 6.34	R (%) (± 0.05 %) [SCI] measured from the uncoated areas before cleaning (plaster+soiling, a) (ii) and after cleaning (uncoated plaster, a) (iii) . R% of the uncoated unsoiled plaster (d) (i) is also shown for reference. The areas belong to the plaster control sections of P1, 5 and 9 (UA) and P3, 7 and 11 (A). The R% of the cleaned areas shows intermediate values between the ones of the US and S areas.	273
Figure 6.35	R (%) (± 0.05 %) [SCI] measured from of the areas coated with beeswax before cleaning (plaster and beeswax+soiling, a) (ii) and after cleaning (beeswax, a) (iii) . R% of the unsoiled plaster coated with beeswax (d) (i) is also shown for reference. The areas belong to the plaster-beeswax control sections of P2, 6 and 10 (UA) and P4, 8 and 12 (A). The R% of the cleaned areas shows intermediate values between the ones of the US and S areas.	273
Figure 6.36	Reflectance (%) (± 0.05 %) [SCI] measured from the areas coated with cold-pressed linseed oil (i) , boiled linseed oil (ii) , shellac6% (iii) , shellac18% (iv) , barite20° (v) and barite60° (vi) after cleaning (AC) are compared to the relevant sections US, S, UA and A. After cleaning the R% was not particularly different in the areas coated with boiled linseed oil (ii) and barite (v and vi) and was intermediate between the US and S values after cleaning for cold-pressed linseed oil (i) and shellac (iii and iv) .	274
Figure 6.37	Reflectance (%) (± 0.05 %) [SCI] measured from of the areas coated with cold-pressed linseed oil (i) , boiled linseed oil (ii) , shellac6% (iii) , shellac18% (iv) , barite20° (v) and barite60° (vi) and beeswax after cleaning (AC) are compared to the relevant sections US, S, UA and A. After cleaning the R% was not particularly different in the areas coated with boiled linseed oil (ii) , shellac18% (iv) and barite (v and vi) , but was intermediate between the US and S values after cleaning for cold-pressed linseed oil (i) and shellac6% (iii) .	275
Figure 6.38	FT-IR spectra acquired on the aged areas coated shellac6% unsoiled (P3e), soiled (P3b) and cleaned (P3b, AC). The spectra are consistent and small differences can be seen.	279
Chapter 7 Frontpage	Image No. 2018LC8071. Detail of the Cast of the Pórtico de la Gloria (REPRO.1866-50), 1866, D. Brucciani. Now in The Ruddock Family Cast Court, Room 46A, V&A. © Victoria and Albert museum, London/as specified by the rights holder. Source: V&A's Collection Management System	285
 VOLUME 2 		
Appendices Frontpage	View of the inner court of Blythe House (London, UK), housing the V&A Archive (VAA). September 2018.	1
Figure A4.1	Figures attached to Patent No. 192112, 19 June 1877, by W. B. Closson. Source: https://worldwide.espacenet.com/	73
Figure A4.2	Figures attached to Patent No. 968505, 23 August 1910, by G. J. Zolnay. Source: https://worldwide.espacenet.com/	80

Figure A4.3	Figures attached to Patent No. 2660776, 1 December 1953, by J. H. Miller. Source: https://worldwide.espacenet.com/	84
Figure A5.1	Presbyter Bruno (REPRO.1873-380), ca. 1873. Photographic record: 2006BK4555. © Victoria and Albert Museum, London/as specified by the rights holder. Source: V&A's Collection Management System.	88
Figure A5.2	Record of the Presbyter Bruno (REPRO.1873-380) acquisition retrieved from the Registry of Reproductions of the V&A Museum (1873). The Registry reports the description of the cast, notes on the purchase, and the price paid. © Victoria and Albert Museum, London/as specified by the rights holder.	88
Figure A5.3	Figure A5.3. Choir screen stucco (REPRO.1873-561), ca. 1873. © Victoria and Albert Museum, London/as specified by the rights holder. Source: V&A's Collection Management System.	89
Figure A5.4	Record of the Choir screen stucco (REPRO.1873-561) acquisition retrieved from the Registry of Reproductions of the V&A Museum (1873). The Registry reports the description of the cast, notes on the purchase, and the price paid for the object. © Victoria and Albert Museum, London/as specified by the rights holder	89
Figure A5.5	Font cast brass (REPRO.1874-29), ca. 1874. © Victoria and Albert Museum, London/as specified by the rights holder. Source: V&A's Collection Management System.	90
Figure A5.6	Left: V&A's objects number 78075. Right: V&A's objects number 1665-1926. Photograph, the font in the Cathedral of Hildesheim, Germany, gelatine silver print, late nineteenth to the early twentieth century. © Victoria and Albert Museum, London/as specified by the rights holder. Source: V&A's Collection Management System.	91
Figure A5.7	Record of the Font cast brass (REPRO.1874-29) acquisition retrieved from the Registry of Reproductions of the V&A Museum (1874). The Registry reports the description of the cast, notes on the purchase, and the price paid for the object. © Victoria and Albert Museum, London/as specified by the rights holder.	91
Figure A5.8	Christ, St. Godehard and St. Epiphanius (REPRO.1874-45), ca. 1874. © Victoria and Albert Museum, London/as specified by the rights holder. Source: V&A's Collection Management System.	92
Figure A5.9	Record of the Christ, St. Godehard and St. Epiphanius (REPRO.1874-45) acquisition retrieved from the Registry of Reproductions of the V&A Museum (1874). © Victoria and Albert Museum, London/as specified by the rights holder.	92
Figure A5.10	Count Ekkehard (REPRO.1875-16), ca. 1875. © Victoria and Albert Museum, London/as specified by the rights holder. Source: V&A's Collection Management System.	93
Figure A5.11	Records of Regilindis, wife of Hermann, Margrave of Meissen (REPRO.1875-17) and count Ekkehard (REPRO.1875-16) acquisition retrieved from the Registry of reproductions of the V&A museum (1875). © Victoria and Albert Museum, London/as specified by the rights holder.	93

Figure A5.12	Regilindis, wife of Hermann, Margrave of Meissen (REPRO.1875-17), ca. 1875. © Victoria and Albert Museum, London/as specified by the rights holder. Source: V&A's Collection Management System.	94
Figure A5.13	Relief Assumption of the Virgin stone (REPRO.1890-80). Plaster cast made by Messrs Jean Pouzadoux, ca. 1890. © Victoria and Albert Museum, London/as specified by the rights holder. Source: V&A's Collection Management System.	95
Figure A5.14	V&A's objects number 76395. Photograph, a plaster cast of a relief depicting The Assumption of the Virgin (REPRO.1890-80), executed under Pierre de Chelles, Notre Dame, Paris, albumen print, late nineteenth century. Albumen print. © Victoria and Albert Museum, London/as specified by the rights holder. Source: V&A's Collection Management System.	96
Figure A5.15	Relief Coronation of the Virgin stone (REPRO.1890-81). Plaster cast made by Messrs Jean Pouzadoux, ca. 1890. © Victoria and Albert Museum, London/as specified by the rights holder. Source: V&A's Collection Management System.	97
Figure A5.16	Relief death of the Virgin stone (REPRO.A.1916-3152). Plaster cast made ca. 1850-1900. © Victoria and Albert Museum, London/as specified by the rights holder. Source: V&A's Collection Management System.	98
Figure A5.17	Relief entombment of the Virgin stone (REPRO.A.1916-3153). Plaster cast made ca. 1850-1900. © Victoria and Albert Museum, London/as specified by the rights holder. Source: V&A's Collection Management System.	99
Figure A5.18	Relief raising of Lazarus stone (REPRO.1864-56). Plaster cast made ca. 1864. © Victoria and Albert Museum, London/as specified by the rights holder. Source: V&A's Collection Management System.	100
Figure A5.19	Left: V&A's objects number PH.2462-1904. Photograph of the plaster cast (REPRO.1864-56) of the relief showing the raising of Lazarus, from Chichester cathedral, possibly a print from a publication, late nineteenth century. Right: V&A's objects number PH.191-1902. Photograph of a relief showing the raising of Lazarus, in Chichester cathedral, possibly a print from a publication, late nineteenth century. © Victoria and Albert Museum, London/as specified by the rights holder. Source: V&A's collection management system.	100
Figure A5.20	Relief Christ at Bethany stone (REPRO.1864-57). Plaster cast made ca. 1864. © Victoria and Albert Museum, London/as specified by the rights holder. Source: V&A's Collection Management System.	101
Figure A7.1	OCEAN is the software that allows the live monitoring of the environmental conditions in the V&A's premises. The map on the right shows the galleries and the location of the data logs.	407
Figure A7.2	Table and picture showing the data logs located on the ground level of the Cast Courts. There are two located in Gallery 46A, one in Galley 46B and three in the corridor in between them.	407

Figure A9.1	XRD diffractograms of samples analysed for this study showed that, despite a few additional peaks that can be seen in some samples, the pattern of gypsum plaster is consistently present. The relevant peaks are provided in Table 4.4. The diffractograms were compared to the references in the databases (Gražulis et al., 2009; Lafuente et al., 2016), for example, R040029 and R060509 from the RRUFF database.	432
Figure A9.2	REPRO.1873-380_6. VLR OM (top left) and BSE (top right) images. EDS mapping (bottom) showing aluminium (Al), calcium (Ca), iron (Fe), potassium (K), sulfur(S), silicon (Si) and titanium (Ti). EDS spectrum (bottom right).	433
Figure A9.3	REPRO.1873-380_7. VLR OM (top) and BSE (middle) images. EDS mapping (bottom) showing aluminium (Al), barium (Ba), calcium (Ca), iron (Fe), potassium (K) and silicon (Si).	434
Figure A9.4	REPRO.1873-561_6. BSE (left) image and EDS mapping (right) showing silicon (Si), barium (Ba) and titanium (Ti).	435
Figure A9.5	REPRO.1875-16_1. VLR (top left) and UVf (top right) OM and BSE (centre) images. EDS mapping (left and bottom) showing carbon (C), sulfur (S), calcium (Ca), iron (Fe), aluminium (Al), barium (Ba), chlorine (Cl) and sodium (Na).	436
Figure A9.6	REPRO.1875-17_2. BSE (top left) image, EDS spectrum (bottom left) and EDS mapping (right) showing lead (Pb), aluminium (Al), chlorine (Cl), silicon (Si) and iron (Fe).	437
Figure A9.7	REPRO.A.1916-3152_1. VLR (top left) and UVf (top right) OM and BSE (centre) images. EDS mapping (bottom) showing lead (Pb), aluminium (Al) and silicon (Si).	438
Figure A9.8	REPRO.1864-56_1. BSE image (top left) and EDS mapping (top right and bottom) showing barium (Ba), strontium (Sr) and zinc (Zn).	439
Figure A9.9	REPRO.1864-56_2. BSE image (top) and EDS mapping (bottom) showing lead (Pb), chlorine (Cl), iron (Fe) and barium (Ba).	440
Figure A9.10	REPRO.1864-57_1. BSE image (left) and EDS mapping (right) showing aluminium (Al), barium (Ba) and silicon (Si).	441
Figure A9.11	Vis and UVf images of control sections P1d (US, UA), P1d (S, UA) P3d (US, A) and P3d (S, A) from t_{13} to t_{37} . Each square corresponds approximately to a 1x1 cm portion of the section.	442
Figure A9.12	Vis and UVf images cold-pressed linseed oil (1-1) coated plates, sections P1e and P3e (US, UA and A) and P1b and P3b (S, UA and A) from t_{26} to t_{37} . Each square corresponds approximately to a 1x1 cm portion of the section.	443
Figure A9.13	Vis and UVf images boiled linseed oil (1-2) coated plates, sections P1f and P3f (US, UA and A) and P1c and P3c (S, UA and A) from t_{26} to t_{37} . Each square corresponds approximately to a 1x1 cm portion of the section.	444

Figure A9.14	Visible and UVf images shellac6% (2-1) coated plates, sections P5e and P7e (US, UA and A) and P5b and P7b (S, UA and A) from t_{26} to t_{37} . Each square corresponds approximately to a 1x1 cm portion of the section.	445
Figure A9.15	Visible and UVf images shellac18% (2-2) coated plates, sections P5f and P7f (US, UA and A) and P5c and P7c (S, UA and A) from t_{26} to t_{37} . Each square corresponds approximately to a 1x1 cm portion of the section.	446
Figure A9.16	Visible and UVf images barite20° (3-1) coated plates, sections P9e and P11e (US, UA and A) and P9b and P11b (S, UA and A) from t_{26} to t_{37} . Each square corresponds approximately to a 1x1 cm portion of the section.	447
Figure A9.17	Visible and UVf images barite60° (3-2) coated plates, sections P9f and P11f (US, UA and A) and P9c and P11c (S, UA and A) from t_{26} to t_{37} . Each square corresponds approximately to a 1x1 cm portion of the section.	448
Figure A9.18	Vis and UVf images of plaster and beeswax sections P2d (US, UA), P2d (S, UA), P4d (US, A) and P4a (S, A) from t_{13} to t_{37} . Each square corresponds approximately to a 1x1 cm portion of the section.	449
Figure A9.19	Visible and UVf images of cold-pressed linseed oil (1-1) and beeswax (4) coated plates, sections P2e and P4e (US, UA and A) and P2b and P4b (S, UA and A) from t_{26} to t_{37} . Each square corresponds approximately to a 1x1 cm portion of the section.	450
Figure A9.20	Visible and UVf images of boiled linseed oil (1-2) and beeswax (4) coated plates, sections P2f and P4f (US, UA and A) and P2c and P4c (S, UA and A) from t_{26} to t_{37} . Each square corresponds approximately to a 1x1 cm portion of the section.	451
Figure A9.21	Visible and UVf images of shellac6% (2-1) and beeswax (4) coated plates, sections P6e and P8e (US, UA and A) and P6b and P8b (S, UA and A) from t_{26} to t_{37} . Each square corresponds approximately to a 1x1 cm portion of the section.	452
Figure A9.22	Visible and UVf images of shellac18% (2-2) and beeswax (4) coated plates, sections P6f and P8f (US, UA and A) and P6c and P8c (S, UA and A) from t_{26} to t_{37} . Each square corresponds approximately to a 1x1 cm portion of the section.	453
Figure A9.13	Visible and UVf images of barite20° (3-1) and beeswax (4) coated plates, sections P10e and P12e (US, UA and A) and P10b and P12b (S, UA and A) from t_{26} to t_{37} . Each square corresponds approximately to a 1x1 cm portion of the section.	454
Figure A9.24	Visible and UVf images of boiled linseed oil (3-2) and beeswax (4) coated plates, sections P10f and P12f (US, UA and A) and P10c and P12c (S, UA and A) from t_{26} to t_{37} . Each square corresponds approximately to a 1x1 cm portion of the section.	455
Figure A9.25	Visible and UVf images of the unaged (UA) and aged (A) sections coated with cold-pressed linseed oil + beeswax (1-1,4) and boiled linseed oil + beeswax (1-2,4) at t_{37} and relevant visual examination notes. Each square corresponds approximately to a 1x1 cm portion of the section.	456

Figure A9.26	FT-IR microscope survey images (1x1 mm), BSE images and high-resolution 3D images (5.3x5.3 mm) of the unaged (UA) and aged (A) sections coated with cold-pressed linseed oil + beeswax (1-1,4) and boiled linseed oil + beeswax (1-2,4) at t_{37} .	457
Figure A9.27	Visible and UVf images of the unaged (UA) and aged (A) sections coated with shellac6% + beeswax (2-1,4) and shellac18% + beeswax (2-2,4) at t_{37} and relevant visual examination notes. Each square corresponds approximately to a 1x1 cm portion of the section.	458
Figure A9.28	FT-IR microscope survey images (1x1 mm), BSE images and high-resolution 3D images (5.3x5.3 mm) of the unaged (UA) and aged (A) sections coated with shellac6% + beeswax (2-1,4) and shellac18% + beeswax (2-2,4) at t_{37} .	459
Figure A9.29	Visible and UVf images of the unaged (UA) and aged (A) sections coated with barite20° + beeswax (3-1,4) and barite20° + beeswax (3-2,4) at t_{37} and relevant visual examination notes. Each square corresponds approximately to a 1x1 cm portion of the section.	460
Figure A9.30	FT-IR microscope survey images (1x1 mm), BSE images and high-resolution 3D images (5.3x5.3 mm) of the unaged (UA) and aged (A) sections coated with barite20° + beeswax (3-1,4) and barite20° + beeswax (3-2,4) at t_{37} .	461
Figure A9.31	From left to right: BSE images, FT-IR survey micrographs (1x1 mm) and the and the HR 3D images (5.3x5.3 mm) of the plaster surfaces coated with beeswax (4) (P6a and P8a) before (S) and after (AC) cleaning with PE-PAM-IMS solution (Sol I).	462
Figure A9.32	From left to right: BSE images, FT-IR survey micrographs (1x1 mm) and the and the HR 3D images (5.3x5.3 mm) of the plaster surfaces coated with beeswax (4) (P10a and P12a) before (S) and after (AC) cleaning with PE-PAM-IMS solution (Sol I).	463
Figure A9.33	Top. FT-IR spectra acquired from the unaged, unsoiled areas (d of P1, 5 and 9) at t_{37} . Bottom. FT-IR spectra acquired from the aged, unsoiled areas (d of P3, 7 and 11) at t_{37} .	464
Figure A9.34	Top. FT-IR spectra acquired from the unaged, soiled areas (a of P1, 5 and 9) at t_{37} . Bottom. FT-IR spectra acquired from the aged, soiled areas (a of P1, 5 and 9) at t_{37} .	465
Figure A9.35	Diffuse reflectance FT-IR spectra acquired from the unaged (UA) P1 control sections (US d, and S a) and aged P3 control sections (US d, and S a).	466
Figure A9.36	FT-IR spectra acquired from unsoiled (unaged P1e and aged P3e) and soiled (unaged P1b and aged P3b) areas of the plaster surface coated with cold-pressed linseed oil (1-1) at t_{37} .	467
Figure A9.37	FT-IR spectra acquired from unsoiled (unaged P1f and aged P3f) and soiled (unaged P1c and aged P3c) areas of the plaster surface coated with boiled linseed oil (1-2) at t_{37} .	468
Figure A9.38	FT-IR spectra acquired from unsoiled (unaged P5e and aged P7e) and soiled (unaged P5b and aged P7b) areas of the plaster surface coated with shellac6% (2-1) at t_{37} .	469

Figure A9.39	FT-IR spectra acquired from unsoiled (unaged P5f and aged P7f) and soiled (unaged P5c and aged P7c) areas of the plaster surface coated with shellac18% (2-2) at t ₃₇ .	470
Figure A9.40	FT-IR spectra acquired from unsoiled (unaged P9e and aged P11e) and soiled (unaged P9b and aged P11b) areas of the plaster surface coated with barite20° (3-1) at t ₃₇ .	471
Figure A9.41	FT-IR spectra acquired from unsoiled (unaged P9f and aged P11f) and soiled (unaged P9c and aged P11c) areas of the plaster surface coated with barite60° (3-2) at t ₃₇ .	472
Figure A9.42	Top. FT-IR spectra acquired from the unaged, unsoiled areas (d of P2, 6 and 10) at t ₃₇ . Bottom. FT-IR spectra acquired from the aged, unsoiled areas (d of P4, 8 and 12) at t ₃₇ .	473
Figure A9.43	Top. FT-IR spectra acquired from the unaged, soiled areas (a of P2, 6 and 10) at t ₃₇ . Bottom. FT-IR spectra acquired from the aged, soiled areas (a of P4, 8 and 12) at t ₃₇ .	474
Figure A9.44	FT-IR spectra acquired from unsoiled (unaged P2e and aged P4e) and soiled (unaged P2b and aged P4b) areas of the plaster surface coated with cold-pressed linseed oil (1-1) and beeswax (4) at t ₃₇ .	475
Figure A9.45	FT-IR spectra acquired from unsoiled (unaged P2f and aged P4f) and soiled (unaged P2c and aged P4c) areas of the plaster surface coated with boiled linseed oil (1-2) and beeswax (4) at t ₃₇ .	476
Figure A9.46	FT-IR spectra acquired from unsoiled (unaged P6e and aged P8e) and soiled (unaged P6b and aged P8b) areas of the plaster surface coated with shellac6% (2-1) and beeswax (4) at t ₃₇ .	477
Figure A9.47	FT-IR spectra acquired from unsoiled (unaged P6f and aged P8f) and soiled (unaged P6c and aged P8c) areas of the plaster surface coated with shellac18% (2-2) and beeswax (4) at t ₃₇ .	478
Figure A9.48	FT-IR spectra acquired from unsoiled (unaged P10e and aged P12e) and soiled (unaged P10b and aged P12b) areas of the plaster surface coated with barite20° (3-1) and beeswax (4) at t ₃₇ .	479
Figure A9.49	FT-IR spectra acquired from unsoiled (unaged P10f and aged P12f) and soiled (unaged P10c and aged P12c) areas of the plaster surface coated with barite60° (3-2) and beeswax (4) at t ₃₇ .	480
Figure A9.50	Focal Plane Array (FPA) full range absorbance images of the uncoated gypsum plaster unaged and unsoiled (P1d) (i) , aged and unsoiled (P3d) (ii) , aged and soiled (P3a) (iii) and aged and cleaned (P3a, AC) (iv) . Although differences can be seen, no consistent observations can be made.	481
Figure A9.51	Focal Plane Array (FPA) full range absorbance images of the gypsum plaster coated with shellac18% and beeswax unaged and unsoiled (P6f) (i), aged and unsoiled (P8f) (ii), aged and soiled (P8c) (iii) and aged and cleaned (P8c, AC) (iv). Although differences can be seen, no consistent observations can be made.	481

Glossary Frontpage

List of casts in the Catalogue of Charles Lorenzi,
Reproductions d'Oeuvres d'Arts. Source: V&A Sculpture
Department Archive.

483

LIST OF ACCOMPANYING MATERIAL AND PUBLICATIONS

Accompanying material

Risdonne, Valentina; Theodorakopoulos, Charis (2021): **Database of results. Materials and techniques for coating of the nineteenth-century plaster casts. A scientific and archival investigation of the Victoria & Albert Museum cast collection.** Northumbria University. Dataset.
<https://doi.org/10.25398/rd.northumbria.14053985>

Risdonne, Valentina; Theodorakopoulos, Charis (2021): **Database of Results. V&A cast of the tombstone of the Presbyter Bruno (REPRO.1873-380).** Northumbria University. Dataset. <https://doi.org/10.25398/rd.northumbria.13469925>

Risdonne, Valentina; Theodorakopoulos, Charis (2021): **Database of Results. V&A cast of a choir screen (REPRO.1873-561).** Northumbria University. Dataset.
<https://doi.org/10.25398/rd.northumbria.13811594>

Risdonne, Valentina; Theodorakopoulos, Charis (2021): **Database of Results. V&A cast of a font (REPRO1874-29).** Northumbria University. Dataset.
<https://doi.org/10.25398/rd.northumbria.13902737>

Risdonne, Valentina; Theodorakopoulos, Charis (2021): **Database of Results. V&A cast of a tympanum (REPRO1874-45).** Northumbria University. Dataset.
<https://doi.org/10.25398/rd.northumbria.14034986>

Risdonne, Valentina; Theodorakopoulos, Charis (2021): **Database of Results. V&A cast of the statue of Count Ekkehard (REPRO1875-16).** Northumbria University. Dataset. <https://doi.org/10.25398/rd.northumbria.14039279>

Risdonne, Valentina; Theodorakopoulos, Charis (2021): **Database of Results. V&A cast of the statue of Regilindis (REPRO1875-17).** Northumbria University. Dataset.
<https://doi.org/10.25398/rd.northumbria.14039306>

Risdonne, Valentina; Theodorakopoulos, Charis (2021): **Database of Results. V&A cast of the relief of The Assumption of the Virgin (REPRO1890-80)**. Northumbria University. Dataset. <https://doi.org/10.25398/rd.northumbria.14040080>

Risdonne, Valentina; Theodorakopoulos, Charis (2021): **Database of Results. V&A cast of the relief of The Coronation of the Virgin (REPRO1890-81)**. Northumbria University. Dataset. <https://doi.org/10.25398/rd.northumbria.14040182>

Risdonne, Valentina; Theodorakopoulos, Charis (2021): **Database of Results. V&A cast of the relief of The Death of the Virgin (REPRO.A.1916-3152)**. Northumbria University. Dataset. <https://doi.org/10.25398/rd.northumbria.14040224>

Risdonne, Valentina; Theodorakopoulos, Charis (2021): **Database of Results. V&A cast of the relief of The Entombment of the Virgin (REPRO.A.1916-3153)**. Northumbria University. Dataset. <https://doi.org/10.25398/rd.northumbria.14040251>

Risdonne, Valentina; Theodorakopoulos, Charis (2021): **Database of Results. V&A cast of the relief of The Raising of Lazarus (REPRO.1864-56)**. Northumbria University. Dataset. <https://doi.org/10.25398/rd.northumbria.14040281>

Risdonne, Valentina; Theodorakopoulos, Charis (2021): **Database of Results. V&A cast of the relief of Christ at Bethany (REPRO.1864-57)**. Northumbria University. Dataset. <https://doi.org/10.25398/rd.northumbria.14040305>

Publications

Risdonne, Valentina; Hubbard, Charlotte; Borges, Victor H. L.; and Theodorakopoulos, Charis (2021). **Materials and Techniques for the Coating of Nineteenth-Century Plaster Casts: A Review of Historical Sources**. *Studies in Conservation*. <https://doi.org/10.1080/00393630.2020.1864896>

Risdonne, Valentina; Hubbard, Charlotte; Puisto, Joanna; and Theodorakopoulos, Charis (2021) **A multi-analytical study of historical coated plaster surfaces: the examination of a nineteenth-century V&A cast of a tombstone**, *Heritage Science* **9**, 70, <https://doi.org/10.1186/s40494-021-00533-0>

LIST OF ABBREVIATIONS AND SYMBOLS

∅	diameter
3D	3-dimensional
A	aged
Å	Ångström (10^{-10})
α^*	CIELAB colour coordinate
AHRC	Art and Humanities Research Council
aq	aqueous
ASTM	American Society for Testing and Materials
b^*	CIELAB colour coordinate
°Bé	Baumé scale degrees
BM	British Museum
BS	British Standard
BSE	Back Scattered Electron
°C	Celsius degrees
ca	<i>circa</i>
CIE	Commission Internationale de l'Eclairage
CDP	Collaborative Doctoral Partnership
Cwt	Hundredweight, centum weight or quintal
ΔE^*_{ab}	CIELAB colour difference
DR	Diffuse Reflectance
E_e	Irradiance (Watt per square meter, W/m^2)
EDS	Energy Dispersive Spectrometry
°F	Fahrenheit degrees
$F(\lambda)$	Kubelka-Munk function
FT-IR	Fourier-Transform Infra-Red
g	gaseous
GC/MS	Gas Chromatography/Mass Spectrometry
GU	Gloss Unit
H_e	radiant exposure (Joule per square meter, J/m^2)
Hz	Hertz
I_e	Radiant intensity (Watt per unit solid angle, W/sr)
IMS	Industrial Methylated Spirit
ISO	International Organization for Standardization
J	Joule
K	Kelvin degrees
kg	kilogram
KM	Kubelka-Munk
l	liquid

l	litre
L*	CIELAB colour coordinate
Lb	Libra, Pound
m	meter
μ	micro (10 ⁻⁶)
min	minutes
M.W.	Molecular Weight
n	nano (10 ⁻⁹)
oz	ounce (plural ounces, ozs)
OM	Optical Microscopy
P	plate
p.	part(s)
P _e	radiant flux
Pa	Pascal
PL	Proper Left
PR	Proper Right
py-GC/MS	pyrolysis–gas chromatography–mass spectrometry
RH	Relative Humidity (%)
s	seconds
s	solid
S	soiled
SCI	Specular Component Included
SCE	Specular Component Excluded
SEM	Scanning Electron Microscopy
SKM	South Kensington Museum
t	time (seconds, s)
t _e	exposure time (seconds, s)
T	Temperature (degree Kelvin, K)
TIC	Total Ion Current
UA	unaged
US	unsoiled
UV	Ultraviolet
v/v	Concentration, volume ratio percentage
V&A	Victoria and Albert Museum
v _s	Symmetrical stretching
v _{as}	Asymmetrical stretching
W	Watt
WI	Whiteness Index
w/w%	Concentration, weight ratio percentage
XRD	X-ray Diffraction
XRF	X-ray Fluorescence
YI ₃₁₃	Yellowness Index E313

The objects studied in this work are historical replicas. The relevance of the study of the replica is advocated throughout the thesis (Billbey & Trusted, 2010) and must be the axiom of this work. The terms 'replica', 'copy' and 'reproduction' are here used as intended by their dictionary meaning as 'something that has been made to be exactly like something else' (Procter, 2000) and therefore moving away from the idea, given by the popular use of these terms, of the copy being a 'forgery' or a 'fake'. On the other hand, the term 'reconstruction' has been used in this thesis to indicate the mock-ups produced in the scientific laboratory to recreate the historic surfaces.

What is referred to as plaster (from the Greek word ἔμπλαστρον, *emplastron*) is an extremely versatile material. It can be used for casting, moulding, dripping, embedding, sculpting, decorating and building (Kemp, 1912; Meilach, 1966). That the Greeks knew the use of plaster is proven by the writings of Theophrastus and other Greek authors. Theophrastus said that plaster was produced by a stone obtained from Syria, called γύψος (*gypsos*). Pliny mentioned gypsum, as having been used by ancient artists. The 'pulverulent' and the 'compact' type of gypsum were known to the Greeks. The compact gypsum was obtained in lumps, which were burnt in furnaces, and then reduced to plaster, which was used for buildings and for making casts.

Plaster cast is a term open to interpretations. Even after defining the field of application, as for example, fine arts in this research, it can be difficult to generate a shared technical terminology for the discussion of plasterwork. The importation into English of the Italian term *stucco* and its anglicised plural *stuccoes*, instead of the Italian plural *stucchi*, shows the lack of appropriate terms for the materials used by plasterers in the English language. To muddle the communication further, the plasterworks' terms were also used with different meanings over time, and it is only in English that the word *stucco* can be rightly used for both decorative plasterwork and architectural renders (Gapper, 1999). To help the contextualization of the research, a brief modern definition of a few recurrent terms is necessary. Bankart (1908) defined *stucco* as the material based on 'carbonate of lime, generally the burnt limestone or chalk of the rocks and hills' and for Kemp (1912) it is a non-durable material used for internal works introduced by the Italians in the UK. 'Plaster of Paris' generally refers to the plaster obtained by burning gypsum (calcium sulfate dihydrate) of various provenances and therefore different compositions, falling in the category of 'gypsum plasters'. For example, 'plaster of Paris' historically refers to gypsum found in the Tertiary strata of Montmartre hill in Paris, which was known since the Roman Period. Millar

(1899) described this gypsum as containing 10 per cent of carbonate of calcium, not always in intimate union with the sulfate, but the term lost its specificity over time. At the turn of the nineteenth century, the sulfate lime found in Derbyshire was the most used in London and England for preparing plaster (Kemp, 1912; Sullivan, 2019). Gypsum plaster, characterised by quite a fragile, brittle, highly hygroscopic and fast setting matter, was in the past generally defined as 'plaster'. Nowadays the term plaster may be used for many chemically different materials, including 'lime plasters', which are generally harder and more durable, slow-setting and relatively less sensitive to water than the gypsum ones. Lime plaster is obtained by burning calcium carbonate (limestone, usually chalk, travertine or marble). Plasters were often combined with aggregate and additives, and the term changed along with the admixture. The Italian word *intonaco* can be also misleading; although in English this refers to plain lime plaster, in Italian this term implied the architectural application rather than only implying a specific composition. The *intonaco* can be both lime- and gypsum-based but it usually has a sand component. Apart from the vocabulary mismatches, the confusion can be also to the result of the lack of specificity and consistency of many authors when describing objects made of *stucco*. Gapper (1999) cites in this regard the examples of Vasari's description of the work of Giovanni da Udine, Pirro Ligorio (c. 1510-83) describing the *stucco* ornaments in a Roman temple in Via Gabinia and others. Gianasso (2014), quotes Gustav Adolf Breymann (1807-1859, German architect), who defined *stucco* as the decorative material for walls and ceilings made of *gesso allumato cotto* (cooked alum gypsum). The compositions and consequently the definition of these materials was primarily affected by the availability of local materials. It must be also highlighted how, since a relevant portion of this work is based on historical literature, it is sometimes challenging to retrieve and specify appropriate terminology for the materials. It is not only the misinterpretation and lack of accurate description of the word plaster in the literature that can be misleading. A wide range of materials was named and described very differently in the technical literature along over the centuries.

Having briefly clarified some terminology, it is necessary to specify that the protagonists of this study are 'historical' or 'artistic' plaster casts, with a special focus on the nineteenth-century ones held at the Victoria and Albert Museum (V&A), in London. The work presented here aims to provide technological and material information on the coating for the nineteenth-century plaster casts, with a special focus on the V&A collection (Patterson & Trusted, 2018). The V&A museum catalogue accession numbers are provided, as related to every V&A object analysed and/or mentioned, as archival information can be retrieved from the V&A website (*V&A Website - Search the Collections*, 2020). The outcomes of this work are relevant for the historian that seeks to understand the technological practices of the workshops of the nineteenth century, for the heritage scientist who works on the characterization of similar collections or tries to understand the materials' deterioration, as well as for the conservators who base their treatments on previous studies.

The Art and Humanities Research Council (AHRC) supported this PhD research as part of a Collaborative Doctoral Partnership (CDP) between Northumbria University's Department of Art and the Victoria and Albert Museum's Departments of Conservation and Sculpture. The Henry Moore Foundation (HMF) has also contributed to the project, providing a travel grant that allowed the visit of numerous archives.

My appreciation is due to Dr Charis Theodorakopoulos (Senior Lecturer in Conservation Science in the Department of Arts) who supervised my work at Northumbria University and always encouraged me. In February 2019, Victor Borges (Head of Sculpture Conservation) and Angus Patterson (Senior Curator in the Department of Sculpture, Metalwork, Ceramics & Glass) replaced Charlotte Hubbard (former Head of Sculpture Conservation) and Dr Holly Trusted (former Senior Curator of Sculpture) as the V&A's supervisors; my gratitude goes to all of them for the continuous support.

My most sincere appreciation is for the work and expertise of Dr Pietro Maiello (Senior Technician and SEM Specialist in the Department of Physics & Electrical Engineering), Simon Neville (Senior Technician in the Department of Engineering and Environment), Dr Karen Haggerty (Senior Technician in Applied Sciences, Faculty of Health and Life Sciences) and Sofia Pascual (Senior Technician in Conservation of Fine Arts) who constantly shared knowledge and supported my lab work at Northumbria University.

I would like to acknowledge the Science Section at the Victoria and Albert Museum, particularly Bhavesh Shah (Scientist (Environment), Conservation & Collections Management) and Dr Boris Pretzel (Head of Science, Conservation and Collections Management), which supported me, providing access to the Environmental data. My appreciation also goes to the conservators of the V&A's Sculpture conservation team, Sarah Healey-Dilkes, Johanna Puisto, Adriana Francescutto Miro and Sayuri Morio, for the insight on their work on the casts collection.

I would like to acknowledge the work of Dr Friedrich Menges, who developed the open-source "Spectragryph - optical spectroscopy software", Version 1.2.14 (2020), which was a hugely helpful tool to process my data.

On a personal note, I want to acknowledge my mentor and friend, Dr Lucia Burgio (Senior Scientist in Conservation Science at the Victoria and Albert Museum), for believing in me and always being my inspiration.

DECLARATION

I declare that the work contained in this thesis has not been submitted for any other award and that it is all my own work. I also confirm that this work fully acknowledges opinions, ideas and contributions from the work of others. The work was done in collaboration with the Victoria and Albert Museum.

Any ethical clearance for the research presented in this thesis has been approved. Approval has been sought and granted by the Faculty Ethics Committee (Submission Ref: 4490) on the 25/01/2018.

I declare that the Word Count of this Thesis is 85,754 words.

Name: Valentina Risdonne

Signature:

Date: 08/01/2022



CHAPTER 1

BACKGROUND AND CONTEXT

[...] Up to our own day the concept of imitation, whether accepted or rejected, has remained the focus of any interpretation of art. [...]' (Barash, 1985)

1.1. INTRODUCTION

The Victoria and Albert Museum (V&A) collection of nineteenth-century plaster casts is one of the most iconic and visited collections in the world.¹ Walking through the museum's Casts Courts, the visitor is filled with a sense of magnificence and variety. The *trait d'union* of such an eclectic collection is the identity of the objects, these all being created as copies of original works of art, but also related to the materiality of the body of the cast, which consists of plaster. The sense of variety, on the other hand, is given by the different origins and the eclectic styles and dimensions of the casts, but also by their deceptive appearances, due to the many different coatings applied to the plaster.

This study aims to understand manufacturing techniques of the Victorian plaster cast makers through the review of technical historical sources, to investigate selected pieces of the V&A collection through the scientific analysis of their coatings, as means to ensure a desired appearance and durability, and eventually to assess the efficacy of a novel conservation treatment through designed experiments to propose a safe and effective methodology for the removal of soils from such surfaces. The development of a scientific procedure for the study of the coatings will facilitate the study of the surface materials of these objects and a better understanding of Victorian manufacturing. Furthermore, this will ensure conscious conservation approaches and support the understanding of the plasterers' workshop practice during the nineteenth century. This material science research falls in a very specific and interdisciplinary area of study, weaving between art and science, curatorial practice and conservation issues.

This introduction (*Sections 1.1 to 1.3*) explores prerequisite knowledge essential to understanding the main body of this thesis and provide the context for the materials object of the study. Due to the broadness of the topic and the scientific focus of this work, this

¹ '2017–18 was a record year for the V&A. For the first time in the museum's history, the V&A attracted over 4 million visitors, with a total of 4,396,557 people visiting V&A South Kensington, V&A Museum of Childhood and Blythe House.' (*Victoria and Albert Museum Annual Report and Accounts 2017-2018, 2018*).

prologue is by no means exhaustive, but it aims to guide the reader towards relevant references and further reading. The historic background drawn here is mostly focused on a European and Victorian context, as most relevant to the objects studied in this work. This setting is followed in *Sections 1.5* and *1.6* by the *Research Rationale* and *Thesis Outline*.

1.1.1. A WORLD OF REPRODUCTIONS

'living in a world of reproductions and replicas has been seen as a defining attribute of late nineteenth-century culture in general' (Foster & Curtis, 2016: 2)

Artistic plaster reproductions are documented since the fifteenth century in Italy when small replicas were utilised in the Italian workshops to inspire artists. Copies were widely used for education purposes in European academies and art schools starting from the seventeenth and eighteenth centuries, and especially after the renewed classicist impetus brought in the early nineteenth century in Britain with the broad circulation of copies of the Parthenon Marbles.

After the idealist neoclassicism of Johann Joachim Winckelmann (1717 -1767), the classical revival sprung during the eighteenth century and lasted into the following century (Barash, 1985).² In 1816 the British Museum acquired the Phidias sculptures to connect with the Pantheon *aura* of greatness. The sculptures and the architectural details, including the friezes, metopes and pediment sculptures, were widely reproduced and sold or donated to art schools and museums (Lending, 2017).³ Collecting archaeological plaster casts has been an interesting topic of discussion for many curators and art critics (Frederiksen & Marchand, 2010; Graepler & Ruppel, 2019; Guderzo & Lochman, 2017; Pearce, 2013): the notion of this kind of collection seems to begin in the eighteenth century following the accumulation of the big collections of marbles and held their 'fine art' status well during most of the nineteenth century. The idea that knowledge could be transferred through the objects was at the base of the proliferation of plaster cast collections in nineteenth-century Britain (Wade, 2019). Creating copies of great works of art for royal and aristocratic collections, by the middle of the nineteenth century, had been evolving for over three centuries. In the UK, the peak of the production and display of reproductions can be framed between the 1851

² Winkelmann's theories should be carefully applied to plaster casts as they cannot be accepted as a precise replacement of an original, the original being made in a much 'noble material' (Barash, 1985).

³ Parthenon Frieze casts travelled as far as the Western Australia Museum and Art Gallery. Bernard Woodward (1846–1916), the museum director, acquired casts of classical art from Brucciani & Co (O'Toole, 2007).

Great Exhibition in London and World War I (Foster & Curtis, 2016; Foster & Jones, 2020a). Throughout the twentieth century, archaeological plaster casts collections began steadily to lose place in the museum, and by the 1970s were merely considered a replacement for the original masterpieces (Pearce, 2013). By this time, the casts themselves were rather the worse for wear, and their dingy appearance matched their declining status. As collection studies have begun to gather force again, the cast collections themselves now advance again to the status of important historical documents in the history of taste and perception, which construct their own legitimate view of the world. Collecting plaster casts was not confined to classical and Renaissance art. Other fields of education made good use of this appreciated practice: anatomy (Gamer, 2019) and palaeontology, anthropology, ethnology and phrenology, and largely also in architecture. The possibility of three-dimensional reproduction made casts preferred to photography. Rieppel (2015: 482) suggests that the casts were ‘a genuine mode of publication in the late nineteenth century’, able to maintain their own materiality.

Plaster figures were a source of inspiration for artists, designers and others (Simon, 2011). During the eighteenth and early nineteenth centuries, designs would usually be taken from engraving. After architects or artists drawings, freelance sculptors or the shops’ owners produced three-dimensional plaster models for the use of manufacturers or craftsmen. Stylish models were often pirated by shops and, when the practice became popular, the businesses started to be blamed for plagiarising others’ designs until and the Garrard’s Act was bought in 1798 to provide copyright.

An extremely lively exchange of works of art was through the action of individuals and collectors, who acquired sculptures for personal interest or decorative purposes, events and celebrations (Wade, 2019). There was a change from the elitism of the eighteenth century, shifting to more popular and accessible art, along with the university education valuing the education of the common man, using models and examples. The spread of the cast collections established during the nineteenth century is far beyond one’s expectation. Colonialism and the spread of European and classical art implemented the build of plaster casts collections in the colonies (Tietze, 1998). A preliminary counting of the plaster casts collections around the world recorded about 260 collections, from very small to huge ones, ranging from different topics (from mathematic models to numismatic to masks of the dead), from Japan to the Netherlands and South Africa. A preliminary list of plaster casts collections in the World is provided in *Appendix 1*.

Classical art cast collections are held in many museums: the Trustees Academy in Edinburgh has a large group purchased from the Albacini firm in 1838 (Davies, 1991); the Museum of Classical Archaeology, Cambridge, founded in 1884, contains well over five hundred casts taken from ancient Greek and Roman sculptures or, in some cases, casts

from casts (Waldstein, 1889); and the Cast Gallery of the Ashmolean Museum has a similar collection (Pearce, 2013). Despite the most famous collections of casts in Britain being held in the largest museums (e.g., V&A, British Museum, The Ashmolean Museum), many 'provincial' institutions acquired plaster casts in the nineteenth century (Foster, 2015; Wade, 2019). The limited chances for the people to travel was a shared concern in many different regions and countries, therefore museums and art schools everywhere acquired and collected replicas of important monuments and works of art to complement their collections and to allow their students to learn and draw from the classical and Renaissance models (*Figure 1.1*) - see for example the case study of The Leeds School of Design in Wade (2019).



Figure 1.1. Ann Macbeth and another woman in a Glasgow School of Art drawing and painting class, both holding palettes, with plaster casts in the background, c. 1912. Glasgow School of Art Archives. Source: The Glasgow School of Art. Archives and Collection. (2020).

1.1.2. AUTHENTICITY, VALUE AND FUNCTION

‘authenticity [...] is an intellectual dead end’ (Emerick, 2014: 3)

Since the Renaissance, Greek and Roman classical antiquity had served as a model of public opinion and taste, and ‘collective memory’, standing as the foundation of the British culture of the time (Fehlmann, 2007).⁴ Baker *et al.* (2010) define this as a ‘reproductive continuum’ or a sort of ‘social memory and witness’, intimately related to Walter Benjamin’s theory of authenticity⁵ and the still-open debate around the art object’s *aura* and its transferability (Dini, 2018). Authenticity, significance and value must be rethought for the replicas. These qualities should not be considered intrinsic to the object but created by the combination of its materiality, past life and contextual relations with time and places. Replicas should be considered instead as ‘extended objects’ characterised by ‘composite biographies’ (Foster & Jones, 2020b). The replicas in the past were exempted from having Benjamin’s quality of *hic et nunc*, here and now, which would link the unicity and originality of the art object to space and time, to the context and the artist (Rotili, 2009). Moreover, the value attributed in the past to the artistic knowledge and expertise was greater than what is recognized today, the modern artistic approaches being more focused on the glorification of the significance of the object and the individuality of the artist, rather than on the technological skills and innovations. Technological and mechanical modern progress for the industrial production of copies has in a way diminished the appreciation of the artisans’ skills. On the other hand, even in 1786 J. W. von Goethe (1749-1832) highlighted the deficiency of life of the plaster copy of the ‘Medusa Rondanini’, when compared to the marble original version, defining the *Verfremdung* (alienation) that the viewer experienced in front of a copy (Rotili, 2009).⁶

The nineteenth-century replicas were never pretending to be the originals. They aspired to be the exact copy of the original, but their creation, circulation, use and after-life define the reason why these ‘models’ are historical objects in their own right, with their own patina of age and use (Foster & Curtis, 2016; Lending, 2017). By noticing the large number and types of replicas produced over the centuries, it is possible to understand how the value given to

⁴ The definition of a ‘sense of a shared past’ was necessary for the built of a feeling of community, linking past and present. ‘This shared past was shaped and manipulated by the contemporary political and economic aspirations, often resulting in the stereotyping and simplification of an imagined past.’ (Fehlmann, 2007).

⁵ For Lowenthal (1999) authenticity is a fluid concept and its definition varies within groups. The discussion about the nature of authenticity brought up the idea of this quality not being an intrinsic, ‘material’ property of the objects, but a construction, ‘informed by the relationship between people, places, and things’ (Jones, 2010).

⁶ Goethe experienced mixed feeling regarding the copies. He criticised and then commented with enthusiasm the production of casts in the workshops. He was himself a plaster casts collector (Rotili, 2009).

the copies changed throughout the ages. In the nineteenth century, the establishment of a commonly accepted canon of art was the main scope of the reproductions. They played a central role in the development of the museums for the V&A and many others, nationally (e.g., Royal Scottish Museum and the National Museum of Antiquities of Scotland in Edinburgh) (Foster, 2015) and internationally (e.g., Römisch-Germanisches Zentralmuseum in Mainz and the Museum of Fine Arts in Boston) (Foster & Curtis, 2016). As suggested by the agenda of the V&A Circulation Department, for example, the production and distribution of replicas were intentionally planned to define the Museums' identities (Foster, 2015).

The relatively low cost of plaster casts allowed new institutions to build up remarkable collections of replicas or to use casts as placeholders for the original works (Disalvo, 2012; Foster & Jones, 2020b; Lending, 2017) and display comprehensive collections in an increasingly competitive international market (Wade, 2019). From the second half of the nineteenth century, when the hierarchy of values of art was at a turning point, the casts lost their significance and value, becoming mere tools for the fine arts and ornamental models.

Another unfortunate use of the casts at the end of the nineteenth century was the production of forgeries (Rotili, 2009).⁷ Art curators, critics and the press questioned the value of casts beyond their role in education. Moreover, there was a concern that the copies could be misinterpreted as 'original' by the viewer. Furious debates sprung by the end of the nineteenth century: in different parts of the World museums professionals were discussing the value of casts, and their role in the arrangement of museums of art (Foster & Curtis, 2016). Cambareri (2011) describes the so-called Boston 'battle of the casts', which is possibly the most famous example of such a diatribe.⁸ From that time, there was a change of attitude to authenticity and copies fell out of favour and began to be questioned. In museums many historic replicas came off the display and, once in the storehouses, they received less care than 'authentic' original objects. Some were sadly destroyed or redistributed somewhere else (Baker, 2010). Flour (2008) cites Summerson (*The Architectural Association*) concerning the Royal Architectural Museum at the beginning of the twentieth century, well conveying the feeling of the times: 'the collection of casts [...] was in the nature of a white elephant – a sad Victorian elephant depressing the aspiration of another age'.

⁷ Alceo Dossena (1878–1937), Icinio Ioni and Fulvio Corsini (1874–1938) were famous artisans in Italy, which deliberately produced casts and moulds from museums to be sold as 'originals' (Rotili, 2009).

⁸ Edward Robinson was a Classical scholar and the Director of the Boston Museum of Fine Arts. In 1905, he was attending the opening of the purpose-built Aberdeen Sculpture Gallery of plaster casts. While he was abroad his staff undermined his agenda, which supported the value of plaster casts. His deputy Matthew Pritchard aimed for aesthetic appreciation of sculpture in preference to its use in education (Cambareri, 2011; Foster & Curtis, 2016).

Responses today are still highly varied as to whether copies are valuable or expendable. The discussion around the perception of reproductions in the Museum provides the chance to rethink the concepts of authenticity and value, historically and contemporarily.⁹ These concepts deeply relate to the value that the observer assigns to the replica, not solely based on the intrinsic qualities of the object (Foster & Jones, 2020a, 2020b).¹⁰ Some museums sold their collections (e.g., the New York Metropolitan Museum of Art in 2006) or transferred them to other institutions. The pressure on display and storage space often requires difficult decisions, which must be made with the awareness of the nuanced historiography of the replicas (Foster & Jones, 2020b). On the other hand, new investments are recently redirected to the redisplay and curation of plaster casts by many institutions (e.g. the New Acropolis Museum and Underground in Athens, the refurbished Galeries de Moulages at the Cité de l'Architecture et du Patrimoine in Paris, the conservation and redisplay of the Albacini and other historic casts at the Edinburgh College of Art, the conservation of the collection of the Real Academia in Madrid, the plaster storage in the National Museum of Wales). Müller in Graepler & Ruppel (2019), for example, describes the unfortunate story of the plaster casts collection of the University of Leipzig, founded in 1840. The collection was subjected to heavy losses during World War II and in 1968 lost its domicile during the redesign of the university campus and was then moved to storage spaces. The collection re-evaluation started only in 1999. From many aspects, the V&A's cast collection is unique, as the museum preserved most of the collection, which has been always on display since its creation (Baker, 1982).

The question of 'why historical replicas matter' (Foster & Curtis, 2016) can broadly raise discussion for many objects rather than plaster cast: electrotypes, drawings, photography and even photocopies. There is a wide range of objects that can be perceived as reproductions: scaled copies or interpretative reconstructions, materials for archaeology or palaeontology, visual media or copies made to replace originals etc. Nowadays the debate around reproductions can and must be also extended to new materials and digital reproductions (photogrammetry, 3D scanning and printing).

⁹ This topic was the topic of *Lasting Impressions* (29th June 2018), a AHRC funded study day organised as part of the dissemination purposes of this PhD research (Risdonne *et al.*, 2018b, 2018a).

¹⁰ Further reading on the process of rethinking and revaluating the replica, and the consequent recommended change of actions and practices can be found in Foster & Jones (2020a and b). An example of project that engages with the concepts of materiality and authenticity can be seen in Hughes *et al.* (2014).

Many museums are updating their policies¹¹ and plans to keep pace with modern digital technologies for recording, documenting and re-creating works of art (Sharpe, 2014).¹² For example, 'New futures for replicas' (Foster & Jones, 2020b) was published in July 2020 to provide guidelines for museums' professionals and academics working with reproductions.

Brown (2016) wrote about the dissemination role of Victorian facsimile and the additional role that copies play nowadays, not only in terms of education but also as acts of preservation. In some cases, historical and modern reconstruction techniques are used together for research (Payne, 2019b; Wachowiak *et al.*, 2009), conservation or restoration purposes.¹³ The creation of the casts can be part of a program to document works of art that were too difficult or fragile to move but considered to be at risk of damage (Payne, 2019a). The V&A's copy of the Trajan's Column (Museum no. REPRO.1864-128) is a popular example of casts that held details partially or completely lost in their originals, having the column in Rome been exposed to pollution and acid rain. In some circumstances the original of the copy has been destroyed, for example, a notable Viking Mammen-style casket, destroyed during the Second World War bombing of Dresden in Germany or a decorated Roman distance slab from the Antonine Wall in Scotland, discovered in 1865 but lost in the Great Chicago fire in 1871 (Keppie, 1998), copies of which exist in several museums (Foster & Curtis, 2016). Depending on the interest and perspective, plaster cast replicas can serve as a replacement for the original, they can have scientific importance as an example of practices and craft technologies, or objects in their own, having their social and economic context and history, as an eloquent and outstanding expression of Victorian taste.¹⁴

¹¹ Along with new technologies for reproductions, new issues related to Copyright were raised (Vulliamy, 2016).

¹² See for example the REACH (Reproduction of Art and Cultural Heritage) programme signed by the V&A, UNESCO, the State Hermitage Museum in St Petersburg, the Warburg Institute in London, the Smithsonian Institution in Washington DC, the Palace Museum in Beijing, the Vorderasiatisches Museum in Berlin, Factum Arte in Madrid, and the Institute for the Preservation of Cultural Heritage at Yale University (Somers-Cocks, 2018). The project evolved out from the exhibition titled 'A world of fragile Parts' (28 May – 27 November 2016). See also the case of the Digital Comparison of nineteenth-century plaster casts and original classical sculpture using 3D scans (Payne, 2015).

¹³ Brendan Cormier, V&A curator of *A world of fragile Parts*, at the Applied Arts Pavilion of the Venice Biennale 2016, exhibited objects ranging from Victorian plaster casts to 3D objects created from photographs.

¹⁴ That is what Foster & Curtis (2016: 8) define as a 'biographical approach' which '[...] enables us to identify how the meaning of things change in different context and through time. It allows for things to have multiple lives, both simultaneously and consecutively, extending beyond a short biography into a long biography.'

1.1.3. PLASTER WORKSHOPS AND FORMATORI

Few plaster shops survive today and several *formatori* (moulds and plaster cast artisans) are still active in some countries.¹⁵ Historically, shops seemed to be regarded as 'less noble' and often not quite a respectable fraction of the artistic manufacturing chain and therefore to be ignored (Wade, 2019). That is one of the possible reasons why finding recipes books belonging to this manufacturing seems to be harder than for other artistic practices.

The spread of Renaissance values and tastes outside the borders of Italy was geographically consistent with the spread of cast collections for instructional purposes. Early examples are given by the French Academy in Rome, established in 1666, which exported a group of its casts to Paris, and the collection of casts acquired in 1649 in Italy by the court painter Diego Velázquez (1599–1660), later transferred to the Royal Academy of Fine Arts of San Fernando, Madrid (Frederiksen & Marchand, 2010). Similar collections began spreading north Europe, and by the end of the seventeenth century, artists' academies were founded in Mannheim, Copenhagen, and Berlin. Plaster casts for teaching academic students about the history of art occur first in Germany in the eighteenth century, and the casts began to be transferred from the artist's atelier and academy to the university. The University of Göttingen, under the influence of Winckelmann himself, opened its new assemblage of casts to students in 1767.

The reproduction in plaster of replicas of archaeological material during the nineteenth century was a significant and profitable business for art collectors and museums. The early manufacturers mostly concentrated on statues after the antique and after sculptors like Rysbrack (1694–1770), Roubiliac (1702–62), Scheemakers (1691–1781), Wilton (1722–1803) and Bacon (1740–99). James Deville (born 1776), William (1782-1843) and George (1783-1843) Bullock practised in Birmingham and Liverpool. Humphrey (1767-1834) and Thomas Hooper (1776-1856), Benjamin and Robert Shout (1778-1823) and lots of Italians, or plasterers of Italian extraction, Federico Nicoli, Anthony Sartini (1789-1823), B. and J. Papera, Giannella were also active at the time. The spread of plasterers' studios and figurers' businesses increased from the early eighteenth century, with its highest point between 1760 and 1825. At that time, this plaster industry to this extent did not exist elsewhere in Europe, it was a British phenomenon, but it had become very lucrative throughout Europe by the 1850s. By the 1780s there were not only many plaster workshops in competition with one another but also large businesses making use of these shops. John Nost (1686-1729) and Andrew Carpenter (1677-1737) famously initiated mass-produced

¹⁵ For example, Andrea Felice is a modern Italian *formatore* (Felice, 2018) and the *Gipsoteca Mondazzi* still produce plaster casts in Torino, Italy (*Gipsoteca Mondazzi*, 2018). In Berlin is active *Gipsformerei* (*Gipsformerei*, 2018), the *Atelier de Moulage* is the workshop of the Royal Museum of Art and History in Brussels (*Atelier de Moulage*, 2018) and Lorenzi produces casts in Paris (*Lorenzi Moulage d'Art*, 2018).

sculptures in Britain in their yard. In 1738 John Cheere (1709-87) introduced mass marketing of plaster casts when he acquired Carpenter's business to produce garden sculptures and busts. He also developed recipes for bronzing, gilding and painting casts milk-white to resemble marble. Peter Vanina or Vannini (1753-70), James Hoskins (1858-59) and Benjamin Grant, Charles Harris (1777-95), Richard and Theodore (1769-74) Parker were also known in Britain. Other active centres of plaster casting were Birmingham, Liverpool, Bristol and Dublin. Dr Quin and James Tassie (1735-99) elaborated a technique for making casts after the antique cameos and intaglios in a vitreous paste. The competition became so intense and the plagiarism so common that many sculptors, above all George Garrard (1760-1826), petitioned to establish plastic arts copyright. The act defined a milestone between the practices of the eighteenth-century plaster shops and the ones of the first quarter of the following century.

Italian 'figure makers' started to move to Britain in the early nineteenth century to produce and sell plaster ornaments and figures for the town and country houses desired not only as decorative pieces but also for the will to commemorate wartime heroes and political leaders.¹⁶ The list of the 'Itinerant Italians' (Wade, 2019) working with plaster in Britain is extensive. The renewed interest in ancient art did not only consist of the study and imitation of the rediscovered antiquities. Those Italian artists that firstly engaged with ancient art also promoted the restoration and preservation of antiquities using replication and dissemination. Francesco Squarcione (c. 1395 – after 1468), for example, was a Paduan painter of the fifteenth century, who used plaster casts for training his pupils. Oronzio Lelli was a famous plasterer in Firenze, appointed plasterer at the Uffizi Galleries; Domenico Brucciani was a *formatore* from Lucca who became the official plasterer of the British Museum after moving to London (Rotili, 2009). Andrew Lawrence 'Lorenzo' Giuntini (c. 1845–1920) was a renowned pupil of Brucciani (Wade, 2019). During the 1820s and 1830s, many businesses closed, due to the rise of cheaper metalwork production, except for Bernasconi and Brucciani who stayed in business until the early 1840s. The last successful figure shop was run by Domenico Brucciani. Sir William Peterson (1856-1921) purchased Brucciani moulds and gave them to the V&A and many were moved to the British Museum (Clifford, 1992).

In Britain, while most of the workshops were in London, many others were elsewhere in the Country and deserve to be further investigated. Sullivan (2019), for example, recently carried a study on the plaster production in Derbyshire over the sixteenth-nineteenth centuries, and Foster (2015) narrated the casts distribution in Scotland.

¹⁶ The purpose of the creation of the plaster cast is fundamental when studying these objects; Frederiksen & Marchand (2010), for example, classified three categories for the use of plaster casts in the antiquity: casts used for the production of sculpture, casts used as copies and casts served as artworks in their own right. The quality and the technique used for the manufacturing the object depend on the destination of the cast.

1.2. THE V&A CAST COURTS AND THE COLLECTION

The V&A Museum can be rightly acknowledged as the greatest decorative art museum in the world, but also as the oldest museum of its kind. The very first introduction of any book, pamphlet or guide about the V&A (Baker, 1982; Cocks *et al.*, 1980; Saumarez-Smith, 1991; *The Victoria and Albert Museum.*, 1991; Williamson, 1996) is most likely to be about the history of the Museum and its collection. Every time, this turns out to be inseparable from the history of the collection of casts and therefore from the Casts Courts.

The V&A's Sculpture collection is as old as the Museum itself, the first acquisition dating 1844.¹⁷ A Selected Committee of Arts and Manufactures was appointed in 1835 'to enquire into the best means of extending a knowledge of the arts and the principles of design among the country (especially the Manufactory Population)' (Scala, 1991; Wainwright & Gere, 2002). In 1837 The School of Design of Ornamental Arts at Somerset House was established on the Committee's suggestion and is considered the precursor of the V&A. The School's teaching programme did not have great success, but the collection acquired its relevance in 1851 when, in the wake of the Great Exhibition, the School was incorporated in the Museum at Marlborough House, then named Museum of Manufactures in 1852. The museum moved to South Kensington in 1857 becoming part of the South Kensington Museum (Williamson, 1996). Among the Museum's primary aims was the 'improvement of public taste in design and the application of fine art to objects of utility' by instrumental casts of architectural and ornamental work (Baker, 1982). This educational purpose does not seem to have been changed during the long history of the museum (*Figure 1.2*). Only in 1899 was the Museum named after Queen Victoria and Prince Albert, both enthusiastic supporters of the collection. Queen Victoria laid the foundation stone of the current V&A building trusting that 'it will remain for ages a Monument of discerning liberality and a source of Refinement and progress' (Cocks *et al.*, 1980).

In its first twenty years, the V&A was so acclaimed that a great number of other institutions were created in its likeness (Cambareri, 2011). The inspiration was not only regarding the public and educational purpose of the museum but very often also the structure and programme itself. The Museum was actively engaged in the promotion of casts much earlier than International Exchange Scheme for the promotion of art: since 1852 a dedicated V&A Circulating Agency encouraged the selling and production of casts, through loans and grants, in many institutions (see for example the case of the Celtic Crosses in Scotland) (Foster, 2015).

¹⁷ Bronze statuette of Icarus, V&A accession number: 379-1844.



Figure 1.2. V&A's 2014 publicity campaign. Photographer: James Medcraft. © Victoria and Albert Museum, London/as specified by the rights holder. Source: *Inspiring Beautiful Free Shoot* (2014).

From 1841, many years before the opening of the Cast Courts, a collection of 'cases of ornamental art of all periods and countries' was being amassed (Baker, 1982). The lack of space appears to have been always an issue, and sometimes the acquisitions were subject to the availability of space. For this reason, the cast collection of the Architectural Museum, which focused on Gothic architectural ornament, was taken on loan only in 1857 (Flour, 2008).¹⁸ Consistent addition of casts was made to the collection and 3,200 plasters of architectural details were transferred from Government stores in 1861. The earliest acquisitions were casts from French and Italian Renaissance originals and Classical art, consisting largely of ornamental details. Figure sculpture was introduced by the early 1860s with the broadening of the collecting policy, although the medieval and Renaissance casts continued favoured to other styles and periods.

During the 1860s, many of the casts were acquired or purchased by selected workshops, but others were obtained through trades with other museums or private donations. The availability of moulds and casts through trade and exchange was surely a determining factor for their acquisition. The change of preferences for different styles, related to periods and countries, was also influenced by the value accorded to plaster casts, the way that the

¹⁸ The debate between the Architectural Museum and the South Kensington Museum, about an architectural cast museum, is complex and was fed by the two museums' rivalry and cohabitation (Flour, 2008).

history of art was perceived and the Museum wider policy and the purposes of the acquisitions - see for example the role of the Circulation agency (Foster, 2015).

The V&A casts were acquired from many different workshops, as documented in the V&A registries, or suggested by the workshop stamp on the casts. For example, by 1864 J. C. Robinson (1824-1913, the Museum's first curator) initiated an extensive campaign for the acquisition of Italian Renaissance casts (Wade, 2019). The cast of the Giovanni Pisano pulpit at Pisa was commissioned to Franchi (1812-74), a London-based craftsman. Italian reproductions were purchased in the 1880s from the workshop of Oronzio Lelli (active ca. 1860-1900) in Florence or commissioned to Franchi or Brucciani (Wade, 2014; 2019).¹⁹ Often the acquisition of 'original' objects and the production of casts happened at the same time. For instance, after several extensive tours of Spain in 1864-65, Robinson obtained original pieces but also casts of monuments such as the fifteenth-century cloister of San Juan de Los Reyes (Toledo) and the massive late twelfth-century Portico de La Gloria (Santiago de Compostela - commissioned to Brucciani). Very few examples represented mannerist and baroque sculpture and several neoclassical works are included too. The cast acquisitions of the 1860s and 1870s also included sixteenth-century German sculpture.

Henry Cole (1808-82, the Museum's first director) was the initiator of the 1864 International Exchange Scheme for the promotion of art (Baker, 1982),²⁰ which resulted in the 'International Convention of promoting universally Reproductions of Works of Art'. Fifteen European princes were persuaded to sign the convention while visiting the Paris International Exhibition in 1867. The Convention for the acquisition of Casts led to the height of popularity of the casts and the V&A collection began to assume the shape and dimension that made such an impression when the Architectural Courts were opened in 1873.

'The Architectural Courts' was the original name of the Cast Courts. They were designed by General H. Scott (1822–1883) to house a comprehensive cast collection of post-classical European sculptures, but also 'original' sculptures. The rooms' massive proportions allowed the display of large monuments not able to be accommodated in galleries of normal dimensions (for example the North Court in SKM in *Figure 1.3*). However, the gallery was still not high enough to accommodate the *Trajan's column* in one piece, even without the surmounting figure of St Peter. The creation of these galleries reflected the widespread educational fervour of the mid-nineteenth century, coupled with the limited opportunities for

¹⁹ Brucciani & Co. in London has been extremely important during the nineteenth century. Many authors described his work, see e.g. Wade (2014; 2019). However, Brucciani was a pretty good self-publicist, and although he was a key figure, especially for the V&A, there are many other important families and workshops in that period.

²⁰ The role of Henry Cole in the history of the Museum is not only relevant to the acquisition of the collection and the Cast Courts but it also fundamental for the building of the SKM itself. Whitehead (2005), for example, highlighted how Cole's travels around Europe influenced the museum's architectural development and neoclassic style.

the students to travel. The classical casts were placed in the temporary exhibitions' room while the Northern European Italian, South American and Indian plasters were divided between the enormous West and East courts (Singh, 2019).



Figure 1.3. South Kensington Museum, North Court, south-west corner, showing the cast of Trajan's Column (REPRO.1864-128), 1868. Stereoscopic albumen print. Photographer: Davis Burton, No. 3 in the London Series. © Victoria and Albert Museum, London/as specified by the rights holder. Source: V&A's Collection Management System.

The galleries housed casts of architectural details and reproductions of mosaics were placed in the central corridor. With the opening of the Courts, much attention was raised by the press and the public, though the reactions were rather mixed.²¹ The collection appears now and then quite eclectic and sometimes confusing. Trusted (2017), formerly V&A Sculpture curator, said:

'When we commenced work on the Cast Courts in 2009, we convened focus groups of members of the public, asking people what they most liked and what they most disliked about the Cast Courts as they then were, before the renovations. Everyone said they liked most the sense of drama and surprise in the Cast Courts, the feeling of the unexpected, and the extraordinary juxtapositions of monuments, which are in reality hundreds of miles apart. When asked what they least liked, those same people said they disliked the sense of confusion, the lack of a narrative, not knowing where to find specific objects, or how to navigate the spaces. In other words what they most liked and what they most disliked was precisely the same.'

²¹ The lack of narrative and the unorganised stack of plaster casts in the Cast Courts was strongly criticized by the contemporaries. This 'unstructured structure', however, might be a remembrance of the *wunderkammer*, popular in the previous century and then forgotten (Baker, 1982).

The two galleries are 24 metres high and house some of the V&A's largest and most popular objects. Since their opening, the Courts and the plaster casts they contain have continued to impress the Museum's visitors; many of these plaster casts, despite being reproductions, have become celebrities in themselves, independently of the monuments of which they are copies. Some of the objects retain a fascinating story, for example, the acquisition of the Michelangelo's *David* (acquired in 1857, V&A accession number: REPRO.1857-161), the mounting of the *Trajan's Column* (acquired in 1864, V&A accession number: REPRO.1864-128) or the challenging acquisition of the *Portico de la Gloria* (V&A accession number: REPRO.1866-50).

‘the new court is indeed a novelty of construction, at it may safely be said that the world does not possess such another’. *Building News*, 25 April 1873 (Williamson, 1996)

Over 39 *formatori*, or cast makers, are represented in the V&A collection and there are more in the literature on casting in plaster (Hubbard, 2015). The most represented manufacturer in the V&A's cast collection is Oronzio Lelli, from Florence. The most impressive and iconic casts were already in the collection by 1873, except for the Architectural Museum's casts that were relocated to South Kensington in 1916. Around 1900, a series of early medieval high crosses and cross-slabs from England, Ireland, Scotland and the Isle of Man cast was added to the collection, despite the shift in interest (*Figure 1.4*). The final addition of casts was after the Crystal Palace burned down, in 1937.

The value of the collection began to be questioned in the 1920s, although by this date the enthusiasm for the cast collection had long faded. The effects of the casting procedure on the objects to be replicated were also questioned in the years before²² and often the use of casts in art schools was discouraged. It is remarkable how the collection survived even when its value was questioned. In 1922, Brucciani's company was renamed 'The Department for the Sale of Casts' when acquired by the V&A Board of Education in 1922. The fortunes of the Cast Courts went through ups and downs during the twentieth century, with the Galleries always having been kept open, apart from a brief period during the Second World War. Bilbey & Trusted (2010) highlight how, due to the early twentieth-century reaction against copying works of art, it is only recently that the collection has begun

²² For example, cast of the *Portico de la Gloria* was produced in 1866 by Brucciani who received 'a certificate from the Dean stating that the work had been done without the slightest damage to the original. Seven years earlier, however, William Burges had complained of the damage done to the original colouring of sculpture by casting' (Baker, 1982).

to be fully appreciated again.²³ A brief timeline of the history of the Museum and the Cast Courts can be found in *Appendix 2*.



Figure 1.4. Painted plaster cast (REPRO.1903-25) of a green sandstone cross (Muiredach's High Cross) purchased from the Dublin Museum in 1903 for £32 10s. © Victoria and Albert Museum, London/as specified by the rights holder. Source: V&A's Collection Management System.

²³ The renewed interest in historical plaster casts in the past 20 years is suggested, for example, by the most recent international conferences on their study (Frederiksen & Marchand, 2010; Graepler & Ruppel, 2019).

1.3. MAKING PLASTER CASTS

To cast means ‘to shape (metal or other material) by pouring it into a mould while liquid’ (Stevenson & Waite, 2011). As mentioned in the *Preface* of this work, depending on the author and the field of application, the word plaster could be misleading and refer either to plaster of Paris or many different mixtures made of different proportions of gypsum, lime and sand (details in *Section 3.1*).

Gypsum had been used in buildings for over five thousand years (Turco, 1990). The use of plaster as casting material goes back to classical antiquity itself since ancient Egypt.²⁴ The Cheope pyramid is made of over 83% of gypsum. Plaster was also employed in ancient Greece and Rome for many different purposes (e.g., making death masks, stucco sculptures and copies of sculptures).²⁵ Plaster was for long associated with death and more specifically with the production of death masks (Wade, 2019). The Romans excelled in the preparation of plaster for coating internal walls²⁶ (Kemp, 1912). According to Plinius, the invention of the casting technique is due to Lysistratus, having this been elaborated for the preparation of the clay models used to produce the marble or bronze copies²⁷ (Rotili, 2009). Historical sources such as Bankart (1908) and Kemp (1912) state that, despite its use since ancient times, plasterwork was not in great use during the Mediaeval times, apart from some notable examples, such as the astonishing Hispano-Islamic ornamental plaster works in the interiors of the celebrated Alhambra Palace of Granada, Spain (Cardell-Fernández & Navarrete-Aguilera, 2006). These authors overlooked the wide-spread and early Mediaeval traditions of the use of plaster in the Middle East regions and beyond (Vanni, 2019), declaring that it is only in the sixteenth century that there is a notable revival of plaster works, especially in Italy, seeing the Renaissance celebrated artists Raffaello Sanzio (1483-1520) and Giovanni da Udine (1487–1564) experimenting with *stucco duro* (Bankart, 1908). This *gesso* (gypsum), or fine hard plaster, soon spread to France, England and all over Europe. More recent research demonstrated that numerous examples of *stucco* can be seen in the early and late Medieval period, in Europe and beyond (Caskey, 2007; Danford, 2016; Nenci, 2006; Pasquini, 2002; Sapin, 2004; Vanni, 2019), despite although technical and scientific research is still scarce on Medieval *stuccoes*.

²⁴ The Ancient Egyptians discovered the composition of practicable plaster and used it freely in the interiors of many of their edifices (Kemp, 1912).

²⁵ For insight on the use of plaster casts in the antiquity see Frederiksen & Marchand (2010).

²⁶ Vitruvius in *De Architectura* described the ancient *stucco* as composed of well-burned and slaked lime, a little fine sand, and some finely ground unburned lime-stone or white marble dust (Kemp, 1912).

²⁷ Luciano, *Juppiter Tragoedus*, 33, ‘Stavo testé con la solita pazienza/ a farmi impegolare da statuari/ il petto e il dorso: impiasticciato avemmi/ intorno al corpo corazza ridicola/ allacciata strettissima per togliere/ bene l'impronta del bronzo’, quoted in P. Toesca, *calco*, in *Enciclopedia italiana Treccani*, Roma 1949, vol VIII, pp. 540 (Rotili, 2009).

Gypsum was first mined commercially in France in Montmartre as late as the 1770s and since then has been commonly known as plaster of Paris, even when not produced there (Smith, 1810; Turco, 1990). It is known also as gypsum, gypsum plaster or *gesso*. The advantage of using plaster is that following slight calcination gypsum can be reduced to a pulverised state to create plaster, which will again become a cohesive solid by being mixed with water and afterwards allowed to dry (Turco, 1990). Due to its qualities, it is fit for the double purpose of making both casts and moulds for forming those casts. Plaster casting can be made with different techniques, by changing the way the mould is made. The most common procedures are produced by using the waste mould, gelatine mould or piece mould. The techniques for making the casts depend mostly on the shape of the subject (Smith, 1810; Wager, 1963) and are described in *Section 3.1.3*. Although in the sixteenth-century plaster casting was considered expensive and difficult, in the following centuries the techniques were simplified and generally were consistent throughout the centuries (Rotili, 2009).

Plaster is also one of the least expensive craft materials. Distinct types and grades of plaster are available for different tasks, differing for specific physical properties such as water required, fineness, hardness, setting time, workability, strength, and surface characteristic. Plaster is most often impure and contains other minerals and impurities (sulfur, iron, silicates and others), which can affect its colour and properties. Even after selecting the proper cast and mould class of materials for a particular purpose, additional factors must be considered. The model's material also affects the outcome and the pre-treatment to be chosen. The texture and hardness of the model surface, the presence of undercuts, as well as the integrity of any paint layer must, for example, be considered to avoid damage during the moulding procedure (Auerbach, 1961; Wager, 1963).

Plaster has traditionally also been modified during or after casting, to impart hardening and water repellence (Bankart, 1908). Properties of the plaster can be modified by adding various materials. Straw, hemp, sawdust, or hair are traditional materials added to improve mechanical properties. For instance, adding small amounts of inorganic acids and their salts (nitrate and chloride salts, sugar, calcium or barium carbonate, glue, stale beer and ammonia) can accelerate the setting time (Bankart, 1908; Smith, 1810; Turco, 1990). This property is otherwise retarded by adding sodium phosphate or sand, organic materials, usually sugar, pectin (ground mallow root), organic acids and their salts or organic colloids, (Megens *et al.*, 2011; Turco, 1990). All additional substances change the setting rate to varying degrees. Alum, marble dust, potassium, borax, animal glue, magnesia, or dextrin were traditional additives used to achieve the increased hardening of set plaster. Organic media in the mixture (e.g., milk and oils), on the other hand, traditionally rendered this hygroscopic material more resistant to water and more easily washable. Generally, coatings of oil, shellac or milk on cast plaster surfaces for the purpose of waterproofing the surfaces

were fairly common, also in combinations with calcium silicate, paraffin or fatty emulsions, barium sulfate, soap treatments, phosphoric acid many others (Megens *et al.*, 2011).

Plaster can be classified following different criteria. For example, a classification can be made considering the purpose of the plaster, which would also affect the chosen qualities.²⁸ By the end of the nineteenth century, Portland cement replaced the use of stucco in ornaments in architecture in England, this material being fairly durable, although less appealing (Kemp, 1912). The number of existing types of plaster increased during the twentieth century, due to the development of new technologies²⁹ leading to the development of modern materials such as Crystacal, Jesmonite and others.

1.3.1. THE COATINGS

By the beginning of the nineteenth century, the interest for the plaster copies was deeply related to the admiration for the ancient art and perfection in shape they carried, but also to the purity of the marble-like white colour,³⁰ at the time regarded as the favourite material of the ancient sculptors.³¹ The study and imitation of the perfection of the ancients, following Winckelmann's lesson, was the route to greatness and the plaster casts were irreplaceable tools, cheaper and easier to produce than the corresponding copies in marble and metal. From the mid-nineteenth century, due to the coeval new archaeological pieces of evidence, which proved the use of polychromies in ancient times, the replicas started to resemble the lost polychromies of the classical objects (Rotili, 2009). Wade (2019) reports about the structure of a typical casting campaign: 'The master was normally the "moulder" (*formatore*); one apprentice was the "cleaner" (*sbavatore*), who polished the images as they came off the mould; another apprentice was the "painter" (*colorista*), who coloured them.' Plaster provided the shape of the original and the deception of the material. Coating and colouring the plaster surface allowed to mimic the surface of the 'originals' made of wood, metal, ivory and more (*Figure 1.5*).

²⁸ Industrial moulding plaster is soft plaster or plaster of Paris. Softest, most porous, has no surface hardening additives, easily carved and best fitted for models and waste moulds. Consistency 60-80 sets in 20+35 minutes. Casting plaster mixes easily, is slightly harder, and develops a hard surface upon drying. Good for the cast to be painted. Consistency 67-80 sets in 20-35 minutes. Art plaster is similar to casting plaster, but not as hard (Kemp, 1912).

²⁹ Hydrocal A-11*: low coefficient of expansion, smooth, hard-surfaced, used for pattern-making industry. A short period of plasticity and stiffens rapidly. Sets in 20 minutes, consistency 45-55. Hydrocal B-11*: low coefficient of expansion, a high degree of plasticity, gradual setting action. Sets in 25-30 minutes, consistency 50. Hydrostone*: one of the very hardest cement, consistency 32-40. Cannot be worked in a plastic state. Sets in 15-25 minutes. Ultracal 30*: harder and stronger of hydrocal. At consistency 37 sets gradually (about 30 minutes) (*Trademarks owned by United States Gypsum Company) (Chaney, 1973).

³⁰ The idea of a perfectly white antiquity, romantically wrong, is due to the loss of the vegetal colour originally on the surface that the sculpture experienced being buried under the soil for long periods.

³¹ The already white plaster casts were sometimes coated to be more resembling to marble (Rotili, 2009).



Figure 1.5. Plaster casts of a lead Statuette figure of a seated girl (A.2-1946) made in the Sculpture Conservation Studio at the V&A to illustrate that plasters can carry many different finishes. © Victoria and Albert Museum, London/as specified by the rights holder.

In the speech for the opening of the Museum of Archaeology of the University of Jena (1907), B. Gräf (1857–1917) said: ‘a cast made of white plaster is sincere, whereas one with colour is a deceptive plaything’ (Bankel, 2004). Opinions on the use of coatings were therefore many and varied. The practice of coating the casts made of plaster during the nineteenth century had the double purpose of changing the appearance of the casts, sometimes to deceive the eye of the observer, and of protecting this porous and water-sensitive material from the environment, therefore making it more durable. Plaster casts produced for schools of arts and as such were rarely coated, as considered expendable. Moreover, the choice of which casts were to be collected or displayed in the different institutions, often guided by regional political agendas and identities, resulted in the variety of coatings, or lack thereof, in casts collections (Foster, 2015). White plaster casts are often favoured in classical and archaeological collections and attempts of recreating lost polychromies in modern days have produced interesting results (Figure 1.6).



Figure 1.6. Plaster cast and reconstruction of the Peplos Kore in the Cambridge Museum of Classical Archaeology. The original (ca 530 BC) now stands in the Acropolis Museum in Athens. © Cambridge Museum of Classical Archaeology.

Collections of non-archaeological material are often coated to mimic the surfaces of the originals. A plaster sculpture can be cleaned, carved, and treated to look like stone, bronze and other most costly materials (Figure 1.7). It can be finished to look like china or earthenware, as a substitute for stone or ceramic. To change the appearance or just to protect, several treatments seemed to be in use. Size or gelatine water or milk were used to close the pores of the plaster, or white shellac, dextrin, beeswax and linseed oil. Recipes for coatings suggest among other materials: animal glue, waxes, tree resins, pigmented

paint. They were used alone, in successive layers or admixtures (Wager, 1963). Schelper in Graepler & Ruppel (2019) reports that the art replicas of the *Gipsformerei* Berlin were offered, until the end of the nineteenth century, either in natural plaster or impregnated with a stearin solution, to provide water resistance and facilitate cleaning. The author suggests that new procedures have been introduced over the years and the casts are also available in a coloured version, as well as with an imitation coating. The patina, either intended or due to the work of time, is an additional factor that should be considered when looking at the plaster casts surfaces. Considerations on the types and depth of conservation treatments should be ethical and not establish a 'fictitious timelessness' (Lending, 2017).



Figure 1.7. Plaster cast of a Putto (CMS number REPRO.1888-519). The plaster is finished to resemble bronze. © Victoria and Albert Museum, London/as specified by the rights holder. Source: V&A's Collection Management System.

1.4. RESEARCH AND CONSERVATION

The first public display of plaster casts was in the already mentioned Great Exhibition in the Crystal Palace in 1851 in Hyde Park (London, UK); in America, cast collecting became an extremely important practice in museums and colleges as shown by the 1904 Louisiana Purchase Exposition in St. Louis, Missouri (Disalvo, 2012). The Haskell & Penny (1981) monograph, 'Taste and the Antique', reaffirmed the value of historical casts, heralding conferences such as 'Plaster casts: making, collecting and displaying from classical antiquity to the present' held at the University of Oxford in 2007, the renovation of the cast gallery at the Ashmolean in 2010 and the 2012 exhibition 'Cast Contemporaries' by artist Chris Dorsett and curator Margaret Stewart at the Edinburgh College of Art (Dorsett & Stewart, 2012). A conference titled 'Plaster and plaster cast: materiality and practice' was organised in 2010 (Sackler Centre, V&A) by Eckart Marchand (The Warburg Institute, London), Majorie Trusted (former Senior Curator of Sculpture, V&A) and Charles Hind (Royal Institute of British Architects). A conference focused on the conservation of plaster casts was held in Göttingen in 2016 and the post-prints were published by Graepler & Ruppel (2019). The trend continues with the 2018 reopening of the V&A Casts Courts and the relevant conference in January 2019 (Celebrating Reproductions: Past, Present and Future).

Research on the materials of plaster casts and innovation on conservation practices is scarce and fragmentary, although available. Many publications are available on the casts' collections and art schools' *gipsoteche*, and many papers discuss the role of these objects in the museum, but it was particularly difficult to retrieve reliable information on the materials of the plaster casts. Although in the past few years an increase in the interest in the materiality of plaster casts can be observed (*Section 1.1.2*), very few scientific researches and case studies on this topic were published, when compared to other cultural heritage materials and objects (Graepler & Ruppel, 2019; Marcinkowski & Zaucha, 2010). Personal discussion with conservators and other professionals suggested that often these researches were not disseminated and/or published and peer-reviewed. This lack could be most likely because of the outdated perception of the casts as 'false'. Moreover, the relative scarcity of historical recipe books for the *formatore* can again be addressed to the 'lower status' of plaster casting if compared with the noble arts (painting, sculpture and architecture), but also to workshops' secrecy on the recipes in the nineteenth century's highly competitive art environment.

Recent studies have tackled aspects of this topic, providing some preliminary results on the materials used for plaster casting (Megens *et al.*, 2011; Payne, 2015, 2019a, 2019b, 2020). Case studies can be helpful to understand the problems encountered by the conservator when dealing with such objects (Cipriani & Fodaro, 2015), but are often unsatisfactory due

to the particularity of the single cases and the huge variety of finishing and conservation issues that can be found on plaster casts. A study of the early twentieth-century plaster models and figures made by Ismael Smith (1886-1972) was undertaken, for example, by Guderzo & Lochman (2017) before the cleaning of the objects with agar-agar, but it is particular to the artist's practices rather than related to the period. Research on building decorative materials, such as plasterworks (Salavessa *et al.*, 2013) and mortars (Luxán *et al.*, 1995), can provide useful insight into the properties of materials also used by the plasterers. For example, Gariani *et al.* (2018) used a multi-analytical approach to characterise the materials of a selection of Renaissance *stucco* reliefs, and Freire *et al.* (2020) used X-Ray Diffraction (XRD), Scanning Electron Microscopy - Energy Dispersive Spectrometry (SEM-EDS) and pyrolysis-gas chromatography-mass spectrometry (py-GC/MS) to analyse *stucco* marble collected in Portuguese buildings, both showing the potentialities of such methodologies. da Silveira Paulo *et al.* (2007) showed the definition, characteristics and methods of application of 'gypsum plaster coatings' in historical buildings, which in this case, refers to *renders* made of plaster. Megens *et al.* (2011) describe the study of twenty plaster casts of different origins from the collection at the National Museum of Antiquities in Leiden (Netherlands), as combined with a selection of analytical preliminary studies, whereas Perusini *et al.* (2009) assessed the treatment and cleaning of nineteenth-century plaster casts from Napoli by a scientific evaluation of the surfaces. Foster in Hunter & Sheridan (2016) briefly discuss the results of physical examination of surviving plaster casts and surface scientific analysis of the original St Andrews Sarcophagus - X-ray fluorescence and Near-Infrared spectroscopy undertaken by the British Museum and Historic Scotland - mostly focussing on the implications of the findings for the archaeological and historical perspectives.

Scientific research on sculptures is usually focused on three major categories: determining sources of raw materials, developing methods of authenticating artefacts, and preservation (Sackler, 2005). Despite the effort in understanding why plaster cast decays and the processes involved, the perception is that much less progress has been made in helping conservators cope with several longstanding conservation problems. These problems can be attributed to the characteristic of the materials, but also to the inappropriate care taken of the casts until now.

By adopting a very general attitude, plaster casts can be considered simple objects made of gypsum. In practice, they can be found raw, untreated or with various finishes; casts can be monochromed, polychromed or gilded and can also hide different inner construction made of metal, wood, fabric, or hemp. Inappropriate storage conditions, protection and handling are often the cause of damage. Due to neglect, casts can become heavily soiled, covered with a thick layer of dirt and dust. The inner constructions that are introduced during the casting process to reinforce and improve the object's durability and stability (steel rods

for limbs or other protruding elements, wooden frameworks for exterior supporting constructions, meshes made of metal, textile or tow for thin layered surfaces) can react differently than plaster to environmental conditions. The issue of cleaning plaster casts is particularly challenging, not fully understood and partially tackled (Pelosi *et al.*, 2013). Established cleaning methods have been problematic when used on plaster. Considering the physicochemical properties of this type of surface, and a cleaning procedure pursuing selectivity and respect for the integrity of the artwork, aqueous solutions are usually not often a viable option because plaster is partially soluble in water, so any moisture accompanied by the slightest removal action can wear away the surface causing irreversible alteration of its original qualities. Besides water solubility, plaster surfaces are extremely fragile. They can be easily eroded by the action of a cotton swab and do not usually react well with the direct contact of poultices, so cleaning options are very limited (Domínguez, 2013). More details on the plaster can be found in *Section 3.1* and more on its properties and relevant conservation practices as reported in the literature can be found in the introduction and discussion of *Chapters 4, 5 and 6*.

The conservation of the V&A's Cast Courts has always been a complex task for the museum's conservators as the collection of casts created by Henry Cole John and Charles Robinson includes an eclectic collection of casts and finishes. The recent renovation of the Italian court involved the redecoration of the walls in the original colour scheme and the restoration of the roof and the floor, causing stress to the objects (movement of the objects and the raising of large amounts of dust). Humidity and natural light have also had an impact on the ageing material. Pollution caused both by early heating and lighting methods within the Museum and by the general quality of London's air directly affect the casts, which for the largest part have been on open display rather than in cases. The casts have been affected by past interventions such as partial or complete coating with paint or resins, dismantling and re-location, and they were also subject to a variety of traditional cleaning methods with varying degrees of success. As much as for the records of the makers and their exact processes, documentation of previous treatments is scant and somewhat scattered. A gradual broader understanding of these aspects has been achieved with the recent project through close visual observation of the objects, limited sampling and analysis campaigns and the gathering of written source materials. The Weston Cast Court (Gallery 46b, also known as Italian Cast Court) was renovated from 2010 to 2014 and its twin, The Ruddock Family Cast Court (Gallery 46a) reopened in November 2018.

The recent renovation of the galleries has allowed new studies and in-depth examinations resulting from the conservation of the collection. This opportunity for systematic research into the techniques of casts, surface coatings, finishes and mould making, together with a review of novel conservation contributions and scientific techniques constitute the backbone of this PhD research (Theodorakopoulos & Hubbard, 2017). Conservation in the Cast

Courts started with the assessment of the condition of the casts: in general, there were several casts displaying signs of serious structural problems, degradation was more evident in the form of cracking and shrinking coatings and paint layers and discoloured and eroded sealants with exposed areas of plaster having darkened considerably due to the absorption and cementation of dirt. Structural issues were often related to the method of construction (Hubbard, 2015). This could be installation-related, for example, the cast of a window from the Certosa of Pavia (V&A accession number: REPRO.1867-39, cast by Pietro Pierotti, then based in Milan) has a large wooden substructure that began to shrink soon after being built, causing cracks and distortions in the plaster. In other cases, it was related to the actual method of casting, for example, Desachy's cast of Michelangelo's Moses (V&A accession number: REPRO.1858-278). Desachy, a formatore based in Paris, patented a technique in 1856 that allowed him to create large scale casts with extremely thin walls by the addition of scrim and timber supports, which resulted in super-lightweight but rather delicate structures. Desachy's cast of Michelangelo's Moses was cast in two halves, at an overall height of almost 2.5 m high. The image shows the thin structure that Desachy was able to achieve even on casts of this scale, which in total only weighs thirty-five kilogrammes. At the left edge of the crossbar that supports the top of this half, carbon fibre webbing has been added to support a broken area of plaster. This is a very lightweight material that now provides extra strength to the load-bearing area. The black layer around the top edge of the joint line has been added as a softener for when the top half is added, protecting both sides of the joint. A variety of cleaning methods were used during the conservation of casts at the V&A. An innovative response to this challenging cleaning has been the development over the past fifteen years of the latex poultice method (Miramón, 2019). Unpublished reports have been produced by students of the City and Guilds of London Art School on BA conservation degree projects related to the V&A's plaster casts and by commissioned contractors, aiming to answer conservation queries, but lacking a common and defined research plan.

An unpublished pilot study was undertaken in the summer of 2016 to test the efficacy of some treatments in use at the V&A Sculpture Conservation. The short project, funded by the Radcliffe Trust and the Henry Moore Foundation (Hubbard & Pretzel, 2016), provided preliminary scientific results on selected techniques, but also showed the necessity of a wider database of information regarding the materials of the casts. Latex poultice produced visually impressive results but raised doubts on the effect of the cleaning product with the surface of the plaster cast and the historical coatings. Reconstructions of plaster and coatings (made following selected historical recipes) were thermally aged (60 °C for

between one and two months) and cleaning products were used on the samples.³² The material removed from the samples was analysed³³ and traces of organic coating and gypsum were detected on the cleaning residues, suggesting that selected cleaning techniques might not be appropriate for some aged coatings. The study highlighted the need for greater understanding and examination of the surfaces of plasters before cleaning and the relative risks of using different cleaning techniques (Hubbard & Pretzel, 2016).

³² The recipes include a range of probable organic coatings: animal glue, linseed oil, white glue, beeswax with glycerine, beeswax with Venice turpentine, shellac.

³³ ATR-FT-IR in-house, Macro ATR-FT-IR at Imperial College and SEM-EDS.

1.5. RESEARCH RATIONALE

The Art and Humanities Research Council (AHRC) Collaborative Doctoral Partnership (CDP) collaboration of Northumbria University with the V&A Museum generated the unique opportunity to examine the iconic collection of the Cast Courts, which has inspired artists and museums around the world for almost two centuries. The research presented in this thesis was undertaken at a very exciting moment for the Casts Courts, following the great reopening of the Galleries in November 2018. Whilst the collection is united by consisting of casts made of plaster, the uniqueness of the collection lies in the variety of the coating applied to casts' surfaces. Conservators reported having found over 84 traditional recipes for the coatings on the surfaces and additives to the plaster when observing the V&A's cast (Hubbard, 2015). Analytical information is in need to support the conservators' observations and literature sources. As understanding and preserving this much-loved collection is fundamental, close observation and conservation of the casts were carried out alongside the renovation of the galleries, leading to a better understanding of the objects' manufacturing, but also spurring many questions on the surfaces' composition. This work is intrinsically multidisciplinary as it stands at the intersections of the research fields of art technology, technical art history, material science and art conservation. Studies on other materials (*Section 1.4*) showed how combining the study of technical literature and with scientific analysis can provide invaluable information for the preservation and conservation of the objects. The audience intended for this work is therefore as varied as its extended field: the difficult task of finding a shared code of communication is here pursued and hopefully achieved. More on the perspectives and methodologies that serve this research, which can be referred to as Technical Art History through the use of Heritage Science, are discussed in *Section 2.1*.

1.5.1. GAP IN KNOWLEDGE

As outlined in *Section 1.4* in this chapter, historical plaster casts' coatings have not been studied in detail. The V&A's Cast Court collection has never been examined systematically from a scientific and material point of view, suggesting that detailed scientific research is required to support the preservation and conservation of the surfaces of the cast and to achieve a better understanding of the objects' manufacturing. While adding information to the knowledge available on the composition and deterioration of these materials, this is also an opportunity to prompt a critical review of the casts manufacturing and the treatments undertaken so far, and to design a scientific methodology for the study of the casts, also based on the understanding of the nineteenth-century literature, that will eventually allow the assessment of conservation treatments within and beyond the Museum.

1.5.2. RESEARCH QUESTIONS

- What were the original historic materials and methods employed to make the nineteenth-century plaster casts? What were the possible purposes of coating the nineteenth-century plaster casts?
- The V&A's collection has a variety of sources in different countries, through direct purchase, exchange and commission. Is it possible to identify differences between recipes used in different countries? The casts have had several periods of treatments since their early display. Can we distinguish between the original coatings and later restorations?
- How does a greater understanding of coatings' colour contribute to understanding the surface deterioration and designing the objects' preservation and conservation?

1.5.3. AIM

The study aims to investigate a selection of nineteenth-century plaster casts from the iconic Victoria and Albert Museum collection through the analysis of their coatings, as a means to ensure a desired appearance and durability, to understand the Victorian manufacturing techniques and eventually to assess the efficacy of a novel conservation treatment to test a new safe and effective methodology for the removal of soils from their surface.

1.5.4. OBJECTIVES

1. Understanding the history of the Cast Courts and the historical coatings background.
2. The thorough review of representative historical technical literature to ensure the understanding of the workshop practices during the nineteenth century.
3. The study of the historical recipes for the coating of the nineteenth-century plaster cast from representative sources, to understand the techniques and materials, as well as hypothesise the purpose of their application and their effect on the preservation of the casts.
4. A complete scientific examination of selected nineteenth-century plaster casts from the V&A collection, to acquire full information on the manufacturing, the structural materials and in particular the coatings. The techniques employed to address these objectives are optical microscopy (OM), XRD, SEM-EDS, micro-Fourier Transformed – Infrared spectroscopy (FT-IR) with chemical mapping and py-GC/MS.

5. The review and comparison of the results of the characterization of the casts, highlighting similarities and differences between cast from different workshops.
6. Following historical recipes, the production of plaster reconstructions, to be used as a substrate for selected coatings. The application of these coatings, their soiling and ageing, to achieve their degradation and therefore a plausible stratigraphy of a nineteenth-century plaster cast.
7. The assessment of the reproductions' surfaces, before and after ageing, by visual examination, technical photography (visible light and ultraviolet fluorescence) and scientific analysis (colourimetry, glossimetry, micro-FTIR with chemical mapping, high-resolution 3D surface measurements) to understand the effects of the degradation on the coated and soiled surfaces.
8. The assessment of the reproductions' surfaces, before and after cleaning the soiling with a selected cleaning treatment, by visual examination, technical photography (visible light and ultraviolet fluorescence) and scientific analysis (colourimetry, glossimetry, micro-FTIR with chemical mapping, high-resolution 3D surface measurements) to understand the efficacy of the cleaning method.
9. The compilation of a comprehensive database of results will provide reference and corpus datasets for relevant future studies.

1.6. THESIS OUTLINE

Chapter 1 describes the *Background and context* of the research, in terms of museum collections and historical background to the collection and the making of plaster casts in the nineteenth century, as based on literature review. A special focus is given to the Victoria and Albert Museum collection, addressing *objective 1*. A list of plaster cast collections can be found in *Appendix 1* and a brief timeline of the V&A's history is available in *Appendix 2*. An overview of research on plaster casts and their conservation is also given in this chapter. The rationale and the justification of this research including the gap in knowledge, the research questions, the research aims, and objectives close the chapter.

Chapter 2 is dedicated to the *Research Methodology*. Theoretical issues such as the role of the replica and the purpose of studying it, challenges in interdisciplinary studies, scientific research and cultural heritage and technical art history are addressed. The rationale of the selected archival resources and analytical techniques for the characterization of the materials of the V&A casts are presented and the methodological approach to the making of accurate historical reproduction is described. This chapter also discusses how this research can lead to improved knowledge of the materials and the techniques in use in the nineteenth century (and therefore to a better knowledge of the society that hosted them) as well as to aid the conservators and museum managers.

Chapter 3 describes the *Historical materials and manufacturing techniques for plaster casting* as described in the selected literature, addressing *objectives 2 and 3*. The properties of the plaster bulk and the historical coatings, as well as their intended purposes, are discussed. A comprehensive description of plaster techniques is given in this Chapter and original quotes from the reviewed literature can be found in *Appendix 3* and *Appendix 4*.

Chapter 4 presents the experimental method, the results and discussion of the *Characterization of the V&A casts* selected for this study. Here, *objectives 4, 5 and 9* are addressed. The techniques employed to address these objectives are OM, XRD, SEM-EDS, FT-IR and py-GC/MS. Archival information on the selected casts can be found in *Appendix 5* and extended analytical results are given in *Appendix 6*.

Chapter 5 incorporates the experimental method to produce accurate plaster reconstructions and the assessment of the surfaces at the different stages of accelerated ageing and soiling. Here, *objectives 6, 7 and 9* are addressed. The reconstructions were produced to evaluate the accelerated ageing, artificial soiling, and subsequent cleaning (*Chapter 6*) of the coated plaster surface. The aim is also to provide the information necessary for the replication of the experiments undertaken in this research, supported by the calculations in *Appendix 8*. Information on the reference environmental condition in the

Cast Courts can be found in *Appendix 7* and additional tables and images can be seen in *Appendix 9*.

Chapter 6 introduces the different approaches undertaken by conservators to care for the plaster casts' surfaces. It continues with the description of the experimental method for the cleaning experimented on the soiled reconstructions, produced as described in *Chapter 5*. Here, *objectives 8* and *9* are addressed. A novel cleaning technique was experimented with compatible solutions, to remove the soil and preserve the coatings. The techniques used to assess the cleaning method were visual examination, technical photography (visible light, ultraviolet fluorescence and SEM) and scientific analysis (colourimetry, glossimetry, FT-IR, high-resolution 3D surface measurements).

Chapter 7 summarises the work, emphasises the main points and findings. It also provides the conclusions and links the work presented throughout the thesis to the research questions, aims and objectives. A thorough discussion on whether the research reached, and to which degree, the research aim, and a future research and conservation outlook is provided.

The full record of results can be found in the database compiled as a result of this research, as referenced in the *List of accompanying material and publications*.



CHAPTER 2

DEFINING A METHODOLOGY

[...] From favoured models to increasingly ignored remnants of defunct teaching methods and styles, to decaying artefacts of the college's past in need of care and preservation.'
(Basile, 2014: 11)

2.1. INTRODUCTION

There are many different perspectives, challenges and opportunities that need to be discussed when defining the methodology for this research. Firstly, the research falls in the interdisciplinary field of heritage science, and this needs some consideration on the approaches, limits and possibilities. The archival research, the characterization of the V&A casts and the study of purpose-made reconstructions are the pillars of this research and constitute the interdisciplinary and multi-analytical methodology. This is also why in this thesis *Chapter 2* describes the 'methodology', probably a concept more familiar to the humanist, and the scientific research 'method' is described at the outset of *Chapters 4, 5 and 6* (Lebedev, 2016). Secondly, the objects, on which the research is based, are historical replicas, meaning that, even before starting to think about the practical approach to the research, some thinking on the different levels of information and meaning carried by these objects must be pondered on. Replicas should be subject to the same scientific, conservation and curatorial processes as other cultural objects (Foster & Jones, 2020b). Some background on the 'discussion about the replica' was given in *Section 1.1.2* and the following paragraphs will also clarify how this can affect the methodology and the possible outcomes of the research.

Art historians aim to try and interpret the art of the past and narrate it. To do so, art historians should be conscious of the value of the research of those who reconstruct materials and investigate their properties (Clarke *et al.*, 2005). The study of works of art using scientific methods dates to the late eighteenth century but expanded exponentially in the late twentieth century. Scientific research devoted to making conservation itself more rational and effective came along sometime later, though it can also be traced back to the nineteenth century (Sackler, 2005). Surprisingly enough, the role of scientific research in the humanities still needs in many cases to be explained and advocated. Art, science, and conservation must constitute nowadays the triangle of a thoughtful and ethical approach to art objects and artistic research. Building an appropriate communication code for the triad scientist-conservator-curator and a considerate understanding of each other's field of

expertise is the base for more significant and efficient research practice in art history and fine arts. 'Art technology' aims to provide knowledge concerning the production methods of works of art or crafts, i.e., machines, materials, studios, techniques, tools etc. (Clarke *et al.*, 2005). Information on this can be derived by the object itself, primary information given directly or indirectly by the artists or craftsman of the object, *realia* (i.e., surviving historical machines, materials and sites and tools related to the production process), secondary, contemporary information (surviving treatises, recipes books and as such) and modern studies in art history, chemistry, conservation etc. and literature on historical sources (Clarke *et al.*, 2005). In line with the above-discussed interdependency art history-science-conservation, the sources mentioned herein are 'sources within context': 'An art technological source never stands alone – there is always a context which is present in various ways' (Clarke *et al.*, 2005). Source research, scientific analysis and reconstruction are therefore the three pillars of art technology.

'The greatest art in the world was done for its place and in its place' J. Ruskin³⁴ cited by Bankart (1908)

There is a range of intrinsic and contextual qualities that must be considered when studying replicas of cultural objects, including their technology of production, authorship, location, materiality, use, social context, accessibility, and biography (Foster & Jones, 2020b). Research based on a 'cultural biographical approach' (Foster & Curtis, 2016) must account for an analysis of the copies relationship to the biography of the object that they replicate and include thought on the way their identity and authenticity are negotiated (*Section 1.1.2*) (Foster & Jones, 2020a).³⁵ Nineteenth-century plaster casts are hence rich in historical information, characterised by composite biographies constructed by the stories of the casts and of the object they replicate (Foster & Curtis, 2016; Foster & Jones, 2020b). The biographical approach enables the identification of how the meanings given to objects change through times and contexts. This approach allows replicas to have 'multiple lives', including their 'short biography' (production, use, and disposal) and their extended one (up to the present) (Foster & Jones, 2020b). The latter end of the extended biography is where the objects are discovered, and how they have come to be the subjects of interpretation (Holtorf, 2002). An additional biographical level of replicas relates to the relationship of the replica to the original and other collections, including their origins (Foster & Jones, 2020a).

³⁴ John Ruskin (1819–1900) was a draughtsman, art patron, watercolourist, philanthropist and he is considered the leading English art critic of the Victorian era.

³⁵ Connections and stories that relate the copies and their original can be drawn - see for example Kupiec (2019) and Reynolds-Kaye (2019).

More generally speaking, the scientific approaches to the collection can also provide new evidence and perspective for future studies and to rethink not only the role of the reproductions in the museum but also the perception of the replica in its own historical context. The value and significance of the replicas must be re-evaluated, particularly when the pressure to dispose of them tends to increase. The study of replicas provides the opportunity to rethink the ideas of value and authenticity (Foster & Curtis, 2016) while studying and comparing 'authentic originals' and 'reproduced originals' in their contemporary different settings, with their changed social values and also their historical ones (Foster & Curtis, 2016, Foster & Jones, 2020a).

With the case study of the St Andrews Sarcophagus, Foster in Hunter & Sheridan (2016), for example, provides a good example of the role that heritage science can and must have in defining the narratives behind replicas and their 'parent objects'. In this piece of research, a great deal of information on British early antiquarian societies was derived by examination of plaster casts, archival and documentary research, and scientific analysis of the original Sarcophagus. Foster also highlighted how the 'fabric of plaster casts' (i.e., its materiality) can help define stories on technologies and craftsmanship while discrediting or confirming established knowledge.

Another example is given by the work of Hughes *et al.* (2014) who report an interdisciplinary project focused on historic buildings or monuments that were the subject of active conservation, in collaboration with the National Trust for Scotland, Historic Scotland and a European research project (HEROMAT). Interviews and forms of participant observation aimed to assess the values attached to deterioration and decay in historic buildings and how decisions about the conservation of materials and science-based interventions are informed by these, also concerning authenticity. A wide range of academic researchers and professionals worked towards informing future conservation policy and practice, ensuring that science-based techniques are used in a culturally sensitive way in conserving the historic environment.

As often happens in the field of heritage science, especially in the museum, this research started from the need of answering the questions of curators and conservators (Theodorakopoulos & Hubbard, 2017). There is a wide literature on the historical study of plaster casts, but very little has been scientifically studied or at least published on the topic (*Section 1.4*). Curators and historians have been relying on archival sources and visual evidence for the interpretation of plaster casts (Frederiksen & Marchand, 2010; Graepler & Ruppel, 2019; Lending, 2017). Conservators base the practices for caring and cleaning plaster casts on experience, common sense and previous case studies (Pelosi *et al.*, 2013). Archival and scientific information on the materials and manufacturing processes can be an invaluable tool for museum professionals. However, as any conservator knows well, it is

impossible to define a unique conservation practice applicable to a class of materials, as the uniqueness of each object and its environment must always be considered. Every object has a unique history, due to its condition of manufacturing, the conditions in which the objects were stored along over the decades (if whether in storage, indoors or outdoors, if on display), and the conservation treatments (the decisions made by the conservators and any unexpected occurrences such as accidents). Moreover, the lack of knowledge of the real potentialities of the analytical techniques may create unattainable expectations (Fratelli & Signorini, 2008). The main outcomes of archival, scientific and technological investigation of the V&A plaster casts, as well as of other cultural heritage objects, are: 1) knowledge of the materials and the manufacturing techniques of the artefact; 2) supporting information for the conservation and preservation of the object; 3) knowledge on the context of the object, past and present (Fratelli & Signorini, 2008).

2.2. THE LITERATURE RESEARCH

‘That an art so extremely interesting and unique as that of the plaster should have escaped record and consideration in any collected form at the present day is to be regretted.’ (Bankart, 1908)

As discussed in *Sections 1.1 to 1.3*, making replicas by plaster casting was an extremely successful and remunerative business during the nineteenth century. This led to workshop secrecy around the art of casting and plastering. Moreover, the ‘lower status’ of this art, when compared with painting, sculpture and architecture, may have resulted in reduced interest in the preservation of documentation on this topic. Until recently, the underestimation of the role of plaster replicas in the museums may also have caused the lack of conservation peer-reviewed papers on the treatments applied to these objects (*Section 1.4*). Archival and historical research on the materials and the manufacturing techniques in use during the nineteenth century to produce plaster casts can support the understanding, display and conservation of these objects. Behind the replicas production, trade, use, and after-life, their networks and relationships reveal the contextual circumstances for their interpretation. Understanding the context explains why and how replicas are valuable, highlighting the specific advantages of a ‘biographical approach’ to their study (Foster & Curtis, 2016).

Archival resources and historical literature were explored to contextualise the technological information, and seventeen manuals or historical books and fourteen patents focused on plaster casting or in some way related to this technology were selected to be reviewed for this study. Literature and archival research are in this case irreplaceable sources of information, and scientific research helps to support this information. The sources described in this section allowed the summary, in *Chapter 3*, of technical information on the materials and manufacturing of plaster casts. Such a wide collection of technical information is solely based on the sources reviewed for this study, meaning that other techniques, methods and materials in use during the nineteenth century might be described in other resources.

2.2.1. THE ARCHIVES

The study of historical replicas offers imperative historical perspectives into the purpose of plaster casts collections in the past, of the related materials, but also information on the relationships between cultural heritage organisations (Foster, 2015; Foster & Curtis, 2016, Frederiksen & Marchand, 2010). Visiting archives, collections or *gipsoteche* can in some

cases uncover information valuable for revealing not only the historic dynamic of the collection but also some unexpected information on the manufacturing and the materials that can be extremely significant for the scientist (Figure 2.1). Moreover, important records may be found in the archives of individual workshops and manufacturers rather than in larger institutions (Foster & Jones, 2020b).

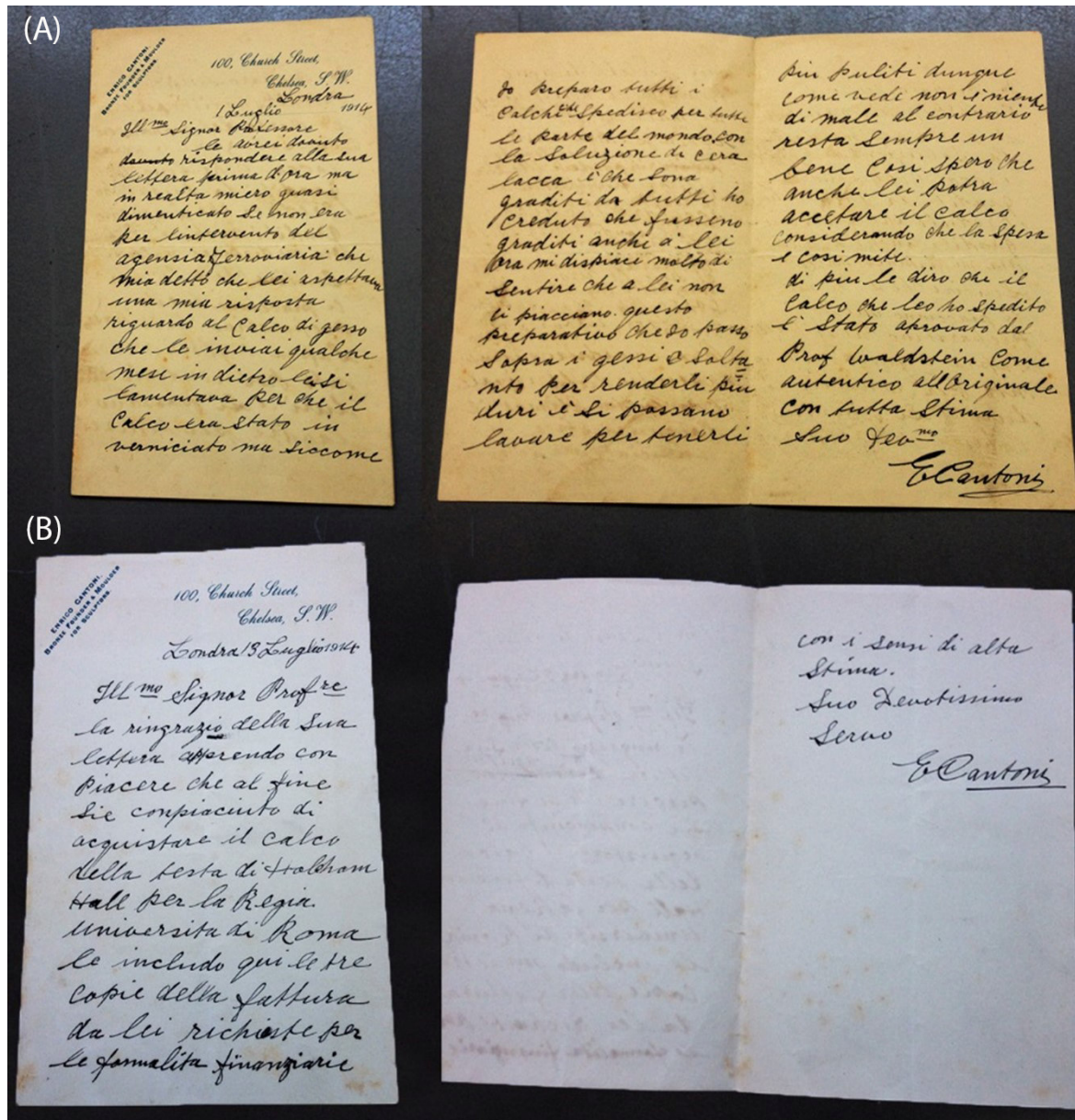


Figure 2.1. Two letters from the Archive of the Museo dell'Arte Classica (Museo dei Gessi) at the University of Sapienza, Rome (Italy). The two letters were written by Enrico Cantoni (c. 1859-1923) to Professor Emanuel Löwy (1857-1938) on the 1st of July (A) and 13th of July (B) 1914.

Letters shared by workshops' and museums' professionals, transportation documents for the casts, and records of modern cleaning treatments can be sources of unexpected pieces of information. Hidden in piles of correspondence, there are many histories to be told. As

an example, *Figure 2.1* shows two letters, from the archive of the *Gipsoteca* or 'Museo dei Gessi' at the University of Sapienza (Rome, Italy), written by Enrico Cantoni (c. 1859-1923) to Prof Emanuel Löwy (1857-1938) on the 1st and 13th of July 1914. Cantoni was an Italian *formatore* based in Chelsea (London, United Kingdom) and Löwy was the eminent Austrian Professor, director of the *Museo dei Gessi* (Rome, Italy). The two letters are written in Italian and suggest that Löwy ordered a cast of a Head from the collection held at Holkham Hall (Norfolk, England), from Cantoni. The cast was coated with *ceralacca* (which translates as sealing wax), according to Cantoni, and the Austrian Professor did not like the appearance of the cast.

Letter written on the 1st of July 1914 (A in *Figure 2.1*):

'Dear Eminent Professor,

I should have answered your letter earlier, but, honestly, I had almost forgotten, if not for the reminder by the railway company, that told me that you were waiting for my answer regarding the Plaster Cast that I sent you a few months ago, that you complained about because the plaster cast has been varnished, but given that I make all the plaster casts that I send around the world with the admixture of shellac³⁶ and that these are liked by everybody, I thought that these would have been liked by you too. Now I am truly sorry to hear that you do not like them. This admixture that I apply onto the casts is only to make them harder, and to make them washable and to keep them cleaner, therefore you can see that this is nothing bad, at the contrary, it is always good then I hope that you will accept the cast considering that the cost is that mild. Moreover, I will tell you that the cast that I sent you was approved by Professor Waldstein³⁷ as authentic to the original.

With all my regards,

Yours E. Cantoni'

Letter written on the 13th of July 1914 (B in *Figure 2.1*):

'Dear Eminent Professor,

Thanks for your letter, as it seems that in the end, you were pleased to buy the cast of the Head of Holkham Hall³⁸ for the Royal University of Rome. I enclose here three copies of the invoice requested by you for the financial formalities with the utmost regard.

Your devoted servant,

E. Cantoni'

³⁶ *Ceralacca* in the terminology used in the original letter. This would translate as 'sealing wax', but it is more likely that Cantoni meant shellac.

³⁷ Sir Charles Waldstein (1856-1927) was an Anglo-American archaeologist; he lectured for many years in Cambridge and was director of the Fitzwilliam Museum

³⁸ Holkam Hall is an eighteenth-century country house in Norfolk, England

The two letters, and also the many invoices in the archive in Rome, suggest a frequent trade of casts from London to Rome and vice versa.³⁹ The letters seem also to suggest that the British practice of coating plaster casts was not that usual in Italy, and also that the casts used to be ‘approved’ by academics ‘as authentic to the original’. The fact that Cantoni refers to a ‘mild cost’ also suggests that the casts were cheap additions to the museum collections. All these snippets of information might open further and deeper archival investigation, and the ones above are just an example of the many opportunities provided in this (almost) unexplored field.

Delivery notes and Museums’ Registries can also provide information on the trades and the specific story of the objects, as well as period photographs and descriptions of the original objects from which the moulds were taken. For example, the pricelists for the plaster casts might suggest that during the nineteenth century the acquisition of plaster casts was due to the low prices of the casts as best substitutes for the ‘real objects’ while the Museum cannot afford to acquire them (Disalvo, 2012). From this perspective, the Museum registries offer invaluable information on the story of the specific object, once in the collection, as well as period photographs and descriptions of the original objects from which the moulds were taken (Figure 2.2).

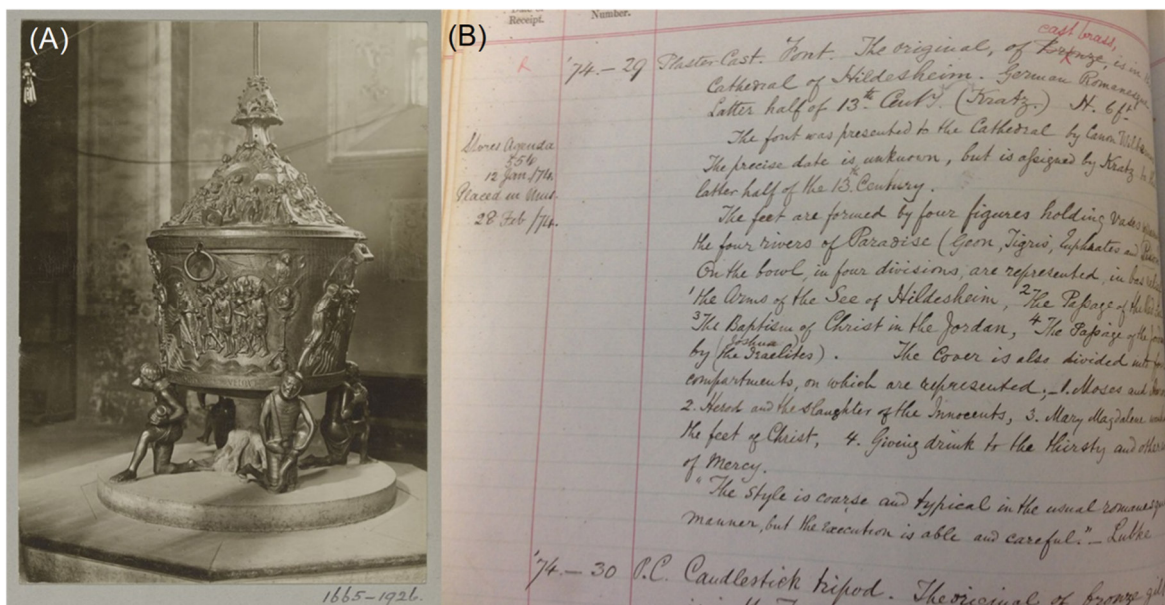


Figure 2.2. (A) V&A’s object number 1665-1926. Photograph, the font in the Cathedral of Hildesheim, Germany, gelatine silver print, late nineteenth to the early twentieth century. Photographic record: 2016JA0650. © Victoria and Albert Museum, London/as specified by the rights holder. Source: V&A’s Collection Management System. (B) Description of the object on the V&A’ Register of Acquisition, 28th of February 1874. From the Archive of the Sculpture Department at the Victoria and Albert Museum, London.

³⁹ Casts trades between Rome and Ireland are documented (Betzer, 2019).

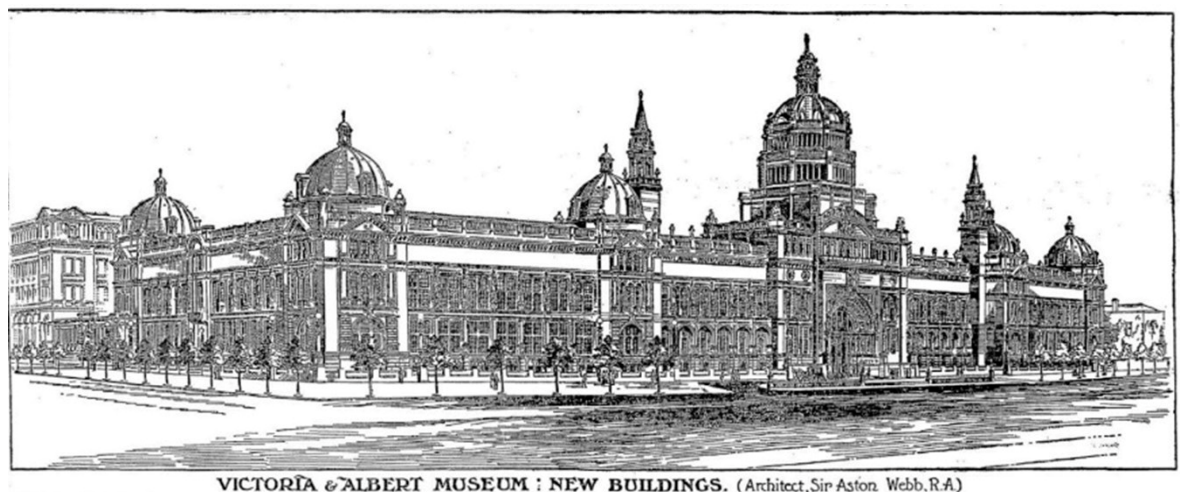
Another archival resource is represented by extracts from historical journals (*Figure 2.3*). The already discussed controversial reaction to the opening of the Cast Courts (*Section 1.2*) can be seen in the press of the time.

‘The boldness of the idea, the height of the apartments, the magnitude of many of the objects with which they are filled, and the beauty of others, all concur to produce a lasting effect.’ (“The Architectural Courts, South Kensington Museum. The Trajan Column and the Portico de La Gloria, Santiago de Compostella,” 1873)

‘[...] the new court, [...] a most instructive chapter in the long and varied history recorded in the collection at South Kensington.’ (“The New Court at South Kensington,” 1873)

‘[...] it may safely be said that the world does not possess such another. [...] some person will, perhaps, be inclined to question the wisdom of erecting a facsimile of a monument like the Trajan Column, and placing it where it will doubtless be an object of wonder to the public, but will be of very limited benefit to the art student, since, though the column is in two pieces, there is much bas-relief that can hardly be distinguished, much less copied [...]’ (“The New Court, South Kensington,” 1873)

‘At South Kensington, in the two great hall which contains the casts and the copies, there is at present the most extraordinary jumble of works [...] that can possible be imagined.’ (“The South Kensington Museum,” 1882)



VICTORIA & ALBERT MUSEUM : NEW BUILDINGS. (Architect, Sir Aston Webb, R.A.)

Figure 2.3. Image taken from 'The Times' (21 November 1908) showing a drawing of the New Building of the Victoria and Albert Museum.

The drawback of the archives is their vastness and their constant expansion: for interdisciplinary research that cannot only rely on the archive investigation, but it is also virtually impossible to explore all the documents held by the archives in some way related to the selected workshop/plasterer. Moreover, by the time research seems to have fulfilled its purpose, new techniques, perspectives and information are added to it: 'It sounds as a lot of work and it is, but it is feasible, and this is the paradox⁴⁰ of conservation' (Price & Doehne, 2011: XIV).

2.2.2. HISTORICAL TECHNICAL LITERATURE AND PATENTS

The practice of writing manuals on the technical arts is as old as the arts themselves. The eighteenth and nineteenth centuries saw a raising interest in medieval artists' manuals especially on the art of painting. In the nineteenth century, many historical texts on all kinds of art techniques were transcribed and published. However, in the twentieth century, there was a drop of interest, concentrating on theory and aesthetics rather than on practice and materials. Since the 1970s, a new and increased appreciation of the historical-material aspects of art has been recorded (Carlyle *et al.*, 1995; Clarke *et al.*, 2005).

'It is somewhat remarkable that, although most of the useful arts and crafts are fairly well represented in the literature of our own and other languages, the trade of the Plasterer – which is one of the most ancient of calling – has not adequate representation in technical literature.' (Kemp, 1912)

Seventeen manuals or historical books focused on plaster casting or in some way related to this technology were reviewed for this study (*Table 2.1*). The books date from the first century BC to 1990 and offer a great variety of material descriptions and definitions, as well as an incredibly interesting range of recipes and treatments. The choice of including references that span in such a wide timeframe, although the focus of this research is the nineteenth-century plaster casts, was made to comply with the flux of transmission of the recipes, that often are quoted or simply repeated (either word-by-word or after interpretation and/or translation) from ancient to modern books. The recipes are often very vague in some parts, and they are quoted in *Appendix 3* and discussed in *Chapter 3*.

⁴⁰ The central paradox in conservation is: 'while progress is necessarily incremental, time and the elements steadily take their toll on cultural heritage, and the window for action to ensure that history is preserved for future generations is limited' (Horie, 2010).

Table 2.1. List of manuals and historical books reviewed for this study.

<i>Source</i>	<i>Date</i>	<i>Reference</i>
The ten books on architecture	30-15 BC	Pollio, (1914)
Il libro dell'arte, o Trattato della pittura	Fourteenth century	Cennini, (1859)
The treatises of Benvenuto Cellini on Goldsmithing and Sculpture	Sixteenth century	Cellini (1967)
The Laboratory. Or School of arts	1740-1810	Smith (1810)
The art of fresco painting: as practised by the old Italian and Spanish masters, with a preliminary inquiry into the nature of the colours used in fresco painting, with observation and notes.	1846	Merrifield (1846)
A descriptive catalogue of the fictile ivories in the South Kensington Museum	1876	Westwood (1876)
Plaster casts and how they are made	1899	Frederick (1899)
Plastering, plain & decorative. A practical treatise on the art & craft of plastering and modelling, including full description of the various tools, materials, processes and appliances employed	1899	Millar (1899)
The art of the plasterer. An account of the decorative development of the crafts chiefly in England from the Sixteenth to the Eighteenth century with chapters on the stucco of the classic period and of the Italian Renaissance also on sgraffito pargetting Scottish Irish and modern plasterwork	1908	Bankart (1908)
The practical plasterer. A compendium of plain and ornamental plaster work	1912	Kemp (1912)
Modelled sculpture and plaster casting	1961	Auerbach (1961)
Plaster casting: for the student sculptor	1963	Wager (1963)
Creating with plaster	1966	Meilach (1966)
Plaster mold and model making	1973	Chaney (1973)
The art of doing: plaster techniques	1985	de Jonge (1985)
Manuale pratico di tecnica pittorica	1989	Piva (2010)
Il Gesso. Lavorazione, trasformazione, impieghi	1990	Turco (1990)

More details are available in Appendix 3 and discussed in the materials' description in Chapter 3.

As already discussed in *Section 1.1*, copyright and intellectual property is intrinsic issue related to the production of plaster casts. It was not solved by the Garrard's Act in 1798 and it is still a topic of discussion today - see for example the case of the scanning of the Nefertiti bust (Charr, 2019).

Patents aim to provide intellectual property, by giving the legal right to their owner to exclude others from selling, using, making, and importing an invention for a set period of years. Historic standards can be also a valuable source of information (*Gypsum - Properties, Definitions and Uses. Vol. 108*, 1921). A selection of fourteen patents was reviewed for this study. The patents date from 1839 to 1981 and were registered in the United Kingdom, Canada and the United States. A summary of the content of the patents can be seen in *Table 2.2* and more details are available in *Appendix 4*.

When referring to and interpreting historical recipes to define or reproduce the technologies of the past, extra care must be taken. While their effects are obvious, recipes for artists may exclude those causes (either 'material' ingredients or 'efficient' instructions) that were considered self-evident. Concentrations and quantities are often vague, and materials are often described through definitions and units no longer in use. The intention of why a material is added is rarely defined. Recipe books are rarely copied word-for-word: they are frequently subject to addition, elimination, and correction, and often mistakes (or wrong translations, as was also suggested in *footnote 36* in this chapter).

The nature of certain variations or errors across the text can often tell us something about the context of the compilation. A change in ingredients used in a recipe could be, on the one hand, due to palaeographical problems that resulted in a word being misunderstood and thus being replaced by another well-known one; on the other, it might also correspond to a deliberate technical improvement suggested by the author of the recipe (Bucklow, 2009; Neven, 2009).

Table 2.2. Description of the patents reviewed for this study.

<i>Patent no.</i>	<i>Date</i>	<i>Office</i>	<i>Authors</i>	<i>Title</i>
1361	09/10/1839	US	J. D. Greenwood, R. W. Keene	Improvement in cements for forming artificial stone, &c.
59154	23/10/1866	US	D. E. Somes	Improved composition for forming useful and ornamental articles
192112	19/06/1677	US	W. B. Closson	Improvement in the art of making molds and their counterparts
308111	18/11/1884	US	J. H. Trickey	Art or process of and composition for making artificial stone
371550	18/10/1887	US	E. T. Laxton	Process of hardening and preserving plaster-of-Paris casts and molds and making them impervious to water, &c.
16840	28/10/1893	UK	A. Cléry	A preservative composition, applicable also for the manufacture of artificial stone, statuary and the like
10658	22/04/1899	UK	W. R. Johnson, G. Nichols	Improvements relating to Gypsum or Plaster of Paris
15204	16/11/1901	UK	A. Wolf	Improvement in Composition for Coating Surfaces
968505	23/08/1910	US	G. J. Zolnay	Process of Making art models, &c.
14378	03/06/1920	UK	W. J. de Bas	Improvement in Plastic composition
446844	24/02/1948	CA	M. C. Dailey, E. W. Duffy	Gypsum Product
2660776	01/12/1953	US	J. H. Miller	Flexible mold for forming statues with spaced legs
1 461 812	19/01/1977	UK	F. F. Koblitz	Modified Gypsum Composition
2 053 184 A	04/02/1981	UK	L. W. Stockton	Improvements in or related to gypsum plaster

More details are available in Appendix 4 and are discussed in the materials' description in Chapter 3.

2.3. SCIENTIFIC INVESTIGATION OF THE V&A CASTS

An introduction to the V&A and its history and how this tightly relates to the cast collection and the Cast Courts was given in *Section 1.2*. This should have provided a general idea of the variety, in terms of geographical provenance and period of manufacturing, but also in terms of ways of acquisition and history of the objects. It seems obvious that it is impossible to fully analyse, during a PhD research, a collection formed by over 4000 casts (Graepler & Ruppel, 2019) and it must be clear that such an enormous collection needs further scientific study than the one provided here. V&A conservators reported that at least 84 traditional recipes for the coatings on the surfaces and additives to the plaster have been observed and over 39 *formatori* have been documented (Graepler & Ruppel, 2019; Hubbard, 2015). The variety of objects and materials and therefore of types of decay may also discourage from providing a general practice in the treatment of these objects. Nevertheless, by selecting three groups of objects, this research aims to provide information on the selected groups' manufacturing and possible differences within the workshops. Moreover, the specific decisions made regarding the objects selected in this study and the reasons why they were made, can enlighten on the method of research to be used in future studies.

2.3.1. THE OBJECTS

The casts selected for this study are individually described in *Appendix 5*. The objects were selected by Charlotte Hubbard (Head of Sculpture Conservation at the V&A until February 2019) by evaluating the accessibility and relevance of the objects, but also the other plans and projects happening in the galleries at the same time of this research. A total of 12 objects and 63 samples were analysed for this study. The objects belong to three different groups, identified by workshop or provenance:

- **Küsthardt Group** consists of six objects made by Friedrich Küsthardt (*Figure 2.4*), cast from details in the Cathedral of Hildesheim and Naumburg Cathedral, Germany. The objects were acquired by the V&A between 1873 and 1875;
- **Notre-Dame Group** consists of four objects (*Figure 2.5*), cast of details of the decorations made by Pierre de Chelles for the Notre-Dame Cathedral in Paris. Two out of four of the casts (REPRO.1890-80 and REPRO.1890-81) were cast by Jean Pouzadoux and acquired by the V&A in 1890. The others (REPRO.A.1916-3152 and REPRO.A.1916-3153) were part of the casts acquired from the Architectural Association in 1916;
- **Franchi Group** consists of two objects acquired by the V&A in 1864 (*Figure 2.6*). The casts were made by Giovanni Franchi and Son in 1851 from medieval reliefs from Chichester Cathedral (Sussex, England).



Figure 2.4. V&A casts of the Küsthardt Group. Dimensions are available in Appendix 5. © Victoria and Albert Museum, London/as specified by the rights holder. Source: V&A's Collection Management System.

The objects selected for the study have been on display in the Galleries for most of the time after being acquired by the V&A. Hubbard in Graepler & Ruppel (2019) suggested that there are several interventions, beyond that of the original casting workshop, which have significantly impacted the conditions of the collection and their surfaces, specifically building developments undertaken at the Museum between 1857 and 1884, the five redecoration schemes for the Cast Courts from 1873-1979 and the conservation intervention to date. After the recent refurbishing of the Casts Courts, the objects were dusted and some of the objects were also subjected to other conservation treatments (Graepler & Ruppel, 2019; Hubbard, 2015). The conservation treatments details on the objects selected for this study are available in *Appendix 5* and were kindly provided by the V&A Sculpture Conservation team. The recent project provided the conservators with the opportunity to work on over 350 plaster casts in the V&A collection, prioritising the structural and surface stabilization of the casts and setting cleaning levels to retain any historic polychromy and surface coating (Graepler & Ruppel, 2019). An appreciation of how an object was made, along with its place in the art historical tradition is just as important to conservation as is an understanding of the chemistry behind the creation of the material and the substances used to clean or repair it (Miller, 2005).



Figure 2.5. V&A casts of the Notre-Dame Group. Dimensions are available in Appendix 5. © Victoria and Albert Museum, London/as specified by the rights holder. Source: V&A's Collection Management System.



Figure 2.6. V&A casts of the Franchi Group. Dimensions are available in Appendix 5. © Victoria and Albert Museum, London/as specified by the rights holder. Source: V&A's Collection Management System.

2.3.2. THE ANALYSIS

A multi-analytical approach was designed for the scientific examination of the V&A casts. The visual examination was followed by the objects' sampling and analysis. The samples were examined with visible light reflectance (VLR) and ultraviolet fluorescence (UVf), optical microscopy (OM) and scanning electron microscopy (SEM). Elemental characterization was carried out with energy-dispersive X-ray spectroscopy (EDS) and further analyses were performed with X-ray diffraction (XRD) and Fourier-transform infrared (FT-IR) spectroscopy with focal plane array (FPA) imaging. Gas chromatography/mass spectrometry (GC/MS) and pyrolysis-GC/MS with extraction methods based on n-propanol followed by pentafluoro propionic anhydride (PFPA), tetramethylammonium hydroxide (TMAH) and 3-trifluoromethylphenyltrimethylammonium hydroxide (m-TFPTAH) were performed to detect organic media. Throughout the study, regular photography and documentation were ensured.

The focus of the analysis undertaken for this research was on the objects' outer layers, as justified by the Aims and Objectives in *Sections 1.5.3* and *1.5.4* at the beginning of this work. This is due to the historical relevance of this class of historical coatings (*Section 1.3.1*), but also to the role that the coated surface(s) play in the processes of degradation and therefore their importance for the conservation decisions. No matter whether the causes of deterioration are physical, chemical or biological, the surface will be the first frontier to be modified both in structure and composition: the way any solid surface interacts with its environment, or with any other surface, is determined by the composition of the outermost atomic layers, suggesting the utmost importance of the understanding of the properties of this layer to perform appropriate care of the materials (Baglioni & Chelazzi, 2013). Exposure of the work of art to the atmosphere will result sooner or later in the growth of nano- or microlayers of different chemical compositions readily adsorbed on the surface. Although bulk and surface compositions may be related to a greater or lesser degree, and the bulk composition of solid materials is generally easily controlled, it is well known that the surface is more affected by its environmental record than by its composition (Baglioni & Chelazzi, 2013).

Due to the lack of previous systematic studies on the interaction of plaster substrates with different classes of coating materials (*Section 1.4*), and due to the large variety of materials that could have been applied (*Section 1.3.1* and *Section 3.2*) the analysis of the casts' surfaces must be approached by defining a broad analytical methodology and referring to studies of other works of art materials (Blasco-López *et al.*, 2015; Cardell-Fernández & Navarrete-Aguilera, 2006; da Silveira Paulo *et al.*, 2007; Gariani *et al.*, 2018). The analytical methodology chosen for the characterization of the materials object of this study was developed by considering the purpose of the study, their characteristics as suggested by

the literature information, the integrity of the museum objects and the availability of equipment during this research. When studying a museum artefact, there are several requirements necessary for selecting an appropriate analytical technique. Non-destructive techniques are preferred to minimise damage to the object of interest. The smallest quantity of material can be collected when the use of destructive techniques is required to obtain the desired information (Rizzutto *et al.*, 2015; Stuart, 2007).

Few case studies published on the cleaning of the plaster casts showed that selected analytical techniques were employed before the cleaning treatments. Analyses were carried out before cleaning treatments of three plaster casts belonging to the Brera collection by Cerea *et al.* (2017); Ángeles Solís Parra described in Graepler & Ruppel (2019) reports the restoration of a large collection of plaster casts, used as teaching material over 350 years, held at the Royal Academy of Fine Arts of San Fernando in Madrid: the restoration was preceded by observation and gamma-graphic study of reinforcements and internal structure. Guderzo & Lochman (2017) indicate that SEM and FT-IR analysis were used for the characterization of the pigments and binders of the polychromed pieces (dated 1907-1932) of the early twentieth-century plaster models and figures made by Ismael Smith (1886-1972) in the laboratory of the Conservation Department of the Museu Nacional d'Art de Catalunya of Barcelona. Results suggest the use of a 'modern' palette: bone black, alizarin red, viridian, ultramarine, Prussian blue, copper blue, cobalt blue, Schweinfurt green, vermilion, chrome red, and chrome yellow, and that shellac, natural resins and drying oils were identified. Final polishing with wax was also found, as well as degradation products such as copper stearates and atacamite. Analytical studies on materials such as *stucco* and other architectural materials demonstrated how effective a multianalytical approach is for the characterization of inorganic and organic materials. For example, Freire *et al.* (2020) analysed *stucco* marble in Portuguese architecture using a multianalytical approach, combining XRD and SEM-EDS for mineralogical and elemental characterization and py-GC/MS to determine the presence of organic compounds. Gariani *et al.* (2018) also approached the analysis of *stucco* materials using a multianalytical approach to have both structural and compositional characterization of the samples. Blasco-López *et al.* (2015) defined a methodology for the study of the micro-layers in historical plasterworks, based on OM, XRD, SEM-EDS and FT-IR. Melita *et al.* (2020) combined visual examination and analyses using FT-IR and py-GC/MS for the characterization of a painted plaster surface before and after laser cleaning. Such an approach is also fundamental since the plaster-coating system object of the characterization in this study is widely unknown and it likely consists of a mixture of organic and inorganic materials (*Section 1.3*).

Before more detailed analysis, an initial visual examination of materials can provide useful information. Important identifying marks on an object, and information regarding colour, production method, surface finish, and degradation (for example in *Figure 2.7* tools marks

and signatures/stamps from the workshops could be seen) can be documented after an examination with a magnifying glass, and assisted by different types of lighting (Stuart, 2007). Information regarding colour, gloss and opacity can be obtained by standard lighting. Raking light can reveal details about cracking, texture and planar distortion. Transmitted light from the verso of an object can show features related to mending, inner structures, tears and watermarks (Sackler, 2005; Stuart, 2007).



Figure 2.7. (A) A closer look at the surface of V&A's object number REPRO.A.1916-3152 shows marks due to the use of tools during manufacturing. (B) A closer look at V&A's object number REPRO.1874-29 shows the stamp of the workshop where the cast was manufactured. © Victoria and Albert Museum, London/as specified by the rights holder.

Regular visible photography is the most traditional and used tool to document all the actions taken on the Museum objects. Unfortunately, although photography has been used in Museums for many purposes for many years, appropriate systematic documentation is often disregarded, leading to loss of information. The appropriate cataloguing and referencing of such records are often subjected to limited time and they could get lost in digital storage and devices. Other forms of photographic documentation, such as with Ultraviolet fluorescence (UVf) light (Figure 2.8) and Infra-Red Reflectance (IRR) or X-rays are often available, but not always a viable option. For example, in this research, only visible images were taken as it was not possible to organise the setting for UVf or IRR images in the Galleries during the refurbishing of the spaces or organise the moving of the objects into the V&A's X-ray photographic room (Veasey, 2019). Colour and dimension reference through a Photography Scale for visible light and subsequent white balancing through an image editing software, Adobe Photoshop® CC 2019 in this study, allow to overcome the lack of consistency and uniformity of the light as related to the time of the day and location of the object to be photographed, and also to contextualise its dimensions (Boylan, 2004) (Section 4.2.2.1). Documentation of the condition of the area before and after the sampling was recorded.

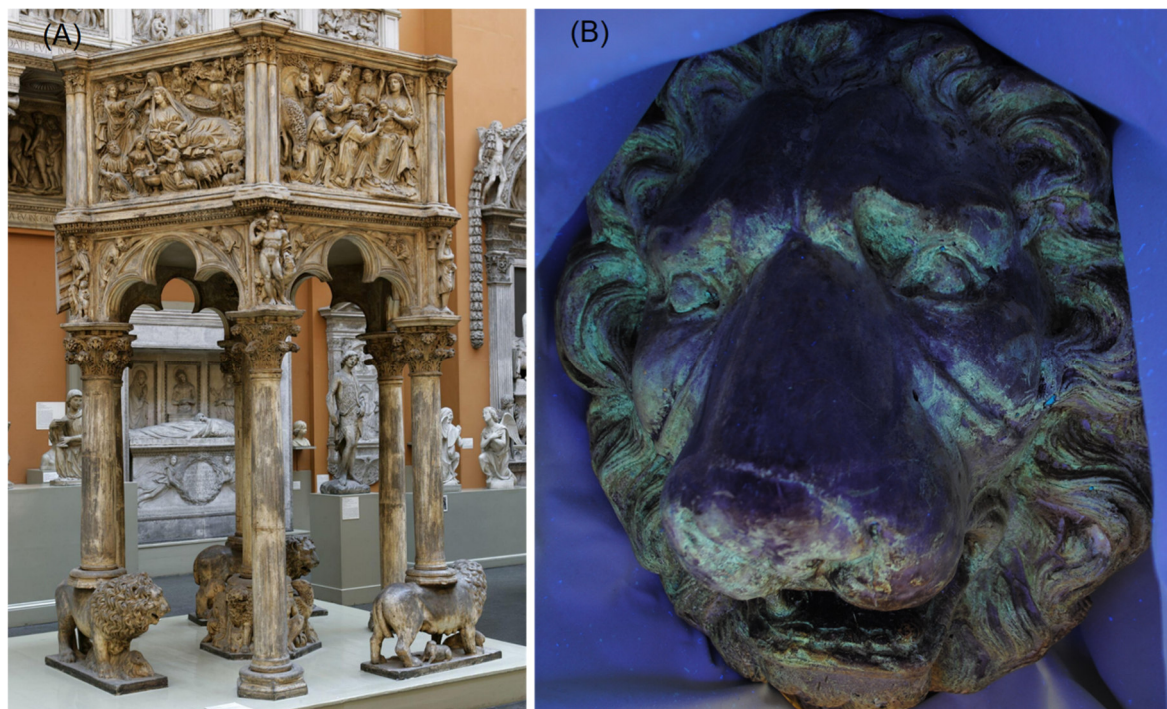


Figure 2.8. Observing details of the V&A plaster cast of the Pisano Pulpit (REPRO.1864-83) (A) with the aid of UV illumination allowed to identify areas that have characteristic fluorescence (B). © Victoria and Albert Museum, London/as specified by the rights holder.

Mapping and recording of the objects were made possible by AutoCAD® rendering. The main purposes of the photographic recording were to ensure that an image appropriate for the AutoCAD® rendering was available and that documentation of the condition of the area before and after the sampling was recorded. Digital documentation of cultural heritage can be pursued by following different methodologies (Ioannides *et al.*, 2018), either 2D or 3D or both: in this study, it was decided to have a 2D mapping of the objects, to reasonably fit the process to the purpose of the recording (mere mapping) and the time availability. The 3D rendering is also possible, but it was not considered necessary for this study. To achieve an appropriate image for the 2D rendering in AutoCAD® it is necessary to photograph the object in a way in which the camera is positioned in a 0° geometry (Ioannides *et al.*, 2018). It was decided to use Autodesk® AutoCAD® 2019 as it is familiar to the researcher but also considering its characteristics: AutoCAD® allows to transform a raster image, made of finite pixels in a vector drawing, where potentially each line is infinitely divisible. The nature of the software ensures a more accurate recording, given that the translation of the original object image is done by also shaping and scaling (Ioannides *et al.*, 2018).

The sampling strategy should always be determined by the question that the analysis aims to answer. As the sensitivity and precision of the analytical methods get even better, when samples need to be taken, the amount required becomes ever smaller. This is good news, but it does mean that there is an ever-increasing concern to ensure that the sample is representative and not contaminated. Possible changes in both structure and composition

in different locations on the surface of an object suggest that the examination of multiple samples is sensible (Sackler, 2005). Small fragments can be mounted as cross-sections and constitute one of the most valuable types of sample, allowing both compositional and structural studies (Ceroni & Elia, 2008; Craddock, 2009). The samples taken for this study were analysed both as they are and as cross-section (*Sections 4.2*).

Optical Microscopy (OM) is a quick method based on the interaction of light with a sample and can inform about the characteristics and structure of a sample. Magnification and resolution depend on the characteristics of the equipment (*Section 4.2.2.2*). A sample can be examined, as it is or cast in a material, with reflected light, transmitted light and via stereomicroscopy (Sandu *et al.*, 2015; Stuart, 2007). UVf microscopy allows investigating the microscopic appearance of a sample under ultraviolet illumination. This provides visual information on the fluorescence of the materials that, in some cases, is particularly distinctive, as is for the case of some varnishes. Due to superficial dirt and grime, fluorescence can be obscured significantly, and a lack of fluorescence does not necessarily indicate the absence of a varnish. Some materials do not fluoresce, including many synthetic resins and most acrylic paints (Pande *et al.*, 2012; Simpson-Grant, 2000).

In the case of coatings applied to a plaster substrate, the relationship between the bulk and the surface layer seems to be more intimate than observed in other museum objects materials (paint and varnish layers appear more well-defined when the substrate is made of canvas, metal or wood) (Carlyle *et al.*, 1995; Roberts, 1968). Historically, artisans have incorporated a large range of natural materials in adhesives, varnishes and the medium of paint layers. These include coniferous resins, seed oils, proteins such as animal glue and casein and plant gums (Sano *et al.*, 2014; Singer & McGuigan, 2007).

Salavessa *et al.* (2013) showed that EDS in conjunction with the images obtained by SEM constitute a great aid for the chemical analysis and the characterization of the crystalline structure of the elements present in *stucco* samples, and Ventolà *et al.* (2011) applied the same analytical technique for the study of mortar samples. In fact, by SEM-EDS it is possible to obtain the image of an object, generated using a beam of electrons, and elemental characterization of very small samples (Moropoulou *et al.*, 2019; Stuart, 2007). The BSE (Back-Scattered Electron) image allows the observation of samples with a great rate of resolution (depending on the surface characteristics and the equipment specifics) even at extremely high magnifications (which is not limited by the light wavelength as in OM) (Creagh & Bradley, 2000). BSE images show a contrast between elements of different atomic numbers (Z): in an SEM BSE image silver (Z=47), for example, appears brighter than lighter elements, such as silicon (Z=14), because more backscattered electrons are emitted from the sample surface in the first case. The High Vacuum mode is usually applied for smaller areas of observation, requires samples irreversible preparation by coating the

sample with conductive material (metals) and provide extremely detailed BSE. The Low Vacuum mode allows the navigation of larger areas of observation, partially sacrificing the definition of the BSE, but eventually allowing the observation of the full stratigraphy of the sample and enabling to keep the sample without the metal coat and therefore still observable under OM etc. (Creagh & Bradley, 2000).

Elemental analysis was performed by EDS and XRD analysis allowed to confirm the nature of crystalline compounds in the samples (Freire *et al.*, 2020; Janssens, 2004; Stuart, 2007). Salavessa *et al.* (2013) and Ventolà *et al.* (2011) proved the use of EDS and XRD to achieve mineralogical, morphological, microstructure and chemical characterization of *stucco* and mortar samples, respectively. Many studies focusing on the structural and compositional analysis of cultural heritage materials have proven the reliability of these techniques (Doménech-Carbó *et al.*, 2008; Kanngießner *et al.*, 2012; Moropoulou *et al.*, 1995). More detailed trace studies (Bianco, 2017; Mendoza Cuevas *et al.*, 2015; Nel *et al.*, 2010) demonstrate the capability of these techniques in the investigation of the provenance of the gypsum used to manufacture the cast. As the focus of the characterization of the V&A casts was mostly on the surface coating, the determination of the trace elements in the inorganic mineral bulk, as showed in Gariani *et al.* (2018), was not considered a priority. In that study, EDS and XRD allowed to provide confirmation of the casts' composition and also to highlight whether any trace element can be distinctively considered as a marker. By determining the distribution of the elements in the sample, through the mapping mode of the SEM/EDS equipment, however, it is possible to identify the presence of materials purposely added to the cast surface (such as pigmented coatings) or the presence of soiling (such as carbon black) or decay products (such as salts efflorescence) (Creagh & Bradley, 2000; Sackler, 2005).

Molecular analysis is the most useful technique when the aim is to characterise organic materials such as binders and varnishes. Some organic materials will undoubtedly be present, but their nature relative abundance can be very diverse. Many extremely sensitive organic analysis techniques exist, such as Fourier-transform infrared spectroscopy (FT-IR) and gas chromatography/mass spectrometry (GC/MS), which can be applied to the characterization of organic residues (Sackler, 2005). The application of such techniques of cultural heritage materials can be found in numerous studies (Aruga *et al.*, 1999; Doménech-Carbó *et al.*, 2008; Sotiropoulou *et al.*, 2018; Svečnjak *et al.*, 2015).

FT-IR is a non-destructive and fast method widely used for the characterization of organic and inorganic materials, allowing the determination of the type or class of material in a sample (resin, wax, bitumen, oil, proteinaceous material). The usefulness of the technique decreases with the complexity and increase of the number of materials in the sample. Binders, fillers and pigments may all be identified using FT-IR (Derrick *et al.*, 2000), but the

interpretation is often complex despite the availability of databases of spectra of cultural heritage materials (Price *et al.*, 2009). A low concentration of organic material within a mostly inorganic sample can make the interpretation of the FT-IR spectra quite challenging. This technique can be complemented with spectroscopic or chromatographic techniques (Azemard *et al.*, 2014). In this research, it was possible to undertake micro-FT-IR mapping and imaging in reflectance mode and attenuated total reflectance (ATR) (Section 4.2.2.4).

GC/MS is one of the most detailed techniques for the identification of organic material (Stuart, 2007). The output is a GC chromatogram that characterises components in terms of their retention times. The elution time can indicate the compound identity by comparison with a database of known compounds, but GC requires volatile compounds and there is no definitive proof of the nature of the separated component of the detected compounds. Identification is often based on retention time on the column, which is not necessarily unique for different compounds (Colombini & Modugno, 2009). MS is a powerful analytical tool able to perform qualitative and quantitative analyses on even a small quantity of samples. It is based on the creation of gas-phase ions and their separation in accordance with their mass-to-charge (m/z) ratios (Stroobant & De Hoffmann, 2001). A single GC/MS system can therefore separate mixtures into their components, isolate them and provide quantitative and qualitative information to help identification (Colombini & Modugno, 2009; Ribechini *et al.*, 2008). Usually, natural polymeric materials have commonly to be broken down into their individual 'building blocks' – fatty acids, sugars, amino acids or whatever – before subjecting these to separation procedures. Furthermore, these individual compounds are themselves not always suitable but need to be derivatized (Colombini & Modugno, 2009). Although GC/MS analytical procedures require a relatively long analysis time and a wet chemical pre-treatment of the samples, they are nowadays unmatched for molecular composition characterization (Aruga *et al.*, 1999; Sotiropoulou *et al.*, 2018; Wei *et al.*, 2013). Many applications of GC/MS to lipid characterization, including the study of lipid degradation processes reported in the conservation science literature (Mills, 1966; Sotiropoulou *et al.*, 2018). Identification and quantification of oils hydrolysed to fatty acids (FAs) is possible (Blasco-López *et al.*, 2015). Methyl esters and ethyl or 2-propyl esters are commonly used in routine lipid analyses. Alkylchloroformates alkylation is quick and can be performed in aqueous solutions; silylation is frequently employed for protein derivatization (Mills, 1966).

The use of pyrolysis and/or several chemical pre-treatments of the samples can be found in literature and are often necessary for correct identification of the sample's components, allowing appropriate separation and fragmentation without pre-treatment (Colombini & Modugno, 2009; Ribechini *et al.*, 2008). An appropriate derivatising agent is necessary for the pyrolysis of glycerolipid materials, to enhance the detectability of FA and dicarboxylic acids, which may appear in an aged paint film as metal soaps, free acids, and esterified with glycerol. The oils and fats usually employed in cultural heritage samples have been

analysed using pyrolysis using tetramethylammonium hydroxide (TMAH), and hexamethyldisilazane (HMDS) by Colombini & Modugno (2009) and Singer & McGuigan (2007). High-performance liquid chromatography (HPLC) (Halpine, 1992) and GC/MS methods involving ethyl chloroformate derivatives of amino acids (Schilling & Khanjian, 1996) have been used for the testing of proteinaceous artists media. Nowik (1995) reported a GC method for the simultaneous analysis of both amino acids and fatty acids which may occur together in mixed paint media and egg tempera. Acid hydrolysis was followed by neutralisation, treatment with ethanol in pyridine and ethyl chloroformate producing both the ethyl esters of fatty acids and the N-(O, S)-ethoxycarbonyl ethyl ester derivatives of the amino acids. The use of t-butyl-dimethyl silyl derivatives (TBDMS) for the simultaneous detection of fatty acids, amino acids and glycerol is reported by Colombini & Modugno (2009) and Šimek *et al.* (1994). GC/MS analysis of amino acids has also been performed with the esterification of the carboxylic acid group as the methyl, n-propyl, isopropyl or n-butyl ester followed by N-acylation with acetyl, trifluoroacetyl or pentafluoro propionyl groups. The use of N-trifluoroacetyl methyl esters is reported by White (1984), N-trifluoroacetyl n-butyl esters by Kenndler *et al.* (1992) and N-trifluoroacetyl n-propyl esters by Aruga *et al.* (1999). In situ thermally assisted methylation with TMAH has been established for the analysis of phenols, carboxylic acids and amines. By mixing the sample with the TMAH solution and evaporating the water, TMA salts are produced, which decompose at higher temperatures to generate phenols, methylated acids and side products due to the decomposition of TMAH. Challinor (2001) reported the hydrolysis and methylation of hydrolysable polymeric material and Anderson & Winans (1991) concluded that this approach is effective for the analysis of diterpenoid acids, but less so for their oxidised derivatives, containing additional carbonyl and/or hydroxyl groups. For these compounds, the interpretation of the results is complicated by the occurrence of side reactions such as eliminations and incorporation of nitrogen. Thermally assisted methylation combined with pyrolysis is valuable for the analysis of small and complex samples, being time-saving and more consistent and sensitive than wet chemical techniques (Pastorova *et al.*, 1997).

In this study, the analysis was performed either by GC/MS or py-GC/MS. Pre-treatment of the samples was achieved through methylation with TMAH and/or with 3-trifluoromethylphenyltrimethylammonium hydroxide and derivatization with *n*-propanol followed by pentafluoro propionic anhydride (PFPA). Pyrolysis and GC/MS data interpretation are based on the evaluation of both molecular markers and chromatographic profiles. Interpreting pyrograms, chromatograms and mass-spectra is complicated and requires experience. The simultaneous incidence of multiple materials in the sample, both organic and inorganic, can impact the formation of the final pyrolysis products, affecting marker formation, chromatographic profiles and also the derivatisation outcome (Colombini & Modugno, 2009). Details on the experimental setting and samples preparation are given in *Section 4.2*.

2.4. SURFACE RECONSTRUCTIONS AND CLEANING TRIALS

Ageing and degradation are always complex processes consisting of multiple reactions and this is especially true if the material is not a pure compound. The characteristics of the objects are crucial in their deterioration and affect the way the environment must be controlled in the museum (Cassar, 1994). Photochemical reactions drive most of the changes that occur on the surface of the objects, due to ageing. A broad classification based on the materials' sensitivity to light can guide the preventive conservator, but it must not be assumed that what is perceived as the same group of objects will degrade equally in the same conditions. For example, for the case of plaster cast, as it is demonstrated in *Chapter 3*, the great variety of materials used for the manufacturing of these objects must suggest great care in deciding the conditions these objects should be kept in. Once again, materials research, including characterization and reconstructions research, provides background information for the case-by-case decision making of the preventive conservator. Salavessa *et al.* (2013), Freire-Lista *et al.* (2015) and Freire *et al.* (2020), amongst many others, demonstrated the effectiveness of reconstruction research for the understanding of the materials properties and deterioration processes. For such research to be as meaningful as possible, it is necessary to recreate a stratigraphy as similar as possible to the one of the objects subject of the study, including the component materials, their ageing and deposited dirt and grime, if present.

The accelerated ageing tests are carried out for three major purposes: to classify materials according to their chemical stability in a conveniently short time, to estimate optimal periods of intervention and preservation - under expected conditions of use or display, and to investigate processes of deterioration (Feller, 1994). The latter aims to understand the chemical reactions or "mechanism" of the degradation and its physical consequences. These purposes ensure the appropriate understanding of the materials' behaviour under specified conditions, which can guide the conservator on the case-by-case choices of care and treatment. Moreover, by performing cleaning trials on the aged reconstructions, recommendations for the care of the objects can be given and the effectiveness of treatments can be evaluated (Wolbers, 1992). The objective of making reconstructions is, therefore, to recreate, as close as possible, the 'real' scenario, including the material composition, as well as the changes that occurred due to the environmental conditions it was kept throughout its life (see for example the thorough review carried by Gold (1994) on bismuth painting).

Reconstruction research can also be used to see whether and how a recipe or technique, described in the technical literature, works and can provide knowledge to support researchers in understanding its applications. By comparison with the results from the characterization of the materials on real objects, it is possible to confirm similarities and

differences in the manufacturing along the periods and within the countries and the workshops. Fritz (1999), for example, demonstrated the opportunities of studying literature and scientific evidence to recreate Magdalenian manufacturing techniques. Research using such methodology was widely explored for paintings (Burnstock & van den Berg, 2014; Galatis *et al.*, 2012; Sano *et al.*, 2014), but less so for other artistic practices.

The methodological approach to the making of accurate historical reconstructions included the production of plain plaster substrates, the application of coatings, as suggested by the historical sources and the results of the V&A casts, their accelerated ageing and artificial soiling (*Chapter 5*). A novel cleaning approach was selected for the removal of soil from the surfaces of the plaster reconstructions (*Chapter 6*). The assessment of the effects of the accelerated ageing and the effectiveness of the cleaning technique was carried by visual evaluation according to EN ISO 4628-1, visible light and ultraviolet fluorescence photography, electron microscopy (SEM), weight measurements (gravimetry), colourimetry (Colour coordinates L, a, b, ΔE), glossimetry and goniometry, elemental analysis (EDS), transmittance, absorbance, and reflectance (FT-IR) and high-resolution (HR) 3D surface measurements.

2.4.1. ACCELERATED AGEING

Accelerated ageing in the laboratory allows obtaining the information required within a much shorter time frame than natural ageing. The test processes and the interpretation of the results must be conceived thoughtfully (Jelle, 2012). It is important to consider the real correlation between the accelerated ageing test's conditions and the museum object's environment for the material being tested. No laboratory test can be specified as a total simulation of real conditions (BS EN ISO 16474-1:2013, BS EN ISO 16474-2:2013) and every accelerated ageing method must be considered an approximated model.

The mutual interaction of the different degradation mechanisms is one of the main reasons why accelerated ageing cannot accurately represent a real-life scenario. The effects and dynamics of one or more of these processes can however be observed in the laboratory. The scale of intrinsic stability to be defined in the cultural heritage materials is so great that no unique accelerated-ageing test method is likely to be efficient. There is a large variety of test procedures that can help rank the relative stability of carefully characterized materials or surrogate systems under the conditions of the test (Feller, 1994). The ageing occurring on a museum object itself can cover a wide range of conditions (for example ageing while on display can be extremely different from ageing in storage), which therefore influence the setting of the accelerated ageing. These concepts and other parameters specified in the next paragraphs and *Appendix 8* are the basis for accelerated ageing. An understanding of

some fundamental principles is important to describe critical aspects of deterioration. The two basic approaches to accelerated ageing are: to attempt to simulate the deterioration of a real object by recreating a specific set of environmental conditions over a specific time or to exaggerate the conditions to induce a specific reaction or decay (Erhardt & Mecklenburg, 1995; Luxford & Thickett, 2011). For example, to obtain specific types of decay, accelerated ageing tests can be performed in terms of freezing/thawing cycles along with wetting/dry cycles (Freire-Lista *et al.*, 2015); these do not fit into the purpose of this study, being these more representative of outdoor ageing. In other studies, accelerated ageing was used as a tool for dating objects (Chiriu *et al.*, 2018).

The objects that the reconstructions in this research aim to reproduce are inspired by the selection of V&A objects analysed for this study (*Section 2.3.1*): they are plaster casts produced in the last decades of the nineteenth century, coated in some way straight after the casting process and aged in the V&A cast galleries for about 150 years. The objects present a layer of dust and soiling, and the possibility of the objects being coated again during the 1920s in the Museum should be also ideally recreated. To achieve such reconstructions (or mock-ups) decisions should be made in terms of materials, approximations, methodology and parameters for accelerated ageing and artificial soiling. By estimating and researching the natural events and conditions in which the object was kept, it is possible to define the experimental conditions for the making of the reproductions and their artificial soiling and accelerated ageing. It is also important to define what kind of environmental conditions the experiment aims to reproduce (galleries or outdoor) and what are the conditions that cannot be recreated (i.e., unpredictable, or unknown events and as such). Examples of such an approach can be found in Pentzien *et al.* (2011), Sano *et al.* (2014) and Willneff *et al.* (2014). As for the purposes of this research, only humidity, temperature and light will be considered.

The measure of the acceleration is given by the acceleration factor (AF). This factor is practically used to define the relationship between the conditions and time of ageing in the 'real scenario' and those in the laboratory. This factor cannot be 'arbitrarily assigned' relating some hours or mega joules of radiant exposure in thermal, weathering or irradiation chamber to the amount of time of actual exposure. Acceleration factors depend significantly on the materials but are also related to the equipment: for instance, light acceleration factors calculated on the ratio of irradiance between a laboratory light source and solar radiation do not account for the effects of moisture, temperature and differences in spectral power distribution between the light sources (BS EN ISO 16474-1:2013). The duration of the test can be set either by calculating the time necessary for the surfaces of the test panels to be subjected to an agreed radiant exposure or by fulfilling an agreed or specified ageing criterion (BS EN ISO 16474-1:2013). Many accelerated-ageing tests continuously expose samples to emission, but exposure under natural conditions is subjected to daylight and

darkness cycles. Continuous exposure or alternating conditions could cause different results, and this aspect has not been extensively investigated (Feller, 1994).

As mentioned above, degradation and ageing processes influence each other's, suggesting that AF_{total} should be the results of several interdependent factors, humidity, temperature, and light in this experiment. In other studies (Jelle, 2012), and especially when weathering chambers that can provide simultaneous UV and thermal ageing are used, this must be taken into consideration. In this study, however, UV and thermal ageing were carried into two different apparatus (*Section 5.2.1.3*), allowing to approximate the two parameters (AF_T and AF_{UV}) as independent. These calculations are of course a strong simplification (*Appendix 8*).

Due to the mechanical characteristics and the chemical composition of the plaster mock-ups prepared for this study, which are highly hygroscopic, the humidity level was kept constant throughout the accelerated ageing and matched to the average relative humidity RH% in the galleries (RH= 43.2%). *Table 2.3* shows the mean data of humidity as recorded in the Cast Courts (see details in *Appendix 7*). The relative humidity of the outside air in the UK tends to average around 80% in winter and 70% in summer. The control of the humidity in the galleries is paramount, and the specified value is normally set at $54\pm 4\%$ RH (Cassar, 1994). Moreover, the effect of moisture in deterioration is difficult to foresee as related to each particular situation. In most of the ageing studied the effects of water seemed to have been monitored, rather than investigated, and it was not possible to find a reliable model for the effect of RH during accelerated ageing (Camuffo & Bertolin, 2012). Feller (1994) reports examples in which the degree of deterioration is directly comparable with the equilibrium concentration of water and other cases in which moisture has little consequence. The hydrolysis of molecular bonds was believed to be the main course of degradation in a polymer, but in some cases, it did not occur in the absence of oxygen (Feller, 1994). This variety of modes of action suggested that the role of moisture in deterioration continues to be far from being understood. *Table 2.3* also shows the mean values of temperature recorded in the Cast Court ($T= 21.52^\circ\text{C}$, *Appendix 7*), which will be set as the reference value for the model of accelerated thermal ageing as described in *Section 5.2* and *Appendix 8*.

Table 2.3. Average values recorded by five sensors located in Galleries 46, 46A and 46B.

No. of sensors	Temperature			Humidity			Time within limits %		
	Mean	Min	Max	Mean	Min	Max	Temperature	Humidity	Overall
5	21.52	14	30.54	43.2	18.2	69.6	67	65.6	43

Data was recorded over a period of 5 years (00:00 25 October 2014 to 00:00 25 October 2019). Temperature in °C and Humidity in RH%.

As for the radiation, aiming to perform reliable and reproducible experiments in this study, it was decided to calculate all the dimensions related to light in terms of radiometry⁴¹ instead of photometry (Oleari, 1998). *Equations 2.1* and *2.2* show, for example, the definitions and conversion between irradiance and illuminance.

$$\text{Irradiance [W/m}^2\text{]} \qquad E_e = \frac{dP_e}{dA} \qquad (2.1)$$

↕

$$\text{Illuminance [lux], [lm/ m}^2\text{]} \qquad E_v = k_m \int_{380}^{780} E_{e,\lambda} V(\lambda) d\lambda \qquad (2.2)$$

where P_e is the radiant flux, A is the area, K_m is constant and equal to 683 lm/W and $V(\lambda)$ is the function of relative spectral luminous efficiency, between the limits of 380 and 780 nm (visible range of the spectrum).

Indoor lighting is traditionally measured in lux and Thomson (2013) defined the traditionally accepted target values of 50 lux for sensitive items and 200 lux for less sensitive items in the museum. Lux units are defined on the Photopic Response Curve $V(\lambda)$, a standardized measure of the human eye's response to light, specified by a unit of illuminance equal to one lumen per square meter (equivalent to 0.093 footcandles). The Curve is a bell-shaped curve that is centred at 555 nm and extends from approximately 400 nm to 700 nm. Relative light levels and relative efficiency of various light sources can be correlated and compared only for purposes of human vision, not for photodegradation. Therefore, the theory of radiometry is considered here a more suitable tool to describe materials ageing processes (Oleari, 1998; Pritchard, 1995).⁴²

Theoretically and besides the specific responses at different wavelengths, the shorter wavelengths are the more potentially damaging. This is formally expressed by the relationship that inversely relates the logarithm of the induced damage to the wavelength - suggested in the 1950s by the U.S. National Bureau of Standards (Harrison, 1961). In terms of the threshold for photochemical damage initiation, which is potentially the most important piece of information for museum professionals, it has been observed that above a certain

⁴¹ The irradiance is the radiant flux incident on a surface per unit area (W/m^2), the spectral irradiance is the irradiance as a function of the wavelength ($\text{W/m}^2 \cdot \text{nm}$), the radiant exposure is time integral of irradiance (J/m^2) and the spectral radiant exposure is the radiant exposure as a function of wavelength ($\text{J/m}^2 \cdot \text{nm}$).

⁴² Several photography test standards specify the use of lux as a means to time radiant dosage. A more appropriate measurement would be to use radiant energy measured in an appropriate spectral region, typically in watts per square meter (W/m^2).

wavelength numerous reactions will not be induced. Theoretically, there is no minimum of intensity (or exposure, i.e., intensity times time) that would determine the end of a photochemical process. UVB ultraviolet radiation, 280 to 315 nm (which is not significantly transmitted by ordinary window glass) has been proven capable of inducing reactions that are different from those that known to occur under ordinary museum conditions (Feller, 1994). Hence, wavelengths equal and below these values should be avoided in most accelerated photochemical testing that aims to reproduce indoor museum conditions. Such settings will rarely have relevance to conservation (Feller, 1994).

Indoor irradiance typically comprises a mixture of artificial light originating from different light sources, such as fluorescent lamps, incandescent lamps, and LEDs, and sunlight that enters through windows and skylights (Müller *et al.*, 2009). Müller *et al.* (2009) have conducted extensive research on the measurement of indoor irradiance, reporting that though indoor irradiance can exceed 500 W/m², 1–10 W/m² are the average orders of magnitude (0.1 W/m² represents the worst-case scenarios in the winter without the use of artificial light). Solar radiation constitutes the major component for surfaces orientated to the window, and for surfaces orientated to the artificial light, the latter will contribute most of the radiation, proportionally to the distance from the source. Sunlight spectral range of irradiance is from 300 up to 4000 nm, whereas the spectral distributions of artificial light are narrower and characteristic of the type of artificial lighting - incandescent lamps have a spectral range of 350 up to 2500 nm, LEDs from 400 up to 800 nm, and fluorescent lamps from 300 up to 750 nm.

The illumination in the Cast Courts is different from anywhere else in the V&A. Due to the complex lighting setting in the Cast Courts, light exposure measurements are not recorded in these galleries, therefore we do not have an exact target reference exposition for the accelerated ageing. The light is coming from multiple sources, natural light⁴³ from the skylight windows and artificial lighting consisting of multiple types of lamps,⁴⁴ such as tungsten and LED. The two sources contribute to the direct and diffused light level at the surface of the object in a gallery (McGlinchey, 1994). All the above considered and not having the possibility of recording the exposure for a meaningful amount of time during this

⁴³ Natural light sources include direct sunlight and indirect (diffuse) sunlight. The CIE (International Commission on Illumination) provides a standard definition of direct sunlight in publication 85, table 4 (1989). This is equivalent to noon, summer sunlight in the Northern Hemisphere. This is also known as Air Mass 1. Numerous ISO and ASTM committees have incorporated this sunlight benchmark in their test methods and specifications. Pleijel, G. (1951) *Daylight in central urban areas*. calculated the yearly average luminous efficacy which was 112 lm/W for the horizontal global radiation. Littlefair, P. J. (1985) 'The luminous efficacy of daylight: a review', *Lighting Research & Technology*, 17(4), pp. 162-182. made a thorough review of the luminous efficacy measurements made during 1955–1984. In most studies, the global luminous efficacy was between 100 and 115 lm/W Vartiainen, E. (2000) 'A comparison of luminous efficacy models with illuminance and irradiance measurements', *Renewable Energy*, 20(3), pp. 265-277..

⁴⁴ Personal communication with Bhavesh Shah, Scientist (Environment) at the V&A. Artificial illumination is currently being changed into LED as to follow standard recommendations.

research, it was decided to use as reference literature data, critically reviewed and adapted to the lighting conditions in the Cast Courts (Littlefair, 1985; Oleari, 1998; Pritchard, 1995).

Theoretically, the irradiance arriving onto the surface of the casts consists in the cumulative contribution of the irradiance of the daylight filtered by a window⁴⁵ (Littlefair, 1985) and the one arriving from the artificial lighting. Comparison between man-made light sources and sunlight filtered through window glass can be found in Quill *et al.* (2004). The radiation emitted from the artificial lighting usually employed in an indoor environment (e.g. tungsten lamps 60-120 W) is significantly lower than the irradiance of sunlight through a window unless the artificial source of light is significantly close to the objects (Oleari, 1998).⁴⁶ It would therefore be possible to approximate the cumulative irradiance equal to the one through the skylights, especially in consideration of the massive skylight in the Cast Courts (Figure 2.9).



Figure 2.9. The Weston Cast Court at the V&A. The massive skylight windows are the major source of light. © Victoria and Albert Museum, London/as specified by the rights holder.

⁴⁵ Window-filtered Sunlight. The shortest of the UV wavelengths are filtered out by window glass and the solar cut off shifts from approximately 295 nm to about 310 nm. Glass that is dirty, thicker, tinted, laminated, or double pane would have even less UV transmission.

⁴⁶ According to the *inverse square law* irradiance is proportional to the intensity I_e inversely proportional to the square of the distance r^2 between the source and the illuminated object, $E_e = I_e/r^2$

Pritchard (1995) demonstrated that the levels of diffuse lighting through windows are also affected by numerous factors, including the shape and dimension of the room, the reflectance of the walls and the presence and reflectance of objects in the room. This value would also be dependent on the position of the target within the room. As the aim of this work is not to design the lighting of the spaces but to approximate the overall radiant exposure in the galleries over a long period, it appears not only easier but also statistically more correct, to provide an average estimation. Long-term data collection is undoubtedly the most accurate and effective approach for setting up reliable databases of daylight illuminance. Measured data can comprise global and diffuse illuminance on a horizontal surface, vertical daylight illuminance facing the four cardinal orientations and sky luminance distributions. For daylighting applications, diffuse illuminance is more important and widely considered and direct sunlight is often excluded (Li, 2010). The distance of the skylight (25 m high) for the floor and its dimension provides diffuse light into the galleries (*Figure 2.9*).

Figure 2.10 shows the Global Horizontal Irradiation (GHI) map for the UK. The Horizontal rather than the Normal Irradiation was used as a reference because the GHI considers the scattering (Pritchard, 1995). The map presents the data of sunlight irradiation arriving on earth in terms of the average daily/yearly sum of GHI covering a period of 25 recent years (1994-2018). The uncertainty in the yearly GHI value is a result of limited potential for regional model validation, due to a lack of high-quality ground measurement data, which is estimated to vary regionally from 4% to 6% approximately.

In London, the yearly sum is 1022 kWh/m² and the daily is 2.8 kWh/m². This value does not consider the presence of the window glass, which is opaque for long-wave infrared radiation and transmits about 90% of the UV and visible light, depending on the characteristics of the glass (Berardi, 2019; Pritchard, 1995). The yearly GHI 1022 kWh/m² should be therefore reduced by about 10%, but it was decided to refer to the overestimated value as the rest of the approximations underestimated the contribution of the reflectance within the room and of the artificial lighting. The total irradiance that is ideally aimed for this ageing experiment is therefore 117 W/m² average annual irradiance. Details on the ageing equipment are provided in *Section 5.2.3* and the calculations related to the physical models defined for the experiments are given in *Appendix 8*.

SOLAR RESOURCE MAP

**GLOBAL
HORIZONTAL
IRRADIATION**
**UNITED
KINGDOM**



DESCRIPTION
This solar resource map provides a summary of the estimated solar resource available for power generation and use in the United Kingdom. It is based on the average daily (hourly) solar radiation data for the period 1950-2015. The underlying solar resource data was obtained from the European Centre for Medium-Range Weather Forecasts (ECMWF) reanalysis data. The effective solar resource is presented at a spatial resolution of 250 m.
There is some uncertainty in the year 2015 data, due to the limited availability of high quality ground measurement data, which is addressed by the use of regional climate model (RCM) data. The underlying solar resource data is presented in the form of a global solar resource map, which is available for all countries and regions. The map was last updated by SolarGIS, under contract to the World Bank, based on solar resource data from SolarGIS and other sources.
For more information, please visit: <http://globalatlas.info>

ABOUT
The World Bank Group has published this solar resource map using data from the Global Solar Atlas (GSA), the largest and most up-to-date map of solar power in our planet. This work is licensed by the World Bank Group under a Creative Commons Attribution-NonCommercial-ShareAlike license. It is part of a global initiative to promote renewable energy and sustainable development. The map was last updated by SolarGIS, under contract to the World Bank, based on solar resource data from SolarGIS and other sources.
For more information, please visit: <http://globalatlas.info>

DISCLAIMER
The World Bank Group and the World Bank Group's member institutions do not warrant the accuracy, completeness, or timeliness of the information contained in this map. The information is provided for general informational purposes only and should not be used for any specific purpose. The World Bank Group and the World Bank Group's member institutions are not responsible for any errors or omissions in this map. The information is provided as is, without any warranty of any kind, express or implied, including but not limited to the accuracy, completeness, or timeliness of the information. The World Bank Group and the World Bank Group's member institutions are not responsible for any damages, including but not limited to, direct, indirect, or consequential damages, arising from the use of this map. The information is provided for general informational purposes only and should not be used for any specific purpose. The World Bank Group and the World Bank Group's member institutions are not responsible for any errors or omissions in this map. The information is provided as is, without any warranty of any kind, express or implied, including but not limited to the accuracy, completeness, or timeliness of the information. The World Bank Group and the World Bank Group's member institutions are not responsible for any damages, including but not limited to, direct, indirect, or consequential damages, arising from the use of this map.

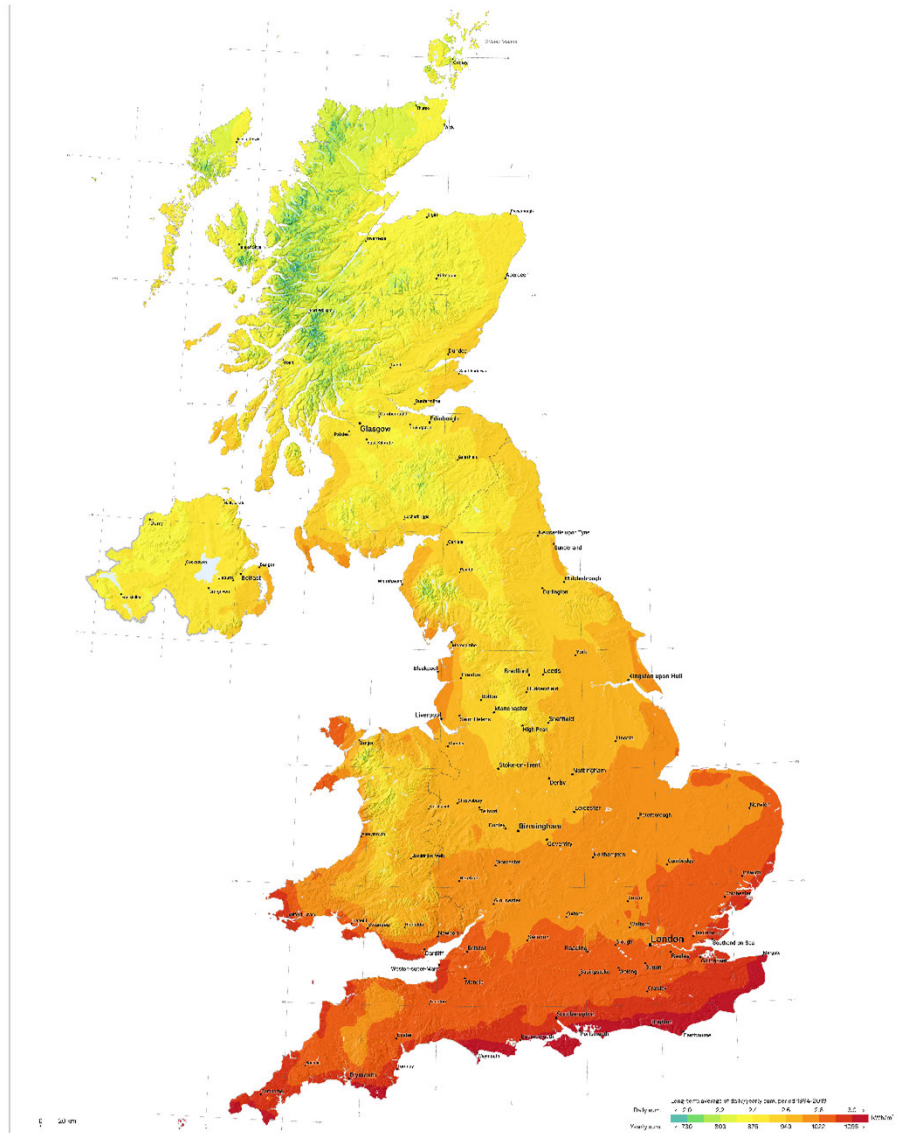


Figure 2.10. Global Horizontal Irradiation map for the UK. © 2019 The World Bank, Source: Global Solar Atlas 2.0, Solar resource data: SolarGIS.

2.4.2. ARTIFICIAL SOILING

In previous experiments carried out in the conservation department at the Victoria and Albert Museum, different methods for artificial soiling were applied and observed. For instance, the pigment lampblack was used, and lard was rubbed onto the surface to create handling grease or grease from burning by-products (Coon, 2009) and Ashrae standard test dust (Batch No4003, a complex mix of mineral/carbon/fibres) was also used (Jones, 2011). For this work, it was decided to apply a soiling mixture produced according to published protocols (Florio & Mersereau, 1955; Getchell, 1955; Wolbers, 1992). The mixture and method described in Galatis *et al.* (2012) was selected to mimic the dust and dirt that inevitably deposit onto the objects' surfaces, as well as the greases carried by visitors and due to historic illumination - candles and as such (Grau-Bové & Strlič, 2013), and more details are available in Section 5.2.5. It is also rather important to define the calculation

method employed to estimate acceleration factors use for the accelerated ageing, to define the experimental parameters and to estimate the required ageing time in the ageing apparatus. Details on the soiling and the experimental parameters set for the accelerated ageing are provided in *Section 5.2.1*.

2.4.3. CLEANING TRIALS

Cleaning in conservation should be generally performed following methods fully tested on the specific material to be treated. Preliminary testing in the laboratory is not always feasible, due to the close deadlines and lack of appropriate analytical equipment. In situ cleaning trials are often the easiest choice. Usually, the most suitable treatment or cleaning procedure for a single object is determined based on the experience of conservators as well as on previous similar works and studies. Objects that have deposits that contain historical information can raise the question of whether it is appropriate to remove them with conservation cleaning procedures. Moreover, a dirt layer could in some way protect the object. Beale *et al.* (1977) suggest that superficial dust and grime can be removed from surfaces with a vacuum and a soft brush and imply that if a coating is suspected, solvent tests must be carried out to determine solubility and possibly to classify or identify the coating material.

When designing surface cleaning of an art object, observation and analysis of the object to understand the materials used to create it and the nature of the soiling on the surface are typically the first steps before treatment. This knowledge supports in planning the cleaning procedure used in the treatment. In circumstances where the characteristics of the soiling and/or the texture and consistency of the object's surface are complex, it can also be crucial to elaborate a method to monitor and measure the efficacy and degree of cleaning of the surface (Wolbers & Little, 2007). Cleaning treatments can be classified based on their principles of interaction with the substrate. They can be grouped into dry methods (mechanical) and wet methods (aqueous and non-aqueous). The cleaning of plasterworks can often be complicated by the presence of surface materials, originating from moulding, patinas and historical or modern treatments. The complexity of the composition and the variety of the materials in use during the moulding and finishing procedures and their mixture prevent the unambiguous interpretation of the alterations (*Chapter 3*). The complexity of the stratigraphy of the plaster casts is due to the porosity of the bulk but also to the procedures of moulding and casting that implies the use of release agents and/or sealants. An introduction to the cleaning approaches as found in the literature can be found in *Section 6.1*.

The objective of performing a cleaning test is to assess the interaction of different cleaning methods and possibly different concentrations (in the case of the use of solvents). The test will enlighten on the depth of the cleaning, the effect on the chromatic characteristics and gloss of the surface layer (Massa & Scicolone, 1991). It is widely accepted that every object of art is a *unicum* from a material perspective. The knowledge and the investigation of the materials will help to define and forecast the modalities of intervention.

During the refurbishment of the Cast Courts (Graepler & Ruppel, 2019; Hubbard, 2015), the removal of dirt from the casts on open display was of particular importance because over the years dirt contributed to the degradation of the surfaces. In the Cast Court refurbishment, for example, before cleaning, small tests were carried out to select the appropriate method. The aim is to remove all the dirt, which has often had become ingrained in the pores of the plaster and trying to remove that, could cause damage to the surface (Hubbard, 2015). According to Hubbard (2015), the selected cleaning techniques took several factors into account including the nature of the plaster substrate (absorbent, porous, fragile and brittle material that is slightly soluble in water), the variety of the coatings on the surface, and their aged nature (which can include partial breakdown and partial or complete loss, and their success at creating a seal on the surface), the presence of later restorations (including consolidation materials and or coatings, which may be partial or total on the surface) and the lack of clear identification of the surface layer(s), relying on solubility tests, microscopy, UV light and empirical observations to aid selection of cleaning materials.

The cleaning techniques have included dry cleaning methods, which are based around the movement of soft dry materials over the surface, where the coating or plaster layer are stable enough to permit such contact. The materials include soft-hair brushes with a vacuum cleaner, PVC sponges, vulcanised rubber sponges, microfibre cloth, phthalate- and latex-free erasers.

Wet techniques have included the application of solvents to the surface on rolled swabs of cotton wool, in a variety of mixtures, depending on the nature of the unwanted material and the solubility and stability of the surface, and the aim is to remove dirt and leave the surface coatings in place. The range of solvents can include white spirit, ethanol, acetone, isopropyl alcohol, water; these may be used on their own or as mixtures, or one followed by another. The treatment relies on the swab not being too wet and being rolled to pick up dirt then changed for a clean one.

Poulticing techniques have relied on the liquid content being held at the surface by a gelling agent or binder including methylcellulose, agar-agar, and latex, or on capillary action of materials such as cellulose pulp. The liquid is held at the surface for a measured time to soften the dirt, which is either absorbed into the poultice or wiped away by another material, such as a swab, sponge or microfibre. The efficacy of this method relies on the appropriate

selection of solvent, but also on the ability of the poulticing medium to retain the solvent at the level of the dirt without it being drawn into the substrate.

Laser (q-switched Nd YAG) has been effectively used on plasters that do not have sealant coatings, as found in the literature (Cerea *et al.*, 2017; Pelosi *et al.*, 2013). Cleaning of plaster often involves more than one technique and can require partial consolidation as part of the process. In this study, it was decided to experiment with a novel cleaning technique (*Section 6.1*), to define an assessment methodology for the cleaning of the plaster casts coated surfaces, rather than assess the efficacy of selected cleaning techniques onto particular surfaces. While defining the assessment methodology, the efficacy of the novel technique on coated plaster surfaces will be experimented too.

Freese *et al.* (2020) have developed a thin hydrogel coating on a flexible polyolefin backing to bring a controlled amount of liquid onto the surface during the cleaning treatment. Surfactant monomers were copolymerized with hydrophilic monomers to ensure covalent immobilization of the amphiphilic species in the hydrogel network, preventing their leaching during the cleaning procedure. These incorporated surfactant moieties are expected to perform like the free surfactant micelles based on the documented hydrophobic aggregation of apolar groups in hydrophilic polymers. Such Polyolefin-Supported Hydrogels have been so far experimented onto painting surfaces and were the supports selected for the application of appropriate solution for the cleaning of the soiled surface reconstruction object of this study (*Chapter 6*).

2.4.4. ASSESSING AGEING AND CLEANING

The methodology described so far gathers its relevance in terms of knowledge for conservators and researchers once the desired outcomes and method of assessment are thoroughly explained. The effects of ageing and subsequent cleaning can theoretically be assessed by following the same protocol but keeping in mind what is acceptable in terms of changes (of appearance and/or properties) after ageing and after cleaning. Apart from the ethical considerations, the efficacy of a cleaning technique can be assessed *in situ* by the conservators through cleaning tests. However, the assessment of the efficacy of cleaning techniques in the science lab is a way to reduce the possibilities available to the conservator, by providing experimental information on the effects of solvents and cleaning techniques on selected materials.

What is desired from a cleaning treatment is for it to be: controllable at every stage, highly effective in the removal of undesired deposits, selective, gradable, and completely considerate of the substrate. Nowadays, cleaning procedures that are proven to be harmless to the environment and the operators are particularly and rightly appreciated

(Price & Doehne, 2011). The choice of the most suitable cleaning methodology should follow the detailed understanding of the substrate characteristics, including the stratigraphy, the constituent materials, and the presence of non-original materials due to conservation and later interventions. The chemical composition of the materials to be removed, the thickness of overlapped layers, the depth of penetration of deposits and the adhesion to the substrate should also be taken into consideration (Gulotta *et al.*, 2014).

The need for a robust analytical methodology to assess ageing and conservation interventions using well-defined performance criteria is emphasised in the literature (Delegou *et al.*, 2018; Rodrigues & Grossi, 2007; Vergès-Belmin, 1996). The effectiveness of a cleaning technique is often subjectively assessed, although a range of objective procedures has been described by many authors (Andrew *et al.*, 1994; Vergès-Belmin, 1996; Werner & Schmitz, 1973; Young & Urquhart, 1992). This is both inevitable and understandable since individual researchers are constrained by the range of techniques that are available to them and the case-by-case demands can widely diverge. Having access to a variety of techniques also has the benefit that the methodology can be customised to suit a specific object and environment (Huertos & León, 1994).

For example, Wolbers & Little (2007) during the conservation of the busts of du Pont de Nemours and Madame Du Pont belonging to the Winterthur Collection assessed the cleaning by measuring the pH, the conductivity and the viscosity of the cleaning solutions. Domínguez (2013), instead, carried observation with confocal microscopy and water vapour permeability tests, before and after the treatments with agar-agar. The objective was to determine morphological changes on the surface, porosity changes and the presence of residues and eventually suggest changes in the concentration and application time. Perusini *et al.* (2009) assessed the cleaning effectiveness of Agar and Laponite RD by OM observation, FT-IR and SEM/EDS onto plaster mock-ups and later tried the preferred cleaning methodology for the cleaning of the plaster cast models made by Antonio Carestiato in 1937 and by Luigi De Paoli in 1890. Salavessa *et al.* (2013) used XRD, EDS, mercury intrusion porosimetry (MIP), Brunauer–Emmet–Teller method (BET) and XRF analysis to assess the properties of the mortars. Melita *et al.* (2020) assessed the efficacy of laser cleaning on lime plaster surfaces by FT-IR and py-GC/MS.

It is unrealistic to imagine that any single method could fit all situations. Nonetheless, it is extremely difficult to evaluate and compare the findings of one researcher with those of another, and there is a need for standardized procedures. The choice of a conservation material/method is based on multiple parameters that mainly consider issues of compatibility between treatments and substrates; however, each application should be both laboratory- and pilot-tested on the scale of the historical work under investigation, to ensure that compatibility requirements are satisfied (Delegou *et al.*, 2018). One of the early

decisions that must be made in planning the assessment protocol is to decide the property to measure as an indication of the extent of ageing and cleaning. Unfortunately, with unfamiliar materials, it is usually not possible to decide in advance which chemical property will be most significant or revealing (Feller, 1994). Given the cultural heritage interest of the materials object of this study and the focus on the surface coating, it is clear that major attention will be given to the changes in the appearance of the surface, including colour, gloss, and roughness. Surface techniques for quantifying rates of decay and surface loss include the use of a micro-erosion meter, profilometry, close-range photogrammetry, laser scanning, and laser interferometry (Price & Doehne, 2011).

All the above considered, in this study, it was decided to combine visual and chemical evaluation parameters to assess the surface of the reconstructions after soiling and ageing and after the cleaning test. Visual assessment was possible via visual evaluation according to EN ISO 4628-1,⁴⁷ Visible light and Ultraviolet Fluorescence photography, scanning electron microscopy (SEM), colourimetry, glossimetry and goniometry (Colour coordinates L, a, b, ΔE , yellowing E313, etc.) and high-resolution 3D surface measurements. Gravimetry (weight measurements) was undertaken to assess the water loss during the experiments and FT-IR allowed to define molecular changes after ageing and the presence of residues after cleaning. Details on the equipment are available in *Section 5.2*.

⁴⁷ EN ISO 4628-1 describes a uniform convention for designating the quantity and size of defects and the intensity of changes by means of rating on a numerical scale ranging from 0 to 5, 0 denoting no defects or changes and 5 denoting changes or defects so severe that further discrimination is not reasonable. In addition to the ratings, the approximate dimensions of the area concerned shall be given, or the proportion of the area concerned compared with the total area, expressed as percentage. Carry out the first assessment under good illumination and without any magnification.

2.5. CONCLUSION

The *Research Methodology* of this work is based on an interdisciplinary approach for the study of the replica to ensure a better understanding of the many layers of information embedded in it. By combining the archival research, the characterization of the V&A plaster casts and the study of purpose-made reconstructions, a methodology for the study of the nineteenth-century coated plaster casts was defined. Seventeen manuals or historical books and fourteen patents focused on plaster casting or in some way related to this technology were selected to be reviewed for this study. A multi-analytical approach was selected for the scientific examination of the surfaces of the V&A casts. The methodological approach for the making of accurate historical reconstructions included the production of plaster substrates, the application of coatings, as suggested by the historical sources and the results of the analysis of the V&A casts, their accelerated ageing and artificial soiling. The study of the reconstructions aimed to highlight the coated plaster characteristics and changes upon ageing, to be used as a reference for future studies on the surfaces of historical plaster casts. A novel cleaning approach was experimented for the removal of soil on the plaster surfaces reproductions. The assessment of the effects of accelerated ageing and the effectiveness of the cleaning technique is expected to allow the understanding of the ageing effects of the selected materials and to define whether the novel cleaning approach is appropriate for these materials. This methodology was designed to improve the knowledge of the materials and the techniques in use for coating the plaster casts in the nineteenth century.



VICTOR . H. WAGER .

CHAPTER 3

HISTORICAL MATERIALS AND TECHNIQUES

FOR PLASTER CASTING

[...] That will be an evil day in which we cease to benefit from the experience, the struggles, the disappointments, the shortcomings, and the failures of those who have worked before us. [...]' (Bankart, 1908)

3.1. MATERIALS, PROPERTIES, AND TECHNIQUES FOR PLASTER CASTING

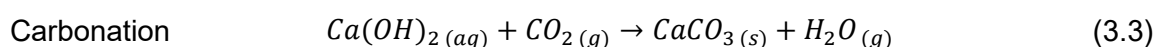
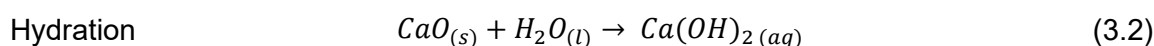
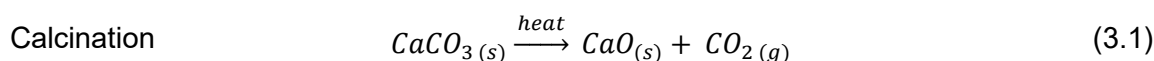
Plaster has always been used as an aid for many branches of art, due to its capability to quickly reproduce works of marble, pottery, and metal, and for its distinctive ability to penetrate every nook and cranny of a shape. Plaster is extremely easy to use and dries very quickly, but it is also fragile and impermanent (de Jonge, 1985). The nature of plaster is more complex than can be assumed at a glance. It is a porous, brittle material that absorbs moisture and dust particles. If it is not sealed, it will alter in appearance dramatically over time and remains susceptible to erosion (Hubbard, 2015). Often it is quite difficult to hypothesise the reactions occurring in the plaster bulk and surface, both for the complexity of the mixtures and the materials intentionally added to the stratigraphy and also because of the contamination occurring at any stage of the manufacturing, also from tools and from the mixing water. Plaster is also one of the best-known fire-resisting materials for building purposes. The use of plaster in art and architecture is surely connected but for many aspects different. For example, in architecture, plaster and *stucco* are considered covering coats (renders) added to a structure already existing, whereas the same terminology relates to different compositions when applied to the fine arts (Kemp, 1912) (see *Preface* and *Glossary*). As sometimes the historical sources could lack specificity, the term 'plaster' will here refer to any calcium sulfate-based mixtures, unless otherwise stated.

3.1.1. GYPSUM AND PLASTER

Plaster is a heterogeneous material that can vary quite fundamentally in chemical composition both for its natural makeup and because of the variety of additives traditionally added to it (Risdonne *et al.*, 2021). Plaster can be mixed with many other materials to obtain different properties and textures, and colour can be added to the mixture or applied on the wet or dry surface. As the word plaster refers to many different preparations, the main chemical types are lime plaster and gypsum plaster.

3.1.1.1. Lime plaster

Lime plaster is made by heating calcium carbonate (limestone) to produce calcium oxide (quicklime) (*Equation 3.1*). Water is added to form calcium hydroxide (slaked lime) which forms the plaster mix (*Equation 3.2*). Lime plaster sets chemically by reacting with carbon dioxide (CO₂) present in the air (*Equation 3.3*) (Lewry & Williamson, 1994; Payne, 2020; Turco, 1990).



Although lime plaster was widely employed in outdoor architectural and decorative details (Sotiropoulou *et al.*, 2018; Ventolà *et al.*, 2011), the historical literature sources suggest that the nineteenth-century plaster casts were mostly produced with plaster made of gypsum (Megens *et al.*, 2011; Payne, 2020; Risdonne *et al.*, 2021).

3.1.1.2. Natural gypsum

Natural gypsum is a mineral constituted by calcium sulfate and two molecules of crystallization water (calcium sulfate dihydrate, CaSO₄·2H₂O). Gypsum is the most abundant natural sulfate, widely present in the earth crust; it is heavily used in industry, as a construction material (plaster, mortar, blocks, additive to Portland cement, etc.), a component of fertilizers and soil conditioners for high sodium soils, and even in the cosmetic (foot creams, shampoos and other hair products) and food (tofu, dough conditioner, brewery, etc.) industries (Aquilano *et al.*, 2016). Gypsum has a sedimentary genesis and deposits can be found in Spain, Egypt, Italy, Russia, Poland, France, Switzerland, France, the United States, Africa, the Middle East, some of the South American states and Canada (Cox *et al.*, 1974; Madonia & Forti, 2003). It is found in the UK in the counties of Derbyshire, Cheshire, Nottingham, Cumberland, and Westmoreland (Millar, 1899; Sullivan, 2019). Gypsum crystallizes in the trimetric group and monoclinic system (spatial group A2/n), commonly a combination of a vertical prism with an oblique prism and with the pinacoid (selenite variety). and the crystals show a ‘tabular’ shape (Cox *et al.*, 1974). Some varieties crystallize in vitreous lamellar masses, in saccharoid masses (chalky alabaster or alabastrite), in fibrous masses (sericolite) or compact masses. The natural variety from Montmartre, also containing calcium carbonate, is also called Montrmatrite (Turco, 1990). Natural gypsum measures 3-3.5 on Mohs’ hardness scale of 1-10 and it has a specific

weight of 28.45-29.28 N/dm³ (Palache *et al.*, 1951). It is easily scratched and highly porous: this material is vulnerable to mechanical damage, discolouration by dirt penetration and softening and disintegration caused by the presence of moisture. The properties of mineral gypsum are summarised in *Table 3.1* and definitions can be found in the *Glossary*.

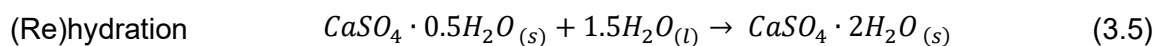
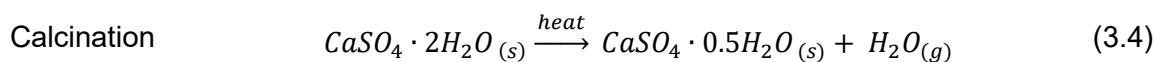
Table 3.1. Summary of gypsum properties.

ABOUT THE GYPSUM MINERAL	
Chemical Classification	Sulfate
Chemical Composition	CaSO ₄ ·2H ₂ O (calcium sulfate dihydrate)
Diagnostic Properties	Cleavage, specific gravity, low hardness
Uses	Used to manufacture drywall, plaster, and joint compound. Also used for agricultural soil treatments.
Physical and Mineralogical Properties	
Colour	Colourless to white, often displaying other hues due to impurities (white, grey, yellow, red, brown); colourless in transmitted light
Transparency	Transparent, translucent, opaque
Lustre	Vitreous, sub-vitreous, silky, pearly, dull
Streak	White
Hardness	2 (Mohs Scale), varies with direction down to 1.5
Tenacity	Flexible
Cleavage	Perfect (eminent), almost micaceous in some samples; on {100} distinct, yielding a surface with a conchoidal fracture; on {011}, yielding a fibrous fracture {001}
Fracture	Splintery, Conchoidal
Density	2.312 - 2.322 g/cm ³
Diaphaneity	Transparent to translucent
Crystallography	
System	Monoclinic
Class (H-M)	2/m - Prismatic
Cell Parameters	a = 5.679(5) Å, b = 15.202(14) Å, c = 6.522(6) Å, β = 118.43°
Ratio	a:b:c = 0.374 : 1 : 0.429
Z	4
Unit Cell Volume	495.15 Å ³ (Calculated from Unit Cell)
Morphology	Thin to thick tabular crystals, {010} with {111} and {120}; also prismatic [001], stout to acicular, with the prism zone often striated. Crystals may have warped surfaces or may be bent or twisted. Rosette-like clusters of lenticular crystals are common. Also found as granular masses, massive beds, and fibrous masses ("satin spar")

Sources: Aquilano *et al.* (2016); Cox *et al.*, (1974); *Gypsum - Properties, Definitions and Uses*, (1921); Palache *et al.*, (1951). Definitions can be found in the *Glossary*.

3.1.1.3. Gypsum plaster

Gypsum plaster is a hemihydrate of calcium sulfate and is prepared by the partial calcination of gypsum (*Gypsum - Properties, Definitions and Uses*, 1921). The water of crystallization held in chemical combination in natural gypsum ($\text{CaSO}_4 \cdot 2\text{H}_2\text{O}$) can be driven off by heat (*Gypsum - Properties, Definitions and Uses*, 1921) (Equation 3.4). When natural gypsum (calcium sulfate dihydrate) is heated to a temperature between 107-200°C,⁴⁸ it loses one molecule and a half, about 75%, of its water of crystallization to become the very reactive hemihydrate (also known as ‘modelling plaster’) (*Gypsum - Properties, Definitions and Uses*, 1921).⁴⁹ During the process of (re)hydration, water is mixed into the gypsum plaster (hemihydrate or dehydrate gypsum), providing a short working time for procedures like casting, before it hardens and reforms into gypsum as a mass of needle-like monoclinic crystals (Aquilano *et al.*, 2016) (Equation 3.5). These crystals are arranged randomly, and their interlocking and intertwining held together at points of contact by intercrystalline attractive forces accounts, at least in part, for the strength of set plaster.



During the setting process, the conversion to the dihydrate is accompanied by the generation of heat (about 3.900 Cal/mol) and a slight increase in volume due to thermal expansion (Barclay, 2002; *Gypsum - Properties, Definitions and Uses*, 1921). The amount of water is crucial; little produce powdery material that crumbles and cracks, whereas too much water, results in a porous material, weak and fragile (Barclay, 2002). The setting process was studied for the first time in 1765 by the French chemist Antoine-Laurent Lavoisier (1743-1794) and more in-depth between 1900 and 1903 by the Dutch chemist Jacobus Henricus van't Hoff (1852–1911) (Meilach, 1966; Turco, 1990). Aquilano *et al.* (2016) provide insights on the differentiation between the morphology derived from the crystal structure – termed structural morphology – and the actual morphology of the crystals as found in nature – termed growth morphology. Growth morphology appears to be dependent on the chemical composition and time, but also the values of the physical parameters relevant to crystallization, such as temperature, supersaturation, pressure, fluid dynamics and the presence of impurities in the mother phase (see *Glossary* for definitions).

⁴⁸ More in details, Turco (1990) indicates 128°C for a first step of the reaction, where the dihydrate sulfate loses 75% of the crystallization water and a second step, occurring at 163°C, where all the water is lost. Heating further, at about 500-600°C, gesso morto (dead gypsum) is obtained, and it does not absorb water. Heating at 1000°C, there is the formation of up to 3% of calcium oxide (quicklime, CaO). At 1360°C the material melts and at 1375°C the complete dissociation occurs (see *Appendix 3* for the reaction).

⁴⁹ Calcium sulfate hemihydrate $\text{CaSO}_4 \cdot \frac{1}{2}\text{H}_2\text{O}$, having specific weight equal 24.52-26.49 N/dm³ and containing 5-7.5% of water.

According to Aquilano *et al.* (2016), gypsum crystallization has recently gained further interest owing to the study of naturally-appearing giant crystals in Naica (Mexico), which have been proven to grow very close to equilibrium. Studies on the rearrangement of the crystals after dehydration and re-hydration are still scant in the literature (Jørgensen & Posneb, 1959; Lewry & Williamson, 1994). There are two allotropic varieties, both highly water-soluble: the fast-setting α and the slow one β . During the setting process, the mixture expands slightly, before returning to near its original volume. This is one of the reasons why it can be used to pick up small details from a sculpture model (Beale *et al.*, 1977; Meilach, 1966; Payne, 2020).

3.1.2. BEFORE CASTING

There are a series of steps, before the actual plastering, modelling or casting, that need to be undertaken to ensure the desired quality of plaster for the job. The quality of the gypsum, the atmospheric temperature, the calcining temperature, the presence of additives, the rate of grinding, the storage conditions and the water/plaster ratio massively affect the setting time and therefore the quality of the final product (Kemp, 1912; Turco, 1990). Some of the causes of the decay are related to the manufacturing of the plaster casts and also to the properties of the final product, influencing its longevity in terms of conservation. Frequent problems are lumps, weak casts, erratic setting times and surfaces that are soft, chalky or full of air holes (*Figure 3.1*). Improper storage of the powdered plaster is a very important variable: it should be stored in a dry space as plaster that has been exposed to moisture will start crystallising and become lumpy. Mixing time also affects the final product: when not all the particles are wet, undermixing occurs and the resulting plaster will not be strong and the surface may be soft and chalky (Meilach, 1966). The temperature of the water is another factor: plaster sets more quickly when the water between 30 °C and 40 °C is used because the point of maximum solubility of gypsum in water lies between these temperatures. As quick setting can be a disadvantage for the plaster stability, room temperature is the safest to use (Barclay, 2002).

Plasters from different regions have different compositions. Gypsum can contain a wide variety of natural impurities, including small amounts of calcium carbonate, clay (hydrous aluminium silicate), iron oxide and rock salt (*Gypsum - Properties, Definitions and Uses*, 1921). Additives are also added to the plaster to alter the working properties, setting times, mechanical characteristics and appearance of the plaster (Cox *et al.*, 1974). According to Bankart (1908), ‘Elm bark and hot barley water (tannin and size) were mixed in the stucco’ used in the Justinian’s Church of the Baptist, Constantinople. [...] In later times at Rochester Cathedral, about the end of the ninth century, bullocks’ blood was mixed in the stucco and mortar. [...] In 1280, at Rockingham Castle, melted wax was used. [...] On

Queen Eleanor's Cross, Charing Cross, London, erected in the thirteenth century, the whites of eggs and strongest wort of malt were mixed with the lime and Calais sand. [...]' About 1324-1327, 'in King Edward II's work at Westminster pitch was mixed in the stucco and mortar. Wax, pitch, urine, beer, and size were also extensively used at that time for the same purpose. [...]'.



Figure 3.1. Detail of a plaster cast of a relief on the outside of Notre-Dame Cathedral in Paris, in the V&A collection (REPRO.1890-80). Uneven distribution of the plaster during the casting process could cause the formation of air pockets as can be seen in the picture (yellow circle). © Victoria and Albert Museum, London/as specified by the rights holder.

The materials are selected for a specific purpose considering the desired performances of these during the processing and their afterlife. Every additive must be carefully and homogeneously mixed in water to be used for the plaster blend so that its action will be uniform and perfectly distributed across the plaster. When selecting an additive to modify the setting time, for example, it might be useful to consider its hardening properties, as it is convenient to obtain desired results with the addition of only one material. In particular, the following effects can be obtained depending on the materials added to the plaster admixture:

- **Acceleration of setting time** is obtained in the presence of alum, potassium, zinc sulfate, nitrate and chloride salts and acids, sugar, calcium and barium carbonate (Bankart, 1908; Turco, 1990; Wager, 1963);
- **Improvement of mechanical or aesthetic properties (texture, density, strength, workability)**. Bankart (1908) says that during Vitruvius' time juice of figs (also mentioned by Pliny), rye dough, hogs' lard, curdled milk and blood were added to improve the plaster mechanical properties. Traditionally also straw, hemp, sawdust, hair were used for this purpose; bulking agents like sand or pulverised marble are blended in the plaster to improve its strength and change its colour and texture (Meilach, 1966; Merrifield, 1846; Millar, 1899). To achieve an improved hardness of the plaster it is possible to incorporate substances capable of combining with each other or with calcium sulfate to the gypsum mixtures, forming compounds with a hardness greater than that of gypsum (treatments with silicates, fluates, carbonates, sulfates, barite, alum etc.) (Merrifield, 1846; Turco, 1990). Substances that do not react, but fill the porosities (gelatine solutions, casein, Arabic gum, albumin, methylcellulose, sodium alginates, emulsions and solutions of synthetic resins, soapy solutions) were also added to the plaster, before or during the mixing, for several purposes (Bankart, 1908; Turco, 1990). Marshmallow root, sodium bisulfite, ammonium triborate, metal oxides and phosphates or sulfates (Turco, 1990) are also additives found in the literature. In this category, there are also additives added to the admixture to achieve improved resistance to water, e.g., glue (Turco, 1990; Wager, 1963).
- **Retarding of the setting time**. Organic materials with a high molecular weight such as glues, caseins, keratins, pectin, albumin, Gum Arabic, gelatine, hydrolysed proteins, molasses, decomposition products of albuminoids, hydrolysis products from animal residues, products of reactions of amino acids with formal aldehyde, powder and marshmallow root, tannin were found in the literature as used for the purpose of retarding the setting time (Bankart, 1908). Substances that decrease the solubility of gypsum such as glycerine, alcohol, acetone, ether, sugar, nitric, acetic, phosphoric, boric, lactic acids and their salts, including alkaline and calcium salts, sodium carbonate also achieve this purpose (Bankart, 1908). Substances modifying the crystalline structure of gypsum such as calcium acetate, magnesium carbonate and calcium and also borax, lime, stale beer, and ammonia have a retardant effect. Additives such as waxy and resinous emulsions, alginates, carboxymethylcellulose and sodium silicate also behave as protective colloids (Turco, 1990).

Imparting tints by adding additives and pigments was never as popular as applying a coloured surface coating for the same purpose (Merrifield, 1846; Smith, 1810; Turco, 1990). This is because the intensity of the colour changes from the wet and dry plaster and calibrating the right proportion of colouring agent in the admixture can be very challenging.

The gypsum mixtures with glue, rubbers, resins, waxy emulsions, acetovinyl resins and other glueing or waterproofing substances, prevent the penetration of the colouring substances, so, in such cases, one must be satisfied with the simple surface dyeing. Craddock (2009) reports the variation in the concentrations of the additives as a way to give a streaking effect, simulating, for example, the graining of stone.

Drawbacks of the addition of additives can be the decomposition of the paint by chemical action, the appearance of efflorescence (see *Glossary*), the formation of cracks and blisters and the loss of adhesion. Turco (1990) and Ordonez & Twilley (1997), for example, suggest that salts can be good retardants and also hardeners, but can cause the formation of saline efflorescence. Impurities or half-baked particles harm the setting of the plaster, causing incomplete crystallization and weakening of the structure. This can be better understood if compared to the effect that salt and other components have on the natural nucleation and growth of natural gypsum, as reported by Aquilano *et al.*, (2016), related to the reduced capacity of the material to absorb water when the impurities are present (Turco, 1990).

Large materials have been found in the plaster casts' structure and were used to provide the casts with a 'backbone' or simply to avoid breaking (Graepler & Ruppel, 2019) (see for example metal rods in *Figure 3.2*). Wager (1963) and Kemp (1912) mentioned the use of fibres, wood and metal nails. Payne (2020) refers to Leonard Alexander Desachy (1845-1864),⁵⁰ who produced hollow casts by applying plaster strengthened with layers of jute inside the mould. This formed a lighter, tougher cast than those constructed from solid plaster. Zolnay (1910) in the patent 'Process of Making art models' mentioned the use of asbestos⁵¹ as reinforcing material, which is also found in Dailey & Duffy (1948) and Koblitz (1977). However, reinforcing materials may deteriorate much more rapidly than plaster itself. Beale *et al.* (1977) referred to the use of rods in the plaster that would leave stains and wood swelling that would create cracks, besides the obvious structural support (see for example *Figure 3.2*). Klosowska & Obarzanowski (2010) observed corroded inner metal structures in damaged areas of several plaster casts in the National Museum of Krakow, leading to swelling of the rusted material that caused cracking of the plaster. Examples of rust stains in plaster casts were also shown by Ángeles Solís Parra in Graepler & Ruppel (2019).

Grinding is described in many different sources and the degree depends on the purpose of the plaster, as it will change its mechanical properties. The moulder should be provided with

⁵⁰ French modeller who patented fibrous plaster casting in 1856.

⁵¹ Fibrous minerals composed of thin, needle-like fibres. Before its dangers were known, asbestos was often used in buildings for insulation, flooring and roofing and sprayed on ceilings and walls. It is now banned in the UK and many other Countries.

at least two grades of plaster, '[...] a fine grade [...] for surfaces, and a larger quantity of a cheaper grade for strengthening moulds and casts [...]' (Frederick, 1899).



Figure 3.2. X-ray photography of the V&A's plaster cast of Michelangelo's Tondo Taddei (REPRO.1902-98) showed that the cast was reinforced with metal rods (A). Side views of the object show that the presence of the rods created cracks (B) and rust stains (C). Images courtesy of Victor Borges. © Victoria and Albert Museum, London/as specified by the rights holder.

3.1.3. PLASTER CASTING

During the nineteenth century, plaster was frequently used in both moulding and casting to transfer images made in plastic materials, such as wax, clay, and later plasticine, into a more durable form that would not shrink or crack upon setting (de Jonge, 1985). Casting involves pouring into a mould a liquid material, which hardens and takes the shape of the mould. Pouring liquid plaster into a mould produces an object with an interior cavity and walls of variable thickness, depending upon how well the plaster was distributed. Air bubbles that may have formed as the plaster was sloshed inside the mould can also weaken the structure. Smaller objects are often made of solid plaster, in which case the mould is filled completely with plaster and allowed to set without agitation (Barclay, 2002). Moulds can be made of sand, clay, cardboard, plaster and new plastic materials (Meilach, 1966).

The water-to-plaster ratio varies, generally one part of water and two of plaster (Meilach, 1966). '[...] Water should be as pure as procurable, and especially free from those salts, which absorb moisture from the atmosphere [...]' (Kemp, 1912). Meilach (1966) recommends adding the water in the mixing bowl first and using room-temperature water, as too hot water would accelerate the setting and cold water would retard it. According to Chaney (1973), liquid plaster to be used for casting should be made from gypsum that was burnt to contain ca. 7% water, as too high temperatures make the gypsum unusable for casting.

There are several different techniques available for plaster casting and which one is used depends on the characteristics of the object to be reproduced, such as its shape and the presence of undercuts, and also on the availability of time and resources. Four main types of casting techniques are discussed here as found in the literature selected for this study (*Section 2.2.2*), but more are known and often related to the individual workshops' practices. The casting techniques are named by the type of mould produced during the moulding process:

- A **waste mould** derives its name from the fact that it must be broken or wasted before the cast can be extracted, whereas several casts can be obtained from a piece or safe mould. Plaster is applied to the model and when set, the model is withdrawn. The mould created is filled with fresh plaster and broken away (Auerbach, 1961; Meilach, 1966; Wager, 1963).⁵² As the mould is one piece, the model must be destroyed to remove it from the mould. Plaster waste moulding is a method used for moulding clay models on the round to obtain a cast or a moulding piece (Millar, 1899). Waste moulds were used

⁵² A coloured layer of plaster is used to indicate where the interface between the mould and the cast is. Kemp (1912), for example, suggests the use of some powder colour – yellow ochre, burnt umber, or light red – to tint the first coat of plaster.

to save the expense of piece moulding clay models, where one cast only is required for making a moulding piece, or for cleaning up the cast before being permanently moulded. Plaster is used for waste moulding models on the round and similar works. Wax is used for small, flat, and delicate work (Millar, 1899). According to Millar (1899), casting wax was used for casting silver or bronze models, also for piece moulding. '[...] The Italian artists use a casting wax made simply of beeswax, Venice turpentine, and finely sifted wood ashes. [...]'

- A **gelatine (jelly or elastic) mould** is made of gelatine.⁵³ The resilience of the material permits making casts with undercuts, no fear of adherence of mould and cast. Many casts can be made, but the gelatine can only be kept for a short time (Frederick, 1899; Kemp, 1912; Wager, 1963). Frederick (1899) suggests working only with 'the best white glue',⁵⁴ or with glue and molasses (proportion of 16 ounces of glue to 14 ounces of molasses) and Kemp (1912) works with 'one part of good glue and two parts of molasses (treacle), by weight, melted together'. Wager (1963) mentions 'rubber jelly' moulds as a recent development and notes that this material is 'more expensive than gelatine, but last indefinitely'.
- A **piece mould** derives its name from being made up of several pieces which placed together form the complete mould, and the mould can be kept indefinitely. Piece moulds are used for reproducing metal, terra-cotta, concrete, wax, or plaster casts from original models that are on the round or undercut, and where it is impracticable to mould them in one piece or two pieces, such as a front and back mould. Various pieces of moulds are made and carefully fitted together (de Jonge, 1985; Kemp, 1912; Wager, 1963). Each section is made individually so it fits perfectly against the section next to it. Pieces are held together by a casing of plaster (called 'mother mould'). All the mould pieces are then greased thoroughly and assembled and tied together. The cast material is poured into the mould through an opening left at the top and allowed to harden. Each piece of the mould is then carefully removed and the finished cast results. Plaster lends itself more freely and is more adaptable for forming a piece mould than either wax, clay, sulfur, or metal. '[...] Its quick setting powers and unshrinkable and plastic nature, combined with its fine and smooth surface, seems to be expressly designed by Dame Nature for this purpose. [...]' (Millar, 1899). These moulds are imperative where moulds have to be kept in stock over a period and for huge objects (Cellini, 1967; Meilach, 1966; Wager, 1963).

⁵³ Gelatine is 'animal jelly, obtained by the prolonged action of boiling water on the organic tissues of the bones, tendons and ligaments, the cellular tissues, the skin and the serous membranes. Glue and size are coarser varieties of gelatine prepared from hoof, hides etc.' (Frederick, 1899).

⁵⁴ The source does not indicate a definition of this material. In modern days this would be understood as polyvinyl acetate – PVAc – adhesive (which would not be suitable), however here it likely refers to some type of purified or 'bleached' animal glue.

- **Wax mould.** Millar (1899) provided four different recipes for producing squeezing wax (see *Appendix 3*). Millar (1899) also provide a recipe for making a wax used for making moulds for plaster casting: '[...] It consists of 1 part pure beeswax, and from 1 to 2 parts of powdered resin, dissolved in a metal pot, over a slow fire, or on a hot plate. [...] The quantity of resin varies according to the quality of the wax. A rich wax will carry more resin than a poor one. Poor wax is improved by adding from 1 to 3 oz. of mutton suet, or best white tallow, to each pound of wax. [...]' Frederick (1899) also describes the wax mould as made of one part of rosin and three parts of white wax (or melt paraffin wax and add a little sweet oil and whiting). Kemp (1912) suggests the following wax admixture: '½ lb. of beeswax, ½ lb. of black resin, and 6 oz. of tallow'.

3.1.4. SEPARATING AGENTS

Gelatine and wax moulds do not require a 'separating interface' between the mould and the original piece, however, these techniques do not produce lasting moulds. As for the piece and waste techniques, the application of a separating agent to the object to be reproduced was immensely important for the success of the procedure (Frederick, 1899). A great variety of separating agents are described in the literature and can be found summarised in *Table 3.2*. The relevance that the use of a separating agent can have on this research on the coatings is related to the use of the separating agent for casting the object investigated and also for further moulding and casting. Pieces of evidence were found by conservators at the V&A, that moulds were produced within the museum casting service from the objects in the cast collection (Graepler & Ruppel, 2019). Although the separating agent cannot be considered itself as a cast's coating layer, the possibility of the separating agent being transferred onto the cast surface during the casting must be taken into account, at least to be able to discriminate between the two.

Table 3.2. Separating agents as found in the historical literature.

Separating agent	Description	Sources
Clay water	Clay and water up to the consistency of cream	Frederick (1899)
Fat (animal)	The fats dissolved by heat, and then sufficient paraffin oil added until of a creamy consistency	Millar (1899)
Lard	Soft lard	Cellini (1967)
	Lard with and without sweet oil; the addition of paraffin oil to these oils renders them softer and cleaner	Millar (1899)
	Equal parts of lard and tallow	Frederick (1899)
Oil	Russian tallow and sweet oil	Millar (1899)
	Chalk oil (also used for wax moulds)	Millar (1899)
	Olive oil	Kemp (1912)
	Automotive oil (30wt)	Chaney (1973)
Shellac	Heated finely ribbed shellac in methylated spirits <i>au bain-Marie</i> without the cork on the bottle. Use cold	de Jonge (1985)
Soap solution	One pint of boiling water with as much white castile soap as will dissolve.	Frederick (1899)
	Green liquid soap	Kemp (1912)
	Boil two large tablespoons of best black soft soap in a pint of water and use cold. Two coats of shellac might be applied while damp and then grease with olive oil mixed with tallow	Wager (1963)
	English crown soap dissolved in warm water and kept available in cool liquid condition	Wager (1963)
	Dissolve liquid (green) soap or a bar of soap in hot water and leaving this to stand for about a day. One part of soap to two parts of water	de Jonge (1985)
Stearic acid	(German plaster) one part of stearic acid (or stearine) melted in a water bath, and about 5 parts of alcohol or benzene	Millar (1899)
	¼ lb. Of melted stearic acid in one pint of kerosene gradually stirred after removing from heat	Chaney (1973)
Suet solution	Dissolve fresh mutton suet by gentle heat, then add as much paraffin oil as will keep it in a soft cream state when cold.	Millar (1899)
Vaseline	Pure or melted with carbon tetrachloride to simplify the spreading	Meilach (1966), de Jonge (1985)
Wax	No specification is given in the source	Meilach (1966)

3.2. FINISHING AND COATINGS

After moulding and casting the objects as desired, many different actions can be taken, depending on the wanted result, including the properties of the surface and its appearance. The cast can be left raw, uncoated, or be subjected to different degrees of sanding and polishing (Auerbach, 1961; Millar, 1899; Turco, 1990). Further treatments could be applied to the finished work to modify its qualities. Gypsum plaster makes excellent casts, capturing fine surface details; however, it is also soft, porous and easily damaged. '[...] Plaster may be stained or painted, stippled or glazed; it may be left near its natural colour or darkened to give the glow of bronze or the sheen and colour of ebony; it may be left matt or it may be polished [...]' (Auerbach, 1961).

Sanding of plaster products can be done in dry conditions (with pumice pieces, with pumice and abrasives in powder and with abrasive papers), with water and or with oil (or any oily materials) (Turco, 1990). The rate of sanding, coarse to fine, and technique used to polish the cast affect the final appearance of the surface, as well as the porosity of the cast (from matt to shiny); the use of tools to remove leftover material can be sometimes still be observed in the finished cast, as seen for example during the observation of a cast of a relief on the outside of Notre-Dame Cathedral in Paris (REPRO.A.1916-3153, *Figure 3.3*). There is a great variety of simple tools that can be used by the plasterer for this purpose. It is possible to make impressions, add textures, dig holes and gouges, sand, smooth and scratch lines into plaster until the last moment (Meilach, 1966). Spatulas, scrapers, plaster rasps, saw-toothed instruments and chippers are finishing tools, wet sponges to wash and smooth and many other instruments to create interesting designs (Kemp, 1912).

According to Auerbach (1961), a new cast will usually take some weeks at least to dry out thoroughly in the air. The quality of the gypsum, the water/plaster ratio and the atmospheric conditions of course have an impact on the drying time. Nevertheless, the application of finishing could have to be done either straight after the casting or even months later, depending on the time availability and other practical factors, such as storage space and conditions. Moreover, as it has been discussed in Graepler & Ruppel (2019), several collections were repainted decades after the production of the cast, as a result of the change in taste of the directorship of the museum, to protect the cast from damage, or to hide and treat superficial damage. Graepler, for example, describes the history of the surface treatments applied on the Göttingen plaster casts since 1765, highlighting how in different moments of the casts' lives, from their production to their conservation, 'the casts might have had been treated with some coating'. Moreover, Ruppel talks about the 1960s campaign that aimed to clean the plaster and also remove the old coats of paint and suggests that the cleaning was followed by the overpainting with white emulsion paint. Grein in Graepler & Ruppel (2019) also mentioned the acquisition of casts of works of archaeology

and art history in 1888 and 1889 in the Ducal Museum in Brunswick. The author reports that initially the casts were white, but they were provided with coatings to mimic the appearance of their original between 1901 and 1916 and that missing parts were also reconstructed by local sculptors. Müller in Graepler & Ruppel (2019) narrated the poor conditions of the collection of casts at the University of Innsbruck, formerly known as the Royal Plaster Museum. At the beginning of the 1950s, the casts were soiled and damaged and were then restored. It was decided in that process to 'coat the casts to resemble their originals' and often a thin layer of wax can be observed onto the surface (Graepler & Ruppel, 2019).



Figure 3.3. Detail of a plaster cast of a relief on the outside of Notre-Dame Cathedral in Paris, in the V&A collection (REPRO.A.1916-3153). A closer look allowed to identify marks and scratches due to the use of tools. © Victoria and Albert Museum, London/as specified by the rights holder.

What is considered to be a finishing layer or a coating for plaster cast is not what we would normally define for other artefacts such as paintings. In these artworks, the substrate (i.e. wood, canvas, etc.) can be covered by one or more preparation layers that are not, in any case, supposed to exist independently as the surface layer, and the finishing or paint layer is applied on top of those (Carlyle *et al.*, 1995; Roberts, 1968). The case for plaster casts is that every treatment applied to their surface can instead be a 'coating' or a finishing layer in itself. A plaster cast, when extracted from the mould, already represents the complete form not depending on the 'building up of layers' on its surface as is the case in the stratigraphy

of a painting. Therefore, every treatment applied to the surface of casts can allegedly be the outer surface layer or coating. Moreover, there is not a 'rule' in terms of the consequentiality of the layers (Auerbach, 1961; Roberts, 1968).

The cast can be coated, for different purposes, and the coating can be equally applied onto unpolished surfaces as well as onto polished ones. Millar (1899) also says that casts that are to be polished by friction with other substances should be made as hard as possible, suggesting that a hardening treatment can be applied *before* the polishing. The coating can be applied by brush, by spray or by dipping the object into a bath of the prepared solution (Turco, 1990). The coating can be applied warm or cold onto the surface of the casts that might be or might not be previously heated (Turco, 1990). Roberts (1968) and de Jonge (1985) suggest that a pre-treatment with a solvent which, penetrating through the cavities and pores, could remove the occluded water and dust (for example abundantly soaking the plaster products with acetone) can be done once or several times. As for coatings that form a film on the plaster surface, their concentration should be 'intermediate', to allow the material to form a film, but at the same time to penetrate the plaster enough to interact with it (Roberts, 1968).

After reviewing the historical sources, it was possible to identify that a material used for coating plaster cast objects can serve multiple purposes at the same time, but it can, however, be generally categorised according to its intended function (Risdonne *et al.*, 2021), which can be:

- Seal the pores,
- Waterproof the surface,
- Hardener the surface,
- Change the appearance.

The above purposes can be achieved with one or more layers of the same or different materials and there is not a well-defined hierarchy or order in which these layers were usually applied. A coating could ideally accomplish multiple desired effects: 'sealing the pores' and 'waterproofing' for example might seem the same action, but, although in some cases the two can be achieved at the same time, one property does not imply the other. The latter interact and penetrate the plaster surface more or less in-depth depending on its chemical characteristics, concentration and density. *Tables 3.3* and *3.4* quote a selection of recipes retrieved from the books and other archive resources reviewed for this study (*Section 2.2*). *Table 3.5* summarises a list of materials encountered in the historical manuals and patents for coating the surface of the plaster casts.

Table 3.3. Summary of recipes as found in the historical literature.

Description	Application	References
Waterproofing the surface		
Boil 1 oz. pure white wax, 2 ozs. Venice turpentine. Add half-pint spirits turpentine (Invented by Mr F. D. Millet)	Brush	Frederick (1899)
The lime sulfate is changed into baryta sulfate and caustic lime using baryta water. Exposure in the air subsequently changes the caustic lime into lime carbonate. This is best worked by using a zinc vessel with a zinc grating 1 ½ m from the bottom, and a close-fitting lid. Soft water, 54 to 77° Fahrenheit. Every 25 gallons of water add 8 lbs. fused oil or 14 lbs. crystallised pure hydrated barium oxide and 0.6 lb. lime. The dipping should be affected with rapidity. Hollow casts after being saturated are filled with the solution and suspended in the bath, and the vessel is closed from two to twelve days, according to the silicate stratum required (Invented by Dr Reissig, of Darmstadt)	Dip or brush	Millar (1899), Kemp (1912)
To harden using the silicate of potash solution, convert the lime sulfate into lime silicate by using a diluted solution of potash Silicate containing free potash. 10% solution of caustic potash in water, heat and add pure silicic acid (free from iron). After cooling the solution deposits silicated potash and alumina. Before using, throw in some pieces of pure potash, or add about 2% of the potash solution (Invented by Dr Reissig, of Darmstadt)	Dip or sponge	Millar (1899), Kemp (1912)
Immerse the cast or throw upon it in a fine spray a hot solution of a soap prepared from stearic acid and soda lye in ten times its quantity, by weight, of hot water (Invented by Jacobsen)	Dip or spray	Millar (1899)
Apply a solution of borax and alum to harden the plaster, and apply soluble precipitates (salts of barium, calcium, and strontium), by which the minutest pores are filled up and the surface rendered hard (Patent by F. von Dechend, 1814-1890)	Brush	Millar (1899)
Mica rendered perfectly white by boiling with hydrochloric acid or calcining, mixed with dilute collodion to the consistency of oil – paint (Invented by Shellhass)	Brush	Millar (1899)
Boil p.6 of linseed oil, p.1 of litharge and p.1 of wax. Brush on hot, when dry second coat. Allow to dry and then polish	Brush	Wager (1963)
Coating paraffin or white wax or spermaceti in white spirit, petrol or petroleum	Brush	Turco (1990)
Waxy encaustics or aqueous wax emulsions (alone or with emulsions of white shellac and resins) These emulsions must be very concentrated or thickened with Arabic gum, alginates, methylcellulose, carboxymethylcellulose, animal glues, etc.	Brush	Turco (1990)
Dry the cast in the oven (80-90°C) and then immerse it in oil or paint (50-60 ° C); the plaster must be impregnated and subsequently dried in a well-ventilated area. It dips again for half the time and dries again (Yellow-brown colour)	Dip	Turco (1990)
A diluted solution of aluminium soap in turpentine and petrol essence	Brush	Turco (1990)
Dissolve casein with hydrated lime or slaked lime. A small amount of barium peroxide can be added to the mixture	Brush	Turco (1990)

Table 3.3. (continued)

Casein p.75, slaked lime p.17, anhydrous sodium carbonate, p.8 barium peroxide p.1.5, water p.280. Peroxide is added eventually. The final product should be used in a maximum of 20 minute	Brush	Turco (1990)
p.3 of rosin in p.5 of water and p.1 of soda. If instead of soda ammonia is required, long heating at 30-100°C is necessary	Brush	Turco (1990)
p.24 alum, p.4 white soap, p.2 Arabic gum, p.6 gelatine (12% solution), p.24 water	Brush	Turco (1990)
p.25 oily paint, p.35 solvent naphtha, p.40 carbon tetrachloride, p.150 denatured alcohol, p.50 soap, p.700 water (apply to keep the product in a water bath)	Brush	Turco (1990)
p.1 fish glue, p.420 water, p.30 sodium sulforicinate, p.49 stearic acid OR p.432 oleic acid, p.122 ammonia at 28° Bé, p.61 denatured alcohol 95% by volume, p.43 aluminium chloride, p.37 calcium chloride, p.305 water)	Brush	Turco (1990)
Paraffin p.20, ozocerite p.30, white-spirit p.20, toluol p.150	Brush	Turco (1990)
Ozocerite p.2.4, paraffin (50-52° C) p.8.9, olein p.2.5, morpholine p.2.2, water p.84	Brush	Turco (1990)
Paraffin p.120, stearic acid p.12, ammonia at 26° Bé p.6, 30% silicone emulsion p.40, water p.180. Paraffin is heated to 55°C, ammonia is added and then water. After cooling, the silicone is added. For the application, it is diluted with water	Brush	Turco (1990)
Ozocerite p.90, ammonium linoleate p.14, water p.400, 30% silicone emulsion p.30	Brush	Turco (1990)
Hardening the surface		
A bath of borax (biborate of soda) applied in the proportion of about one pound to every gallon of boiling water (Patent: Process of hardening and preserving plaster-of-Paris casts and molds and making them impervious to water)	Dip	Laxton (1887)
A bath of melted pure white wax, paraffine by preference, as this keeps its whiteness better than any other (Patent: Process of hardening and preserving plaster-of-Paris casts and molds and making them impervious to water)	Dip	Laxton (1887)
A neutral soap of stearic acid and caustic soda is prepared and dissolved in about ten times its weight of hot water.	Dip or brush	Millar (1899)
Equal parts of stearine and resin and containing per each kilogramme, 0.20 grammes of bitumen, preferably jew's pitch, 0.50 grammes of benzoin, preferably from Sumatra, 0.05 grammes of creosote, preferably from beech and also if it is desirable any colouring matter. Heated in a proper recipient to a complete solution and suitably stirred to produce a homogeneous mixing of composition. In the bath for 5 to 30 minutes, depending on the nature, thickness etc. of the article as well as the degree of hardening desired. This composition may be employed for decorating purposes being capable of being made in various colours by the addition of suitable colours [...] (Patent)	Brush	Wolf (1901)

Table 3.3. (continued)

<p>[...] a compound made of gum, beeswax, and gasolene, the latter rendering the molded article impervious, washable, and extraordinarily hard. [...] raw asbestos pulp, kaolin, whiting, or plaster of Paris with dissolved glue, flour paste, and linseed oil, all in such proportions as to yield a paste of about the consistency of dough. The above plastic layer is then backed by strips 2 of sheet asbestos, adhesively applied thereto. [...] The above product is then permitted to dry, and when dry it is saturated with heated paraffin, oxide of lead, and a suitable pigment by which it is rendered impervious, washable, and of the desired colour (Patent)</p>	Brush	Zolnay (1910)
<p>Immerse a plaster cast object in a saturated solution of alum at 90 °C</p>	Dip	Wager (1963)
<p>40-50% silicone solution in water p.5, potassium silicate p.15, water p.80</p>	Dip or brush	Turco (1990)
<p>Dry and heated casts are sprayed with a concentrated ammonia solution that helps the subsequent action of hardening baths based on alkaline borates and salts capable of forming double salts with those of ammonia</p>	Spray and dip	Turco (1990)
<p>Immersion in an ammonium triborate solution is obtained by saturating a concentrated and warm solution of boric acid with ammonia.</p>	Dip	Turco (1990)
<p>Small objects are dried in an oven at 100°C and then immersed in a 20-30% silicate solution (sodium silicate with silica and oxide ratio 3.2-3.3)</p>	Dip or brush	Turco (1990)
<p>Applying a saturated borax solution in water (120g salt in crystals for each litre of water)</p>	Dip or brush	Turco (1990)
<p>Slaked lime 2 p., Casein 8 p., Water 90 p.</p>	Dip or brush	Turco (1990)
<p>Casein 5 p. Slaked lime 5 p. Arabian gum 1 p. Sodium silicate 4 p. Water 70-100 p.</p>	Dip or brush	Turco (1990)
<p>The objects dried in the oven are immersed, while still having a temperature of 70-80 ° C, in a hot saturated solution of barite (barium oxide), then they start to dry again by repeating the treatment several times</p>	Dip or brush	Turco (1990)
Non-specified Purposes		
<p>Coats with hot glue sizing – the first being quite thin. Allow this to dry thoroughly and cover it with one or more coat of white shellac</p>	Brush	Frederick (1899)
<p>White wax dissolved in olive oil, or paraffin wax. Polish with French chalk and cotton wool</p>	Brush or dip	Millar (1899)
<p>White beeswax and glycerine. Polish with French chalk and cotton wool or sable hair brushes</p>	Brush or dip	Millar (1899)
<p>Plaster gauged with milk and water</p>	Brush or dip	Millar (1899)
<p>Dissolve ½ oz. of soft soap in 1 quart of water and 1 oz. of white wax. Polish with a soft rag and French chalk</p>	Brush or dip	Millar (1899)

Table 3.3. (continued)

Coat of white shellac, then a good coating of boiled soft soap, and polish a soft dry rag	Brush	Millar (1899)
1 gill of Copal varnish with 1 oz. of patent driers and turpentine	Brush	Millar (1899)
p.100 water, p.12 best hard shellac, and p.4 of borax. Used alone or mixed with a small portion of linseed oil and a few drops of turpentine	Brush	Millar (1899)
Dissolve India rubber in naphtha	Brush	Millar (1899)
Melt ½ oz. of tin and ½ oz. of bismuth. Add ½ oz. of mercury. Add the white of an egg	Brush	Millar (1899), Wager (1963)
Powered micaceous iron ore is mixed with cement, lime or plaster in a pasty or moist condition to which colouring matters may be added. A sample of the micaceous iron ore used (in the dry conditions consisted of: silicic acid and small stones (7.24%), iron oxide (Fe ₂ O ₃ , 80.17%), Aluminum oxide (5.16%), Calcium Oxide (0.40%), sulfur in the form of sulphide (4.30%), Magnesia (1.33%), loss in calcining (1.28%), the remainder (not determined, 0.12%). Objects made of this composition may be worked, just as stone, with a chisel without losing their metallic lustre. It may vary within the limits of p.1 of ore to p.1 of cement, lime or plaster and p.1 of ore to p.10 of cement, lime or plaster (Metallic lustre)	-	de Bas (1920)
White shellac, an ounce in a pint of methylated spirit	Brush or dip	Wager (1963)
Dextrin, an ounce of powder dissolved in a pint of water	Brush or dip	Wager (1963)
Two ounces of beeswax heated and melted into half a pint of glycerine, and thinned with turpentine	Brush or dip	Wager (1963)
Stearin or paraffin wax dissolved in turpentine, 1 ounce to half pint	Brush or dip	Wager (1963)
Paraffin or white wax or spermaceti in white spirit, petrol or petroleum	Brush	Turco (1990)
Waxy encaustics or aqueous wax emulsions (alone or with emulsions of white shellac and resins). Very concentrated or thickened with Arabic gum, alginates, methylcellulose, carboxymethylcellulose, animal glues, etc.	Brush	Turco (1990)

p.=part(s), °C=Celsius degrees, °F=Fahrenheit degrees, °Bé =Baumé scale degrees. The recipes are retrieved from the sources analysed for this study, divided by the purpose of the coating (waterproofing, hardening or others) was applied for. Quantities, concentration, and percentages are quoted from the original recipes. Most often is not defined whether the % concentration is in weight or volume. The lack of detailed instruction in the original source could be overcome only by reproducing and testing the recipes. More information is available in Appendices 3 and 4.

The purpose of **sealing the pores** is generally achieved by most of the materials used for coating, with different results depending on the characteristics of the material (such as porosity and roughness of the substrate and viscosity of the coating) and the concentration of the coating. Physical and chemical interactions between the plaster substrate and the coating material are fundamental and will be further discussed along with the results in *Chapters 4, 5 and 6*. In general, to close the pores of the plaster casts there is a wide range of materials described in the literature that can be applied onto the plaster surface and they work either by penetrating the pores and filling them - (A) in *Figure 3.4* - rather than by creating a film onto the surface and consequently preventing the dust and moisture from entering into the pores - (C) in *Figure 3.4*. Every intermediate scenario - for example (B) in *Figure 3.4* - is also possible and dependent on the properties discussed of the plaster and coating.

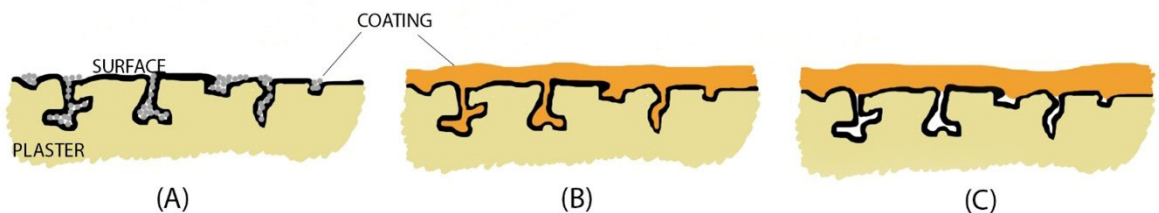
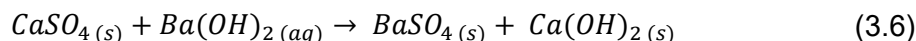


Figure 3.4. Simplified drawing representing the possible interactions of the coating with the porous plaster surface. The material applied onto the surface can penetrate the pores without forming a film (A), penetrate the pores and form a film on the surface (B) or form a film without penetrating the surface (C).

The formation of a film involves the conversion of a liquid phase, in which the film-forming material may be present in solution or as an emulsion or be in the molten state, into a solid laminal system (Massa & Scicolone, 1991). Depending on the nature of the compounds involved, the formation of the solid system may be the result of a physical change or a chemical reaction, or a combination of both (Masschelein-Kleiner, 1985). The effectiveness of the coating also depends on two properties, permeability and porosity, which are caused by many factors, the principal ones being the nature of the materials in the coating layer, how the film is formed and the processes that take place during ageing. The permeability of a film is its ability to allow the passage of a fluid (gas, vapour, liquid). The collection of holes, pores, fissures, breaks and cracks present in a film is responsible for its porosity (Masschelein-Kleiner, 1985).

Broadly, it is possible to categorise the surface **waterproofing treatments** as waterproofing film-forming materials and materials that react with gypsum producing an insoluble compound. The task of making the casts resistant to water or 'washable' was investigated for a long time. According to Millar (1899), in 1878, F. von Dechend (1814-1890), of Bonn,

obtained a patent for “making plaster casts washable without injury” by using a solution of borax (sodium borate) and alum (hydrated double sulfate salt of aluminium) and the latter application of soluble precipitates (salts of barium, calcium, and strontium). The chemical reaction employed by F. von Dechend can be described as:



An interesting review on the development of this technique was made by Payne (2020), who cites Brannt & Wahl (1919) on two methods and also discuss the technological developments in the treatment of plaster casts through the invention of machines during the nineteenth century. Millar (1899) also mentioned that Jacobsen⁵⁵ made the cast washable with lukewarm soap-water ‘by immersing them or throwing upon them in a fine spray a hot solution of a soap prepared from stearic acid and soda lye in ten times its quantity, by weight, of hot water’ and Shellhass⁵⁶ recommendation of coating plaster casts with a compound of finely powdered mica and collodion. In the mid-nineteenth century, scientific research into the investigation of protective treatments for casts was supported by the Prussian Government and a prize was awarded to Dr W. Reissig,⁵⁷ of Darmstadt, for his development of a method for treating casts such that they would become water-resistant. This involved converting the surface of the calcium sulfate cast into either barium sulfate or silicate, both of which are insoluble compounds. Dr Reissig, of Darmstadt, suggested that this could be achieved ‘[...] (1) by converting the lime sulfate into baryta sulfate and caustic or carbonate of lime, or (2) by changing the lime sulfate into lime silicate using potash silicate. [...]’ (Kemp, 1912; Millar, 1899). Auerbach (1961) and Wager (1963) report traditional film-forming treatments with waxes, drying oils and varnishes as very effective for waterproofing, also providing translucent appearance and a fine aesthetic effect. Modern authors, such as Turco (1990) and de Jonge (1985) mention the use of solutions of elastic rubber or natural and synthetic rubber and silicones. More recipes to achieve waterproofing are summarised in *Table 3.3*.

The purpose of **hardening** the surface can be achieved with different methods. Traditional methods are mentioned by Wager (1963) and Millar (1899) and patents that focussed on this can also be found: Laxton (1887) patented a ‘Process of hardening and preserving plaster-of-Paris casts and molds and making them impervious to water, Wolf (1901) suggested an [...] Improvement in Composition for Coating Surfaces to be used for hardening, agglomerating, coating or decorating different porous materials and

⁵⁵ It is unclear who is the person mentioned by Millar. It could be Jens Peter Jacobsen (1847 – 1885, Danish novelist, poet, and scientist), Antonio Nicolo Gasparo Jacobsen (1850 – 1921, Danish-born American maritime artist) or David Jacobsen (1821 – 1871, Danish artist)

⁵⁶ No reference found; it is not clear who is mentioned by Millar.

⁵⁷ Mentioned by multiple sources, but no background information available.

manufactured article [...]’ and Zolnay (1910) patented ‘[...] a compound made of gum, beeswax, and gasolene, the latter rendering the molded article impervious, washable, and extraordinarily hard [...]’. In some cases, finishing is recommended without specifying the final result or purpose. For example, Millar (1899) and Wager (1963) describe ‘a beautiful varnish’: ‘[...] by fusing $\frac{1}{2}$ oz. of tin and $\frac{1}{2}$ oz. of bismuth in a crucible. Melt together, then add $\frac{1}{2}$ oz. of mercury. When perfectly combined, take the mixture, allow it to cool, and add the white of an egg. The casts must be dry, and free from stains or dust [...]’. Another ‘good varnish’ is made by mixing 1 gill of Copal varnish with about 1 oz. of patent driers and turpentine and a shellac varnish is made by mixing 100 parts water, 12 parts best hard shellac, and 4 parts of borax. This is used alone or mixed with a small portion of linseed oil and a few drops of turpentine. A rubber varnish can be obtained by dissolving Indian rubber in naphtha (Millar, 1899).

Changing the appearance of the plaster surface can be done following numerous recipes (Table 3.4) and the effects achieved can be as many as the materials available to the sculptor. Recipes to provide a good gloss, for example, are mentioned by Millar (1899) and Wager (1963). Millar (1899) and Frederick (1899) suggest that a cast can be made **white**, or ‘whiter’, after coating (Figure 3.5). Polychromed statues can also be reproduced in plaster and a few examples can be seen in the V&A collection (Figure 3.5).



Figure 3.5. (A) Plaster cast from one of the shields on the Royal Albert Hall (REPRO.1901-16). White plaster cast. (B) A plaster cast of an Effigy of Isabella of Angouleme (REPRO.A.1938-4). Painted plaster cast. © Victoria and Albert Museum, London/as specified by the rights holder. Source: V&A’s Collection Management System.

Millar (1899) suggests colouring the surface of a cast by using watercolour when a dry surface is to be imitated (the watercolour might require several coats), oil-colours when the surface is moist. Gypsum is ideal for the application of paint materials, but attention must be paid to the interaction between gypsum and paint (Turco, 1990). A specific recipe to achieve a light-yellow coloured surface is reported by Frederick (1899) and one for a lead colour by de Jonge (1985). Often the casts' surface is intended to perfectly mimic the material of the original object. Marble, wood and metals (gold, silver and bronze) can be beautifully reproduced on the white matter (*Figure 3.6*). Recipes for achieving the appearance of artificial stone, a porcelain effect, or the appearance of terracotta and an old ivory finish are quoted in *Table 3.4*.

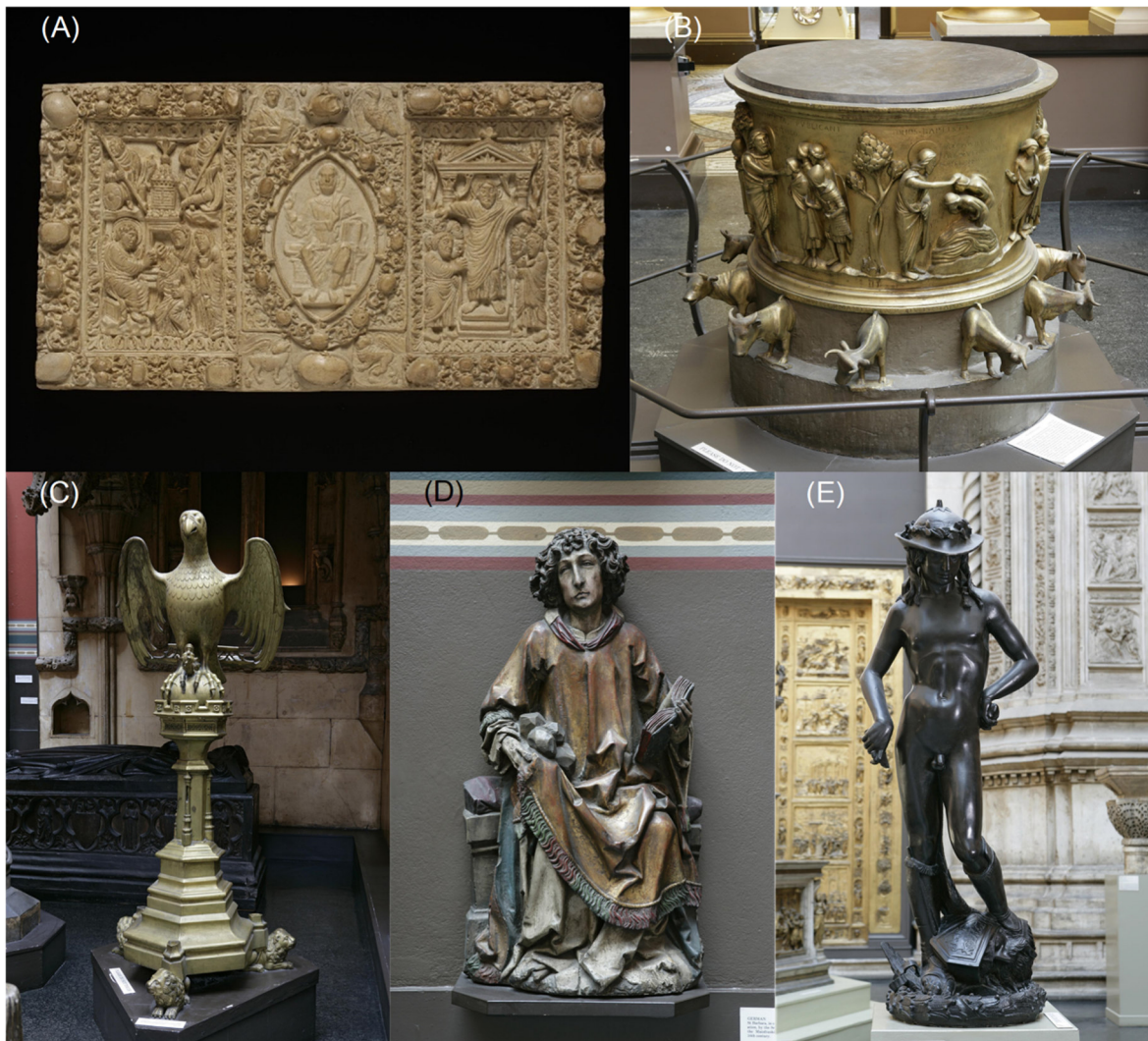


Figure 3.6. (A) A plaster cast of the lid of a casket (REPRO.1873-235). The plaster is finished to resemble ivory. (B) A plaster cast of a font (REPRO.1877-1). The plaster is finished to resemble gold. (C) A plaster cast of a Lectern (REPRO.1872-65). The plaster is finished to resemble brass. (D) A plaster cast of a wooden statue of St Stephen (REPRO.1906-3). The plaster is finished to resemble painted wood. (E) A plaster cast of Donatello's David (REPRO.1885-197). The plaster is finished to resemble bronze. © Victoria and Albert Museum, London/as specified by the rights holder. Source: V&A's Collection Management System.

Table 3.4. List of recipes used to achieve the desired appearance onto a plaster cast surface.

Effect	Recipe	References
<i>Artificial stone</i>	(patent) (1) muriatic acid 40 parts, tin 30 parts, sal ammoniac 30 parts. The tin is first dissolved in the acid, after which the sal ammoniac is incorporated in small pieces in the mixture. (2) pulverised freestone 50 parts, zinc oxide 20 parts, pounded glass 15 parts, powdered marble 10 parts, calcined magnesia 5 parts. The above ingredients are intimately mixed and passed through a fine sieve to form a powder which is reduced to a pasty consistency with the above liquid (1), this paste is applied with a trowel to the surface (building front, inner or outer wall) which is to receive a damp proof covering, layer or coating. After a very short space of time this paste becomes very hard and assumes the appearance of stone and after being well set it is as hard as flint and has a smooth polished surface which can be rapidly painted if required ordinarily. Or it may mix any suitable coloring material, dye or pigment with the above powder (2) to impart to the hardened coating either a plain color or a marbled, veined or motley surface. [...] generally for all casting and moulding purposes for which plaster of Paris is generally used, my improved paste being manipulated in exactly the same manner as the latter and producing ornaments of fine appearance having a hard surface and being made to assume when required by the judicious addition of suitable colors the appearance of marble, granite or other ornamental stone	Cléry (1896)
	500 litres of water, 7 kg of alum, 6 kg of slaked lime, 1 kg of yellow ochre. To this mixture is added 1 kg of strong paste dissolved in 5 litres of hot water and 900 kg of gypsum and 450 kg of fine sand, free of clay, are diluted there	Turco (1990)
<i>Bronze</i>	(bronze paint) mastic varnish and bronze powder	Frederick (1899)
	A coat, or coating of powder-colour mixed with milk or casein, followed by some slight polishing with cotton wool which has been dabbed into some talc (French chalk)	Auerbach (1961)
	Give the plaster cast a coat of white polish. When this has dried thoroughly, pour some of the polish into a saucer and mix into it some burnt amber and give the cast a not too thick but free coating of this mixture. Now get some good gold-bronze powder of a full rich warm colour. Using a little of the white polish as a vehicle a dragging fresh bronze powder into it, touch up all the prominences of the cast with the gold bronze. If this operation has been carried out successfully, the cast will now have very much the appearance of a real bronze before being treated for colour. Then get a lump of beeswax and shred it finely into the top of a tin or other small receptacle, with a knife. Just cover this pile of wax shreds with some turpentine and leave it to soak overnight. By the next morning, the wax should have dissolved, turning the mixture into a thickish and nearly transparent, somehow jelly-like substance. Into this solution, mix whatever colour you have in mind for the final bronze	Auerbach (1961)

Table 3.4. (continued)

	Artists' oil colour straight from the tube will serve well here; a Prussian blue with burnt sienna will give a rich green base with immense depth of tone whether it verges toward the olive or the blue side. Modification to the colour can, of course, be made by adding some yellow ochre or viridian. The whole mixture should be transparent rather than opaque. It is best to use a hog's hairbrush for this operation and to spread the coloured wax very evenly and not too thickly, by stippling hard over the whole surface and into all the crevices. This will be shiny when wet and will become matt when dry. It can be then polished with a very soft cloth. When it is completely dry another polishing can be made with French chalk. If beeswax is not available almost any wax in paste form – not liquid – will serve	Auerbach (1961)
	Need powder colour, burnt umber, emerald green, lamp black, reds and blues and a medium for floating these on. Use a gold size (thinned with turpentine and linseed oil) or shellac. Need metal powders, bronzes, golds, coppers, medium cellulose lacquer or shellac. After bronzing, wax to protect	Wager (1963)
	Gold, silver or bronze paint can be bought in either liquid or solid form	de Jonge (1985)
	(ancient bronze) 56 p. Burnt shadow earth, 15 p. Green, 5 p. Prussian blue, 15 p yellow ochre, 5 p. Chrome yellow, 4 p. Burnt sienna earth diluted with 60 p. The essence of turpentine, 25-30 p. Copal paint and 10 p drying oil. Treat first with shellac varnish and then with the aforementioned mixture. To emphasize more shiny areas, a wax dissolved in turpentine is added	Turco (1990)
	Soap solution (50g of white soap in 500g of water) is combined with a 10% copper sulfate solution and the green precipitate formed (copper soap), after filtration, it is dried completely. The mixture is prepared: copper soap (15 p.), white wax (15 p.) And linseed oil (30 p.) For which the pieces previously heated in a stove at 100-150°C are treated. If you add 5-20% of iron sulfate, from bluish brown it becomes greenish-brown. With this, the plaster becomes hard and waterproof	Turco (1990)
Colours	Light yellow or buff is easily obtained by linseed oil, which tints the plaster, makes it resistant to water and durable and hard. The oil can be applied with a slightly tint (e.g. Yellow ochre, raw sienna) or a wax-like surface can be obtained (immersing the cast in warm oil for ten or twelve hours)	Frederick (1899)
	Watercolours for a dry surface and oil colour for a moist one	Millar (1899)
	Shellac application before application of tempera' (dry powdered colour with the yolk of an egg)	Bankart (1908)
	The lead colour is achieved by using graphite powder, asphalt lacquer, wax, black vinyl emulsion paint, turpentine-based oil	de Jonge (1985)
	For a yellow-brown colour dry the cast in the oven (80-90°C) and then immerse it in oil or paint (50-60°C); the plaster must be impregnated and subsequently dried in a well-ventilated area. It dips again for half the time and dries again	Turco (1990)

Table 3.4. (continued)

	Using metal sulfates. The plaster objects are soaked with diluted solutions of these salts, left to dry and then treated with barite water, sulphide or other barium or calcium salt. With the same metal acetates or sulfates, the plaster can be dyed by following their application by treatment with phenolic dyes in alkaline ammoniacal medium or other alkaline earth hydrates. Oxidation colors such as pyrogallol, paraphenyldiamine, etc. They can be usefully applied by making alkaline or neutral solutions with the presence of catalysing substances and then exposing them to light.	Turco (1990)
	Soluble colouring materials remain more bright if added to the mass of the plaster with rubber, resins, silicates, fats, sodium casein, glue, etc.	Turco (1990)
	Greases penetrate gypsum deeply enough that they can be used to obtain good transparent dyes with a very pleasant, lively, very bright and washing-resistant effect. A fatty dye dissolves hot in a mixture of paraffin, stearin, spermaceti and similar substances, in which the pieces of plaster are immersed, keeping the temperature at 100°C for half an hour. The mixture is left to cool down to 30-40°C and heated to 100°C again, repeating this operation three or four times. Dye and waterproofing are obtained simultaneously with grease and solvent dyes the acid and substantive dyes in a diluted solution of silicates, rubber, glue, sugar, dextrin, are ideal for surface work.	Turco (1990)
	Good deep penetration of the colouring solutions is also obtained by first heating the pieces in the oven for 7-9 hours and then immersing the pieces for a few minutes in a saturated solution of potassium sulfate and then in a solution of chromium alum, sulfate ferrous, zinc sulfate, manganese sulfate. After about 24 hours they withdraw and are left to dry in the air.	Turco (1990)
<i>Copper</i>	It is also known to mix the plaster with a metallic powder, for example with iron filings or finely divided zinc, and to treat objects cast or moulded of this material with a solution of metallic salt, to obtain a metallic, more particularly copper, external coating	de Bas (1920)
<i>Gilding</i>	Gilding is often unsuccessful, but possible: gold leaf can be applied to any painted or shellacked surface and gold paint can be used for the details	Frederick (1899)
<i>Gloss</i>	4 lbs. Of clean water, 1 oz. Of pure curd soap, 1 ½ oz. Pure white beeswax. Polish with cotton	Millar (1899)
	Boil 2 parts stearine, 2 parts Venetian soap, 1 part of pearl ash, 30 parts of a solution of caustic potash and water	Millar (1899), Wager (1963)
<i>Ivory</i>	Rub the surface with paraffin or wax candle and polishing with silk. Beeswax with an equal amount, or a little more, of turpentine, gives a good finish	Frederick (1899)
	White wax dissolved in olive oil, or paraffin wax. Polish with French chalk and cotton wool. If the polished casts are left in a smoky room	Millar (1899)

Table 3.4. (continued)

	Two coats of clear linseed oil, and kept for a while in a smoky room	Millar (1899)
	To apply a coat or coatings, of white polish alone, is the simplest method of giving a slightly ivory and polished appearance to the cast. A little raw umber, yellow ochre or another colour may be added to the polish to give variety and warmth.	Auerbach (1961)
	Little yellow ochre, raw umber or black, applied sparingly just before the final polish, will give an old ivory effect. Rub the colour well into the hollows and wipe off high spots. [...] a final polish with French chalk will give a good lustre	Wager (1963)
	Heat the plaster cast and dip it in stearic acid	de Jonge (1985)
	Indispensable to have gypsum plaster or very white gypsum, the objects must be heated in the oven at 100-120 ° c to make them anhydrous and favour the penetration of waxy substances. They are immersed in a paraffin or stearin bath with spermaceti. The yellowish shade is obtained by dyeing the waxes with traces of bitumen or aniline dyes with fats or Judean bitumen dissolved in turpentine essence	Turco (1990)
<i>Marble</i>	A smooth surface can be obtained by mixing the plaster with a weak solution of gum Arabic. It will have a marble appearance if saturated with milk. Melted stearin can be applied. The finest quality of plaster mixed with turpentine can be used as a paint	Frederick (1899)
	Clean skimmed milk, and with a clean soft brush coat the figure until it will absorb no more. Gently blow off all superfluous milk from the face of the object. Plaster gauged with milk and water will enable the casts to be polished.	Millar (1899)
	Heated bath composed of a solution of brimstone and boiled linseed oil or equivalent oil (in some cases the oils might be omitted). When the articles remain a sufficient time in the heated bath, they are taken out and put into an oven heated to about from 125° to 150° and allowed to remain there two or three days, and gradually cooled off; or they may be put in a paper when taken out of the bath and allowed to stand for about a week in an airy room. After this the articles are polished by the same process as marble is polished, they are taking a very high and smooth polish similar to it. I may add that in experimenting I have added litharge, glue, soda-ash, or potash to the brimstone for boiling the composition in; but I prefer the brimstone alone, or it and boiled linseed or equivalent oils or varnish	Trickey (1884)
	The basic acetates of metallic salts provide the most stable and pleasant colours and also the most suitable for imitating marble	Turco (1990)
<i>Porcelain</i>	White plaster is mixed with magnesium oxide (or zinc) and after complete hardening, the pieces formed are drenched with a solution of phosphoric acid or with calcium acid phosphate. Excellent results are also obtained with aluminium oxide or alumina	Turco (1990)
<i>Silver</i>	Finely ground mica powder mixed with colloidal	Frederick (1899)

Table 3.4. (continued)

<i>Terracotta</i>	Venetian, light or Indian red. It is better to give the cast a coat of white polish first. Start by applying the main colour desired opaquely and then work over the top of this colour with very thin washes, glazes or scumbles of lighter colours, finally using just a little French chalk and a wad of cotton wool. Alternatively, a little powder colour mixed with some glue size to hold it together and a little gilders' whiting (or a touch of titanium white	Auerbach (1961)
	The plaster is mixed with slaked fat lime in small quantities and mixed with a dilute solution of iron sulfate. Particular nuances can be obtained with further surface treatments	Turco (1990)
<i>White</i>	[...] white lead thinned with turpentine is preferred by many to zinc white. [...] lead does not have the whiteness of the zinc, but it can be applied much more quickly	Frederick (1899)
	Give it a coat of linseed oil, and give another coat, and French polish. Make smooth with white size, and varnish with hard white varnish.	Millar (1899)
<i>Wood</i>	To make a model look like wood, varnish the plaster with wax or wood stain	de Jonge (1985)

p. = part(s). The recipes are retrieved from the sources analysed for this study. Quantities, concentration, and percentages are quoted from the original recipes. Most often is not defined whether the % concentration is in weight or volume. The lack of detailed instruction in the original source could be overcome only by reproducing and testing the recipes. More information is available in Appendices 3 and 4.

Table 3.5. Summary of the materials encountered in the historical sources reviewed for this study and their intended purpose.

MATERIAL	PURPOSE	REFERENCE
Alum solution at 90 °C	Hardening	Wager (1963)
Aluminium soap in turpentine and petrol essence	Waterproofing	Turco (1990)
Alum, white soap, Arabic gum, gelatine and water	Waterproofing	Turco (1990)
Ammonia solution, alkaline borates and salts	Hardening	Turco (1990)
Ammonium phosphate and oxalate	Sealing the pores	Turco (1990)
Ammonium tetraborate solution	Hardening	Turco (1990)
Animal or vegetable oils	Sealing the pores	Turco (1990)
Baryta water	Waterproofing, hardening	Millar, (1899), Kemp (1912), Turco (1990)
Barium chloride	Sealing the pores	Turco (1990)
Barite and oxalic acid	Waterproofing, hardening	Turco (1990)
Beeswax and curd soap	Polishing	Millar, (1899)
Beeswax, glycerine and turpentine	-	Wager (1963)
Boiled linseed oil	-	Auerbach (1961)
Borax (biborate of soda)	Hardening	Laxton (1887)
Borax, alum and salts of barium, calcium or strontium	Waterproofing, hardening	Millar, (1899)
Borax and water	Hardening	Turco (1990)
Casein with hydrated lime or slaked lime (optional barium peroxide)	Waterproofing	Turco (1990)
Casein, slaked lime, anhydrous sodium carbonate, barium peroxide and water	Waterproofing	Turco (1990)
Calcic casein	Waterproofing, hardening	Turco (1990)
Caustic potash in water and pure silicic acid	Waterproofing, hardening	Millar, (1899), Kemp (1912)
Copal varnish, patent driers and turpentine	-	Millar, (1899)
Dextrin and water	-	Wager (1963)
Drying oils	Waterproofing	Turco (1990)
Fish glue, water, sodium sulphuricinate and stearic acid	Waterproofing	Turco (1990)
Fluates	Sealing the pores	Turco (1990)
Glue and white shellac	Polishing	Frederick (1899)
Greasy and synthetic paints	Sealing the pores	Turco (1990)
Gum, beeswax, and gasoline	Waterproofing, hardening	Zolnay (1910)
Hair lacquer	Sealing the pores	de Jonge (1985)
India rubber and naphtha	-	Millar, (1899)
Lead acetate	Sealing the pores	Turco (1990)
Lead white and turpentine	Colouring	Frederick (1899)
Linseed oil	Imitating	Millar, (1899), Wager (1963)
Linseed oil and litharge	Waterproofing	Wager (1963)
Linseed oil, French chalk, white size	Imitating	Millar, (1899)
Natural and synthetic elastic rubber (dissolved in suitable solvents)	Sealing the pores, waterproofing	Turco (1990)

Table 3.5. (continued)

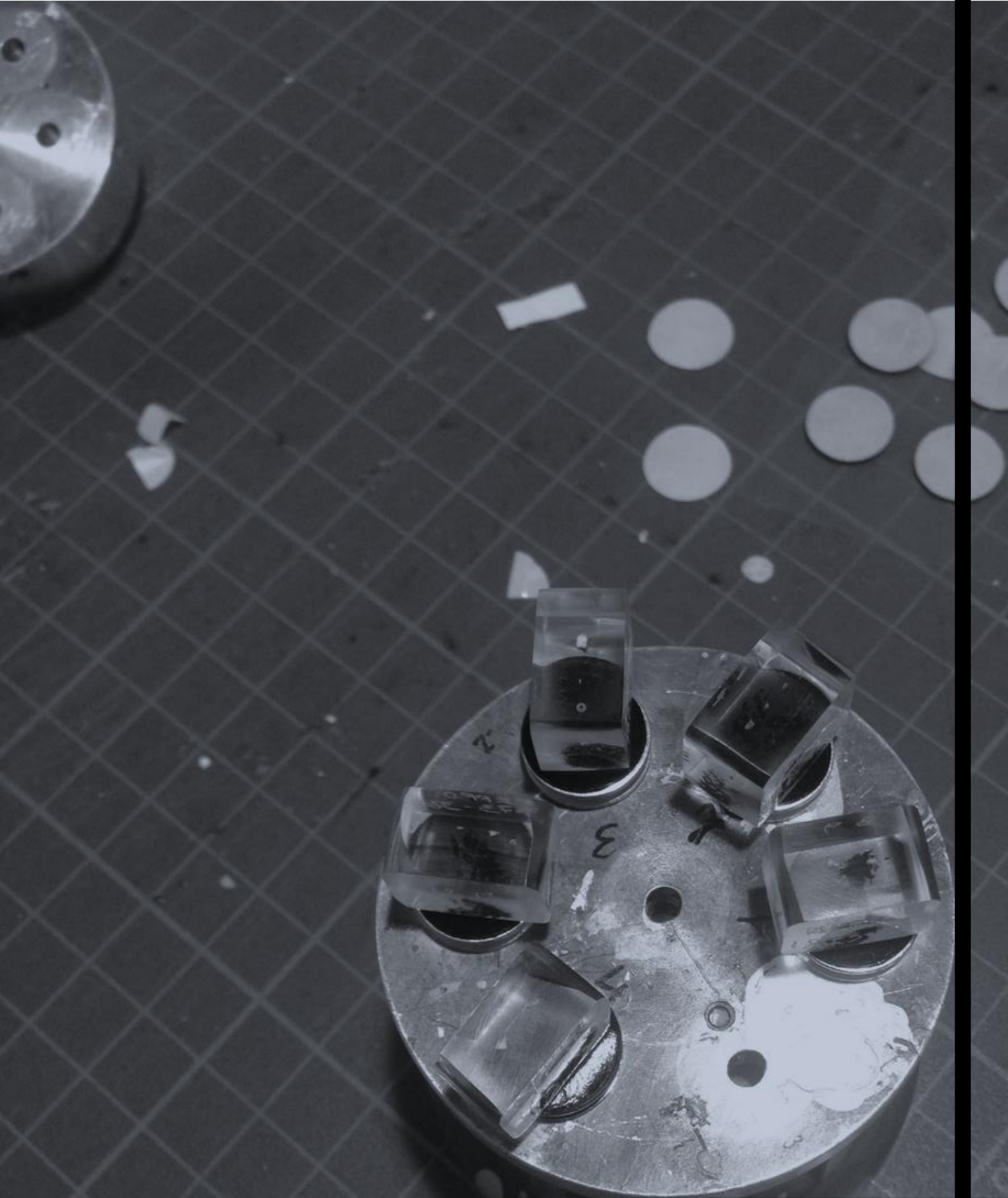
Magnesium fluosilicates	Waterproofing, hardening	Turco (1990)
Mica (calcined) and collodion	Waterproofing	Millar, (1899)
Oil-colours	Colouring	Millar, (1899)
Oily paint, solvent naphtha, carbon tetrachloride, denatured alcohol, soap and water	Waterproofing	Turco (1990)
Oleic acid, ammonia, denatured alcohol, aluminium chloride, calcium chloride and water	Waterproofing	Turco (1990)
Ozocerite, paraffin, olein, morpholine and water	Waterproofing	Turco (1990)
Ozocerite, ammonium linoleate, water, silicone emulsion	Waterproofing	Turco (1990)
Paraffin and oxide of lead	Waterproofing, hardening, colouring	Zolnay (1910)
Paraffin, or stearin, bath with spermaceti and bitumen or aniline dyes with fats or Judean bitumen dissolved in turpentine essence	Imitating ivory	Turco (1990)
Paraffin, ozocerite, white-spirit and toluol	Waterproofing	Turco (1990)
Paraffin, stearic acid, ammonia, silicone emulsion, water	Waterproofing	Turco (1990)
Paraffin, wax candle, beeswax and turpentine	Imitating ivory	Frederick (1899)
Paraffin wax, followed by French chalk	Polishing	Millar, (1899)
Paraffin in white spirit, petrol or petroleum	Polishing	Turco (1990)
Potassium and sodium silicates	Hardening	Turco (1990)
Rosin, water and soda	Waterproofing	Turco (1990)
Shellac and colour	Imitating	Bankart (1908)
Shellac, water and borax (optional linseed oil and turpentine)	-	Millar, (1899)
Silicate solution	Sealing the pores, hardening	Turco (1990)
Skimmed milk	Imitating	Wager (1963), Millar, (1899)
Skimmed milk and water	Polishing	Millar, (1899)
Slaked lime	Hardening	Turco (1990)
Sodium carbonate	Waterproofing, hardening	Turco (1990)
Sodium chloride	Sealing the pores	Turco (1990)
Soaps (stearates, oleate, calcium steropalmitate, iodine, ammonium stearates, etc.)	Sealing the pores	Turco (1990)
Spermaceti in white spirit, petrol or petroleum	Polishing	Turco (1990)
Stearic acid	Imitating ivory	de Jonge (1985)
Stearic acid, caustic soda	Waterproofing, hardening	Millar, (1899)
Stearic acid, soda lye and hot water	Waterproofing	Millar, (1899)
Stearine, Venetian soap, pearl ash, caustic potash	Polishing, hardening	Millar, (1899), Wager (1963)

Table 3.5. (continued)

Sulfates (zinc, ferrous and magnesium)	Hardening	Turco (1990)
Synthetic resins (in solution or emulsion)	Sealing the pores	Turco (1990)
Tin, bismuth, mercury and egg	-	Wager (1963)
Water-colour	Colouring	Millar, (1899)
Wax and turpentine	-	Auerbach (1961), Wager (1963)
Waxes (melted or in solution with appropriate solvents)	Sealing the pores	Turco (1990)
Waxy encaustics or aqueous wax emulsions (alone or with emulsions of white shellac and resins)	Polishing	Turco (1990)
White beeswax and glycerine, followed by French chalk	Polishing	Millar, (1899)
White shellac and methylated spirit	-	Wager (1963)
White shellac, followed by boiled soft soap	Polishing	Millar, (1899)
White wax	Polishing	Millar, (1899)
White wax and olive oil, followed by French chalk	Polishing	Millar, (1899)
White wax and soft soap, followed by French chalk	Polishing	Millar, (1899)
White wax and Venice turpentine	Polishing	Frederick (1899)
White wax in white spirit, petrol or petroleum	Polishing	Turco (1990)
White wax or paraffin	Hardening	Laxton (1887)

3.3. CONCLUSION

This Chapter provides an overview of the manufacturing techniques and the materials used for producing and coating the nineteenth-century plaster casts. The review of the selected recipes' books (*Appendix 3*) and the patents (*Appendix 4*) allowed a better understanding of the availability, application and properties of the materials (see summary in *Table 3.5*) used to produce plaster casts in the nineteenth century. A great variety and quantity of recipes for making and coating the casts were found in the selected historical technical literature (*Section 2.2*). Two types of plaster were consistently described in the literature: lime and gypsum plaster. Gypsum plaster (*Section 3.1.1.3*) is suggested as the most used material for making plaster casts. Four main types of casting techniques were found in the literature, named after the type of moulds they use: waste, gelatine, piece and wax mould. Numerous mineral inclusions are documented in the gypsum plaster mixture (*Section 3.1.1.3*) and inorganic and organic additives can be accidentally or intentionally added to it (*Section 3.1.1.2*). When intentionally added, the additives are intended to accelerate or retard the setting time or improve mechanical properties. Four main types of casting techniques were found in the literature, named after the type of moulds they use: waste, gelatine, piece and wax. A range of separating agents, from oils, soaps and resins to clay water, that may have been used during the casting processes were also listed. The main purposes for applying the coating in the nineteenth century were identified in the historical literature and patents: sealing the pores, waterproofing the surface, hardening the surface, and changing the appearance. Often a type of coat was applied to serve multiple purposes. A list of materials that can be found in the surface layer(s) of the historical plaster casts is finally provided. More than eighty organic and inorganic materials, pure or in combination with each other's, were mentioned in the over a hundred recipes found in the selected literature. Knowledge of the historical techniques, as based on the selected historical literature, provides the researcher with the necessary background to support the characterization of the materials found in the museum objects (*Chapter 4*). Moreover, considerations on the properties and interaction of the materials will support the discussion of the ageing (*Chapter 5*) and cleaning (*Chapter 6*) of the surfaces of the historical plaster casts. This chapter addresses **objectives 2** and **3** described in *Section 1.5.4*.



CHAPTER 4

CHARACTERIZATION OF THE V&A CASTS

4.1. INTRODUCTION

The Cast Courts are the only galleries in the V&A which remained with their original use. They currently house about 350 casts whereas many more are in storage. The casts range in size from over 18 metres tall to only 35 centimetres and over 39 makers have been documented. The methods and recipes used are inevitably varied according to the different makers. Most of the coatings have changed on ageing. Their visual appearance has become darker and their gradual breakdown has resulted in patchy, eroded surfaces (Graepler & Ruppel, 2019). Over the years, the casts have been cared for in various ways. This has ranged from complete dismantling and re-installation, and partial or complete re-coating with paint or tree resins, to a variety of cleaning methods with varying degrees of success. This history, in addition to the variety in the manufacture, contributes to the differences in condition between the objects.

All the above considered, it appears clear how unpredictable is the composition of the surfaces and more generally of the stratigraphy of these understudied objects. As described in *Section 2.3.2* multianalytical approaches have proven effective in studies on similar materials (Blasco-López *et al.*, 2015; Gariani *et al.*, 2018), but still had been limited in their application to the study of historical plaster casts. A multianalytical approach was designed considering the unpredictability of the findings, as supported by the literature discussed in *Section 2.2*, and tested in this chapter. The presented methodology focussed on the characterization of the surface layers of the selected V&A plaster casts. Three groups of objects were selected for the analysis and were identified as Küsthardt Group (*Figure 2.4*), Notre-Dame Group (*Figure 2.5*) and Franchi Group (*Figure 2.6*). The methodology and rationale of the characterization of the V&A casts are described in *Section 2.3*. Optical Microscopy (OM) and Scanning Electron Microscopy (SEM) allowed the definition of the stratigraphy, X-ray diffraction (XRD) and Energy Dispersive Spectroscopy (EDS) the mineralogical and elemental characterization, and Fourier Transformed-InfraRed spectroscopy (FT-IR) and pyrolysis-Gas Chromatography/Mass Spectrometry (py-GC/MS) the identification of the organic components.

4.2. EXPERIMENTAL METHOD

The analyses were chosen to ensure the understanding of the coating materials, which was the purpose of the research. However, a sample of incoherent dirt and dust was taken from the base of *REPRO.1873-380* (*Section 4.3.1*) and a sample of plaster bulk was taken from a deep crack of *REPRO.1873-380* (*Section 4.3.2*) to confirm the expected composition of the substrate. Trace analysis to investigate the provenance of the object were not performed in this study, being beyond the scope. All the samples were taken to represent the stratigraphy of the object from the surface to 0.5-1.0 mm towards the bulk.

4.2.1. SAMPLING

A total of 63 samples (*Table 4.1*) were taken from the selected areas with the aid of brushes, No15 scalpel blades and tweezers. The utmost attention was given to ensure that the samples were collected limiting contamination and stored in chemically clean glass vials. For this reason, vials were kept in clean containers away from dust or other contaminations. The sampling areas were determined by accessibility and the significance of the area. As little quantity as possible was taken, to suffice for the analysis and never larger than 1 mm across, without affecting the appearance of the object. The samples were taken from areas of pre-existing loss and undercuts or marginal areas. Details of the sampling location were noted and accompanied by any relevant observation. The samples' description and location for each of the objects can be found in the individual reports of analysis in *Appendix 6*.

Processing was necessary for some of the analysis of the samples (Colombini & Modugno, 2009; Mills & White, 2012; Singer & McGuigan, 2007) (*Section 4.2.3*). When appropriate, each sample was split into two so that one fragment could be cast in resin and the other could be analysed by other techniques. The fragments that were cast in resin were observed by OM and analysed by SEM-EDS and FT-IR. Unmounted samples were either pulverised for XRD analysis, by lightly and repeatedly squeezing the fragment between two glass slides, or otherwise processed for GC/MS and py-GC/MS analysis (*Section 4.2.3*).

Table 4.1. Sample numbers as related to the Museum number, divided by group.

MUSEUM NO.	TITLE	DATE	SAMPLE NOS.*
Küsthardt Group			
REPRO.1873-380	Copy of a Tombstone	1873	REPRO.1873-380_1 to 13
REPRO.1873-561	Copy of Part of a Choir Screen	1873	REPRO.1873-561_1 to 6
REPRO.1874-29	Copy of a Font	1874	REPRO.1874-29_1 to 6
REPRO.1874-45	Copy of a Tympanum	1874	REPRO.1874-45_1 to 5
REPRO.1875-16	Copy of a statue - Count Ekkehard	1875	REPRO.1875-16_1 to 4
REPRO.1875-17	Copy of a statue - Regilindis, wife of Hermann, Margrave of Meissen	1875	REPRO.1875-17_1 to 4
Notre-Dame Group			
REPRO.1890-80	Copy of a Relief - The Assumption of the Virgin	1890	REPRO.1890-80_1 to 4
REPRO.1890-81	Copy of a Relief - The Coronation of the Virgin	1890	REPRO.1890-81_1 to 4
REPRO.A.1916-3152	Copy of a Relief - The death of the Virgin	1850-1900	REPRO.A.1916-3152_1 to 4
REPRO.A.1916-3153	Copy of a Relief - The Entombment of the Virgin	1850-1900	REPRO.A.1916-3152_1 to 4
Franchi Group			
REPRO.1864-56	Copy of a Relief - The Raising of Lazarus	1851	REPRO.1864-56_1 to 5
REPRO.1864-57	Copy of a Relief - Christ at Bethany	1851	REPRO.1864-56_1 to 4

* The samples were numbered as follows: MUSEUM ACCESSION OBJECT NUMBER_PROGRESSIVE SAMPLE NUMBER.

4.2.2. INSTRUMENTATION

4.2.2.1. Photographic equipment

Regular visible photographs were taken with a Panasonic DCM-FZ38 camera under the gallery's normal illumination (i.e. diffuse lighting, skylight window natural light and mixed artificial illumination). Colour and dimension reference was ensured through the Past Horizons® Credit Card Photography Scale. The images were processed by Adobe Photoshop® CC 19 and white-balanced through the Past Horizons® Credit Card Photography Scale. The objects were also rendered in Autodesk® AutoCAD® 2019 for mapping purposes. Images of the details of the casts and the sampling procedure are shown in *Appendix 6*, along with the AutoCAD® renderings.

4.2.2.2. Microscopies

A StereoZoom® LEICA S6D stereomicroscope was used to observe the samples, to understand the shape of the samples, the position of the layers in the stratigraphy and to decide the processing of the sample. The Leica S6D Stereomicroscope has a 10x eyepiece and the objective magnification goes from 0.63x to 4.00x.

Optical Microscopy (OM) was performed with an Olympus BX51 Metallurgical Microscope equipped with four objectives (magnification of x5, x20, x50 and x100), and an x10 eyepiece. In many instances, a small amount of white spirit was applied on the surface of the cross-section to improve the saturation under the microscope. The microscope is equipped with a 6-cube filter turret which allows to operate the system in reflected visible light (brightfield and darkfield mode) and reflected UV light (365 nm) using a 100 W mercury burner. The attached camera is DP70-12.5 Million Pixel Resolution Digital Camera. The visible images were white processed with the Olympus image software. The magnification was selected for each sample, to achieve the optimal observation of the stratigraphy and the scale defines the samples' dimensions.

Scanning Electron Microscopy coupled with Energy Dispersive Spectroscopy (SEM-EDS) was performed with a field emission TESCAN MIRA 3 with a gigantic chamber. The SEM is equipped with: secondary electron detector (SE), secondary electron in-beam detector (In-beam SE), back-scatter detector (BSE), back-scatter in-beam detector (In-beam BSE), cathodoluminescence detector (without wavelength detection) (CL), plasma chamber/sample cleaner and software Alicona 3D imaging. For the EDS analytical part, it has an Oxford Instruments setup: Software: AztecEnergy, X-ray detector X-Max 150 mm² and X-ray detector X-Max Extreme, low energy detector for thin films, high resolution and low voltage. Most of the samples were analysed by SEM-EDS Low Vacuum Mode (10-15 Pa) and when high vacuum (1.5×10^{-2} Pa) was used, the samples were adhered to the support with silver (Ag) paint and coated with platinum (Pt, 5 nm thick). This special treatment, which could be also done by the application of gold and/or carbon as coatings on its surface, has the purpose of increasing the sample conductivity. EDS Mapping in Low Vacuum Mode and data processing were performed with Aztec Oxford software.

4.2.2.3. X-Ray Diffractometry (XRD)

XRD analyses were performed with a Rigaku SmartLab SE equipped with a HyPix-400, a semiconductor hybrid pixel array detector and a Cu (copper) source. The analyses were performed in Bragg-Brentano geometry mode, with 40 kV tube voltage and 50 mA tube current. The diffractograms were processed with SmartLab II software. The data was compared to RUFF (Lafuente *et al.*, 2016) and COD (Gražulis *et al.*, 2009) databases.

4.2.2.4. *Fourier Transformed-InfraRed Spectroscopy (FT-IR)*

A Perkin Elmer Frontier FT-IR spectrometer (350 cm^{-1} at the best resolution of 0.4 cm^{-1}) was used, equipped with a diamond crystal (refractive index 2.4, depth of penetration $2.01\text{ }\mu\text{m}$ at 45° and 1000 cm^{-1}) for ATR measurements and combined with a Spectrum Spotlight 400 FT-IR microscope equipped with a 16×1 pixel linear mercury cadmium telluride (MCT) array detector standard with InGaAs array option for optimised NIR imaging. Spectral images from sample areas are possible at pixel resolutions of 6.25, 25, or $50\text{ }\mu\text{m}$. The Perkin Elmer ATR imaging accessory consists of a germanium crystal (refractive index 4.0, depth of penetration $0.66\text{ }\mu\text{m}$ at 45° and 1000 cm^{-1}) for ATR imaging. These run with Perkin Elmer Spectrum 10™ software and with SpectrumIMAGE™ software. The spectra obtained from them were interpreted through the aid of databases for conservation materials (Price *et al.*, 2009; Vahur *et al.*, 2016) and studies published on relevant materials (Azemard *et al.*, 2014; Melita *et al.*, 2020; Sarkar & Kumar, 2001; Toniolo *et al.*, 2009).

FT-IR imaging has emerged as an excellent new analytical approach to the study of cross-sections and complex specimens (Prati *et al.*, 2010; Van der Weerd *et al.*, 2002; van Loon & Boon, 2004) and reflectance techniques may be used for samples that are difficult to analyse by the conventional transmittance method (Khoshhesab, 2012). This technique provides information about the spatial distribution of characteristic functional groups in a cross-section. A false colour plot is used to represent the distribution of a particular absorption band across the surface of different colours. The spectra were plotted in absorbance rather than in percent transmission for several reasons: humans are better in interpreting upward-facing peaks than downward-facing peaks and absorbance is plotted in a logarithmic scale (this enables to detect weak signals next to very strong ones), which is traditionally used in the case of quantitative analysis, and might be necessary to appreciate small contributions in the complex spectra of the museum objects (Derrick *et al.*, 2000; Stuart, 2007). The Kubelka Munk (KM) transformation is the most often used theory to describe and analyse diffuse reflectance (DR) spectra and it was applied to all the spectra acquired in DR mode. For most materials, the reflected energy is only 5–10 %, but in regions of strong absorptions, the reflected intensity is greater. As the samples selected for this study mostly consist of inorganic materials with an expected small contribution of organic material, small organic vibrations are expected in the IR spectrum.

The FT-IR spectra acquired in diffuse reflectance from the cross-sections show broad bands rather than sharp and defined peaks, due to the complexity of the mixtures containing several components and to the several diffuse reflections. The overlapping of the contributions of bending and stretching vibrations of organic and inorganic components and the variety of components in the sample constitute the challenge of the characterization of these materials.

4.2.2.5. *pyrolysis- Gas Chromatography/Mass Spectrometry (py-GC/MS)*

The instrument is a Thermo Focus Gas Chromatographer with DSQ II single quadrupole mass spec using Electronic Ionisation (EI). The column currently installed is an Agilent DB5-MS UI column (ID: 0.25 mm, length: 30 m, df: 0.25 μ m, Agilent, Santa Clara, CA, USA). Carrier gas: helium. Detector temperature: 280 °C, Injector temperature: 250 °C. It can be used with the Pyrola 2000 Platinum filament pyrolyser (PyroLab, Sweden) attachment or in split/splitless mode. Detection: Total Ion monitoring (TIC).

1 μ l of the sample was injected directly into the column for the GC/MS and placed on the Pt filament for the py-GC/MS. The inlet temperature to the GC was kept at 250 °C. The helium carrier gas flow rate was 1.5 ml/min with a split flow of 41 ml/min and a split ratio of 27. The MS transfer line was held at 260 °C and the ion source at 250 °C. The pyrolysis chamber was heated to 175 °C, and pyrolysis was carried out at 600 °C for 2 s for all the samples.

Thermal Programme (1). (PaintpyrolysisTMAH30m.meth) Seg1 start at 2.40 Scan events MS, Heated zones Ion Source 250 °C, Detector Gain $1.21 \cdot 10^5$ (Multiplier Voltage 1025 V). Oven: Initial temp 40 °C hold 4 minutes Ramp 1 10.0 °C/min (rate), until 250 °C, hold 15 min. Mode: splitless.

Thermal Programme (2). (PaintpyrolysisTMAH30m.meth) Seg1 start at 2.40 Scan events MS, Heated zones Ion Source 250 °C, Detector Gain $1.21 \cdot 10^5$ (Multiplier Voltage 1025 V). Oven: Initial temp 40 °C hold 4 minutes Ramp 1 10.0 °C/min (rate), 250 °C, hold 45 min.

Thermal Programme (3). (ProteinBM_Valentina.meth) Seg1 start 13.00 Scan events MS, Heated zones Ion Source 250 °C, Detector Gain $1.21 \cdot 10^5$ (Multiplier Voltage 1025 V). Oven: Initial temp 60 °C hold 2 minutes Ramp 1 6.0 °C/min (rate), 250 °C, hold 0 min. Ramp 2 25 °C/min, 300 °C, 20 min hold. Mode: split

The acquisition was carried out in a Total Ion Count mode, where all ions in the range 38-550 m/z were monitored. The data were examined and processed using Thermo Scientific XcaliburTM 2.2 version.

4.2.3. SAMPLE PROCESSING

4.2.3.1. Processing for stratigraphy observation and analysis

The resin used for embedding samples was Alec Tiranti® Ltd clear casting resin: a Clear Casting Resin AM– Styrene ($C_6H_5CH=CH_2$) and Methyl methacrylate ($CH_2=C(CH_3)COOCH_3$) / Polyester Resin (Product Code: 405-210) and Liquid Hardener 50g - BUTANOX M-50 Methyl ethyl ketone peroxide (MEKP), solution in dimethyl phthalate ($(C_2H_3O_2)_2C_6H_4$ (Product Code: 405-810) in a ratio of 4 mL : 50 μ L. The resin required 48 hrs to cure. A rubber mould was produced with Alec Tiranti® RTV-101 Silicone Rubber and Cat '28' (CA28 curing agent). It was made to cast the samples in a cube-like shape (ca. 3.0x3.0x1.5 cm), which would provide the support of samples by ensuring that the sample stratigraphy is parallel to the surface where the cube is positioned onto.

The fragments were positioned in the mould in a way that the stratigraphy would be parallel to the surface that would be exposed by polishing and then embedded in resin. However, being the samples extremely small and made of a porous material, they often moved during the curing and hardening of the resin making the positioning of samples challenging. As shown in *Figure 4.1*, the samples were observed under the stereomicroscope and positioned (surface layers facing down and as close as possible to the shape side chosen for the sample observation) in the hole half-filled with dry resin. Then, the samples were covered with the resin until filling the cube-shaped rubber mould. After curing, the resin 'cubes' were extracted from the mould and polished with a polisher/grinder Metaservice 2000 using Buehler CarmbiMet Carbide SiC abrasive paper, from 180 Grit, to 600 and finishing with the 1000 Grit. The final polish was obtained with nylon paper and Alumina suspension (Agar Scientific Micropolish Alumina 0.3 μ m – B8226). It was observed that the transparency of the cubes was somehow affected by temperature, being opaquer during the colder days (samples of REPRO.1864-56 and 57, REPRO.1890-80 e 81).

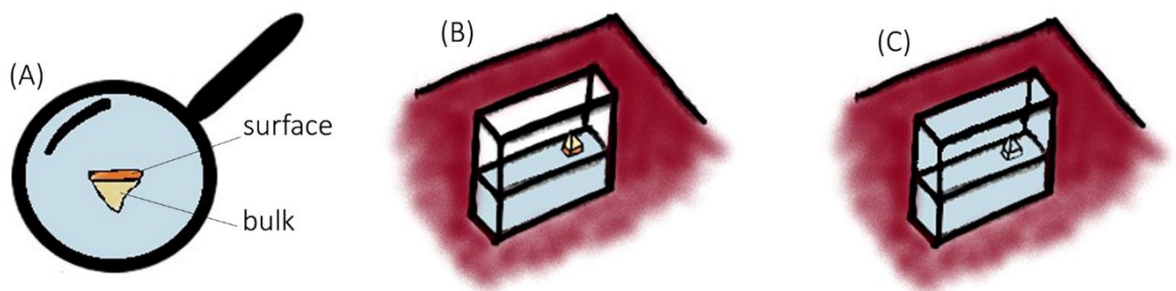


Figure 4.1. The image summarises the steps performed to cast the samples in polyester resin. The sample was observed under the stereomicroscope (A), positioned in the hole half-filled with dry resin (B) and covered with casting resin until filling the whole cube-shaped hole (C).

4.2.3.2. Processing for GC/MS and py-GC/MS

Due to the unknown composition of the samples, more than one method found in the scientific literature for GC/MS and py-GC/MS was experimented (*Section 2.2.3*) (Colombini & Modugno, 2009; Mills & White, 2012; Singer & McGuigan, 2007). The methods assigned to the different samples are summarised in *Table 4.2*. A brief description of the GC/MS program and the samples' quantities are also provided in *Table 4.2*, while described in *Sections 4.2.2.5* and *4.2.3.2*. The samples were processed in Thermo Scientific™ Reacti-Vials™, which are small Glass Reaction Vials, resistant to heat and reagents.

Sample preparation for GC/MS:

- **Derivatization with *n*-propanol and pentafluoropropionic anhydride (PFPA)**

Mills & White (2012) suggest a method by which is possible to prepare methyl esters of the acids and convert the amino groups to their trifluoro-acetates. Singer & McGuigan (2007) suggest the use of *n*-propanol followed by pentafluoropropionic anhydride (PFPA) to facilitate the simultaneous analysis of both fatty acids and amino acids in acid hydrolysates of egg tempera and other mixed artists' paint media. This application has also proven effective in the detection of the oxidised diterpenoids which, if found, are an indication of the presence of pine resin. The amino acids are analysed as *N*-pentafluoropropionyl *n*-propyl esters and the fatty acids and diterpenoid acids as *n*-propyl esters. This combination of reagents allows the amino acids to completely elute before the appearance in the chromatogram of the propyl esters of the fatty acids and diterpenoids which allow the analysis of lipids and resin. For the extraction 1N sulphuric acid is usually used with heating at 100°C for 10-12 hrs (Mills, 1966; Mills & White, 2012; Singer & McGuigan, 2007).

PROCESS: 1 mg of sample, ground between two glass slides, was pulverised and placed in Reacti-Vial. 150 µL of Hydrochloric acid (HCl) were added to hydrolyse the sample (Reacti-Vial cap on during this step). Nitrogen was used to remove the excess Oxygen in the vial. The vial was left in a heating block at 90°C for 3 days, the vial was put in a glass vacuum desiccator for 24 hours to remove the acid. 180 µL of propan-1-ol : acetyl chloride (3:1) were added in the Reacti-Vial, the sample was heated at 110 °C for 45 minutes (cap on), the temperature was lowered to 50°C for about 30 min, the cap was removed and the vial was filled with nitrogen to vaporise the reagent excess and dry out the sample. The residue was dissolved in 50 µL 0.2% pyridine. 150 µL of dichloromethane (DCM) and 150 µL perfluoropropionic anhydride (PFPA) were added and the sample was heated at 110°C for 15 minutes (cap on).

Sample preparation for py-GC/MS:

- Methylation with Tetramethylammonium hydroxide (TMAH)** is one of the most used reagents for online methylation of acidic and alcoholic moieties. Pyrolysis in the presence of TMAH gives rise to the hydrolysis of ester bonds, followed by the formation of tetramethylammonium salts, which are subsequently subjected to thermal dissociation, leading to the formation of the corresponding methyl derivatives (*Figure 4.2*). Although the TMAH thermochemolysis (TMH) method has been extensively applied to the characterisation of materials used in the realisation and restoration of works of art, the strong alkalinity of TMAH may cause problems in the interpretation of pyrograms. The main limitations of this technique are related to decarboxylation reactions undergone by carboxylic acids, the isomerisation of polyunsaturated fatty acids, the formation of dehydration products, and the α -methylation of acidic moieties. TMAH can also induce decomposition of the stationary phase of the gas chromatographic column (Challinor, 1991; Challinor, 2001).

PROCESS: The sample was ground between two glass slides and about 0.5 mg were positioned onto the Pt filament and directly derivatised in an aliquot of 1 μ l of 25 % (wt) in methanol tetramethylammonium hydroxide.

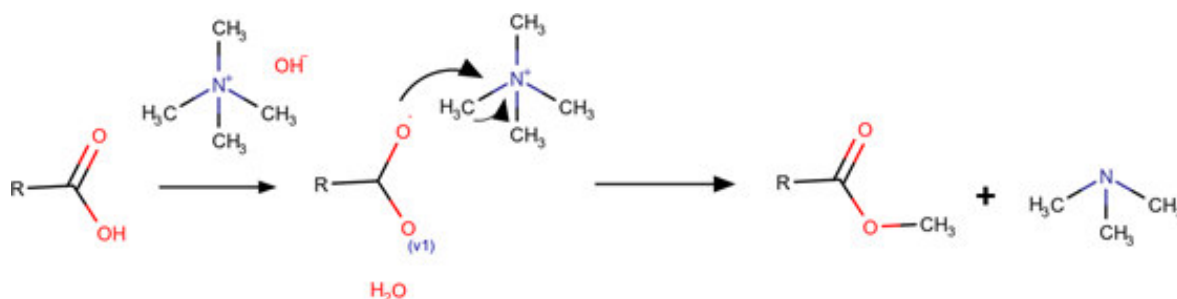


Figure 4.2. Proposed mechanism of methylation of carboxylic acids with TMAH.

- Methylation with 3-trifluoromethylphenyltrimethylammonium hydroxide**
 3-Trifluoromethylphenyl trimethylammonium hydroxide has been used in a 5% solution aqueous solution and also as a 5% solution in methanol as a reagent to derivatise lipids in biological mixtures by converting triglycerides into the methyl esters of fatty acids. The methanolic reagent, available commercially as MethPrep II (5% wt in Methanol, CAS number 68254-41-1, C₁₀H₁₄F₃NO m-TFPTAH) has since been widely used for the analysis of artists' media where it is useful for the analysis of both seed oils and natural resins which contain diterpenoid acids or triterpenoid acids such as moronic acid from mastic. The reagent is alkaline and will therefore hydrolyse the lipid polymer present in dried artists' paint films to yield the 3-trifluoromethylphenyltrimethyl ammonium salts of

the saturated fatty acids cleaved from the polymer. The fatty acid salts of this compound are then converted to fatty acid methyl esters (FAME, type of fatty acid ester that is derived by transesterification of fats with methanol) at a lower temperature, about 200-250°C which is the typical temperature of the injection port in an ordinary GC and hence the pyrolysis attachment is not necessarily required. At 250°C, the typical temperature of the injection port of a GC instrument, the salt will yield the methyl esters of the fatty acids via a nucleophilic substitution reaction (Figure 4.3). According to Singer & McGuigan (2007), this method is routinely used to analyse oils and resins from painted or varnished art objects. However, the method will not detect amino acids or proteins (Singer & McGuigan, 2007).

PROCESS: method (1). 1-3 drops of MetPrep II, depending on sample size, is added to the sample in a Reacti-Vial. The solution was heated gently in a heating block set at 60°C for 24 hours; method (2). 0.3 mg of sample in 30 µl of MetPrep II is heated gently in a heating block set at 60°C for 24 hours in a Reacti-Vial.

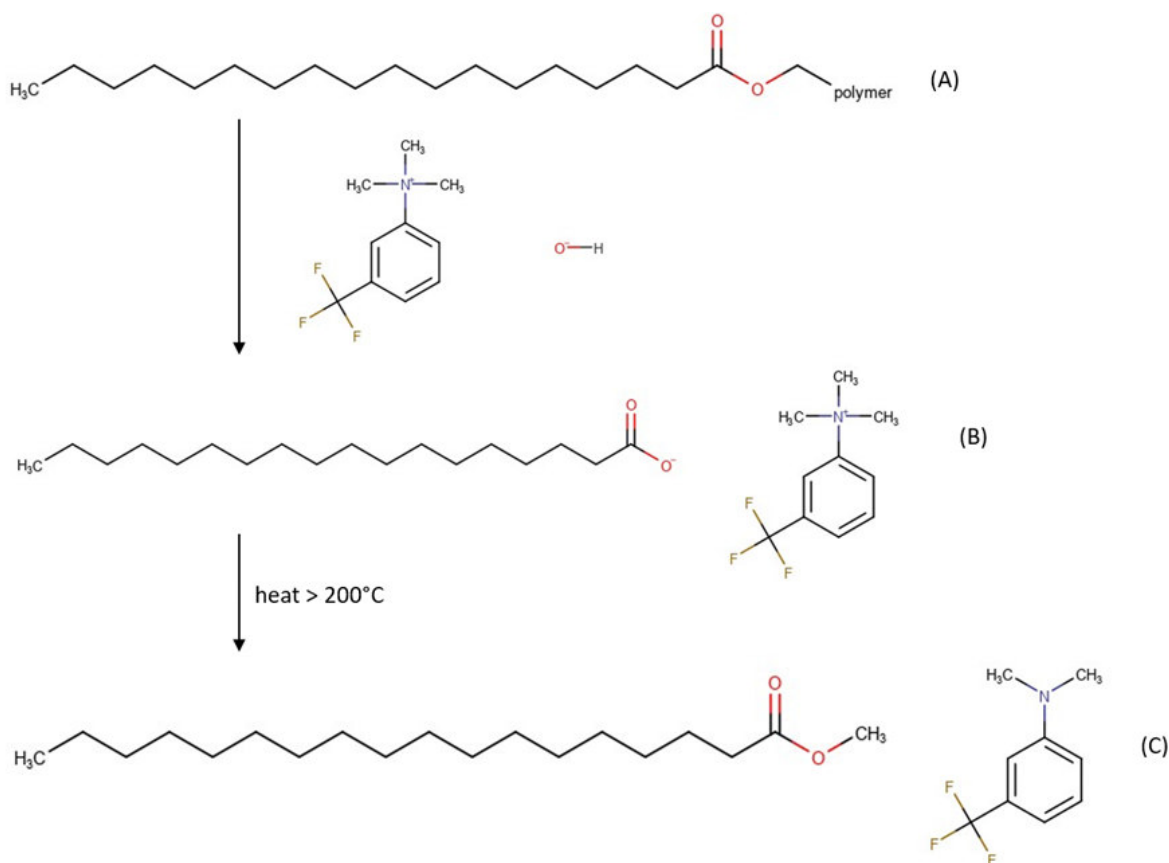


Figure 4.3. Proposed mechanism of methylation with 3-(Trifluoromethyl)phenyltrimethylammonium Hydroxide (A → C).

Table 4.2. Summary of methods used for GC/MS samples preparation and equipment settings.

SAMPLE	SAMPLE PREP METHOD	THERMAL PROGRAMME
REPRO.1873-380_2-02	Py-TMAH-GC/MS, 2 µl Meth Prep II (2) solution, 1 µl TMAH	(1)
REPRO.1873-380_3-01	Py-TMAH-GC/MS, 1 µl TMAH	(1)
REPRO.1873-380_3-02	Py-TMAH-GC/MS, 1 µl TMAH	(1)
REPRO.1873-380_3-03	Py-TMAH-GC/MS, 5 µl Meth Prep II (2) solution, 1 µl TMAH	(1)
REPRO.1873-380_3-04	Py-TMAH-GC/MS, 10 µl Meth Prep II (2) solution, 1 µl TMAH	(1)
REPRO.1873-380_3-05	Py-TMAH-GC/MS, 10 µl Meth Prep II (2) solution, 1 µl TMAH	(1)
REPRO.1873-380_4-01	Py-TMAH-GC/MS, 1 µl TMAH	(1)
REPRO.1873-380_4-02	GC/MS, 1 µl PFPA solution	(3)
REPRO.1873-380_4-03	GC/MS, 1 µl PFPA solution	(3)
REPRO.1873-380_4-04	GC/MS, 1 µl PFPA solution	(3)
REPRO.1873-380_5-01	Py-TMAH-GC/MS, 1 µl Meth Prep II (1) solution, 1 µl TMAH	(1)
REPRO.1873-380_5-02	Py-TMAH-GC/MS, 2 µl Meth Prep II (2) solution, 1 µl TMAH	(1)
REPRO.1873-380_8-01	Py-TMAH-GC/MS, 1 µl Meth Prep II (1) solution, 1 µl TMAH	(1)
REPRO.1873-380_8-02	Py-TMAH-GC/MS, 2 µl Meth Prep II (2) solution, 1 µl TMAH	(1)
REPRO.1873-380_9-01	Py-TMAH-GC/MS, 1 µl Meth Prep II (1) solution, 1 µl TMAH	(1)
REPRO.1873-380_9-02	Py-TMAH-GC/MS, 2 µl Meth Prep II (2) solution, 1 µl TMAH	(1)
REPRO.1873-380_10-01	GC/MS, 1 µl PFPA solution	(3)
REPRO.1873-380_10-02	GC/MS, 1 µl PFPA solution	(3)
REPRO.1873-380_11-01	GC/MS, 1 µl PFPA solution	(3)
REPRO.1873-380_11-02	GC/MS, 1 µl PFPA solution	(3)
REPRO.1873-380_13-01	Py-TMAH-GC/MS, 2 µl Meth Prep II (2) solution, 1 µl TMAH	(1)
REPRO.1873-380_13-03	Py-TMAH-GC/MS, 2 µl Meth Prep II (2) solution, 1 µl TMAH	(1)
REPRO.1864-56_2-01	Py-TMAH-GC/MS, 2 µl TMAH	(2)
REPRO.1864-57_4-01	Py-TMAH-GC/MS, 2 µl TMAH	(2)
REPRO.1873-561_6-01	Py-TMAH-GC/MS, 2 µl TMAH	(2)
REPRO.1874-29_4-01	Py-TMAH-GC/MS, 2 µl TMAH	(2)
REPRO.1874-45_2-01	Py-TMAH-GC/MS, 2 µl TMAH	(2)
REPRO.1875-16_4-01	Py-TMAH-GC/MS, 2 µl TMAH	(2)
REPRO.1875-17_3-01	Py-TMAH-GC/MS, 2 µl TMAH	(2)
REPRO.1890-80_4-01	Py-TMAH-GC/MS, 2 µl TMAH	(2)
REPRO.1890-81_4-01	Py-TMAH-GC/MS, 2 µl TMAH	(2)
REPRO.A.1916-3152_3-01	Py-TMAH-GC/MS, 2 µl TMAH	(2)
REPRO.A.1916-3153_3-01	Py-TMAH-GC/MS, 2 µl TMAH	(2)

4.2.4. DATABASE FORMATION

An analysis report for each of the objects analysed was provided for dissemination within the V&A conservators and curators and can be seen in *Appendix 6*. Individual datasets for the analysis were also deposited in the Northumbria University Figshare repository (see *List of accompanying material and publications*). A full database of results in a spreadsheet format and with plots and images was compiled and deposited, to make the research outputs available in a citable, shareable and discoverable manner (Risdonne & Theodorakopoulos, 2021).

4.3. RESULTS AND DISCUSSION

It was observed in other studies that several layers could constitute the stratigraphy of the historical plaster casts. For example, Ángeles Solís Parra described in Graepler & Ruppel (2019) that from one to five layers were identified on historical plaster casts. All the samples analysed for this study consistently showed at least three layers in the stratigraphy: the bulk, an interface layer, and a surface or coating layer (*Figure 4.4*). Several samples showed more layers as sampled from areas of repairs or having additional varnish layers (*Section 4.3.4*).

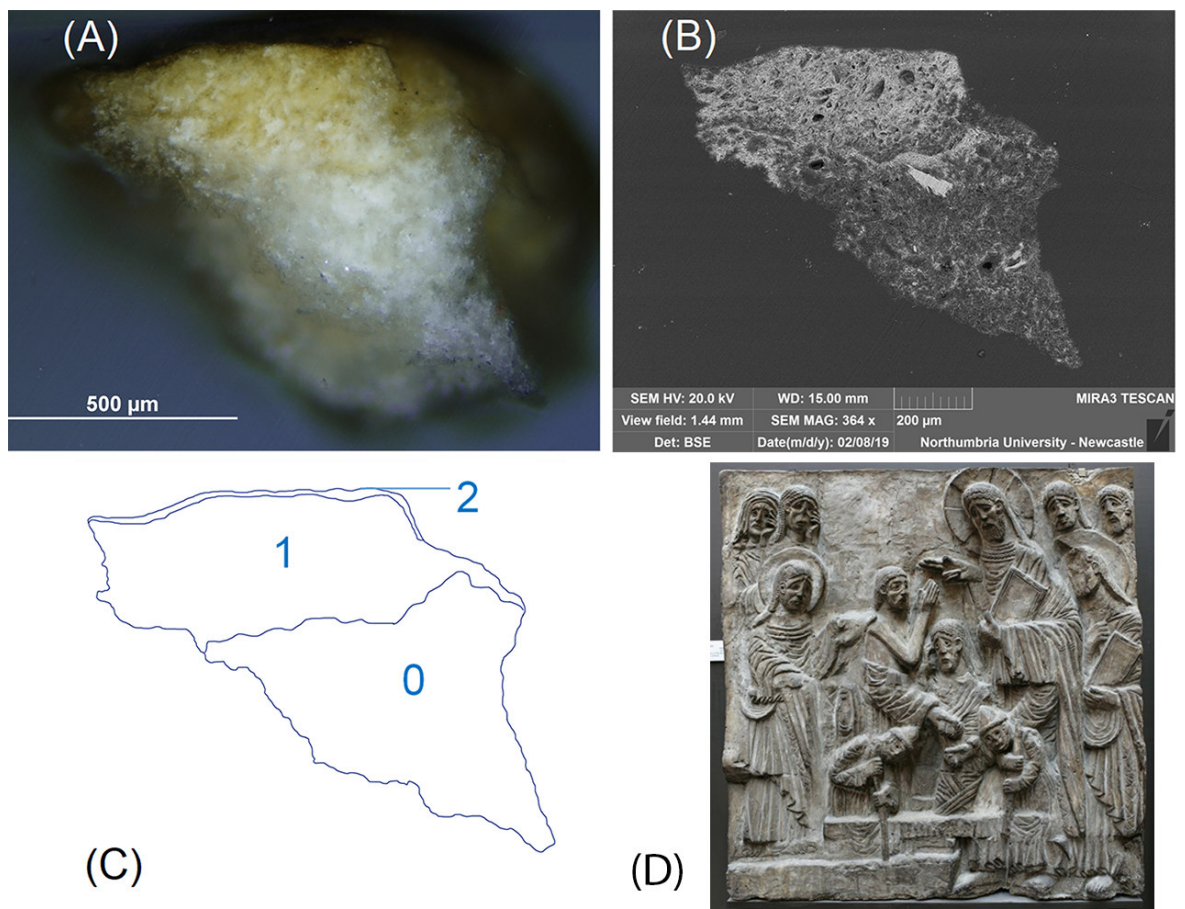


Figure 4.4. VLR OM (A) and BSE (B) images and outline of the layers (C). Sample 4 taken from REPRO.1864-57 (D) (Raising of Lazarus, object dimensions 122.0X117.0 cm) clearly shows the substrate (plaster bulk, layer 0) and the coating (layer 2). Layer 1 is the interface, where the coating has penetrated the plaster bulk (yellow under VLR and denser in the BSE image).

The coating layers are not well defined and visible in the stratigraphy. Most often, the outermost layer appears dark under visible illumination, as the portion of the coating that was exposed to the environment reacted with the air, pollutants and UV radiation resulting in the oxidation of the coating. A large portion of the coating appeared to be absorbed by the porous plaster bulk and it was identified as an interface layer. The interface was observed in the VLR and UVf images, but also in the BSE images: the coating, by filling the

pores or hardening the surface of the cast made the gypsum plaster 'denser'; it is also possible that the outer portion is of a different quality of plaster than the bulk, and would then appear slightly different from the rest of the bulk, although the elemental composition is the same (Figure 4.5).

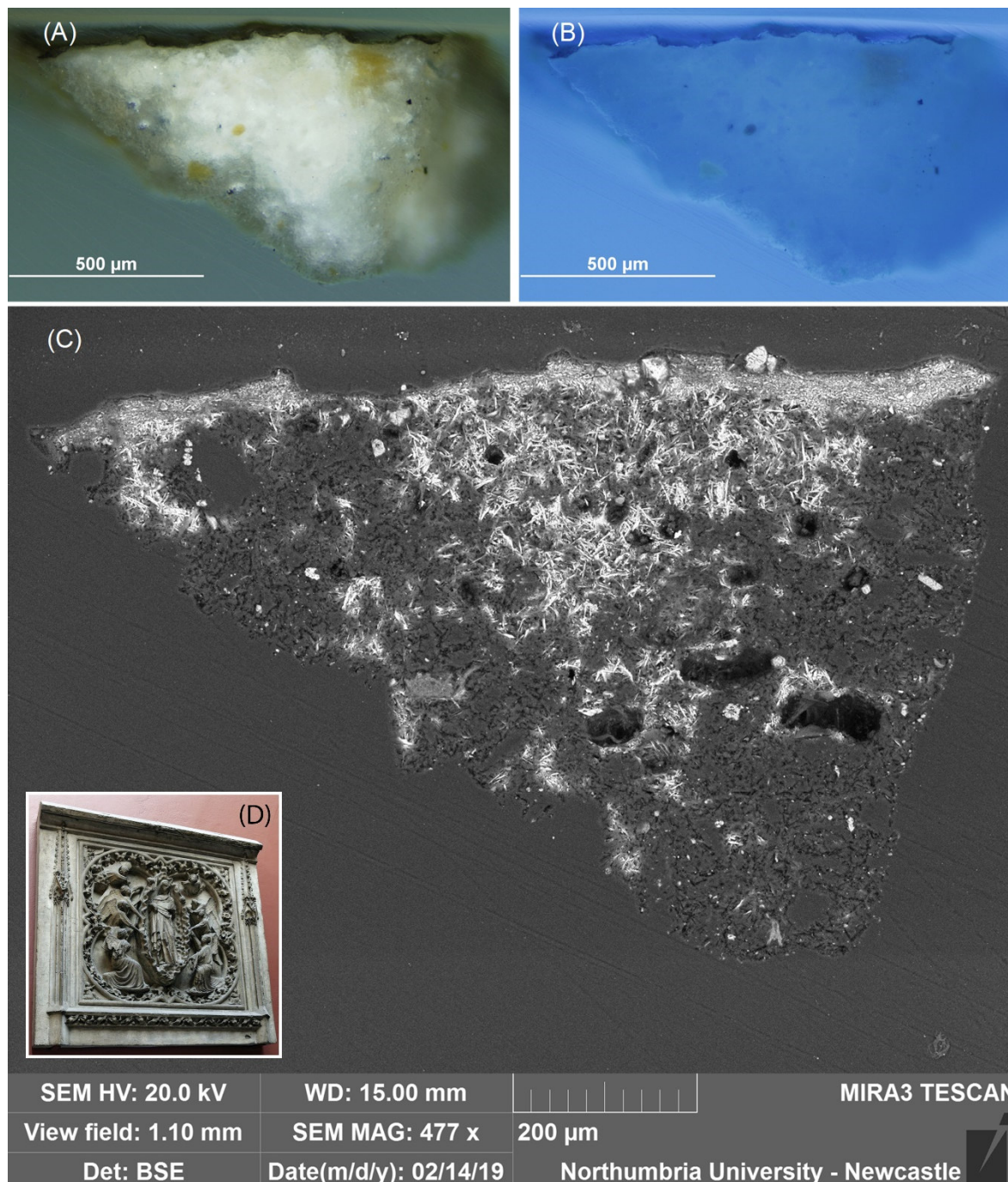


Figure 4.5. In sample REPRO.1890-80_2 no differences in the elemental distribution were observed but the top layer appears denser. VLR (A), UVf (B) and BSE (C) images. The sample was taken from REPRO.1890-80 (D) (Assumption of the Virgin, object dimensions 152.5X160.0 cm).

4.3.1. DUST

Dust in museums' galleries might consist of fine particles of textile, skin, soot, silica and salt crystals, which can move from place to place and settle on the surface of an object (Coon, 2009; Thomson, 2013). Particles that enter from outside the museum are produced by burning fuels and are tarry, sooty and acidic as they absorb sulfur dioxide (SO₂) and can contain traces of metals causing further deterioration on the surface and catalyse chemical reactions on surfaces (Hackney, 1984; Thomson, 2013). Dirt can be dust that has bound firmly to a surface as well as grease from other sources which changes the appearance of an object (Coon, 2009).

The characterization of the dust, dirt, grime and other deposits was beyond the scope of this study. Nonetheless, the deposits on REPRO.1873-380 were sampled (sample REPRO.1873-380_1) and analysed to have a better understanding of the contaminants present in Gallery 46A and, eventually, be able to discriminate which elements found on the surface can be traced back to the environmental dust in the galleries. Under the microscope, the deposits seemed to comprise fibres of various colours (red, green, blue), as shown in *Figure 4.6*. Despite the complexity of the signal, ATR/FT-IR analysis (*Figure 4.6* and *Table 4.3*) highlighted that the dust is made of: sulfates, showing the asymmetric bending modes and symmetric and asymmetric stretching of SO₄²⁻, and the ν_2 H₂O of the sulfates (Melita *et al.*, 2020; Miliani *et al.*, 2012), carbonates indicated by the out-of-plane bending and asymmetrical stretching vibration peaks of O–C–O (Hajji *et al.*, 2017; Melita *et al.*, 2020) and unidentified organic material(s) indicated in the 1200-1300 cm⁻¹ area (ν CN), amine peaks, the CO vibration signal and the CH vibrational modes (Derrick *et al.*, 2000; Vahur *et al.*, 2016).

Table 4.3. ATR/FT-IR peaks identified in the spectra acquired in the dust sample (REPRO.1873-380_1).

Peaks (cm ⁻¹)	Assignment
435	δ SO ₄ ²⁻
600	δ SO ₄ ²⁻
667	δ SO ₄ ²⁻
875	out-of-plane δ O–C–O
1005	ν SO ₄ ²⁻
1105	ν SO ₄ ²⁻
1360	ν CN aromatic amine
1425	ν O–C–O
1580	δ NH of amine I
1620	ν_2 H ₂ O
1680	ν_2 H ₂ O
1714	ν CO of esters
2852	ν CH
2917	ν CH

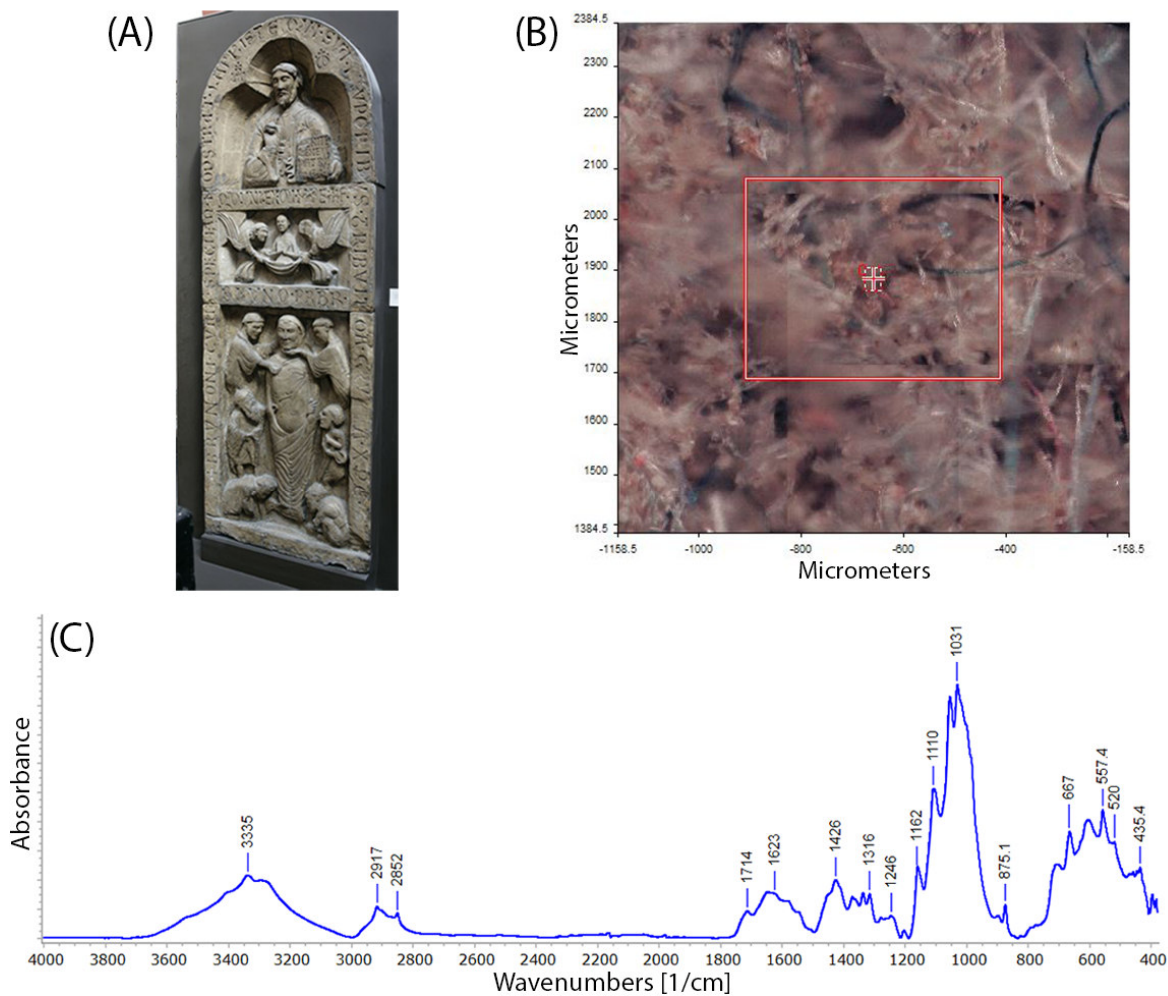


Figure 4.6. Sample 1 was taken from REPRO.1873-380 (Tombstone of the Presbyter Bruno, object dimensions 218.5X77.0 cm) (A). Fibres of different colours are visible in the micrograph (B) taken with the FT-IR microscope. ATR/FT-IR analysis of the dust (C) shows the presence of several contributions including sulfates, carbonates and organic material. Assignment of significant peaks can be seen in Table 4.3.

Overall, the presence of sulfates and carbonates can be justified by material generated during building works, and the fibres and organic contribution may have been derived from visitors (fibres and other residues of human interaction - skin, oils and as such) (Derrick *et al.*, 2000; Kumar & Rajkumar, 2014; Price *et al.*, 2009).

Previous research on the assessment of surface cleaning techniques in the V&A was based on the presence of gypsum in the material removed by cleaning techniques under assessment, to ensure that the removal of the dirt did not accidentally also partially tackle the plaster substrate (Hubbard & Pretzel, 2016). Due to such relevant sulfate contribution in the dust, it appears that such an approach to the assessment of the cleaning cannot be considered consistent.

4.3.2. PLASTER BULK

An understanding of the composition of the bulk of the objects was necessary to discriminate the materials belonging to the bulk from the ones deriving from the coatings. As in all the samples the 'substrate' or 'plaster bulk' was analysed as part of the stratigraphy in the cross-section, one sample (REPRO-1873-380_2) was taken from a deep crack of the casts, hoping that it would be representative of the bulk only.

As suggested by the historical sources (*Section 3.1.1*) and previous studies (Jones, 2011; Mahmoud *et al.*, 2012; Megens *et al.*, 2011), it was expected that the plaster bulk would consist of dihydrate calcium sulfate (gypsum plaster), with some quantity of contaminants (at the mineral level or deriving from the manufacturing) and additives (inorganic and organic). Isella *et al.* (2017), for example, analysed casts and found that calcium sulfate dihydrate ($\text{CaSO}_4 \cdot 2\text{H}_2\text{O}$) constituted 90% of the bulk together with traces of quartz (SiO_2) and bassanite (calcium sulfate mineral), a small percentage of organic material and calcite (CaCO_3) and rutile (TiO_2) in the upper layers, possibly deriving from historical or modern coatings. Phosphorus (P), magnesium (Mg), silicon (Si) and aluminium (Al) were also detected on the surface, possibly due to the presence of newberyite $\text{Mg}(\text{HPO}_4) \cdot 3\text{H}_2\text{O}$, as a deterioration product. On the other hand, Melita *et al.* (2020) identified a plaster cast belonging to the British Museum collection as made of lime plaster and Gariani *et al.* (2018) found that the Renaissance *stucco* Madonna composition was closer to the gypsum plaster cast, whereas they were expected it to be made of lime plaster.

REPRO-1873-380_2 was studied under the SEM in high vacuum mode, which provided higher resolution and magnification than the low vacuum mode (*Figure 4.7*). The drawback of the high vacuum mode is that non-conductive samples must be coated with a thin layer of conductive coating (Pt in this analysis) which would make the sample not reusable for other types of analysis. The *tabular* structure of the gypsum plaster was recognised in high vacuum in this sample, but it was also visible in the plaster bulk of almost all the samples analysed in low vacuum mode (*Figure 4.7*). Despite the shape of the crystals observed in the BSE images being consistent with gypsum plaster, it cannot be uniquely identified by its crystals' shape alone. EDS spectra (*Figure 4.8*) showed calcium (Ca), sulfur (S), and oxygen (O) in all the samples, suggesting calcium sulfate, and other elements were also observed, depending on the sample. Gypsum is a sedimentary rock; unlike igneous rocks, most sediments are made up of a very small selection of minerals, of which quartz, feldspars, clay minerals and carbonates and sulfates are by far the most important (Cox *et al.*, 1974). Gypsum shows a tabular crystallization – crystals somewhat flattened in one direction, which is also common in barite and feldspars. The continuous readjustment of sedimentary minerals causes the contaminations and impurities found in these materials' quarries. Silica in sediments is largely held in quartz (SiO_2), while the alumina is concentrated in clay

minerals and feldspars. The arenites (sandstone) are siliceous sediments composed mainly of quartz. Limestones, including dolomite (Mg-rich carbonate rocks), comprise some 25 wt% of sedimentary deposits. The term limestone is commonly used for rocks containing 50 wt% or more of calcium carbonate (Cox *et al.*, 1974). Celestite (SrSO_4) is also a common impurity in gypsum quarries. The shape and degree of the formation of the crystals, according to Aquilano *et al.* (2016), can be affected by the presence in the mineral gypsum of water in the crystals and around them, salts such as halite (NaCl) and other additives (Section 3.1).

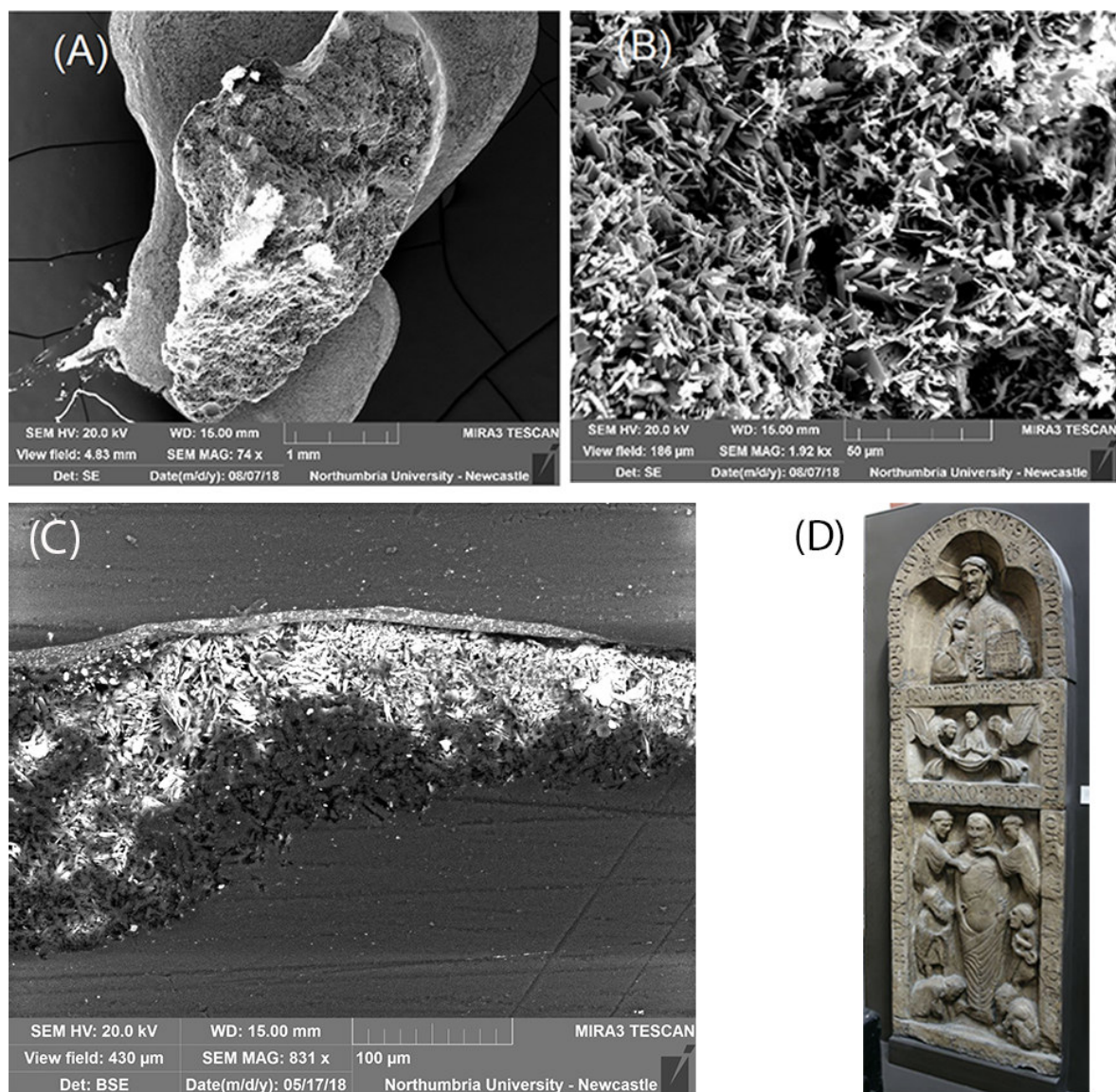


Figure 4.7. Sample 2 was adhered with Ag paint and coated with Pt (A) and analysed in SEM high-vacuum mode, which allowed to observe the tabular mineral structure of gypsum plaster (B). The structure can be also seen in the cross-sections analysed in SEM low-vacuum mode (REPRO-1873-380_4) (C). The samples were taken from REPRO.1873-380 (Tombstone of the Presbyter Bruno, object dimensions 218.5X77.0 cm) (D).

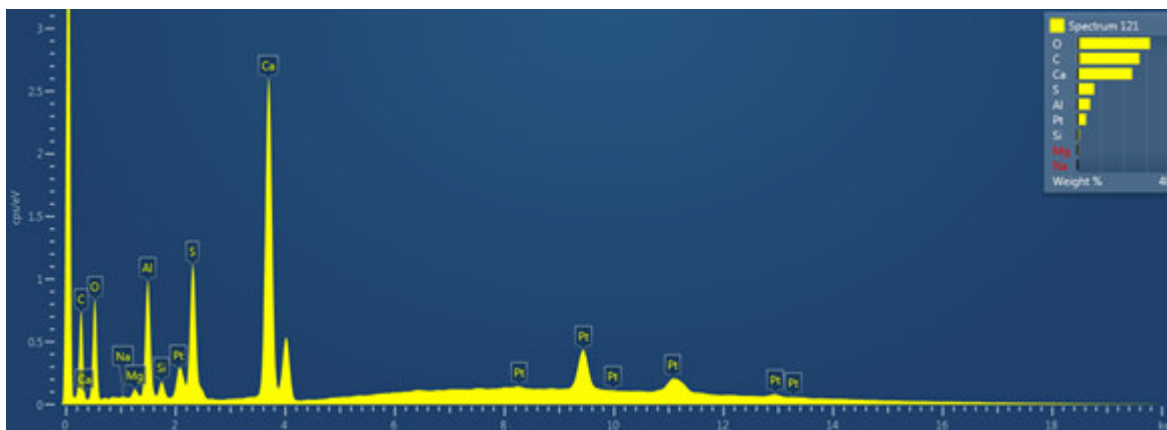


Figure 4.8. EDS spectrum of sample REPRO-1873-380_2 shows that the plaster bulk is made of calcium sulfate (Ca, S and O) and contains Si, Al, Na and Mg.

Literature (Beran, 2002; Cox *et al.*, 1974; Hanor, 2000) suggests that in well-crystallized specimens the determination of crystal system can aid the identification and the provenance determination, despite the complex mixture of materials used by the plasterer. Most often, trace analysis is more effective to determine the provenance of the objects as specific concentrations of trace elements can be characteristic of a mineralogical region (Gariani *et al.*, 2018). Trace analysis was not performed in this research as being beyond the scope.

The gypsum plaster identity, suggested by the elemental composition, was confirmed by XRD by comparison with relevant scientific literature (see *Appendix 9*). References from the databases (Gražulis *et al.*, 2009; Lafuente *et al.*, 2016) and other studies (Serafima *et al.*, 2016) allowed the comparison of the diffractograms and indicated that the analysed samples showed the same XRD pattern of gypsum references (for example R040029 and R060509 from the RRUFF database shown in the supplementary material in *Appendix 9*). No additional phases were investigated, but it is possible that running larger quantities of samples for prolonged analysis time would have highlighted more components, which at this stage of the research were beyond the scope.

The mineralogical identification must be supported by the classification on a chemical basis, i.e., native elements, sulfides, halides, oxides, carbonates, sulfates, phosphates, tungstates, silicates (Cox *et al.*, 1974). EDS analysis and EDS mapping of all the samples analysed for this study suggested that the plaster bulk largely consisted of Ca, S and carbon (C) and O were also detected in all the samples, being from the environment, the casting resin that was absorbed by the porous sample and the organic component (*Figures 4.7 and 4.9*). Peaks characteristic of the casting polyester resin can be also seen at 1312 cm^{-1} (δ OH phenol) and 1760 cm^{-1} (δ CH aromatic) in the FT-IR spectrum (*Figure 4.10 and Table 4.4*).

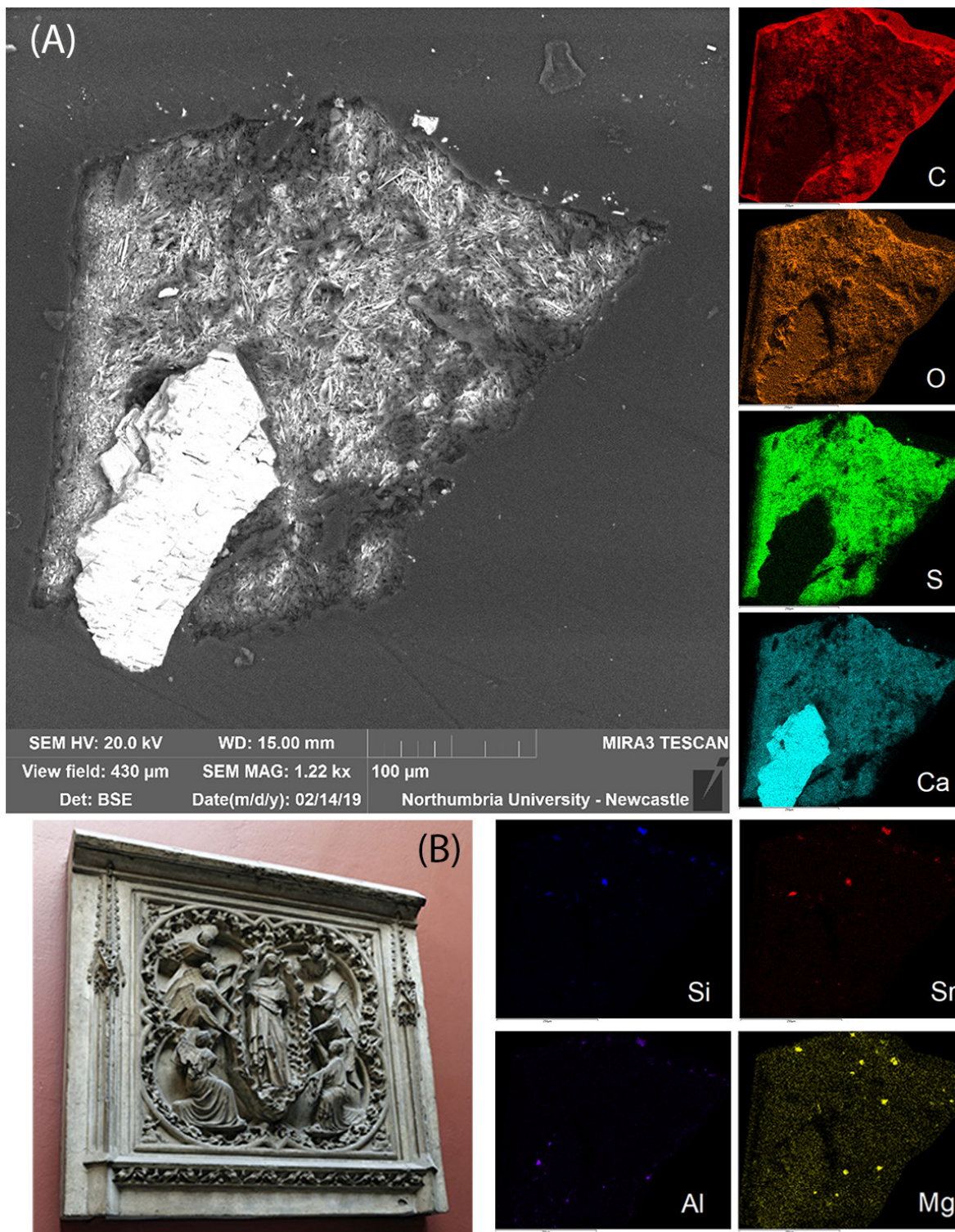


Figure 4.9. Sample REPRO.1890-80_1: BSE image (A) shows the tabular mineral structure of the calcium sulfate and the EDS mapping indicates that the sample largely consisted of calcium sulfate (Ca, S, O) and several other inclusions (Al, Mg, Si, Sr). C and O are also present due to the environment and to the casting polyester resin. The sample was taken from REPRO.1890-80 (Assumption of the Virgin, object dimensions 152.5X160.0 cm) (B).

The main infrared bands for some common minerals can be found in several publications (Beran, 2002; Derrick *et al.*, 2000; Hofmeister & Bowey, 2006; Ross & Farmer, 1974) and can be important for the identification of simple mixtures. In this study, this information cannot be definitive for such characterization once again due to the complexity of the organic-inorganic mixture. Aluminium (Al) was detected in all the samples and often can be due to the 0.3 μm Alumina Suspension, but it was often also observable in combination with silicon (Si) (Figure 4.9), which may imply that it is part of Si-Al clay minerals. In many samples, manganese (Mg), strontium (Sr), titanium (Ti) and iron (Fe) were also detected in the bulk (Figure 4.9). Si-O clay minerals are suggested by the presence of IR peaks in the 900-1200 cm^{-1} region (Figure 4.10, Table 4.4, and references in Figure 4.11).

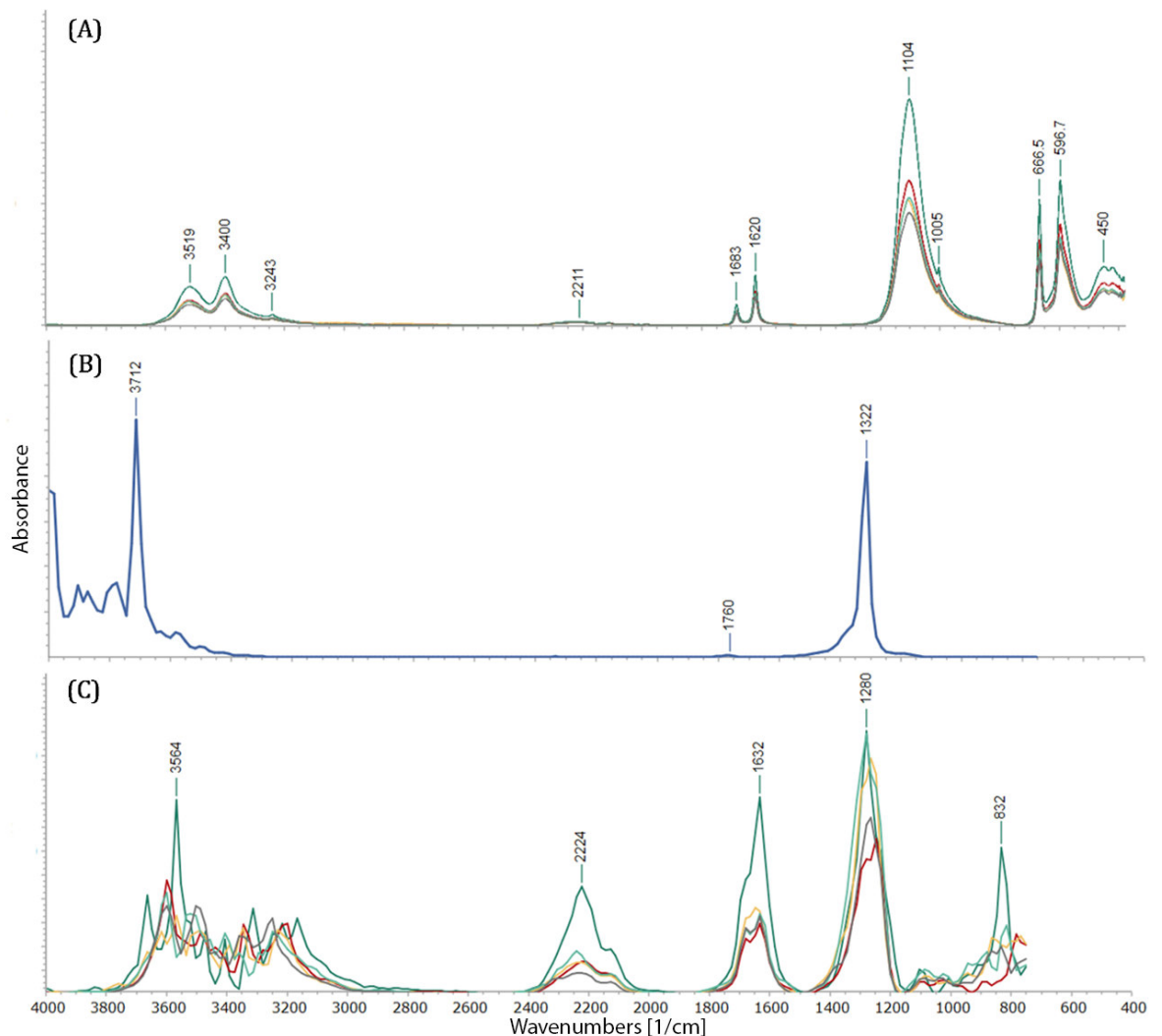


Figure 4.10. FT-IR spectra acquired in ATR mode (gypsum plaster reference) (A), and in DR of polyester casting resin reference (B) and plaster bulk of the objects (C) (REPRO.1873-380_2).

Table 4.4. FT-IR peaks identified in the spectra acquired from the gypsum plaster reference (A), the polyester casting resin reference (B) and plaster bulk of the objects (C) (REPRO.1873-380_2) shown in Figure 4.10.

Peaks (cm ⁻¹)			Assignment
(A)	(B)	(C)	
450			δ SO ₄ ²⁻
597			δ SO ₄ ²⁻
667			δ SO ₄ ²⁻
		832	
1005			ν SO ₄ ²⁻
1105			ν SO ₄ ²⁻
		1280	
	1322		δ OH phenol
1620		1632	ν ₂ H ₂ O
1683			ν ₂ H ₂ O
	1760		δ CH aromatic
2211		2224	overtone
3243			ν OH
3400			ν OH
3519		3564	ν OH
	3712		ν OH

Calcite (calcium carbonate, CaCO₃) is considered an important accidental and intentional additive to plaster mixtures (Melita *et al.*, 2020) as also shown in historical sources (Risdonne *et al.*, 2021; Sullivan, 2019; Turco, 1990) and was also clearly observed in the EDS mapping of several samples (Figure 4.9). References for FT-IR peaks of calcite (Figure 4.11) suggest that an O-C-O ν₂ out-of-plane bending mode band at 850-900 cm⁻¹ of the C-O bending mode, a ν₁ at about 1088 cm⁻¹, a strong band at 1440-53 cm⁻¹ (ν₃ CO₃ stretching mode of carbonate) and also 1780 cm⁻¹ are expected (Anastasiou *et al.*, 2006; Böke *et al.*, 2004; Legodi *et al.*, 2001; Tatzber *et al.*, 2007). FT-IR analysis (Figure 4.10 and Table 4.4) also allowed to identify gypsum plaster (CaSO₄·0.5H₂O), as the peaks characteristic of bending and stretching of SO₄²⁻ at 1005 and 1105 cm⁻¹, and the ν₂ H₂O related to the sulfate at 1620 and 1680 cm⁻¹ were observed.

A minor variation of the position of the FT-IR peaks can be observed for several reasons, one of which is the local substitution of elements such as Mg and Pb in the gypsum structure. Small changes and shifts are also expected due to the variability of diffuse reflection signals when compared to the transmission references (Derrick *et al.*, 2000). El Hazzat *et al.* (2019), for example, carried out thermal experiments on artificial gypsum that can be useful to understand that changes, although small, can be observed in the XRD pattern and FT-IR bands. A certain degree of variability should be considered when looking at the results of the XRD and FT-IR analysis of the plaster bulk as the calcining at different temperatures might have influenced the crystal growth and mineral structures. In the FT-IR spectra, the absorption of the inter- and intra-molecular water is correlated to gypsum hydration, also related to the manufacturing temperatures (see also Sections 3.1 and 5.3). As reported in Manfredi *et al.* (2015) and Miliani *et al.* (2012), the strong and broad band at

2000-2500 cm^{-1} is due to the combination of bending and vibration modes of H_2O ($\nu_1 + \nu_3$ and $2\nu_3$) related to the presence of gypsum (centred at 2200 cm^{-1}) and other minerals. These overtones are particularly intense in the diffuse reflectance spectra.

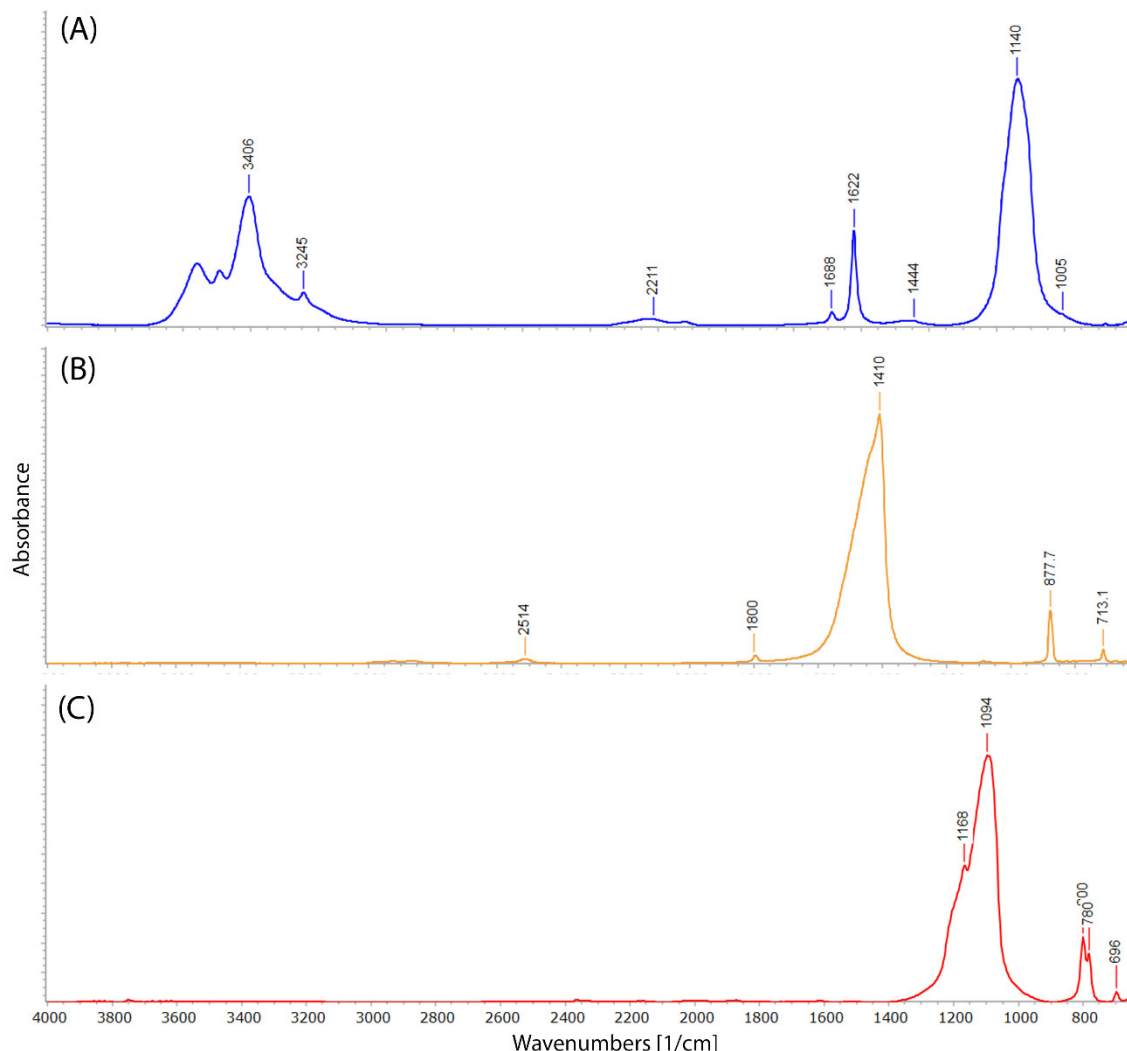


Figure 4.11. FT-IR reference spectra of gypsum (IMP00024 Gypsum, from chalk sample, Kremer, 5815, GCI, tran) (A), calcite (IMP00108 Calcite, source unknown, PMA, tran) (B) and silica (IMP00322 Quartz, silica, Forbes: Howe&French, 187, SCC, tran) (C) from the IRUG database (Price et al., 2009).

The FT-IR analysis of REPRO.1873-380_2 (Figure 4.10 and Table 4.4) did not suggest that organic material is present in the plaster bulk. However, py-TMAH-GC/MS of this sample (Figure 4.12) showed small fragments due to derivatization (evolved at a retention time of 3.03 to 16.99 min) and markers characteristic of a pine resin (**5** and **6** in Figure 4.12 and Table 4.5) (Colombini & Modugno, 2009; Mills & White, 2012; Singer & McGuigan, 2007; Van der Doelen, 1999). The presence of methyl palmitate (**2**) and stearate (**3**) (Figures 4.12 and 4.13) and the value of the ratio of their relative abundance ($P/S = 2.15$) might suggest that the resin has been mixed with oil, but the small relative abundance of methyl azelate (**1**)

suggests that the fatty acids (FA) are either from a non-drying oil, another source of lipids or naturally present in the resin (Colombini & Modugno, 2009; Singer & McGuigan, 2007). The unique identification of oils is in these samples impeded by the predominance of the inorganic matrix, as will be further discussed in *Section 4.3.3*.

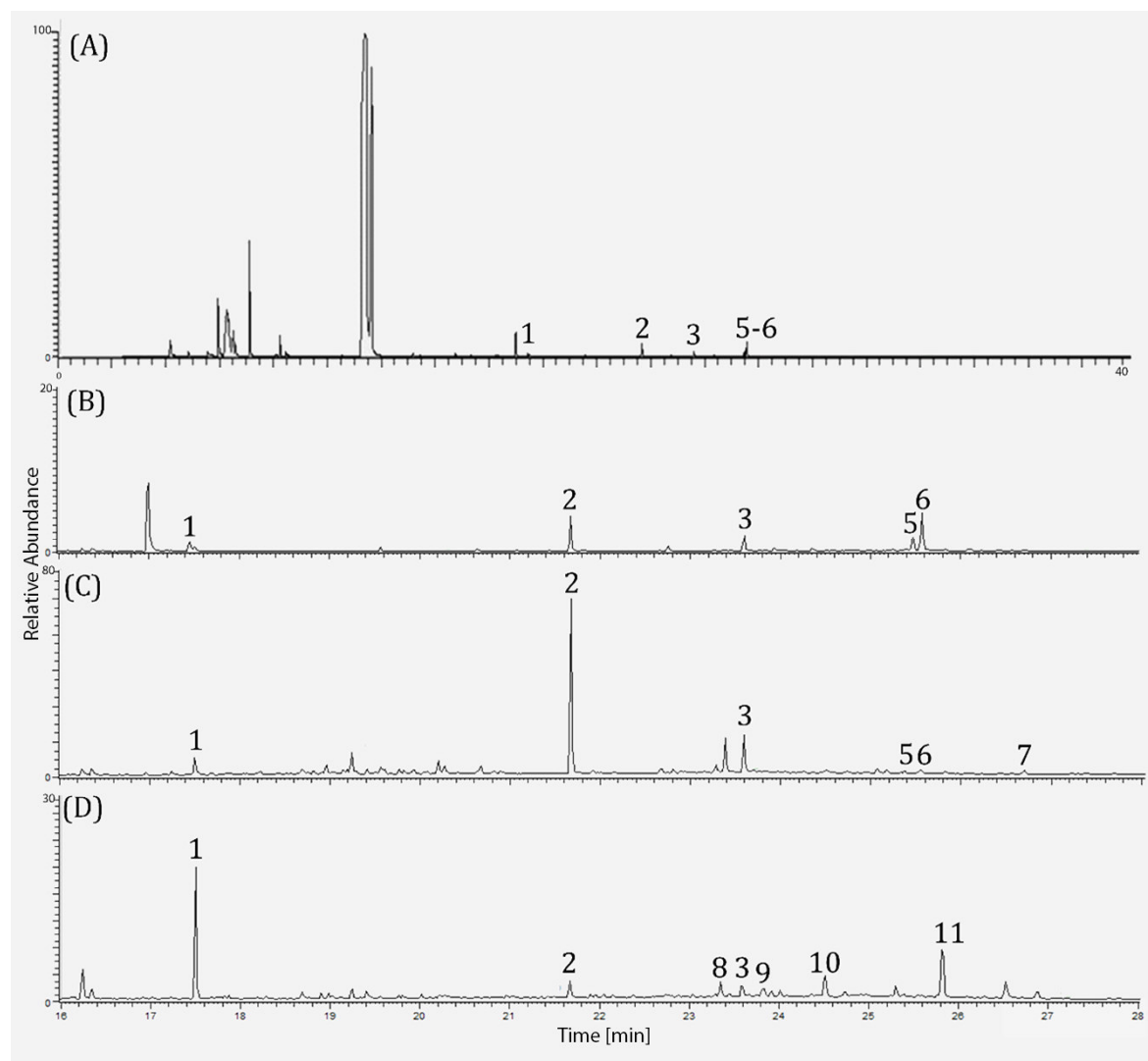


Figure 4.12. py-GC chromatograms of three samples: sample from the plaster bulk only (A-B) (REPRO.1873-380_2) and another sample (C) (REPRO.1873-561_6) showing markers of diterpenic resin and FAs; a sample (D) (REPRO.1890-81_4) showing shellac resin markers. (A): 0-40 min and (B-D): 16-28 min. Labels' assignments are described in Table 4.5.

Table 4.5. GC/MS markers used to characterise the organic component.

Label	Marker	m/z	RT* (min)
1	Fatty acid Methyl azelate (A)	42, 58, 74 (100), 87, 120, 138, 152, 171, 185	16.68-
			17.52
			21.68-
2	Methyl palmitate (P)	55, 74(100), 87, 101, 129, 145, 185, 199, 227, 239, 270	21.70
3	Methyl stearate (S)	74 (100), 87, 129, 143, 199, 255, 298	23.60- 23.62
4	Diterpene resin Methyl 7-oxo-15-hydroxy-dehydroabietic acid	58(100), 71, 85, 115, 149, 207, 219, 251), 270, 299, 331	22.79
			25.47
			25.57
			26.72
5	Methyl 7-Oxodehydroabietic acid	44, 58, 74, 87, 129, 171, 187, 207, 239, 253(100), 281, 299, 314, 328	
6	Methyl dehydroabietate	141, 155, 197, 239(100), 253, 314	
7	Methyl oxo-dehydroabietic acid	44(100), 79, 115, 165, 191, 207, 227, 267, 281, 342	
8	Shellac Jalaric acid	59, 69, 83, 87, 105, 121, 135, 145, 167, 179, 191, 203, 208, 231, 247, 262(100), 275, 307, 322	23.35
			23.82
			24.53
			25.54-
			26.52
9	Shelloic acid	55, 71, 97, 109, 137, 169, 201(100), 231, 261, 291, 304, 336	
10	Shelloic acid	59, 79, 91, 129, 169, 206, 229, 238, 260, 288, 305, 320(100), 337	
11	Aleuritic acid	44, 55, 71(100), 81, 109, 137, 159, 201, 207, 239, 312, 327	
12	Phthalic compound Phthalic anhydride	45, 55, 71(100), 85, 101, 111, 142, 147, 156	10.67-
			13.67
			16.35
13	Dimethyl phthalate	58, 77, 92, 104, 133, 163(100), 194	

* Retention Times (RT) are specific to the experimental conditions and characteristics of the equipment used. In this study, RT of the same component varies ± 0.50 depending on the sample.

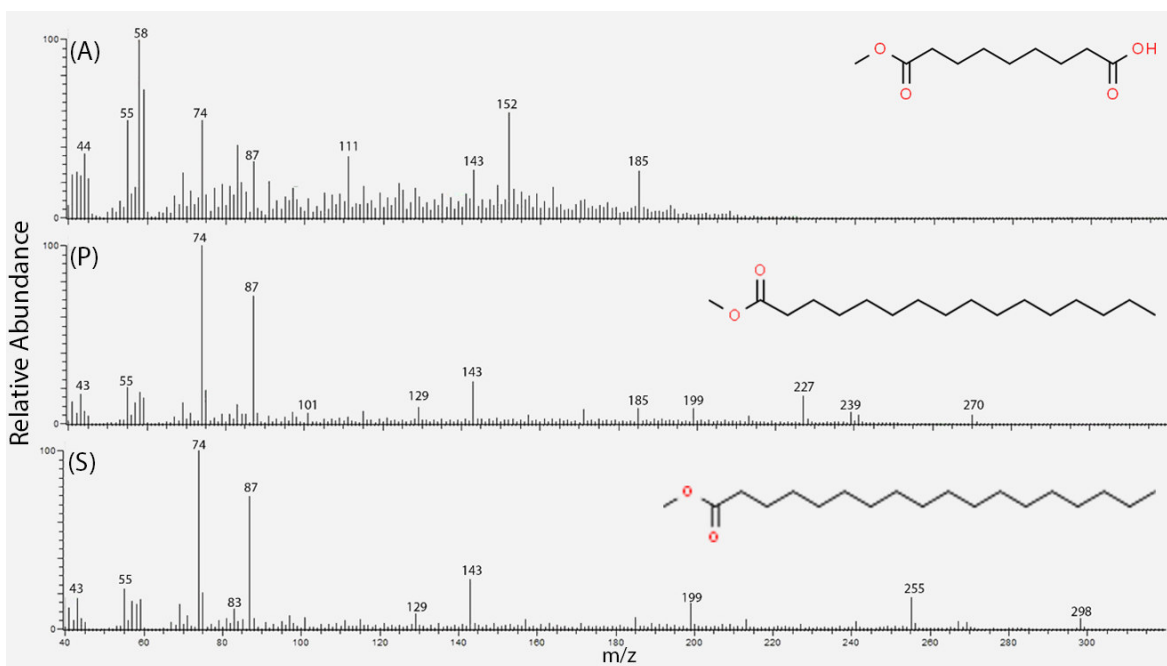


Figure 4.13. EI-MS of methyl azelate (A) (1), methyl palmitate (P) (2) and methyl stearate (S) (3). The list of peaks can be seen in Table 4.5.

4.3.3. COATINGS AND INTERFACE WITH THE SUBSTRATE

The outermost layer observed in all the samples is rarely well defined and most often a relatively thin darker layer should be considered as oxidized coating and dirt, whereas the interface layer, shown for example in *Figures 4.4* and *4.14*, is representative of a portion of coating diffused in the bulk.

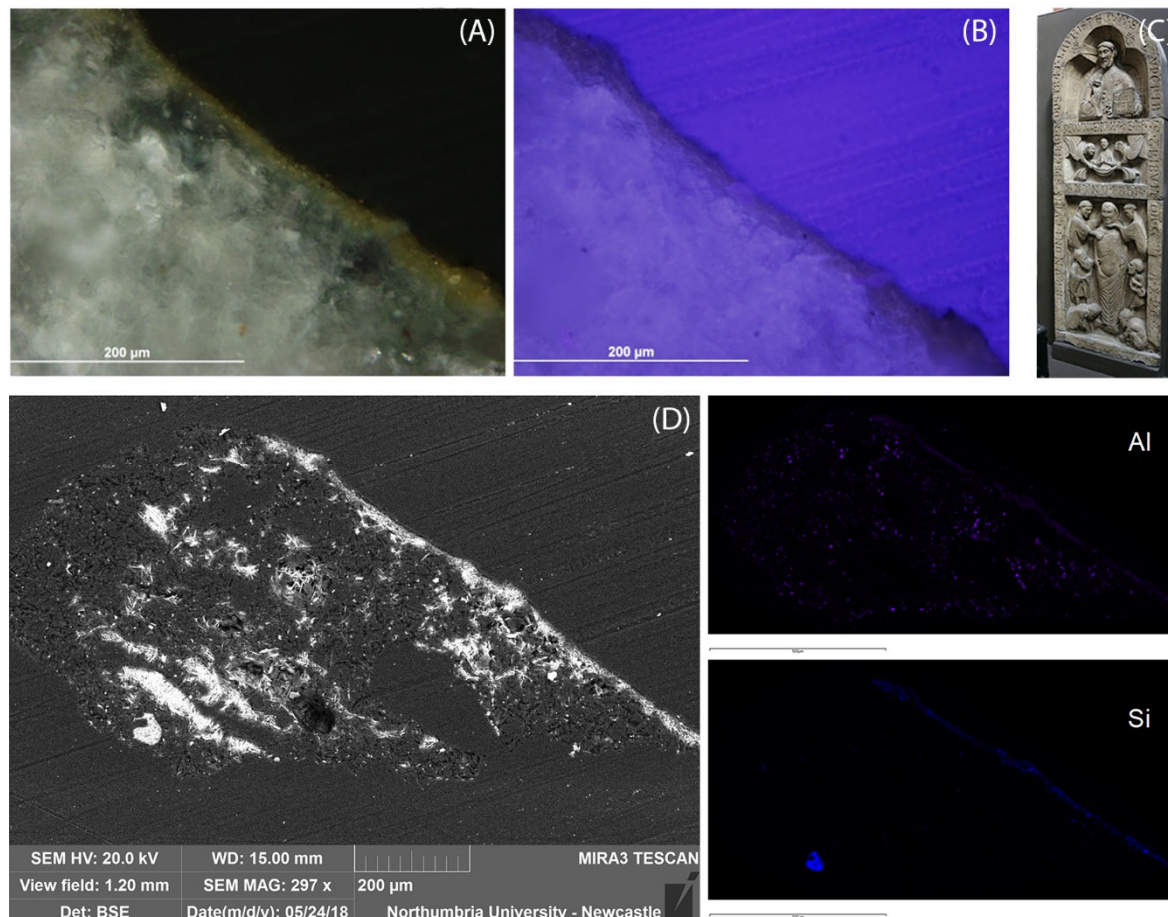


Figure 4.14. Example of Si-Al and diterpenic resin coating (REPRO.1873-380_11). VLR (A) and UVf (B) OM images, BSE image (D) and EDS mapping showing Al and Si. The sample was taken from REPRO.1873-380 (Tombstone of the Presbyter Bruno, object dimensions 218.5X77.0 cm) (C).

The identification of the elemental composition of the surface layer was possible by EDS mapping, which highlighted the elemental distribution in a layer fashion when present. Calcium sulfate was detected in the surface layers of all the samples, often together with other elements. Si and Al were observed in the EDS mapping of the outermost layer of several samples (*Figures 4.14*, *4.15* and *4.16*). It is possible to hypothesise that the presence of Si and Al can be due either to the use of clay water as a separating agent (Auerbach, 1961; Frederick, 1899) or to the use of the silicate mineral pigment kaolinite $\text{Al}_2\text{Si}_2\text{O}_5(\text{OH})_4$ (*Figure 4.17*) to tone the surface (Millar, 1899). In some of the samples, a significant Mg

component can be also seen in the surface together with Al and Si, suggesting that 'French chalk' (talk, mostly containing Mg and Si, but also Al) could have been used to polish the surface (Auerbach, 1961; Millar, 1899; Wager, 1963). Other samples contain Si, Al and Sr (Figure 4.15).

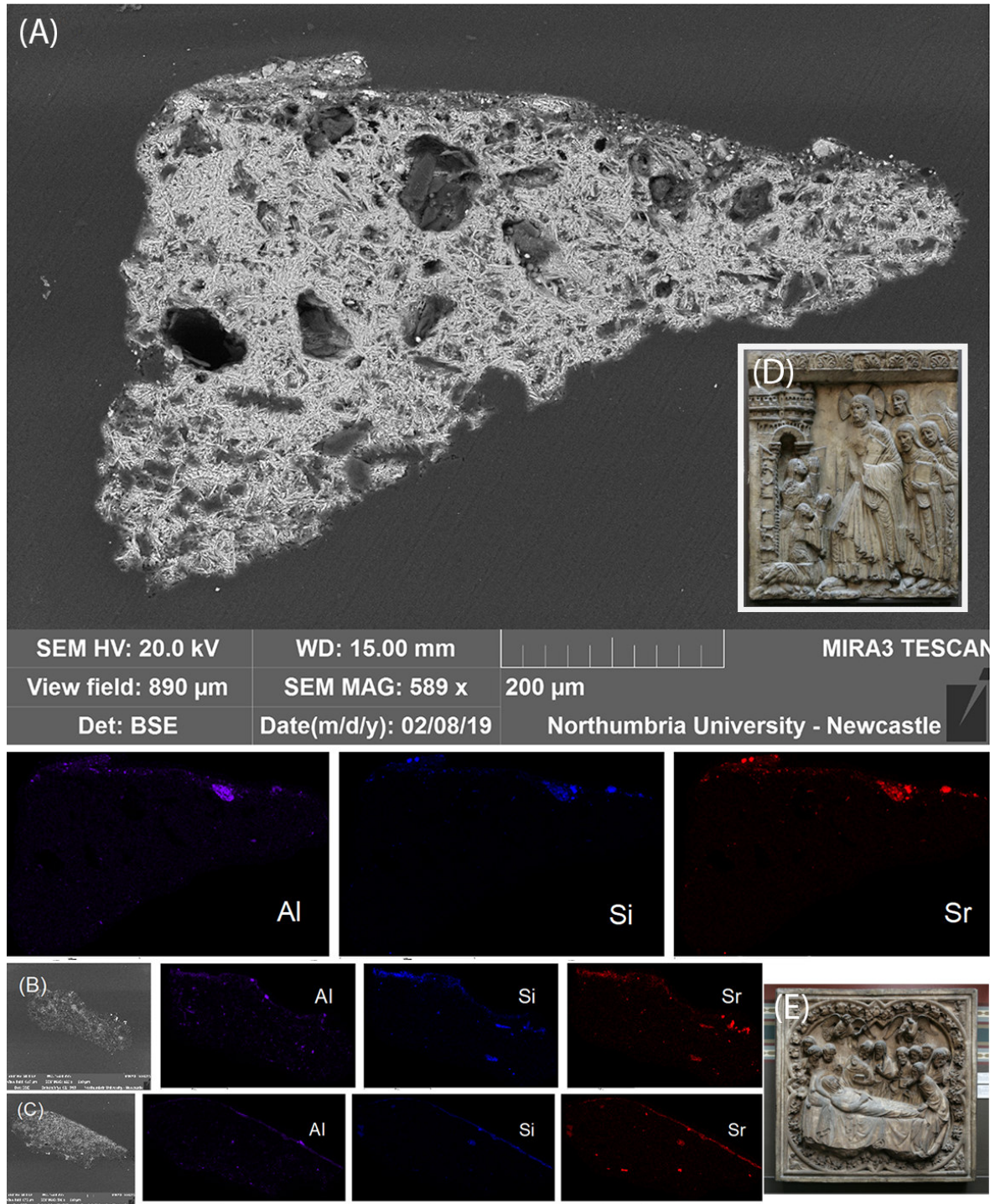


Figure 4.15. Examples of Si-Al-Sr and diterpenic resin coating. REPRO.1864-57_2 (A), REPRO.A.1916-3152_3 (B) and REPRO.A.1916-3152_4 (C) BSE image and EDS mapping showing Al, Si and Sr. The samples were taken from REPRO.1864-57 (Christ at Bethany, object dimensions 135.0X112.0 cm) (D) and REPRO.A.1916-3152 (Death of the Virgin, object dimensions 90.0X86.0 cm) (E).

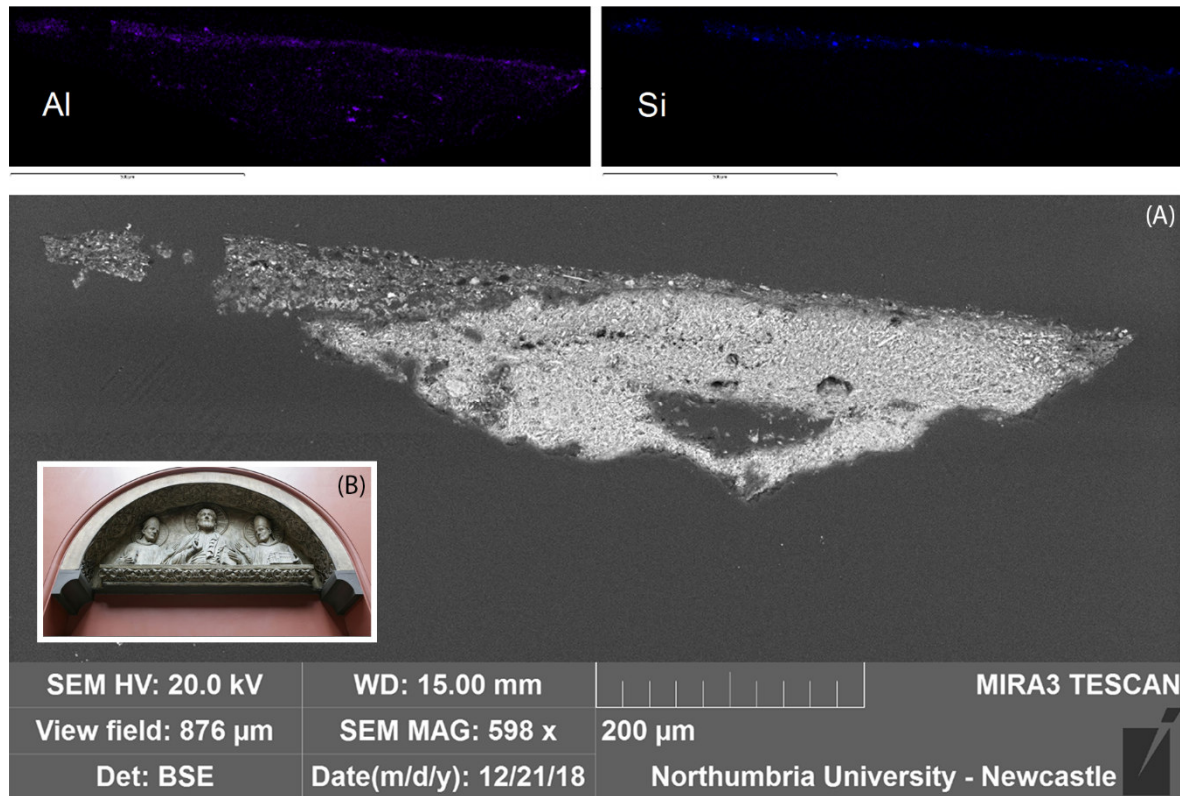


Figure 4.16. Example of Si-Al and shellac coating (REPRO.1874-45_2). BSE image (A) and EDS mapping of Al and Si are shown. The sample was taken from REPRO.1874-45 (Christ, St. Godehard and St. Epiphanius, object dimensions 107.0X213.5 cm) (B).

Apart from the characterization of the elemental composition, particularly important was the identification of the organic media. Organic materials are more subject to degradation than inorganic ones, and being able to identify natural substances and their degradation products is a challenge. Organic materials could have undergone various modifications (e.g. oxidation, photodecomposition, and microbial digestion) over time. Identifying a small amount of a protein (in the order of tens of picomoles) represents a difficult problem for traditional methods of chemical analysis. The situation is even more complicated when a protein mixture of the variable composition should be identified in a complex matrix containing dyes, oils, inorganic pigments, lime, etc. In this study, FT-IR and GC/MS analysis were combined to characterise the organic media in the plaster samples. FT-IR spectra were inconclusive due to the broadness of the bands that resulted from the diffuse reflectance signal and the presence of numerous components in the sample. The broad bands did not allow to characterise specific organic components but were however indicative of the presence of classes of materials. As the results of the EDS suggested the presence of gypsum, calcite and clay minerals, FT-IR reference spectra of these materials (Figure 4.11) (Derrick *et al.*, 2000; Price *et al.*, 2009; Vahur *et al.*, 2016) were used to skim the peaks in the spectra acquired from the objects. Reference spectra for the casting resin

(*Figure 4.10*) were also acquired. This was particularly important because, as discussed above, the porous samples absorbed the casting resin when in the liquid state. The recipes also helped to select references to navigate our spectra. Just as the presence of functional group bands can be used to select potential matches, the absence of a functional group band is used to eliminate potential groups of materials. It is important to note that ageing can cause significant changes to the infrared bands of certain binding media. As salt efflorescence is a common degradation phenomenon observed on the surface of the plaster and building materials (Baglioni & Chelazzi, 2013), references for the identification of these products were also taken into account. Calcium oxalate is for example suggested as a degradation product by Toniolo *et al.* (2009) but cannot be identified in the FT-IR spectra acquired for this study due to the broadness of the bands: the characteristic peaks of calcium oxalate (1648 cm^{-1}) are expected close to the calcium sulfate vibrations (1620 and 1680 cm^{-1}).

GC/MS was particularly important to allow the identification of organic materials. A mass spectrometer is an excellent tool for clearly identifying the structure of a single compound but is less useful when presented with a mixture (Colombini & Modugno, 2009). Most often the full GC pattern that would characterise a fresh or even aged pure sample prepared in the laboratory, is not present in the materials sampled from cultural heritage objects. The interpretation of the chromatograms and mass spectra or even only the assignment of a few components that may be considered 'markers' is the key to the characterization of unknown samples (*Table 4.5*). The GC expected from a fresh material was not always detected, but this can be due to the natural degradation of the molecules or to the derivatization processes applied to the already degraded organic material, as suggested in Coelho *et al.* (2012), Colombini *et al.* (2003) and Colombini & Modugno (2009) (*Figure 4.12*).

It has been suggested that the intensity of the FA peaks can change, as affected by matrix effects due to the presence of inorganic pigments in organic media (Chiavari *et al.*, 2005; Poli *et al.*, 2014). In this study, it is possible that this effect is amplified, as the organic component is less than the inorganic portion. This is likely to also influence the small relative abundance of the markers in the chromatograms.

Extensive literature is available on the study of oil paint surfaces: seed oils such as linseed oil, walnut oil and poppy seed oil are common oils to be found in the paints and these three oils can be distinguished by the palmitic acid to the stearic acid ratio in the hydrolysed lipid (Colombini & Modugno, 2009; Mills, 1966; Mills & White, 2012). The ratios are calculated through the integrated areas of the relative abundances of the FAs in the GC. The integration is often provided as a tool in the software attached to the GC equipment, but any spectral or mathematical software (such as MatLab®) would also suffice. The prevalence of the inorganic component over the organic component also raised doubts on the validity in

this case of the ratios of the abundance of fatty acids (FA) (Figure 4.13) for the identifications of organic materials (Colombini & Modugno, 2009). In other words, the presence of inorganic pigments would change the palmitate/stearate acids ratio (P/S) and therefore invalidate the correlation which allows the determination of the type of lipid compounds. Table 4.6 shows the ratios calculated in this study, which are not consistently comparable to the ones commonly used in the references (Colombini & Modugno, 2009). Schilling & Khanjian (1996) also showed, for example, that exposure of oil paint specimens to heat and light significantly increased the concentrations of most dicarboxylic fatty acids, whereas the amount of azelaic acid increased only slightly. Surprisingly, exposure to heat and light reduced the concentrations of saturated fatty acids in oil paints. Test results of samples from oil paintings were consistent with the trends established by the exposed oil paint specimens. However, due to the lack of previous studies on the effects of the predominance of the inorganic portion over the organic component on the abundances of the FAs in the chromatogram, further research on this topic is required.

Table 4.6. P/S and A/P ratios calculated in the samples analysed by (py-)GC/MS. Relevant samples processing and analytical details are described in Sections 4.2.2 and 4.2.3.

Sample	P/S	A/P
REPRO.1873-380_2	2.16	0.68
REPRO.1873-380_3	1.10	0.55
REPRO.1873-380_4	2.60	0.87
REPRO.1873-380_5	0.19	3.02
REPRO.1873-380_8	0.32	0.41
REPRO.1873-380_9	0.34	0.15
REPRO.1873-561_6	2.81	0.17
REPRO.1874-29_4	1.22	1.15
REPRO.1874-45_2	0.91	0.54
REPRO.1875-16_4	1.78	2.89
REPRO.1875-17_3	1.79	2.42
REPRO.1890-80_4	1.75	0.92
REPRO.1890-81_4	1.53	3.92
REPRO.A.1916-3152_3	1.90	0.55
REPRO.A.1916-3153_3	1.48	-
REPRO.1864-56_2	1.30	-
REPRO.1864-57_4	0.93	3.70

Overall, no protein material was identified in the samples analysed for this study. Small amino acid fragments were identified in several GC/MS chromatograms, but the rarity of their presence suggests that either a very small quantity of proteinaceous material was added or that the amino acids are the ones naturally present in the resins (Colombini & Modugno, 2009). The identification of natural materials containing proteins, such as animal glues, casein, egg, horn and ivory, is aided by the characteristic FT-IR bands due to the protein characteristic amide group: amide I and II bands at 1650 and 1550 cm^{-1} , respectively (Derrick *et al.*, 2000; Fabian, 2002; Stuart, 2007). The amide I band is mainly associated

with the C=O stretching vibration and is directly related to the backbone conformation. Amide II results from the N-H bending vibration and from the C-N stretching vibration. These were not consistently observed in the FT-IR spectra acquired in this study.

In general, two types of organic materials were identified in the objects, namely diterpenic (such as sandarac, copal, rosin or colophony) and shellac resins.

The FT-IR spectra of natural resins (*Figure 4.17*) can vary significantly depending on the tree species, manufacturing and degradation of the resin; however, an overview of characteristic peaks is provided in *Table 4.7*. Resins are mostly composed of terpene molecules and can be classified into diterpenic and triterpenic resins (Azemard *et al.*, 2014). The cyclic ring structure of resins of plant origin produces a spectrum with C–H stretching bands at higher wavenumbers than oils. These bands tend to be broader than those observed for oils and waxes because of the presence of more methyl (CH₃) end groups and a variety of molecular environments for the methylene (CH₂) groups. Resins also show a distinctive broad band in the 2700–2500 cm⁻¹ range due to O–H stretching of a dimerised carboxyl group. These compounds also produce carbonyl stretching bands near 1700 cm⁻¹. To differentiate resins, the fingerprint region may be used. Terpenic resins generally photochemically degrade by different kinds of oxidation reactions and polymerization. Shellac, a resin of insect origin, also shows distinctive bands in the FT-IR spectra (*Table 4.7*), as shown in the literature (Derrick *et al.*, 2000). The C–H stretching bands appear at similar wavenumbers to those of oils and there is a small olefinic band at 1636 cm⁻¹. The C=O stretching band of shellac is a doublet with peaks at 1735 and 1715 cm⁻¹ due to the ester and the acid, respectively. The alcohol, acid and ester groups produce C–O stretching bands at 1040, 1163 and 1240 cm⁻¹, respectively.

Due to the complexity of the FT-IR spectra (*Figures 4.18* and *4.19*) acquired from the samples in this study, the assignment of the broad bands in the spectra was challenging; nonetheless, the spectra were compared, and it was often helpful to note the *absence* of a characteristic vibration. The absence of the CH vibrations in the 2700–3000 cm⁻¹, for example, can suggest that no organic material is present in the analysed sample. *Figures 4.18* and *4.19* show examples of spectra acquired from samples where diterpenic resin (REPRO.A.1916-3152_3) and shellac (REPRO.1890-81_4) were confirmed by py-GC/MS. It is hardly possible to identify the components of the sample by looking at the FT-IR spectra only. However, working backwards, if a range of materials can be hypothesised and skimmed as constituting the samples, it is possible to assign the peaks, consistently with the references and peaks suggested in *Figure 4.17* and *Table 4.7*, for example, and the characteristic peaks defined for gypsum (*Figure 4.10*) and other inorganic materials (*Figure 4.11*).

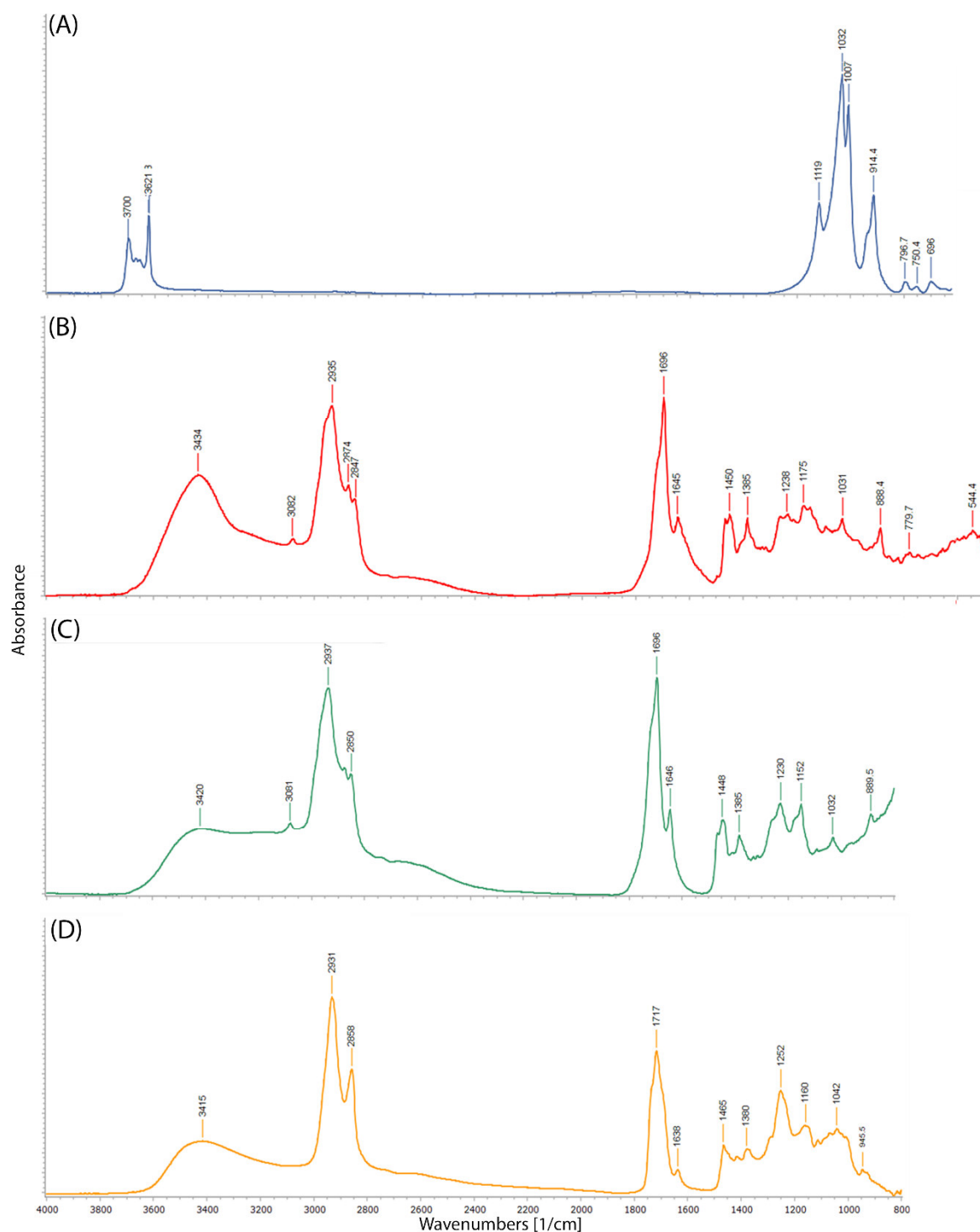


Figure 4.17. Examples of FT-IR reference spectra of kaolin (IMP00109 Kaolin pigment, hydrous, Eglehard, ASP 600, PMA, tran) (A), sandarac (INR00056 Sandarac AF Suter GCI tran) (B), copal (INR00011 Copal Sarmi from *Agathis alba* Roy. Trop. Inst, CIA) (C) and shellac (INR00008 Shellac *Lacifer lacca* SAM M Jahan Ethno41 GCI tra) (D) from the IRUG database (Price et al., 2009).

Table 4.7. Summary of FT-IR peaks characteristic of the organic materials identified by GC/MS, according to literature*.

Peak (cm ⁻¹)				Assignment
Diterpenic resin	Triterpenic resin	Shellac	Oil	δ(CH ₂) v(C–O–C) ether
888	1035			
		1040		v(C–O) alcohol
		1163		v(C–O)
		1240		v(C–O) ester
1386	1378-84			δ(CH ₃)
			1418	v(C–O)
1445-8	1455			δ(CH ₃)
		1636		olefinic
1644				v(C=C)
	1639-58			vinyl
1690-1718	1706-13	Doublet 1715 and 1735	1730-50	v(C=O)
2844				v(C–H)
2870				v(C–H)
2936				v(C–H)
2990-3050	2990-3050			v(-C=C-)
3070-88	2650-3079			v(=C–H)
	3425-46			v(O–H)

* (Azemard et al., 2014; Colombini & Modugno, 2009; Derrick et al., 2000; Sarkar & Kumar, 2001; Vahur et al., 2016)

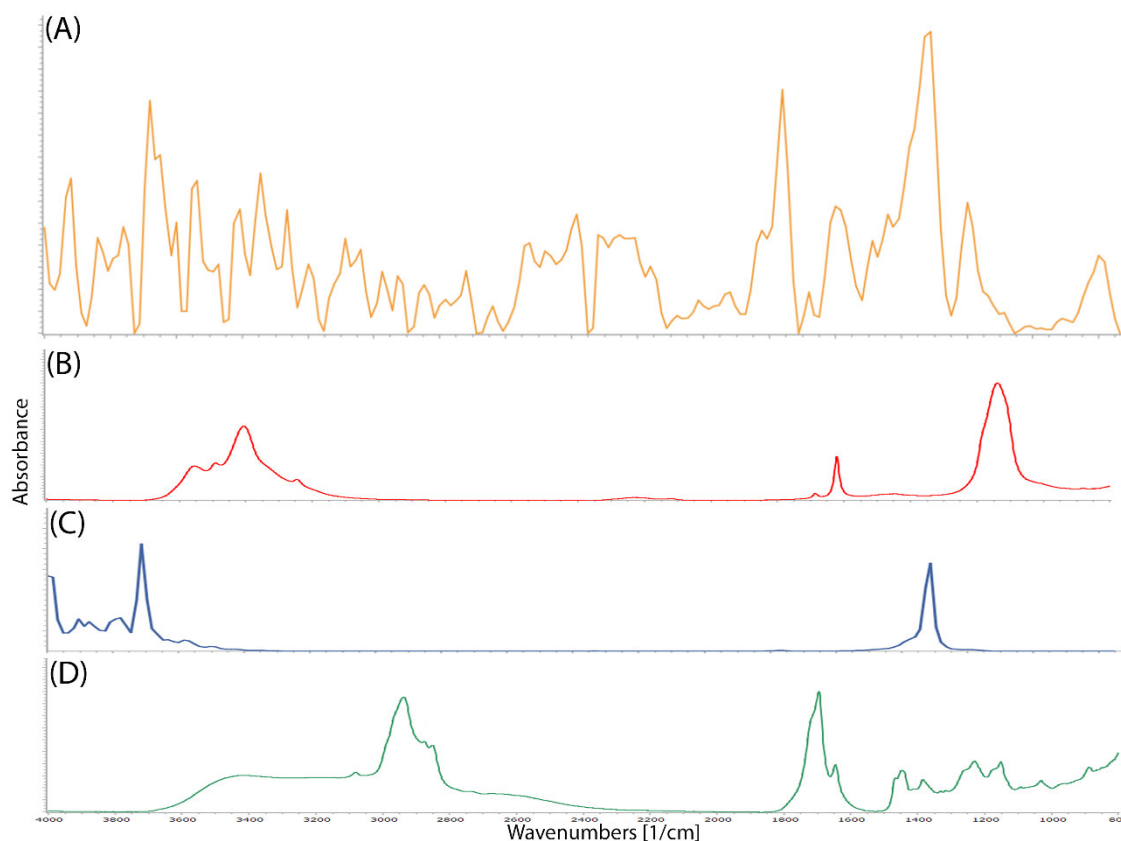


Figure 4.18. Diffuse Reflectance (DR) FT-IR spectrum acquired from a sample in which diterpenic resin was confirmed by py-GC/MS (REPRO.A.1916-3152_3) (A) and reference spectra of gypsum (B), polyester resin (C) and copal (D) shown in Figures 4.11 and 4.17.

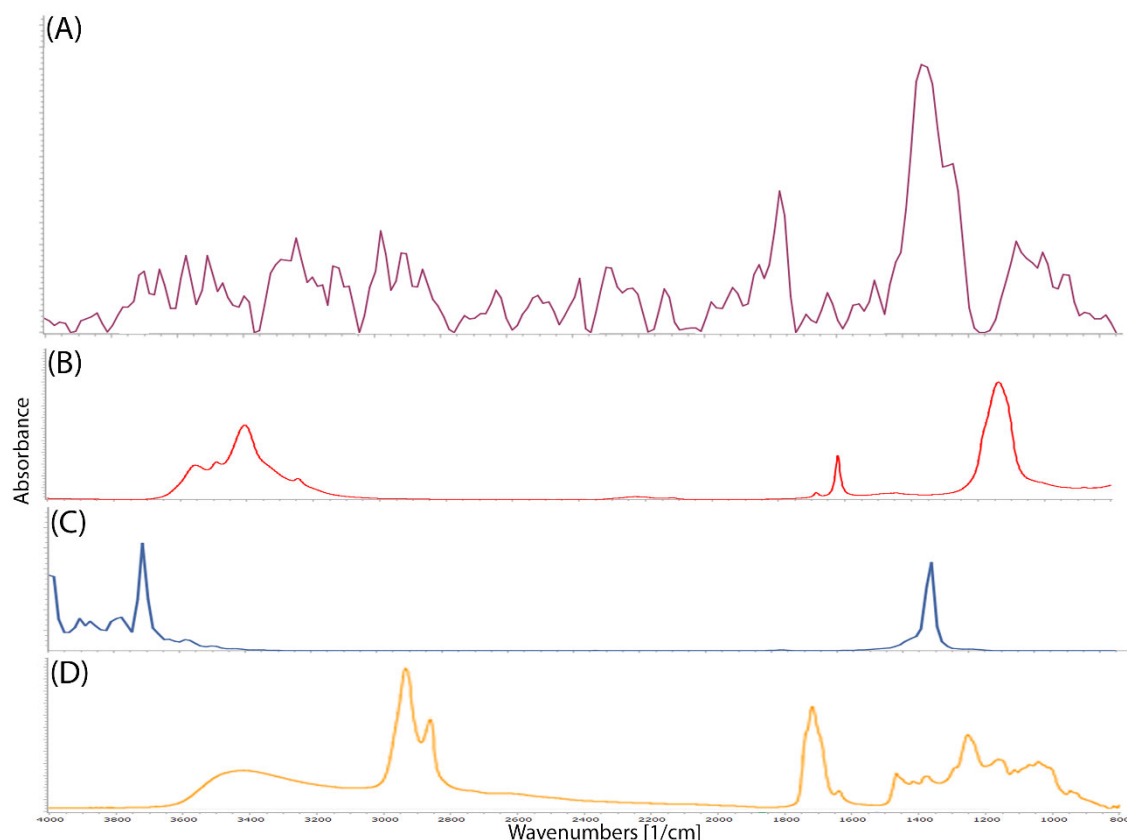


Figure 4.19. Diffuse Reflectance (DR) FT-IR spectrum acquired from a sample in which shellac was confirmed by py-GC/MS (REPRO.1890-81_4) (A) and reference spectra of gypsum (B), polyester resin (C) and shellac (D) shown in Figures 4.11 and 4.17.

The diterpenic resin was identified by py-GC/MS as characteristic markers were observed in the GC (Table 4.5 and Figure 4.12) and the relevant MS spectra were supported by the literature (Figure 4.20) (Colombini & Modugno, 2009; Mills & White, 2012; Scalarone *et al.*, 2003). The presence of methyl palmitate (**2**) and stearate (**3**) was detected in all the samples and the P/S ratio varies significantly from sample to sample (Table 4.6). Methyl azelate (**1**) is not always present in the chromatogram, and when present, it is not very abundant. The resin can have been mixed with an oil or the FAs can be derived from another source of lipids or naturally present in the resin (Colombini & Modugno, 2009). Thus, the P/S and the A/P ratios cannot be used for the assignment of lipids in this study.

In a few samples where the diterpene markers were detected, py-TMAH-GC/MS also showed few betullin-like triterpene markers (Colombini & Modugno, 2009; Van der Doelen, 1999) or markers for dammar resin (e.g. 20, 24-epoxy-25-hydroxy-dammaran-3-ol) suggesting that, as diterpene and triterpene molecules are rarely found together in a plant resin, a birch, dammar or mastic is additionally present in the stratigraphy. As the presence of the triterpene markers was rare, their relative abundance small and no other indication

was found, it is impossible to better define the identity of this material at this stage and further analysis is required.

Shellac can be relatively easily identified by UVf OM due to the characteristic pink-orange fluorescence colour that can be seen in *Figure 4.21* and the other UVf OM images of the objects containing shellac (*Figure 4.22*). Py-TMAH-GC/MS chromatogram markers characteristic of **shellac** namely jalaric acid (**8**), shelloic acid (**9**), shellolic acid (**10**), aleuritic acid (**11**) and other C15 fragments (*Figure 4.23*) (Colombini & Modugno, 2009; Mills & White, 2012; Singer & McGuigan, 2007). Methyl azelate (**1**), methyl palmitate (**2**) and stearate (**3**) were also detected. Shellac and drying oils were also detected, for example, on plaster cast surfaces (containing Ca, Sr and Fe) by Fodaro *et al.* (2014). In one of the objects (REPRO.1874-29), Cu was detected in the outermost layers by EDS mapping and shellac was observed in the same layer in the UVf OM image, and confirmed by py-GC/MS. The use of powdered copper and shellac has been suggested for a brass finish by Wager (1963) and de Bas (1920).

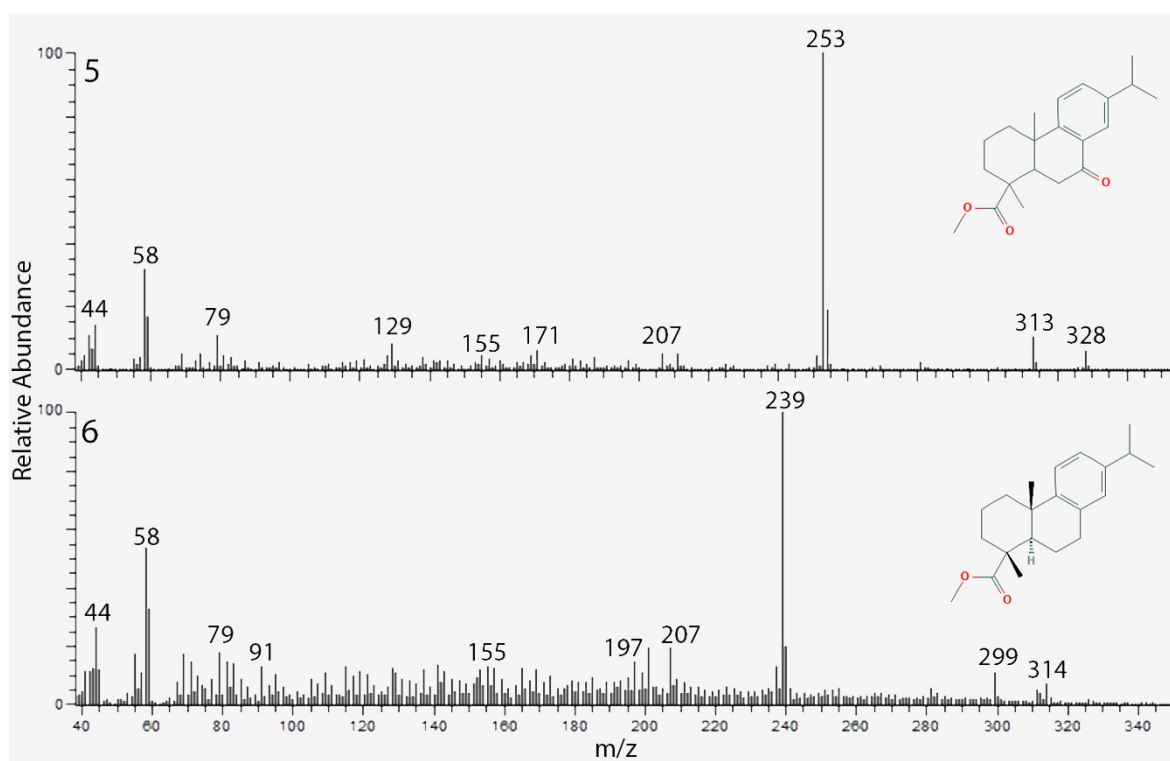


Figure 4.20. EI MS of methyl 7-Oxodehydroabietic acid (5) and methyl dehydroabietate (6). A list of peaks can be seen in Table 4.5.

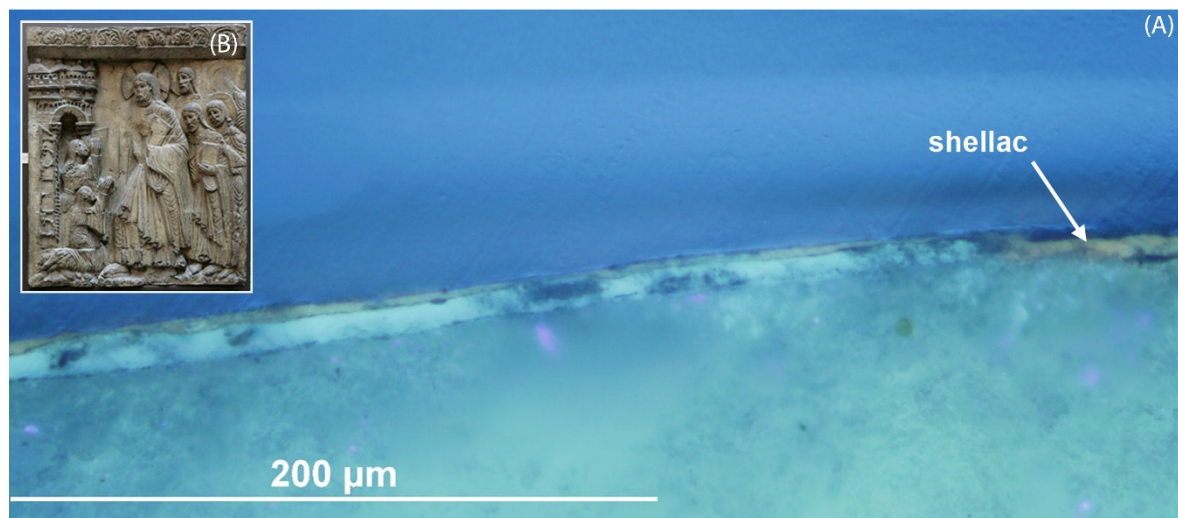


Figure 4.21. REPRO.1864-57_3 UVf image (A) showing a white fluorescing coating and a layer fluorescing pink-orange, which is consistent with shellac. The samples were taken from REPRO.1864-57 (Christ at Bethany, object dimensions 135.0X112.0 cm) (B).

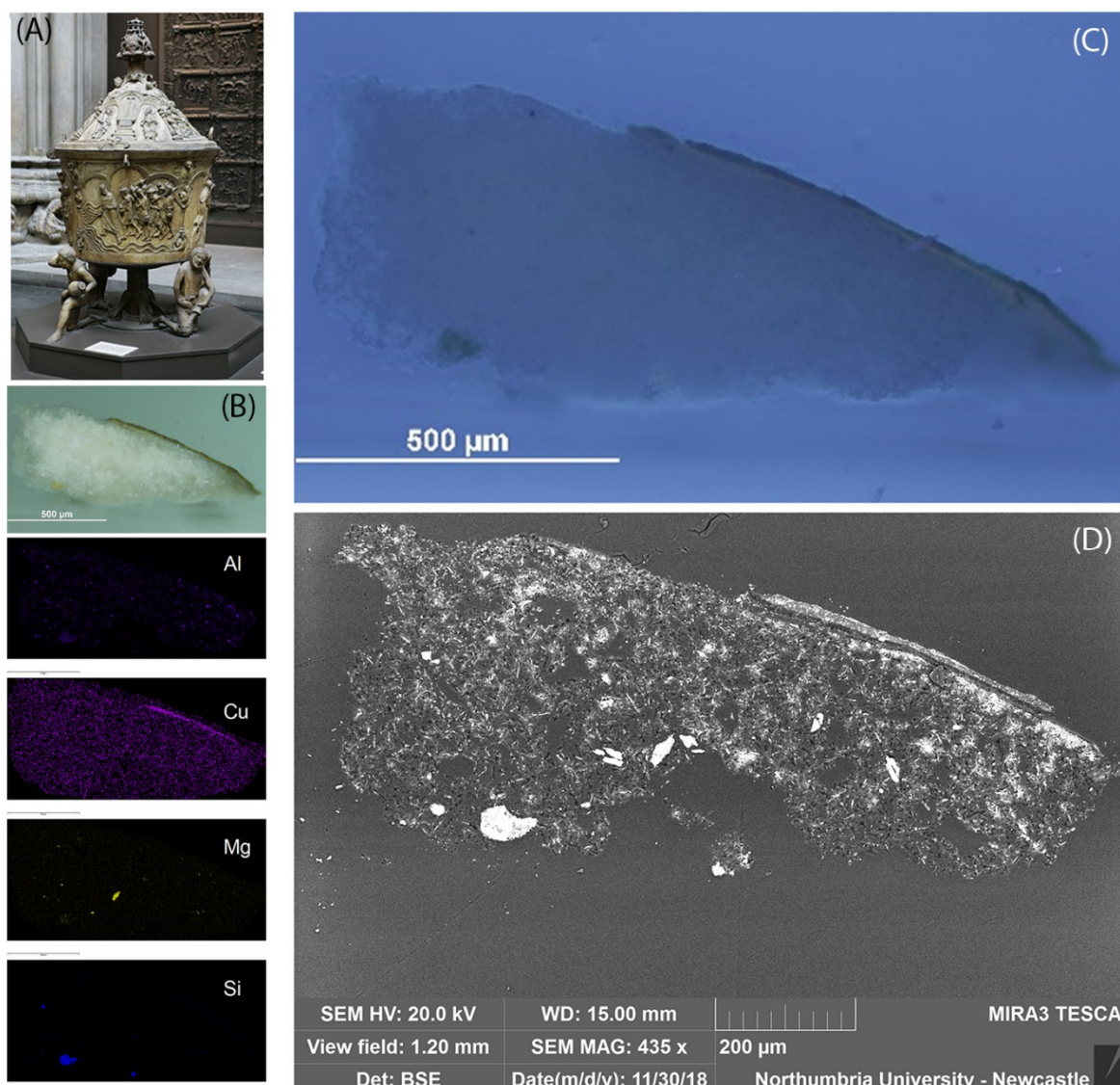


Figure 4.22. Sample 1 from REPRO.1874-29 (Brass font, object dimensions 183.0X990.0 cm) (A) shows a Cu and shellac coating. VLR (B) and UVf (C) OM, BSE (D) images and EDS mapping showing Al, Cu, Mg and Si.

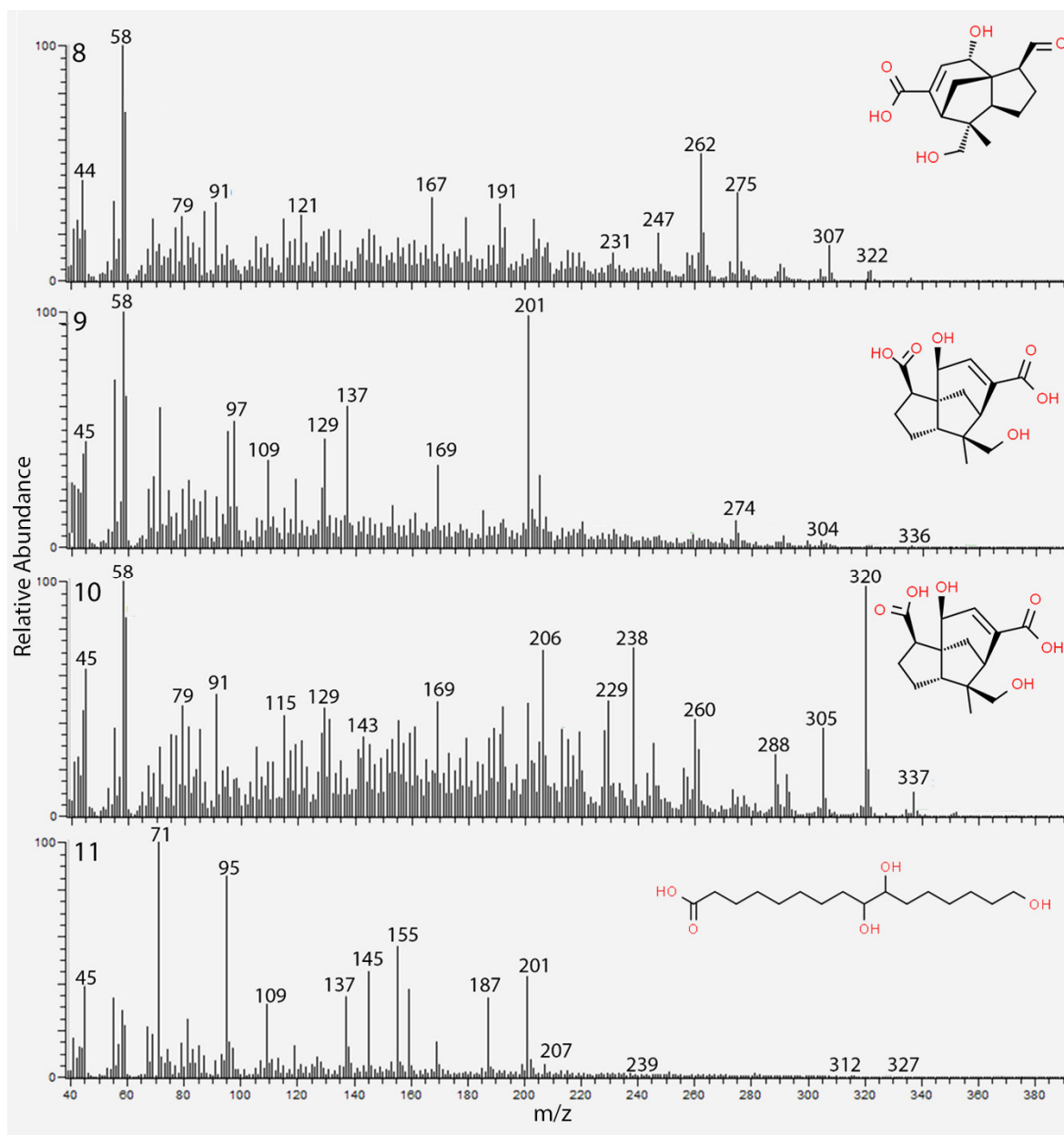


Figure 4.23. EI-MS of jalaric acid (8), shelloic acid (9), shellolic acid (10) and aleuritic acid (11). The list of peaks can be seen in Table 4.5.

Table 4.8 shows a summary of the characteristics observed in the coating layer. By considering all said until now, three types of coatings were identified:

- Si-Al and diterpene resin,
- Si-Al and shellac,
- Cu and shellac.

Other types of surface layers were also observed on top of the bulk-interface-coating stratigraphy defined up until now and were considered later additions (as observed over a layer of dirt) or a replacement of the original coating when damaged. In a few cases, the stratigraphy of one sample appears totally different from the others in the same object and

showed different inclusions and/or several layers, suggesting that the sample was taken from an area of repair or filling. In several samples, phthalic anhydride (**12**) and dimethyl phthalate (**13**) (Figure 4.24) were found in the samples showing a different coating and/or stratigraphy. Phthalic compounds can indicate the presence of a range of different twentieth-century materials; in conservation, they can be found, for example, in alkyd paints, polyvinyl adhesives and BEVA®371 and cellolyn (Horie, 2010). Given that the phthalates were detected in samples in which layers of barium (Ba), zinc (Zn), Ti or Fe were also observed, it seems more likely that alkyd paints have been used for the retouching or repaint of damaged areas. V&A conservators have confirmed that polyvinyl adhesives, BEVA®371 and cellolyn have not been used in the casts, but more analysis is required for confirmation. Overpaints, repaints and fillings are listed and briefly discussed in Section 4.3.4 and more examples are shown in Appendix 9.

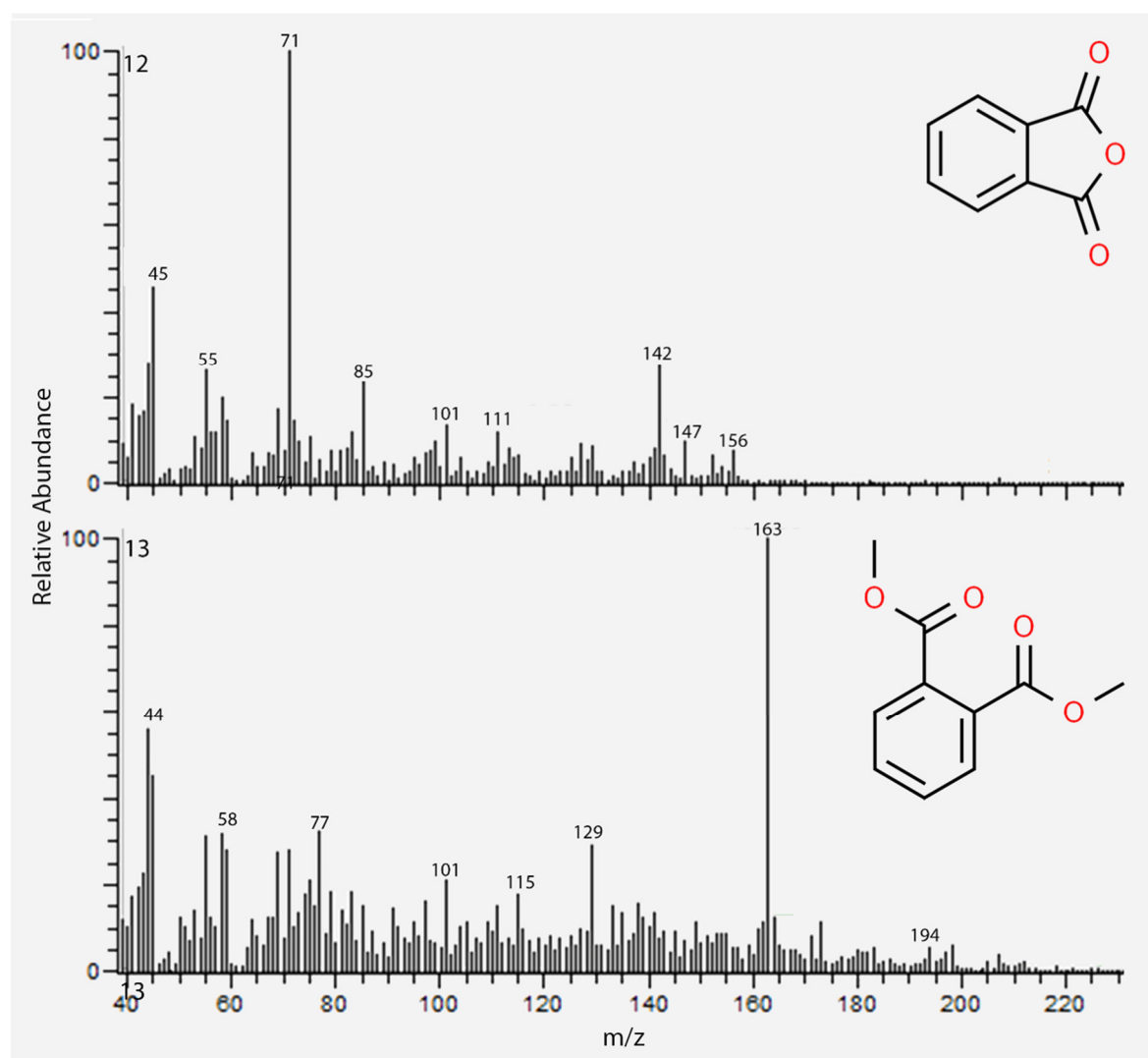


Figure 4.24. EI-MS of phthalic anhydride (12) and dimethyl phthalate (13). The list of peaks can be seen in Table 4.5.

Table 4.8. Summary of features observed in the samples analysed. Samples codes described in Table 4.1.

Sample*	Type of coating				
	Si-Al	Other elements**	Diterpene resin*	Triterpene resin	Shellac
REPRO.1873-380_3	✓		✓		
REPRO.1873-380_5			✓		
REPRO.1873-380_8	✓		✓		
REPRO.1873-380_10	✓				
REPRO.1873-380_11	✓	K			
REPRO.1873-380_12	✓				
REPRO.1873-380_13	✓		✓		
REPRO.1873-561_1-5			✓		
REPRO.1874-29_1	✓	Cu			✓
REPRO.1874-29_2					✓
REPRO.1874-29_3					✓
REPRO.1874-29_4					✓
REPRO.1874-29_5					✓
REPRO.1874-45_2	✓				✓
REPRO.1874-45_4	✓				
REPRO.1875-16_4	✓			✓	✓
REPRO.1875-17_1	✓	Ti			
REPRO.1875-17_3				✓	
REPRO.1890-80_1	✓				
REPRO.1890-80_2	✓				
REPRO.1890-80_3	✓				
REPRO.1890-80_4	✓		✓		
REPRO.1890-81_1	✓	Mg			
REPRO.1890-81_2	✓	Mg			
REPRO.1890-81_3	✓	Mg			
REPRO.1890-81_4	✓	Mg			✓
REPRO.A.1916-3152_3	✓	Sr	✓		
REPRO.A.1916-3152_4	✓	Sr			
REPRO.A.1916-3153_1	✓				
REPRO.A.1916-3153_3	✓	Fe	✓		
REPRO.1864-57_2	✓	Sr			
REPRO.1864-57_3	✓				✓

* The samples that are not listed here either did not show any difference in the surface layer or are shown in Table 4.10, as identified as areas of repair.

** Several trace elements were detected in the surface layer. In this column, only the elements visible in the EDS mapping in a layer shape are listed.

4.3.4. AREAS OF RETOUCHING OR REPAIR

Several samples, that were likely taken from areas of repair or retouch, showed different characteristics than samples taken from original layers of the objects. Two types were identified: type a in *Table 4.9* represents a stratigraphy that is entirely different from the one observed in the majority of the samples, suggesting that new materials were added to the cast to fill an area of loss (*Figure 4.25*); type b in *Table 4.9* represents the samples showing the aforementioned bulk-interface-coating stratigraphy and additional layer(s) of varnish or paint, indicating that the surface was re-coated to cover surface damage (*Figure 4.26*). Additional representative images of the retouch or repair areas can be seen in *Appendix 9* and their characteristics are summarised in *Table 4.9*.

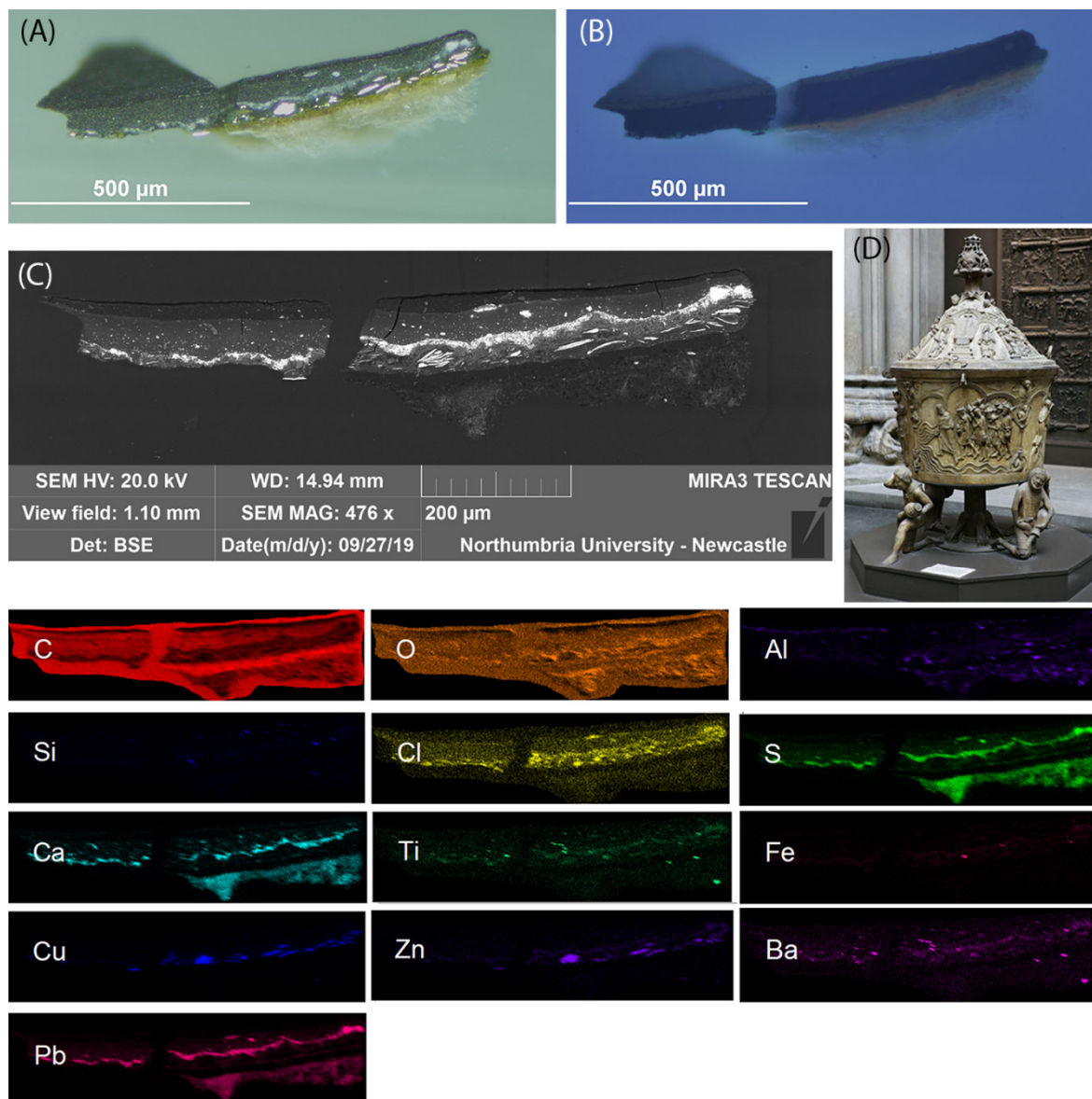


Figure 4.25. Sample 6 taken from REPRO.1874-29 (Brass font, object dimensions 183.0X990.0 cm) (D). VLR (A) and UVf (B) OM and BSE (C) images. EDS mapping showing C, O, Al, Si, Cl, S, Ca, Ti, Fe, Cu, Zn, Ba and Pb.

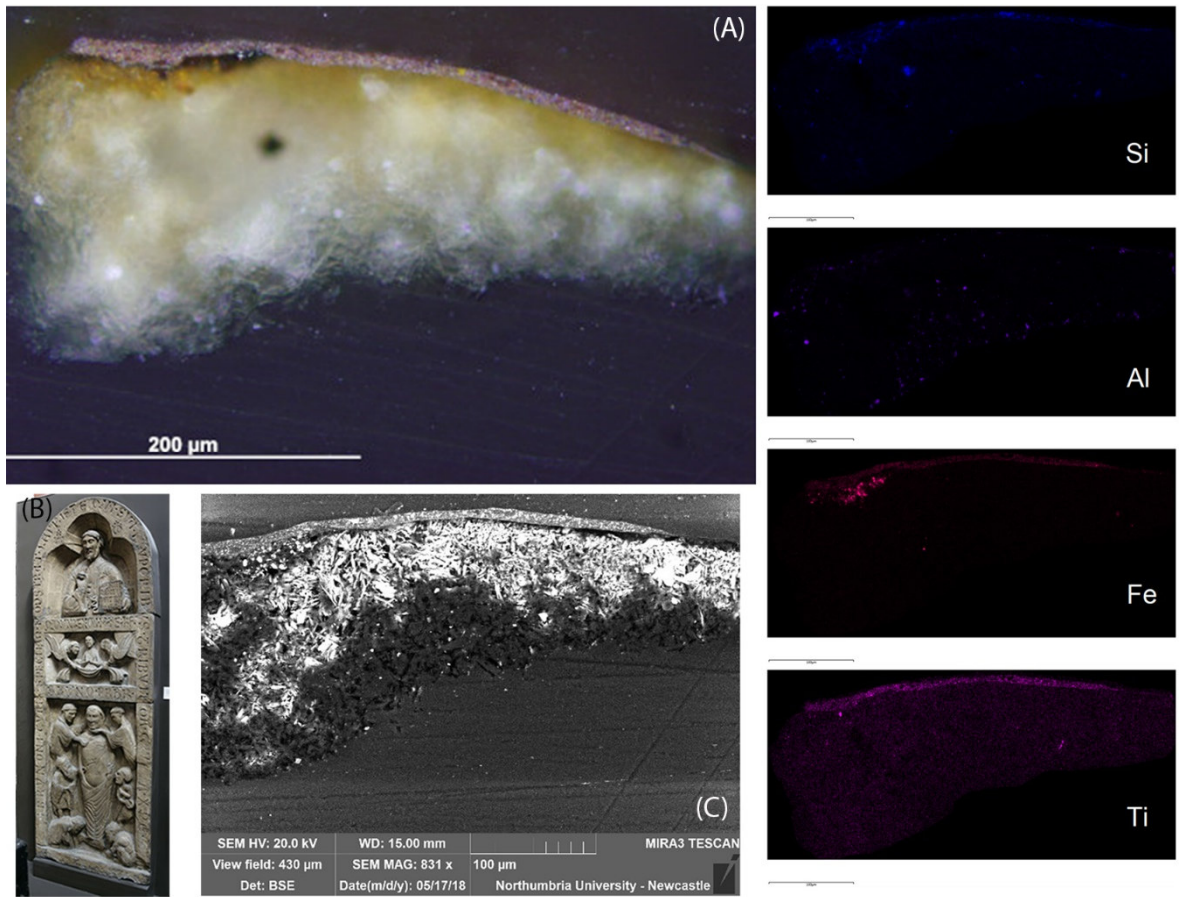


Figure 4.26. REPRO.1873-380_4. VLR OM (A) and BSE (C) images. EDS mapping showing Si, Al, Fe and Ti. The sample was taken from REPRO.1873-380 (Tombstone of the Presbyter Bruno, object dimensions 218.5X77.0 cm) (B).

Table 4.9. Summary of features observed in the samples taken from areas of repair. Samples codes described in Table 4.1.

Sample	Type*	Composition	Notes
REPRO.1873-380_4	b	Fe, Si and Ti; diterpenic resin, phthalate markers	Purple under VLR OM
REPRO.1873-380_6	a	Al-Si, Ti, K and Fe	Large orange and black particles visible in the VLR OM
REPRO.1873-380_7	a	Ba, Fe, Al and Si	Large orange and black particles visible in the VLR OM
REPRO.1873-380_8	b		White fluorescence in UVf OM
REPRO.1873-380_9	b		White fluorescence in UVf OM
REPRO.1873-380_12	b		White fluorescence in UVf OM
REPRO.1873-380_13	b		White fluorescence in UVf OM
REPRO.1873-561_6	b	Si, Ba and Ti, diterpenic resin	Yellow in the VLR OM
REPRO.1874-29_6	a	Calcium sulfate, Pb and Ba, Ti and Al. Brass fillings (Zn and Cu) and traces of Cl. Shellac	Several layers
REPRO.1874-45_5	b	Si, Al and Ti	
REPRO.1875-16_1	b	Si, Mg, Al and Ba, shellac	
REPRO.1875-16_2	b	Si, Mg, Al and Ba, shellac	
REPRO.1875-17_1	b	Ti	
REPRO.1875-17_2	b	Calcium sulfate and Pb, Si, Cl, Fe, Ba, Na, Zn, Ti and P	
REPRO.A.1916-3152_1	a	Calcium sulfate, Pb and Si-Al inclusions; traces of Cl, Al, Si and Fe	White in the VLR OM
REPRO.A.1916-3152_2	a	Calcium sulfate, Pb and Si-Al inclusions; traces of Cl, Al, Si and Fe	White in the VLR OM
REPRO.A.1916-3153_4	a	Ba, Zn, Na and traces of Fe and Cl	White in the VLR OM
REPRO.1864-56_1	a	Sr, Ba and Zn	White in the VLR OM and slightly fluorescent under UVf
REPRO.1864-56_2	a	Calcium sulfate, Pb and Fe, Ba, Cl, phthalate compound	
REPRO.1864-57_1	b	Al, Ba and Si	

* a= the stratigraphy is entirely different from the one observed in the rest of the samples; b= the original stratigraphy is observed underneath the additional layer(s).

4.4. SIMILARITIES AND DIFFERENCES WITHIN THE GROUPS

The objects selected for the characterization in this study, despite being manufactured in different workshops, show a similarly simple stratigraphy. The objects were selected as they showed neutral coatings, rather than polychromed and more complicated patterns. This choice was due to the lack of extensive previous analytical examination of the casts and considering that the characterization of simpler stratigraphies can facilitate the development of the method and pave the way for further studies.

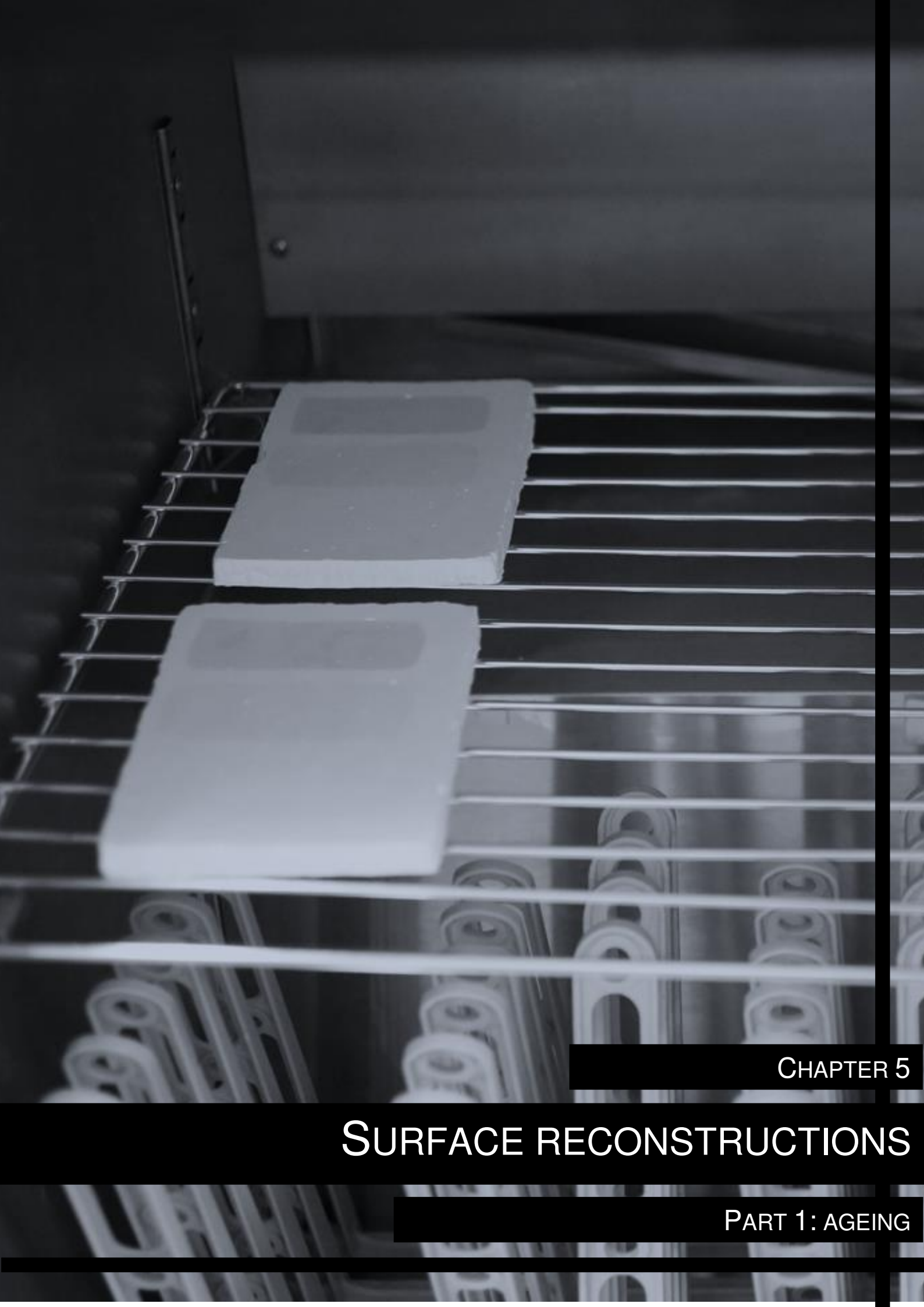
In summary, the stratigraphy of the samples is quite consistent, featuring a 'substrate' layer, an 'interface' layer and a coating 'dark' layer, likely a combination of aged coating and dust. On top of these, some samples feature additional layers, having been overpainted or having been sampled from an area of repair. The bulk of the object is made of gypsum plaster, which contains several types of inclusions (including silicates and carbonates). *Table 4.10* shows a summary of these findings divided by group. It is possible to notice that the presence of a particular type of inclusions (for example Mg, Sr, Fe or Ti) was not consistently observed in the groups, but was particular to individual objects. A larger sampling campaign combined with trace analysis might highlight such differences, which were beyond the scope of this study. The fact that only two types of coatings were largely observed in the samples and that these are not defining of the different groups suggests that Si, Al, shellac and diterpene resin were possibly used in the nineteenth century to achieve the limestone/stone appearance that unites the selected objects. Due to the diffusion of the organic media in the bulk, it is not possible to determine whether the media were applied before, after or bound to the Si-Al compound. Only object REPRO.1874-29, which is a copy of a brass font, showed a coating made of copper and shellac, possibly more suitable to achieve the brass appearance. Several samples taken from areas of repair or repaint showed similar traits in their stratigraphy, even in different objects. This could constitute an interesting topic for further research, as it might allow the identification of the different restoration campaigns in the Cast Courts and highlight their materials and methodology.

Table 4.10. Summary of findings divided by group. Objects' Museum accession numbers shown in Table 4.1.

	Object	Bulk	Coating	Areas of repair
Küsthardt Group	REPRO.1873-380	Gypsum plaster, Si, Al and Ca inclusions	Si and Al, diterpenic resin medium	Areas of repairs consist of overpaints containing phthalates and inpaints containing Si or Ba
	REPRO.1873-561	Gypsum plaster, Si, Al and Ca inclusions	Si and Al, diterpenic resin medium	Area of overpaint containing Si, Ba and Ti
	REPRO.1874-29	Gypsum plaster, Si, Al and Ca inclusions	Si and Al, traces of Cu, Cl, Zn, Fe, P, Mg and K, the medium is shellac.	Sample 6 appears different from the rest of the samples, presenting extra layers, and it is possible that this area was repaired
	REPRO.1874-45	Gypsum plaster, Si, Al and Ca inclusions	Si and Al and shellac resin	<i>Not sampled</i>
	REPRO.1875-16	Gypsum plaster, Si, Al and Ca inclusions	Si and Al and shellac resin	Sample 1 appears different from the rest of the samples, presenting two extra layers, one of which is made of Ba-based paint
	REPRO.1875-17	Gypsum plaster, Si, Al and Ca inclusions	Si and Al and triterpene marker	Sample 2 appears different from the rest of the samples, containing Pb in all the layers and Fe and Cl in the surface layer
Notre-Dame Group	REPRO.1890-80	Gypsum plaster, Si-, Ca- and Mg-based inclusions	Mg, Si, and Al; the organic medium is oxidised diterpene resin	<i>Not sampled</i>
	REPRO.1890-81	Gypsum plaster, Si-, Ca- and Mg-based inclusions	Mg, Si, and Al; the organic medium is shellac	<i>Not sampled</i>
	REPRO.A.1916-3152	Gypsum plaster, Si-, Ca- and Mg-based inclusions	Samples 1 and 2, taken from the front-facing side of the relief shows a significant concentration of Pb (and Si and Al too). White-blue fluorescing coating, containing a diterpenic resin.	<i>Not sampled</i>
	REPRO.A.1916-3153	Gypsum plaster, Si-, Ca- and Mg-based inclusions	Si and Al, the triterpene organic medium mixed with drying oil or just one of these	Sample 2 appears different from the rest of the samples, containing Pb in all the layers and Fe and Cl in the surface layer
Franchi Group	REPRO.1864-56	Gypsum plaster, Si-Sr-K-Al silicates	Wax or resin penetrated in the bulk	Sample 1 is made of gypsum plaster and toned with Ba, Zn and Sr paint. Sample 2 is made of gypsum plaster containing Pb, contains phthalates and Fe, Ba and Cl
	REPRO.1864-57	Gypsum plaster, Si, Ca and Al inclusions	Dust/dirt can be seen underneath the coating layers suggesting that the coatings were applied sometime after the manufacturing of the cast. Coating taken from the reverse or the edge of the object contains Si, Al and Ba or Sr. Two different coatings, one of which is shellac-based	<i>Not sampled</i>

4.5. CONCLUSION

A complete scientific examination of selected nineteenth-century plaster casts from the V&A collection, based on a multi-analytical approach allowed to shed light on the materials constituting the surface layers. Twelve plaster casts, grouped according to the workshop and provenance (Küsthardt, Notre-Dame and Franchi Group), were observed and documented. 63 samples were taken from areas of pre-existing damage. The analytical method employed included OM, XRD, SEM-EDS, FT-IR and py-GC/MS. The analyses were undertaken to establish the stratigraphy and the layer compositions of the objects. Characterisation, interpretation, and further information was supported by the materials and techniques which are described in historical sources and determined workshop practices as deduced by similarities and differences observed in the samples. The stratigraphy in all objects was consistently made of three layers: a bulk, a coating and their interface. Several types of additional coatings were observed, which must have been applied at a later stage after the construction of the casts when seen over a layer of dirt. The bulk is made of dihydrate calcium sulfate (gypsum plaster). Between the surface layers and the bulk, there is an interface layer that was formed upon the absorption of these coatings into the top layers of the plaster bulk. The coating layer was a mixture of oxidised organic medium and dirt. In most of the samples, the surface layer contains silicon and aluminium, possibly due to the use of clay water as a separating agent or a clay mineral pigment to tone the coating. The medium was identified as made of pine or shellac resins. By reviewing and comparing the results of the characterization of the casts, through an extensive database, it was possible to highlight that the differences observed within the groups cannot be considered distinguishing of the different workshops. Nonetheless, the multianalytical method selected for the analysis of the nineteenth-century V&A plaster casts has proven effective for the identification of the inorganic and organic components of the historical coatings applied to the plaster surfaces. This suggests that larger analysis campaigns based on this multi-analytical protocol have the potentiality of providing information on the workshop practices. In this chapter, **objectives 4, 5 and 9** described in *Section 1.5.4* are addressed.



CHAPTER 5

SURFACE RECONSTRUCTIONS

PART 1: AGEING

5.1. INTRODUCTION

The experimental strategy described below is designed to ensure a systematic method to reproduce possible stratigraphies of nineteenth-century plaster casts. The variety of materials used by *formatori* during the nineteenth century cannot be comprehensively represented in this study; therefore, a selection of materials was made based on findings on historical technical sources and patents (*Section 3.2*), as well as the analysis of the V&A casts (*Section 4.3*). The complexity of the composition of the stratigraphy of a historical plaster cast is due to the variety of the materials used during the steps of moulding – namely in the plaster bulk, inorganics such as sulfates, clays and carbonates, and organic, such as resins, oils and glues –, finishing – namely inorganic, such as sulfates and silicates, and organic such as oils, resins and waxes – and their mixtures (Auerbach, 1961; Risdonne *et al.*, 2021; Turco, 1990). The decay of the component materials, resulting in salts and carboxylates, and further contamination due to more recent moulding or conservation treatments should have led to additional compositional complexity. A representative example is the case of the acquisition of the V&A cast of the *Portico de la Gloria* (Baker, 1982). Additives to slow or quicken the setting of the plaster, or to improve mechanical properties of the plaster casts were usually added into the wet mixture before casting (Millar, 1899; Risdonne *et al.*, 2021; Wager, 1963). As the aim of this research was to study the coatings, the investigation of the effects of possible additives in the bulk of the plaster was beyond the scope.

Four different types of coatings were selected for this study, as frequently found in the historical technical literature (*Table 3.5*) and several layers of the V&A objects analysed for this study (*Table 4.6*, *Sections 4.3* and *4.4* and *Appendix 6*): linseed oil, shellac, barite solution and beeswax.

5.1.1. LINSEED OIL

Linseed oil is extracted from the herbaceous plant flax (*Linum usitatissimum L.*) and has numerous applications in painting, varnishes, wood treatment and linoleum due to its drying properties. Linseed is grown in several geographic areas, but the major world producers are Canada, China, Kazakhstan, India, and Europe (Symoniuk *et al.*, 2016) and the oil

pressed from the seeds displays natural variation in the composition that reflects the growing, agronomic and environmental conditions (Gunstone, 2011). Flax oilseeds contain about 36–40% of oil (Dlugogorski *et al.*, 2012). There are four varieties of linseed oil sold in the market, including raw, boiled, stand and refined linseed oils (Dlugogorski *et al.*, 2012). Raw linseed oil (cold-pressed) refers to pure oil with no additional treatment and with no additives, while boiled linseed oil is produced by adding a mixture of hydrocarbon solvents and metallic dryers to speed its drying time. *Boiled oil* is a well-known trade name, even though the process does not involve boiling raw oil, whereas the stand linseed oil is processed by heating the oil to about 300°C, over a few days in the absence of oxygen. During this process, a polymerisation reaction occurs, increasing the oil's viscosity. It means that stand or polymerised oil has been boiled to make it unreactive and more viscous. The oil consists almost exclusively of the esters of glycerol (C3 alcohol with three hydroxyl groups, one on each carbon atom) and five fatty acids, two of them saturated, C16 palmitic and C18 stearic, and three unsaturated, oleic, linoleic, and linolenic, exhibiting one, two and three double bonds, respectively (Gunstone, 2011). Several studies have been undertaken to investigate the oxidation of the components in linseed oil (Dlugogorski *et al.*, 2012; Lazzari & Chiantore, 1999; Oyman *et al.*, 2005; Symoniuk *et al.*, 2016). These studies led to establishing a generally good understanding of the overall radical chain reactions that operate in the oxidation process. Numerous analytical methods have been applied to identify and quantify the chemical changes during oxidation, the gaseous and liquid products, and the catalytic effect of metal dryers. The chemical structure of the triacylglycerols in the oil determines the reactivity of the species in the radical chain reactions. The significant catalytic pathways proceed either through the decomposition of hydroperoxides or the formation of coordination complexes (Grehk *et al.*, 2008). Linseed oil forms a continuous film with good optical and mechanical properties after being spread out in a thin layer. It cures slowly in the air without using a catalyst as the double bonds of the unsaturated acids in the oil react with oxygen in the air and with one another to form a polymeric network that determines the drying power of such oils, resulting in the liquid layer evolving to a solid film (Dlugogorski *et al.*, 2012; Lazzari & Chiantore, 1999). The drying reaction of linseed oil continues for many years even when the oil film seems to completely dry in a few days and the presence of glycerides as plasticisers can moderate the hardening process (Lazzari & Chiantore, 1999). The oil can gain up to 40% of its original weight during oxidation in the drying process with some weight loss due to the decomposition and disappearance of volatile compounds during oxidation reaction and the presence of metals and anti-oxidants affects the oxidation processes (Dlugogorski *et al.*, 2012). Detailed studies on the different types of oxidation and degradation of linseed oil have gone so far as to define the step by step mechanism by the use of a great variety of thermal and spectroscopic techniques (De Viguerie *et al.*, 2016; Dlugogorski *et al.*, 2012; Grehk *et al.*, 2008; Lazzari & Chiantore, 1999; Oyman *et al.*, 2005; Symoniuk *et al.*, 2016).

These studies describe reactions of thin films of linseed oil and, despite not being fully representative of the plaster-linseed oil system, are greatly important to support and complement the results herein discussed. Linseed oil and boiled linseed oil were found in the technical historical literature (Auerbach, 1961; Frederick, 1899; Millar, 1899; Wager, 1963). Linseed oil would have been the best match in several of the analysed objects, but it was demonstrated that it could not be uniquely assigned (*Section 4.3.3*).

5.1.2. SHELLAC

Shellac is described in the literature as a cross-linked oligomer (MW \approx 1000 Da), a purified product of lac, a natural resinous material secreted by the parasitic insect *Kerria lacca* on various host trees in India, Thailand, and Myanmar (Maria Perla Colombini & Modugno, 2009; Farag & Leopold, 2009). Broken branches are sold as *stick lac* and, after grinding and washing with water to eliminate wood and red pigments (*lac dye*), *seedlac* is obtained. Purification of *seedlac* gives the more homogeneous product known as *shellac* (Colombini *et al.*, 2003). At the end of the sixteenth century, shellac was introduced into Europe and has been widely used since as an adhesive, sealing, insulating and coating material for several applications, including the production of musical instruments, the protection of vinyl records, and the insulation of radios and electrical tools (Tamburini *et al.*, 2017). Shellac colours range from deep red to pale gold. Currently, shellac is still used as a wood-finishing material and a coating for pharmaceuticals and food products. Shellac has also been used in the field of conservation, as a varnish for wooden objects (*French polish*) and mural paintings, or as an adhesive for ceramics (Derrick *et al.*, 2000). Shellac is a mixture of resin (70–80%), wax (6–7%) and colourant molecules (4–8%) (Tamburini *et al.*, 2017). Shellac in its refined form is a polyester type of resin consisting of two aliphatic hydroxy acids (butolic acid, ca 8%, and aleuritic acid, ca. 35%) with several related sesquiterpenoid carboxylic acids (jalaric, ca. 25%, and laccijalaric acids, ca 8%, and their reduction and oxidation products). The relative amounts of these acids and how the corresponding esters are formed differ for the “soft” and “hard” resin, with the “soft” resin generally having a lower molecular weight and the “hard” resin constituting the backbone of the material. The composition varies depending on the insect species as well as the host tree from which the raw material is obtained. Shellac is insoluble in water, glycerol, hydrocarbon solvents and esters but dissolves readily in alcohol, aqueous solution of alkalis, organic acids and ketones (Sharma *et al.*, 1983). The stability and degradation behaviour of natural resins have been investigated by many authors (Coelho *et al.*, 2012; Colombini *et al.*, 2003; Poli *et al.*, 2014) for their important role in conservation chemistry but resin compositions and related degradation issues are not completely understood.

Shellac was found in the technical historical literature, also called *white polish*, and to be mixed with a methylated spirit (Auerbach, 1961; Bankart, 1908; Millar, 1899; Wager, 1963). Meilach (1966) highlights that shellac could turn slightly yellow and the use of orange shellac must be avoided. In several of the V&A casts analysed, shellac was observed in the stratigraphy and detected by pyrolysis-Gas Chromatography/Mass Spectrometry (*Section 4.3.3*).

5.1.3. *BARITE*

Barium sulfate (BaSO_4) commonly referred to as barite or baryte, is used widely because of its high specific gravity, opaqueness to X-rays, inertness and whiteness. The barite mineralogical group consists of baryte, celestine, anglesite, and anhydrite (Sifontes *et al.*, 2015). Barite is one of the most important fillers used in the plastics, rubber, lithographic ink, paint industries, linoleum, oilcloth and pharmaceutical formulations. As a pigment, barium white can be obtained by the mineral barite, but can also be made artificially, and then called *blanc fixe*, as discovered in the late nineteenth century. Blanc fixe is a white, opaque pigment composed of zinc sulfide and barium sulfate (Derrick *et al.*, 2000). Barite is suggested as an inorganic coating in several recipes and patents (*Section 3.2*). also discussed in modern reviews (Payne, 2020) and largely discussed for electric engineering and building science, as related to indoor and outdoor coatings (renders) (Freire *et al.*, 2015). Turco (1990) suggests that the hardening and waterproofing efficacy of barite lays in its ability to react with the calcium sulfate, modifying the outer gypsum plaster surface in barium sulfate, harder and more resistant to water than the calcium type. As discussed in *Section 4.3*, the assignment of such an element to a particular layer must be cautious as barium is a natural contaminant of mineral gypsum (Cox *et al.*, 1974; Mahmoud *et al.*, 2012).

Barite solutions were found in the technical historical literature in Millar (1899), Kemp (1912) and Turco (1990). According to Turco (1990), barium oxide (BaO) would absorb water and carbon dioxide (CO_2) from the air, turning into hydroxide (caustic barite) and barium carbonate, which will then react with gypsum and produce calcium carbonate, harder than the sulfate. Payne (2020) also highlighted the use of barite solutions for the conservation of plaster casts in the nineteenth century. Despite the expectations and the fact that barium was detected in most of the casts by Energy-dispersive X-ray spectroscopy (EDS) analysis, EDS mapping did not suggest that a barite solution was applied on the surface of the casts. Barium-containing surface layers were only observed in areas of repair, suggesting that more modern colours used by conservators contained barium (*Section 4.3.4*).

5.1.4. BEESWAX

Beeswax is produced by many species of bees, the most common being *Apis mellifica*. It is secreted from the organs of the worker bees and is used in the formation of the cells of the honeycomb (Derrick *et al.*, 2000). Wax may be obtained by melting the combs in hot water and straining to remove impurities that may contain resins, sugars, and other plants materials. The waxes from various localities vary considerably in colour and texture and chemical composition. The colour ranges from light yellow to dark brown. The darker varieties can be bleached by exposure to light and air, or ozone or hydrogen peroxide. Beeswax contains about 10% hydrocarbons in addition to alcohols, acids and ester. Chemical identification of beeswax in archaeological samples is generally based on the detection of characteristic solvent-soluble molecular constituents, including a series of odd-numbered linear hydrocarbons (C21-C33), even-numbered free fatty acids (C22-C30) and long-chain palmitate esters in the carbon range C40-C52 (Regert *et al.*, 2001). Contemporary beeswax shows a characteristic recognizable pattern of n-alkanes of which heptacosane (C27) is the major compound of esters with the main constituent that contains 46 carbon atoms, and of free fatty acids, of which lignoceric acid (C24) is predominant (Regert *et al.*, 2001). To better understand the decay of beeswax, laboratory degradation experiments accelerated by temperature were performed on contemporary beeswax in several studies (Čížová *et al.*, 2019; Liu *et al.*, 2019; Regert *et al.*, 2001; Svečnjak *et al.*, 2015). These experiments yield new insights into the evolution of fatty acid, n-alkane and ester patterns, which depend both on chemical and physical mechanisms, but raised the question of the effect of high temperatures used for the accelerated ageing (Regert *et al.*, 2001) on the chemical decay of the wax. Low molecular weight phenolic compounds, both benzoic and cinnamic acid derivatives, are formed during beeswax degradation.

Beeswax was found in technical historical literature (Auerbach, 1961; Millar, 1899; Wager, 1963). For example, Frederick (1899) suggests that beeswax with an equal amount of turpentine can be used to finish the casts. Beeswax was one of the materials initially hypothesised as used for the coating of the V&A casts selected for this study and considered as traditional materials used by the conservators.⁵⁸ Although beeswax was not detected in the objects of this study (*Section 4.3.3*), it was considered as a coating for the historical reconstructions presented below.

The following sections describe a study of the making and the ageing of coated plaster casts. Furthermore, it provides a multianalytical physicochemical study for the assessment of the surfaces as well as the visual and molecular post-ageing modifications.

⁵⁸ Personal communication with Charlotte Hubbard, former V&A Head of Sculpture Conservation until 2019.

5.2. EXPERIMENTAL METHOD

The experimental method for the making of the coated plaster surface reconstructions (*Section 5.2.1*) and the description of the instrumentation for the assessment (*Section 5.2.2*) of surfaces ageing is given in this section.

5.2.1. COATED PLASTER SURFACE RECONSTRUCTIONS

5.2.1.1. Plaster substrates

A rubber mould was purposely made with Alec Tiranti® RTV-101 Silicone Rubber and Cat '28' curing agent to produce rectangular shaped plaster plates (length: 9.5 cm, width: 14.0 cm and depth: 1.0 cm). The thickness of the plaster support (hereafter 'plate', P) was chosen to ensure that it would represent a theoretically infinite thickness, as in a plaster cast the thickness of the plaster bulk is infinitely greater than the thickness of the coating.

Twelve plaster plates (P1 to P12) were prepared with Formula Saint Gobain Fine Casting Plaster. The raw and dry plaster was mixed with deionized (DI) water (pH= 7.00 at T= 18.1 °C) in the traditional 'island' method (Meilach, 1966) by evenly sprinkling the plaster over the entire surface of the water, allowing it to settle and continuing in this way until little island started to appear above the water level (*Figure 5.1*). After letting the mixture settle for a couple of seconds, it was mixed to a double cream consistency (Coon, 2009).

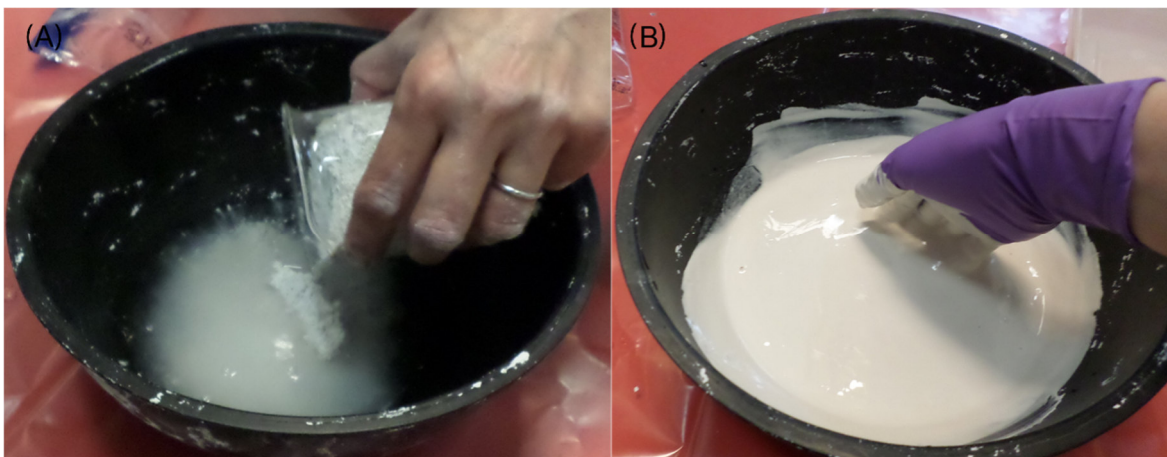


Figure 5.1. Plaster was added to the water in the traditional 'island' method (A) until a creamy consistency was achieved (B).

The water-to-plaster ratio (expressed in terms of 100 parts of plaster) (*Section 3.1*) aimed for the mixture was the one suggested by Meilach (1966) (50:100), and Turco (1990) (45:100). The weights were measured for each of the mixtures (*Table 5.1*). Three ‘control’ plaster ‘cubes’ (C1, C2 and C3) were also made in the mould prepared for casting the V&A casts’ samples in resin (*Section 4.2.4*), to have a reference for the weight variation of the plaster without any coating during the experiments (*Appendix 8*). The water-to-plaster ratio and the setting and drying conditions were kept constant for all the samples, as this would ensure an almost constant porosity, which might affect the properties of the coatings. A follow-up study would be desirable to add these variables.

Table 5.1. Quantities and times for the preparation of the plaster plates.

MIXTURE	WATER [g]	GYPSUM [g]	WATER-PLASTER RATIO (:100)	MIXING TIME [min]	SETTING TIME [min]	NOTES*
1	53.57	86.51	61.93	4	11	Not used
2	63.66	125.18	50.85	5	9	Not used
3	84.61	167.66	50.46	3	8	P1`
4	87.22	170.77	51.07	4	8	P2
5	87.07	172.52	50.47	4	6	P3, C1, C2
6	94.46	193.79	48.74	4	12	P4, C3
7	76.84	157.77	48.70	4	10	P5
8	79.26	161.67	49.03	2	8	P6
9	86.70	176.42	49.15	3	10	P7
10	87.42	178.99	48.84	3	12	P8
11	86.47	172.91	50.0`1	4	10	P9
12	87.02	176.20	49.38	4	9	P10
13	86.61	176.52	49.07	5	10	P11
14	88.10	178.16	49.45	3	11	P12

* P=plate, C=cube

5.2.1.2. Coatings

The coatings were applied to a support made of plaster. Each of the three different types of traditional coatings (linseed oil, shellac and barite water) was prepared following two different recipes, resulting in two different types or concentrations. An additional coating of beeswax was prepared following a selected recipe. The coatings are described below:

Coating (1) Linseed oil (applied with the aid of a brush, without dilution)

(1-1) Cold-pressed linseed oil (C. Roberson & Co., Code: CR32225J);

(1-2) Boiled Linseed Oil: Kremer Pigmente, 79424, Verkochter Leinollack, transparent.

Coating (2). Shellac (white shellac - Kremer Pigmente, 60471, Schellack Dreiring - in methylated spirit - Fisher Chemical M/4450/25, Methylated Spirit, IDA 99, 99% (v/v), Pure, Industrial Methylated Spirit IMS, 74 0.P., IMS - prepared by mixing the components and waiting until complete dissolution)

(2-1) (hereafter named 'shellac6%') 6 wt% solution was obtained by dissolving 3.15 g of white shellac in 50.10 g of IMS, as inspired by Wager (1963);

(2-2) (hereafter named 'shellac18%') 18 wt% solution was obtained by dissolving 10.85 g of white shellac in 50.60 g of IMS, to obtain a thicker solution.

Coating (3). Barite solutions (two different recipes inspired the following solutions of water (deionised water at 18 °C) and barite (barium hydroxide: Kremer pigmente, 64080)

(3-1) (hereafter named 'barite20°') 100 g of water, 5.58 g of crystallised pure hydrated barium oxide and 0.24 g of calcium hydroxide (powder, Sigma-Aldrich CAS No.: 1305-62-0) were mixed and stirred until dissolution at room temperature (about 20° C), as inspired by Millar (1899) quoting Dr Reissig experiment;

(3-2) (hereafter named 'barite60°') Turco (1990) suggests the use of *acqua di barite*, which is prepared, according to Salomone (1947), by dissolving barium hydroxide in 20 times its weight of warm water. The solution was therefore prepared by mixing 100 g of water and 5 g of crystallised pure hydrated barium oxide onto a heating unit (set at 60°C) and stirred until the solution was homogeneous.

Coating (4). Beeswax The solution was prepared by mixing 50 ml of beeswax (Kremer 62210 Beeswax, bleached, CAS No: 8012-89-3, corresponding to 28.90 g) in 50 ml of oil of turpentine (Sigma Aldrich Oil of Turpentine purified, corresponding to 135.30 g) onto a heating block until dissolution. The solution was applied warm (ca. 60 °C).

5.2.1.3. *Accelerated ageing equipment and parameters*

Thermal and humid exposure was undertaken in a Mercia Scientific MGF8401 Excell Humidity cabinet MER 180 SCN/RH. The cabinet allows a controlled temperature in a range +10 °C to +40 °C (better than +/- 2 °C) and humidity-controlled up to 75% (+/- 5% variation). A humidified air source (micro-mist) is achieved by utilising a series of ultrasonic oscillations beneath a small reservoir of water; the micro-mist is then circulated within the cabinet. The relative humidity (RH) was kept at 43.2% throughout the experiment and the temperature was 40 °C that was the maximum for the chamber.

Accelerated light ageing was run with a Q-Sun Xenon Xe-1 Test Chamber with a single 1800W (X-1800) Xenon–arc lamp equipped with two filters (Daylight and Window-Q) to cut radiation below 420 nm (irradiance 1.0 W/m² @420 nm). The xenon arc lamp covers 270–800 nm with a close match for sunlight. The filters coupled reproduces the spectral power distribution (SPD) of the sunlight, particularly in the important low-wavelength region of the UV spectrum (CIE No. 85:1989) or to simulate daylight that has passed through window glass (BS EN ISO 16474-1:2013). The temperature inside the Q-Sun chamber did not exceed 21 °C.

The timescale of the whole experiment is provided in *Section 5.2.1.5*, and *Tables 5.2* and *5.3*. The accelerated ageing times were set to compromise the experimental time available with the objective to achieve changes onto the plaster-coating surfaces (see *Sections 2.4.1*, *5.2.1.5* and *5.4*).

5.2.1.4. Artificial soiling

The following procedure was based on the study experimented with and published by Galatis *et al.* (2012). The dry portion of the soiling mixture was combined first and consisted of: carbon black pigment (Kremer Pigmente, wt.% 0.23), iron oxide pigment (Kremer Pigmente, wt.% 0.06), gelatine powder (VWR, code number: 24350, wt.% 1.14), soluble starch (wt.% 1.14), Portland Type I cement (B&Q Blue Circle Mastercrete Handy Pack Cement, wt.% 1.99), silica gel (Sigma-Aldrich Fumed Silica gel powder, S5130, wt.% 0.20), kaolin (Kremer Pigmente, 58250, wt.% 2.28). The wet portion was therefore added and consisted of high-grade mineral (paraffinic) oil (Sigma-Aldrich, 18512, wt.% 1.82), olive oil (wt.% 1.05) and white spirit (SLS scientific laboratory supplies, CHE3886, wt.% 90.09). The soiling was undertaken by spraying the admixture with an airbrush (*Figure 5.2*).

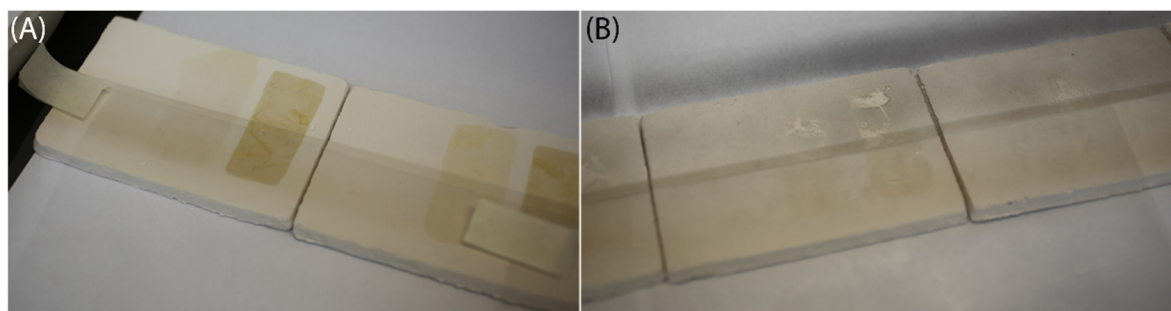


Figure 5.2. The bottom halves of the plaster plates were protected with Melinex® sheets (A) while the top half was airbrushed with the artificial soiling solution (B).

5.2.1.5. The build-up of the stratigraphy

After drying (gravimetric evaluation - *Section 5.2.2.1*), the twelve plaster plates were coated and aged. The linseed oil (1), shellac (2) and barite (3) coatings were applied on different plates following the recipes described in *Section 5.2.1.2*. The coating's area was equal to 21 cm². Each plate featured a control section (no coating applied) and two different coated sections (types 1 and 2). The application was made by brush and the amount of coating applied was visually decided. A total of four identical plates was obtained for each of the coatings (1), (2) and (3). An additional beeswax (4) coating was applied on two out of the four identical plates to recreate a later application of a coating, as suggested by Hubbard in Graepler & Ruppel (2019). Two plates for each of the traditional coating (1, 2 and 3), with and without coating (4), were aged as described in *Section 5.2.1.3* and detailed in *Table 5.2* and *Table 5.3*, whilst their identical ones were kept in room conditions.⁵⁹ Artificial soiling was applied onto the plates' top halves by airbrush (*Section 5.2.1.4*), either halfway through the thermal ageing, for the plates that were not going to be coated with the coating (4), or before the light ageing, for the plates coated with the coating (4). The sections on the plates were named as shown in *Figure 5.3*. Based on the rationale in *Section 2.4.1*, the accelerated ageing times were ultimately decided by compromising time availability with the objective to achieve changes onto the plaster-coating surfaces (see also *Section 5.4*). The steps at different times t_z ($z = 0$ to 38) and the corresponding event and time interval are shown in *Table 5.3*. For each t_z a gravimetry measurement was recorded (*Section 5.3.1*). The total time of artificial ageing is 130746 min (90 days, 19 hours, 6 minutes). The total time of natural ageing of the plates that did not undergo accelerated ageing was of 452024 min (313 days, 21 hours, 44 minutes). As for the plates that were aged in thermal and light chambers the natural ageing time is therefore 452024 min minus the time in the ageing chambers and equal to 321278 min (223 days, 2 hours, 38 minutes).

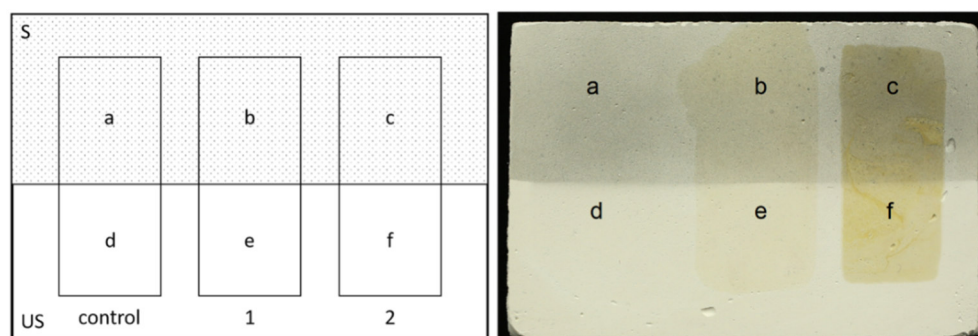


Figure 5.3. The scheme of the sectors on the plates (left). The sectors were named from a to f. S= soiled, US= unsoiled. On the right is shown an example: on P1, P1b is the sector coated with (1-1) and soiled (S).

⁵⁹ Recorded with a Meaco HK100 (sensor 1) and a Testo 608-H1 (sensor 2) thermohygrometers.

Table 5.2. Scheme of the plates (P), including coatings and ageing.

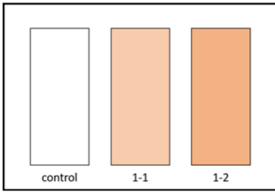
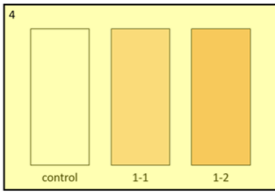
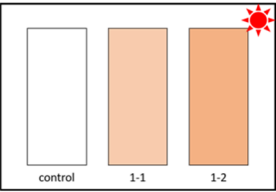
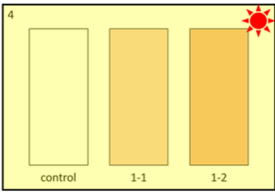
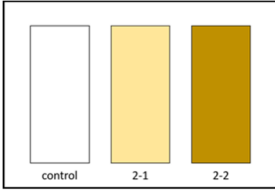
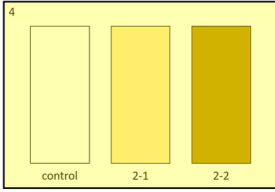
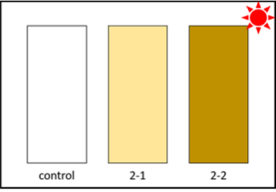
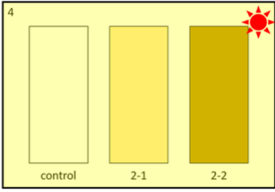
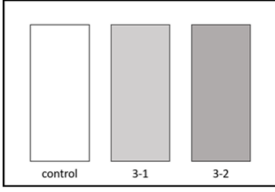
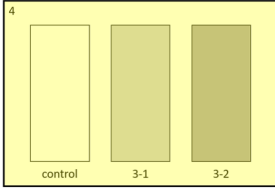
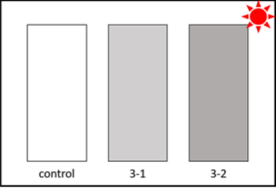
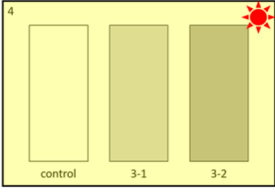
LINSEED OIL (1)		PLATES 1, 2, 3, 4	
			
P1 Control (no coating) (1-1) 2 coats of cold-pressed linseed oil (1-2) 2 coats of boiled linseed oil Naturally aged for 452024 min	P2 Control (no coating) (1-1) 2 coats of cold-pressed linseed oil (1-2) 2 coats of boiled linseed oil (4) 2 coats of beeswax Naturally aged for 452024 min	P3 Control (no coating) (1-1) 2 coats of cold-pressed linseed oil (1-2) 2 coats of boiled linseed oil Naturally aged for 321278 min Accelerated ageing 130746 min	P4 Control (no coating) (1-1) 2 coats of cold-pressed linseed oil (1-2) 2 coats of boiled linseed oil (4) 2 coats of beeswax Naturally aged for 321278 min Accelerated ageing for 130746 min
SHELLAC (2)		PLATES 5, 6, 7, 8	
			
P5 Control (no coating) (2-1) 2 coats of 6 wt% shellac in IMS (2-2) 2 coats of 18 wt% shellac in IMS Naturally aged for 452024 min	P6 Control (no coating) (2-1) 2 coats of 6 wt% shellac in IMS (2-2) 2 coats of 18 wt% shellac in IMS (4) 2 coats of beeswax Naturally aged for 452024 min	P7 Control (no coating) (2-1) 2 coats of 6 wt% shellac in IMS (2-2) 2 coats of 18 wt% shellac in IMS Naturally aged for 321278 min Accelerated ageing for 130746 min	P8 Control (no coating) (2-1) 2 coats of 6 wt% shellac in IMS (2-2) 2 coats of 18 wt% shellac in IMS (4) 2 coats of beeswax Naturally aged for 321278 min Accelerated ageing for 130746 min
BARITE (3)		PLATES 9, 10, 11, 12	
			
P9 Control (no coating) (3-1) 6 coats of cold barite solution (3-2) 6 coats of warm barite solution Naturally aged for 452024 min	P10 Control (no coating) (3-1) 6 coats of cold barite solution (3-2) 6 coats of warm barite solution (4) 2 coats of beeswax Naturally aged for 452024 min	P11 Control (no coating) (3-1) 6 coats of cold barite solution (3-2) 6 coats of warm barite solution Naturally aged for 321278 min Accelerated ageing for 130746 min	P8 Control (no coating) (3-1) 6 coats of cold barite solution (3-2) 6 coats of warm barite solution (4) 2 coats of beeswax Naturally aged for 321278 min Accelerated ageing for 130746 min

Table 5.3. Steps and time intervals (Δt) of the surface reconstructions making and ageing.

t	event	Δt
0	Plaster poured in the mould	-
1	Plates extracted from the mould	(1-0) Setting time, variable, see Table 5.1
2	Plates placed in storage	(2-1) ca. 200 min
19	Plates let dry at room temperature	(19-2) 71756 min (49 days, 19 hours, 56 minutes)
26	Application of coatings (1), (2), (3)	(26-19) 174 min
28	Coatings let dry at room temperature	(28-26) 185640 min (128 days, 22 hours)
29	All the plates in the thermal chamber	(29-28) 40140 min (27 days, 21 hours)
30	Application of soiling. The Plates that were not going to be coated with (4) were soiled at this stage	(30-29) 182 min
31	Plates in the thermal chamber	(31-30) 50249 min (34 days, 21 hours, 29 minutes)
32	Plates at room temperature and application of coating (4)	(32-31) 4267 min (2 days, 23 hours, 7 minutes)
33	Application of soiling. The P coated with (4) were soiled at this stage	(33-32) 139 min
36	Plates at room temperature	(36-33) 10229 min (7 days, 2 hours, 29 minutes)
37	All the plates in the light chamber	(37-36) 40357 min (28 days, 0 hours, 37 minutes)
38	Plates at room temperature until analysis	(38-37) 48878 min (33 days, 22 hours, 38 minutes)

5.2.2. EVALUATION

5.2.2.1. Gravimetry

Gravimetric measurements were taken throughout the preparation of the plates to evaluate the water loss as well as the effects of thermal and light ageing on the coatings. The measurements were taken with a JJ-BC Series Electronic Analytical Balance (JJ224BC, capacity 220 g, resolution 0.1 mg). To evaluate the effects of the ageing on the weight of the coatings, the % weight loss of the reference plaster cubes (C1, 2 and 3) was used to correct the weight of the plaster (P1 to 12) to observe the effects of the ageing on the coatings only. For every cube 30 weight measurements (nos. 0-29) were taken, so that each measurement was assigned a weight ($w_{C,j}$) at a time ($t_{C,j}$) ($j= 0\dots 29$). The weight measurements taken from the plates at t_z ($z= 0$ to 38) have a unique correlation with the weight measurements taken from the cubes at t_j ($j= 0$ to 29) (Table 5.3). The error of these weight measurements is given by the resolution (r) of the JJ-BC Series Electronic Analytical Balance and is equal to 0.1 mg. The weight loss % ($\Delta w_{C,0-j}\%$) of the cubes at $t_{C,j}$, relative to the initial weight $w_{C,0}$ at $t_{C,0}$, represents the water loss during the drying process and was measured as follows:

$$\Delta w_{C,0-j}\% = \frac{(w_{C,0} - w_{C,j})}{w_{C,0}} \cdot 100 \quad (5.1)$$

The weight loss % ($\Delta w_{c,0-j}$) of the cubes for each $t_{c,i}$ was used to apply a correction to the gravimetry measurements w_z taken from the twelve plaster plates (P1 to 12) at t_z ($z = 0 \dots 38$). Such correction was applied to observe the effects of ageing on the weight of the coatings only. The differences in the shape and size of the plates and the cubes (and therefore the different surface area-volume ratio) would have suggested that the rate of weight loss is different between the plates and cubes, but by looking at the plates and cubes gravimetry data, it was possible to assume that the rate is very similar. As the $w_{c,j}$ at $t_{c,j}$ of the cubes has a unique correspondence to the w_z at t_z measured on the plates, a point by point correction was applied and calculated as follows:

$$w'_z = w_z - \left(\frac{w_z \cdot \Delta w_{c,0-j} \%}{100} \right) \quad (5.2)$$

where w'_z is the weight of the plate, at time t_z , after the correction, w_z is the weight of the plate, at time t_z without correction and the weight loss % ($\Delta w_{c,0-j} \%$) of the cubes at $t_{c,j}$ correspondent to t_j . The data for the gravimetry of the plates were then normalised to the initial value w_0 and 100 by defining:

$$w''_z = \frac{w'_z}{w'_0} \cdot 100 \quad (5.3)$$

where $w'_z = (w'_1 \dots w'_{38})$ and w''_z is the z th normalised data shown in *Section 5.3.1*. A more detailed discussion on the calculations for the normalization of the gravimetry data and the error propagation is described in *Appendix 8*.

5.2.2.2. Visual Examination

The visual evaluation was carried according to EN ISO 4628-1 BSI Standards, on the evaluation of degradation of coatings. The British Standard (BS) was chosen to obtain a standardised designation of quantity and size of defects, and intensity of uniform changes in appearance. The BS provides that the first assessment of defect is carried out visually, without any magnification and defines several categories which aim to the designation of the quantity of defects, in the form of discontinuities or other local imperfections in the coating, scattered over the test area in a more or less even pattern, the average size, or order of magnitude, of defects, and the intensity of uniform changes, in the appearance of the coating, such as colour changes. The categories are rated from 0 to 5, and the BS provides a detailed description of each rating and category. The type of defect and its size or intensity (I0-5) shall be expressed together with the approximate dimensions of the area concerned, or its proportion of the total area expressed as a percentage (S0-100% of the

total area). Even upon the BS specification, visual examination remains dependant on the operator, but the use of the BS allows improved uniformity of parameters. In other words, in addition to describing the type of decay, it is essential to measure its extent or the area it covers; its severity, or how advanced the decay is; and the rate of decay over time.

5.2.2.3. *Visible (vis) and Ultraviolet fluorescence (UVf) reflectance*

Reflectance images of the plaster plates were taken at every stage of their preparation and artificial ageing to ensure that every detectable change was recorded under visible or ultraviolet illumination. A Canon EDS 6D camera allowed both visible light and UVf photography. For visible illumination two OSRAM DULUX L 55W/840 lamps were placed following a 45°/45° geometry. For UV illumination two UV lamps 8000K NARVA LT36W/073 Blacklight Blue were placed using a 45°/45° geometry. For UVf reflectance imaging, the camera was equipped with a UV filter Kodak Wratten 2E (52 mm Pitch: 0.75). All the images were taken along with the Colour Photography Chart #13.

5.2.2.4. *Scanning Electron Microscopy (SEM)*

Scanning Electron Microscope (SEM) analysis was performed with a field emission TESCAN MIRA 3 with gigantic chamber. The SEM is equipped with a backscatter detector (BSE), which was used to obtain BSE images of the surfaces through the software Alicona 3D imaging. The plates were analysed by SEM Low Vacuum Mode (10-15 Pa).

5.2.2.5. *Colourimetry*

For colourimetric analysis, a spectrophotometer CM-2600d (Konica Minolta) was used. The spectrophotometer operates with an illuminating system $d_i:8^\circ$, $d_e:8^\circ$, the specular component can be optionally included (SCI) and excluded (SCE) and conforms to CIE No. 15, ISO 7724/1, ASTM E 1164, DIN 5033 Teil 7 and JIS Z 8722 condition and standards. The spectrophotometer is equipped with three pulsed xenon lamps, a $\varnothing 55$ mm integrating sphere and a silicon photodiode array detector. It operates in a 360-740 nm range (10 nm pitch) and a 0-175% reflectance range. The data were acquired in both SCI and SCE modes. Three measurements for each examined area were averaged to obtain each data point. The reflectance R data obtained were in the visible range (360-740 nm) and the $L^*a^*b^*$ colour space. The data were exported with the software SpectraMagic NX. The difference of colour was then calculated according to the CIE 1976 and CIE 2000 colour

spaces (Oleari, 1998), providing ΔE_{ab} and ΔE_{00} respectively. The colour difference ΔE_{ab}^* CIELAB 1976, between two points 1 and 2, is defined by:

$$\Delta E_{ab}^* = \sqrt{(L_1^* - L_2^*)^2 + (a_1^* - a_2^*)^2 + (b_1^* - b_2^*)^2} \quad (5.4)$$

where the difference is calculated between two colours with coordinates (L_1^*, a_1^*, b_1^*) and (L_2^*, a_2^*, b_2^*) . L^* is the lightness, ranging from 100 (brightest white) to 0 (darkest black), a^* defines the green-red (negative to positive) value and b^* the blue-yellow (negative to positive) value. The colour difference CIEDE2000 ΔE_{00} is equal to:

$$\Delta E_{00} = \sqrt{\left(\frac{\Delta L'}{k_L S_L}\right)^2 + \left(\frac{\Delta C'}{k_C S_C}\right)^2 + \left(\frac{\Delta H'}{k_H S_H}\right)^2 + R_T \left(\frac{\Delta C'}{k_C S_C}\right) \left(\frac{\Delta H'}{k_H S_H}\right)} \quad (5.5)$$

where $\Delta L'$, $\Delta C'$ and $\Delta H'$ are the lightness, chroma and hue differences between two points, respectively. The parametric weighting factors k_L , k_C , and k_H and compensation factors S_L , S_C and S_H can be calculated from the CIELAB coordinates. Detailed definitions of the parent parameters of these equations and their individual propagated errors are shown in *Appendix 8*. The Yellowness Index (YI) ASTM E313 (Oleari, 1998; Steven, 2005) and the Whiteness Index (WI) (CIE 2004) (Kotwaliwale *et al.*, 2007; Oleari, 1998), for D65/10°, were also calculated as follows:

$$YI_{E313} = \frac{100(1.3013X - 1.1498Z)}{Y} \quad (5.6)$$

$$WI = Y + 800(0.3138 - x) + 1700(0.3310 - y) \quad (5.7)$$

where $x = X/(X+Y+Z)$ and $y = Y/(X+Y+Z)$, and X , Y and Z are the CIE Tristimulus values and based on the CIE (Y, x, y) coordinates (Oleari, 1998). Conversion equations to obtain X , Y , Z values from CIELAB coordinates, are particularly complicated, but several codes for such conversion are available online as provided by spectrophotometers suppliers. The conversion codes used here are provided by HutchColor (Copyright © 1995 - endoftime HutchColor, LLC).

5.2.2.6. Glossimetry

A Rhopoint IQ™ Glossmeter was used for glossimetry measurements. It conforms to ISO 2813, ASTM D523, ASTM D2457, DIN 67530, JIS 8741, ISO 7668 and 20°/60° or 20°/60°/85° versions are available. Measurement range 12.75° - 27.25°, angular resolution: 0.02832°, resolution: 0.1 gloss units (GU). The Rhopoint IQ™ Glossmeter at 20° also allowed goniometry measurements using a diode array to measure the distribution of reflected light $\pm 7.25^\circ$ from the specular reflection angle in steps of 0.02832°.

As the plaster surfaces, even after glossy coatings resulted in low-gloss values, no meaningful goniometry measurements were achieved (*RHOPOINT Instruments Manual*, 2020). Other parameters, which would have been available for highly glossy surfaces (haze, DOI, RIQ and Rspec, see *Glossary*) were also not available for the plaster surfaces. Three measurements, all taken with 20°/60°/85° sensors, were obtained from every area analysed. The 85° sensor results are considered for matt surfaces which measure below 10 GU at 60°. Mean values of three readings were considered as representative of the considered areas. The change of gloss at 85° was calculated as the percentage difference between the mean value calculated on the unaged (UA) sample's area and the aged (A) value (in a before/after fashion), as follows:

$$\Delta Gloss \% = \frac{(Gloss_A - Gloss_{UA})}{Gloss_{UA}} \cdot 100 \quad (5.8)$$

5.2.2.7. High Resolution (HR) 3D surface measurements

A Bruker Alicona G5 Infinite Focus (IF) system for conducting HR 3D surface measurements. The IF system reconstructs a 3D image from a number of 2D images that have been captured between the lowest and highest focal plane, combining the small depth of focus of an optical system with vertical scanning to provide topographical and colour information. Scan area and scan heights were up to 100 x 100 x 100 mm and vertical and lateral resolutions were down to 10 and 440 nm, respectively. It should be noted that the colour scales are particular to the individual HD 3D images in this manuscript and the database because, due to the large variability of the depth of the focal plane, a unified or normalised scale would have caused a reduced resolution (see for example *Figure 5.13* in the results *Section 5.3.3*). The system is equipped with 5x, 10x, 20x, 50x and 100x objective lenses.

Besides the 2D and 3D images, the system automatically provides roughness profiles and measurements defined as the 'average arithmetic roughness of the surface (R_a), the root mean square of the surface roughness (R_q)' and the 'average of the tallest peak to the depth

of the lowest valley from each or subsection of a surface measurement (R_z). The measurement on the plaster surfaces was taken with the 10x objective (vertical resolution 0.219 μm and lateral resolution 3.914 μm) and an area of 5.3 x 5.3 mm was measured, and the results were processed with the software Bruker Measure Suite 5.35.

5.2.2.8. *Fourier-transform infrared spectroscopy (FT-IR)*

The FT-IR equipment and parameters are consistent with the description in *Section 4.2.2.4* (page 119). For the assessment of the coated plaster surfaces, a minimum of three spectra was acquired in diffuse reflectance for each region of interest.

5.2.3. *DATABASE FORMATION*

A database of results in Microsoft Excel format was compiled and deposited in the Northumbria University Figshare repository, to make the research outputs available in a citable, shareable and discoverable manner (Risdonne & Theodorakopoulos, 2021).

5.3. RESULTS AND DISCUSSION

The steps of the making and ageing of the plaster surfaces can be fully appreciated in the gravimetry plot in *Figure 5.4*. Analysis results and observations are shown and discussed here and refer to these steps ($t_z= 0$ to 38, described in *Table 5.3*, page 174) also correspondent to the gravimetry measurements) and the plate number and section that are detailed in *Table 5.2*, page 173.

As the accelerated ageing conditions may vary among laboratories, the interlaboratory comparison of the analytical results may be complex (Van der Doelen, 1999). For example, according to Feller (1994) although Xenon-Arc radiation, filtered to resemble sunlight or daylight through window glass, has become the most widely accepted source in tests of general photochemical stability, in other cases, artificial ageing setups, which use fluorescent tubes, can be self-constructed in the different laboratories. A thorough comparison of the experimental settings and results is therefore particularly important. In the coating discussion below, the ageing of the surfaces was evaluated by observing the differences between the identical surfaces aged with or without accelerated ageing, therefore defining a before/after ageing scenario.

Visible Reflectance, UVf, BSE, FT-IR microscope survey micrographs and HR 3D images were acquired to generate references for the uncoated (control sections), unsoiled (US) and soiled (S), unaged (UA) and aged (A) plaster plate surfaces. Sections d and a of plates P1 (UA) and P3 (A) are shown hereafter in the results as representative of the control sections for all the plates without beeswax and they are consistent with the d and a areas on plates 5, 7, 9 and 11 (control sections).

The detailed vis reflectance and UVf images taken from the US and S coated sections at t_{26} , just after the application of the coating, to t_{37} , just before the analysis (see *Table 5.3*, page 174, for details of the experiment timeline), of the unaged and aged surfaces are shown in *Appendix 9*. The effects of accelerated ageing on the coated plaster surfaces were evaluated at t_{37} , by comparing the identical unaged and aged sections.

5.3.1. GRAVIMETRY

From the making of the plaster plates at t_0 to the application of the coatings (t_{19-26}) (*Table 5.3*, page 174), it was observed that the majority of the water loss happened before t_6 (*Figure 5.4(B)*), within the first 12 days, when the plaster dried out and the water either evaporated or reacted with the powdered gypsum to grow the plaster structure (Aquilano *et al.*, 2016; Cox *et al.*, 1974; Hanor, 2000).

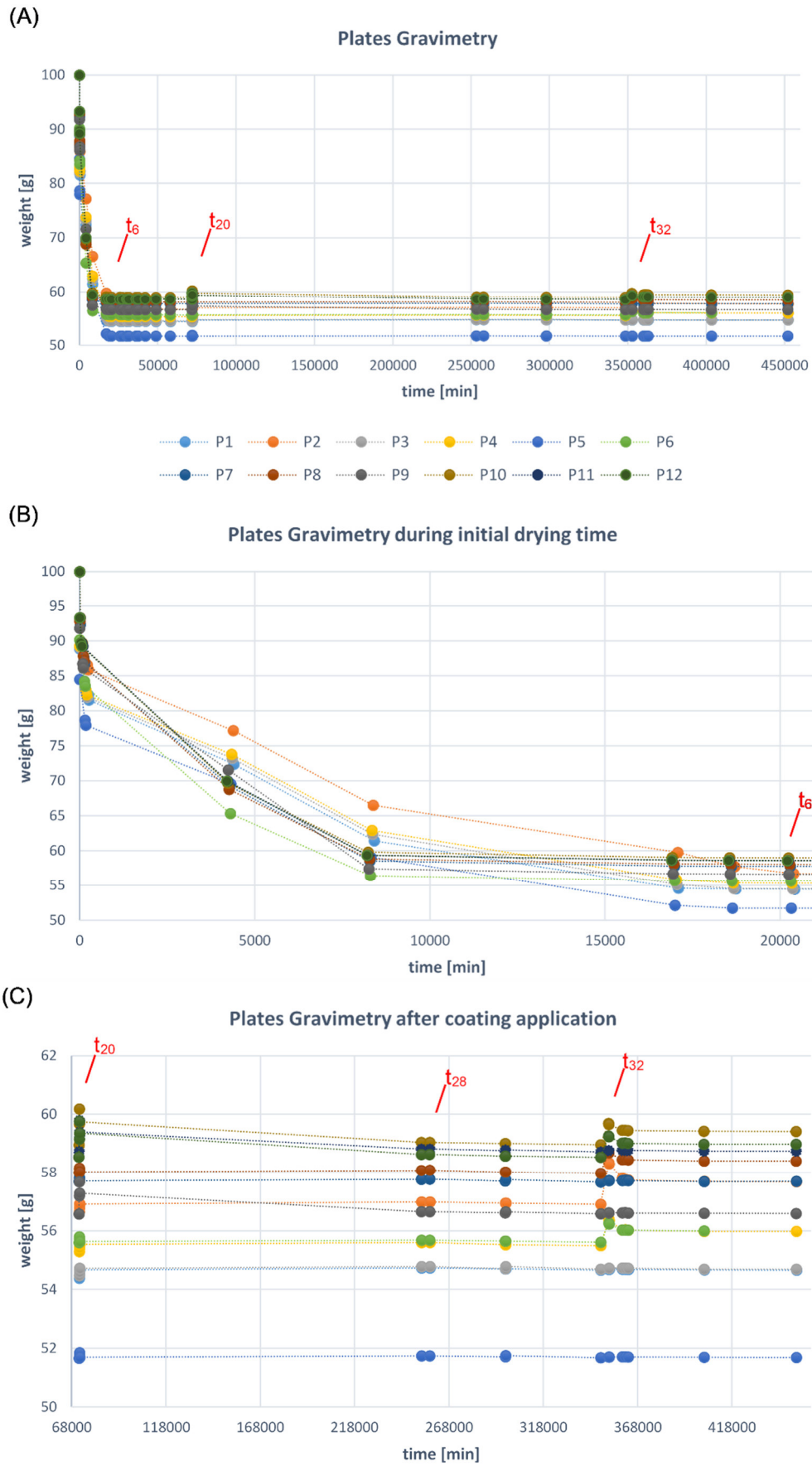


Figure 5.4. Plots of the gravimetry data of the twelve plaster plates (P1-12), for the whole experiment from t_0 to t_{38} (A), corrected and normalised as described in Section 5.2.2.1. The initial drying time from t_0 to t_6 is shown in (B) and after coating application from t_{19} and t_{38} (C). t_{20} marks the application of the linseed oil (1), shellac (2) and barite (3) coatings, t_{28} the beginning of the accelerated ageing and t_{32} the application of the beeswax coating (4) P2, 4, 6, 8, 10 and 12. For details and t_z labels refer to Table 5.3 on page 174.

Figure 5.4 shows the gravimetry data of the twelve plates (P1-12) from t_{19} , just before the application of the linseed oil (1), shellac (2) and barite (3) coatings. t_{28} marks the beginning of accelerated ageing (*Table 5.3*, page 174). It is possible to observe the weight increments due to the application of these coatings (1, 2 and 3) on all the plates from t_{20} and due to the application of the beeswax coating (4) at t_{32} on P2, 4, 6, 8, 10 and 12; small weight increments can be also seen due to the application of the artificial soiling at t_{30} (P1, 3, 5, 7, 9 and 11) and t_{33} (P2, 4, 6, 8, 10 and 12) (*Tables 5.2 and 5.3*, pages 173-4). Each weight increment is followed by a gradual and relatively slow loss of weight, related to the drying of the coating(s), but overall, no clear differences can be observed between the weight variations of the unaged and aged plates. This can be also due to the small weight of the coatings applied when compared to the overall weight of the plates.

5.3.2. VISUAL EXAMINATION, VISIBLE (VIS) REFLECTANCE AND ULTRAVIOLET FLUORESCENCE (UVF) IMAGING

Figures 5.5 to 5.11 (pages 184-187) show the visible reflectance and UVf photographs of the unaged and aged sections and the visual evaluation (EN ISO 4628-1 BSI) observation, relevant to the same areas, are discussed hereafter. The visual evaluation according to BSI standards is defined in *Section 5.2.2.2* and described in the results in terms of area percentile (S0-100%) and intensity (I0-5) of change. Images of control sections d and a of the plates at t_{13} to t_{37} (*Table 5.3*, page 174) can be found in *Appendix 9* and the database (Risdonne & Theodorakopoulos, 2021). The colour and fluorescence variations observed are due to the ageing of the plaster, but partially also to simultaneous colour contrast phenomena (Oleari, 1998).

Cold-pressed linseed oil (1-1) after accelerated ageing showed discolouration (S100%, I3) for the unsoiled (US) and discolouration (S100%, I2) for the soiled (S) sections under visible illumination (*Figure 5.5*, page 184). The bright light-blue fluorescence almost disappeared after accelerated ageing. The aged and soiled area (b) has an increased porosity, which could be due to the complete drying of the surface, more visible in the soiled portion when compared to the unsoiled section.

Boiled linseed oil (1-2) appears slightly discoloured after accelerated ageing, for both the unsoiled (US) (S100%, I3) and soiled (S) (S100%, I3) sections (*Figure 5.6*, page 184), as similarly observed for cold-pressed linseed oil. The bright light-blue fluorescence colour under UV remains unchanged upon ageing. In the unsoiled areas, it is possible to observe slightly more saturated patterns (indicated by the arrows in *Figure 5.6*, page 184), which appear to be caused by a locally reduced absorption of the coating by the plaster. This phenomenon, which would have been caused by local differences in the plaster structure

and porosity, also appears in the soiled areas, as the soiling mixture did not fully adhere to the surface in those regions.

Shellac6% (2-1) (*Figure 5.7*, page 185) and shellac18% (2-2) (*Figure 5.8*, page 185) are slightly discoloured (S100%, I1) after accelerated ageing, for both the unsoiled (US) and soiled (S) sections. The light-blue fluorescence dulled after ageing. The aged and soiled areas (b and c) show increased porosity, probably due to the complete drying of the surface, more visible in the S than in the US section. On the unaged and soiled area (P7b and c) the soiling mixture has not adhered uniformly, suggesting that the shellac coating has been absorbed unevenly by the plaster.

Barite20° (3-1) (*Figure 5.9*, page 186) and barite60° (3-2) (*Figure 5.10*, page 186) appear to be slightly whitened (S100%, I1) after accelerated ageing, for both the unsoiled (US) and soiled (S) sections. The UV fluorescence of the inorganic coating was not particularly intense since application and faded after ageing.

In the Vis and *UVf* images of the plates coated with beeswax (*Figure 5.11*, page 187), the soiling mixture highlighted the brush marks. Upon ageing, the colour of the soiled section slightly faded, and the brush marks are less noticeable. As for the *UVf* images, the changes of the fluoresce of beeswax during its drying and ageing are shown in *Appendix 9*. At t_{37} (*Table 5.3*, page 174) no relevant changes can be observed in the plaster-beeswax control sections.

Further details for the sections, where the plaster was coated with linseed oil, shellac, barite and beeswax and lists of more visible and *UVf* images along with the relevant visual examination notes are shown in *Appendix 9*. In summary, cold-pressed linseed oil (1-1) and beeswax (4) is subjected to light discoloration after ageing and reduced fluorescence. The interaction between boiled linseed oil (1-2) and beeswax (4) resulted in a surface, yellow under visible illumination and light blue fluorescent under UV. The surface appears lightly and unevenly discoloured after ageing and the intensity of the fluorescence increased significantly and unevenly. No significant differences can be seen in the shellac6% (2-1) and shellac18% (2-2) and beeswax (4) section in the visible images, that show a light discoloration. On the other hand, in these sections, the bright blue fluorescence under UV disappeared after ageing, more or less evenly. Some degree of whitening is observed in both the barite20° (3-1) and barite60° (3-2) and beeswax (4) and the bright blue fluorescence under UV disappeared after ageing.

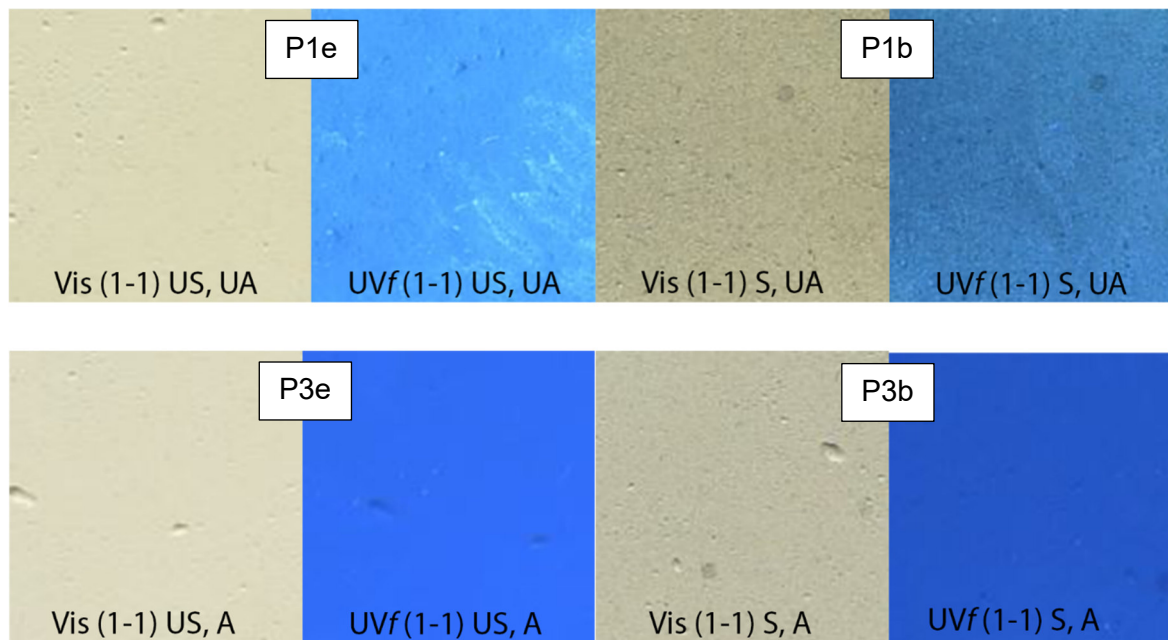


Figure 5.5. Vis and UVf images of the unaged (UA) sections P1e and P1b and the aged (A) sections P3e and P3b of the cold-pressed linseed oil coating (1-1) at t_{37} . Each square is 1x1 cm. Cold-pressed linseed oil after accelerated ageing showed discolouration for the soiled (S) sections under visible illumination and the bright light-blue fluorescence almost disappeared. The aged and soiled area (b) has an increased porosity.

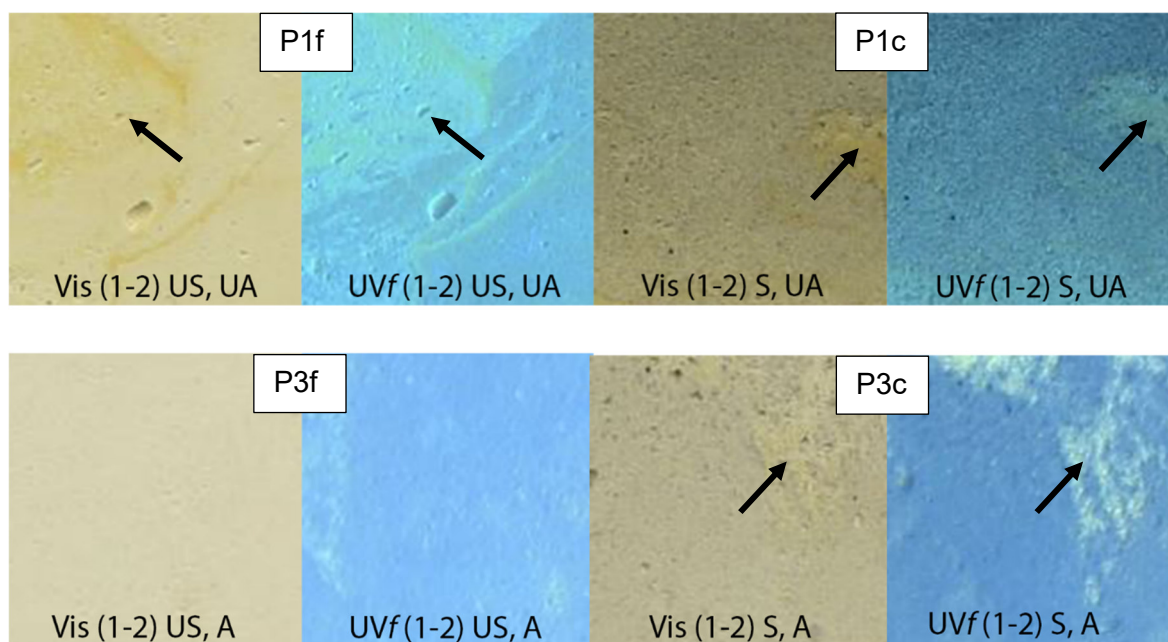


Figure 5.6. Vis and UVf images of the unaged (UA) sections P1f and P1c and the aged (A) sections P3f and P3c of the boiled linseed oil coating (1-2) at t_{37} . Each square is 1x1 cm. Boiled linseed oil appears slightly discoloured after accelerated ageing under visible illumination, but the bright light-blue fluorescence colour under UV remains unchanged upon ageing. The arrows indicate areas where the coating was not absorbed by the substrate.

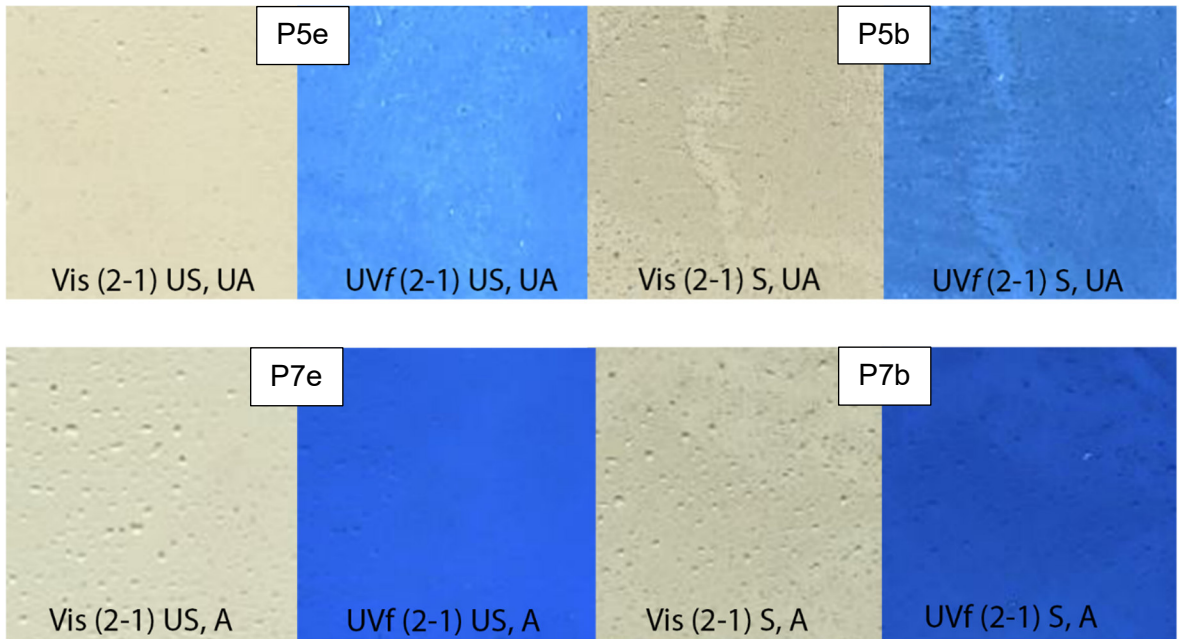


Figure 5.7. Vis and UVf images of the unaged (UA) sections P5e and P5b and the aged (A) sections P7e and P7b of the shellac6% coating (2-1) at t_{37} . Each square is 1x1 cm. Shellac6% is slightly discoloured under visible light and the light-blue fluorescence dulled, after ageing. The aged and soiled area (b) shows increased porosity, probably due to the complete drying of the surface.

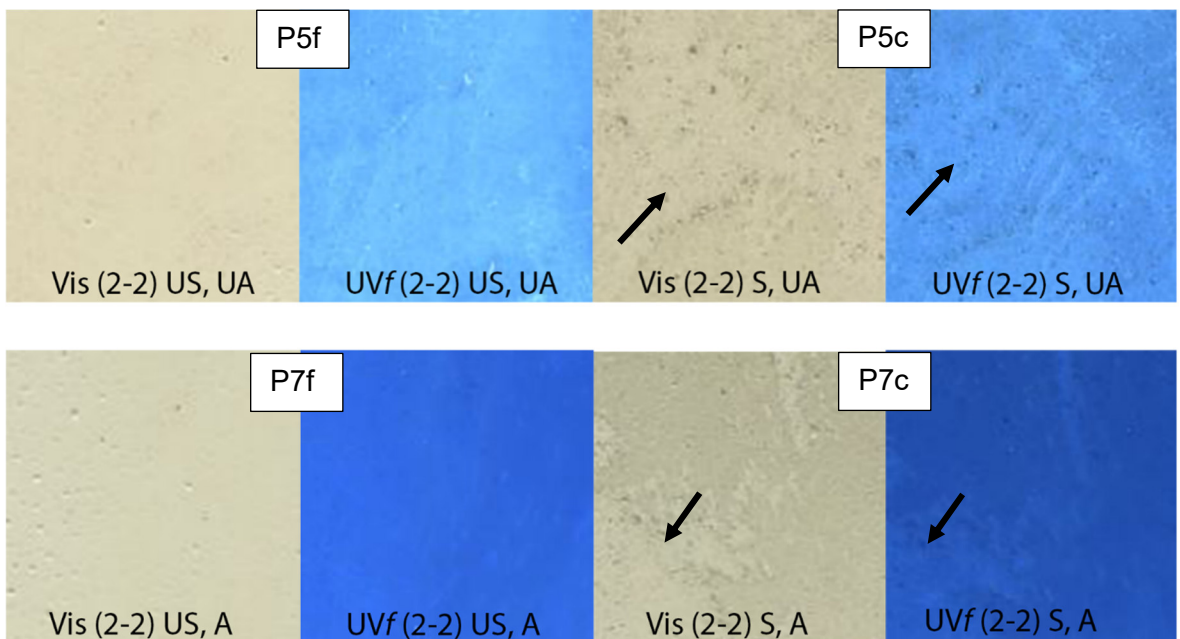


Figure 5.8. Vis and UVf images of the unaged (UA) sections P5f and P5c and the aged (A) sections P7f and P7c of the shellac18% coating (2-2) at t_{37} . Each square is 1x1 cm. Shellac18% is slightly discoloured under visible light and the light-blue fluorescence dulled, after ageing. In the soiled area (c), the arrows in the image show that the soiling mixture has not adhered uniformly, suggesting that the shellac coating has been absorbed unevenly by the plaster.

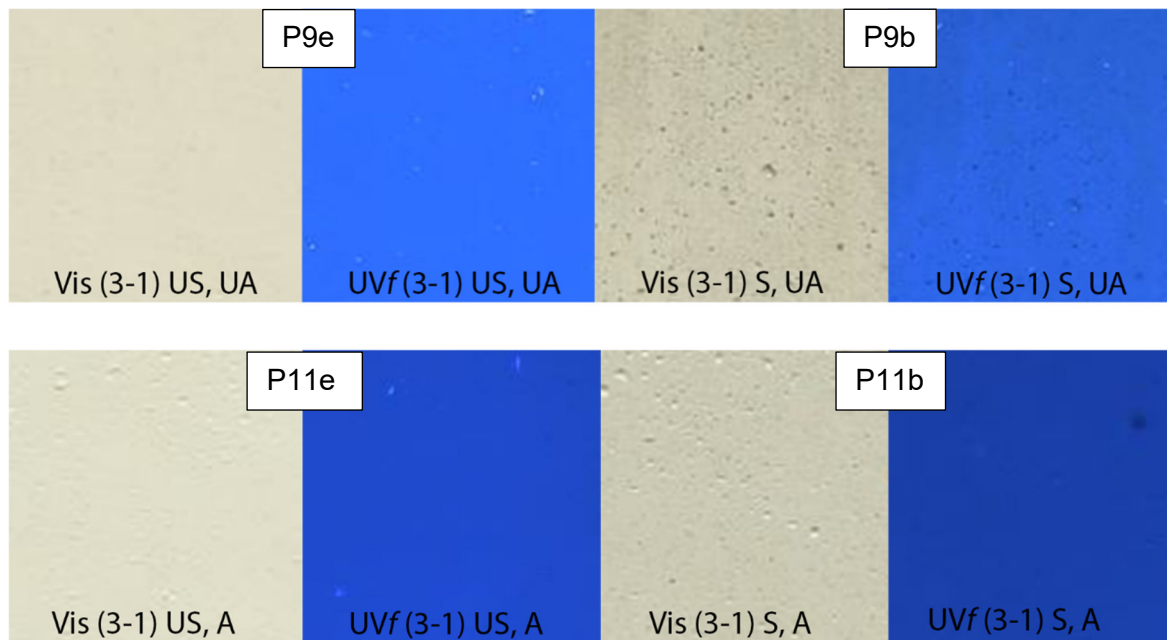


Figure 5.9. Vis and UVf images of the unaged (UA) sections P9e and P9b and the aged (A) sections P11e and P11b of the barite20° coating (3-1) at t_{37} . Each square is 1x1 cm. Under visible light, barite20° appears to be slightly whitened after accelerated ageing, and the UV fluorescence was not particularly intense.

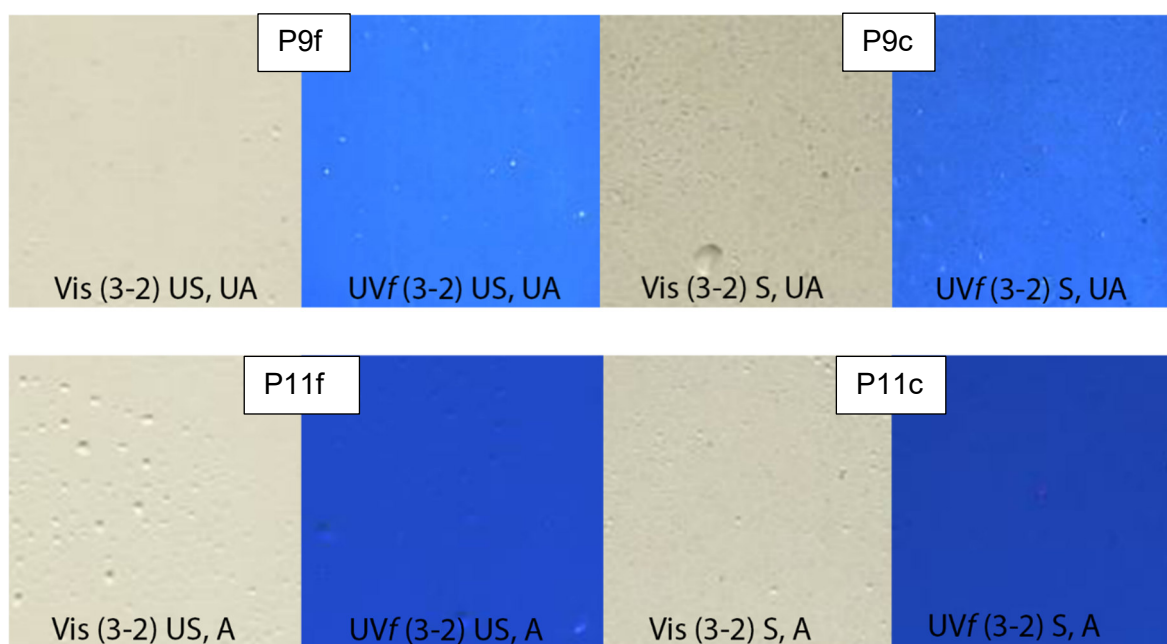


Figure 5.10. Vis and UVf images of the unaged (UA) sections P9f and P9c and the aged (A) sections P11f and P11c of the barite60° coating (3-2) at t_{37} . Each square is 1x1 cm. Under visible light, barite60° appears to be slightly whitened after accelerated ageing, and the UV fluorescence was not particularly intense.

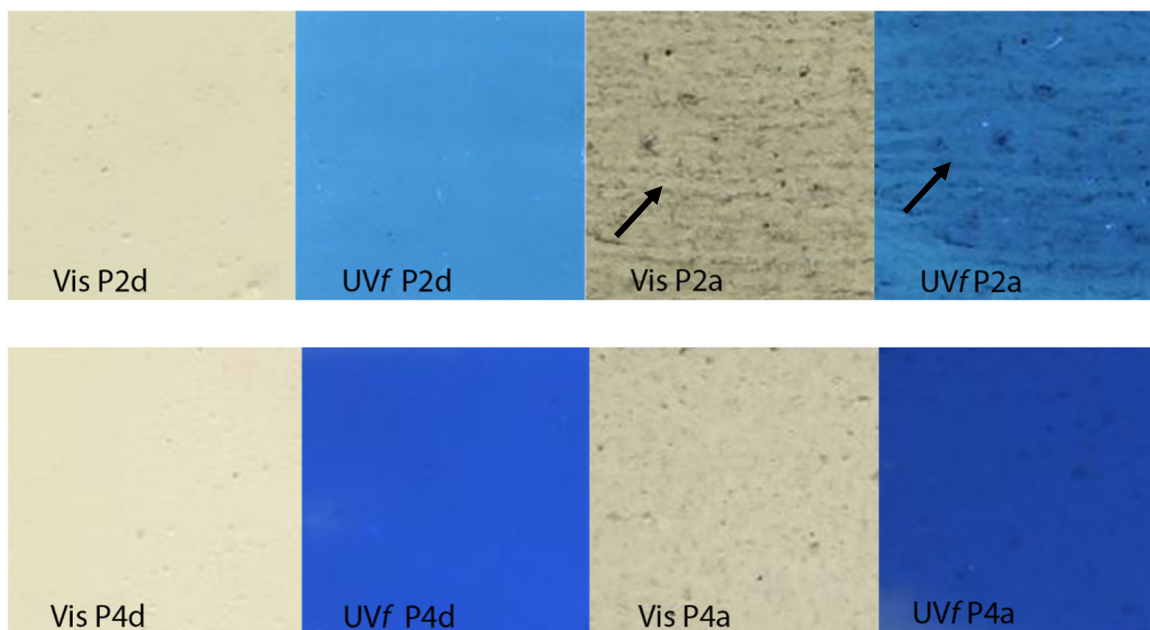


Figure 5.11. Vis and UVf images (1x1 cm) of sections P2d (plaster and beeswax, US, UA), P2a (plaster and beeswax, S, UA), P4d (plaster and beeswax, US, A) and P4a (plaster and beeswax, S, A) at t_{37} . Each square is 1x1 cm. The arrows point to the brush marks highlighted by the presence of the soiling mixture. Upon ageing, the colour of the soiled section slightly faded, and the brush marks are less noticeable (P4a).

5.3.3. TOPOGRAPHICAL AND MORPHOLOGICAL STUDIES

In the unsoiled (US) (for example P1d and P3d) and the soiled (P1a and P3a), control sections the ‘tabular’ structure typical of gypsum plaster (Cox *et al.*, 1974) can be observed in the BSE images (Figure 5.12, page 189). No significant differences can be observed between the regular crystal-like structure of the unaged and aged (P1 vs. P3) areas, aside from an increased presence of ‘voids’ (or ‘pores’) after ageing, possibly due to increased drying of the surface related to affect the thermal and light chambers.

The FT-IR survey micrographs (Figure 5.12, page 189) acquired alongside the FT-IR spectra and the HR 3D images (Figure 5.13, page 190) provide a better appreciation of the appearance of the pores and how they seem to have been partially filled, or at least covered, by the artificial soiling applied onto the plates in the control sections. The BSE and the micrographs show clearly the artificial soiling particles in the control sections as well as in all the other sections where artificial soiling was applied.

The discolouration from a darker to a lighter tone observed in the visible pictures of the areas coated with cold-pressed linseed oil (1-1) (Figure 5.14, page 191) and boiled linseed oil (1-2) (Figure 5.15, page 191) after ageing can be also seen in the survey micrographs and is further discussed in the colourimetry data (Section 5.3.4). The ‘tabular’ structure of gypsum plaster (Aquilano *et al.*, 2016; Cox *et al.*, 1974) is still visible in the BSE images despite the coats of cold-pressed linseed oil. This suggests that in this case the linseed oil did not form a solid film onto the plaster surface but penetrated and filled the pores and would also be

consistent with the lack of significant gloss increase observed after the coating application onto the plaster surface (*Section 5.3.4*). The BSE images of the unaged (P1) and aged (P3) sections show that the mineral structure of plaster appears more defined and more pores are present, possibly due to the more advanced drying stage of the aged plaster-coating surfaces. No significant differences can be observed in the HR 3D images (*Figures 5.16 and 5.17*, page 192), supporting the assumption that the cold-pressed linseed oil penetrated the plaster.

Shellac6% (2-1) (*Figure 5.18*, page 193) and shellac18% (2-2) (*Figure 5.19*, page 193) also showed discolouration in the visible pictures, also seen in the micrographs of the unaged and aged areas. BSE images show the 'tabular' structure of gypsum plaster (Aquilano *et al.*, 2016; Cox *et al.*, 1974), still visible despite the coats of shellac6%, which seems to have filled the pores. This suggests that, as also observed in this case of the linseed oil coatings, shellac did not form a solid film onto the plaster surface but penetrated and filled the pores and would also be consistent with the lack of significant gloss increase observed after the coating application onto the plaster surface. No clear differences can be observed after ageing in the BSE images. The mineral structure appears slightly tighter, possibly as the shellac coating, while drying, 'glued' together with the structure. No significant differences can be observed in the HR 3D images (*Figures 5.20 and 5.21*, page 194), but the soiled section appears somehow more even.

The discolouration observed in the visible pictures of the areas coated with barite20° (3-1) (*Figure 5.22*, page 195) and barite60° (3-2) (*Figure 5.23*, page 195) is not particularly visible in the micrographs of the unaged and aged areas. In the BSE images, the structure of the mineral barite solution appears brighter (barium, Ba, has a higher atomic number than that of calcium, Ca, and for this reason, the BSE image is brighter), and the needle-like structure, similar to the 'tabular' structure of gypsum plaster (Aquilano *et al.*, 2016; Cox *et al.*, 1974) is tighter and finer. The presence of such a structure suggests that barite water did indeed change the surface structure of the gypsum plaster substrate as suggested in the technical literature (Turco, 1990). In barite60° the higher temperature during the making of the solution seems to have allowed the growth of larger crystals, visible in the BSE image. No obvious changes in this structure can be observed in the BSE image upon ageing. No significant differences can be observed in the HR 3D images (*Figures 5.24 and 5.25*, page 196), and the surfaces, apart from the presence of pores in the soiled sections, appear uniform throughout their area.

Interestingly, whereas the 'tabular' structure typical of gypsum plaster (Cox *et al.*, 1974) was still visible in the sections coated with linseed oil, shellac and barite, the mineral structure cannot be seen after the application of beeswax (*Figures 5.26 and 5.27*, pages 197-8). The BSE images of unsoiled (US) control sections P2d and P4d show a coherent and smooth

surface with an orange-peel like appearance. The same can be observed in the relevant soiled sections (P2a and P4a). Brush marks are visible in the HR 3D images (*Figure 5.26*, page 197) and upon ageing, the marks are not as visible.

In the micrographs, the changes of colour described above for the sections coated with linseed oil, shellac, barite and beeswax can also be seen. In these images, the coherent coat of beeswax appears to have created a uniform film onto the surface. This is also visible in the BSE images where, as also observed in the control sections, the structure of the plaster is no longer visible, and the surface shows a uniform orange-peel pattern. Interestingly, the beeswax coat prevents the BSE image to show the bright signal of barium in the barite-beeswax coated sections. All images are available in *Appendix 9* and the database (Risdonne & Theodorakopoulos, 2021). Brush marks are visible in all the beeswax coated sections, particularly in the soiled sections, where the soiled mixture enhanced the marks. The brush marks are particularly visible in the HR 3D images and seem to partially fade after ageing in several sections, possibly due to the drying and shrinking of the beeswax coating.

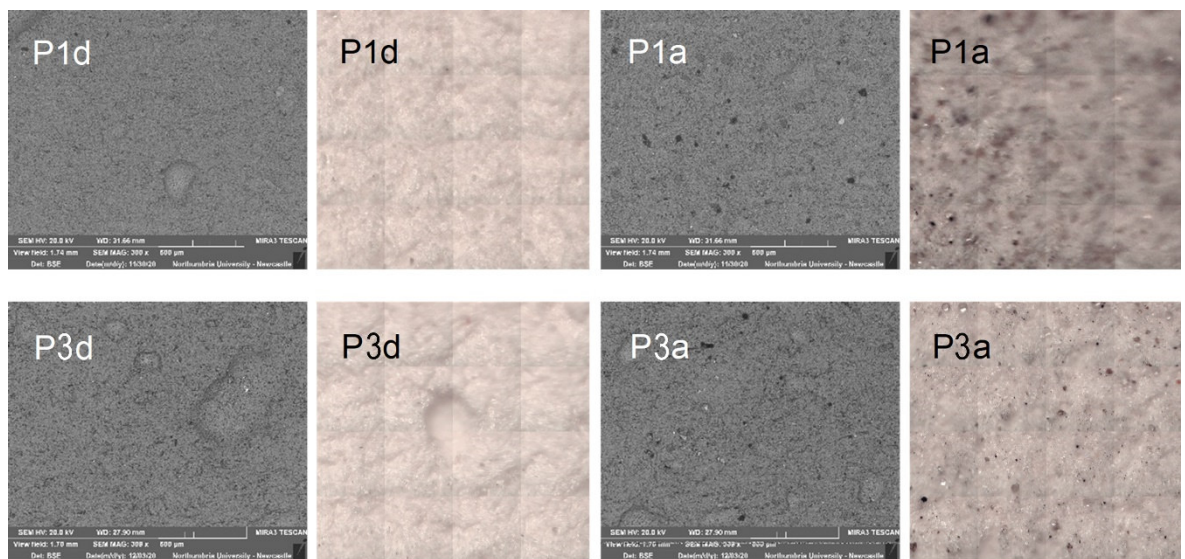


Figure 5.12. BSE (SEM MAG: 300x) (left) and FT-IR microscope survey (1x1 mm) (right) micrographs of control unaged (top) sections P1d (US) and P1a (S), and aged (bottom) sections P3d (US) and P3a (S) at t_{37} . Only an increased presence of 'voids' (or 'pores') after ageing is observed (P1 vs. P3).

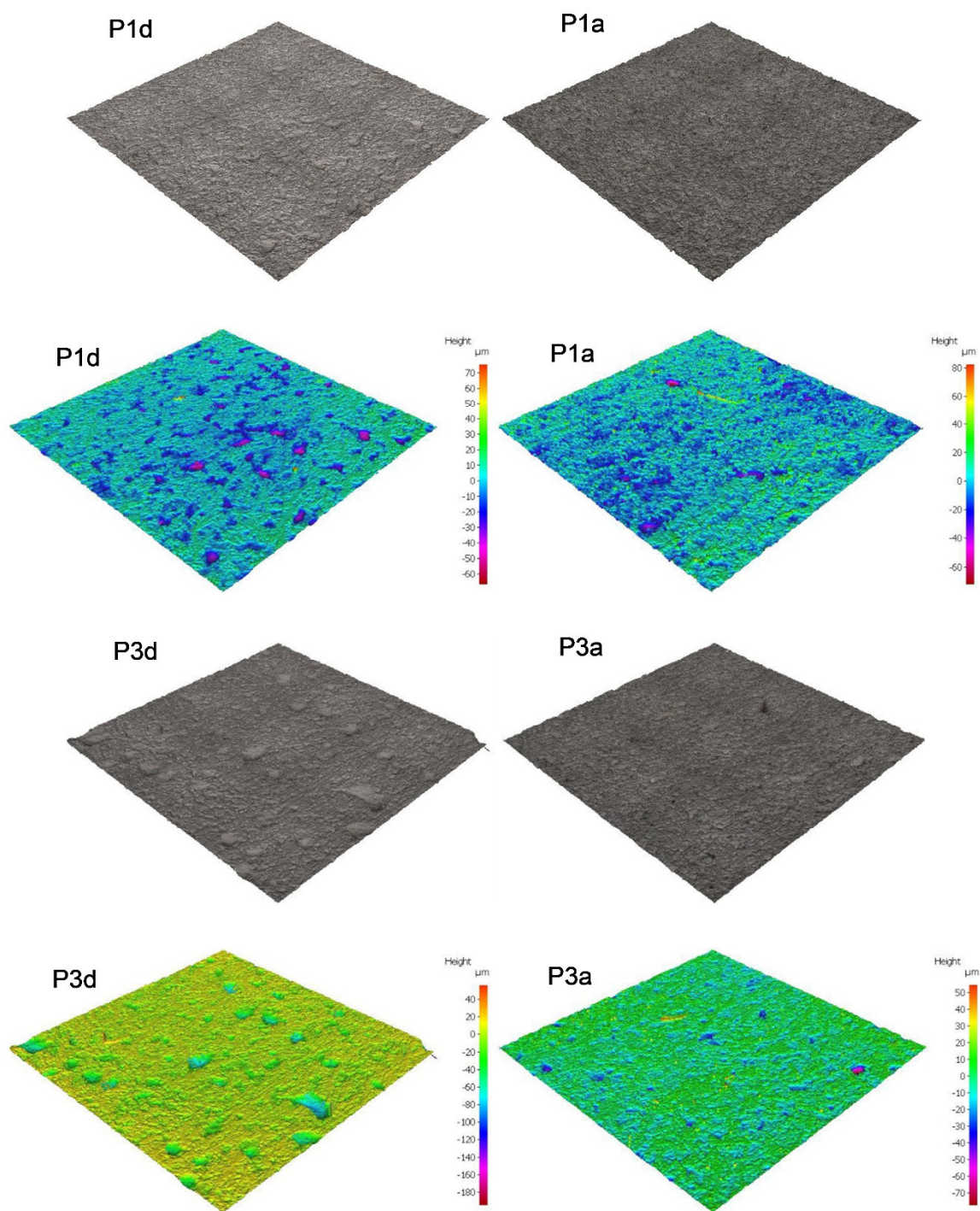


Figure 5.13. HR 3D images (5.3x5.3 mm) of sections P1d (only plaster, US, UA), P1a (only plaster, S, UA), P3d (only plaster, US, A) and P3a (only plaster, S, A) at t_{37} . An increased presence of 'voids' (or 'pores') after ageing is observed (P1 vs. P3), possibly due to further drying of the surface.

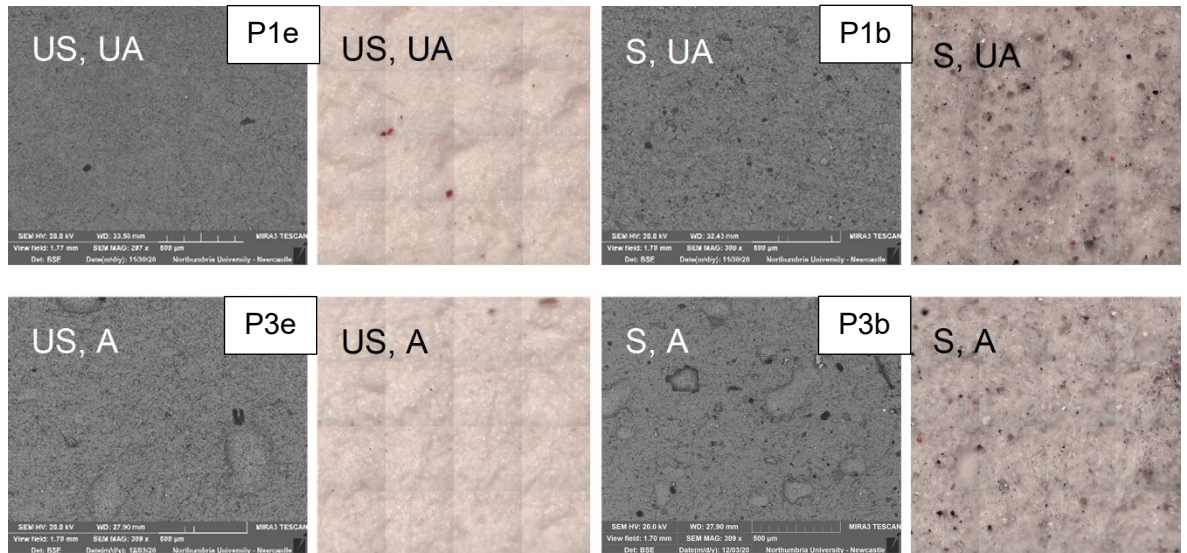


Figure 5.14. BSE (SEM MAG: 300x) (left) and micrographs (1x1 mm) (right) images of unaged (top) sections P1e (US) and P1b (S), and aged (bottom) sections P3e (US) and P3b (S) coated with cold-pressed linseed oil at t_{37} . The discolouration from a darker to a lighter tone after ageing can be seen in the micrograph. The 'tabular' structure of gypsum plaster is visible in the BSE images despite the coats.

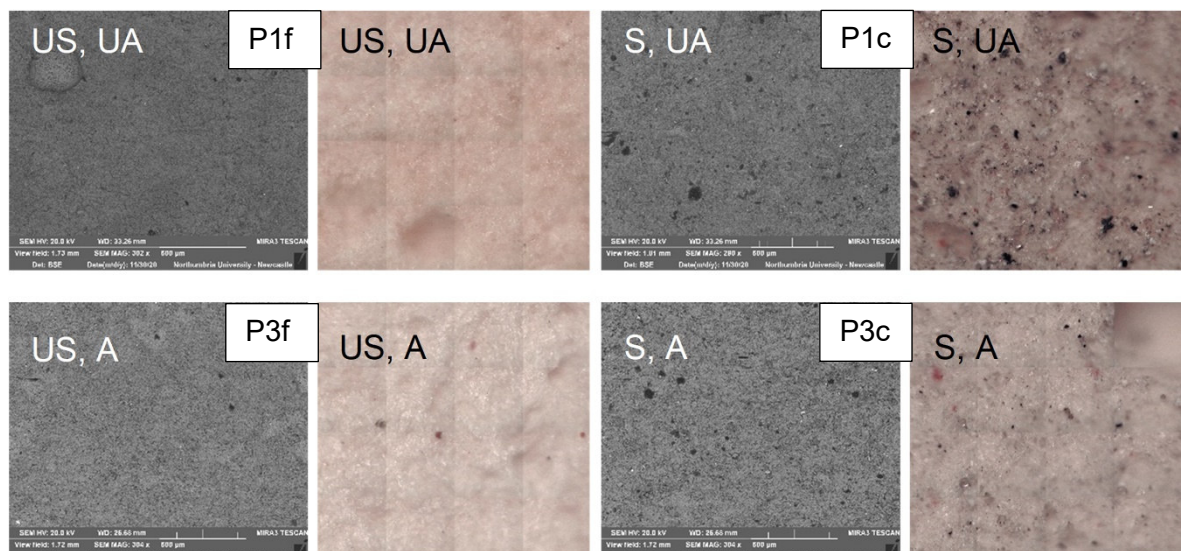


Figure 5.15. BSE (SEM MAG: 300x) (left) and micrographs (1x1 mm) (right) of unaged (top) sections P1f (US) and P1c (S), and aged (bottom) sections P3f (US) and P3c (S) coated with boiled linseed oil at t_{37} . The discolouration from a darker to a lighter tone after ageing can be seen in the micrograph. The 'tabular' structure of gypsum plaster is visible in the BSE images despite the coats.

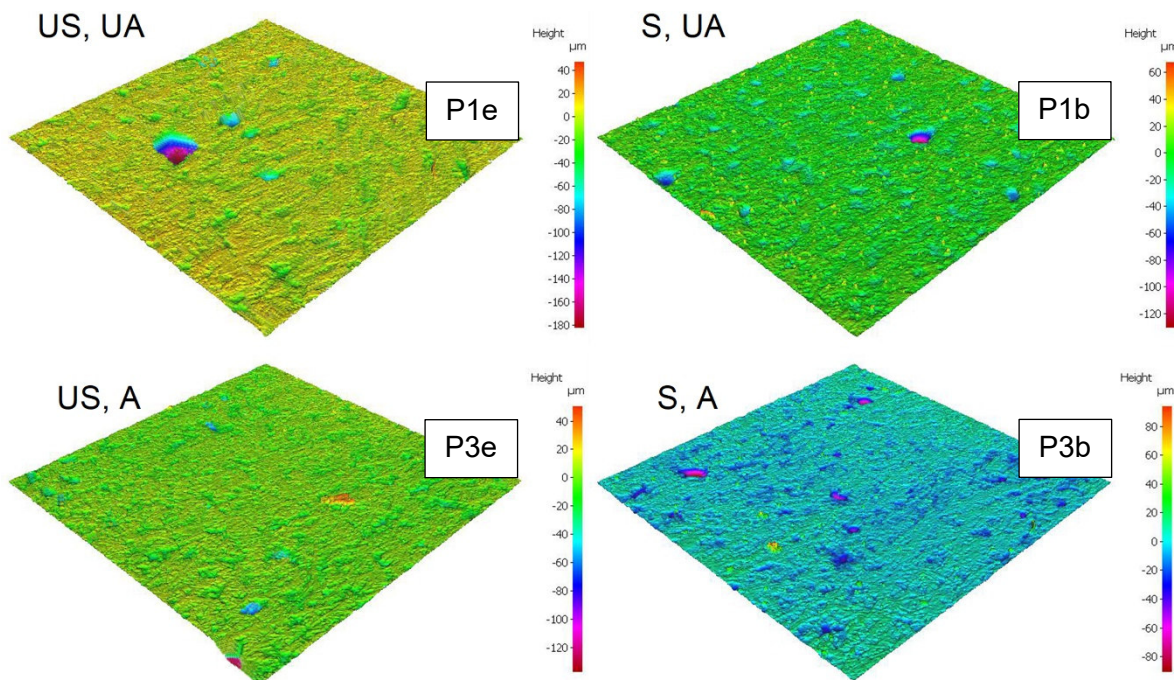


Figure 5.16. HR 3D images of sections e (US) and b (S), on P1 (UA) and P3 (A), coated with cold-pressed linseed oil at t_{37} . No significant differences can be observed in the HR 3D images, supporting the assumption that the cold-pressed linseed oil penetrated the plaster.

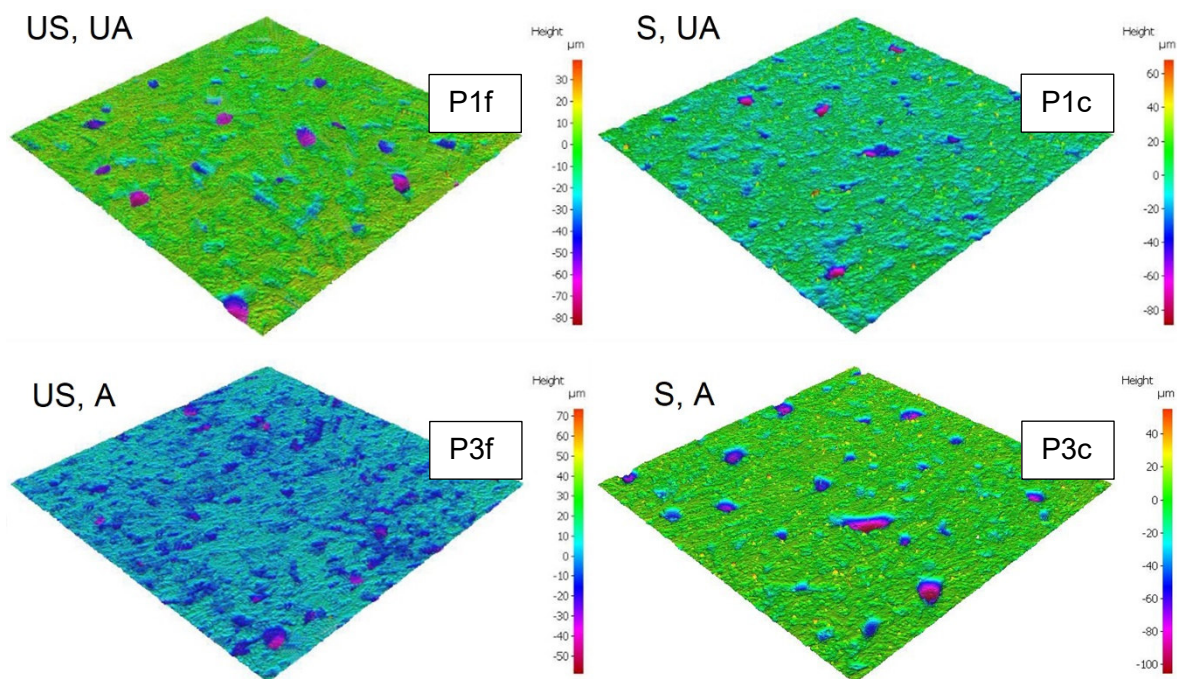


Figure 5.17. HR 3D images of sections f (US) and c (S), on P1 (UA) and P3 (A), coated with boiled linseed oil at t_{37} . No significant differences can be observed in the HR 3D images, supporting the assumption that the boiled linseed oil penetrated the plaster.

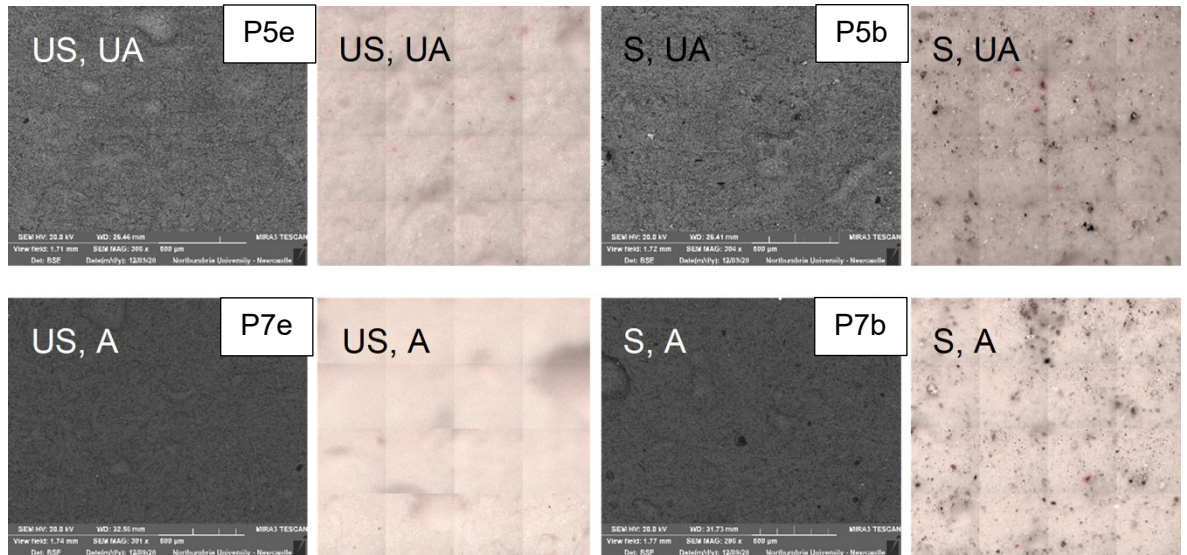


Figure 5.18. BSE (SEM MAG: 300x) (left) and micrographs (1x1 mm) (right) of unaged (top) sections P5e (US) and P5b (S), and aged (bottom) sections P7e (US) and P7b (S) coated with shellac6% at t_{37} . The discoloration from a darker to a lighter tone after ageing can be seen in the micrograph. The 'tabular' structure of gypsum plaster can be seen in the BSE images (see Section 3.1.1).

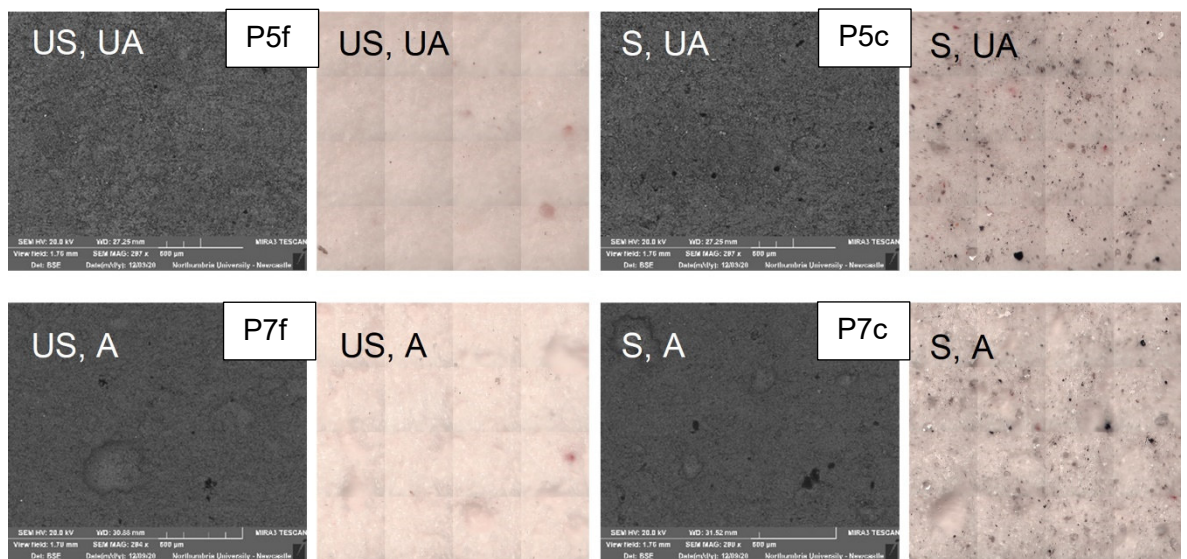


Figure 5.19. BSE (SEM MAG: 300x) (left) and micrographs (1x1 mm) (right) of unaged (top) sections P5f (US) and P5c (S), and aged (bottom) sections P7f (US) and P7c (S) coated with shellac18% at t_{37} . The discoloration from a darker to a lighter tone after ageing can be seen in the micrograph. The 'tabular' structure of gypsum plaster can be seen in the BSE images (see Section 3.1.1).

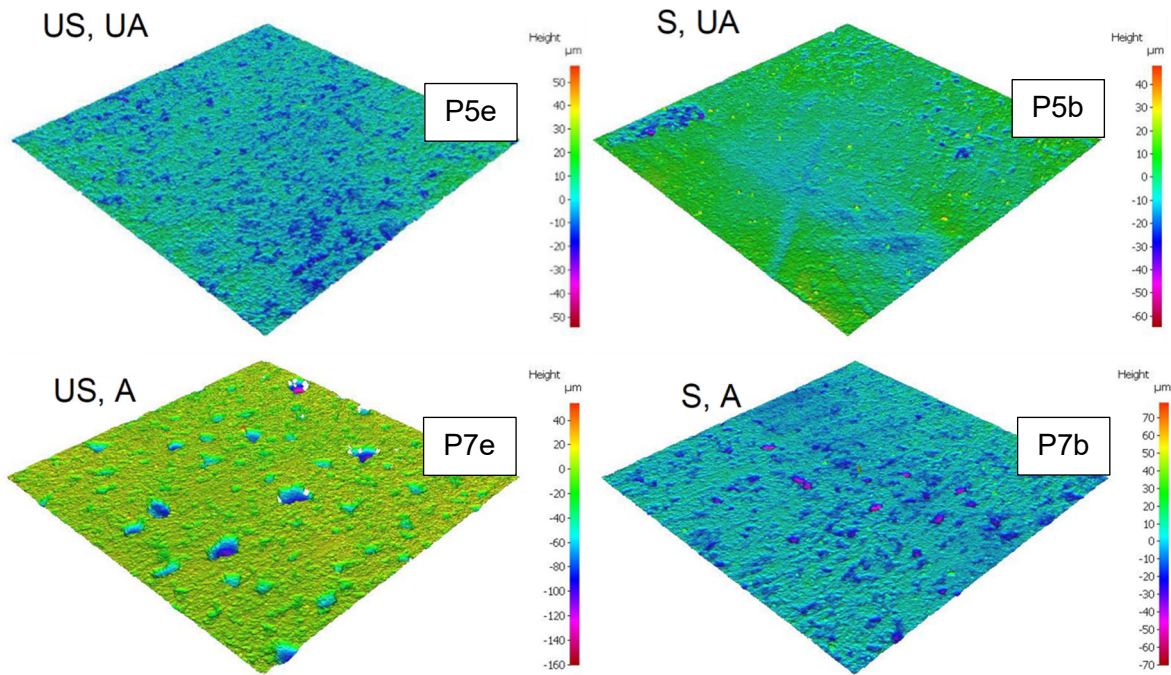


Figure 5.20. HR 3D images of sections e (US) and b (S), on P5 (UA) and P7 (A), coated with shellac6% at t_{37} . No significant differences can be observed in the HR 3D images, but the soiled section appears somehow more even.

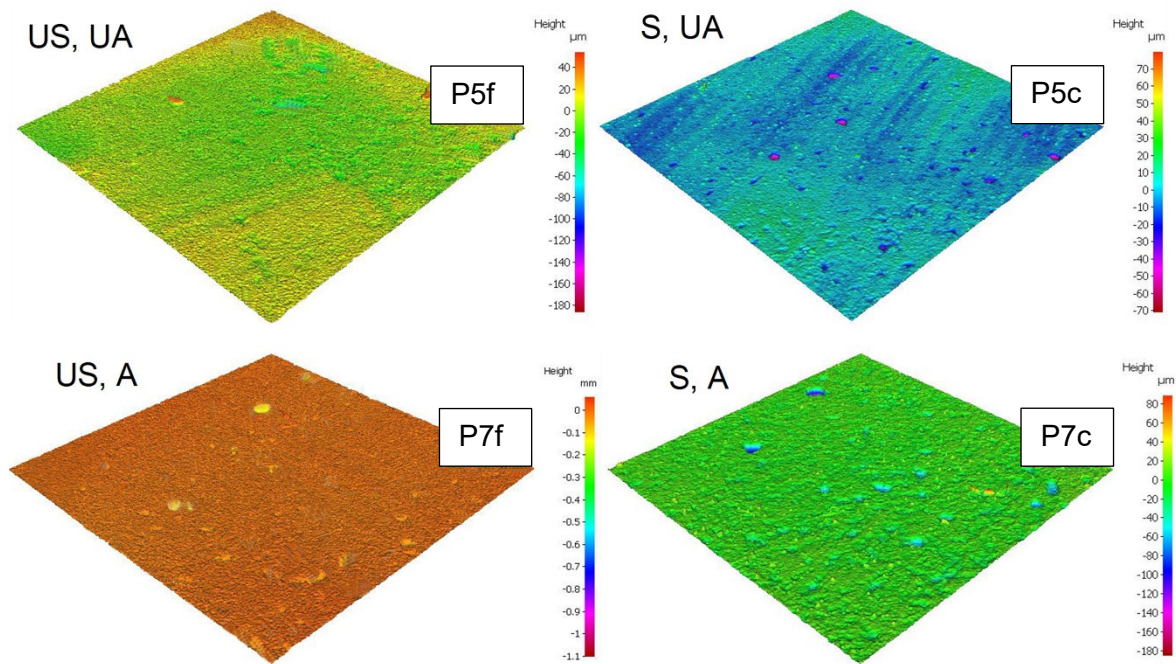


Figure 5.21. HR 3D images of sections f (US) and c (S), on P5 (UA) and P7 (A), coated with shellac18% at t_{37} . No significant differences can be observed in the HR 3D images, but the soiled section appears somehow more even.

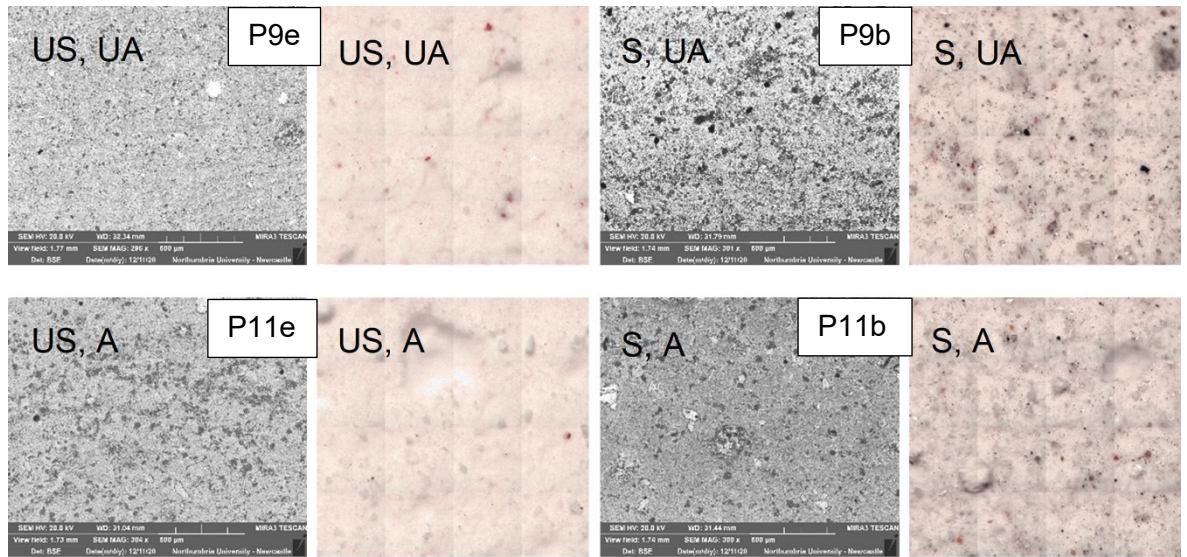


Figure 5.22. BSE (SEM MAG: 300x) (left) and micrographs (1x1 mm) (right) of unaged (top) sections P9e (US) and P9b (S), and aged (bottom) sections P11e (US) and P11b (S) coated with barite20° at t_{37} . In the BSE images, the structure of the mineral barite solution appears brighter (barium, Ba, has a higher atomic number than that of calcium, Ca, and for this reason, the BSE image is brighter), and the needle-like structure, similar to the 'tabular' structure of gypsum plaster (Aquilano et al., 2016; Cox et al., 1974) is tighter and finer. No obvious changes in this structure can be observed in the BSE image upon ageing.

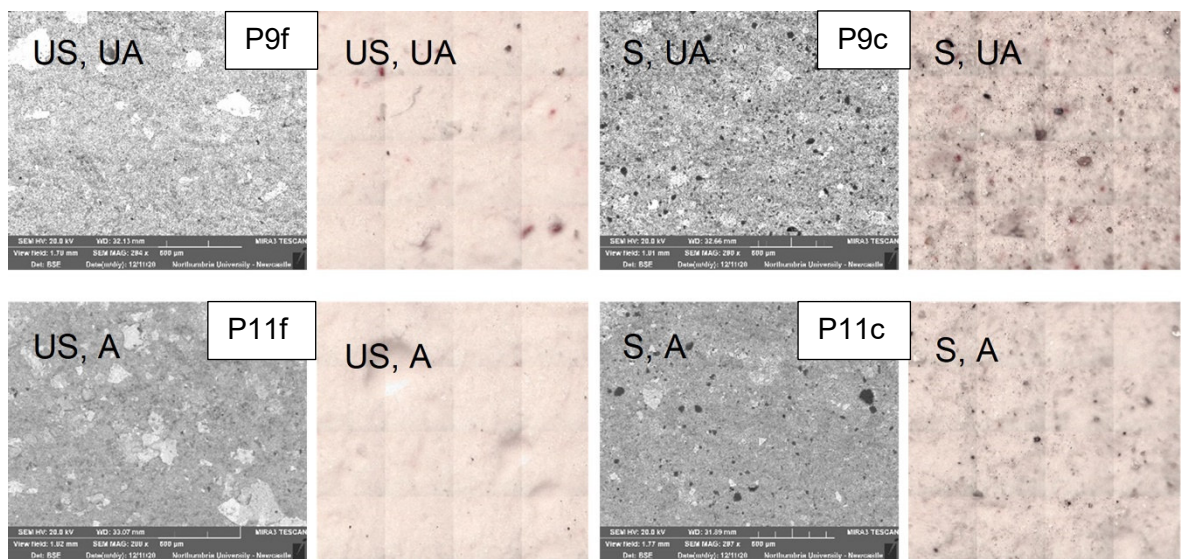


Figure 5.23. BSE (SEM MAG: 300x) (left) and micrographs (1x1 mm) (right) of unaged (top) sections P9f (US) and P9c (S), and aged (bottom) sections P11f (US) and P11c (S) coated with barite60° at t_{37} . In the BSE images, the structure of the mineral barite solution appears brighter (barium, Ba, has a higher atomic number than that of calcium, Ca, and for this reason, the BSE image is brighter), and the needle-like structure, similar to the 'tabular' structure of gypsum plaster (Aquilano et al., 2016; Cox et al., 1974) is tighter and finer. No obvious changes in this structure can be observed in the BSE image upon ageing.

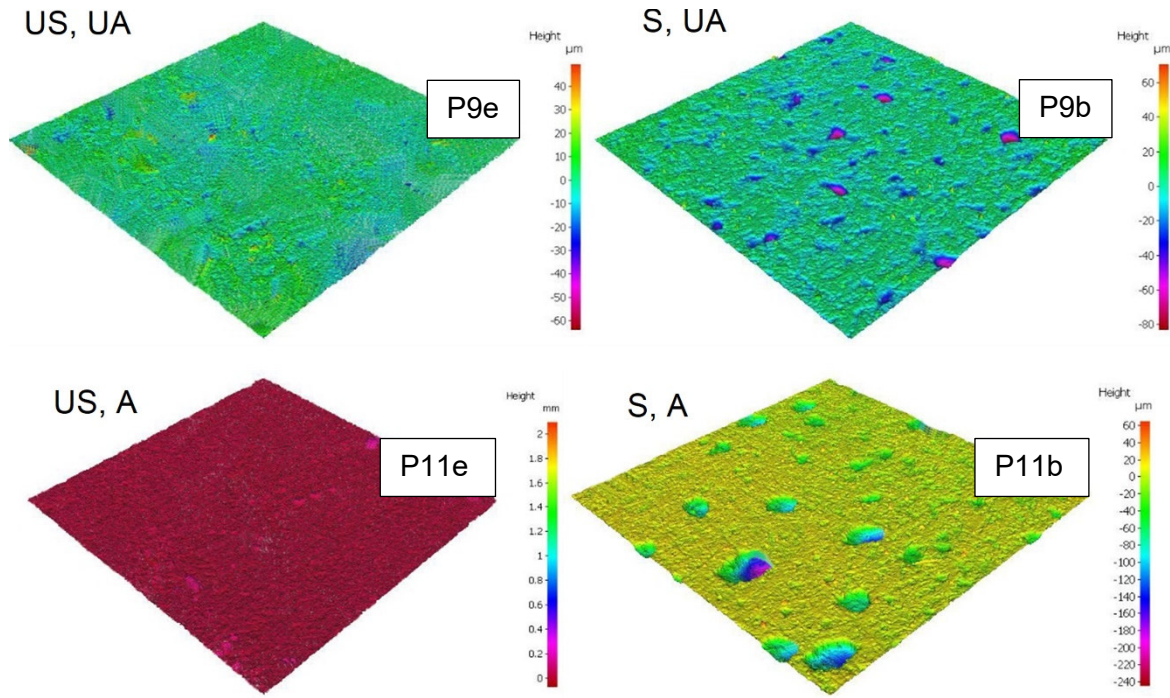


Figure 5.24. HR 3D images of sections e (US) and b (S), on P9 (UA) and P11 (A), coated with Barite20° at t_{37} . The surfaces, apart from the presence of pores in the soiled sections, appear uniform throughout their area and consistent before and after ageing (P9 to P11 of the relevant area).

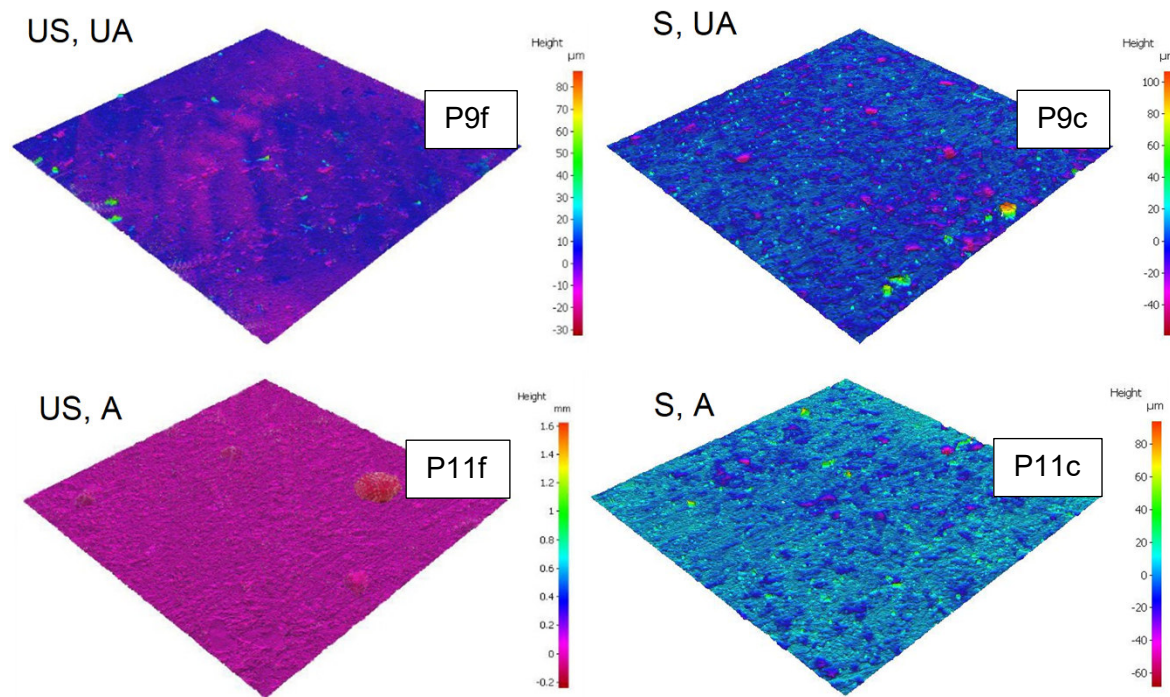


Figure 5.25. HR 3D images of sections f (US) and c (S), on P9 (UA) and P11 (A), coated with barite60° at t_{37} . The surfaces, apart from the presence of pores in the soiled sections, appear uniform throughout their area and consistent before and after ageing (P9 to P11 of the relevant area).

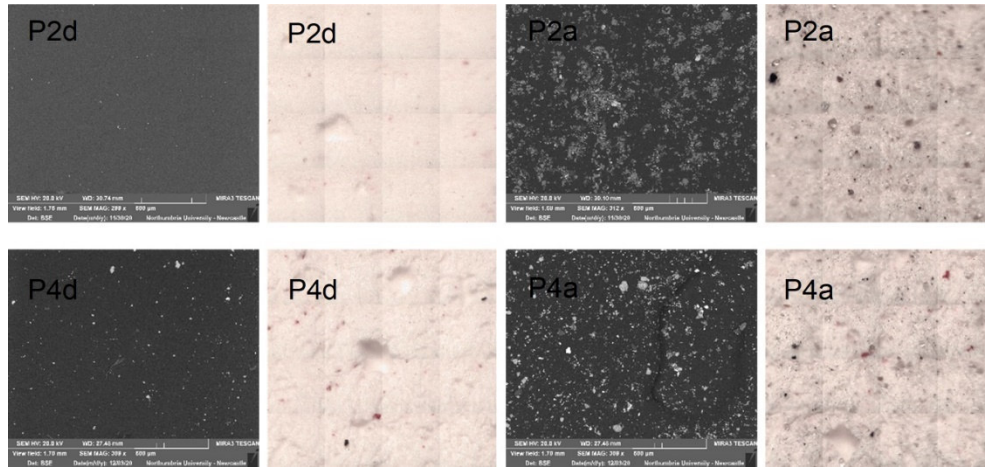


Figure 5.26. BSE (SEM MAG: 300x) (left) and micrographs (1x1 mm) (right) of unaged sections P2d (plaster and beeswax, US, UA) and P2a (plaster and beeswax, S, UA) and aged sections P4d (plaster and beeswax, US, A) and P4a (plaster and beeswax, S, A) at t_{37} . The gypsum plaster structure cannot be seen after the application of beeswax and the surfaces show a coherent and smooth surface with an orange-peel like appearance.

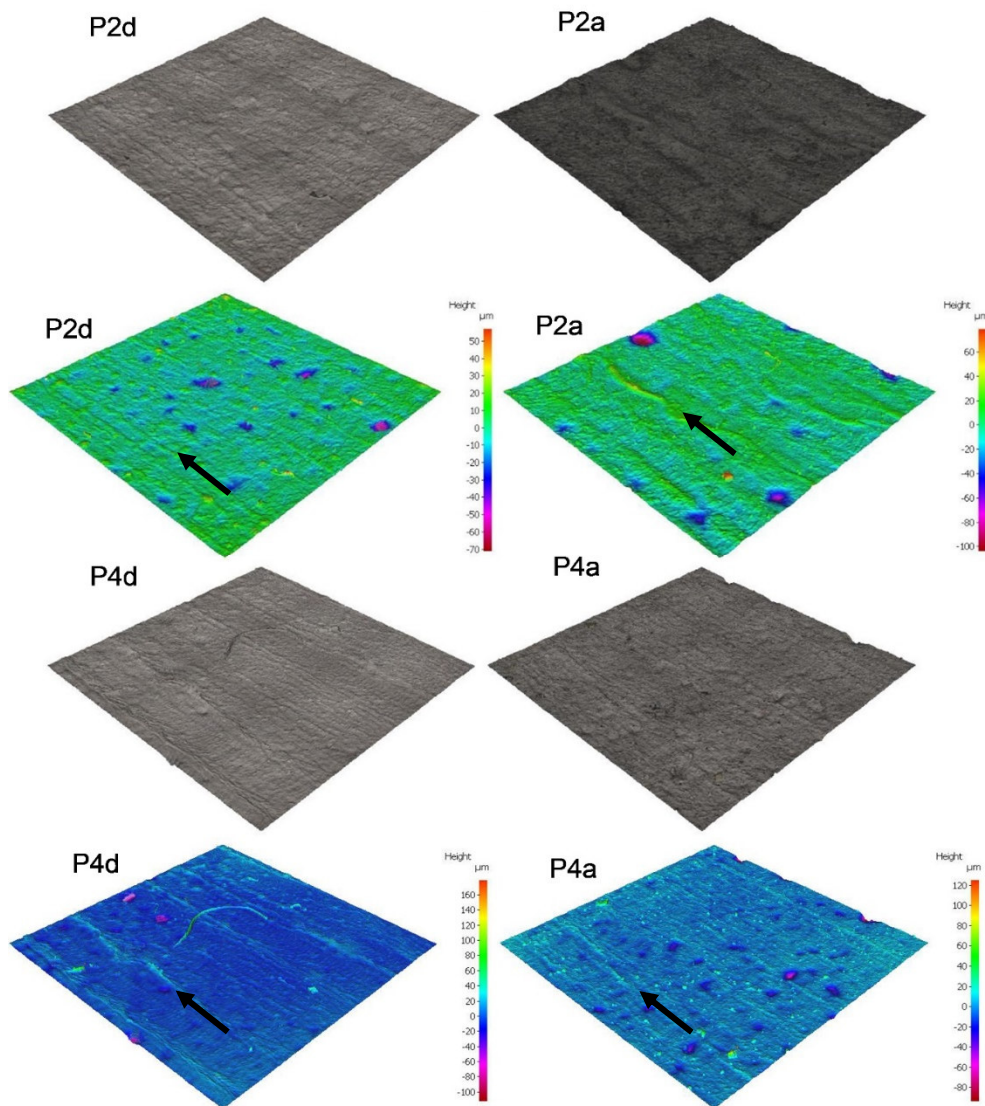


Figure 5.27. HR 3D images (5.3x5.3 mm) of plaster-beeswax control sections P2d (US, UA), P2a (S, UA), P4d (US, A) and P4a (S, A) at t_{37} . Brush marks are visible in the HR 3D images (black arrows) and upon ageing, the marks are not as visible.

5.3.4. COLOUR, GLOSS, AND ROUGHNESS MEASUREMENTS

Reflectance R% and colourimetric measurements in the CIELAB colour space ($L^* a^* b^*$) were acquired in SCI and SCE modes. In the SCE measurement mode, the specular light is excluded from the outside only diffusing light. SCI mode includes both the specular and diffused reflected light and is ideal for computer colour matching and monitoring colour quality. The measured value is the overall objective colour of the object, regardless of the surface condition of the object. The SCE measurement mode, which excludes specularly reflected light, is used to evaluate the colour of an object which correlates to visual perception. The two modes produced almost identical results in the measurement acquired in this study, as can be seen in the raw data in the database (Risdonne & Theodorakopoulos, 2021). The results shown hereafter are the ones acquired in SCI mode.

For R%, L^* , a^* , b^* and Gloss 85° three measurements for each examined area were averaged to obtain each data point. The ΔE_{00} was calculated (Equation 5.5, page 177) and is shown here (Figure 5.28) as it has been proven more precise than ΔE^*_{ab} (Equation 5.4, page 177) (Oleari, 1998). Yellow Index (YI_{313}) and White Index (WI) were calculated as shown in Equations 5.6 and 5.7 (Kotwaliwale *et al.*, 2007; Oleari, 1998; Steven, 2005). Only YI_{313} is herein discussed (Figure 5.29) since the samples were not white enough to consider the WI values within the range of validity. Percentage gloss difference (Δ Gloss %, Equation 5.8, page 178) before/after ageing (with/without accelerated ageing) was calculated, and the detailed dataset can be found in the database (Risdonne & Theodorakopoulos, 2021). However, this parameter is not discussed in the results in this chapter as its large, propagated error made the percentage gloss difference inefficient. This is mostly due to the small gloss values whose size is in the same range as the error itself. R_a and R_z were provided by the Bruker Alicona G5 InfiniteFocus (IF) system software. Detailed error propagation definitions can be seen in Appendix 8 and the database (Risdonne & Theodorakopoulos, 2021).

Figures 5.28 and 5.29 summarise the changes in colour and the yellow component based on the ΔE_{00} and YI_{313} values (Table 5.4), comparing all the coated sections. The most significant changes of colour can be seen in the areas coated with linseed oil (US and S), soiled shellac18% (2-2) and soiled barite60° (3-2). The rest of the sections show changes under or close to the smallest noticeable difference. The changes in YI are overall small before/after ageing, indicating a small decrease in the yellow component. The bleaching observed here can be due to the characteristics of the substrate, which has mostly absorbed the coatings, the thickness of the coating and the length of the ageing procedure, but also to initial bleaching of the surfaces upon ageing before the expected yellowing (Colombini & Modugno, 2009; Derrick *et al.*, 2000; Horie, 2010; Kumarathanan *et al.*, 1992;

Theodorakopoulos *et al.*, 2007). Detailed discussion on the individual coatings is provided hereafter.

Table 5.4. Colour changes according to CIE formulae ΔE_{00} and Yellow Index (YI_{313}) [SCI] before/after ageing.

Coating	ΔE_{00} ($\pm 0.4\%$)		YI_{313}			
	US	S	US, UA	S, UA	US, A	S, A
Linseed oil(1-1)	2.20	4.25	1.94	3.31	1.80	2.64
Linseed oil(1-2)	7.43	8.23	3.18	5.45	2.15	3.52
Linseed oil(1-1)+beeswax	1.57	1.86	1.99	3.09	1.89	2.82
Linseed oil(1-2)+beeswax	4.55	1.03	2.57	4.09	3.34	3.98
Shellac(2-1)	1.50	1.22	1.87	2.55	1.76	2.30
Shellac(2-2)	1.40	4.80	2.03	2.46	1.90	2.64
Shellac(2-1)+beeswax	1.41	4.03	1.97	2.71	1.83	2.82
Shellac(2-2)+beeswax	2.04	2.34	2.05	3.09	1.84	2.92
Barite(3-1)	0.89	0.96	1.66	2.21	1.61	2.11
Barite(3-2)	0.58	3.77	1.67	2.39	1.64	1.97
Barite(3-1)+beeswax	0.56	0.98	1.73	2.52	1.70	2.58
Barite(2)+beeswax	0.57	0.98	1.72	2.74	1.69	2.62

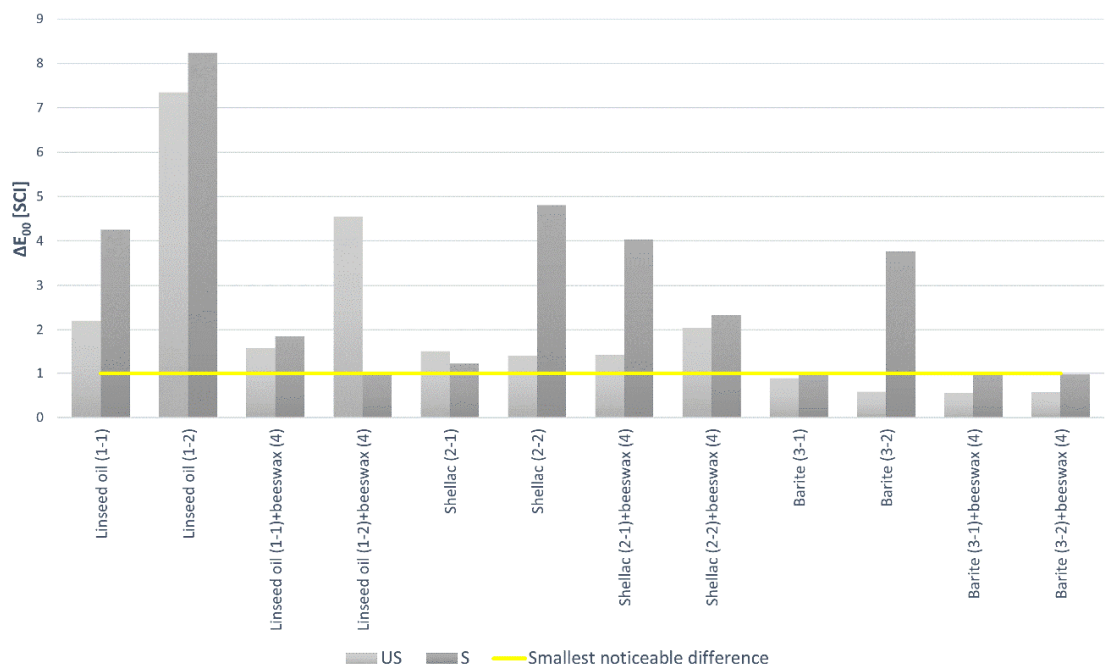


Figure 5.28. Colour changes before/after ageing according to CIE formula ΔE_{00} ($\pm 0.4\%$) [SCI]. The most significant changes can be seen in the areas coated with linseed oil, unsoiled (US) and soiled (S) and soiled shellac18% (2-2) and barite60° (3-2). The rest of the sections show changes under or close to the smallest noticeable difference.

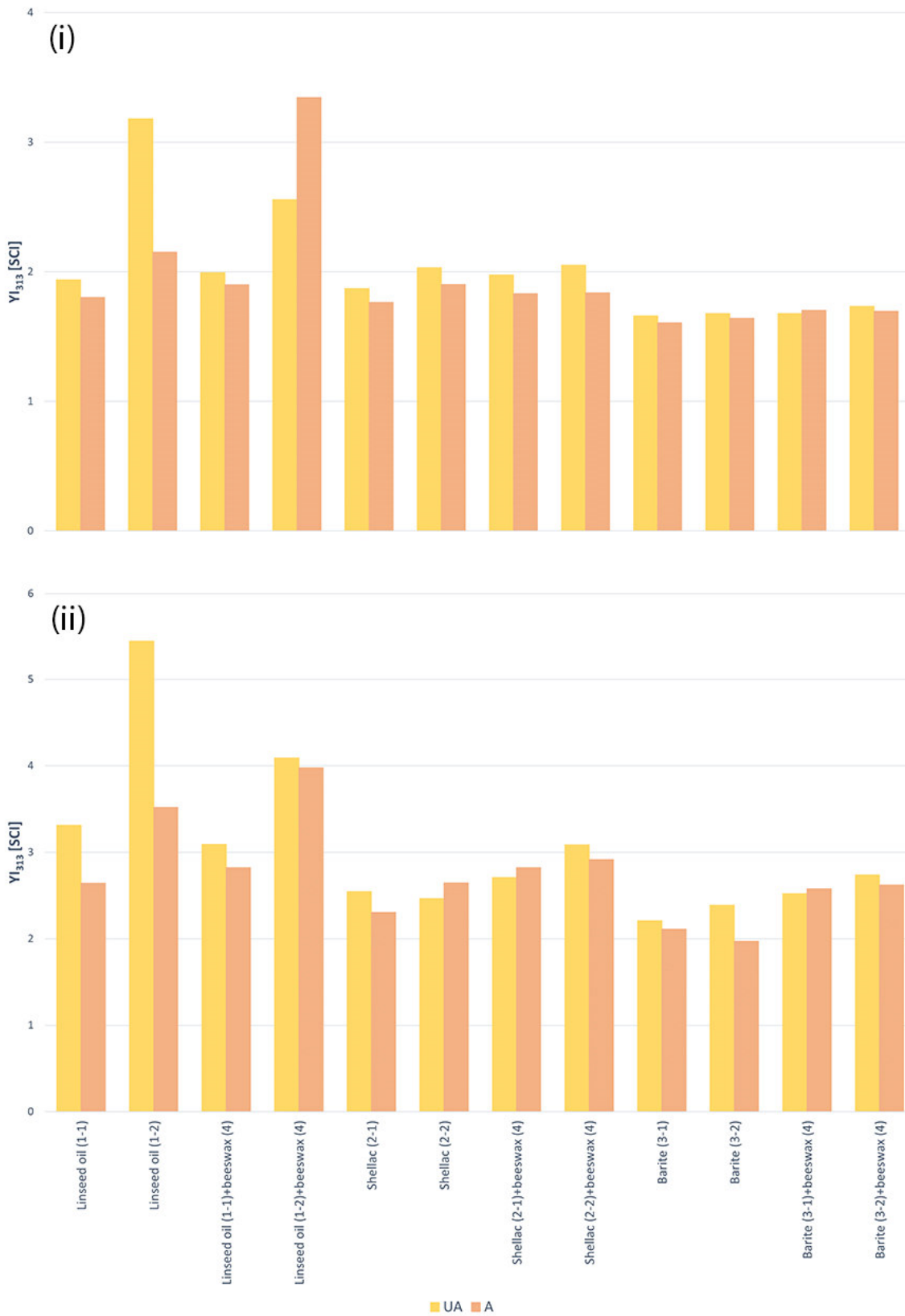


Figure 5.29. Yellow Index (YI_{313}) [SCI] of the unsoiled (i) and soiled (ii) sections. The changes in YI are overall small before (UA)/after (A) ageing, indicating a small decrease in the yellow component. In a few exceptional cases (e.g., boiled linseed oil+beeswax) the YI increases after ageing.

5.3.4.1. Control plaster plates (uncoated and beeswax)

Table 5.5 summarises the measurements acquired from the control sections d (US) and a (S) of the unaged (P1, 5 and 9) and aged (P3, 7 and 11) plates. The data in Table 5.5 are shown as intervals from the minimum and maximum values of the identical areas in the different plates. Changes of colour are extremely small in the control section, but differences can be observed in the lightness, as shown by the changes in R% (Figure 5.30) and L* (Figure 5.31) between the unsoiled and soiled areas. The Gloss85° values suggest that the gloss of the aged surfaces is slightly higher than the gloss of the unaged areas, in both the unsoiled (d) and soiled (a) sections. Only between P9d and P11d a decrease of gloss is observed, suggesting that this is related to the manufacturing of P9 and that overall an increase of gloss is expected on unsoiled and soiled plaster surfaces after ageing. It is possible to notice that the range of Gloss85°, R_a and R_z values is relatively wider for the soiled areas (a). These parameters are affected by the local porosity of the surface, but also by the presence of artificial soiling particles.

The reflectance and colourimetric measurements of the plates coated with beeswax are summarised in Table 5.6. After ageing, an overall increase of the R% in the short wavelengths of the visible spectrum for the unsoiled areas, whereas a small increase can be seen across the spectrum for the soiled sections, however, the R% appears consistent between the unaged and aged sections (Figure 5.32). Gloss85°, L*, a* and b* remain overall consistent before/after ageing in the relevant areas. R% and L* show that the soiled areas are darker than the unsoiled ones (Figures 5.32 and 5.33). R_a shows no significant differences and R_z values show larger changes, possibly due to the variability given by the presence of the brush marks observed in Sections 5.3.2 and 5.3.3.

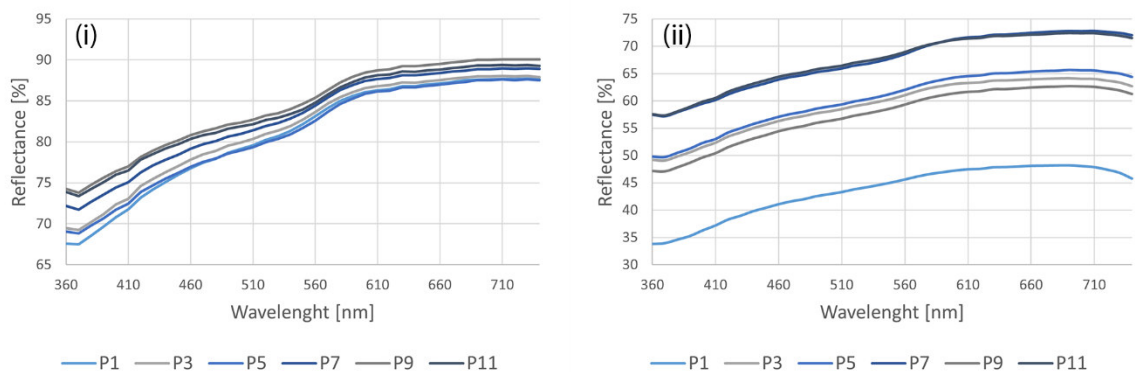


Figure 5.30. Reflectance (%) (± 0.05 %) [SCI] of the d (unsoiled - US) (i) and a (soiled - S) (ii) plaster control sections of P1, 5 and 9 (unaged - UA) and P3, 7 and 11 (aged - A) at t_{37} showing that the surfaces are darker after the application of the soiling.

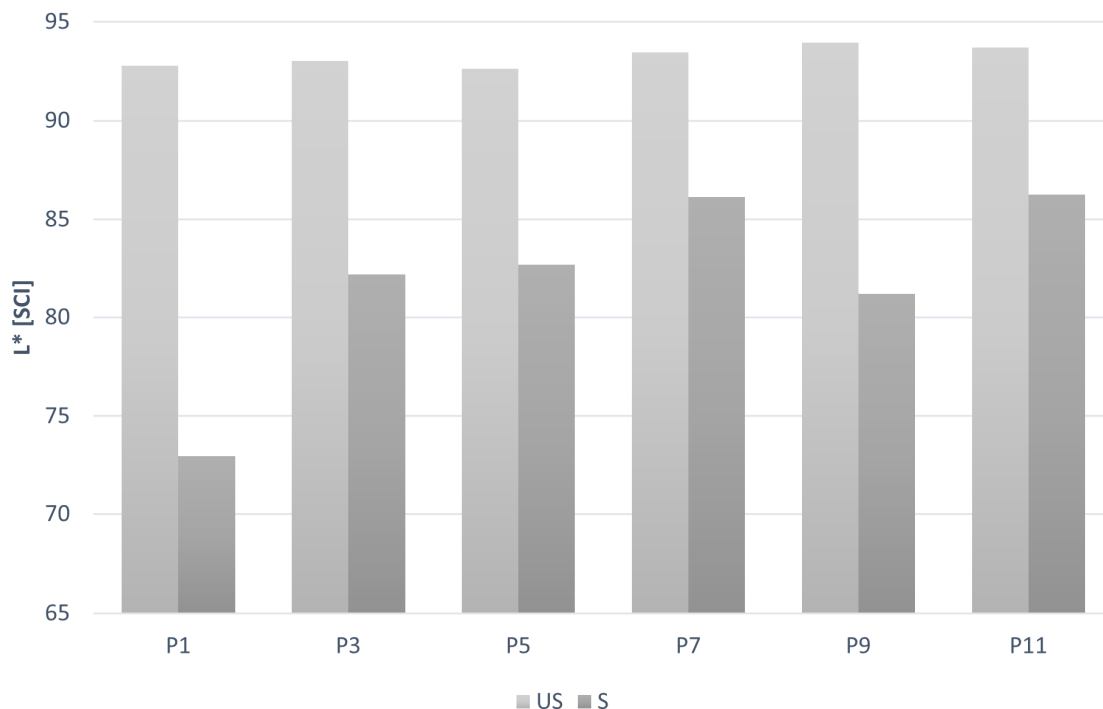


Figure 5.31. L^* (± 0.05) measurements of the d (unsoiled - US) and a (soiled - S) control sections of P1, 5 and 9 (unaged - UA) and P3, 7 and 11 (aged - A) at t_{37} . L^* is relatively constant across the US control sections, UA and A, and varies in the S areas.

Table 5.5. Summary of measurements acquired from the control sections d (unsoiled - US) and a (soiled - S) of the unaged (P1, 5 and 9) and aged (P3, 7 and 11) plates at t_{37} (plates description in Table 5.2).

		P1, 5 and 9		P3, 7 and 11	
		d	a	d	a
R [%] (± 0.05 %)	min	67.50	33.84	69.26	88.02
	max	73.81	49.72	73.38	89.35
L* (± 0.05)	min	92.63	72.95	93.03	82.15
	max	93.93	81.19	93.68	86.13
a* (± 0.001)	min	1.41	0.95	1.42	1.12
	max	1.63	1.27	1.52	1.53
b* (± 0.01)	min	3.72	4.83	3.63	4.17
	max	5.02	5.44	4.60	4.67
YI₃₁₃	min	1.66	1.66	1.67	2.09
	max	1.76	3.29	1.73	2.39
Gloss85° [GU] (± 0.1 GU)	min	0.33	0.31	0.53	0.48
	max	2.06	0.57	1.15	1.49
R_a [µm] (± 0.3 µm)	min	2.00	4.79	3.13	1.54
	max	4.85	7.18	5.35	5.30
R_z [µm] (± 0.05 %)	min	16.26	39.76	21.21	15.82
	max	43.33	54.07	39.91	51.27

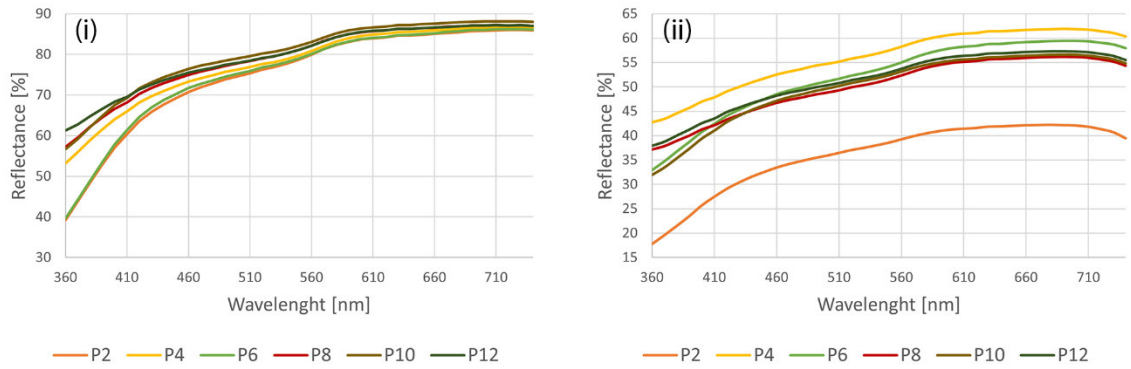


Figure 5.32. Reflectance (%) (± 0.05 %) of the d (unsoiled - US) (i) and a (soiled - S) (ii) plaster-beeswax (4) control sections of P2, 6 and 10 (unaged - UA) and P4, 8 and 12 (aged - A) at t_{37} showing that the R% of the surfaces is consistent in the UA and A areas. The surfaces are darker after the application of the soiling.

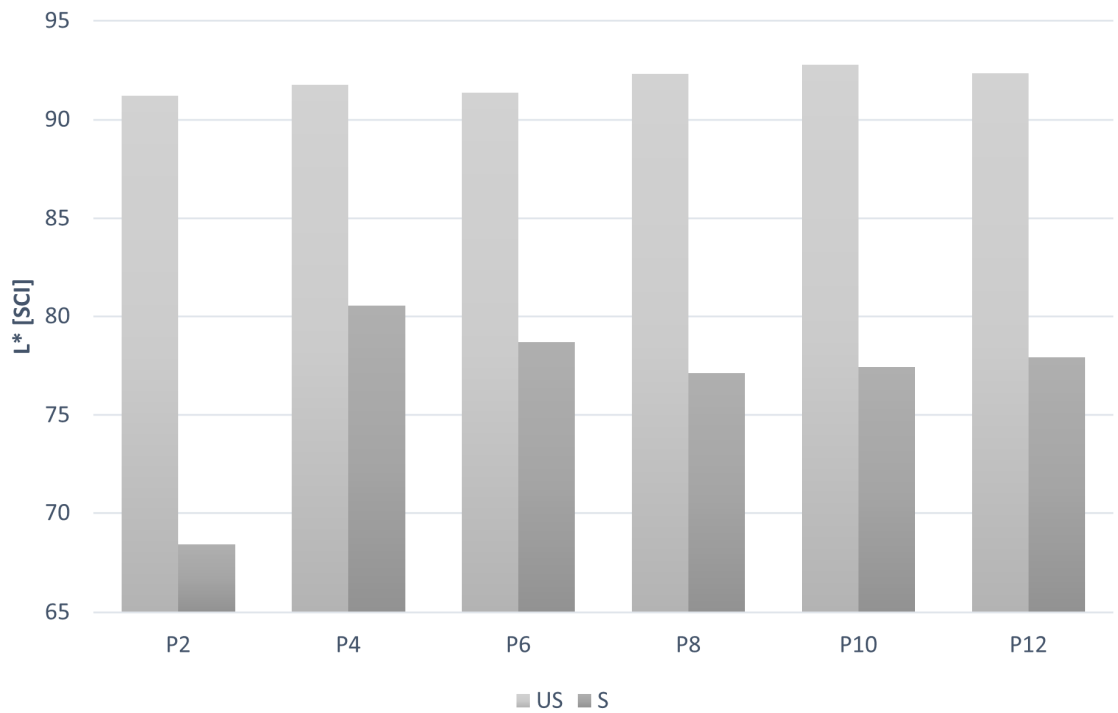


Figure 5.33. L^* (± 0.05) measurements of the d (unsoiled - US) and a (soiled - S) sections of P2, 6 and 10 (unaged - UA) and P4, 8 and 12 (aged - A) at t_{37} . L^* is relatively constant across the US control sections, UA and A, and varies in the S areas.

Table 5.6. Summary of measurements acquired from the control sections *d* (unsoiled - US) and *a* (soiled - S) of the unaged (P2, 6 and 10) and aged (P4, 8 and 12) plates at t_{37} (plates description in Table 5.2).

		P2, 6 and 10		P4, 8 and 12	
		<i>d</i>	<i>a</i>	<i>d</i>	<i>a</i>
R [%] (± 0.05 %)	min	39.28	17.56	53.20	37.20
	max	88.17	59.44	87.20	61.94
L* (± 0.05)	min	91.21	68.31	91.74	77.13
	max	92.78	78.67	92.34	80.53
a* (± 0.001)	min	1.30	1.02	1.45	1.37
	max	1.38	1.57	1.61	1.58
b* (± 0.005)	min	5.6	6.81	5.45	5.87
	max	8.01	8.07	6.42	6.22
YI₃₁₃	min	1.77	2.82	1.79	2.58
	max	1.93	4.11	1.85	2.91
Gloss_{85°} [GU] (± 0.1 GU)	min	1.19	0.88	1.37	0.79
	max	2.14	1.07	1.45	1.11
R_a [µm] (± 0.3 µm)	min	1.28	2.12	1.22	1.90
	max	3.68	2.98	2.46	3.16
R_z [µm] (± 0.05 %)	min	10.99	20.55	9.22	24.49
	max	29.80	27.90	18.30	44.72

5.3.4.2. Plaster plates coated with linseed oil

In the area coated with cold-pressed linseed oil (1-1) and boiled linseed oil (1-2) R% is significantly higher across the visible spectrum for the unsoiled sections and the aged areas show higher R% than the unaged ones (Figure 5.34).

The larger differences can be observed in the shorter wavelengths of the visible spectrum. The lightness (L*) increases after ageing and the b* value decrease, suggesting less-yellow surfaces (also confirmed by YI₃₁₃) (Figure 5.35 and Table 5.7). The overall change of colour in the unsoiled areas is smaller than the one calculated in the soiled areas (Figure 5.28 and Table 5.4, page 199). Changes in the R_a and R_z values suggest that the roughness of the aged areas, when compared to the unaged ones, is significantly higher in the soiled areas and slightly lower in the unsoiled areas. By comparing the data acquired from P1 and P3 to the identical plates P2 and P4 where an additional layer of beeswax was applied it was observed that all the US sections are whiter than the relevant S areas, UA and A. Only the area where beeswax was applied on top of boiled linseed oil shows significant changes in R%, with the US aged area becoming darker than the relevant unaged one (Figure 5.28, Tables 5.10 and 5.11, pages 199-200).

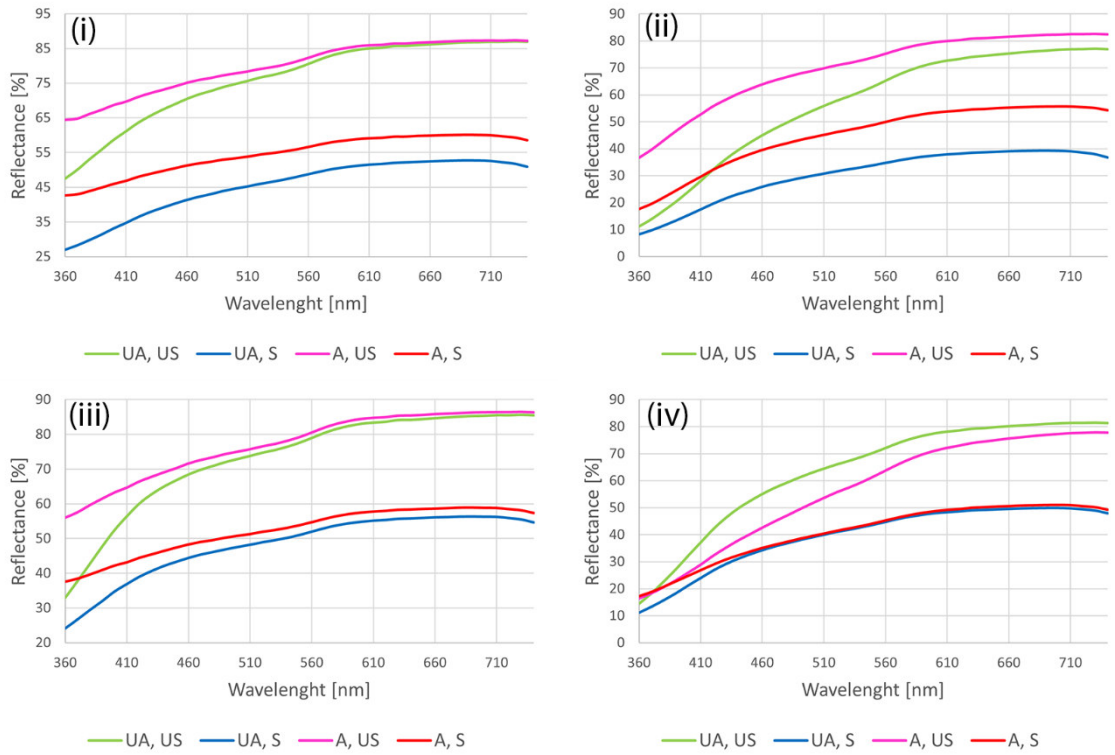


Figure 5.34. Reflectance (%) ($\pm 0.05\%$) of unsoiled – US, and soiled - S sections, on P1 (UA) and P3 (A), coated with cold-pressed linseed oil (1-1) (i) and boiled linseed oil (1-2) (ii) at t_{37} and relevant surfaces (iii and iv) with an additional layer of beeswax (4) on P2 (unaged - UA) and P4 (aged - A). All the US sections are whiter than the relevant S areas, UA and A. Only the area where beeswax was applied on top of boiled linseed oil shows significant changes in R%, with the US aged area becoming darker than the relevant unaged one.

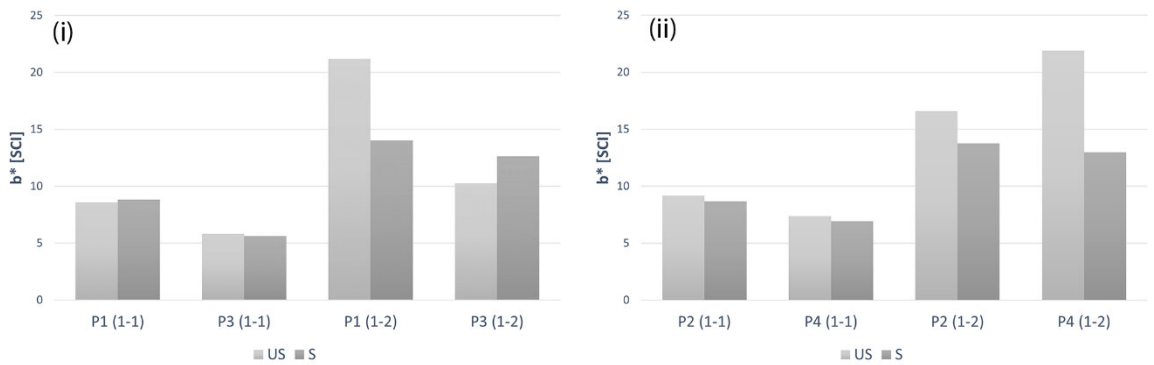


Figure 5.35. b^* (± 0.01) measurements of unsoiled – US, and soiled - S sections, on P1 (unaged - UA) and P3 (aged - A), coated with cold-pressed linseed oil (1-1) (i) and boiled linseed oil (1-2) (ii) at t_{37} and relevant surfaces with an additional layer of beeswax (4) on P2 (UA) and P4 (A). In all the sections the b^* value is reduced after ageing. Only in the coating boiled linseed oil-beeswax and increase of the yellow component can be seen.

Table 5.7. Summary of measurements acquired from the sections e and f (unsoiled - US) and b and c (soiled - S) coated with cold-pressed (b and e) and boiled linseed oil (c and f) of the unaged (P1) and aged (P3) plates at t_{37} (plates description in Table 5.2).

		P1				P3			
		e	b	f	c	e	b	f	c
R [%] (± 0.05 %)	min max	47.52 87.01	26.98 52.77	11.24 77.11	8.30 39.31	64.42 87.38	42.66 60.17	36.69 82.53	17.71 55.76
L* (± 0.05)		91.43	74.77	83.40	64.76	92.36	79.65	88.91	75.34
a* (± 0.001)		1.50	1.14	2.6	1.32	1.55	1.24	1.54	1.46
b* (± 0.01)		8.58	8.80	21.18	14.02	5.82	5.63	10.27	12.61
YI₃₁₃		1.94	3.31	3.17	5.45	1.80	2.64	2.15	3.52
Gloss_{85°} [GU] (± 0.1 GU)		0.26	0.25	1.01	0.20	0.51	0.05	0.49	1.01
R_a [μm] (± 0.3 μ m)		2.55	4.91	2.49	6.57	4.13	4.45	3.15	4.40
R_z [μm] (± 0.05 %)		18.11	39.17	23.33	47.81	24.90	34.23	24.44	45.45

5.3.4.3. Plaster plates coated with shellac

The L* values of the shellac6% (2-1) and shellac18% (2-2) (Table 5.8) aged sections are slightly higher than the L* of the relevant unaged areas. R% is significantly higher across the visible spectrum for the unsoiled sections and the aged areas show higher R% than the unaged ones, with the larger differences observed in the shorter wavelengths (Figure 5.36). The a* and b* values of the aged sections are lower, suggesting a smaller yellow component and a smaller red component (Figure 5.37). This is also confirmed by the lower values of the YI₃₁₃ of the aged areas when compared to the relevant unaged areas (Figure 5.29, page 200).

The overall change of colour in the unsoiled areas and the shellac6% soiled area is small and more relevant in the shellac18% soiled area (Figure 5.28 and Table 5.4, page 199). Almost irrelevant changes can be seen in the R_a values before/after ageing in shellac6%. Only the R_z value of the unsoiled aged section (P7e) is significantly higher than the relevant unaged section (P5e), suggesting a wide difference between the higher and lower data points in the roughness profile.

Although the values of gloss_{85°} of the plaster surfaces coated with shellac18% are still extremely small, they are higher than the values observed with the linseed oil and shellac6%, possibly suggesting that the higher density of the coating produced a glossier surface (greater rate of surface homogeneity can be particularly observed in the aged areas).

Interestingly, in shellac18% the HR 3D images show the brush marks due to the application of the coating, which disappeared after ageing, possibly due to the effect of drying and continued absorption of the coating in the substrate. While the R_a and R_z values of the unsoiled areas decreased after ageing, the soiled sections increased. Small changes can be observed in the areas coated with shellac and beeswax, but the overall trend is consistent (Figures 5.36 and 5.37, Tables 5.10 and 5.11).

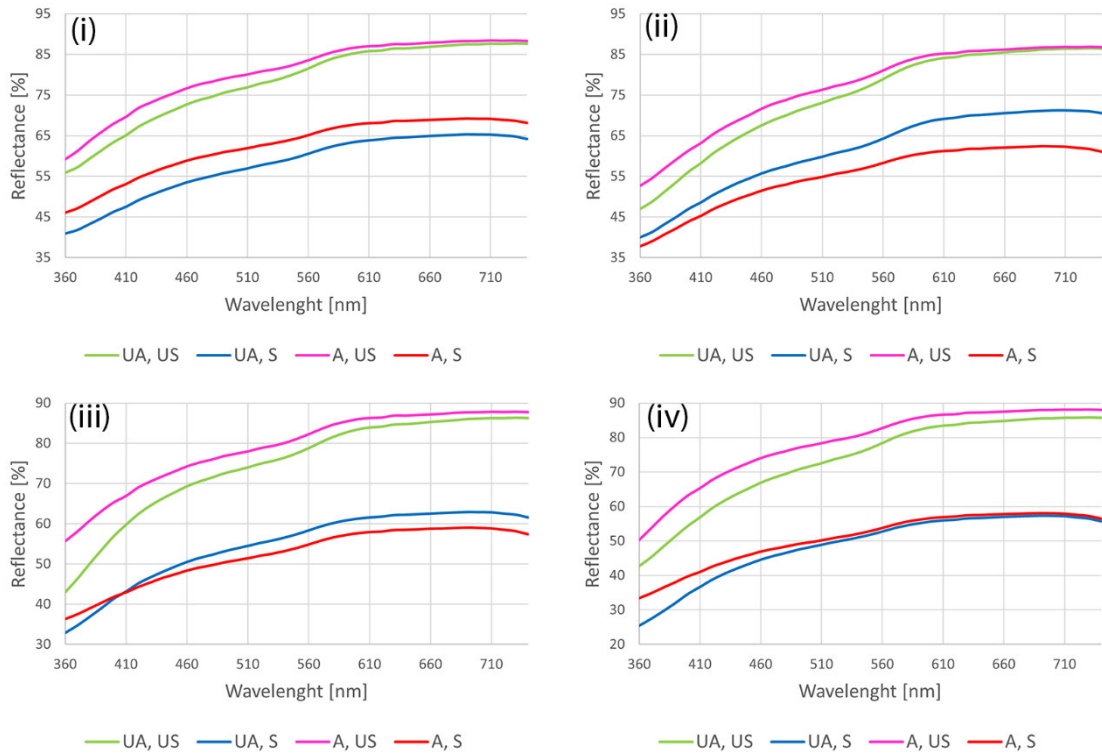


Figure 5.36. Reflectance (%) ($\pm 0.05\%$) unsoiled – US, and soiled - S sections, on P5 (unaged - UA) and P7 (aged - A), coated with shellac6% (2-1) (i) and shellac18% (2-2) (ii) at t_{37} and relevant surfaces (iii and iv) with an additional layer of beeswax (4) on P6 (UA) and P8 (A). All the US sections are whiter than the relevant S areas, UA and A.

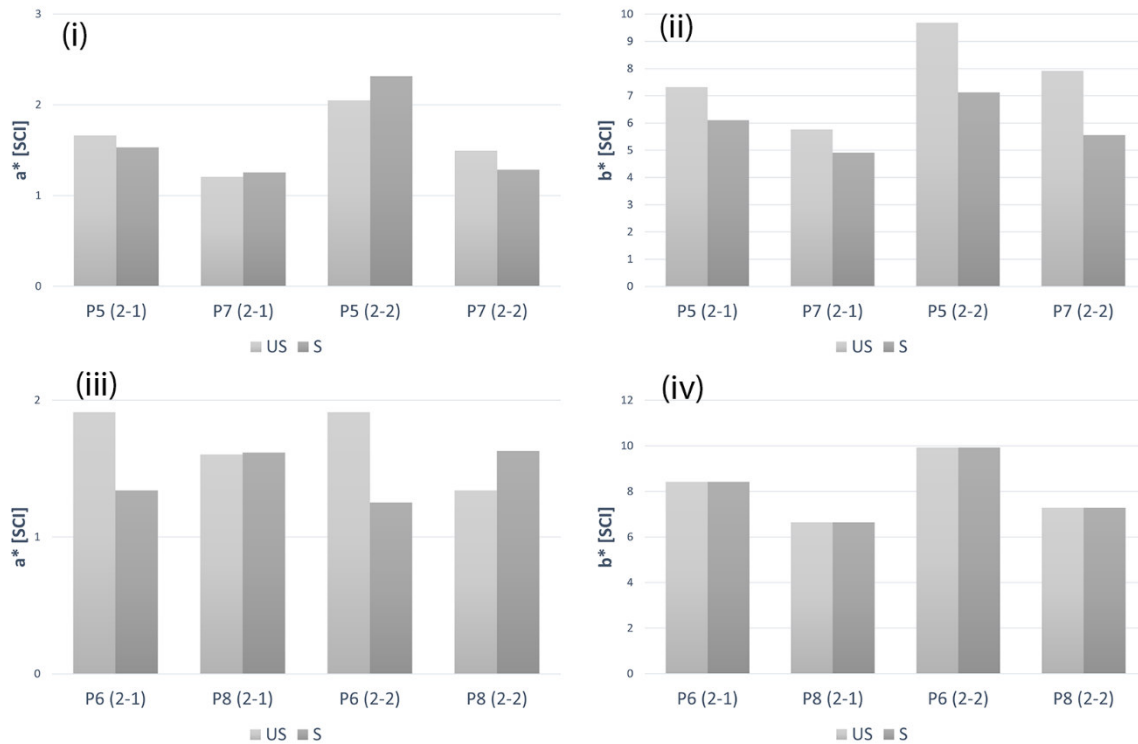


Figure 5.37. a^* (± 0.001) (i and iii) and b^* (± 0.01) (ii and iv) measurements of unsoiled – US, and soiled - S sections, on P5 (unaged - UA) and P7 (aged - A), coated with shellac6% (2-1) and shellac18% (2-2) at t_{37} and relevant surfaces with an additional layer of beeswax (4) on P6 (UA) and P8 (A). a^* and b^* decrease in all the sections after ageing.

Table 5.8. Summary of measurements acquired from the sections e and f (unsoiled - US) and b and c (soiled - S) coated with shellac6% (b and e) and shellac18% (c and f) of the unaged (P5) and aged (P7) plates at t_{37} (plates description in Table 5.2).

		P5				P7			
		e	b	f	c	e	b	f	c
R [%] (± 0.05 %)	min	55.93	40.93	46.95	40.02	59.18	46.02	52.67	37.78
	max	87.70	65.34	86.46	71.20	88.44	69.23	86.90	62.44
L* (± 0.05)		91.96	81.73	90.62	83.72	92.97	84.22	91.69	80.49
a* (± 0.001)		1.66	1.53	2.05	2.31	1.21	1.25	1.49	1.28
b* (± 0.008)		7.33	7.15	9.68	8.55	5.76	6.11	7.91	7.13
YI₃₁₃		1.87	2.55	2.03	2.46	1.76	2.30	1.90	2.64
Gloss85° [GU] (± 0.1 GU)		1.36	0.42	1.73	1.43	0.73	0.75	1.42	0.62
R_a [µm] (± 0.3 µm)		3.59	2.68	3.24	2.29	3.64	3.59	2.18	5.04
R_z [µm] (± 0.05 %)		25.12	23.90	36.30	22.33	35.20	22.81	19.68	51.72

5.3.4.4. Plaster plates coated with barite

A very small difference across the spectrum is observed before/after ageing in the barite20° (3-1) and barite60° (3-2) coated areas (Table 5.9). The aged areas of barite20° show a slightly higher R% (Figure 5.38) and b* values decreased upon ageing; the YI₃₁₃ values appear overall unchanged (Figure 5.29, page 200). The overall change of colour in the unsoiled areas and the barite20° soiled area is below visible and more relevant in the barite20° soiled area (Figure 5.28 and Table 5.4, page 199). A very small difference across the spectrum is observed before/after ageing in the R% (Figure 5.38) and the L* values in the unsoiled sections of barite60° (Figure 5.39), whereas the aged, soiled areas showed a significantly higher R% and L*; the b* values decrease upon ageing and YI₃₁₃ values appear overall unchanged (Figure 5.29, page 200). Changes in roughness can be appreciated in the R_a and R_z values before/after ageing. The roughness increases upon ageing for the unsoiled section and the soiled barite20° decrease and the soiled barite60° increase. No significant changes can be observed in the areas coated with barite and beeswax (Tables 5.10 and 5.11).

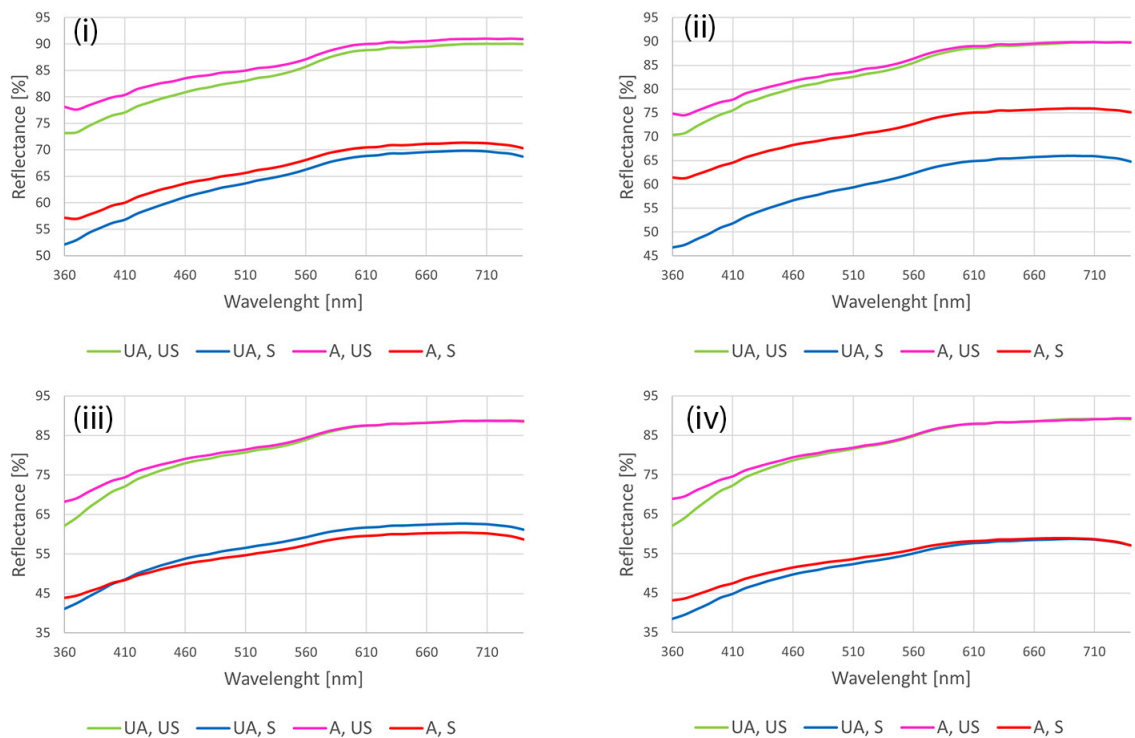


Figure 5.38. Reflectance (%) ($\pm 0.05\%$) unsoiled – US, and soiled - S sections, on P9 (unaged - UA) and P11 (aged - A), coated with barite20° (3-1) (i) and barite60° (2-2) (ii) at t_{37} and relevant surfaces (iii and iv) with an additional layer of beeswax (4) on P10 (UA) and P12 (A). The surfaces did not relevantly change after ageing and the most significant changes in R% can be seen between the US and S areas.

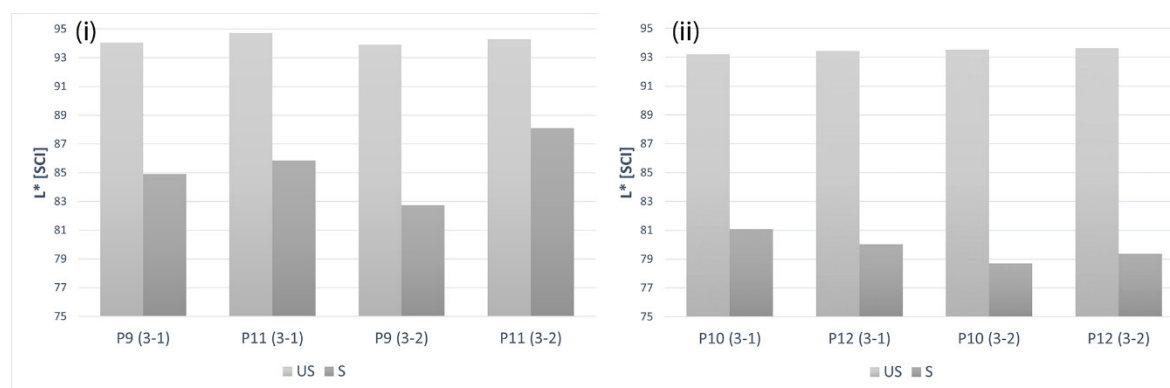


Figure 5.39. L^* measurements of unsoiled – US, and soiled - S sections, on P9 (unaged - UA) and P11 (aged - A), coated with barite20° (3-1) (i) and barite60° (3-2) (ii) at t_{37} and relevant surfaces with an additional layer of beeswax (4) on P10 (UA) and P12 (A). The L^* values are consistent with and without the beeswax coating.

Table 5.9. Summary of measurements acquired from the sections e and f (unsoiled - US) and b and c (soiled - S) coated with barite20° (b and e) and barite60° (c and f) of the unaged (P9) and aged (P11) plates at t_{37} (plates description in Table 5.2).

		P9				P11			
		e	b	f	c	e	b	f	c
R [%] (±0.05 %)	min	73.21	52.13	70.39	46.76	77.59	57.01	74.54	61.29
	max	90.07	69.86	89.82	65.97	91.02	71.39	89.91	75.95
L* (±0.05)		94.06	84.9	93.92	82.74	94.72	85.85	94.29	88.09
a* (±0.001)		1.35	1.09	1.28	1.18	1.28	1.15	1.16	1.11
b* (±0.008)		3.83	4.91	4.26	5.56	2.93	4.06	3.65	3.89
YI₃₁₃		1.66	2.21	1.68	2.39	1.61	2.11	1.64	1.97
Gloss85° [GU] (±0.1 GU)		0.69	0.02	1.06	0.62	0.37	0.19	1.05	0.98
R_a [µm] (±0.3 µm)		1.11	4.66	1.44	2.97	2.94	2.80	2.25	5.00
R_z [µm] (±0.05 %)		13.15	45.14	18.42	41.49	26.66	29.72	16.67	44.65

Table 5.10. Summary of measurements acquired from the unsoiled, unaged (P2, 6 and 10) and aged (P4, 8 and 12), plates at t_{37} (plates description in Table 5.2). P2 and 4 are coated with linseed oil and beeswax, P6 and 8 with shellac and P10 and P12 with barite.

		P2		P4		P6		P8		P10		P12	
		e	f	e	f	e	f	e	f	e	f	e	f
R [%] (± 0.05 %)	min	33.3	14.5	56.0	16.4	42.9	42.7	55.6	50.2	62.1	62.0	68.2	68.9
		8		6	6	9	1	4	6	9	4	1	2
	max	85.5	81.4	86.5	77.9	86.3	85.8	87.8	88.0	88.9	89.2	88.7	88.9
		9	2	1	1	4	8	0	7	7	1	5	4
L* (± 0.05)		90.7	87.0	91.4	82.5	90.7	90.3	92.3	92.4	93.2	93.5	93.4	93.6
		8	5	9	9	6	8	1	6	1	3	3	3
a* (± 0.001)		1.4	1.52	1.80	3.73	1.91	1.91	1.60	1.34	1.40	1.14	1.35	1.25
b* (± 0.005)		9.17	16.5	7.37	21.8	8.42	9.93	6.64	7.28	4.96	5.04	4.30	4.41
			8		9								
YI₃₁₃		1.99	2.56	1.90	3.34	1.98	2.05	1.83	1.84	1.73	1.72	1.70	1.69
Gloss85° [GU] (± 0.1 GU)		0.37	1.04	0.51	2.11	0.44	1.95	1.93	2.84	0.28	1.10	1.14	2.19
R_a [μm] (± 0.3 μ m)		2.20	2.89	1.89	2.18	1.72	3.00	3.64	2.18	2.12	.95	2.22	2.71
R_z [μm] (± 0.05 %)		24.2	27.7	13.4	97.6	23.2	25.0	35.2	19.6	15.2	20.4	19.1	33.0
		1	0	6	2	1	2	0	8	0	1	8	6

Table 5.11. Summary of measurements acquired from the soiled, unaged (P2, 6 and 10) and aged (P4, 8 and 12), plates at t_{37} (plates description in Table 5.2). P2 and 4 are coated with linseed oil and beeswax, P6 and 8 with shellac and P10 and P12 with barite.

		P2		P4		P6		P8		P10		P12	
		b	c	b	c	b	c	b	c	b	c	b	c
R [%] (± 0.05 %)	min	24.2	11.2	37.6	17.1	32.9	25.4	36.2	33.3	41.1	38.4	43.8	43.1
		1		5	9	1	2	8	8	0	2	5	7
	max	56.2	49.8	58.9	51.0	62.9	57.2	59.0	58.0	62.6	57.8	60.3	58.9
		9	4	4	1	2	8	1	5	9	4	6	7
L* (± 0.05)		76.7	71.8	78.4	72.2	80.4	77.1	78.5	77.8	81.0	78.6	80.0	79.3
		4	7	9	9	5	6	3	8	7	9	2	7
a* (± 0.001)		1.44	1.29	1.63	1.89	1.34	1.25	1.62	1.63	1.02	1.23	1.20	1.08
b* (± 0.005)		8.67	13.7	6.91	12.9	8.27	9.36	7.02	7.58	5.68	5.86	4.96	4.82
			7		8								
YI₃₁₃		3.09	4.09	2.82	3.98	2.71	3.09	2.82	2.92	2.52	2.74	2.58	2.62
Gloss85° [GU] (± 0.1 GU)		0.47	0.41	0.64	0.79	0.27	0.61	0.93	1.47	0.34	0.57	0.25	1.11
R_a [μm] (± 0.3 μ m)		2.78	3.93	1.89	1.76	2.39	2.25	3.59	5.04	1.86	1.34	2.12	3.55
R_z [μm] (± 0.05 %)		36.5	49.8	18.1	20.3	27.6	19.5	22.8	51.7	18.0	19.8	14.2	27.6
		3	3	1	4	0	7	1	2	0	4	5	3

5.3.5. FOURIER-TRANSFORM INFRARED SPECTROSCOPY (FT-IR)

ATR/FT-IR spectra were acquired from all the plaster plates at t_{12} (Table 5.3, page 174) before the application of the coatings and the accelerated ageing (Figure 5.40). All the spectra showed the peaks characteristic of gypsum plaster (Table 5.12), as supported by the literature (Al Dabbas *et al.*, 2014; Anastasiou *et al.*, 2006; Derrick *et al.*, 2000; Manfredi *et al.*, 2015; Price *et al.*, 2009; Serafima *et al.*, 2016). Differences in the intensity of the peaks can be observed in Figure 5.40 and are due to the different contact of the ATR on the uneven plaster plate surfaces. The range of the ATR mode ($380\text{-}4000\text{ cm}^{-1}$) is instrumentally slightly wider than the one of the spectra acquired in diffuse reflectance mode ($650\text{-}4000\text{ cm}^{-1}$).

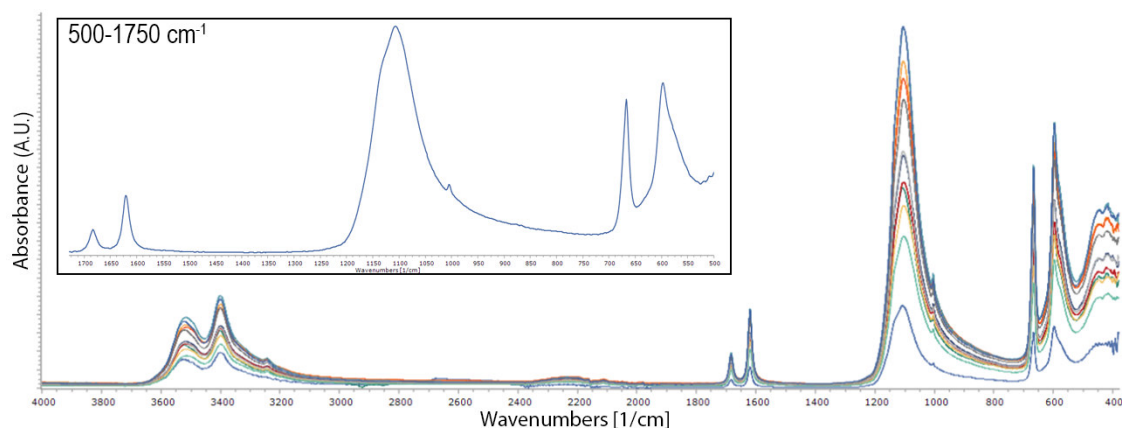


Figure 5.40. ATR/FT-IR spectra acquired from all the plaster plates at t_{12} and close-up (in the black rectangle) of the $500\text{-}1750\text{ cm}^{-1}$ region of one of the spectra. The peaks positions are summarised in Table 5.12.

Table 5.12. ATR/FT-IR bands and relevant assignments of the spectra acquired from the plaster substrate at t_{12} .

FT-IR band [cm^{-1}]	Assignment
420-50	$\nu_{\text{ab}} \text{SO}_4$
597	δSO_4
667	δSO_4
1005	$\nu_{\text{s}} \text{SO}$
1105	$\nu_{\text{as}} \text{SO}$
1620	$\nu_2 \text{H}_2\text{O}$
1680	$\nu_2 \text{H}_2\text{O}$
2224	Overtone H_2O
3232	νOH
3400	νOH
3520	νOH

5.3.5.1. *Unsoiled and uncoated plaster plates*

FT-IR spectra acquired from the unaged and unsoiled areas of the uncoated plaster surface (d of P1, 5 and 9) at t_{37} (Table 5.3, page 174) in diffuse reflectance mode suggest that the plaster substrate is characterised by the same peaks highlighted in Table 5.12. Small differences in intensity and positions of the peaks can be observed between the spectra acquired with different FT-IR modes. These differences are related to the characteristics of FT-IR mode and result from the interactions of specular and scattered signal but are also related to the characteristics and contaminations of the spot analysed. The diffuse reflectance spectra are expected to be very similar to those obtained from transmission mode, but overtones and combination bands increase their signals because many reflections occur (Derrick *et al.*, 2000). The interpretation of the vibrational profiles is often difficult because of the appearance of distortions concerning the spectra acquired in transmission. The distortion arising from the volume and surface reflection can in some cases be corrected by using Kubelka–Munk (KM) and Kramers–Kronig (KK) theories, but in the case of complex morphology and heterogeneity of the surface, like for real artworks, their use is limited (Manfredi *et al.*, 2015; Morris, 1963).

The transmission spectra were acquired at t_{12} whereas the diffuse reflectance spectra were acquired at t_{37} (Table 5.3). Table 5.13 summarises the most relevant peaks observed in control sections d of P1, 5, and 9 at t_{37} . Several differences observed from the transmission and diffuse reflectance results are related to the drying of gypsum plaster and consequent changes in the mineral structure.

According to Morris (1963), in the region of 1000 to 1300 cm^{-1} most metallic sulfates, IR absorption occurs, and the 1005 cm^{-1} peak of gypsum is due to the forced fit of the sulfate ion in the hexagonal crystal lattice formed when the monoclinic crystals of the dihydrate are dehydrated to the hemihydrate. Morris (1963) showed that the 1005 cm^{-1} absorption should disappear when the hexagonal crystals of hemihydrate are dehydrated to either hexagonal anhydrous calcium sulfate or orthorhombic anhydrous calcium sulfate. In the spectra of the unaged unsoiled control sections, the peaks at 1005 and 1105 cm^{-1} are still present, but significantly weaker, relatively to the rest of the vibrations (Risdonne & Theodorakopoulos, 2021).

Small shifts towards higher frequencies are consistent with the literature (Bishop *et al.*, 2014; Morris, 1963; Ross & Farmer, 1974). The presence of the strong band, duplet or triplet in 1230-80 cm^{-1} area, despite differing from the results shown in ATR mode, is still consistent with the S-O vibration range defined by Morris (1963). The decreased intensity of the 1005 and 1105 cm^{-1} and the raise of the strong peak(s) at 1230-80 cm^{-1} is therefore due to the rearrangement of the mineral structure of gypsum during the drying of the plaster substrates. The other absorption maxima (Table 5.13) in the infrared spectra of calcium

sulfate hydrates are due to water molecules bonded to the sulfate or perturbations of the S-O stretch due to the forced fit of the sulfate ion in a crystallographic lattice site and were consistently observed in the spectra (Al Dabbas *et al.*, 2014; Anastasiou *et al.*, 2006; Kling & Schiffer, 1969; Morris, 1963; Seidl *et al.*, 1969). The gypsum plaster overtones centred around the three peaks at 2208, 2336 and 2360, due to the combination of bending and vibration modes of H₂O ($\nu_1 + \nu_3$ and $2\nu_3$) and related to the presence of gypsum appear stronger in DR spectra (Manfredi *et al.*, 2015; Serafima *et al.*, 2016). Bishop *et al.* (2014) highlighted that a small shift towards higher frequencies can be observed for ν_1 and ν_2 from gypsum (calcium sulfate dihydrate) to bassanite (calcium sulfate hemihydrate) to anhydrite (anhydrous calcium sulfate) in transmission spectra (Ross & Farmer, 1974). Such a shift can be observed in the spectra presented in Morris (1963) and would be similarly expected for diffuse reflectance spectra.

The same range of considerations can be applied to the relevant aged plates (section d of P3, 7, 11) when compared with the ATR spectra acquired at t_{12} (see *Table 5.3*, page 174). As the FT-IR spectra of the unaged and aged spectra at t_{37} were acquired with the same conditions and parameters the differences between the aged and unaged identical areas can be due to local imperfections. Overall, these minor changes are not consistent enough across the whole batch of spectra to be considered characteristic of the ageing processes.

5.3.5.2. *Soiled uncoated plaster plates*

The most significant peaks of the soiled sections (a) of the unaged (P1, 5, 9) and aged (P3, 7, 11) sections are summarised in *Table 5.13*. The characteristic peaks of gypsum plaster were also visible in the spectra of the soiled areas (a). These peaks were not assigned to a specific molecular vibration due to the complexity of the artificial soiling mixture, but also as it did not appear particularly important for the scope of the analysis and the comparison of the spectra. In addition to the extra peaks highlighted in the soiled areas, inorganic material in the soiling mixture had surely contributed to the band at 1100-1300 cm⁻¹, as this is the region of sulfates and carbonates vibrations (Derrick *et al.*, 2000).

Table 5.13. FT-IR bands and relevant assignments of the spectra acquired from unsoiled areas (d of P1, 3, 5, 7, 9 and 11) and soiled areas (a of P1, 3, 5, 7, 9 and 11) at t_{37} .

FT-IR band [cm^{-1}]				Assignment
(d) P1, 5 and 9	(a) P1, 5 and 9	(d) P3, 7 and 11	(a) P3, 7 and 11	
688	687	704	680-90	δ SO ₄
736	720-30	736	710-50	S ion
	832		800-30	
			860	
			910-60	
			1000	ν_{1s} SO
			1056	
1005		995		ν_{1s} SO
1105	1105	1088	1105	ν_{as} SO
1230-80	1230-80	1230-80	1230-80	ν_3 SO
	1320-60		1320-60	
1620	1620	1630	1630	ν_2 H ₂ O
1680	1680	1690	1690	ν_2 H ₂ O
	1740		1740	
2220-2360	2220-2360	2220-2360	2220-2360	Overtone H ₂ O
	2400		2400	
	2800-3000		2800-3050	
3200-50	3200-50	3200-50	3200-50	ν OH
3400	3400	3400	3400	ν OH
3530-90	3530-90	3530-90	3530-90	ν OH
3665	3665	3665	3665	ν OH
3776	3776	3776	3776	ν OH

5.3.5.3. Plaster plates coated with cold-pressed linseed oil

Unaged and unsoiled cold-pressed linseed oil on gypsum plaster substrate (P1e) is characterised by the peaks described in Table 5.14 and supported by previous studies (Grehk *et al.*, 2008; Shreve *et al.*, 1950; Sinclair *et al.*, 1952). As the analysed coating did not consist of a pure sample but was applied on the plaster substrate, overlapping of the contributions from the inorganic substrate and the organic coating can be seen.

The peaks at 704 cm^{-1} and 820 cm^{-1} have been respectively tentatively assigned to the *cis*-ethylenic hydrogen vibration and bending by Sinclair *et al.* (1952), but vibrations due to the bending in molecules containing S²⁻ and SO₄²⁻ might contribute to broadening the band in this area (Table 5.12). Weak contribution at 1005 cm^{-1} related to the SO symmetric vibration can be seen, but the 1105 cm^{-1} asymmetric vibration is either absent or has shifted to about 1090 cm^{-1} . In the 1200-1350 cm^{-1} either a sharp peak centred at 1245 cm^{-1} with a shoulder at 1350 cm^{-1} or a duplet, at 1230 cm^{-1} and 1280 cm^{-1} can be seen and is consistent with the S–O vibration as discussed for the plaster substrate.

Contributions from the organic coating, however, are possible in this area: according to Guillén *et al.* (2003), bands associated with stretching vibration of the C–O ester groups and with the bending vibration of the CH₂ group at 1163 cm^{-1} and 1238 cm^{-1} and symmetrical bending vibrations of the CH₃ groups at 1376 cm^{-1} are characteristic of

vegetable oils. Guillén *et al.* (2003) also determined that the IR spectra of the majority of vegetable oils studied in their laboratory showed a band near 1118–1120 cm^{-1} , whose frequency increases and intensity decreases as the degree of unsaturation of the sample increases. The absence of this band in an oil spectrum, therefore, indicates that the oil is highly unsaturated, as observed in linseed oil spectra.

The duplet at 1620 and 1680 cm^{-1} assigned to the vibrations in the water molecule and related to the presence of the sulfate can be also observed in the sections coated with cold-pressed linseed oil. However, the contribution of the organic coating must not be excluded: Guillén *et al.* (2003) suggested that vibrations of disubstituted cis C=C of the unsaturated acyl groups, appears at 1653 cm^{-1} .

The C=O ester peak is mostly centred at 1710 cm^{-1} , although in other spectra this peak appeared shifted to 1730 or 1750 cm^{-1} . Gypsum plaster overtone in the 2100-2350 area can be seen and are due to the combination of bending and vibration modes of H₂O ($\nu_1 + \nu_3$ and $2\nu_3$) (Manfredi *et al.*, 2015; Serafima *et al.*, 2016).

The spectral feature at 2860 cm^{-1} and 2927 cm^{-1} represent the C–H stretching (symmetric and asymmetric, respectively) of CH₂ and the shoulder on the 2927 cm^{-1} peak at 2956 cm^{-1} represent the asymmetric C–H stretching of CH₃ (Grehk *et al.*, 2008; Shreve *et al.*, 1950; Sinclair *et al.*, 1952). Absorption maxima of water vibration in the 3000-3600 cm^{-1} region for calcium sulfate and linseed oil have been consistently identified by several authors (Al Dabbas *et al.*, 2014; Anastasiou *et al.*, 2006; De Viguerie *et al.*, 2016; Grehk *et al.*, 2008; Guillén *et al.*, 2003; Kling & Schiffer, 1969; Morris, 1963; Seidl *et al.*, 1969). For example, Morris (1963) identified characteristic peaks due to the presence of water at 3390 and 3530 cm^{-1} for the di-hydrate calcium sulfate and 3540 and 3600 cm^{-1} for the hemihydrate. Mallégol *et al.* (1999) reported that in drying oils the OH stretching vibration of alcohols lies around 3470 cm^{-1} ; this, however, cannot be separated from that of the hydroperoxides (maximum at 3425 cm^{-1}), which are postulated to be the major products responsible for the broad band in the OH range when oxidation starts. In this study, for the unaged plaster-linseed oil samples, spectra showed several peaks in the 3000-3600 cm^{-1} region. The maxima are inconsistently observed in this region in the spectra acquired from the same area, suggesting that the OH vibrations are caused by different contributors, namely gypsum and linseed oil.

The spectra acquired from the unaged and soiled plaster-cold pressed linseed oil areas (P1b) showed most of the peaks discussed above for the relevant unsoiled areas. Additional peaks, due to the soiling mixture are highlighted in *Table 5.14* and have not been assigned, as discussed also for the control sections. Several bands assigned to cold-pressed linseed oil showed differences in intensity in the spectra acquired from the relevant soiled areas. An increase of intensity was observed in the 1200-1350 cm^{-1} , suggesting that the soiling

mixture contributes to the vibration in this region. The decrease of intensity in other regions, such as in the 2800-3000 cm^{-1} and 3100-3600 cm^{-1} areas, suggest that the soiling covering the surface partially reduced the reflectance characteristic of the plaster-coating surface. The same range of changes was observed in the spectra acquired from the aged and soiled plaster-cold pressed linseed oil areas (P3b) when compared with the relevant unsoiled areas (P3e), and are summarised in *Table 5.14*.

Several studies have been focused on the ageing and oxidation processes of linseed oil (Chiavari *et al.*, 2005; De Viguerie *et al.*, 2016; Marinescu *et al.*, 2014; Symoniuk *et al.*, 2016). No references for the ageing of the plaster-linseed oil system is available in the literature, as most of the studies were carried either on thin coat applied onto glass slides or on easel paintings. By comparing the FT-IR spectra of the aged cold-pressed linseed oil to the unaged relevant spectra it was observed that:

- the peaks at 704 cm^{-1} and 820 cm^{-1} seemed to have slightly shifted, approximately at 720 and 770-780 cm^{-1} and the intensity is slightly higher;
- weak contribution at 1005 cm^{-1} related to the SO symmetric vibration can be still seen, but the 1105 cm^{-1} asymmetric vibration is absent;
- in the 1200-1350 cm^{-1} the sharp peak centred at 1245 cm^{-1} , duplet, or triplet discussed for the unaged oil, can be still seen although appear significantly weaker;
- the duplet at 1620 and 1680 cm^{-1} assigned to the vibrations in the water molecule and related to the presence of the sulfate seems to be overall unvaried;
- the 1710-40 cm^{-1} ester CO vibration is still visible, although lower in intensity;
- gypsum plaster overtone in the 2100-2350 area can be seen and are overall unvaried;
- symmetric and asymmetric C–H stretching at 2860 cm^{-1} and 2927 cm^{-1} are extremely weak, almost disappeared, after ageing;
- the intensity of water vibration peaks in the 3000-3600 cm^{-1} region increased in the 3000-3400 cm^{-1} and decrease in the 3400-3600 cm^{-1} , consistently with the drying of gypsum plaster and mineral rearrangement as observed by Morris (1963). Changes related to the ageing of the oil in this region due to the formation of hydroperoxides (Lazzari & Chiantore, 1999; Mallécol *et al.*, 1999, 2000; Meneghetti *et al.*, 1998; Oyman *et al.*, 2005) were not visible. This can suggest that the path of oxidation and degradation of linseed oil might be affected by the presence of the inorganic substrate.

Table 5.14. FT-IR bands and relevant assignments of the spectra acquired from unsoiled (unaged P1e and aged P3e) and soiled (unaged P1b and aged P3b) areas of the plaster surface coated with cold-pressed linseed oil (1-1) at t_{37} .

FT-IR band [cm^{-1}]				Assignment
P1e	P1b	P3e	P3b	
700-20	705-80	720-30	700-40	δ SO ₄ /v CH
800-20		760-90	800	δ CH
	865			
		910		
	950			
1005-30		1005-50		ν_{1s} SO
			1067	
1090	1101			ν_{as} SO
1245	1245	1245	1235	ν SO/ ν CH ₂
	1280		1280	
1350		1375	1345	ν SO/ δ CH ₃
1616-32		1616-32	1616-48	ν_2 H ₂ O
1690	1695	1660-90	1680	ν_2 H ₂ O
1710-40	1715	1744	1715	ν CO (TAG)
2110-2330	1980-2200	2130-2330	1990-2340	Overtone H ₂ O
2860	2860	2860 (vw)		ν_s CH ₂
2927	2927	2927 (vw)		ν_{as} CH ₂
2956	2942	2956 (vw)		ν_{as} CH ₃
			2990	
		3010-50		ν <i>cis</i> C=CH
3100	3050-3100	3150-3250	3150-3300	ν OH
3200-50	3200-50	3280-3380		ν OH
3340				ν OH
	3450	3420-3500		ν OH
3500-3600	3500-3600	3500-3600	3500-3600	ν OH
3650	3650	3650		ν OH

TAG= Triacetyl glycerol; vw= very weak.

5.3.5.4. Plaster plates coated with boiled linseed oil

References on the molecular vibrations characteristics of boiled linseed oil can be found elsewhere (Marinescu *et al.*, 2014; Samain *et al.*, 2011), but most of the studies on molecular characterization of aged and unaged linseed oil seemed to have been carried on raw linseed oil. Unaged and unsoiled boiled linseed oil on the gypsum plaster substrate is characterised by the peaks described in Table 5.15. By comparing the unaged cold-pressed linseed oil (P1e) and boiled one (P1f) (Figure 5.41) it was possible to determine that the spectra are quite similar and the vibrations described for the cold-pressed linseed oil were also found for the boiled oil. Differences were observed however in terms of a small variation of intensity, particularly in the 3000-3600 cm^{-1} , where the lower intensity of the boiled linseed oil ν OH bands might suggest a lower content of water in these samples.

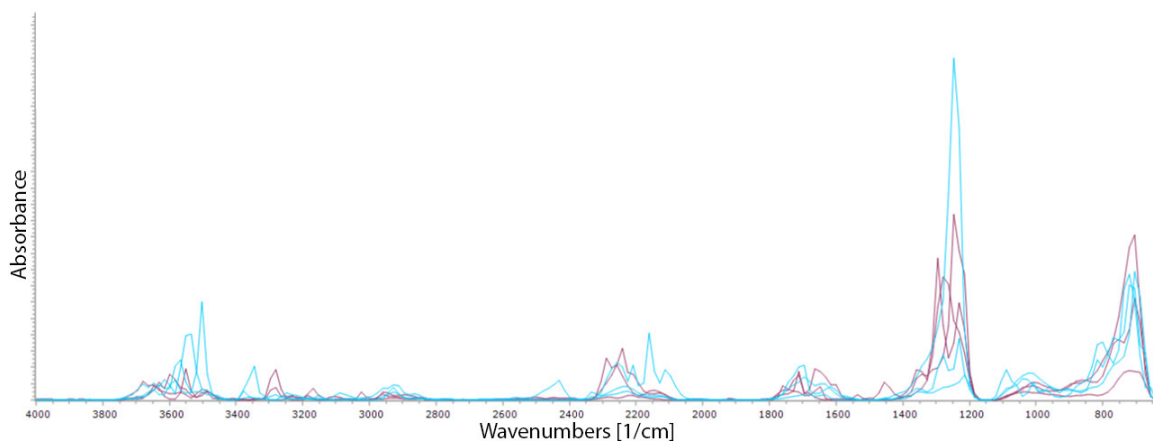


Figure 5.41. Diffuse Reflectance (DR) FT-IR spectra acquired from areas of the unsoiled and unaged plaster surfaces coated with cold-pressed linseed oil P1e (1-1), light blue spectra, and with boiled linseed oil P1f (1-2), purple spectra, at t_{37} .

Following up the observations on the change upon ageing on the plaster surfaces coated with the cold-pressed linseed oil, by comparing the FT-IR spectra of the aged, boiled linseed oil to the unaged relevant spectra, the following was observed:

- the peak at 704 cm^{-1} has not shifted and appears more intense in the aged section, an additional shoulder at $768\text{-}810\text{ cm}^{-1}$ has however emerged;
- the contribution at 1005 cm^{-1} related to the SO symmetric vibration has intensified and the 1105 cm^{-1} asymmetric vibration is either absent or has shifted to the $1070\text{-}80\text{ cm}^{-1}$;
- the peak centred at 1245 cm^{-1} shows a shoulder at 1358 cm^{-1} and is overall unchanged in intensity;
- of the duplet at 1620 and 1680 cm^{-1} assigned to the vibrations in the water molecule only the peak centred at 1620 cm^{-1} is visible;
- the $1710\text{-}40\text{ cm}^{-1}$ ester CO vibration is unchanged;
- gypsum plaster overtone in the $2100\text{-}2350$ area can be seen but is lower in intensity;
- symmetric and asymmetric C–H stretching at 2860 cm^{-1} and 2927 cm^{-1} are unchanged in intensity but have slightly shifted, after ageing;
- the intensity of OH vibration peaks in the $3000\text{-}3600\text{ cm}^{-1}$ region appears overall unvaried.

The spectra acquired from the unaged and soiled plaster-cold pressed linseed oil areas (P1c) showed most of the peaks discussed above for the relevant unsoiled areas (P1f). Additional peaks, due to the soiling mixture are highlighted in *Table 5.15* and have not been assigned, as discussed also for the control sections. Several bands assigned to linseed oil

showed differences in intensity in the spectra acquired from the relevant soiled areas. The bands in the 650-1100 cm^{-1} appear overall constant in intensity, whereas the intensity of the contributions in the 1200-1300 cm^{-1} and 2100-2300 cm^{-1} region is less intense in the soiled areas, suggesting that the soiling covering the surface, partially reduced the reflectance characteristic of the plaster-coating surface. In other regions, the soiling contributed to the vibration, such as in the 2800-3000 cm^{-1} and 3400-3700 cm^{-1} region. The same range of changes was observed in the spectra acquired from the aged and soiled plaster-cold pressed linseed oil areas (P3c) when compared with the relevant unsoiled areas (P3f) and are summarised in *Table 5.15*.

Table 5.15. FT-IR bands and relevant assignments of the spectra acquired from unsoiled (unaged P1f and aged P3f) and soiled (unaged P1c and aged P3c) areas of the plaster surface coated with boiled linseed oil (1-2) at t₃₇.

FT-IR band [cm^{-1}]				Assignment
P1f	P1c	P3f	P3c	
704-50	705-80	704	704-30	δ SO ₄ /v CH
		768-810	780-800	
860	860-90		860	δ CH
	970-90		930	
1005	1009	1005-50	1005-20	ν_{1s} SO
	1088		1067	
	1105	1070-80	1002	ν_{as} SO
1245	1230-45	1235-50	1210-60	ν SO/ ν CH ₂
1280	1280-95		1295	
1356		1358	1345	ν SO/ δ CH ₃
	1330-90			
	1420-80		1440	
	1570-90		1520	
1600-65	1630-65	1616-32	1616	ν_2 H ₂ O
1690			1695	ν_2 H ₂ O
1710-40	1727-50	1710	1745	ν CO (TAG)
		1790	1780	
2140-2290	2130-2330	2200-2390	2110-2320	Overtone H ₂ O
2860	2848-64	2848-80	2865	ν_s CH ₂
	2890-2910			
2927	2927	2945	2915	ν_{as} CH ₂
2956	2944		2944	ν_{as} CH ₃
	2975			
3020		2990	2990	ν <i>cis</i> C=CH
3140-3200	3050-3180	3150-3250	3050-3250	ν OH
3230-80	3250-3330	3280-3360	3280-3360	ν OH
3500-3600	3500-3600	3440-3600	3400-3600	ν OH
3680	3650	3680	3650-80	ν OH

5.3.5.5. *Plaster plates coated with shellac*

In the plaster plates coated with shellac, the characteristic peaks (Coelho *et al.*, 2012; Colombini *et al.*, 2003; Derrick *et al.*, 2000; Poli *et al.*, 2014; Sarkar & Kumar, 2001) can be observed along with and/or overlapping the bands assigned to the plaster substrate.

The peaks characteristic of gypsum described for the control sections can be still seen in the unsoiled and unaged section coated with shellac6% (P5e) including the S-O stretch vibrations (ν), the *cis*-ethylenic hydrogen vibration and bending at 705 cm^{-1} and 820 cm^{-1} (the latter overlapped with the CH out-of-plane bending), and vibrations due to the bending of in molecules containing S^{2-} and SO_4^{2-} might contribute to broadening the band in this area. Weak contribution at 1005 cm^{-1} related to the SO symmetric vibration can be seen, but the 1105 cm^{-1} asymmetric vibration is either absent or has shifted to about $1060\text{--}90\text{ cm}^{-1}$, possibly due to the contribution of the unresolved band at 1032 cm^{-1} of the COC vibration of acetal/dioxolane linkage of shellac. In the $1200\text{--}1300\text{ cm}^{-1}$, the broad band, duplet or triplet is due to β OH of aliphatic carboxyl and hydroxyl groups, overlapped with ν CO of $-\text{COOR}$ and with the S-O vibration as discussed for the plaster substrate. In the $1300\text{--}1456\text{ cm}^{-1}$ region, the C-H bending bands of shellac can be seen. The duplet at 1620 and 1680 cm^{-1} assigned to the vibrations in the water molecule and related to the presence of the sulfate has shifted at 1632 and 1660 cm^{-1} can be also observed in the sections coated with shellac6%, due to the contribution of the C-C stretching band and the C=O stretching band of the $-\text{COOH}$, observed at $1712\text{--}30\text{ cm}^{-1}$. Gypsum plaster overtone in the $2120\text{--}2336\text{ cm}^{-1}$ area can be seen and are due to the combination of bending and vibration modes of H_2O ($\nu_1 + \nu_3$ and $2\nu_3$) (Manfredi *et al.*, 2015; Serafima *et al.*, 2016). The CH_3 and CH_2 vibrations were respectively observed at $2863\text{--}78$ and $2944\text{--}60\text{ cm}^{-1}$ in the plaster-shellac6% area. A crowded and varied range of peaks was observed in the $3100\text{--}3600\text{ cm}^{-1}$ region (O-H stretching bands), due to both gypsum plaster and shellac.

By comparing the FT-IR spectra of the aged shellac6% (P7e) to the unaged relevant spectra, the following was observed:

- the peaks at between 750 and 940 cm^{-1} disappeared;
- the $1000\text{--}1120\text{ cm}^{-1}$ contributions are overall unchanged;
- contrarily to what has been reported by Poli *et al.* (2014), the OH band at 1256 cm^{-1} increased in the aged plaster-shellac6% spectra;
- the contributions in the $1280\text{--}1460\text{ cm}^{-1}$ and the $1620\text{--}80\text{ cm}^{-1}$, as well as the C=O stretching band and gypsum overtones, are overall unchanged;

- symmetric and asymmetric C–H stretching at 2863-78 and 2944-60 cm^{-1} are extremely weak after ageing and the asymmetric one has shifted to 2912-27 cm^{-1} ;
- the O–H stretching vibration peaks intensity in the 3000-3600 cm^{-1} region decreased in the 3000-3400 cm^{-1} region and decreased in the 3400-3600 cm^{-1} .

The spectra acquired from the relevant soiled, unaged and aged, plaster-shellac6% areas (P5b and P7b) showed most of the peaks discussed above. Additional peaks, due to the soiling mixture are highlighted in *Table 5.16* and have not been assigned, as discussed before.

Table 5.16. FT-IR bands and relevant assignments of the spectra acquired from unsoiled (unaged P5e and aged P7e) and soiled (unaged P5b and aged P7b) areas of the plaster surface coated with shellac6% (2-1) at t₃₇.

FT-IR band [cm^{-1}]				Assignment
P5e	P5b	P7e	P7b	
			680	δ SO ₄
705	720	700-40	690-704	δ SO ₄ /v CH
767			720-60	δ CH
850-920	800		870-900	δ CH
	890			
	990	990	970	
1005	1005	1010-20	1005	v _{1s} SO
1060-90	1070	1040-80	1030-80	v _{as} SO
	1101			v _{as} SO
1217	1216	1224	1216-23	v SO/ v CH ₂
1248	1248	1245-55	1230-50	v SO/ v CH ₂
1264	1264	1262-70		v SO/ v CH ₂
1292	1296		1280	v SO/ v CH ₂
1340-90	1354	1312-1380	1305-50	v SO/ δ CH ₃
	1414		1410	
1456				δ_{as} CH ₂ and CH ₃
1530-90				v ₂ H ₂ O, v C-C
1632	1616	1632	1632	v ₂ H ₂ O, v C-C
	1648			
1660		1670		v ₂ H ₂ O, v C-C
	1695	1688	1690	v ₂ H ₂ O, v C-C
1712-30	1712	1721-35	1727-57	v CO
2120-2336	2110-2350	2110-2400	2120-2350	Overtone H ₂ O
2863-78	2862	2860 (vw)	2864	v _s CH ₂
	2912-27	2927 (vw)	2935	v _{as} CH ₂
2944-60		2960 (vw)	2952	v _{as} CH ₃
3120	3140-3230	3150-3360	3130-3380	v OH
3210				v OH
3250-3340	3300-75			v OH
3423-3500	3450-3520	3450	3440-3650	
3550-3650	3570-3660	3558		v OH
		3640		v OH
		3664		
		3703		
		3704		

vw= very weak.

Unaged and unsoiled shellac18% on gypsum plaster substrate (*Table 5.17*) is characterised by the following bands:

- between 680 and 752 cm^{-1} a duplet or a band centred at 704 cm^{-1} , due to SO_4 vibrations and CH vibrations and out-of-plane bending;
- a broad band between 980-1090 cm^{-1} possibly associated at the gypsum peaks at 1005 and 1105 cm^{-1} and the 1032 cm^{-1} of the COC vibration of shellac;
- in the 1200-1300 cm^{-1} , the broad band, duplet or triplet is due to β OH of aliphatic carboxyl and hydroxyl groups, overlapped with ν CO of $-\text{COOR}$ and with the S-O vibration as discussed for the plaster substrate;
- unresolved peaks at 1361-75 (δ_s of CH_3) and 1413-54 cm^{-1} (δ_{as} of CH_2 and CH_3);
- peak at 1615, 1660 and 1695 cm^{-1} are related to the duplet assigned to the vibrations in the water molecule and related to the presence of the sulfate and also due to the contribution of the C-C stretching band and the C=O stretching band of the $-\text{COOH}$;
- contributions at 1744 and 1760-75 cm^{-1} the aliphatic hydroxy acids and the complex mixture of mono and polyesters respectively;
- gypsum plaster overtones in the 2100-2350 cm^{-1} area can be seen and are due to the combination of bending and vibration modes of H_2O ($\nu_1 + \nu_3$ and $2\nu_3$)
- 2800-3100 cm^{-1} C-H stretching bands, particularly at 2863-79 and 2927-44 cm^{-1} (CH_3 and CH_2 vibrations, respectively);
- 3200-3600 cm^{-1} wide and numerous O-H stretching bands.

Very few differences can be noticed between the unaged (P5f) and aged (P7f) unsoiled areas coated with shellac18% (2-2). Particularly in the 1600-1800 cm^{-1} after ageing an increment in the 1680-1750 cm^{-1} can be seen and in the overtones region the 2360 cm^{-1} becomes sharp and more intense and another at 2390 cm^{-1} arises. Whilst the 2800-3100 cm^{-1} C-H stretching bands are slightly weaker in the aged areas, the O-H stretching bands in the 3200-3600 cm^{-1} region are much more intense and a distinct, sharp band arises at 3776 cm^{-1} .

The spectra acquired from the relevant soiled, unaged and aged, plaster-shellac18% areas (P5c and P7c) showed most of the peaks discussed above. Additional peaks, due to the soiling mixture are highlighted in *Table 5.17* and have not been assigned, as discussed before.

Table 5.17. FT-IR bands and relevant assignments of the spectra acquired from unsoiled (unaged P5f and aged P7f) and soiled (unaged P5c and aged P7c) areas of the plaster surface coated with shellac18% (2-2) at t_{37} .

FT-IR band [cm^{-1}]				Assignment
P5f	P5c	P7f	P7c	
688				δ SO ₄
704	704-720		700-70	δ SO ₄ /v CH
752	760	750-830		δ CH
	867			
980-1040	980-1050	975-90	990	ν_{1s} SO
1090	1070	1055	1060-95	ν_{as} SO
	1101			ν_{as} SO
1216	1218	1223	1224	ν SO/ ν CH ₂
1248	1235	1240	1232-48	ν SO/ ν CH ₂
1278	1264	1264		ν SO/ ν CH ₂
	1294	1280	1305	ν SO/ ν CH ₂
1361-75	1328-44	1327	1336-1344	δ_s CH ₃
1413	1410-90		1414	δ_{as} CH ₂ and CH ₃
	1550			
1615	1632	1629	1623-40	ν_2 H ₂ O, ν C-C
1660		1660		ν_2 H ₂ O, ν C-C
1695		1690		ν_2 H ₂ O, ν C-C
1744	1712	1704-27	1720-44	ν CO
1760-75	1745			ν CO
2100-2350	2100-2360	2120-2450	2120-2400	Overtone H ₂ O
2863-79	2850-95	2860	2857	ν_s CH ₂
2927-44	2920-44	2927-44	2919-50	ν_{as} CH ₃
3050-3245	3130-3350	3160-3700	3050-3400	ν OH
3490-3670	3440-3710		3440-3710	ν OH
		3776	3776	ν OH

5.3.5.6. Plaster plates coated with barite

Consistently with the mentioned literature (Derrick *et al.*, 2000), Table 5.18 shows that the plaster-barite^{20°} surfaces, unsoiled and unaged (P9e), are characterised by FT-IR absorption of barium sulfate. The small contribution in the 1550-1600 cm^{-1} range is possibly due to diffuse reflectance distortion or contamination. The only significant change upon ageing of the plaster-barite unsoiled surfaces is that the absorption in the 1000-1300 cm^{-1} is relevantly weaker. As for the soiled sections, changes can be observed in the intensities in some of the FT-IR spectra bands and a few additional absorptions contributes due to the soiling mixture and highlighted in Table 5.18.

5.3.5.7. Plaster plates coated with beeswax

In the plaster-beeswax unaged and aged control sections, a complex range of peaks can be observed, including the characteristic IR absorption bands of beeswax described in the literature (Derrick *et al.*, 2000; Regert *et al.*, 2001) and the peaks assigned to the plaster substrate. The regions in which the absorptions are observed are consistent throughout the control samples, but the position of the individual peaks varies. FT-IR characteristic

absorption bands of the plaster surfaces coated with linseed oil, shellac, barite and beeswax are overall located in the regions identified for the control sections, as suggested by the sources. The full range of spectra can be seen in *Appendix 9* and the database (Risdonne & Theodorakopoulos, 2021). Overall, the peaks characteristic of gypsum plaster, the coating (linseed oil, shellac or barite) and beeswax, described above and in the previous sections, were detected in the FT-IR spectra of the unsoiled, unaged sections. The relevant aged section shows overall the same pattern, although a few bands are slightly shifted. The FT-IR spectra of the soiled sections linseed oil-beeswax show a few additional peaks and an overall decrease of intensity in the 3100-3600 cm^{-1} region. The aged sections shellac-beeswax show overall the same pattern, although a few bands are slightly shifted and there is a significant decrease of intensity in the 700-1600 cm^{-1} and 3200-3400 cm^{-1} regions and characteristic peaks at 3705 and 3776 cm^{-1} ; an increase of intensity in the 700-1000 cm^{-1} region was observed in the relevant soiled sections. The aged sections barite-beeswax also show the characteristic peaks at 3705 and 3776 cm^{-1} .

Table 5.18. FT-IR bands and relevant assignments of the spectra acquired from unsoiled (unaged P9e,f and aged P11e,f) and soiled (unaged P9b,c and aged P11b,7c) areas of the plaster surface coated with barite20° (3-1) and barite60° (3-2) at t_{37} .

FT-IR band [cm^{-1}]								Assignment
P9e	P9b	P11e	P11b	P9f	P9c	P11f	P11c	
		760-80	767	780-800		775	760-80	δ SO ₄
			790-830	830-40			825-80	δ SO ₄
887	890	880		890	890	857-80		ν_{1s} SO
				920-50		927-52	920-60	
995	960	944-	980-	990-	990-	975-95		ν_{1s} SO
		1030	1000	1030	1020			
	1090-	1095	1095			1123	1155	ν_{as} SO
	1120							
1160-8	1150-60	1170-80	1136-75	1175	1173	1160-70	1175-90	ν_{as} SO
1190-	1190-	1200-24	1200-20	1190-	1200	1200-10	1210-24	ν_{as} SO
1213	1200			1200				
					1216-32	1255-80	1240-60	ν_{as} SO
				1275-95	1288			ν_{as} SO
	1340	1450-	1424-	1476	1500	1440	1415-25	
		1500	1500					
	1520-50	1530	1530-50	1530	1536-50	1490-	1470-90	
						1520		
1552-68				1560		1545-60	1535	
1593-	1560-	1560-	1592	1582		1570-90	1590	
1600	1600	1600						
1622-40	1624-40	1624-32	1610-40	1610-30	1610-25	1610-40	1615-50	ν_3 SO, ν_2 H ₂ O
1680-	1665-80	1688-	1664-	1650-90	1663-80	1663-	1665-80	ν_2 H ₂ O
1710		1711	1712			1700		
	1714			1727			1750	
				1790		1790	1790	
2100-	2120-	2100-	2100-	2100-	2100-	2100-	2100-	Overtone H ₂ O
2300	2290	2300	2300	2300	2300	2300	2300	
2336	2340	2345	2336	2340	2336	2336	2336	Overtone H ₂ O
2360	2360	2360	2360	2360	2360	2360	2360	
		2500	2520	2510	2500	2500	2500	
3200-	3150-	3150-	3150-	3070-	3200-	3100-	3100-	ν OH
3400	3400	3400	3400	3400	3400	3450	3450	
3575-	3520-	3450-	3450-	3500-	3480-	3490-	3490-	ν OH
3690	3650	3660	3660	3664	3665	3650	3650	
3720	3710	3705	3700	3705	3700	3705	3705	ν OH
3776	3776	3776	3776	3778	3776	3776	3776	ν OH

5.4. CONSIDERATIONS ON ACCELERATED AGEING

Accelerated ageing methods have proven effective and are particularly popular in research in fields such as coating engineering and food science, however, their application in cultural heritage science is challenging. In this study, to approximate the natural ageing of the surface of the objects displayed in the casts courts for 150 years, coated plaster surfaces should be aged in the thermal chamber and light chamber described in *Section 5.2.3* for a time given by the acceleration factors (*Section 2.4.1*).

The model is imperfect, and, without a strong background set of reference data, it is built on simplifications. Ideally, the chemical, physical and mechanical properties of the materials used in coatings and their interaction with the substrate should be also considered.

It is impossible to obtain acceleration factors high enough to perform such experiments in a reasonable time, as demonstrated in *Appendix 8*, without performing extreme conditions in the chamber, which would then initiate reactions that did not happen on the naturally aged surfaces (Feller, 1994). Based on the considerations outlined in *Section 2.4.1*, the simplified physical model detailed in *Appendix 8* and the equipment characteristics described in *Section 5.2.3*, it has been calculated that to perform 150 years of thermal ageing, under the discussed conditions, it would be necessary to keep the thermal chamber from 4.04 to 27.78 years, corresponding to the higher and lower acceleration factor, respectively.

By basing the calculation on the simplified model and working backwards it is possible to calculate that 90389 minutes (62 days, 18 hours, 29 minutes) of accelerated ageing corresponded to about 1278982 minutes (888 days, 4 hours, 22 minutes) of ageing if we select a mid-value of 110 kJ/mol for the activation energy, but ensuring at least 487989 minutes (338 days 21 hours 9 minutes) of ageing when we assume that the activation energy is equal to a minimum value of 70 kJ/mol (Risdonne & Theodorakopoulos, 2021). To achieve a 150-year ageing, it would be necessary to keep samples in the Q-Sun Chamber for 58.34 years (*Appendix 8*).

To mediate the experimental time available and also to achieve changes onto the plaster-coating surfaces, the light accelerated ageing of 40357 min (28 days, 0 hours, 37 minutes) was therefore performed, corresponding to 71 days, 20 hours, 39 minutes of irradiation in the real case scenario, according to the theoretical model discussed in *Chapter 2* and *Appendix 8*. Despite the impossibility of reproducing the thermal and light ageing of the plaster-coating surfaces aged for 150 years, it is believed that the purpose of obtaining the drying of the surfaces and the coatings, as well as changes on the surface, was achieved.

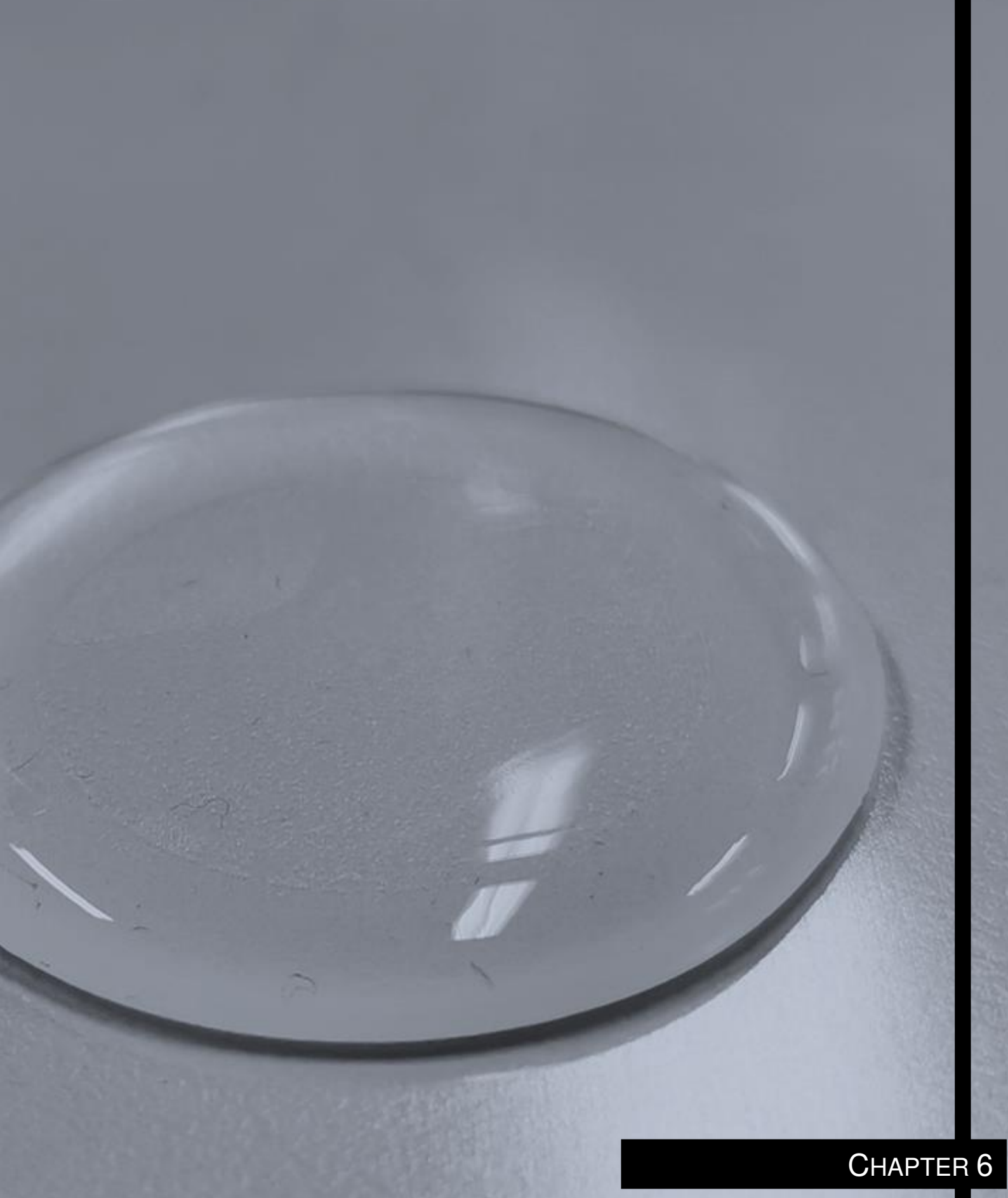
Given the limits of recreating long ageing times in the laboratory, it appears clear that the only viable method for future studies would be to extrapolate the data beyond the time limits,

such as is nowadays pursued with predictive analytics methods. This approach was beyond the scope of this study, but it would surely provide new perspectives in future studies on the degradation of cultural heritage materials. The additional challenge given by the complexity of the composition of the samples, will require extensive analytical research and can be intimidating, but can be overcome and it is necessary for the advancement in the accelerated ageing application in cultural heritage studies.

5.5. CONCLUSION

In this chapter, **objectives 6, 7 and 9** (*Section 1.5.4*) were addressed. By reconstructing a few selected plausible stratigraphies for nineteenth-century plaster casts, based on the historical literature and analysis of the V&A casts, it was possible to compare coated and uncoated plaster surfaces before and after ageing and observe changes in the appearance, colour, and texture, and also in the molecular structure of the plaster-coating (and optionally dust) system. Twelve plaster mock-up plates were selectively coated with linseed oil, shellac, or barite water. An additional beeswax coating was applied to add to the stratigraphy the option of later treatments. The resulting coated plaster mock-ups were accelerated aged and artificial soiled, and their appearance and physicochemical condition was evaluated. Visual assessment was possible via visual evaluation according to EN ISO 4628-1, Visible light (vis) and Ultraviolet Fluorescence (UVf) photography, scanning electron microscopy (SEM), colourimetry, glossimetry, goniometry and high resolution (HR) 3D surface measurements. Gravimetry was undertaken to assess the water loss during the experiments and Fourier-Transform Infrared spectroscopy (FT-IR) allowed to define ageing-induced molecular changes. During the drying of the plaster plates, most of the water was lost within the first 12 days when the plaster dried out and the water either evaporated or reacted with the powdered gypsum to grow the plaster structure. Small weight increments were observed after the application of the coating(s) and the artificial soiling, followed by a gradual and relatively slow loss of weight, related to the drying of the coating(s). The uncoated plaster surfaces showed little changes after ageing, including an increased presence of pores in the aged areas, possibly due to increased drying, and a small increase of gloss. The FT-IR pattern of the uncoated plaster is consistent with the scientific literature and most of the FT-IR peaks characteristic of gypsum plaster are present (*Section 5.3.5.1*). Plaster surfaces coated with linseed oil were slightly discoloured after accelerated ageing, for both the unsoiled and soiled sections. These surfaces fluoresced bright light-blue before ageing and the fluorescence almost disappeared for the raw linseed oil after ageing. The molecular structure of gypsum plaster and linseed oil were identified in the FT-IR spectra and small shifts and changes in intensity were observed after ageing. The symmetric and asymmetric C–H stretching vibrations became extremely weak after ageing for the raw linseed oil. The FT-IR pattern of the boiled linseed oil showed more stability to ageing in the boiled linseed oil than in the raw oil (*Section 5.3.5.4*). Shellac resin visible colour discoloured after accelerated ageing and the light-blue fluorescence dulled. After ageing, whilst the FT-IR C–H stretching bands were slightly weaker, the -OH stretching bands were much more intense and a distinct, sharp hydroxyl band arose (*Section 5.3.5.5*). Given these observations and because there have not been previous studies on these phenomena in shellac-coated plaster surfaces, further studies are required to address the reduction in C–H stretching vibration frequencies. Barite coatings slightly ‘bleached’ after accelerated

ageing, possibly due to the BaSO_4 deposition upon drying. The mineral structure of barite was observed in the BSE images, suggesting that the chemical structure of the surface was indeed modified by the barite solution, as suggested by the literature. Linseed oil and shellac did not form a solid film onto the plaster surface but penetrated and filled the pores, whereas beeswax formed a coherent film. Upon ageing, the colour of the soiled section coated with beeswax faded to some extent and the brush marks observed in the unaged section are less noticeable. Overall, the peaks characteristic of gypsum plaster, the coating (linseed oil, shellac or barite) and beeswax were all observed in the FT-IR spectra of the unsoiled, unaged sections (*Section 5.3.5*). The relevant aged section showed the same pattern, although a few bands were slightly shifted.



CHAPTER 6

SURFACE RECONSTRUCTIONS

PART 2: CLEANING

6.1. INTRODUCTION

Conservation of casts is challenging due to the nature of the material, which is vulnerable and porous, sensitive to moisture and prone to mechanical damage and absorbing dirt and humidity. There are several characteristics of the plaster objects that may affect their condition and conservation:

- the characteristic porosity of plaster is dependent on the water-to-plaster ratio during the making of the plaster (*Section 4.1.3*). Reducing the amount of water shortens the setting time and the period of plasticity (Barclay, 2002). The higher the temperature of calcination and the less water is added, the denser and the less porous is the resulting crystal structure (Turco, 1990). An inhomogeneous mix, trapped air, or excess water in a mould can create areas of varying porosity within a cast. The porosity of the cast also constitutes an 'open window' for damaging external factors such as dust and stains that, once in the pores, are difficult to remove as often deeply embedded within the intercrystallite spaces of the material (Barclay, 2002; Beale *et al.*, 1977; Wolbers & Little, 2007). Aged plaster is softer and much more open-pored than a newly-cast surface;
- plaster is naturally absorbent, because of its porosity (Chaney, 1973). The water-absorbing behaviour (WAB) and the pore size distribution can be indicative of its sensitivity to water determining its propensity to future deterioration (Vandevoorde *et al.*, 2012, 2013). Absorbed water from the air can freeze and expand, leading to weakening and pulverising the plaster as well as causing loss of coatings if present (Freire-Lista *et al.*, 2015). Mould, surface grime or stains can be also carried deeper into the bulk by humidity and many liquid cleaning methods (Perusini *et al.*, 2009). Because water is so easily absorbed, dirt or other contaminants dissolved in the water will be readily and irreversibly migrated into the plaster;
- plaster is soluble in water by 2.41 g/L. Water allowed into the plaster pores will cause softening and the solubilisation of salts. Thus, soaking or washing plasters in water upon conservation treatments should only be reserved for extreme circumstances where non-aqueous treatments have failed or were inappropriate (Isella *et al.*, 2017). Gypsum plaster always contains rock salt (sodium chloride) or other water-soluble sulfates;
- the mechanical properties of plaster casts are also very important. The solidity of the hardened mass depends on the felting of the crystals (less or greater according to the amount of water used for the mix) (Chaney, 1973; Turco, 1990). The excess water

evaporating leaves voids or pores and it is the porosity in the mass that results in a weak structure. The compressive resistance of properly baked plaster is approximately 8.5 kg/cm² when gauged with neat water, and approximately 11.5 kg/cm² when gauged with lime water (Chaney, 1973; Turco, 1990). The strength of cast plaster is reduced because of its solubility in water (Millar, 1899). The soft nature of the plaster means that treatments to seal the surface are very important.

6.1.1. CLEANING PLASTER CASTS

Cleaning is one of the most delicate, complex and high-risk treatments in conservation, which is dependent on the compatibility of the treatment materials with the surface and bulk layers of the object. An ideal approach to conservation cleaning would start with the analysis of the object to understand the materials used to create it, and the nature of the soiling or the contaminants on the surface (Wolbers & Little, 2007). This information aids in designing a compatible system to be used in the treatment. Before any action to prevent or remedy the deterioration of the substrate can be taken, it is necessary to understand the properties of the object's materials and what is causing deterioration. Conservation has been for a long time an empirical process rather than a scientific practice. Conservators and restorers had to face conservation issues by relying on their skill, intuition, and creativity, using a "trial and error" approach. Today there are progressively more conservation workshops that take advantage of the progress that science and technology made in the second half of the twentieth century (Baglioni & Chelazzi, 2013). The characteristics of the plaster surfaces make the approach to the conservation of casts particularly challenging. Conservation treatments including surface cleaning, consolidation and impregnation, mending, repairs and filling are constantly under review by the conservators that approach these objects. Being the focus of this research on the coated surfaces of the Victorian casts, special attention is herein given to surface cleaning.

There is not a single method of treatment universally adopted and recommended for cleaning uncoated and coated plaster surfaces. Determining whether a cast has a finishing layer applied is particularly important, as the coating can change the properties of the surface, as shown in *Section 5.3*. The variability of the coatings (*Section 3.2*) leads to the wide range of methods for the cleaning of plaster objects surfaces, both painted and unpainted (André, 1977; Barclay, 2002; Beale *et al.*, 1977; Wolbers & Little, 2007). Several authors have emphasized the damage that can be caused by cleaning: loss of surface, staining, deposition of soluble salts, or making the stone more vulnerable to pollutants or biological growths (Andrew *et al.*, 1994; MacDonald *et al.*, 1992; Maxwell, 1992; Young & Urquhart, 1992). Bare plaster is particularly sensitive to surface treatments: while water could be effective in cleaning a plaster surface, it should be used sparingly as it could

damage the plaster. Interaction with water will create tide lines and staining to the surface of plaster due to its porosity and hygroscopicity. Before cleaning coated plaster casts, it is important to consider whether the surface layers must be preserved or removed. The decision would be depended on the historical meaning and the condition of these layers. Generally, plaster objects with a coating present fewer problems as they are often more durable than uncoated ones (Barclay, 2002). However, the deterioration of the coating could be an issue, especially if it caused a change in the appearance of the surface and it is difficult to remove as diffused in the plaster. From a morphological point of view, the original surface may be present under a layer of soot or black crust. From the chemical perspective, the surface cannot be considered original, having undergone a series of changes as the surface equilibrates with its varying environment (Smith *et al.*, 2008; Vergès-Belmin, 1996).

Traditional methods for cleaning plaster casts often suggest washing off dirt with clear running water and soft rubbing with brushes or sponges (Clérin, 1988; Rathgen, 2013). Badde in Graepler & Ruppel (2019) reports on the reinstallation and preventive conservation plans on the plaster cast busts in the Rococo Hall of the Duchess Anna Amalia Library in Weimar. In this case, previous conservation strategies consisted of the subsequent overpainting of the soiled surfaces, whereas more recently the casts were cleaned with a vacuum cleaner and soft brushes. Hast in Graepler & Ruppel (2019) reports the recent cleaning project of the casts in the Ny Carlsberg Glyptotek in Copenhagen. The treatment history suggested a range of procedures, including dusting, cleaning with a dust sponge, applying magnesium oxide pastes, or even hiding an unpleasant dirty or damaged plaster surface with an overcoat of shellac resin or paint. The total immersion of the plaster object in water for a few hours, until the plaster is fully soaked, is another method reported, but it is rarely found advocated (Clérin, 1988). Casts that received such a treatment would be heavily compromised by the formation of efflorescence and loss of cohesion of the bulk of the plaster casts. Beale *et al.* (1977) also suggest that, since plaster is very absorbent and one does not want to drive a softened or dissolved coating material into the surface of a porous plaster, care must be taken to remove the coating so that it will not be "soaked in".

Graen in Graepler & Ruppel (2019) refers that during the restoration campaign, after 1996, of the Jena plaster casts, different cleaning methods and substances were in use, including laponite, natural rubber and milk. The dry removal of dirt films has been suggested by way of sanding (Rathgen, 2013). Thorough cleaning of the surface through the use of different kinds of rubbers and micro sandblasting with very fine abrasives is also found in the literature (Pelosi *et al.*, 2013). According to Isella *et al.* (2017) a dry cleaning on a decayed gypsum surface, using synthetic rubber or a sponge, kneads the soiling onto the gypsum matrix. This is a drawback because it produces an uneven cleaning level, which gives the impression of a stained surface.

Laser cleaning is routine for several applications (Dajnowski *et al.*, 2009). Lasers do not entail physical contact with the surface and therefore can lead to the cleaning of very delicate surfaces. There are no solvents or water to redistribute potentially harmful salts. Nd:YAG laser cleaning is a dry cleaning method that is currently under investigation for heavily soiled plaster, showing in many cases very positive results (Cerea *et al.*, 2017; Fodaro *et al.*, 2014; Pelosi *et al.*, 2013). Guidelines for the cleaning of plasterworks finished with intentional patinations are however unavailable. In Italy, Nd:YAG lasers have been used for the cleaning of plastered surfaces (Fratelli & Signorini, 2008) and described the case studies of the cleaning of the head of Ennio Mantegani (dated 1923), the façade of the Priorato di Sant'Orso in Aosta (1494-1506) and the sixteenth-century casts of Palazzo Grimani di Santa Maria Formosa in Venezia. Isella *et al.* (2017) report the same technique for the cleaning of the casts of the Flora Farnese, The Velletri Pallas and the Barberini Faun in the Academy of Fine Arts of Brera in Milan.

It appears that many treatments found in the literature were potentially damaging for the surface patina; these types of invasive approaches were possibly in practice due to the old undervaluation of casts. Turco (1990), for example, rates cleaning processes with increasing intensity: from rubbing with a mash of cold water and starch to rubbing as above with 5 wt% ammonia followed by rapid treatment with water and also cold brush washing with 10 wt% acetic acid bath. Cleaning has always been a high-risk task and taking no action at all is always one of the options to be considered. The types of material used and the interactions must always be taken into consideration (Bertasa *et al.*, 2017).

Poultice-cleaning techniques on plaster using paper pulp, methylcellulose thickened aqueous solutions, corn-starch pastes or other highly absorbent materials are designed to cause unwanted foreign material to be carried into the poultice material rather than into the plaster (Klosowska & Obarzanowski, 2010). For example, Uhlenhuth (1879) and Rathgen (2013) list an entire range of gel-like and paste systems, which are accounted for in plaster cleaning. Frederick (1899) reports that cleaning of the unpainted cast can be done using Milbane Paste (C. Hennecke Company, Milwaukee, Wis.) or a thick layer of warm starch, applied and peeled off. Conservator Rosanna Moradei described the cleaning procedure of a group of plaster casts through a general dusting with soft brushes and the following treatment with wood pulp followed by a dip in deionised water (Fratelli & Signorini, 2008). Formaldehyde was added to prevent the growth of moulds. The use of agar-agar pastes, employed in the same manner as starch pastes, is also frequently discussed in the relevant literature (Bertasa *et al.*, 2017; Cremonesi, 2013; Cremonesi & Casoli, 2017; Domínguez, 2013; Graepler & Ruppel, 2019; Guderzo & Lochman, 2017; Sansonetti *et al.*, 2012). Perusini *et al.* (2009) tested Agar and Laponite RD cleaning methods on plaster mock-ups and suggested that extra care should be taken concerning the water absorption. Parra in Graepler & Ruppel (2019) described the cleaning of the plaster casts at the Royal Academy

of Fine Arts of San Fernando with Anjusil[®], a latex-based material. The early collection of casts were used as teaching material for a long time and recently were restored and studied.

Gel technology for art conservation, introduced in the 1980s (Wolbers, 2000), is now established as a means to provide enhanced control and sufficient monitoring of cleaning treatments (Baglioni & Chelazzi, 2013). Aiming to achieve improved control of the liquid that interacts with the plaster surfaces, it is hereby assessed the efficacy of a novel cleaning method developed by Theodorakopoulos and Jonas (Freese *et al.*, 2020; Mateescu *et al.*, 2017), which consists of thin acrylamide-based polymer networks that are covalently bonded to flexible polyolefin sheets. The perspective of applying novel thin surface-attached might allow exploring the action of sub-micron water application on the sensitive surfaces.

6.1.2. POLYOLEFIN-SUPPORTED HYDROGELS

The choice of surface-attached hydrogels for the cleaning of plaster cast mock-ups was based on several appealing characteristics of these materials, which might help to overcome the limitations given by the properties of the plaster surfaces. Due to the plaster water-absorbing behaviour (WAB) and its solubility in water, the technique was selected because it maximises the cleaning efficacy while it minimises the liquid exposure of the treated surfaces as well as the time of the gel action on the surface (Mateescu *et al.*, 2017). Surface-attached gels are based on covalently bonded polymer networks on solid substrates to yield a robust gel film. By anchoring the polymer network to a substrate, the mechanical stability of these gels is substantially increased and handling is greatly improved. Photo-crosslinked polymer networks are prepared from polyacrylamide (PAM) and N-(4-benzoylphenyl) acrylamide copolymerised with acrylates and methacrylates of polyethoxylated (PEO) surfactants on corona-treated PE sheets. The PE-supported copolymer networks can be swollen with aqueous solutions to form sub-micron-thin hydrogel films. The swelling behaviour is strongly determined by the crosslink density of the network and anchor density of the surface attachment, specifically for very thin films in the micrometre range. Surface-attached hydrogels combine the robust network architecture of 3D bulk polysaccharide gels, with the high surface-to-volume ratio of microgels, allowing rapid water and solute exchange between the gel matrix and the surrounding medium. The thin-film format provides full control over the amount of water into the gel matrix upon swelling, that can be released from such a layer system, which is considerably less compared to bulk gels. The PAM layer serves as a liquid reservoir. Surface contaminants and soiling are mobilized and solvated by the liquid from the hydrogel, dissolved species diffuse into the swollen polymer network, while mobilized soil particles stick to the hydrogel surface (Mateescu *et al.*, 2017). With the removal of the PE-PAM sheet in the final process step, these entities are withdrawn from the surface. Released soils that are pulled on the

surface upon application remain unbound and can be readily removed by gently rolling a dry cotton swab after the peeling off of the PE-PAM film. In this chapter, the cleaning efficacy of PE-PAM hydrogel systems is evaluated on plaster coated surfaces reconstructions. The method was designed to test the potentialities of the PE-PAM hydrogel systems on plaster surfaces; if the films would be proven effective on the reconstruction, further testing would be recommended to take into account the practicalities of the use of these materials for the removal of soils on historical plaster casts.

6.2. EXPERIMENTAL METHOD

6.2.1. CLEANING METHOD

6.2.1.1. pH and conductivity measurements

pH and conductivity (σ) of the unaged and aged plaster surfaces were measured by the use of agarose swollen in Deionised (DI) water, Horiba LAQUA twin compact pH meter (LAQUA twin -pH-22, accuracy ± 0.1 pH) and Horiba LAQUA twin compact conductivity meter (LAQUA twin-EC-22, accuracy $\pm 2\%$).

The procedure for preparing agarose gels started by mixing 1 g of Gensieve LE agarose powder (cat no. H19365) and 50 ml of DI water (pH= 7.4, T= 18.3°C, σ = 0.007 mS/cm) (Sansonetti *et al.*, 2012). The solution was microwaved at high heat for 30 s, stirred and heated 4 more times for 10 s. After cooling, the solution was heated for 20 s. The agarose solution was then poured on a silicon mould, aiming to obtain a disk shape (A in *Figure 6.1*). For every pH and conductivity measurement, an agarose gel plug (B in *Figure 6.1*) was cut with a 2.5 mm specimen puncher and left on the surface of the coated plaster mock-ups (C in *Figure 6.1*). After 2 minutes the gel plug was taken with the aid of tweezers and placed in the pH and conductivity meters for the measurements.

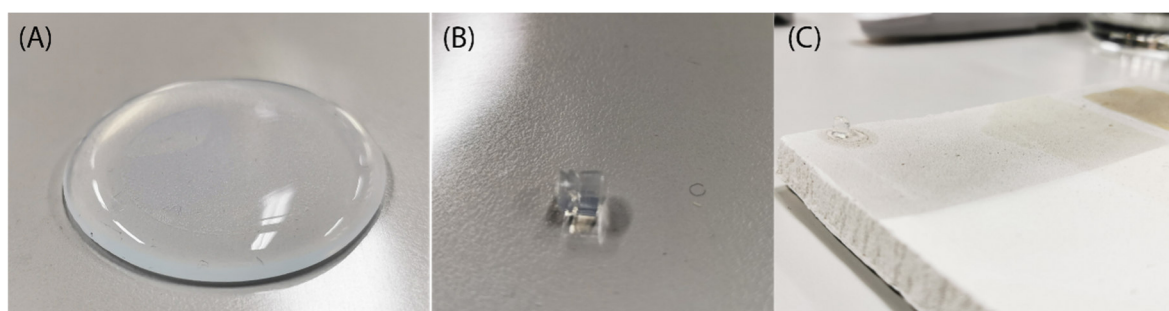


Figure 6.1. The disk made of agarose (A) was cut into plugs (B) to measure the pH and conductivity of the surfaces (C).

6.2.1.2. The solutions

Solutions were prepared with the following materials: DI water (pH 7.4, 18.3 °C, 0.007 mS/cm); Sigma-Aldrich triethanolamine (TEA, CAS-No. 102-71-6), $C_6H_{15}NO_3$, sodium hydroxide (CAS-No. 1310-73-2), NaOH, citric acid (CAS-No. 77-92-9), $HOC(COOH)(CH_2COOH)_2$ and Ethylenediaminetetraacetic acid (CAS-No. 60-00-4), $(HO_2CCH_2)_2NCH_2CH_2N(CH_2CO_2H)_2$; VWR Chemicals BDH 100% glacial acetic acid (27013AU), CH_3COOH ; Honeywell Fluka™ concentrate hydrochloric acid (for 1 L standard

solution, 1.0 M HCl, CAS-No. 7647-01-0); Fisher Chemical methylated spirit (IDA 99), 99% (v/v), Pure, (Industrial Methylated Spirit, IMS, CAS-No. 64-17-5). *Table 6.1* shows the solutions prepared for swelling the surface attached gels.

Table 6.1. The solutions prepared for the tests.

Sol	Composition	pH*	σ [mS/cm]**
A	50 mL Di water 0.75 mL of TEA 1M acetic acid until pH stabilises at 8	8	1.04
B	50 mL Di water 0.75 mL of TEA 1M acetic acid until pH stabilises at 8.5	8.5	0.75
C	50 mL Di water 2.5 mL of TEA 1M hydrochloric acid	9	1.78
D	50 mL Di water 0.85 mL concentrated hydrochloric acid TEA to stabilise at pH 6	6	29.80
E	50 mL Di water 0.25 mL glacial acetic acid 1M sodium hydroxide to stabilise at pH 5.5	5.5	4.08
F	50 mL Di water 0.25 mL concentrated acetic acid 1M sodium hydroxide to stabilise at pH 5	5	3.36
G	50 mL Di water 1 g citric acid TEA to stabilise at pH 8	8	8.45
H	50 mL Di water 1 g EDTA 1M sodium hydroxide to stabilise at pH 8.5	8.5	9.84
I	15 mL Di water 35 mL IMS	6.5	0.005

* accuracy ± 0.1 ; ** accuracy $\pm 2\%$.

6.2.1.3. Cleaning tests

Preliminary tests allowed to choose the type of PAM to use and the solution to be used for the different areas of the plates, as also related to the pH and conductivity measurements. To choose the appropriate solution, preliminary tests were carried by dipping a cotton swab in a solution appropriate for the surface according to the pH values and rubbing it on a side of the area examined (A in *Figure 6.2*). Two types of PE-PAM hydrogels were available: PAM₁₅ and PAM_{E3-15}. '15' refers to the 15 min time of the UV exposure necessary for the PAM network to cross-link (Freese *et al.*, 2020; Mateescu *et al.*, 2017). The only difference between the two types is that the PAM_{15-E3} network contains E3 ECOSURF™ LF surfactant (*ECOSURF™ LF Specialty Surfactants*, 2012) that was copolymerised with polyacrylamide. To decide between the two hydrogels, preliminary test areas were performed on P1a (UA, S, plaster surface) and P1c (UA, S, boiled linseed oil coated plaster surface) and the

relevant aged sections P3a and P3c. The PE-PAM films were cut into 0.5 cm squares (B in Figure 6.2). The cut films were dipped into the solution. The excess of the free-running solution was wiped from the side of the PE backing so that only the solution that swelled the PAM film was applied onto the coated plaster substrate. Preliminary tests that relied on visual assessment of the cleaning efficacy led to the final choice of the solution and the PAM systems. To assess whether the PE-PAM needed to include the co-polymerised surfactant (E3) or not, small sections (0.5x0.5 cm) of PE were cut, dipped in a chosen solution (Sol B) and tested on P3a and P3c (Figure 6.2).

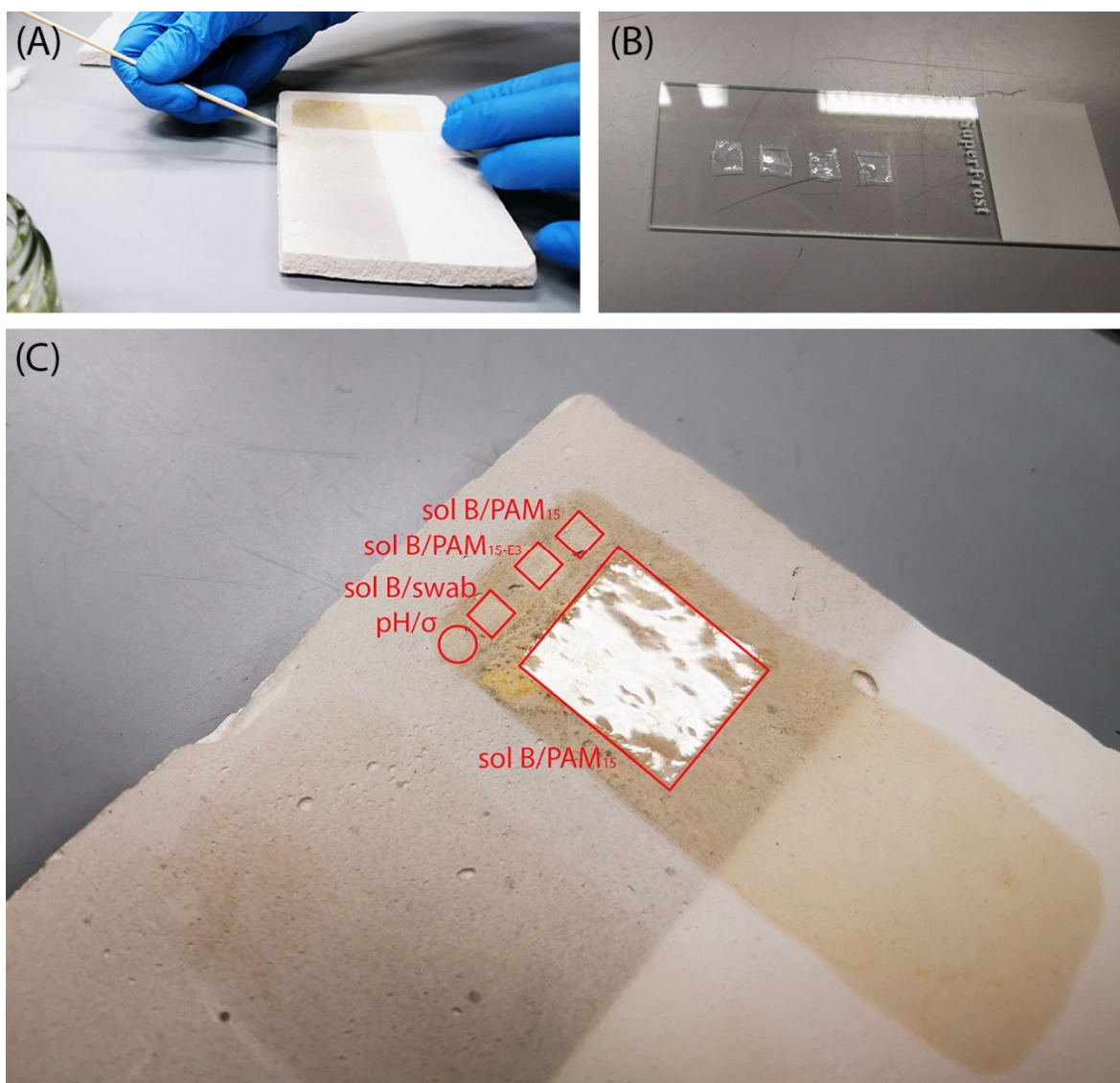


Figure 6.2. Preliminary tests to choose the solution were undertaken with the aid of a swab (A) and small cuts (0.5x0.5 cm) of the PE (B). For example, in P3c (C), it can be seen the areas where the pH and conductivity (σ) measurements were taken, the areas where sol B was used with a cotton swab, with PAM_{15-E3} and PAM₁₅. The test area (2x2 cm) was cleaned with sol B and PAM₁₅.

As no differences were observed between the two tested areas, the PAM films without the copolymerised surfactant were selected. Further preliminary tests were undertaken with a cotton swab and the efficacy of the different solutions was visually assessed. Accurate cleaning tests to larger test areas of 4 cm² (square 2x2 cm) were carried out with the selected PAM-solution systems (C in *Figure 6.2*). The size of the PE-PAM gels cuts was decided to allow a comparable surface coverage that would fit into the coated, soiled section. After 1 minute of contact, the PE-PAM films were removed from the surface and the dissociated soil particles were removed by gently rolling a dry cotton swab on the surface. To assess the cleaning efficacy of the PE-PAM systems, one application was carried out.

6.2.2. EVALUATION OF THE CLEANING EFFICACY

Evaluation of the cleaning efficacy was carried out visually according to EN ISO 4628-1 (*Section 5.2.2.2*), Visible light (Vis) and Ultraviolet Fluorescence (UVf) imaging, scanning electron microscopy (SEM), colourimetry, glossimetry and high-resolution (HR) 3D surface measurements. Fourier-Transform Infrared spectroscopy (FT-IR) was undertaken to define whether the removal of the soil can be appreciated through molecular changes. Instrumentation is detailed in *Sections 5.2.7 to 5.2.13*.

6.2.3. DATABASE FORMATION

A database of results in Microsoft Excel format was compiled and deposited in the Northumbria University Figshare repository, to make the research outputs available in a citable, shareable and discoverable manner (Risdonne & Theodorakopoulos, 2021).

6.3. RESULTS AND DISCUSSION

Liquid-based cleaning methods that operate with the direct application of the liquid onto the surfaces, such as by the use of cotton swabs, do not allow an accurate dosage of the amount of liquid applied. A minimal wetting would mean that the disadvantages of liquid-based cleaning would be critically reduced if not eliminated (Angelova *et al.*, 2016; Domingues *et al.*, 2013; Domínguez, 2013; Wolbers, 2000). This property has been researched in many studies designed for the development of novel cleaning techniques, but it is still under investigation. Angelova *et al.* (2016) for example, argue that the water uptake in young and aged acrylic emulsion paints, evaluated by NMR relaxometry, during exposure to a range of thickened and gelled cleaning treatments (agar gels – 1 and 4 wt% -, methylcellulose, Pemulen-TR2 gel, polyvinyl acetate borax gels) is more or equal to the one measured after swab cleaning. In this research, it was highlighted that the main advantage to agar is reduced mechanical action relative to swab cleaning and that this advantage is somewhat lost if a follow-ups swab-clearance step is necessary to remove surface grime dissolved by the agar gel or to remove chelating agents delivered to the surface by the gel. Furthermore, agar gels are commonly applied as brushed-on warm solutions which may result in a larger release of water to the paint surface, softening of the paint, and softening and melting of the surfactants. The results of this work raised questions on the use of gels on water-absorbent surfaces, but more should be investigated on the topic.

One of the advantages of the use of the PE-PMA is the small quantity of liquid interacting with the surface, which seems appealing for the cleaning of water-sensitive surfaces such as gypsum plaster. Water load studies showed 0.005–0.05 mL/cm² uptake for tested PE-PAM hydrogels (Mateescu *et al.*, 2017). The copolymerised polyethoxylated surfactant in the PAM films almost doubled the water uptake, but still, the results provide a very selective method. The negligible liquid, despite maximising the solubilisation effects due to the advanced architecture of the surface attached gels, eliminates the time for the solution to be diffused into the bulk since diffusion competes with evaporation. Therefore, this method combines the advantages of dry-cleaning methods, such as UV pulsed lasers (Theodorakopoulos & Zafirooulos, 2009), nano-technology (Baglioni & Chelazzi, 2013) and aqueous cleaning (Wolbers, 2000). Since all surfactants are copolymerised there are no post-cleaning residues of the polymer network and the surfactant.

The efficacy of the selected surface cleaning method was evaluated by comparing the characteristics of the soiled plaster surfaces (a, b, c in *Figure 5.3*) before and after the cleaning with the PE-PMA hydrogels.

6.3.1. pH, CONDUCTIVITY AND PRELIMINARY TESTS

Among the various types of cleaning techniques – mechanical, physical, chemical and optical methods – the approach based on the use of pure or mixed solvents has played and continues to play a very important role. To be compatible with hydrogels the selected cleaning solution must be aqueous. Besides the nature of the solute and of the solvent, which determines the intermolecular interactions, other factors can affect the solubility of a material in a certain solvent. These are temperature, pressure, presence of electrolytes, the physical state of the solute, the formation of complexes, and other chemical reactions (Cremonesi, 1999, 2004).

When dealing with the cleaning of artistic or architectural surfaces the aim is to remove soil and dirt from the artefact, by using solvents or aqueous solutions that can solubilize the “unwanted” molecules from their solid aggregation state without affecting the original materials. This is the basis for the term “selective cleaning” (Cremonesi, 2004). For an accurate approach to surface cleaning, conductivity and pH measurements are the fundamentals for determining the characteristics of the surface and the appropriate solution. The pH of the surface indicates at which pH a solution can swell and/or dissolve the surface and the soiling (Cremonesi, 1999; Wolbers, 2000). Conductivity is determined to either induce or prevent ionization of inorganic compounds in the surface (Cremonesi, 1999; Hughes & Sullivan, 2016; Wolbers, 2000). The effects of conductivity-adjusted solutions are distinctly advantageous for moisture-sensitive surfaces and can improve the performance of local wet treatments when using swabs, poultices, and rigid polysaccharide gels (Hughes & Sullivan, 2016). Starting from this information the different approaches to surface cleaning can be undertaken, designing the solution according to pH and conductivity.

The solution must therefore be appropriate for the preservation of the surface and the removal of the soil. There are a few options in terms of reaction mechanism:

- Neutral organic solvents, depending on the similarity of the polarity of the surface, which relies on a physical process (ketones, alcohols, hydrocarbons) and based on the *Teas* solubility diagram (Feller, 1976);
- aprotic dipolar solvents are characterised by strong ionising and dissociative properties. Typically, acids and bases can promote this dissociative action, but strong aprotic solvents can do this too. This is a chemical-physical mechanism of solubilisation;
- another chemical-physical mechanism of solubilisation uses the property of water to create hydrogen bonding;
- acids and basis use a chemical mechanism of solubilisation, by promoting the acidic and basic properties of other materials.

Solubilisation is also enhanced in aqueous solutions by chelating agents, which clamp inorganic materials, surfactants that lower the surface tension of water and enzymes (Cremonesi, 1999, 2004).

pH and conductivity measurements were acquired from the plaster surfaces (plates P1 to P12, *Table 5.3*). The soiled uncoated surfaces of gypsum plaster showed variable values of pH and conductivity (*Tables 6.2* and *6.3*). This is possibly related to the local porosity of the plaster surface, which influences the quantity of soil locally absorbed. No consistent changes in the pH and conductivity can be seen on these surfaces upon ageing. Given the variability of these values, three different solutions (Sol A, B and D) were tested on the uncoated surfaces with the PAM hydrogels. The solutions were promptly absorbed by the uncoated plaster surface, raising doubts on the efficacy of the solubilisation power of the solution in this case.

Linseed oil, shellac and barite were expected to be sensitive to aqueous solutions (sol A to H in *Table 6.1*) (Izzo *et al.*, 2014; Nardelli *et al.*, 2021); as for the plates coated with beeswax, a slightly different solution was needed. The long hydrocarbon chains of beeswax represent a difficulty for the swelling of the surface, although the polarity of beeswax improves the interaction with the solution (Gramtorp *et al.*, 2015). A solution of IMS and DI water (sol I in *Table 6.1*) was compatible with the PE-PAM hydrogels and at the same time able to loosen the soils from the wax coating (Gramtorp *et al.*, 2015).

The cleaning tests were undertaken on the soiled areas (a, b, c); however, the pH and conductivity of the unsoiled areas (d, e, f) were also measured to understand the effect of the soiling mixture on the surfaces (*Table 6.2*). Overall and despite a few exceptions, the pH of the soiled areas is higher than the pH of the relevant unsoiled areas. Differences in the pH before/after ageing are small and varied. The conductivity appears significantly inconsistent in the soiled areas, possibly due to the variability given by the presence of the soiling mixture, and ranges from 0.015 to 0.309 mS/cm. In line with the pH and conductivity measurements, the solutions were preliminarily tested on a side of the area to be cleaned with the PE-PAM hydrogel. The pH of the selected solutions was matched to the pH of the surfaces as can be seen in the preliminary tests summarised in *Table 6.3*. All the solutions except for Sol I (IMS+water) are characterised by high conductivity values from 0.75 to 29.80 mS/cm. The high conductivity enables free acids to be drawn out of the superficial structure more quickly and more thoroughly (Hughes & Sullivan, 2016; Wolbers, 2000).

Table 6.2. pH* and conductivity** (σ) measurements of the surfaces of the plates.

Coating		Section Unaged		Section Aged			
		pH	σ [mS/cm]	pH	σ [mS/cm]		
Soiled	Uncoated	P1a	6.78	0.18	P3a	6.13	0.04
	Cold-pressed linseed oil	P1b	9.62	0.08	P3b	9.19	0.06
	Boiled linseed oil	P1c	8.58	0.04	P3c	6.71	0.03
Unsoiled	Uncoated	P1d	6.2	0.05	P3d	5.83	0.05
	Cold-pressed linseed oil	P1e	5.68	0.03	P3e	5.84	0.05
	Boiled linseed oil	P1f	4.72	0.03	P3f	5.91	0.01
Soiled	Uncoated	P2a	7.76	0.02	P4a	6.73	0.03
	Cold-pressed linseed oil	P2b	6.17	0.02	P4b	7.67	0.05
	Boiled linseed oil	P2c	7.61	0.02	P4c	7.94	0.04
Unsoiled	Uncoated	P2d	6.67	0.03	P4d	6.83	0.04
	Cold-pressed linseed oil	P2e	6.26	0.03	P4e	6.67	0.05
	Boiled linseed oil	P2f	6.15	0.03	P4f	5.98	0.07
Soiled	Uncoated	P5a	5.54	0.31	P7a	5.95	0.22
	Shellac6%	P5b	5.97	0.09	P7b	5.25	0.04
	Shellac18%	P5c	6.08	0.06	P7c	5.27	0.08
Unsoiled	Uncoated	P5d	6.67	0.13	P7d	5.59	0.08
	Shellac6%	P5e	6.8	0.06	P7e	4.91	0.06
	Shellac18%	P5f	6.06	0.13	P7f	4.7	0.21
Soiled	Uncoated	P6a	8.52	0.10	P8a	8.47	0.07
	Shellac6%	P6b	8.09	0.06	P8b	9.15	0.05
	Shellac18%	P6c	6.65	0.06	P8c	9.12	0.06
Unsoiled	Uncoated	P6d	6.03	0.09	P8d	6.87	0.04
	Shellac6%	P6e	5.79	0.06	P8e	6.12	0.04
	Shellac18%	P6f	6.23	0.06	P8f	5.8	0.05
Soiled	Uncoated	P9a	6.44	0.07	P11a	6.34	0.04
	Barite20°	P9b	6.91	0.07	P11b	9.00	0.12
	Barite60°	P9c	8.76	0.06	P11c	8.64	0.04
Unsoiled	Uncoated	P9d	6.22	0.07	P11d	7.31	0.03
	Barite20°	P9e	8.03	0.05	P11e	8.23	0.03
	Barite60°	P9f	6.96	0.03	P11f	7.03	0.04
Soiled	Uncoated	P10a	6.51	0.04	P12a	6.97	0.06
	Barite20°	P10b	8.95	0.06	P12b	8.45	0.06
	Barite60°	P10c	7.8	0.04	P12c	9.13	0.06
Unsoiled	Uncoated	P10d	6.94	0.05	P12d	7.32	0.06
	Barite20°	P10e	6.19	0.03	P12e	6.39	0.09
	Barite60°	P10f	6.18	0.03	P12f	6.22	0.09

* accuracy ± 0.1 ; ** accuracy $\pm 2\%$.

Table 6.3. Preliminary tested solutions according to the pH and conductivity of the soiled surface.

Surface	Condition	pH	σ [mS/cm]	Tested solutions	Chosen solution
Uncoated gypsum plaster	Unaged	5.54-6.44	0.07-0.31	P1a: Sol B; P5a: Sol E, Sol D; P9a: Sol A, Sol C, Sol H.	P1a: Sol B; P5a: Sol D; P9a: Sol A.
	Aged	5.95-6.34	0.04-0.22	P3a: Sol A, Sol B; P7a: Sol D; P11a: Sol A, Sol C, Sol H.	P3a: Sol B; P7a: Sol D; P11a: Sol A
Cold-pressed linseed oil	Unaged	9.62	0.08	Sol H, Sol G	Sol H
	Aged	9.19	0.06	Sol H, Sol G	Sol H
Boiled linseed oil	Unaged	8.58	0.04	Sol B	Sol B
	Aged	6.71	0.03	Sol B	Sol B
Shellac6%	Unaged	5.97	0.09	Sol E, Sol D	Sol D
	Aged	5.25	0.04	Sol D	Sol D
Shellac18%	Unaged	6.08	0.06	Sol E, Sol D, Sol A	Sol D
	Aged	5.27	0.08	Sol D	Sol D
Barite20°	Unaged	6.91	0.07	Sol A, Sol C, Sol H	Sol A
	Aged	9.00	0.12	Sol A, Sol C, Sol H	Sol H
Barite60°	Unaged	8.76	0.06	Sol A, Sol C, Sol H	Sol H
	Aged	8.64	0.04	Sol A, Sol C, Sol H	Sol H
Beeswax	Unaged	6.17-8.95	0.02-0.10	Sol I	Sol I
	Aged	6.73-9.15	0.03-0.07	Sol I	Sol I

6.3.2. VISUAL EXAMINATION, VISIBLE (VIS) REFLECTANCE AND ULTRAVIOLET FLUORESCENCE (UVF) IMAGING

Figures 6.3 to 6.18 (pages 249-256) show the visible (Vis) and ultraviolet fluoresce (UVf) images taken from the accelerated aged plaster casts before cleaning at t_{37} (Table 5.3, page 174) and after cleaning. For comparison, the unsoiled relevant section is also shown in the images. In the same image, the unaged surface on the left and the relevant aged one can be seen on the right. A summary of the plates and sections can be found in Table 5.2 (page 173).

The PE-PAM hydrogels achieved a remarkable removal of the soil from the uncoated gypsum surfaces (Figures 6.3 to 6.5): the appearance of the cleaned surface is closer to the unsoiled reference than to the appearance of the soiled portion. A relative unevenness of the removal of soil in the area was expected due to the locally different absorption and

porosity of the plaster surface. This could be overcome by subsequent PE-PAM hydrogel applications or further cleaning. Differential adherence of the PE sheet onto the irregular surface could also be another reason. The PE-PAM hydrogels are novel products that allow the appropriate material selection and synthesis parameters (Mateescu *et al.*, 2017). For example, modifying or changing the backing with a heavier support film could improve the adherence of the hydrogels onto the plaster substrate.

The cleaning tests were effective on the soiled surfaces coated with linseed oil (*Figures 6.6 to 6.7*). As discussed in *Section 5.3* (from page 180), linseed oil does not form a film, leaving the plaster structure exposed to some degree. Overall, the removal of soils appeared more effective on the aged surfaces, because the unaged oil is not completely dry and softer, and the soil particles have better contact. For example, a larger part of the surface of the particles should be covered by the oil. In contrast, aged/dried oil films result in less oil/soil particle interface, making it is easier to mobilise the particle. The cleaning procedure, by removing the soil, seems to have enhanced the fluorescence of the surface.

The same observations made for the soiled surfaces coated with linseed oil were made for the surfaces coated with shellac (*Figures 6.8 and 6.9*), although the one application of the PE-PAM gels was slightly less efficient in the latter. On the other hand, the surfaces coated with barite solution (*Figures 6.10 and 6.11*) appeared to have similar issues discussed for the uncoated plaster surfaces: removal has not been as effective as for the surfaces coated with linseed oil. In the surfaces coated with barite, the Water Absorbance Behaviour (WAB) of the sulfate surface, did not allow the retention of the solution onto the surface. Once again, fluorescence appeared increased, which could however be a temporary effect due to the wetting of the surface.

Cleaning with the PE-PAM hydrogels showed very positive results on the surfaces coated with beeswax (*Figures 6.12 to 6.18*). Cleaning was more even and effective on the aged sections if compared with the unaged sections. This can be because the soil mixture was much more adhered to the tackier fresh beeswax than to the aged beeswax. The fact that cleaning was more effective in this case can be due to the filming properties of beeswax (*Section 5.3*): during the application the hydrogel-solution was retained onto the surface, therefore having the time to interact and react with the coating. As was also observed in *Section 5.3*, the brush marks were visible on the unaged surfaces and still visible after the cleaning test. Changes in fluorescence upon cleaning were observed and were varied.

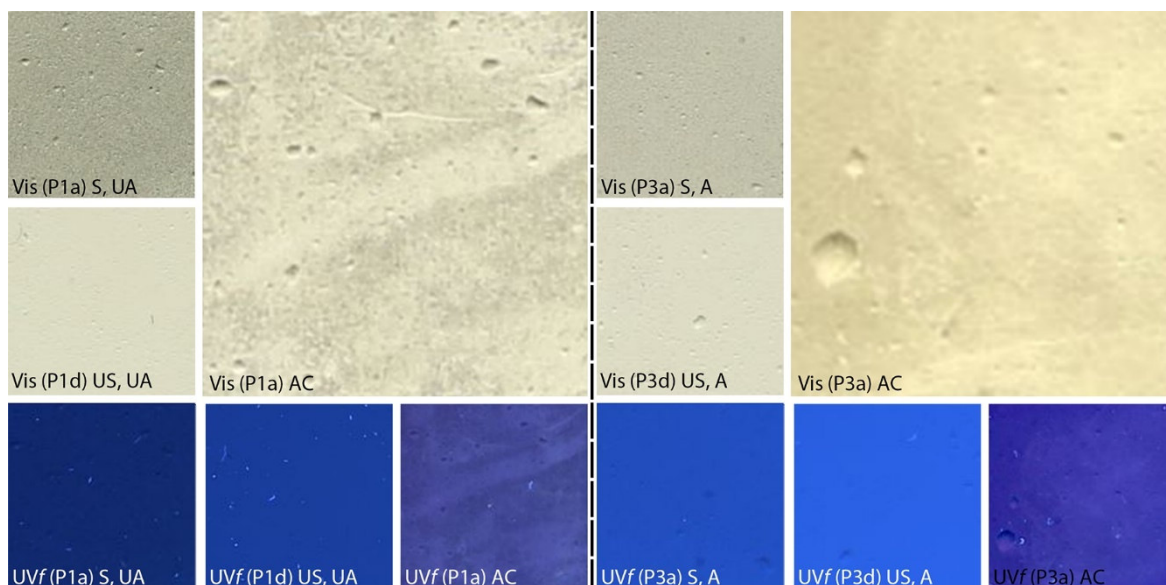


Figure 6.3. Photographs (2x2 cm) taken under Vis and UV illumination of the uncoated gypsum plaster surfaces (areas P1a and P3a). The labels on the photographs indicate the type of illumination and if the image was acquired from unaged (UA) or aged (A) plates, before (S) or after (AC) cleaning with PE-PAM-TEA solution pH 8.5 (Sol B). The relevant unsoiled (US) sections P1d and P3d are also shown.

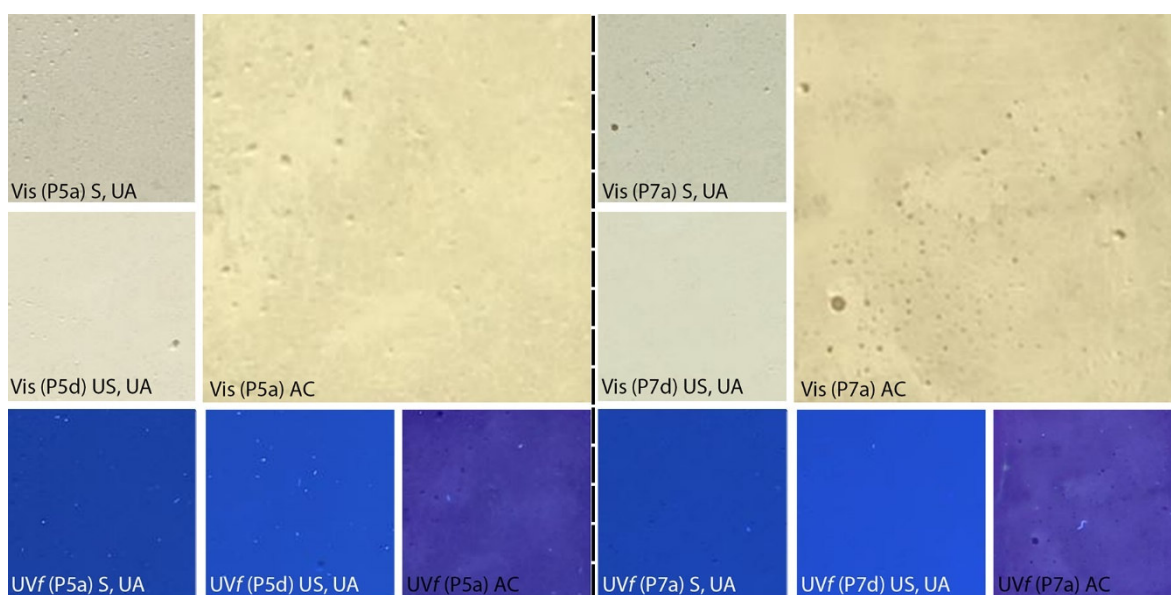


Figure 6.4. Photographs (2x2 cm) taken under Vis and UV illumination of the uncoated gypsum plaster surfaces (P5a and P7a). The labels on the photographs indicate the type of illumination and if the image was acquired from unaged (UA) or aged (A) plates, before (S) or after (AC) cleaning with PE-PAM-HCl solution pH6 (Sol D). The relevant unsoiled (US) sections P5d and P7d are also shown.

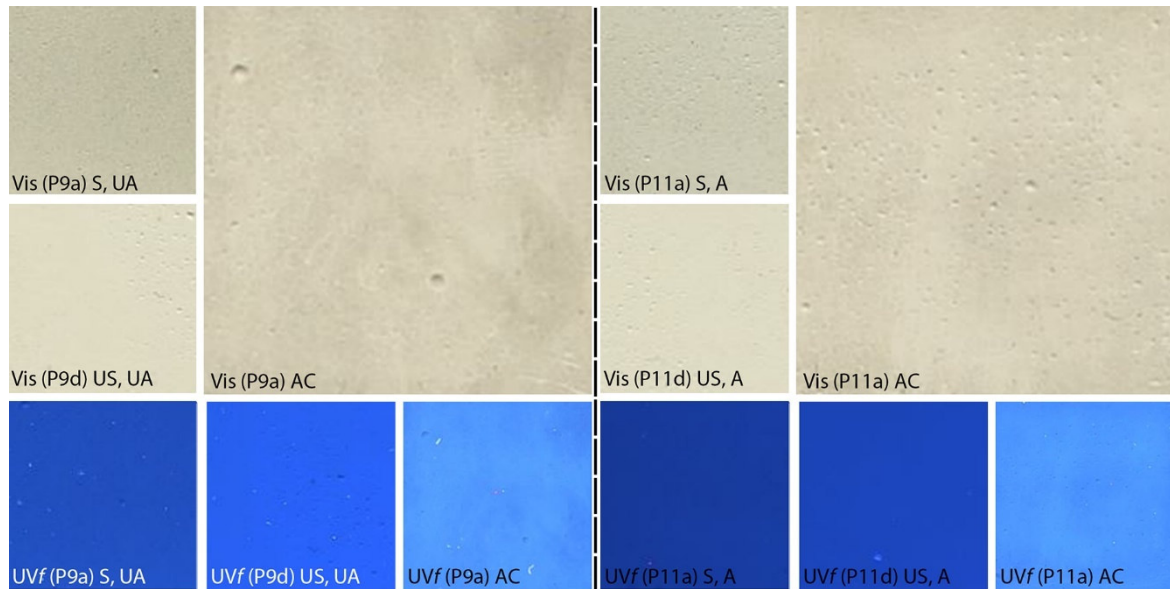


Figure 6.5. Photographs (2x2 cm) taken under Vis and UV illumination of the uncoated gypsum plaster surfaces (P9a and P11a). The labels on the photographs indicate the type of illumination and if the image was acquired from unaged (UA) or aged (A) plates, before (S) or after (AC) cleaning with PE-PAM-TEA solution pH 8 (Sol A). The relevant unsoiled (US) sections P9d and P11d are also shown.

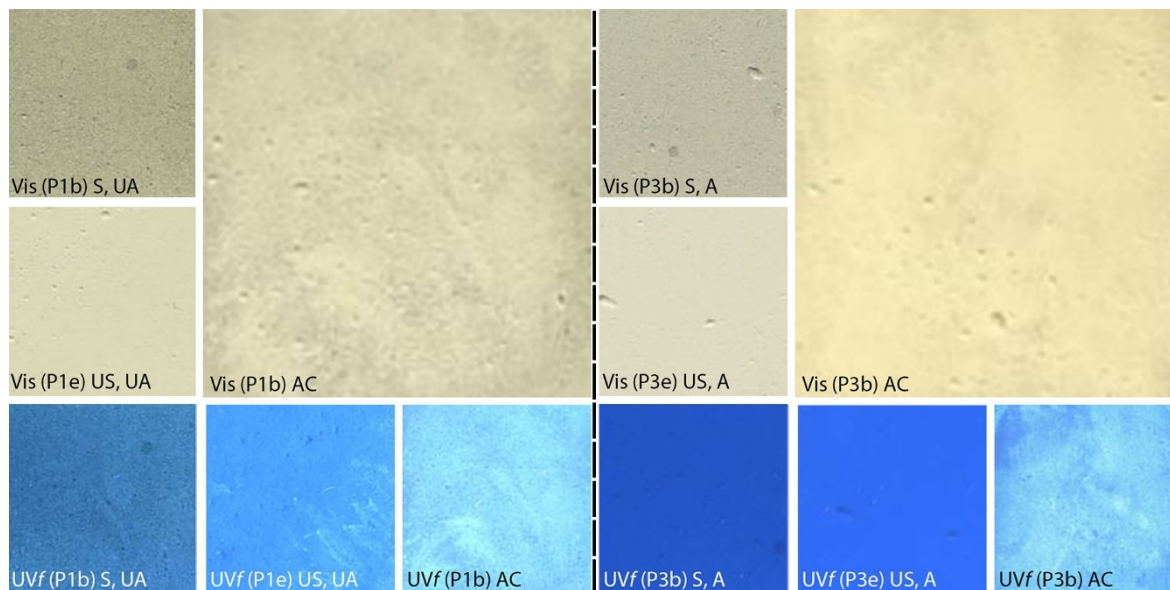


Figure 6.6. Photographs (2x2 cm) taken under Vis and UV illumination of the gypsum plaster surfaces coated with cold-pressed linseed oil (1-1) (P1b and P3b). The labels on the photographs indicate the type of illumination and if the image was acquired from unaged (UA) or aged (A) plates, before (S) or after (AC) cleaning with PE-PAM-EDTA solution pH 8.5 (Sol H). The relevant unsoiled (US) sections P1e and P3e are also shown.

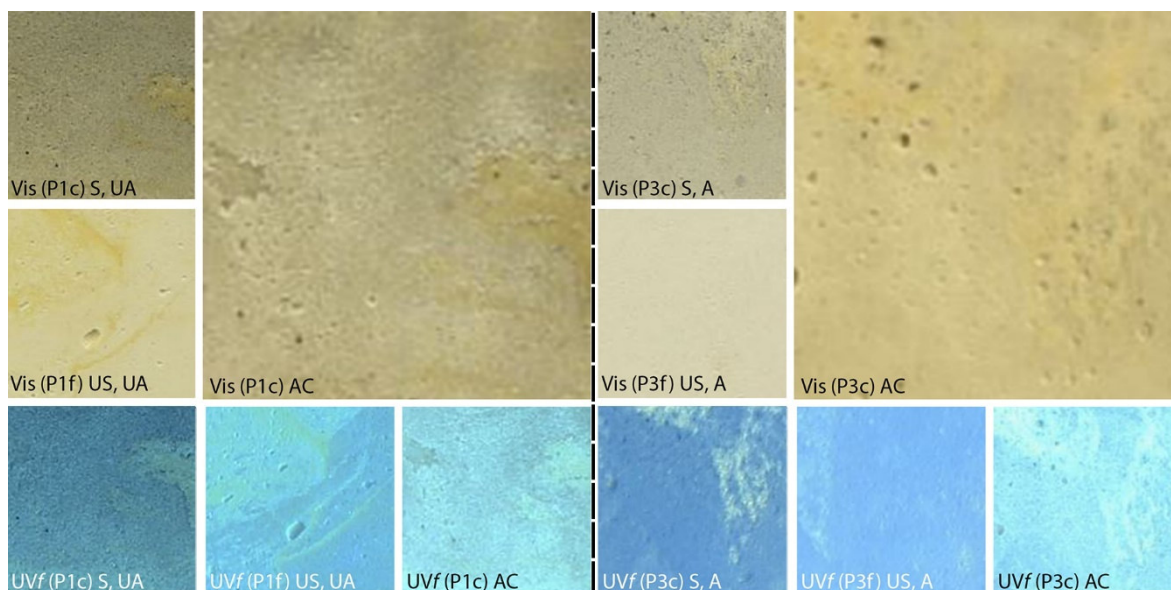


Figure 6.7. Photographs (2x2 cm) taken under Vis and UV illumination of the gypsum plaster surfaces coated with boiled linseed oil (1-2) (P1c and P3c). The labels on the photographs indicate the type of illumination and if the image was acquired from unaged (UA) or aged (A) plates, before (S) or after (AC) cleaning with PE-PAM-TEA solution pH8.5 (Sol B). The relevant unsoiled (US) sections P1f and P3f are also shown.

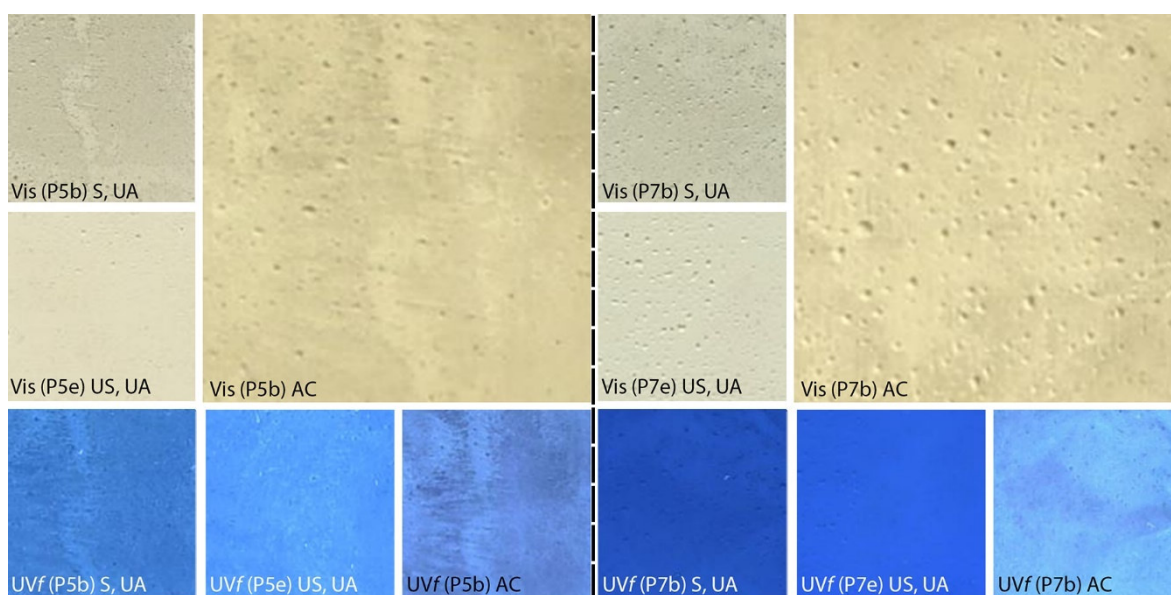


Figure 6.8. Photographs (2x2 cm) taken under Vis and UV illumination of the gypsum plaster surfaces coated with shellac6% (2-1) (P5b and P7b). The labels on the photographs indicate the type of illumination and if the image was acquired from unaged (UA) or aged (A) plates, before (S) or after (AC) cleaning with PE-PAM-HCl solution pH 6 (Sol D). The relevant unsoiled (US) sections P5e and P7e are also shown.

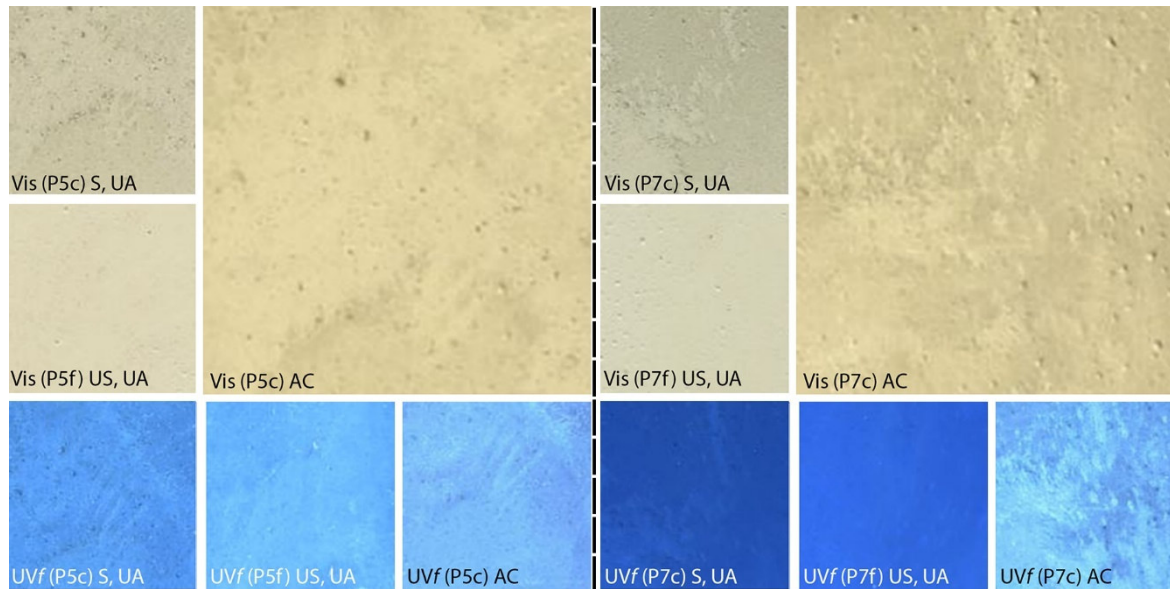


Figure 6.9. Photographs (2x2 cm) taken under Vis and UV illumination of the gypsum plaster surfaces coated with shellac18% (2-2) (P5c and P7c). The labels on the photographs indicate the type of illumination and if the image was acquired from unaged (UA) or aged (A) plates, before (S) or after (AC) cleaning with PE-PAM-HCl solution pH 6 (Sol D). The relevant unsoiled (US) sections P5f and P7f are also shown.

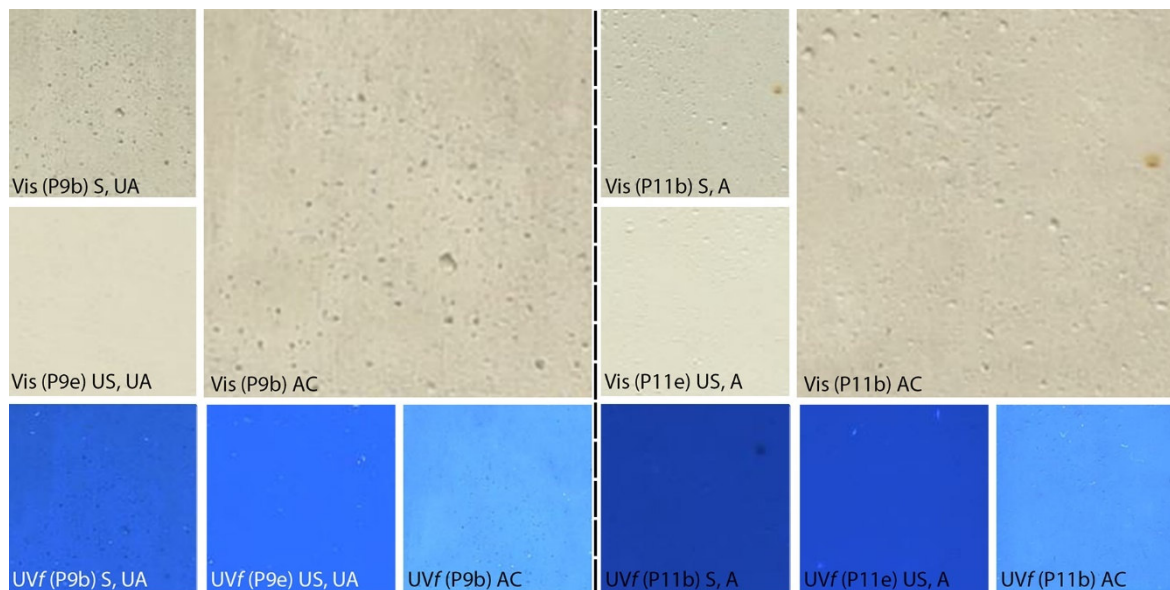


Figure 6.10. Photographs (2x2 cm) taken under Vis and UV illumination of the gypsum plaster surfaces coated with barite20° (3-1) (P9b and P11b). The labels on the photographs indicate the type of illumination and if the image was acquired from unaged (UA) or aged (A) plates, before (S) or after (AC) cleaning with PE-PAM-TEA solution pH 8 (Sol A) (for the UA area) and PE-PAM-EDTA solution pH 8.5 (Sol H) (for the A area). The relevant unsoiled (US) sections P9e and P11e are also shown.

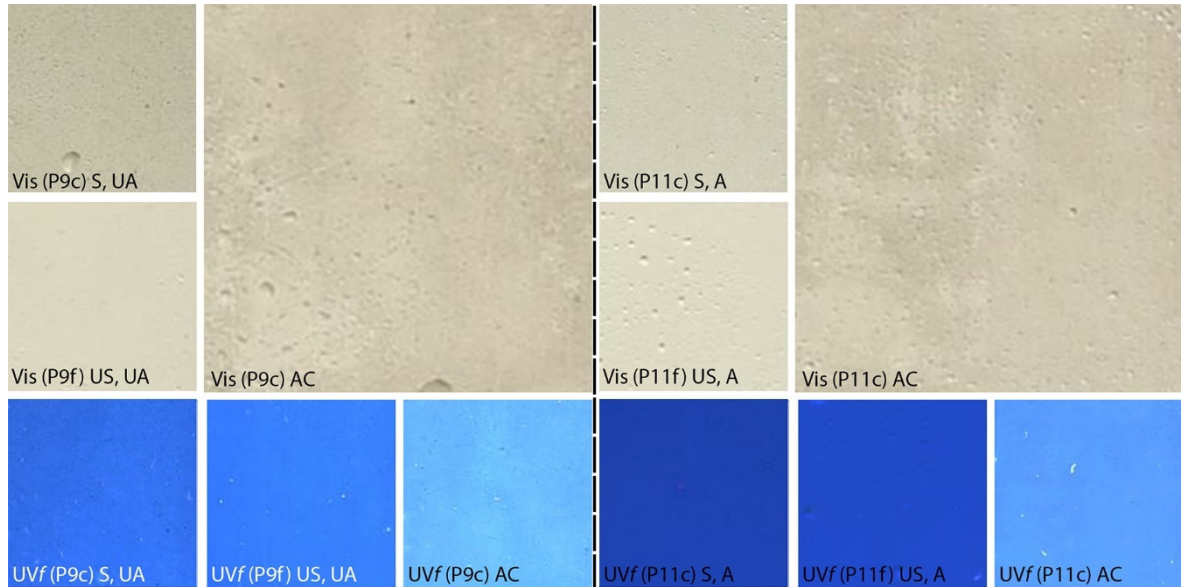


Figure 6.11. Photographs (2x2 cm) taken under Vis and UV illumination of the gypsum plaster surfaces coated with barite60° (3-2) (P9c and P11c). The labels on the photographs indicate the type of illumination and if the image was acquired from unaged (UA) or aged (A) plates, before (S) or after (AC) cleaning with PE-PAM-EDTA solution pH 8.5 (Sol H). The relevant unsoiled (US) sections P9f and P11f are also shown.

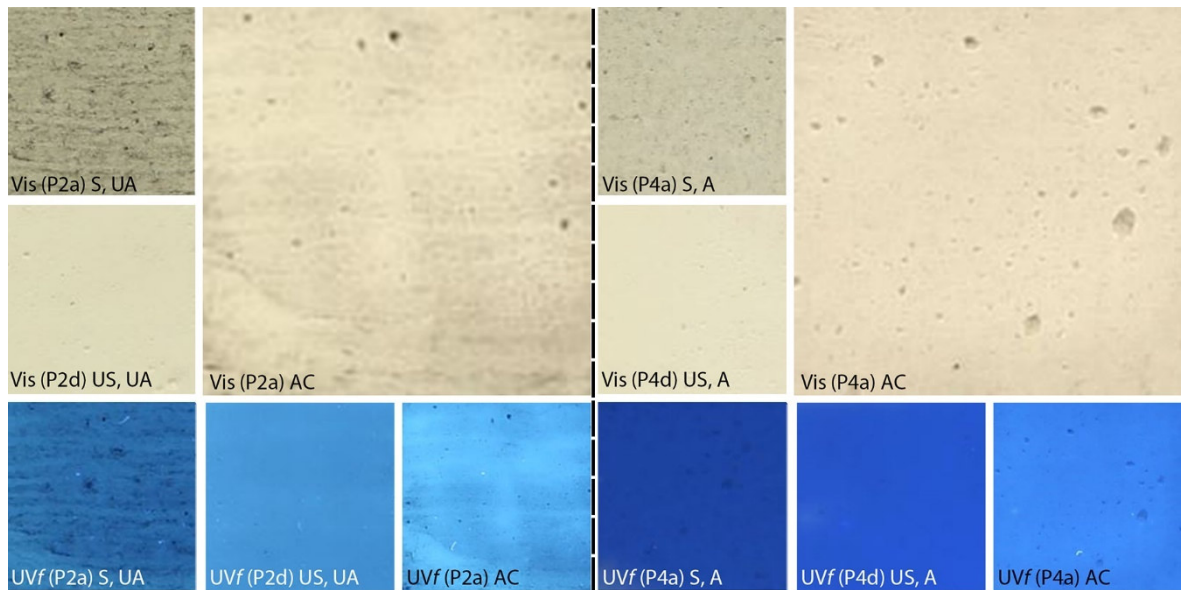


Figure 6.12. Photographs (2x2 cm) taken under Vis and UV illumination of the gypsum plaster surfaces coated with beeswax (4) (P2a and P4a). The labels on the photographs indicate the type of illumination and if the image was acquired from unaged (UA) or aged (A) plates, before (S) or after (AC) cleaning with PE-PAM-IMS solution (Sol I). The relevant unsoiled (US) sections P2d and P4d are also shown.

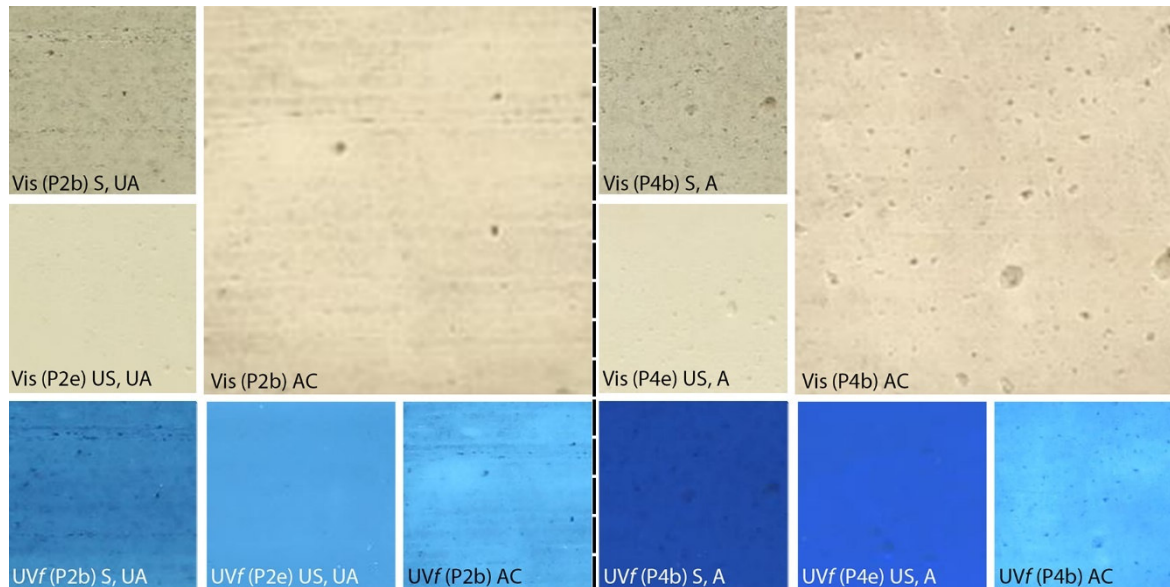


Figure 6.13. Photographs (2x2 cm) taken under Vis and UV illumination of the gypsum plaster surfaces coated with cold-pressed linseed oil (1-2) and beeswax (4) (P2b and P4b). The labels on the photographs indicate the type of illumination and if the image was acquired from unaged (UA) or aged (A) plates, before (S) or after (AC) cleaning with PE-PAM-IMS solution (Sol I). The relevant unsoiled (US) sections P2e and P4e are also shown.

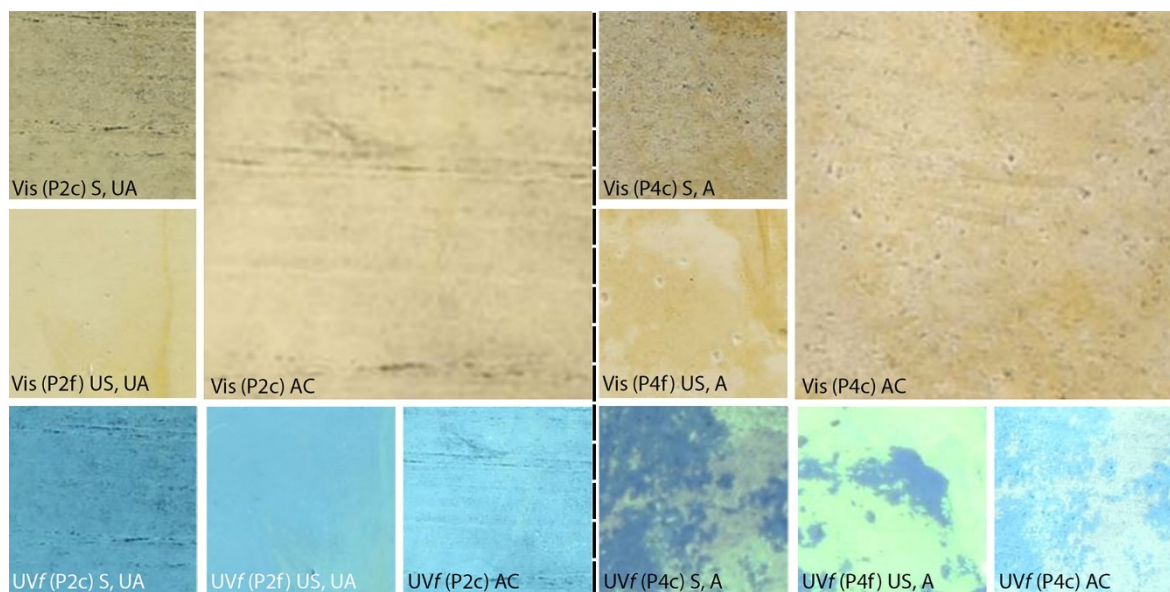


Figure 6.14. Photographs (2x2 cm) taken under Vis and UV illumination of the gypsum plaster surfaces coated with boiled linseed oil (2-2) and beeswax (4) (P2c and P4c). The labels on the photographs indicate the type of illumination and if the image was acquired from unaged (UA) or aged (A) plates, before (S) or after (AC) cleaning with PE-PAM-IMS solution (Sol I). The relevant unsoiled (US) sections P2f and P4f are also shown.

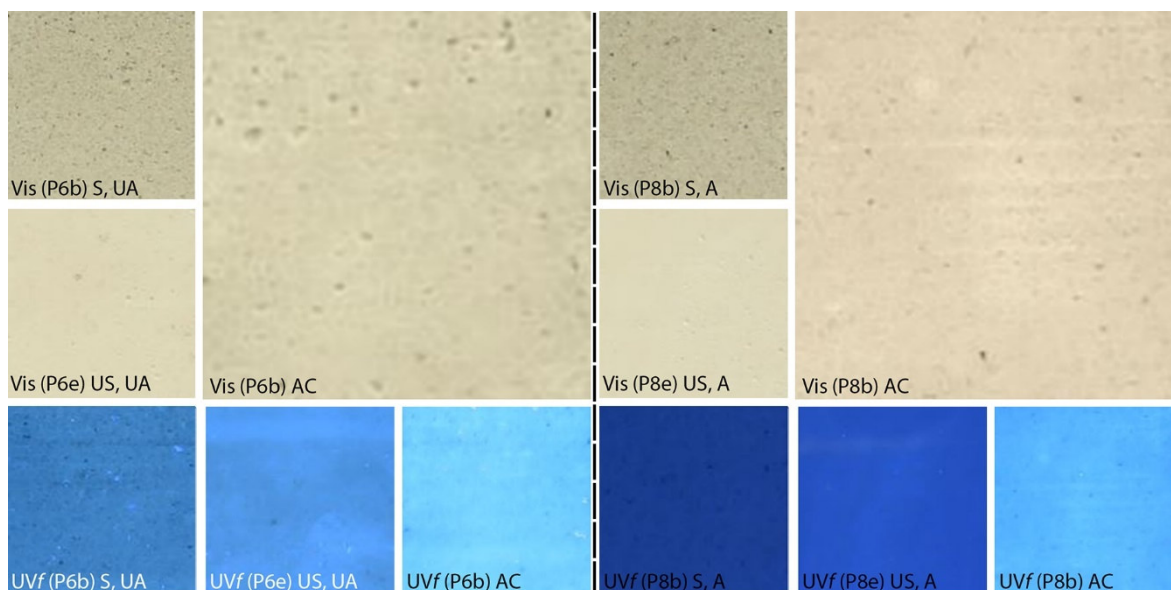


Figure 6.15. Photographs (2x2 cm) taken under Vis and UV illumination of the gypsum plaster surfaces coated with shellac6% (2-1) and beeswax (4) (P6b and P8b). The labels on the photographs indicate the type of illumination and if the image was acquired from unaged (UA) or aged (A) plates, before (S) or after (AC) cleaning with PE-PAM-IMS solution (Sol I). The relevant unsoiled (US) sections P6e and P8e are also shown.

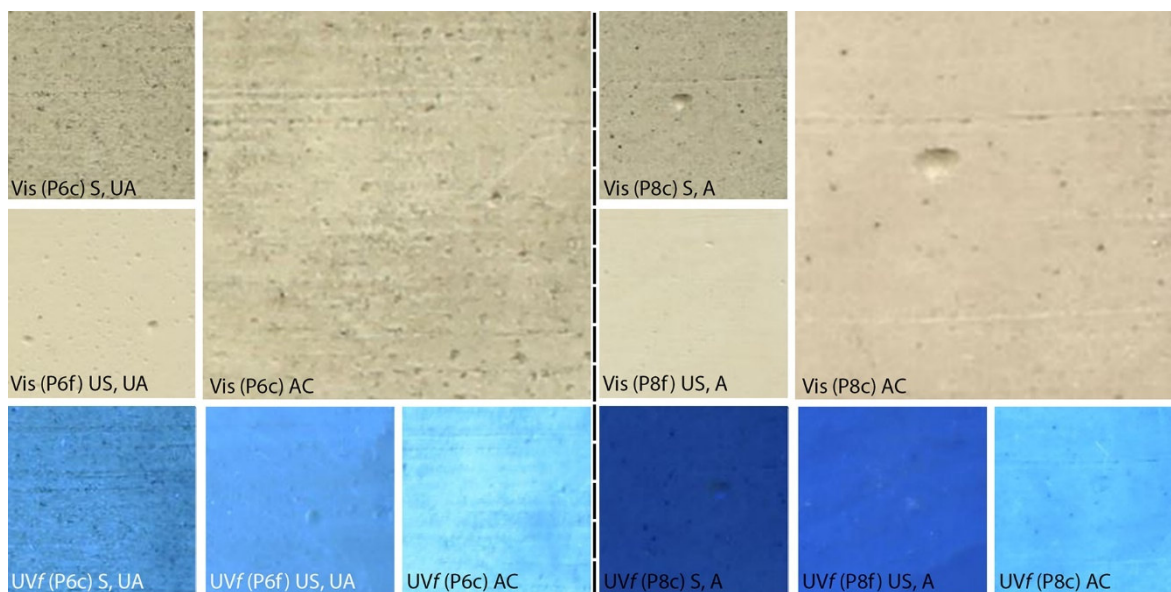


Figure 6.16. Photographs (2x2 cm) taken under Vis and UV illumination of the gypsum plaster surfaces coated with shellac18% (3-2) and beeswax (4) (P6c and P8c). The labels on the photographs indicate the type of illumination and if the image was acquired from unaged (UA) or aged (A) plates, before (S) or after (AC) cleaning with PE-PAM-IMS solution (Sol I). The relevant unsoiled (US) sections P6f and P8f are also shown.

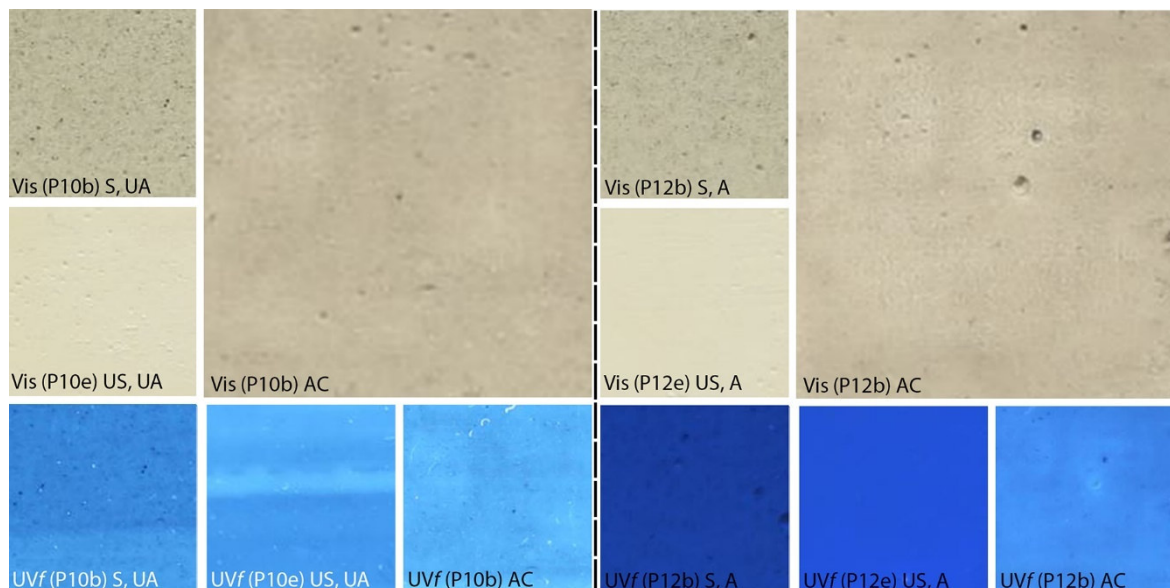


Figure 6.17. Photographs (2x2 cm) taken under Vis and UV illumination of the gypsum plaster surfaces coated with barite_{20°} (3-1) and beeswax (4) (P10b and P12b). The labels on the photographs indicate the type of illumination and if the image was acquired from unaged (UA) or aged (A) plates, before (S) or after (AC) cleaning with PE-PAM-IMS solution (Sol I). The relevant unsoiled (US) sections P10e and P12e are also shown.

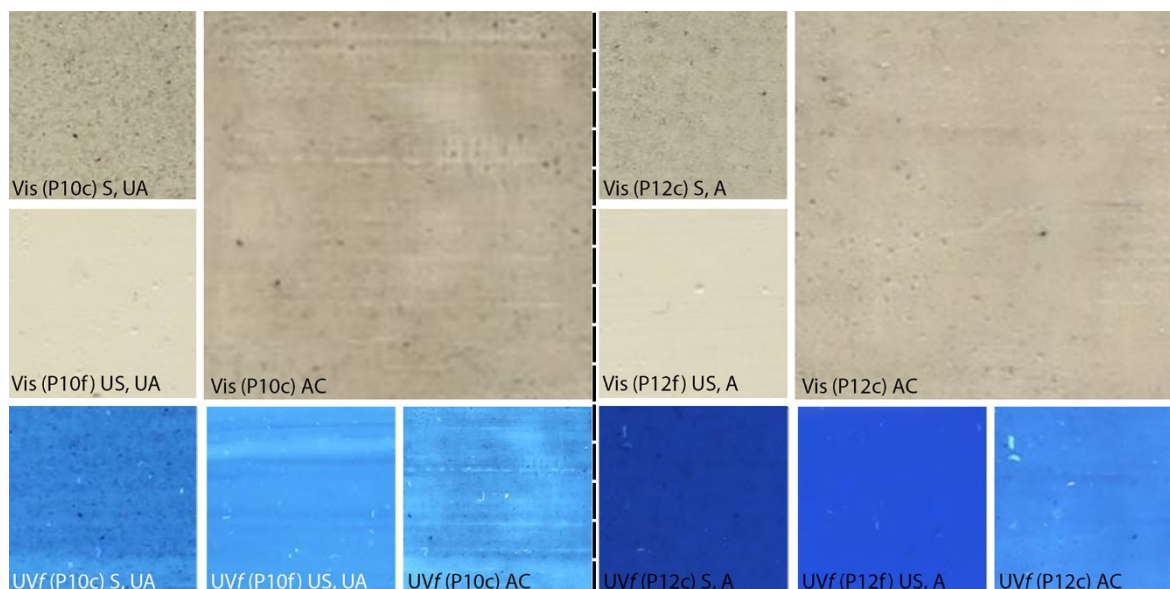


Figure 6.18. Photographs (2x2 cm) taken under Vis and UV illumination of the gypsum plaster surfaces coated with barite_{60°} (3-2) and beeswax (4) (P10c and P12c). The labels on the photographs indicate the type of illumination and if the image was acquired from unaged (UA) or aged (A) plates, before (S) or after (AC) cleaning with PE-PAM-IMS solution (Sol I). The relevant unsoiled (US) sections P10f and P12f are also shown.

6.3.3. TOPOGRAPHICAL AND MORPHOLOGICAL STUDIES

Changes in the surface appearance and the removal of the soil can be also observed in the BSE images, the FT-IR survey micrographs and the HR 3D images (*Figures 6.19 to 6.27*, pages 258-73). The effect of the cleaning on the uncoated plaster surfaces can be observed in *Figures 6.19 to 6.21* (pages 258-60). A reduction of the quantity of the black particles of soil observed in the BSE images and the micrographs is clear in all the images. The unevenness of the effects of cleaning is observed in P1a (AC) and P3a (AC) in the HR 3D images in *Figure 6.19*. The smoothing of the surface was seen and could be due to the removal of the soil, the mechanical action of the swab, but also to minor re-dissolution of the uncoated surface plaster surface in the aqueous solution, despite the negligible amount of liquid introduced (Klimchouk, 1996). Each spot of the area cleaned with PE-PAM hydrogels (2x2 cm) received less than 1 μm of liquid ($10^{-6} \mu\text{L} / \mu\text{m}^2$). The partial dissolution would explain the resulted change of shape of the superficial structure in the BSE images from P1a before and after cleaning (*Figure 6.19*). The same can be also observed in *Figures 6.20 and 6.21*.

Figures 6.22 and 6.23 (pages 261-2) of the surfaces coated with linseed oil showed similar characteristics with the uncoated plaster surfaces. The smoothing effect observed for the uncoated can be seen in the surfaces after cleaning. As already observed in the vis and UVf images, the cleaning of the boiled linseed oil was less effective than the cleaning of the cold-pressed linseed oil. This is shown by the micrographs, in which some soils can still be seen after cleaning. The same considerations can be made for the surfaces coated with shellac (*Figures 6.24 and 6.25*, pages 263-4) although the smoothing effect was less pronounced, possibly because of a harder and drier surface. A reduced amount of soiling was observed in the micrographs of the sections coated with barite (*Figures 6.26 and 6.27*, pages 265-6) and very few changes were observed in the texture of the surface.

The PE-PAM hydrogels in combination with IMS solution (Sol I) have proven effective for soil removal from the plaster surfaces coated with beeswax (*Figure 6.28*, page 267). The soil mixture seemed to have been almost entirely removed from both the unaged and aged areas. The soil that was not removed was mostly located in the pores (see for example black arrow in *Figure 6.28*, page 267). It is possible that a second application could have removed that too. Few micro-scratches can be seen in the micrographs and the HR images of the unaged areas, and are likely due to the soft consistency of the fresh wax and the rolling action of the cotton swab. Micro-scratches were not noticed in the aged, harder surfaces. Overall, the cleaning appeared more homogeneous and effective in the aged areas. The surfaces that were coated first with linseed oil (1), shellac (2) or barite (3) and then with beeswax (4) and cleaned with PE-PAM-Sol I showed the same characteristics discussed for the surfaces coated with beeswax only (additional images can be seen in *Appendix 9* and in the database of results, Risdonne & Theodorakopoulos, 2021).

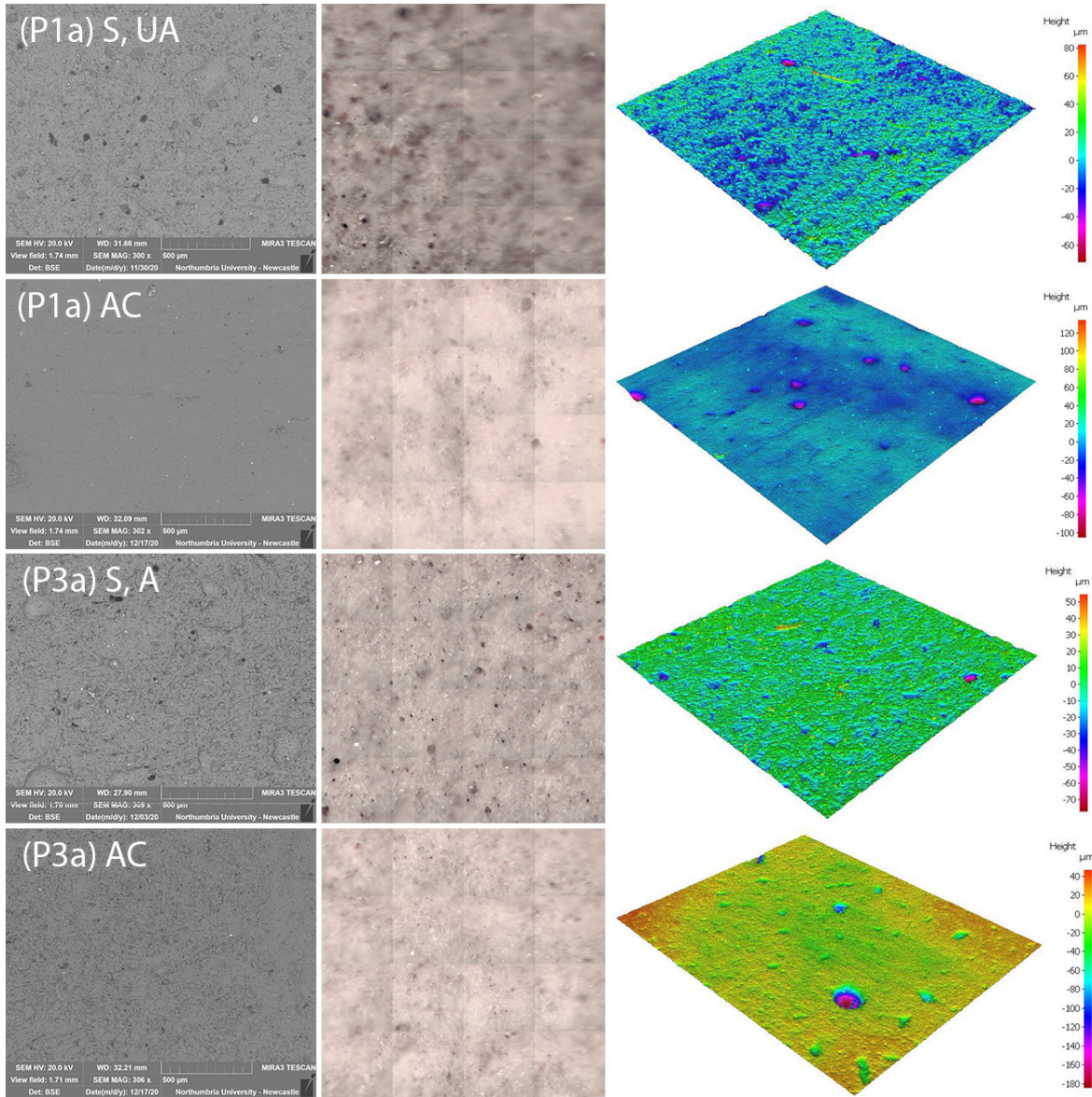


Figure 6.19. From left to right: BSE images (SEM MAG: 300x), FT-IR survey micrographs (1x1 mm) and the HR 3D images (5.3x5.3 mm) of the uncoated gypsum plaster surfaces (P1a and P3a) before (S) and after (AC) cleaning with PE-PAM-TEA solution pH8.5 (Sol B). A reduction of the quantity of the black particles of soil can be seen after cleaning in all the images. The 3D images highlight the removal of the soiling, but also some unevenness of the surface after cleaning. The smoothing of the surface can be seen in the BSE images after cleaning.

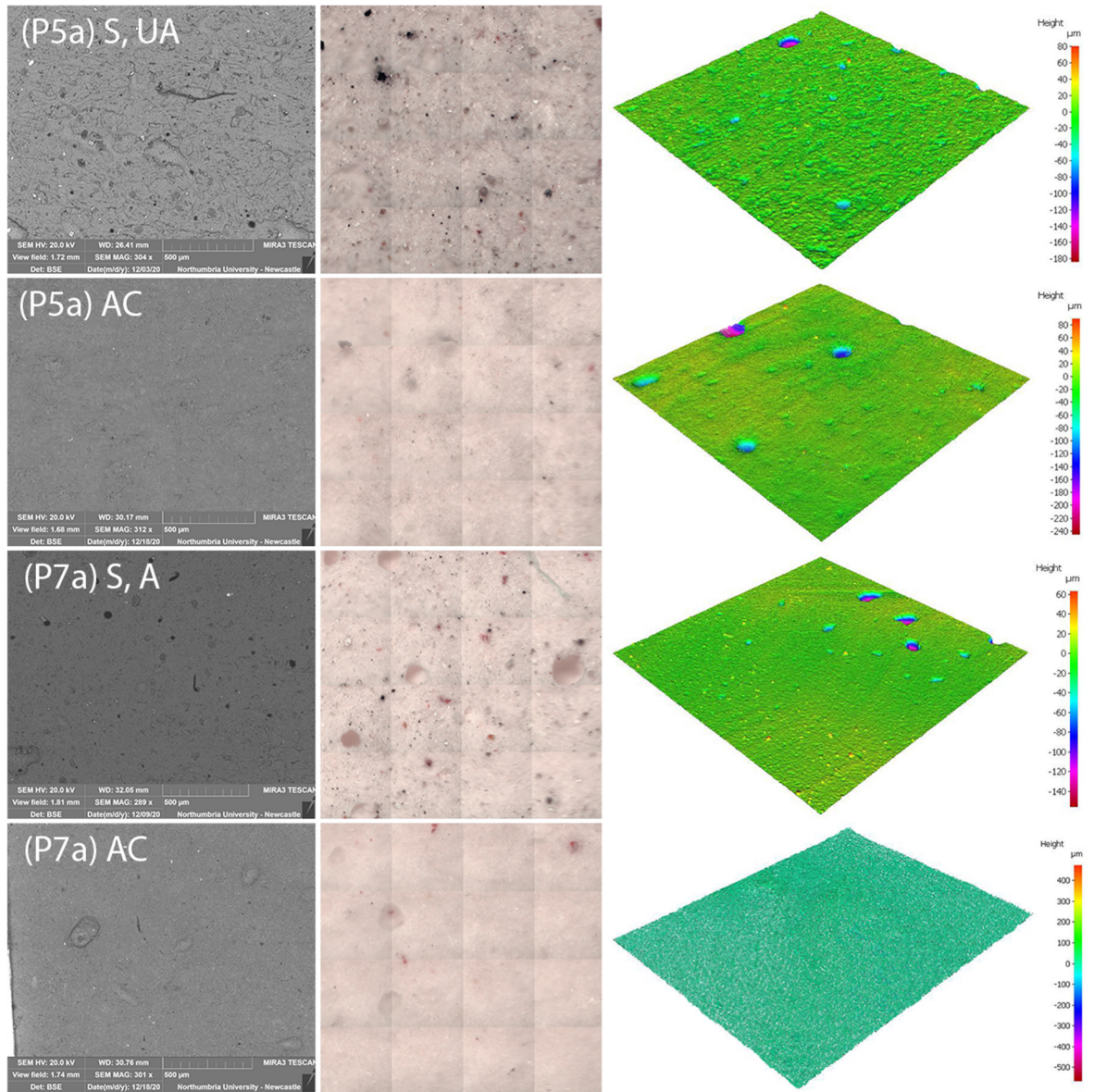


Figure 6.20. From left to right: BSE images (SEM MAG: 300x), FT-IR survey micrographs (1x1 mm) and the HR 3D images (5.3x5.3 mm) of the uncoated gypsum plaster surfaces (P5a and P7a) before (S) and after (AC) cleaning with PE-PAM-TEA solution pH 8 (Sol A). A reduction of the quantity of the black particles of soil can be seen after cleaning in all the images. The smoothing of the surface can be seen in the BSE images after cleaning.

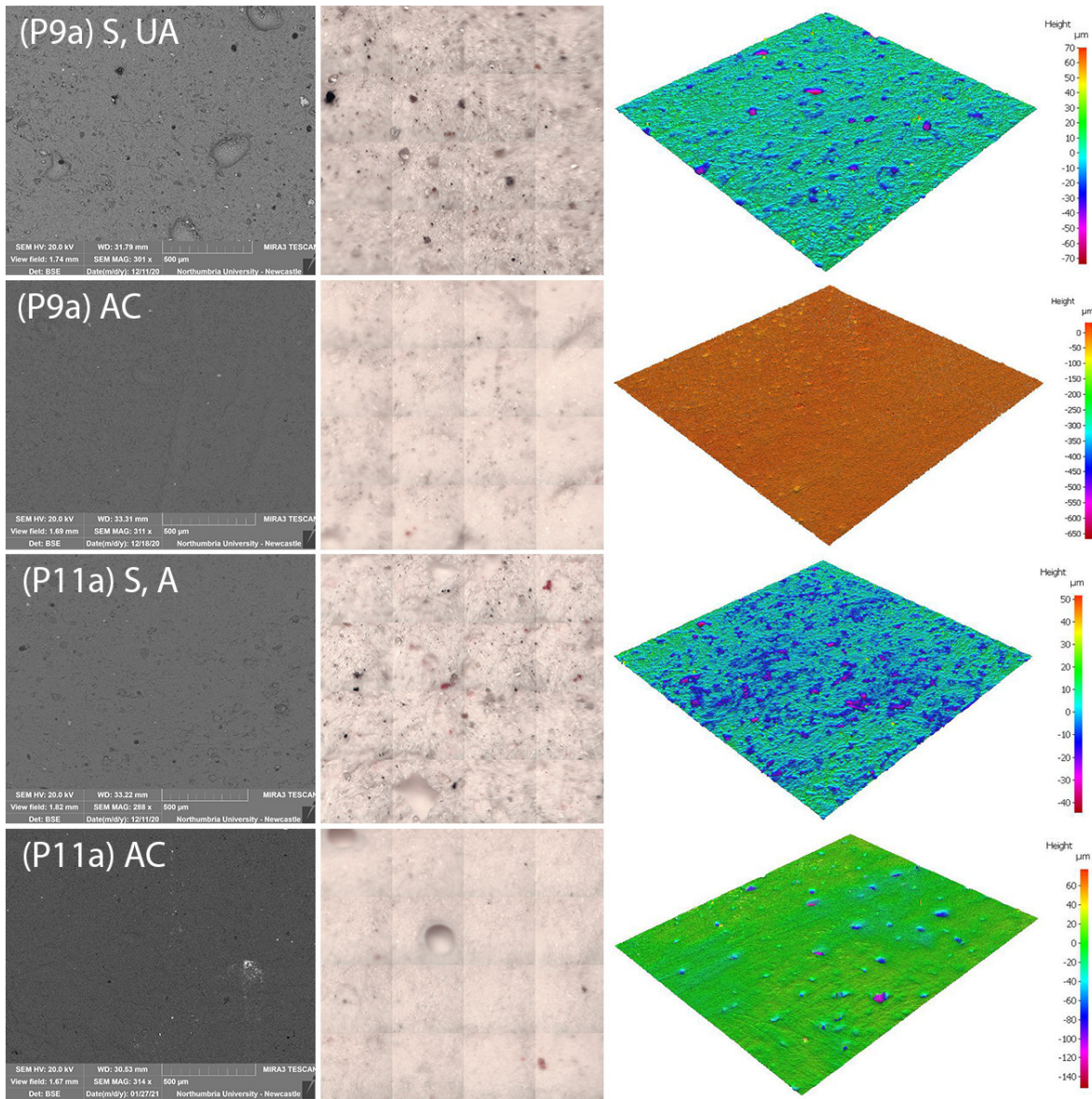


Figure 6.21. From left to right: BSE images (SEM MAG: 300x), FT-IR survey micrographs (1x1 mm) and the HR 3D images (5.3x5.3 mm) of the uncoated gypsum plaster surfaces (P9a and P11a) before (S) and after (AC) cleaning with PE-PAM-HCl solution pH 6 (Sol D). A reduction of the quantity of the black particles of soil can be seen after cleaning in all the images. The smoothing of the surface can be seen in the BSE images after cleaning.

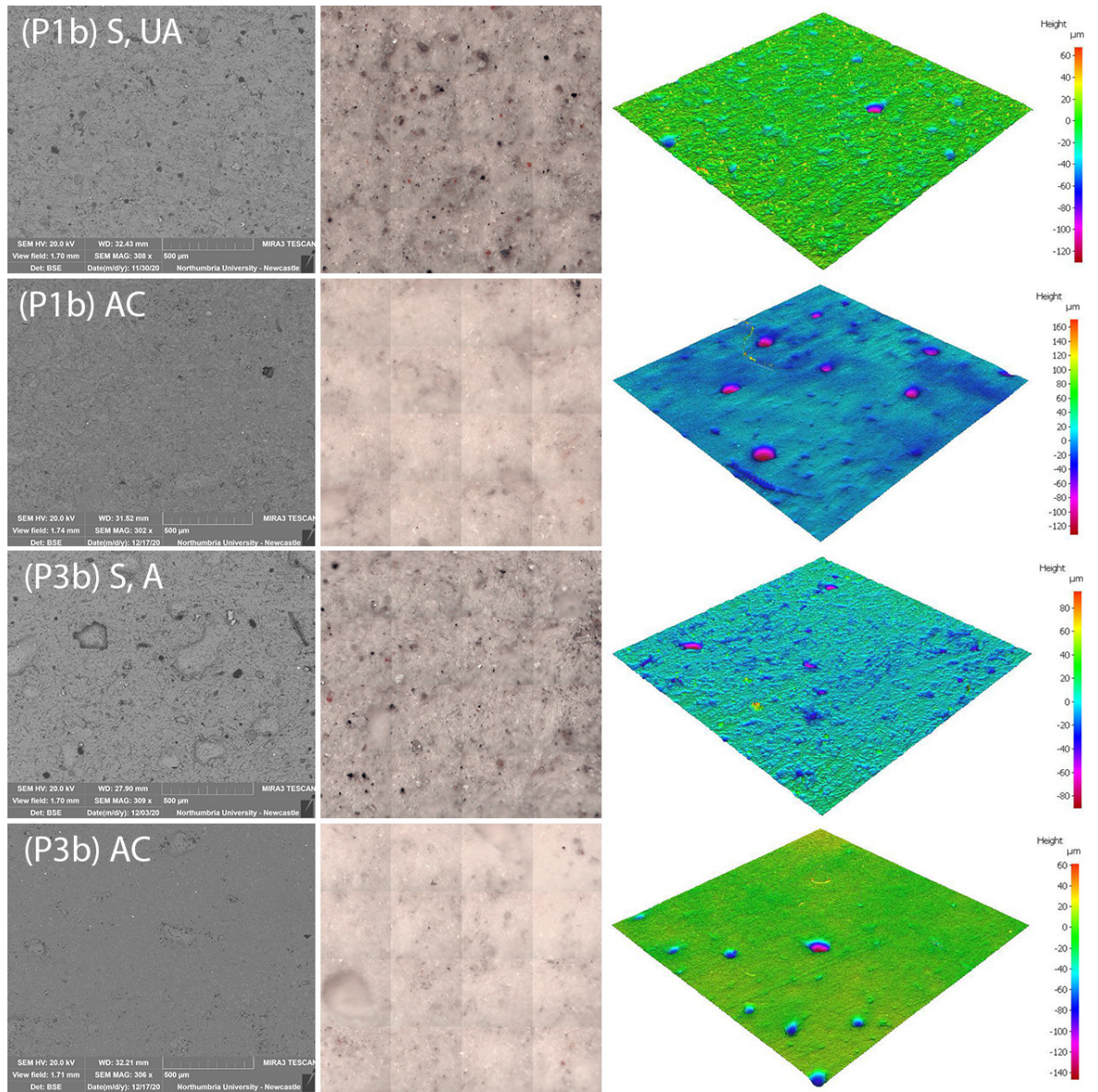


Figure 6.22. From left to right: BSE images (SEM MAG: 300x), FT-IR survey micrographs (1x1 mm) and the HR 3D images (5.3x5.3 mm) of the plaster surfaces coated with cold-pressed linseed oil (1-1) (P1b and P3b) before (S) and after (AC) cleaning with PE-PAM-EDTA solution pH 8.5 (Sol H). A reduction of the quantity of the black particles of soil can be seen after cleaning in all the images. The 3D images highlight the removal of the soiling, but also some unevenness of the surface after cleaning. The smoothing of the surface can be seen in the BSE images after cleaning.

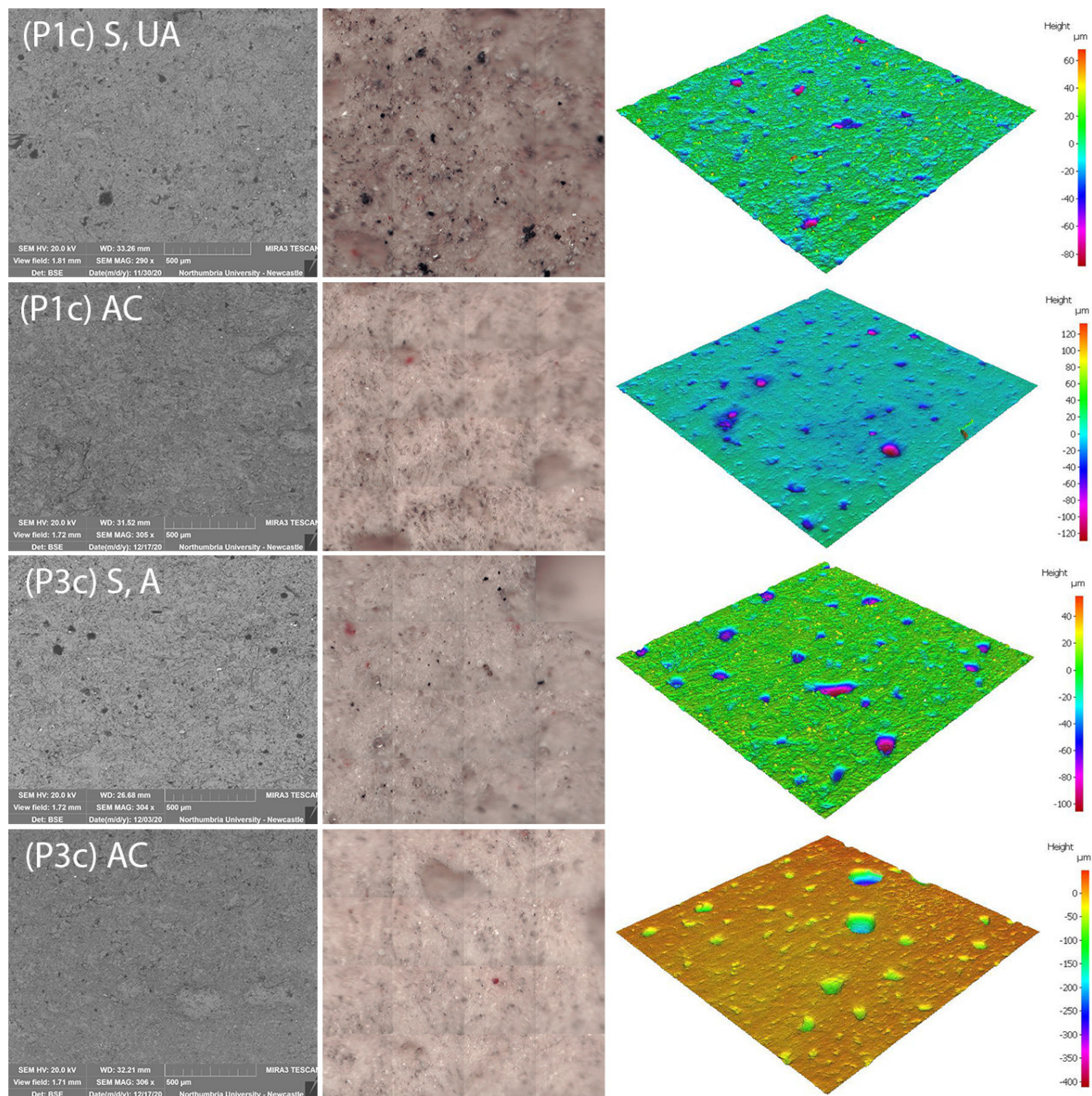


Figure 6.23. From left to right: BSE images (SEM MAG: 300x), FT-IR survey micrographs (1x1 mm) and the HR 3D images (5.3x5.3 mm) of the plaster surfaces coated with boiled linseed oil (1-2) (P1c and P3c) before (S) and after (AC) cleaning with PE-PAM-TEA solution pH 8.5 (Sol B). A reduction of the quantity of the black particles of soil is observed, but the cleaning of the boiled linseed oil was less effective than the cleaning of the cold-pressed linseed oil and some soiling can still be seen in the images. The 3D images highlight some unevenness of the surface after cleaning and the smoothing effect is less pronounced.

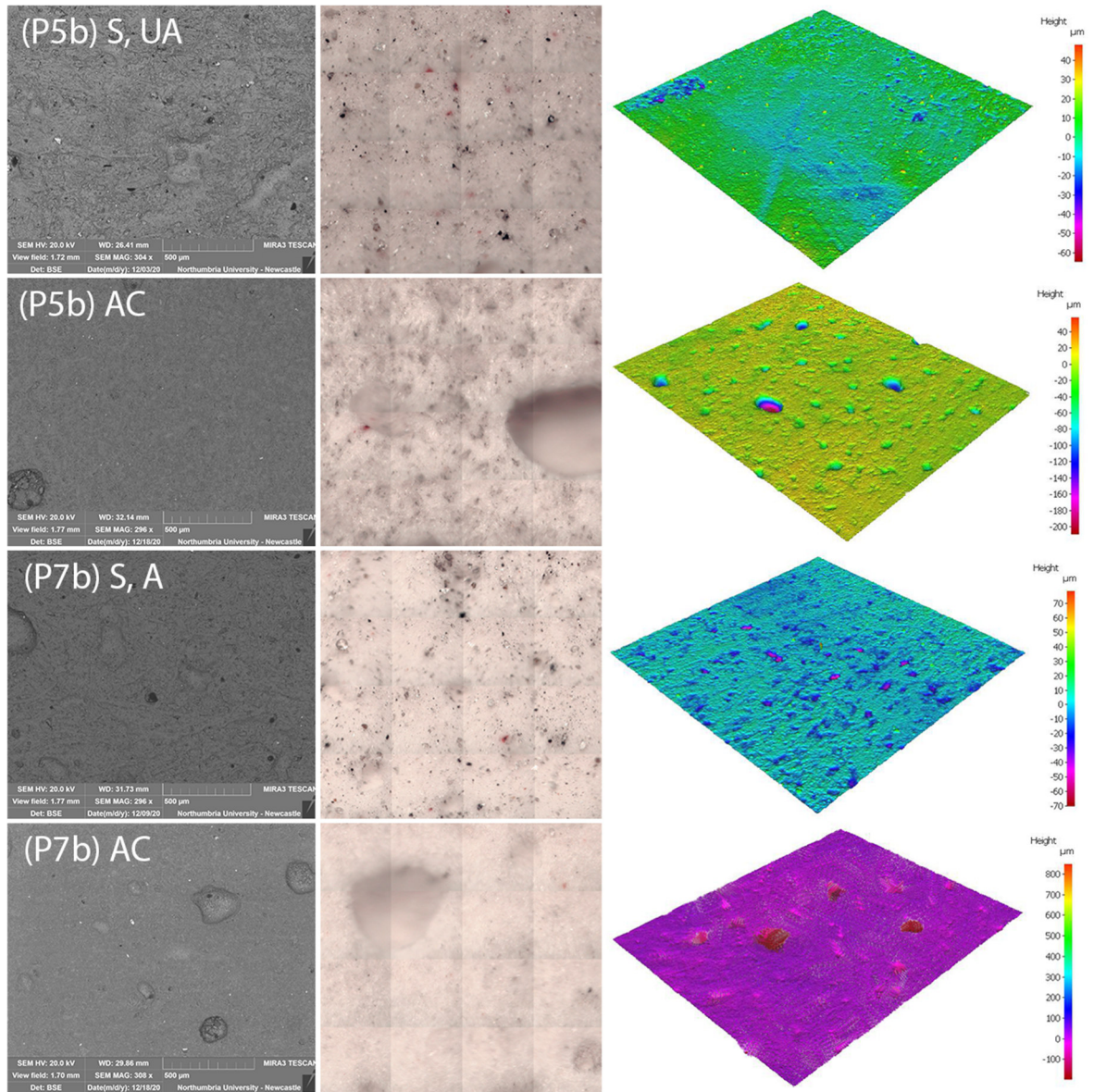


Figure 6.24. From left to right: BSE images (SEM MAG: 300x), FT-IR survey micrographs (1x1 mm) and the HR 3D images (5.3x5.3 mm) of the plaster surfaces coated with shellac6% (2-1) (P5b and P7b) before (S) and after (AC) cleaning with PE-PAM-HCl solution pH 6 (Sol D). A reduction of the quantity of the black particles of soil can be seen after cleaning in all the images. The cleaning was less effective in the unaged areas, as can be observed in the images of the P5b, where soiling particles can still be seen. The smoothing effect shown in the previous images was less pronounced for the areas coated with shellac, possibly because of a harder and drier surface.

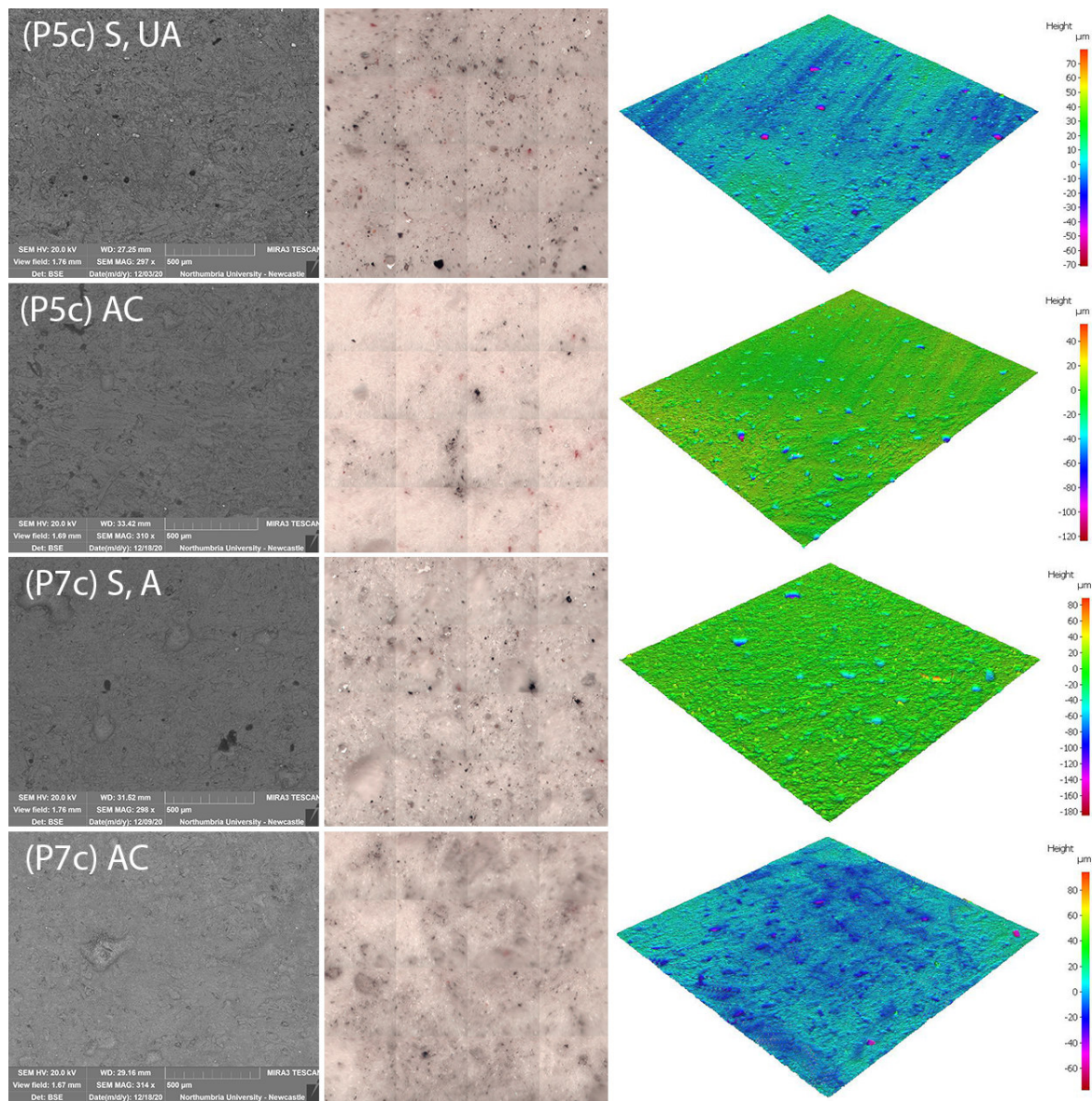


Figure 6.25. From left to right: BSE images (SEM MAG: 300x), FT-IR survey micrographs (1x1 mm) and the HR 3D images (5.3x5.3 mm) of the plaster surfaces coated with shellac18% (2-2) (P5c and P7c) before (S) and after (AC) cleaning with PE-PAM- HCl solution pH 6 Sol D. A reduction of the quantity of the black particles of soil can be seen after cleaning in all the images. A reduction of the quantity of the black particles of soil can be seen after cleaning in all the images. The cleaning was less effective in the aged areas, as can be observed in the images of the P7c, where soiling particles can still be seen. The smoothing effect shown in the previous images was less pronounced for the areas coated with shellac, possibly because of a harder and drier surface.

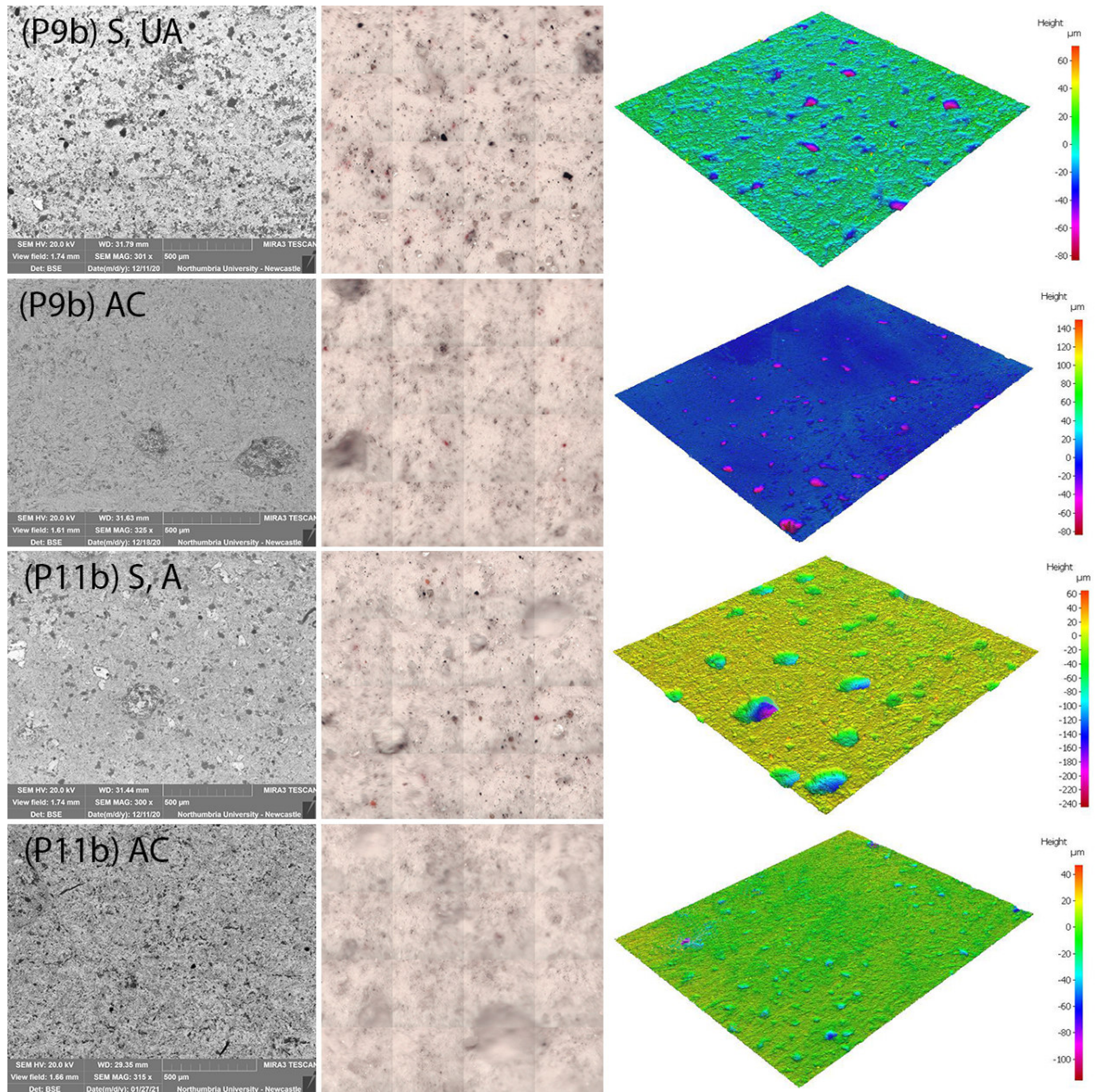


Figure 6.26. From left to right: BSE images (SEM MAG: 300x), FT-IR survey micrographs (1x1 mm) and the HR 3D images (5.3x5.3 mm) of the plaster surfaces coated with barite20° (3-1) (P9b and P11b) before (S) and after (AC) cleaning with PE-PAM-TEA solution pH 8 (Sol A) and -EDTA solution pH 8.5 (Sol H). A reduction of the quantity of the black particles of soil can be seen after cleaning in all the images, and overall very few changes were observed in the texture of the surface.

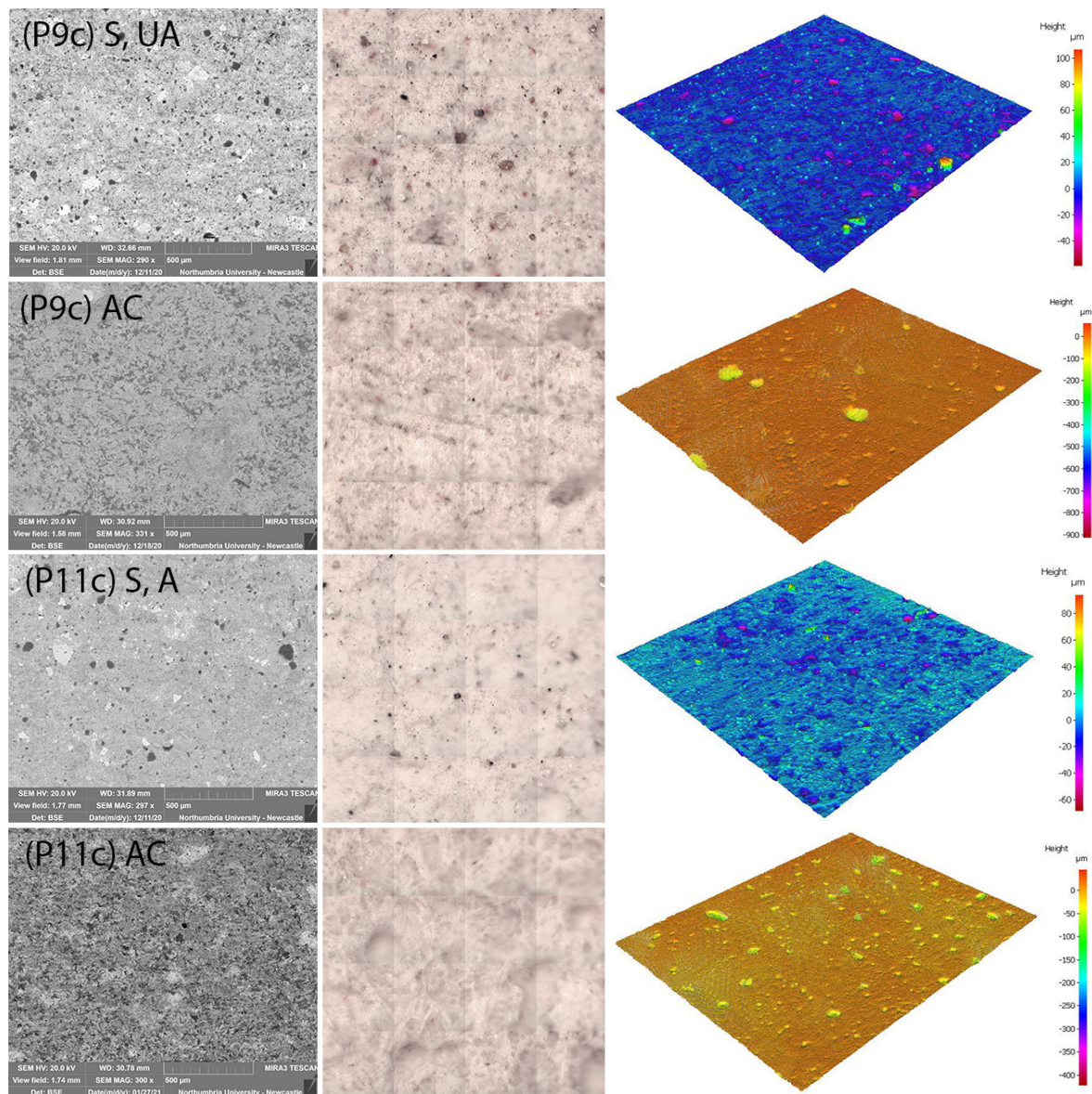


Figure 6.27. From left to right: BSE images (SEM MAG: 300x), FT-IR survey micrographs (1x1 mm) and the HR 3D images (5.3x5.3 mm) of the plaster surfaces coated with barite60° (3-2) (P9c and P11c) before (S) and after (AC) cleaning with PE-PAM-EDTA solution (Sol H). A reduction of the quantity of the black particles of soil can be seen after cleaning in all the images, and overall very few changes were observed in the texture of the surface.

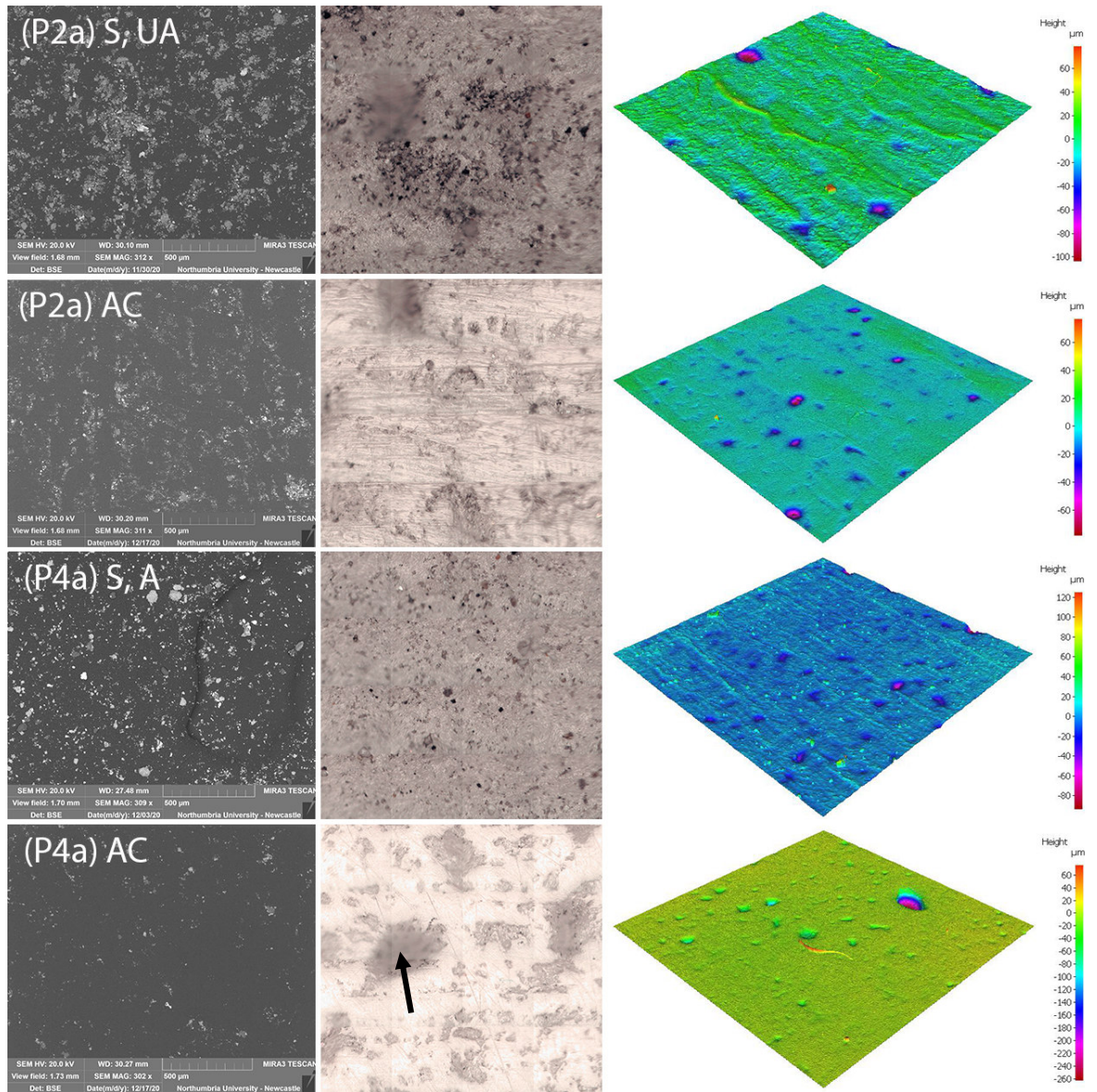


Figure 6.28. From left to right: BSE images (SEM MAG: 300x), FT-IR survey micrographs (1x1 mm) and the HR 3D images (5.3x5.3 mm) of the plaster surfaces coated with beeswax (4) (P2a and P4a) before (S) and after (AC) cleaning with PE-PAM-IMS solution (Sol I). The soil mixture seemed to have been almost entirely removed from both the unaged and aged areas. The soil that was not removed was mostly located in the pores (see for example black arrow in micrograph of area P4a after cleaning). Overall, the cleaning appeared more homogeneous and effective in the aged areas.

6.3.4. COLOUR, GLOSS, AND ROUGHNESS MEASUREMENTS

Reflectance R% and colourimetric measurements in the CIELAB colour space were acquired in SCI and SCE modes but only the SCI data are shown since both SCI and SCE modes generated the same readings (Risdonne & Theodorakopoulos, 2021).

For R%, L*, a*, b* and Gloss85° three measurements for each examined area were averaged to obtain each data point. The ΔE_{00} (Equation 5.5, page 177) is shown in Figures 6.29 and 6.30 (Oleari, 1998). The Yellow Index (YI₃₁₃) was determined (Equation 5.6, page 177) and is shown in Figure 6.31 (Kotwaliwale et al., 2007; Oleari, 1998; Steven, 2005). Gloss measurements are shown in comparison with the soiled areas before cleaning and the

unsoiled relevant areas. Roughness measurements (R_a and R_z , *Section 5.2.2.7*, page 178) were provided by the Bruker Alicona G5 InfiniteFocus (IF) system software. Detailed error propagation definitions can be seen in *Appendix 8* and the database (Risdonne & Theodorakopoulos, 2021).

The most relevant changes in colour after cleaning the soiled areas (*Figure 6.29*) were observed on the areas coated with linseed oil and shellac, with or without beeswax. Colour changes below or close to the *smallest noticeable difference* ($\Delta E_{00} \approx 1$), which defines the limit of the visual perception, were recorded for the areas coated with shellac18% and beeswax (P6c and P8c) and most of the areas coated with barite.

Figure 6.30 highlights that the colour difference between the unsoiled and soiled sections after cleaning is visible and significant. The yellowness of the surfaces can be appreciated by looking at the compared YI_{313} values of the unsoiled and soiled sections before and after cleaning (*Figure 6.31*). The YI values were generally small, and the higher values can be seen for the areas coated with linseed oil and linseed oil-beeswax. The YI values of all the soiled areas were higher than the ones of the relevant unsoiled areas and generally decreased after cleaning. In a few exceptions, particularly in the areas coated with shellac and beeswax, an increase of YI can be seen. In all the areas, the YI were higher in the cleaned areas when compared to the unsoiled sections. This may be due to the yellowing of the surface after ageing, after the initial bleaching (*Section 5.3*).

The resulting gloss of the surface after the removal of the soil would depend on several factors. These include the action of the cleaning materials and their interaction with the soiling and the underlying surface, the mechanical action of the cotton swab and also the own gloss of the original unsoiled plaster substrate. This is demonstrated in *Tables 6.4 to 6.9* and the post-cleaning gloss is shown in *Figure 6.32*. Although the gloss changes before and after soiling vary in the different sections, all readings indicated a significant increase in gloss post-cleaning, particularly in the areas coated with beeswax, possibly due to the cotton swab rolling. This is also suggested by the fact that in several historical manuals it is recommended to polish to surface with fabric after the application of coatings to provide a good gloss (Bankart, 1908; Risdonne *et al.*, 2021; Wager, 1963). On the other hand, the gloss increase in all samples tested, was still low, in the range defining matte surfaces. Regardless, care is suggested during the post-cleaning mechanical removal.

In contrast, the roughness of the surfaces was reduced post-cleaning as shown in *Figure 6.33*. The R_a values of the unsoiled, soiled and the cleaned sections showed that the surfaces were smoothed after cleaning. In a few cases (e.g., P12a and P6b) an increase of roughness is seen, and it can be due to the local porosity. The after-cleaning values can be seen in *Tables 6.4 to 6.9*, the unsoiled and soiled in *Tables 5.5 to 5.11*.

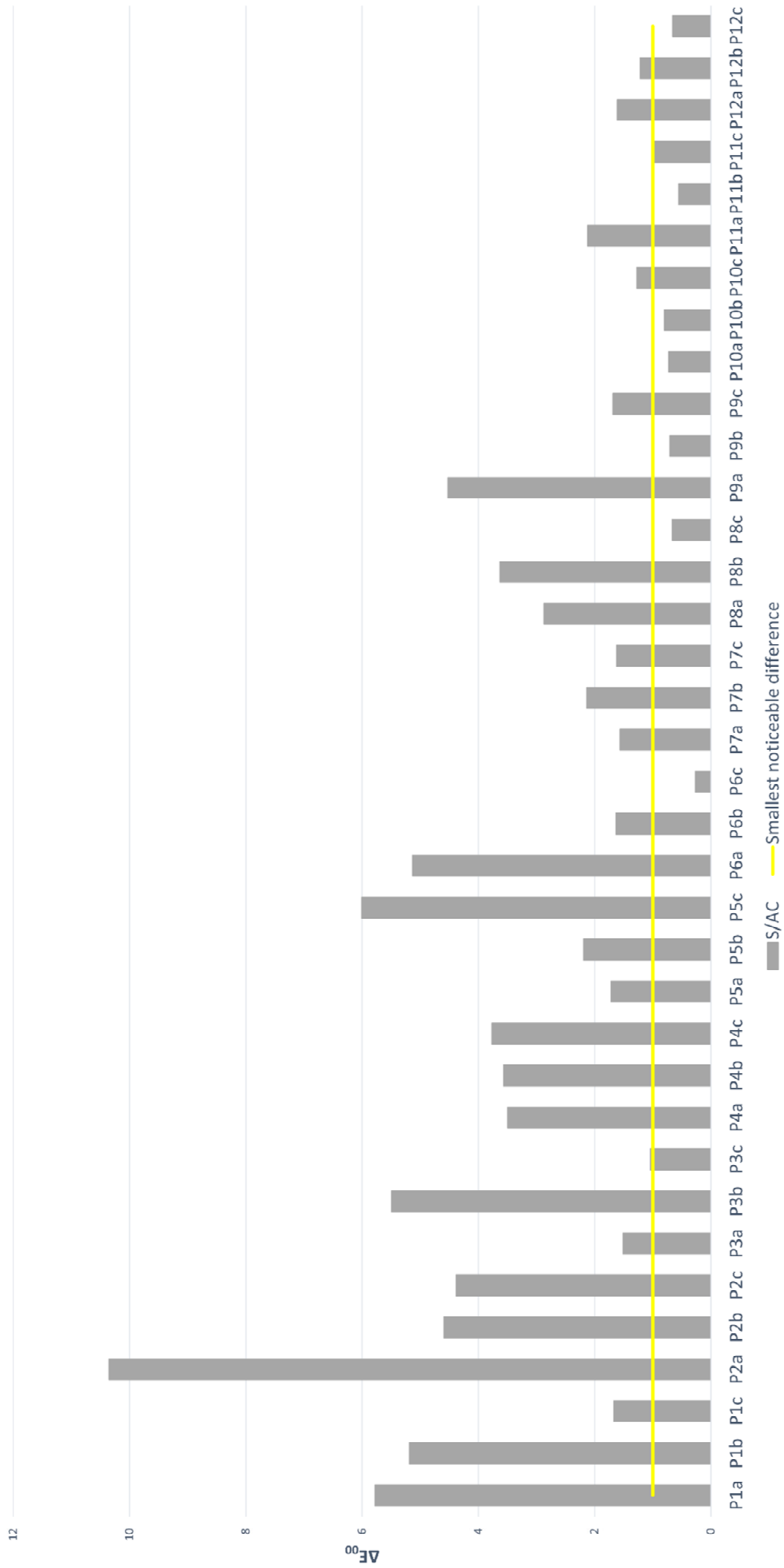


Figure 6.29. Colour changes before(S)/after(AC) cleaning according to CIE formula ΔE_{00} ($\pm 0.4\%$) [SCJ]. The colour change after cleaning is visible in most of the sections. Only in a few areas (P6c, P8c, P9b, P8c, P9b, P10b, P10a, P11b, P12c) the cleaning did not cause a change higher than the smallest visible difference.

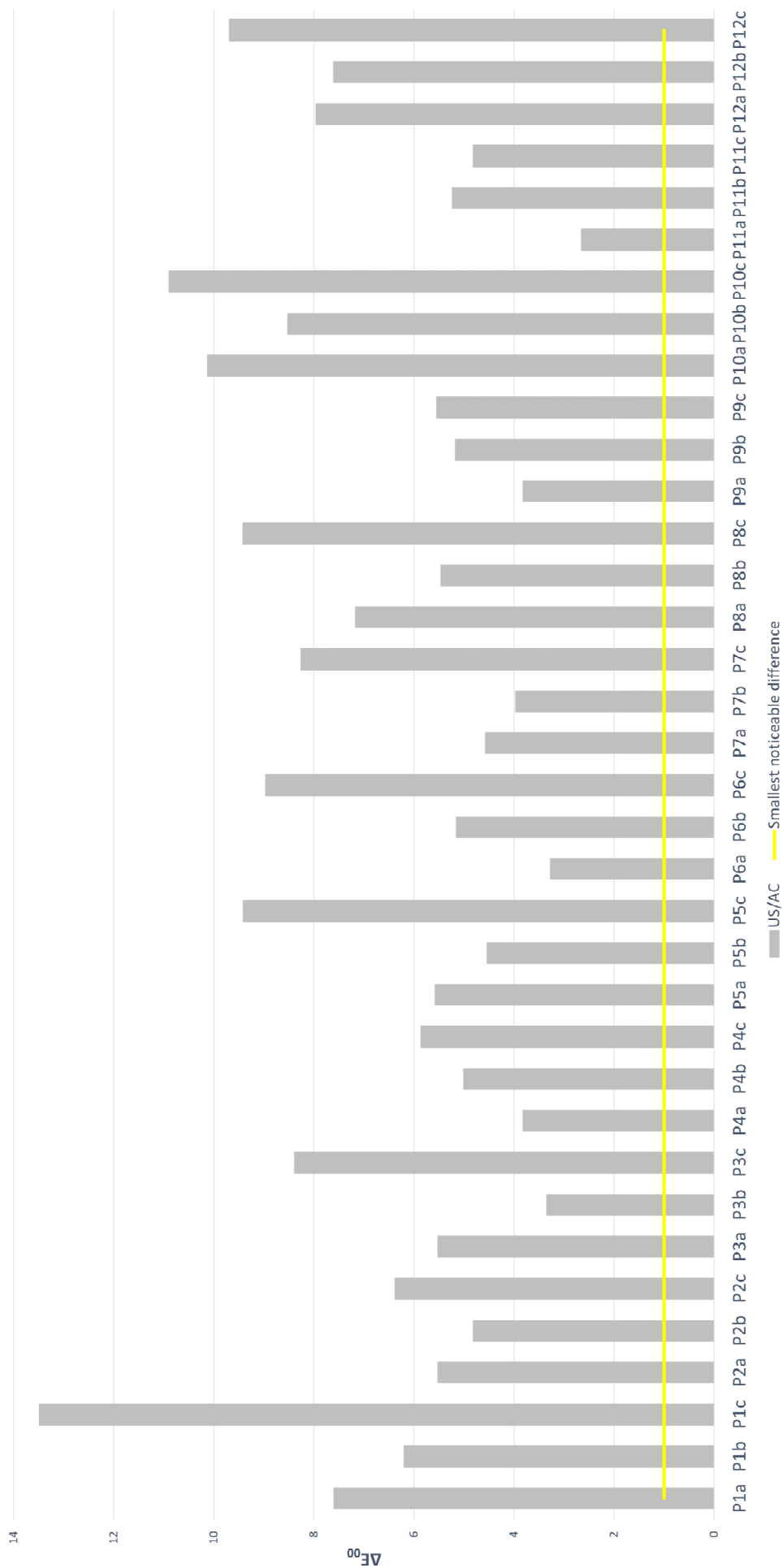


Figure 6.30. Colour differences between the unsoiled (US) areas and the soiled areas after cleaning (AC) according to CIE formula $\Delta E_{00} (\pm 0.4\%) [SCIJ]$. Despite changes in colour after cleaning were observed, as shown in Figure 6.35, the difference in colour between the unsoiled and cleaned areas is noticeable. This is also due to other factors, such as continued ageing and the wetting of the surfaces.

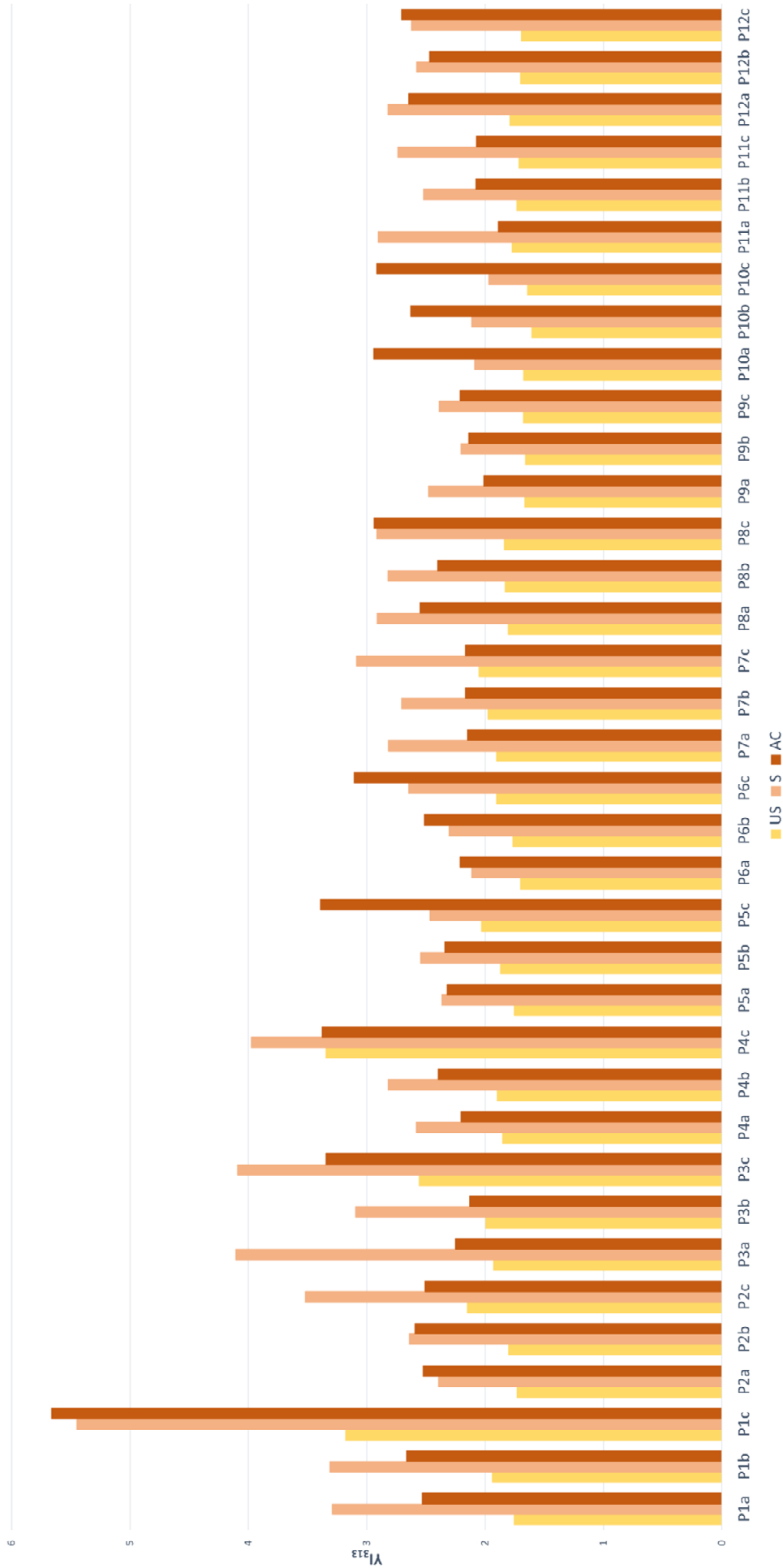


Figure 6.31. Yellow Index (YI_{313}) [SCI] of the unsoiled (US) and soiled sections before (S) and after cleaning (AC). All the soiled sections show a higher YI than the unsoiled relevant section. In most of the sections a decrease of yellowness in the soiled areas before(S)/after(AC) cleaning can be seen. In a few areas (P1c, P2a, P5c, P6a, P6b, P6c, P8c, P10a, P10b, P10c, P12c) an increase of yellowness in observed after cleaning. This can be due to the yellowing of the surface due to ageing, after an initial bleaching highlighted in Section 5.3.

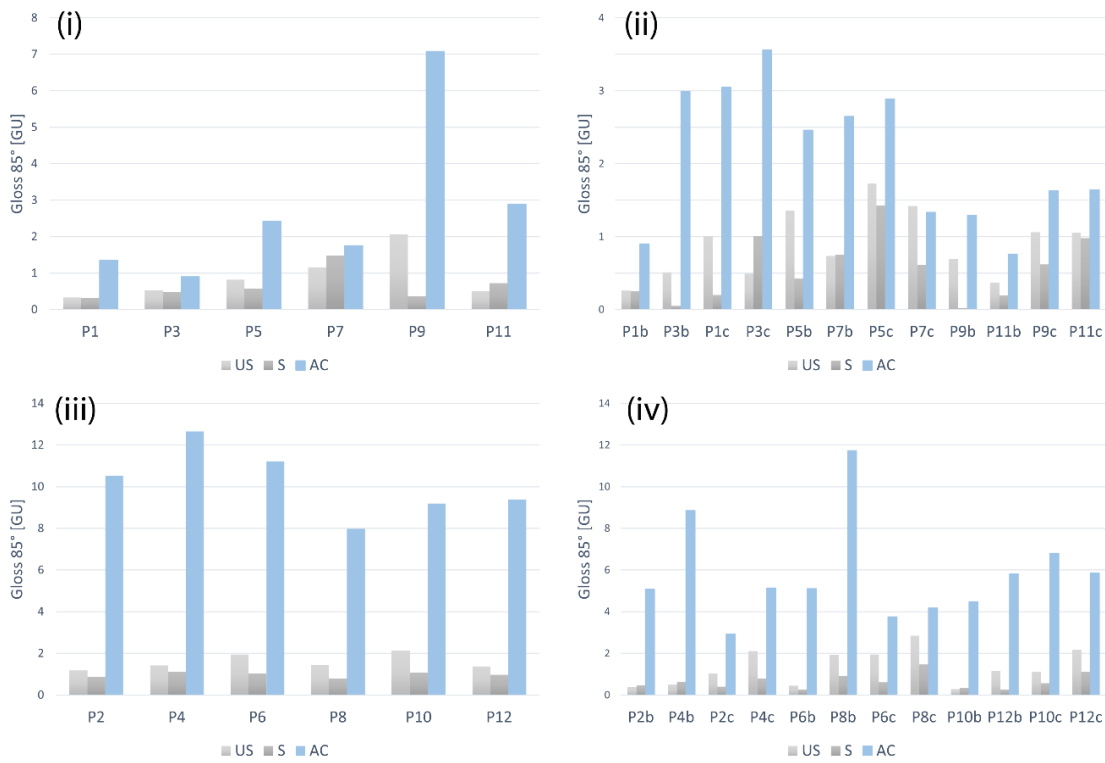


Figure 6.32. Gloss_{85°} of the sections US (grey), S (dark grey) and AC (blue) showed that a significant increase of gloss is achieved after cleaning. The AC values can be seen in Tables 6.4 to 6.9, the US and S in Tables 5.5 to 5.11. Plot (i) shows Gloss_{85°} of the uncoated plaster sections, (ii) of the sections coated with linseed oil, shellac and barite and (iii) and (iv) the respectively relevant sections also coated with beeswax.

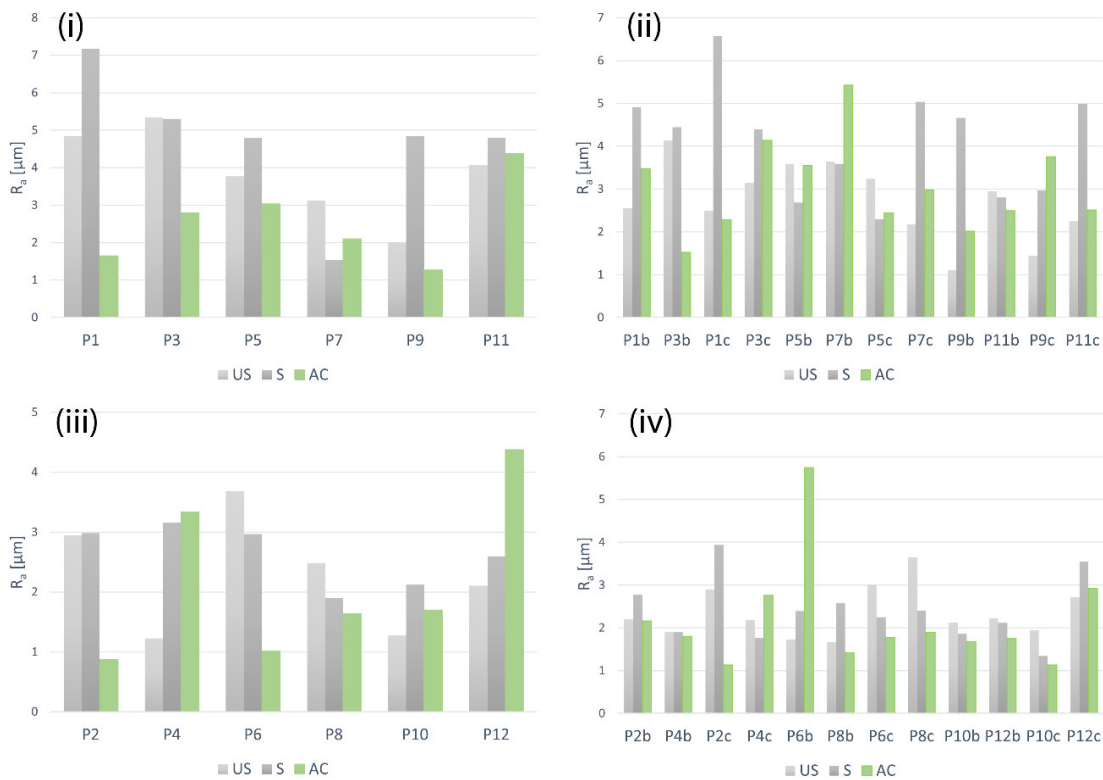


Figure 6.33. R_a of the sections US (grey), S (dark grey) and AC (green) showed that overall, the surfaces were smoothed after cleaning (AC). In a few cases (e.g., P12a and P6b) an increase of roughness is seen, and it can be due to the local porosity. The AC values can be seen in Tables 6.4 to 6.9, the US and S in Tables 5.5 to 5.11. Plot (i) shows R_a of the uncoated plaster sections, (ii) of the sections coated with linseed oil, shellac and barite and (iii) and (iv) the respectively relevant sections also coated with beeswax.

Reflectance (%) (± 0.05 %) (Figures 6.34 to 6.37) measured after cleaning from the areas coated with linseed oil, shellac and barite are compared to the relevant sections unsoiled, soiled, unaged and aged. After cleaning the R% was not particularly different in the areas coated with boiled linseed oil (1-2) and barite (3-1 and 3-2), but was intermediate between the unsoiled and soiled values after cleaning for cold-pressed linseed oil (1-1) and shellac (2-1 and 2-2).

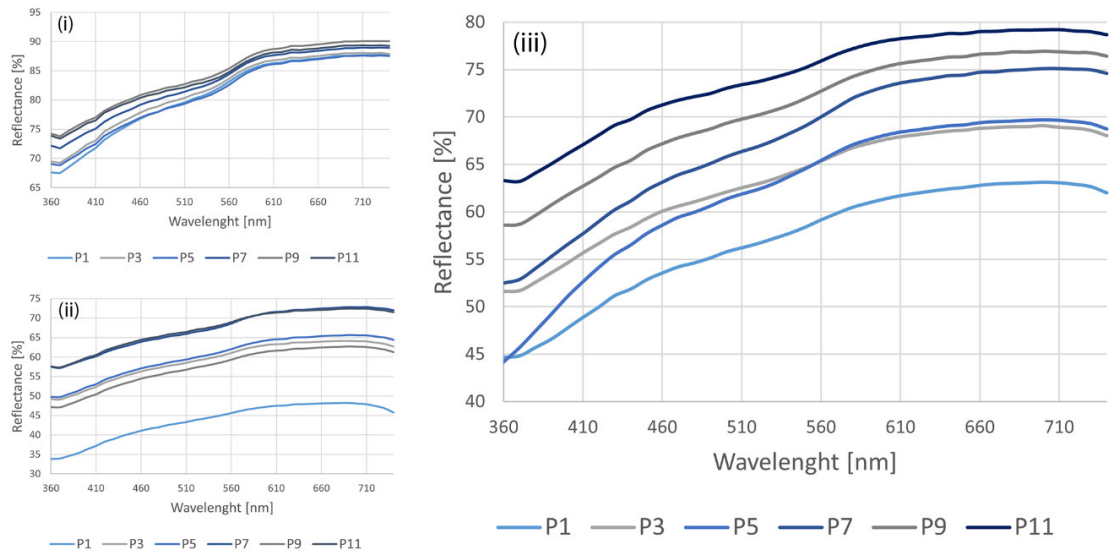


Figure 6.34. R (%) (± 0.05 %) [SCI] measured from the uncoated areas before cleaning (plaster+soiling, a) (ii) and after cleaning (uncoated plaster, a) (iii). R% of the uncoated unsoiled plaster (d) (i) is also shown for reference. The areas belong to the plaster control sections of P1, 5 and 9 (UA) and P3, 7 and 11 (A). The R% of the cleaned areas shows intermediate values between the ones of the US and S areas.

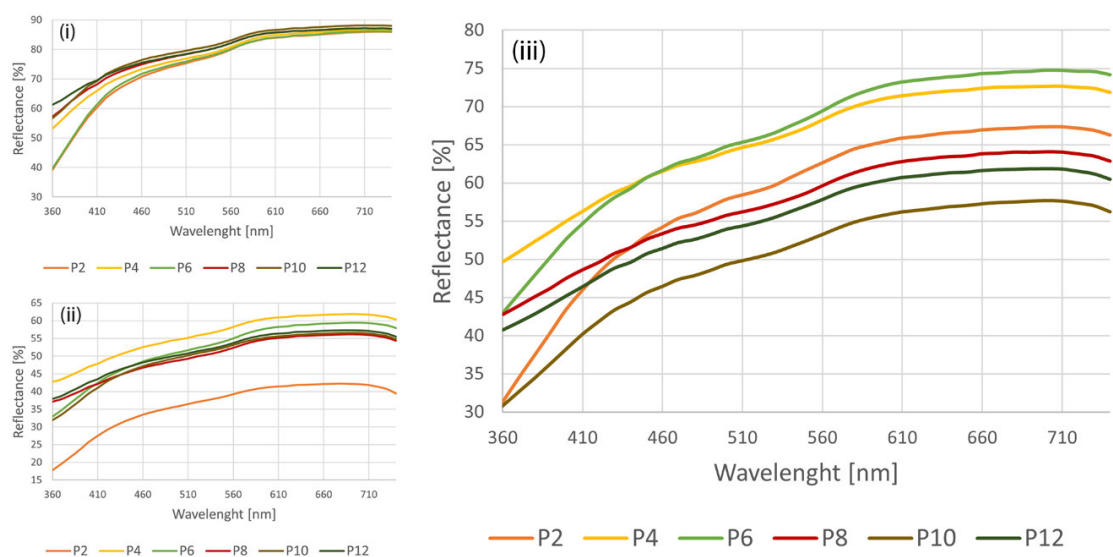


Figure 6.35. R (%) (± 0.05 %) [SCI] measured from of the areas coated with beeswax before cleaning (plaster and beeswax+soiling, a) (ii) and after cleaning (beeswax, a) (iii). R% of the unsoiled plaster coated with beeswax (d) (i) is also shown for reference. The areas belong to the plaster-beeswax control sections of P2, 6 and 10 (UA) and P4, 8 and 12 (A). The R% of the cleaned areas shows intermediate values between the ones of the US and S areas.

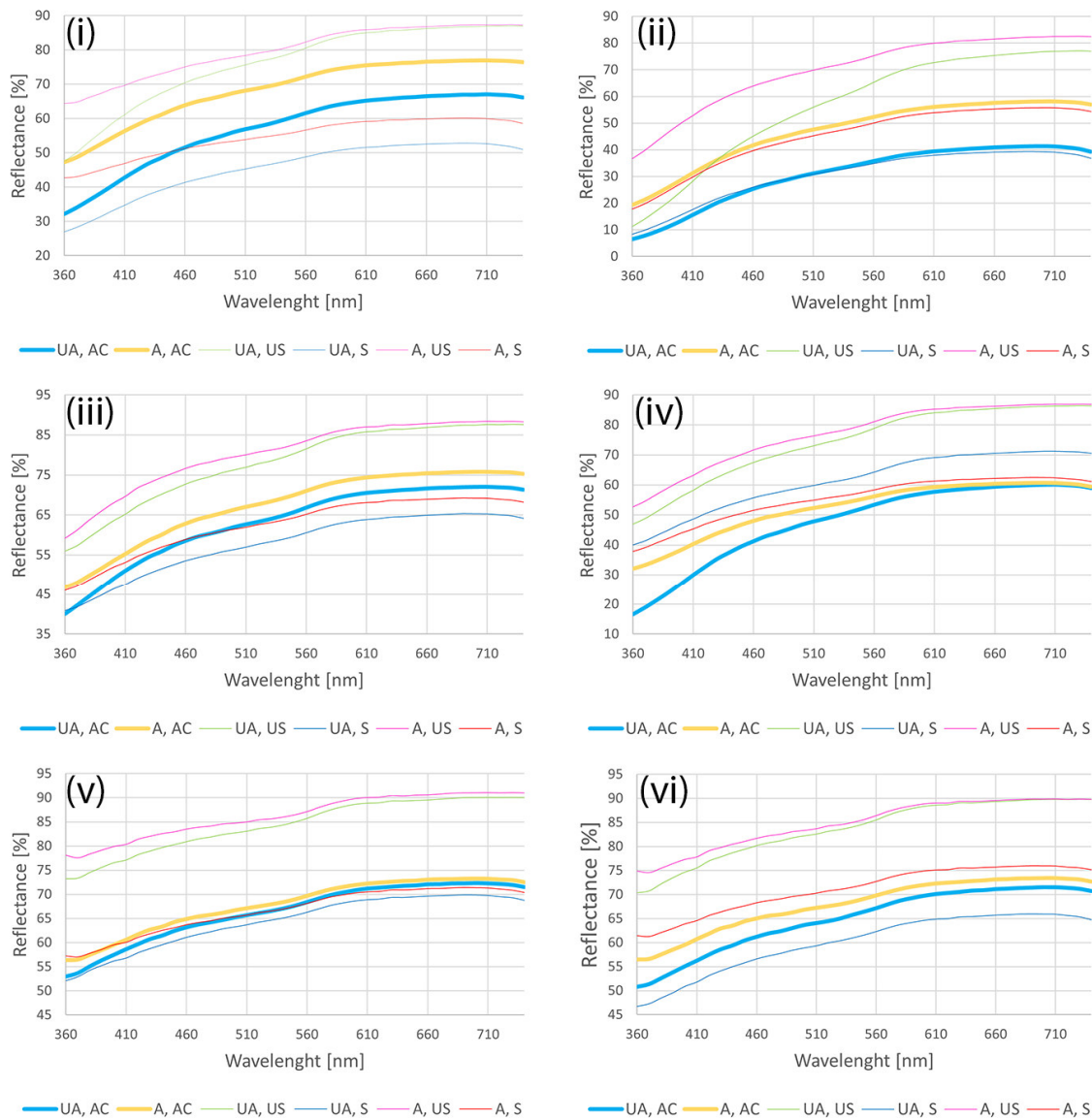


Figure 6.36. Reflectance (%) (± 0.05 %) [SCI] measured from the areas coated with cold-pressed linseed oil (i), boiled linseed oil (ii), shellac6% (iii), shellac18% (iv), barite20° (v) and barite60° (vi) after cleaning (AC) are compared to the relevant sections US, S, UA and A. After cleaning the R% was not particularly different in the areas coated with boiled linseed oil (ii) and barite (v and vi) and was intermediate between the US and S values after cleaning for cold-pressed linseed oil (i) and shellac (iii and iv).

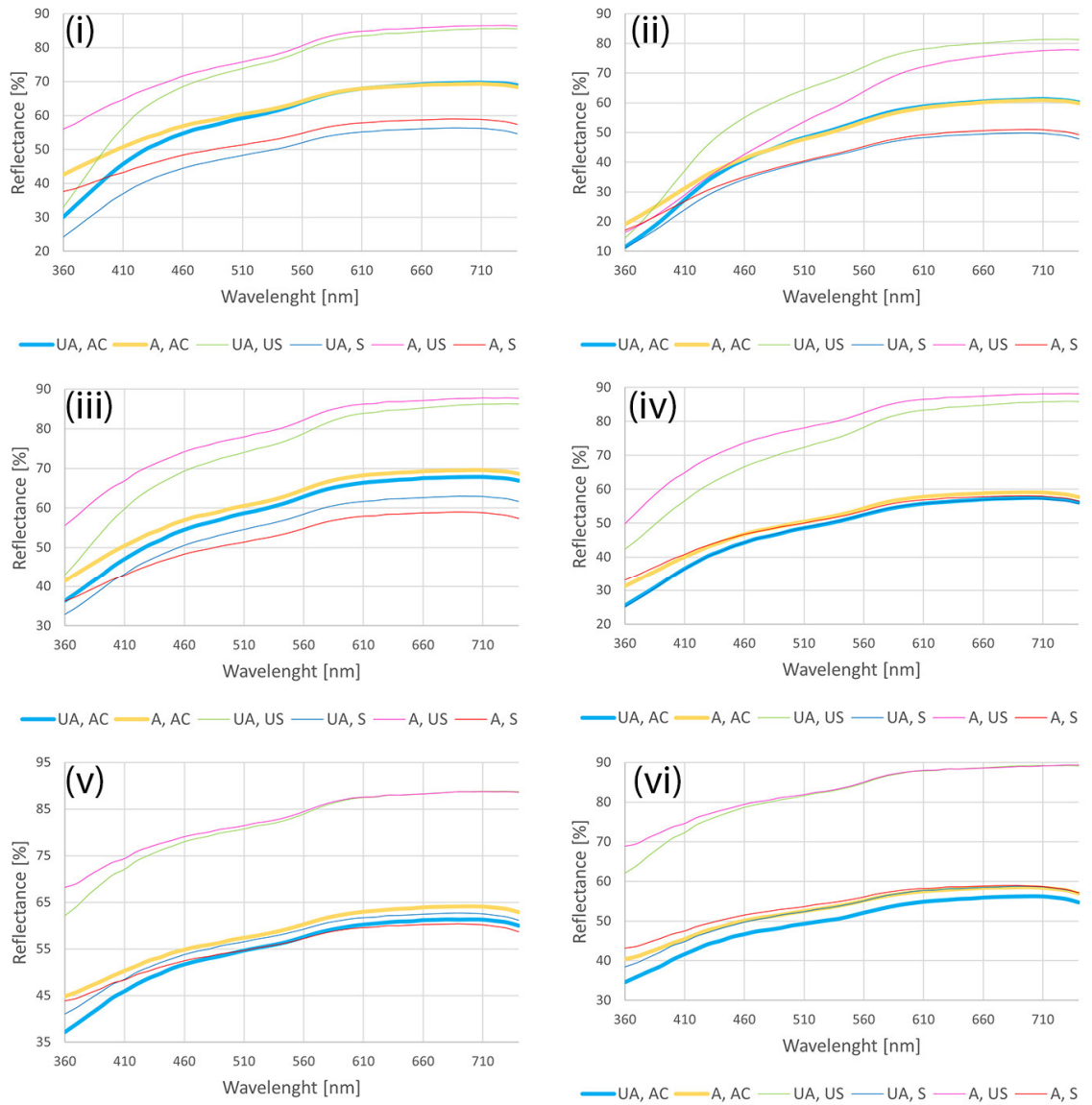


Figure 6.37. Reflectance (%) (± 0.05 %) [SCI] measured from of the areas coated with cold-pressed linseed oil (i), boiled linseed oil (ii), shellac6% (iii), shellac18% (iv), barite20° (v) and barite60° (vi) and beeswax after cleaning (AC) are compared to the relevant sections US, S, UA and A. After cleaning the R% was not particularly different in the areas coated with boiled linseed oil (ii), shellac18%(iv) and barite (v and vi), but was intermediate between the US and S values after cleaning for cold-pressed linseed oil (i) and shellac6% (iii).

Table 6.4. Summary of measurements acquired from the uncoated plaster surfaces a (S) of the unaged (P1, 5 and 9) and aged (P3, 7 and 11) plates after cleaning.

		P1	P3	P5	P7	P9	P11
R [%] (± 0.05 %)	min	44.63	51.62	44.20	52.49	58.61	63.29
	max	63.14	69.10	69.69	75.12	76.95	79.19
L* (± 0.05)		81.01	84.35	84.25	86.66	88.03	89.56
a* (± 0.001)		1.31	1.23	1.36	1.68	1.32	1.05
b* (± 0.01)		5.65	5.05	6.51	6.26	4.91	3.98
YI₃₁₃		2.53	2.25	2.32	2.15	2.01	1.89
Gloss85° [GU] (± 0.1 GU)		1.35	0.90	2.42	1.75	7.08	2.89
R_a [μm] (± 0.3 μm)		1.65	2.80	3.03	2.10	1.27	4.38
R_z [μm] (± 0.05 %)		10.27	20.46	17.87	12.14	8.70	30.87

Table 6.5. Summary of measurements acquired from the plaster surfaces coated with linseed oil, sections b (1-1) and c (1-2), unaged (P1) and aged (P3), after cleaning.

		P1b	P3b	P1c	P3c
R [%] (± 0.05 %)	min	44.48	47.30	6.65	19.34
	max	67.06	76.95	41.41	58.08
L* (± 0.05)		82.01	87.58	65.42	76.68
a* (± 0.001)		1.33	1.73	1.47	1.16
b* (± 0.01)		10.11	7.53	16.68	12.55
YI₃₁₃		2.66	2.13	5.66	3.34
Gloss85° [GU] (± 0.1 GU)		0.90	2.99	3.05	3.56
R_a [μm] (± 0.3 μm)		3.48	1.52	2.29	4.13
R_z [μm] (± 0.05 %)		28.52	9.98	15.74	28.01

Table 6.6. Summary of measurements acquired from the plaster surfaces coated with shellac, sections b (2-1) and c (2-2), unaged (P5) and aged (P7), after cleaning.

		P5b	P7b	P5c	P7c
R [%] (±0.05 %)	min	40.02	46.81	16.66	32.06
	max	71.99	75.80	60.09	60.72
L* (±0.05)		84.87	87.03	77.23	79.15
a* (±0.001)		1.56	1.21	1.54	1.16
b* (±0.01)		7.96	7.52	14.05	8.88
YI₃₁₃		2.34	2.17	3.39	2.17
Gloss85° [GU] (±0.1 GU)		2.46	2.65	2.89	1.33
R_a [µm] (±0.3 µm)		3.55	5.43	2.44	2.98
R_z [µm] (±0.05 %)		23.33	31.70	18.42	16.04

Table 6.7. Summary of measurements acquired from the plaster surfaces coated with barite, sections b (1-1) and c (1-2), unaged (P9) and aged (P11), after cleaning.

		P9b	P11b	P9c	P11c
R [%] (±0.05 %)	min	52.98	56.37	50.78	56.52
	max	72.31	73.22	71.52	73.44
L* (±0.05)		85.93	86.58	85.26	86.63
a* (±0.001)		1.24	1.18	1.34	1.19
b* (±0.01)		4.89	4.40	5.57	4.34
YI₃₁₃		2.14	2.08	2.21	2.07
Gloss85° [GU] (±0.1 GU)		1.29	0.76	1.63	1.64
R_a [µm] (±0.3 µm)		2.01	2.49	3.75	2.51
R_z [µm] (±0.05 %)		15.76	14.30	20.88	16.63

Table 6.8. Summary of measurements acquired from the plaster surfaces coated with beeswax (4) a (S) of the unaged (P2, 6 and 10) and aged (P4, 8 and 12) after cleaning.

		P2	P4	P6	P8	P10	P12
R [%] (±0.05 %)	min	31.30	49.67	42.94	42.78	30.83	40.71
	max	67.33	72.66	74.75	64.06	57.69	61.85
L* (±0.05)		82.67	85.73	86.28	81.24	77.52	80.16
a* (±0.001)		1.29	1.57	1.70	1.73	1.46	1.54
b* (±0.01)		8.38	6.11	7.20	6.28	7.50	6.50
YI₃₁₃		2.52	2.20	2.21	2.55	2.94	2.65
Gloss85° [GU] (±0.1 GU)		10.53	12.65	11.21	7.98	9.19	9.38
R_a [µm] (±0.3 µm)		0.87	3.34	1.01	1.64	1.70	1.57
R_z [µm] (±0.05 %)		6.11	26.42	7.17	9.97	10.82	9.67

Table 6.9. Summary of measurements acquired from the plaster surfaces coated with coatings (1, 2 or 3) and beeswax (4) a (S) of the unaged (P2, 6 and 10) and aged (P4, 8 and 12) after cleaning.

		P2b	P4b	P2c	P4c	P6b	P8b	P6c	P8c	P10b	P12b	P10c	P12c
R [%] (±0.05 %)	min	30.1 8	42.5 7	11.4 7	19.1 8	36.3 3	41.3 9	25.4 7	31.2 2	37.1 9	44.8 6	34.5 8	40.3 8
	max	69.6 6	69.3 6	61.2 6	60.9 4	67.8 3	69.5 6	57.4 5	59.0 9	61.3 7	64.1 3	56.2 4	58.5 0
L* (±0.05)		83.3 4	83.6 9	77.6 4	77.3 8	82.8 2	83.8 1	76.9 7	78.1 6	80.1 4	81.6 6	76.9 8	78.7 8
a* (±0.001)		1.75	1.76	1.38	2.07	1.52	1.75	1.42	1.69	1.18	1.38	1.50	1.20
b* (±0.01)		9.14	7.20	15.6 9	13.9 2	8.30	7.47	9.32	8.43	6.25	5.44	6.08	5.43
YI₃₁₃		2.59	2.40	2.51	3.38	2.61	2.40	3.11	2.94	2.63	2.47	2.92	2.71
Gloss85° [GU] (±0.1 GU)		5.08	8.86	2.91	5.13	5.10	11.7 3	3.75	4.17	4.47	5.81	6.80	5.86
R_a [µm] (±0.3 µm)		2.16	1.80	1.13	2.75	5.74	1.42	1.78	1.89	1.68	1.76	1.13	2.92
R_z [µm] (±0.05 %)		11.3 7	13.8 1	5.88	19.2 7	38.0 9	9.26	11.4 7	11.6 6	10.4 4	11.6 1	8.91	15.9 3

6.3.5. FOURIER-TRANSFORM INFRARED SPECTROSCOPY (FT-IR)

The FT-IR molecular characteristics of the uncoated plaster surfaces and the areas coated with linseed oil, shellac, barite water and beeswax, unsoiled and soiled were discussed in *Section 5.3.5* (page 212). No consistent changes in the FT-IR patterns were highlighted on the surfaces after cleaning. The unique identification of peaks related to the soiling admixture that might have disappeared after cleaning was not possible in this case as the peaks assigned to the soiling were many and varied. Overall, the molecular fingerprint of the analysed areas is unchanged after cleaning. An example is shown in *Figure 6.38* and the full record can be seen in the database (Risdonne & Theodorakopoulos, 2021)

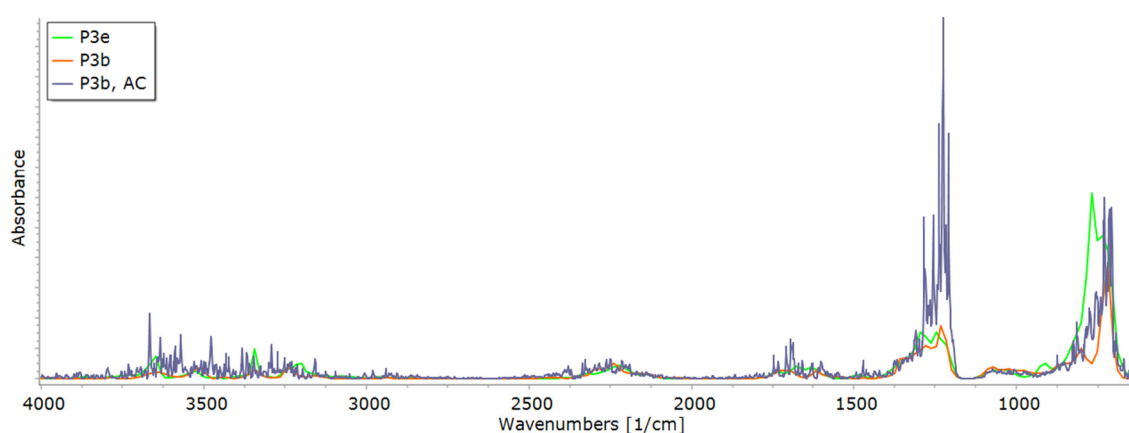


Figure 6.38. FT-IR spectra acquired on the aged areas coated shellac6% unsoiled (P3e), soiled (P3b) and cleaned (P3b, AC). The spectra are consistent and small differences can be seen.

6.3.6. SUMMARY OF RESULTS

A summary of the results discussed in this chapter is provided in *Table 6.10*, to further recap the findings and highlight the effectiveness of the polyolefin-supported hydrogels (PE-PAM) in combination with the solutions described in *Section 6.2.1.2* (pages 239-40) for the removal of soiling from the different mock-up coated plaster surfaces. Details to support and understand the observations in the summary below can be found in *Sections 6.3.1 to 6.3.5*.

Table 6.10. Summary of observations on the effectiveness of the polyolefin-supported hydrogels (PE-PAM) in combination with the solutions described in Section 6.2.1.2 (pages 239-40) for the removal of soiling from the different mock-up coated plaster surfaces.

Surface	Condition	Solution	Effectiveness*	Observations
Uncoated gypsum plaster	Unaged	P1a: Sol B; P5a: Sol D; P9a: Sol A.	++, uneven	Smoothing
	Aged	P3a: Sol B; P7a: Sol D; P11a: Sol A	+++	Smoothing
Cold-pressed linseed oil	Unaged	Sol H	++	Smoothing
	Aged	Sol H	+++	Smoothing
Boiled linseed oil	Unaged	Sol B	+	Smoothing
	Aged	Sol B	++	Smoothing
Shellac6%	Unaged	Sol D	+, uneven	Smoothing
	Aged	Sol D	++, uneven	Smoothing
Shellac18%	Unaged	Sol D	++, uneven	Smoothing
	Aged	Sol D	+, uneven	Smoothing
Barite20°	Unaged	Sol A	-/+	Uneven absorption of the cleaning solution
	Aged	Sol H	-/+	Uneven absorption of the cleaning solution
Barite60°	Unaged	Sol H	-/+	Uneven absorption of the cleaning solution
	Aged	Sol H	-/+	Uneven absorption of the cleaning solution
Beeswax	Unaged	Sol I	++	Soil in the pores, micro-scratches
	Aged	Sol I	+++	Soil in the pores, micro-scratches

* the effectiveness of the cleaning method is in this table rated in terms of progressively positive (+, ++, +++) or negative (-, --, ---) outcome.

6.4. CONCLUSION

Plaster characteristics, such as porosity and water absorption behaviour, greatly affect the casts deterioration and must be considered when selecting an appropriate surface cleaning treatment. The novel cleaning technique selected in this study is based on the use of polyolefin-supported hydrogels (PE-PAM), which was chosen to allow minimal wetting, critically reducing the disadvantages of liquid-based cleaning on liquid-sensitive surfaces. The hydrogels were used to remove the soil applied onto the coated plaster surfaces mock-ups and preserve the coatings. Aqueous solutions were selectively prepared to swell the surface coatings and remove the soil. The assessment of the effectiveness of the cleaning method was carried based on the visual, morphological and spectral evaluation. The cleaning after one application showed positive results, with the partial removal of the soil. It was particularly effective in the less porous areas, which were the ones coated with beeswax. In these areas, the cleaning procedure achieved the removal of a significant portion of the soiling just after one application. The best results were observed in the aged areas, where the soil was less attached to the coating. The uncoated areas and the areas coated with barite seemed to have absorbed the solutions too quickly for the cleaning method to be fully effective. A partial dissolution and recrystallization of the plaster substrate have been postulated in these areas, despite the minimal quantity of liquid released by the hydrogels (*Section 6.3.3*). This leaves the possibility of greater liquid-induced damage on the plaster surfaces when traditional wet methods are used. Testing the polyolefin-supported hydrogels on plaster surfaces showed promising results, suggesting that further development of this method could unfold novel approaches for the removal of soils from historical plaster casts. In this Chapter, **objectives 8** and **9** were addressed.



CHAPTER 7

CONCLUSIONS

7.1 THE RESEARCH QUESTIONS

This study aimed to investigate a selection of nineteenth-century plaster casts from the iconic Victoria and Albert Museum collection through the analysis of their coatings, applied to ensure a desired appearance and durability, to understand the Victorian manufacturing techniques. In addition, a novel conservation treatment was tested to assess the efficacy of new safe and effective methodologies for the removal of soils from their surfaces.

The practice of making replicas with plaster was extremely popular in the nineteenth century and often the casts were coated to improve the surface properties or to change the casts' appearance. Despite the popularity of the practice, historical plaster casts' coatings have not been studied in detail so far. Research on plaster casts and their conservation has been largely undertaken with a case-by-case approach, and scientific background information on the casts is scarce and fragmentary. The V&A's Cast Court collection has never been examined systematically from a scientific and material point of view, although a lot has been invested in its conservation in the latest 20 years, suggesting that detailed scientific research was required to support the preservation and conservation of the surfaces of the casts and to achieve a better understanding of the objects' manufacturing (*Chapter 1*).

The Art and Humanities Research Council (AHRC) Collaborative Doctoral Partnership (CDP) of Northumbria University with the V&A Museum generated the unique opportunity to examine the collection of the Cast Courts, which has inspired artists and museums around the world for almost two centuries. While adding information to the knowledge available on the composition and deterioration of these materials, this was also an opportunity to prompt a critical review of the casts manufacturing and the treatments that have been undertaken so far, and to design a scientific methodology for the study of the casts, also based on the understanding of the nineteenth-century literature, that may be employed for the evaluation of conservation treatments within and beyond the Museum.

The research questions of the research were:

- What were the original historic materials and methods employed to make the nineteenth-century plaster casts? What were the possible purposes of coating the nineteenth-century plaster casts?
- The V&A's collection has a variety of sources in different countries, through direct purchase, exchange and commission. Is it possible to identify differences between

recipes used in different countries? The casts have had several periods of treatments since their early display. Can we distinguish between the original coatings and later restorations?

- How does a greater understanding of coatings' colour contribute to understanding the surface deterioration and designing the objects' preservation and conservation?

The research methodology was based on an interdisciplinary approach which was presented in *Chapter 2*, and allowed to achieve the following:

- the understanding of the nineteenth-century historical practices for coating plaster casts through archival research (*Chapter 3*);
- the characterization of the surface layers of the V&A plaster casts through scientific investigation (*Chapter 4*);
- the preparation, accelerated ageing and study of purpose-made reconstructions (*Chapter 5*);
- the cleaning of the reconstructions with novel surface-attached nano-thin gel films (*Chapter 6*).

Beyond the evidential specificity, this research allowed to define a methodology for the study of the nineteenth-century coated plaster casts. This work is intrinsically multidisciplinary as it stands at the intersections of the research fields of art technology, technical art history, material science and art conservation and every chapter relate to the other. This research can lead to improved knowledge of the materials and the techniques in use in the nineteenth century (and therefore to a better knowledge of the society that hosted them) as well as to aid the conservators and museum managers.

7.2 HISTORIC MATERIALS AND THEIR PURPOSES

The investigation of the history of the Cast Courts to understand the historical coatings background represented **Objective 1** of this work. This was achieved in Chapter 1, where several topics related to the background to the study of the replica, historical plaster casts and the Casts Courts, were discussed. The preliminary background research also allowed to understand the importance of making plaster casts in the nineteenth century, the variety of the collections in the world and the relevance of the V&A collection. Furthermore, the research undertaken for the background allowed informed decisions on the selection of the historical literature for the review (*Chapter 2*).

Objective 2 consisted in the thorough review of representative historical technical literature to ensure the understanding of the workshop practices during the nineteenth century; **Objective 3** was the study of the historical recipes for the coating of the nineteenth-century plaster cast from representative sources, to understand the techniques and materials, as well as hypothesise the purpose of their application and their effect on the preservation of the casts. These objectives were achieved in *Chapter 3* through the review of the historical sources.

Archival resources and historical literature were explored to contextualise the technological information, and seventeen manuals or historical books and fourteen patents focused on plaster casting or in some way related to this technology were selected to be reviewed for this study (*Chapter 3*). V&A conservators reported having found more than 84 traditional recipes for the coatings on the surfaces and additives to the plaster when observing the V&A's cast. The review of the selected recipes' books and the patents allowed a better understanding of the availability, application and properties of the materials used to produce plaster casts in the nineteenth century. A great variety and quantity of recipes for making and coating the casts were found in the selected historical technical literature.

Two types of plaster were consistently described in the literature: lime and gypsum plaster. Gypsum plaster is suggested as the most used material for making plaster casts. Numerous mineral inclusions are documented in the gypsum plaster mixture and inorganic and organic additives can be accidentally or intentionally added to the plaster mixture. When intentionally added, the additives are meant to accelerate or retard the setting time or improve mechanical properties. Four main types of casting techniques were found in the literature, named after the type of moulds they use: waste, gelatine, piece and wax. A range of separating agents, from oils, soaps and resins to clay water, that may have been used during the casting processes was also listed. The main purposes for applying the coating in the nineteenth century were identified in the historical literature and patents: sealing the pores, waterproofing the surface, hardening the surface, and changing the appearance.

Often a type of coat was applied to serve multiple purposes. More than eighty organic and inorganic materials, pure or in combination with each other's, were mentioned in the over a hundred recipes retrieved for this study.

The selected sources ranged from the first century to the 1990s and it was interesting to observe that many recipes recur across the sources, suggesting that many practices were established, despite the secrecy of the workshops. Nonetheless, no mention to workshop specific practices was found in the manuals.

Analytical information is in need to support the conservators' observations and literature sources. As understanding and preserving this much-loved collection is fundamental, close observation and conservation of the casts were carried out alongside the renovation of the galleries, leading to a better understanding of the objects' manufacturing, but also spurring many questions on the surfaces' composition.

7.3 ORIGINAL AND MODERN MATERIALS

A complete scientific examination of selected nineteenth-century plaster casts from the V&A collection, to acquire full information on the manufacturing, the structural materials and in particular the coatings constituted **Objective 4**. The techniques employed to address this objective are optical microscopy (OM), XRD, SEM-EDS, Fourier Transformed – Infrared spectroscopy (FT-IR) and py-GC/MS. **Objective 5** was the review and comparison of the results of the characterization of the casts, highlighting similarities and differences between cast from different workshops. These objectives were addressed in *Chapter 4*.

The multi-analytical approach was designed for the scientific examination of the V&A casts, allowing to identify the stratigraphy and characterise the inorganic and organic components of the surface layers (*Chapter 4*). Twelve plaster casts, grouped according to the workshop and provenance (Küsthardt, Notre-Dame and Franchi Group), were observed and documented. The analytical method employed included Optical microscopy (visible and ultraviolet, VLR OM and UVf OM), Scanning Electron Microscope-Electron Dispersive X-ray Spectroscopy (SEM-EDS), X-ray Diffraction (XRD), Attenuated Total Reflectance (ATR) and Diffuse Reflectance Imaging (DRI) Fourier Transform Infrared (FT-IR) Spectroscopy, Gas Chromatography / Mass Spectrometry (GC/MS) and Pyrolysis GC/MS. The analyses were undertaken to establish the stratigraphy and the layer compositions of the objects.

The stratigraphy in all objects was consistently made of three layers: a bulk, a coating and their interface. Several types of additional coatings were observed, which must have been applied at a later stage after the construction of the casts when seen over a layer of dirt. The bulk is made of calcium sulfate (gypsum plaster). Between the surface layers and the bulk, there is an interface layer that was formed upon the absorption of these coatings into the top layers of the plaster bulk.

The coating layer was a mixture of oxidised organic medium and dirt. In most of the samples, the surface layer contains silicon and aluminium, possibly due to the use of clay water as a separating agent or a clay mineral pigment to tone the coating. The medium was identified as made of pine or shellac resins. By reviewing and comparing the results of the characterization of the casts, through an extensive database, it was possible to highlight that the differences observed within the groups cannot be considered distinguishing of the different workshops. Nonetheless, the multianalytical method selected for the analysis of the nineteenth-century V&A plaster casts has proven effective for the identification of the inorganic and organic components of the historical coatings applied to the plaster surfaces.

It was therefore possible to observe differences in the stratigraphy of the objects and discriminate the materials in the layers. In a few instances, additional layers were observed, and it was possible to postulate later intervention when modern materials were identified.

7.4 TOWARDS THE ASSESSMENT OF DETERIORATION OF PLASTER CASTS COATINGS

The production of plaster reconstructions, following historical recipes, to be used as a substrate for selected coatings (*Section 5.2.1.2*, page 169), followed by the application of these coatings, their soiling and ageing (*Sections 5.2.1.3 to 5.2.1.5*, pages 170-73) constituted **Objective 6**. This aimed to achieve the surfaces degradation and therefore a plausible stratigraphy of a nineteenth-century plaster cast. **Objective 7** was the assessment of the reproductions' surfaces, before and after ageing, by visual examination, technical photography (visible light and ultraviolet fluorescence) and scientific analysis (colourimetry, glossimetry, FT-IR, high-resolution 3D surface measurements) to understand the effects of the degradation on the coated and soiled surfaces. These objectives were addressed in *Chapter 5*.

By reconstructing a few selected plausible stratigraphy of a nineteenth-century plaster cast, based on the historical literature and analysis of the V&A casts, it was possible to observe and assess the changes of the coated plaster surfaces upon ageing. Such methodology can be applied to the many different coating described in the historical literature and the results of the assessment can guide the choices for the preservation and conservation of the cast. This study allowed to compare coated and uncoated plaster surfaces before and after ageing and observe numerous changes in the appearance, colour, and texture, and also in the molecular structure of the plaster-coating (and optionally dust) system. The uncoated plaster surfaces showed little changes after ageing, including an increased presence of pores in the aged areas, possibly due to increased drying of the surface related to affect the temperature, relative humidity and light chambers, and a small increase of gloss. The molecular pattern of the uncoated plaster was consistent with the scientific literature and most of the FT-IR peaks characteristic of gypsum plaster were present. Plaster surfaces coated with linseed oil appeared to be slightly bleached after accelerated ageing, for both the unsoiled and soiled sections. These surfaces fluoresced bright light-blue before ageing and the fluorescence almost disappeared after accelerated ageing for the raw linseed oil and was unchanged in the boiled one. It was shown that linseed oil penetrated the pores, rather than forming a film onto the plaster surface. The molecular structure of gypsum plaster and linseed oil were identified in the FT-IR spectra and small shifts and changes in intensity were observed after ageing. A change in intensity of the symmetric and asymmetric C–H stretching, which becomes extremely weak after ageing, was also highlighted for the raw linseed oil. The molecular pattern of the boiled linseed oil showed more stability to ageing in the raw oil. Shellac resin visibly discoloured after accelerated ageing and the light-blue fluorescence dulled. Shellac did not form a solid film onto the plaster surface but penetrated and filled the pores. After ageing, whilst the C–H

stretching bands were slightly weaker, the -OH stretching bands were much more intense and a distinct, sharp hydroxyl band raised. Barite coatings slightly bleached after accelerated ageing. The mineral structure of barite was observed in the BSE images, suggesting that the chemical structure of the surface was indeed modified by the barite solution. The surfaces coated with beeswax retained the molecular characteristics of the plaster substrate and the other coating (linseed oil, shellac and barite water), which added up to the features characteristic of beeswax. Upon ageing, the colour of the soiled section coated with beeswax slightly faded and the brush marks observed in the unaged section are less noticeable. Interestingly, whereas the 'tabular' structure typical of gypsum plaster was still visible in the sections coated with linseed oil, shellac and barite, the mineral structure could not be seen after the application of beeswax, which seemed to have formed a coherent and smooth film on the surface with an orange-peel like appearance in the BSE images. Overall, the peaks characteristic of gypsum plaster, the coating (linseed oil, shellac or barite) and beeswax were all observed in the FT-IR spectra of the unsoiled, unaged sections. The relevant aged section showed overall the same pattern, although some changes were observed as discussed in *Section 5.3.5* (page 212). Small shifts and changes in intensity were generally due to the ageing of the organic component and the drying of the organic or inorganic coating (for the case of the barite solution) and the inorganic bulk (the plaster support).

It was shown that the methodology can effectively highlight differences in the surfaces before and after ageing. This information can be used as a reference for the characterization of aged materials on plaster casts surfaces, but also to add knowledge on the deterioration processes of the plaster and coating(s) system.

7.5 DESIGNING PRESERVATION AND CONSERVATION

The assessment of the reproductions' surfaces, before and after removing the soiling with a selected cleaning treatment was undertaken by visual examination, technical photography (visible light and ultraviolet fluorescence) and scientific analysis (colourimetry, glossimetry, FT-IR, high-resolution 3D surface measurements). This aimed to understand the efficacy of the cleaning method and was addressed in *Chapter 6 (Objective 8)*.

A novel cleaning approach was selected for the removal of soiling deposits from the surfaces of the plaster reconstructions and to evaluate the efficacy of the method as well as to design a method for the evaluation of cleaning treatments.

Plaster characteristics such as porosity and water absorption behaviour greatly affected the casts deterioration and must be considered when selecting an appropriate surface cleaning treatment. The novel cleaning technique selected in this study was based on the use of polyolefin-supported hydrogels (PE-PAM), which was chosen to allow minimal wetting, critically reducing the disadvantages of liquid-based cleaning on liquid-sensitive surfaces. The hydrogels were used to remove the soil applied onto the coated plaster surfaces mock-ups and preserve the coatings. Aqueous solutions were selectively prepared to swell the surface coatings and remove the soil. The assessment of the effectiveness of the cleaning method was carried based on the visual, morphological and spectral evaluation. The cleaning after one application showed positive results, with the partial removal of the soil. It was particularly effective in the less porous areas, which were the ones coated with beeswax. In these areas, the cleaning procedure achieved the removal of a significant portion of the soiling just after one application. The best results were observed in the aged areas, where the soil was less attached to the coating. The uncoated areas and the areas coated with barite seemed to have absorbed the solutions too quickly for the cleaning method to be fully effective. Observations made on the appearance of the plaster surface post-cleaning (*Section 6.3.3, page 257*) led to the hypothesis that a partial dissolution and recrystallization of the plaster substrate occurred, despite the minimal quantity of liquid released by the hydrogels. This leaves the possibility of greater liquid-induced damage when compared to other methods requiring more wetting. More studies to follow up on these observations are required for a deeper understanding of the interactions between the wet agents and the plaster surfaces. The promising results of the use of thin hydrogel films suggest that further testing can be undertaken for the removal of soil on historical casts by using this method.

7.6 THE DATABASE AND FUTURE PERSPECTIVES

The compilation of a comprehensive database of results, which will provide reference and corpus datasets for relevant future studies, was cumulatively achieved in *Chapters 3 to 6*, constituting **Objective 9**. The database of results in Microsoft Excel format was compiled and deposited in the Northumbria University Figshare repository, to make the research outputs available in a citable, shareable and discoverable manner (Risdonne & Theodorakopoulos, 2021).

This research is the first step towards a new methodological approach for the study of historical plaster surfaces. Due to the novelty of the field, the research, while providing an extensive range of findings, also spurred further questions for new perspectives and approaches. It has been discussed at the opening of this work how replicas, and more specifically plaster casts, are and will continue to be an important element of the world's cultural heritage (*Section 1.1*). New understandings of the replicas can highlight new stories related to the object materiality and craftsmanship while challenging the notions of authenticity and value (*Section 1.1.2*), eventually questioning and possibly redesigning heritage and museum practices (Foster & Jones, 2020).

Relevantly to the archival investigation, further research including technical literature from other regions, including Asia and the Middle-East, as well as investigation on the technologies for making casts (and eventually coating them) for other types of collections (classical archaeology collections, anthropological, numismatic and so forth) can widen the understanding of the practices. Archival material belonging to the individual workshops, despite the secrecy of the artisans, can potentially provide insights on the individual and characteristic practices. There are many collections of plaster casts in the world and studying the material of their coatings can provide further information on the manufacturing practices of the workshops. By looking at casts produced in other periods than the nineteenth century, it would be possible to highlight differences in manufacturing across periods, if any. Due to the replicas identity as 'extended objects' (Foster & Jones, 2020), their 'composite biographies' also required to be studied as related to the lives of the copies and original.

In terms of analysis and characterization of original and modern materials, a broader campaign of sampling, particularly focused on the areas of repair might provide more details on the materials used during the conservation campaigns in the cast courts, therefore providing references for future characterizations. Moreover, further analysis in the laboratory, focused on the making of standards and references for coating applied to plaster surfaces, particularly for XRD, GC/MS and FT-IR datasets, seems remarkably important and long overdue. Such pieces of research would be immensely helpful for future studies

as well as for routine museum analysis. For example, currently available references for GC/MS analysis of cultural heritage materials have limited application for complex samples, particularly for the cases when the sample consists mostly of inorganic matter (Chiavari *et al.*, 2005; Poli *et al.*, 2014). The presence of inorganic material is believed to have an effect on the relative abundances of the fatty acids, impeding the use of the palmitic/stearic and azelaic/palmitic ratios commonly in use in the literature for determining the class of oils or fats in the sample (Colombini *et al.*, 2009). Moreover, the current protocols for characterization of cultural heritage samples as cross-sections, using microscopy in the visible and UV regions, requires casting samples in polyester or epoxy resin. These embedding media are chosen for their desirable optical qualities, but they are characterised by several FT-IR peaks in the 3000-2800 cm^{-1} and 1800-1100 cm^{-1} regions, where traditional and modern art media in the preparation and paint layers have their fingerprint signals (Derrick, 2000). Therefore, the presence of the casting resin mostly impedes, or at least complicates, the identification and discrimination of organic components in the layers (Martin de Fonjaudran *et al.*, 2008; Prati *et al.*, 2012). Subtracting or deconvolving the reference spectrum of the casting resin to avoid the contribution of the casting resin from the spectra does not provide the best result, as this operation can remove some of the overlapping peaks that belong to the sample itself. In future studies, it would be desirable to experiment with different casting methods to eliminate interferences caused by the presence of the casting resin in the porous plaster samples. Extrapolating the Focal Plane Array images from the first or second derivative could also improve the resolution of the peaks. Several recent studies aimed to investigate alternative casting methods, for example by using KBr/NaCl embedding (Mazzeo *et al.*, 2007; Prati *et al.*, 2013) or cyclododecane coating before resin embedding (Martin de Fonjaudran *et al.*, 2008; Prati *et al.*, 2012). In these studies, the samples were analysed by ATR-FT-IR, a technique that offers enhanced resolution and increased signal if compared with the reflectance FT-IR analysis performed on the cross-sections in this study. The contact between the sample and ATR crystal is essential for results with high signal-to-noise (Rosi *et al.*, 2019) but this cannot be ensured, nor sensible, when the samples are soft or prone to crumble, as for the case of the plaster samples.

The methodology designed for the evaluation of ageing of coated plaster surfaces can be applied to the many different coating described in the historical literature and the results of the assessment can guide the choices for the preservation and conservation of plaster cast. Many other variables, such as pollutants or outdoor conditions, and different models for ageing could be experimented with and contribute, together with the results presented here, to define the preventive conservation measures for the care of plaster casts. A deeper understanding of the mechanism of the reactions and the processes occurring during the deterioration of the coated plaster surfaces is anticipated to build on this first study, and

provided that scientific data will be made available in the form of databases or publications, will eventually lead to the understanding of the deterioration of these surfaces.

The methodology for the evaluation of the effectiveness of the novel technique for the removal of soils from the plaster surfaces has proven effective. FT-IR potentiality must be further explored for this scope. The use of PE-PAM hydrogel has shown positive results and highlighted once more how important is water control for the cleaning of water-sensitive surfaces. Further testing is suggested for the use of PE-PAM hydrogel for the removal of soil on plaster surfaces. Additional difficulties such as the curved and irregular shapes of the plaster sculptures and the adherence and timings of the procedure, as well as other types of coatings can be tested to have a full understanding of the cleaning method efficacy and limits. Moreover, this work also ought to inspire and contribute to future guidelines for cleaning studies on soiled model plaster samples.

The importance of designing such methodologies is also built on the new contemporary re-evaluation of the casts, which 'merit the same care as other objects and places' (Foster & Jones, 2020). This renewed perception will positively impact conservation practitioners and heritage scientists as well as the public and communities that engage with the objects' biographies. This work will contribute to increasing knowledge and understanding of the intersection between scientific material analysis, conservation and cultural value. The results will inform the application of heritage science to problems associated with material degradation and decay. These results should also eventually contribute to the development of professional policy and practice within heritage organisations.

- Abdel-Baset, M., Zhou, Y., & Hezam, I. (2019). Use of a sine cosine algorithm combined with Simpson method for numerical integration. *International Journal of Mathematics in Operational Research*, 14(3), 307–318. <http://dx.doi.org/10.1504/IJMOR.2019.099381>
- Al Dabbas, M., Eisa, M. Y., & Kadhim, W. H. (2014). Estimation of gypsum-calcite percentages using a Fourier transform infrared spectrophotometer (FTIR), in Alexandria Gypsiferous Soil-Iraq. *Iraqi Journal of Science*, 55(4B), 1916–1926. <https://www.iasj.net/iasj/article/98517>
- Anastasiou, M., Hasapis, T., Zorba, T., Pavlidou, E., Chrissafis, K., & Paraskevopoulos, K. M. (2006). TG-DTA and FTIR analyses of plasters from byzantine monuments in Balkan region. *Journal of Thermal Analysis and Calorimetry*, 84(1), 27–32. <https://doi.org/10.1007/s10973-005-7211-9>
- Anderson, K. B., & Winans, R. E. (1991). Nature and fate of natural resins in the geosphere. I. Evaluation of pyrolysis-gas chromatography-mass spectrometry for the analysis of natural resins and resinates. *Analytical Chemistry*, 63(24), 2901–2908. <https://doi.org/10.1021/ac00024a019>
- André, J. M. (1977). *The restorer's handbook of sculpture*. New York: Van Nostrand Reinhold. ISBN-13: 978-0442202378
- Andrew, C., Young, M., & Tonge, K. H. (1994). *Stone cleaning: a guide for practitioners*. Aberdeen: Historic Scotland Edinburgh. ISBN: 0748008748
- Angelova, L. V., Ormsby, B., & Richardson, E. (2016). Diffusion of water from a range of conservation treatment gels into paint films studied by unilateral NMR: Part I: Acrylic emulsion paint. *Microchemical Journal*, 124, 311–320. <https://doi.org/10.1016/j.microc.2015.09.012>
- Aruga, R., Mirti, P., Casoli, A., & Palla, G. (1999). Classification of ancient proteinaceous painting media by the joint use of pattern recognition and factor analysis on GC/MS data. *Fresenius' Journal of Analytical Chemistry*, 365(6), 559–566. <https://doi.org/10.1007/s002160051522>
- Atelier de Moulage*. (2018). Retrieved from: <http://www.kmkg-mrah.be/plaster-cast-workshop-0> (last accessed: 27/03/2021)
- Aquilano, D., Otálora, F., Pastero, L., & García-Ruiz, J. M. (2016). Three study cases of growth morphology in minerals: Halite, calcite and gypsum. *Progress in Crystal Growth and Characterization of Materials*, 62(2), 227–251. <https://doi.org/10.1016/j.pcrysgrow.2016.04.012>
- Auerbach, A. (1961). *Modelled sculpture and plaster casting* (A. Barnes Ed.). New York: Thomas Yoseloff. ISBN-13: 9780498019517
- Azemard, C., Vieillescazes, C., & Ménager, M. (2014). Effect of photodegradation on the identification of natural varnishes by FT-IR spectroscopy. *Microchemical Journal*, 112, 137–149. <https://doi.org/10.1016/j.microc.2013.09.020>

- Baglioni, P., & Chelazzi, D. (2013). *Nanoscience for the Conservation of Works of Art* (Vol. 28). Royal Society of Chemistry. ISBN: 1849735662
- Baker, M. (2010). The reproductive continuum: plaster casts, paper mosaics and photographs as complementary modes of reproduction in the nineteenth-century museum. In Frederiksen, R. & Marchand, R. E. (eds.), *Plaster Casts: Making, Collecting and Displaying from Classical Antiquity to the Present*, 485–500. Berlin: De Gruyter.
- Baker, Malcolm. (1982). *The History of the Cast Courts*. V&A Masterpieces Series. <http://www.vam.ac.uk/content/articles/t/the-cast-courts/> (last accessed: 27/03/2021)
- Bankart, G. P. (1908). *The Art of the Plasterer. An Account of the Decorative Development of the Craft, Chiefly in England from the XVIth to the XVIIIth Century, with Chapters on the Stucco of the Classic Period and of the Italian Renaissance, Also on Scraffito, Pargeting, Scot.* London: BT Batsford. ISBN-13: 978-9333148054
- Bankel, H. (2004). *I colori del bianco: policromia nella scultura antica* (Vol. 1). Roma: De Luca Editori d'Arte. ISBN: 8880166336
- Barash, M. (1985). *Theories of Art: From Plato to Winckelmann*. New York University Press. ISBN1-3: 9780814710609
- Barclay, R. L. (2002). *Care of Objects made of plaster of Paris*. CCI notes. Retrieved from: <https://www.canada.ca/content/dam/cci-icc/documents/services/conservation-preservation-publications/canadian-conservation-institute-notes/12-2-eng.pdf> (last accessed: 27/03/2021)
- Basile, J. (2014). Facsimile and Originality: Changing Views of Classical Casts in Arts Education and Art History. *International Journal of the Arts in Society: Annual Review*, 8(1). 11–30.
- Beale, A., Craine, C., & Forsythe, C. (1977). *The conservation of plaster casts*. Paper Presented at the Preprints of Papers Presented at the Fifth Annual Meeting of the AIC, Boston: Mass. 30 May-2 June 1977.
- Beran, A. (2002). Infrared spectroscopy of micas. *Reviews in Mineralogy and Geochemistry*, 46(1), 351–369. <https://doi.org/10.2138/rmg.2002.46.07>
- Berardi, U. (2019). Light transmittance characterization and energy-saving analysis of a new selective coating for in situ window retrofit. *Science and Technology for the Built Environment*, 25(9), 1152–1163. <https://doi.org/10.1080/23744731.2019.1620546>
- Bertasa, M., Chiantore, O., Poli, T., Riedo, C., di Tullio, V., Canevali, C., Sansonetti, A., & Scalarone, D. (2017). A study of commercial agar gels as cleaning materials. *Gels in the Conservation of Art*, 11–18.
- Betzer, S. (2019). Canova, 1816: marble, plaster, surface. *The Sculpture Journal*, 28(3), 315–419.
- Bianco, L. (2017). Techniques to determine the provenance of limestone used in Neolithic Architecture of Malta. *Romanian Journal of Physics* 62, 901, 1-10.

- Bilbey, D., & Trusted, M. (2010). The question of casts': collecting and later reassessment of the cast collections at South Kensington. In Frederiksen, R., & Marchand, E. (eds.), *Plaster casts: Making, Collecting, and Displaying from Classical Antiquity to the Present*, 465–483. Berlin: De Gruyter.
- Bishop, J. L., Lane, M. D., Dyar, M. D., King, S. J., Brown, A. J., & Swayze, G. A. (2014). Spectral properties of Ca-sulfates: Gypsum, bassanite, and anhydrite. *American Mineralogist*, 99(10), 2105–2115. <https://doi.org/10.2138/am-2014-4756>
- Blasco-López, F. J., Alejandre, F. J., & Flores-Alés, V. (2015). Methodology for characterising microlayers in historical plasterwork. *Construction and Building Materials*, 93, 463–470. <https://doi.org/https://doi.org/10.1016/j.conbuildmat.2015.05.135>
- Böke, H., Akkurt, S., Özdemir, S., Göktürk, E. H., & Caner Saltik, E. N. (2004). Quantification of $\text{CaCO}_3\text{--CaSO}_3\cdot 0.5\text{H}_2\text{O--CaSO}_4\cdot 2\text{H}_2\text{O}$ mixtures by FTIR analysis and its ANN model. *Materials Letters*, 58(5), 723–726. <https://doi.org/https://doi.org/10.1016/j.matlet.2003.07.008>
- Boylan, P. J. (2004). *Running a museum: a practical handbook*. Paris: ICOM. ISBN: 92-9012-157-2
- Brannt, W. T., & Wahl, W. H. (1919). *Techno-chemical Receipt Book: Containing Several Thousand Receipts and Processes, Covering the Latest, Most Important and Most Useful Discoveries in Chemical Technology and Their Practical Application in the Arts and the Industries*. New York: HC Baird & Company Incorporated.
- Brown, G. M. (2016). *Art in the age of digital reproduction*. <https://www.ft.com/content/74ffab6e-1b55-11e6-b286-cddde55ca122> (last accessed 27/03/2021)
- BS EN ISO 16474-1:2013. (2013). British Standard. *Paints and Varnishes - Method of Exposure to Laboratory Light Sources. Part 1: General Guidance*.
- BS EN ISO 16474-2:2013. (2013). British Standard. *Paints and Varnishes - Method of Exposure to Laboratory Light Sources. Part 2: Xenon-Arc Lamps*.
- Bucklow, S. (2009). *Impossible recipes. Sources and Serendipity. Testimonies of Artists' Practice*. London: Archetype. ISBN: 9781904982524
- Burnstock, A., & van den Berg, K. J. (2014). Twentieth-century oil paint. The interface between science and conservation and the challenges for modern oil paint research. In Burnstock, A., de Keijzer, M., Krueger, J., Learner, T., de Tagle, A., Heydenreich, G., van den Berg, K.J. (eds.), *Issues in Contemporary Oil Paint*, Springer, 1–19. ISBN: 9783319101002
- Cambareri, M. (2011). Italian Renaissance sculpture at the Museum of Fine Arts, Boston: the early years. In Marshall, C. R. (ed.), *Sculpture and the Museum*, Routledge. 95–114. ISBN: 9781138268371
- Camuffo, D., & Bertolin, C. (2012). Towards standardisation of moisture content measurement in cultural heritage materials. *E-Preservation Science*, 9, 23–35. ISSN: 1581-9280
- Cardell-Fernández, C., & Navarrete-Aguilera, C. (2006). Pigment and plasterwork analyses of Nasrid polychromed lacework stucco in the Alhambra (Granada, Spain). *Studies in Conservation*, 51(3), 161–176. <https://doi.org/10.1179/sic.2006.51.3.161>

- Carlyle, L. A., Barrett, S., Stulik, D. C., Glanville, H., Massing, A., Woodcock, S. A., Federspiel, B., Woudhuysen-Keller, R., Darrah, J. A., & Duffy, K. I. (1995). *Historical painting techniques, materials, and studio practice: preprints of a symposium*, University of Leiden, the Netherlands, 26–29 June 1995. Getty Publications.
- Caskey, J. (2007). Liquid Gothic: Uses of Stucco in Southern Italy. *Reading Gothic Architecture*, Brepols Publishers, 111–122. <https://doi.org/10.1484/M.SVCMA-EB.3.1318>
- Cassar, M. (1994). *Museums environment energy*. Her Majesty's Stationery Office. ISBN-13: 978-0112905196
- Cellini, B. (1967). *The treatises of Benvenuto Cellini on goldsmithing and sculpture* (Translation). Dover Publication, Inc. ISBN-13: 978-1162938875
- Cennini, C. (1859). *Il Libro dell'arte, o Trattato della pittura. Di nuovo pubblicato, con molte correzioni e coll'aggiunta di più capitoli tratti dai codici fiorentini* (Milanesi, C. & Milanesi, G. eds.). Firenze: Le Monnier.
- Cerea, S., Mancini, F., Ruppen, V., Isella, E., Bonelli, D., & Sansonetti, A. (2017). Pulitura laser su tre calchi in gesso dell'Accademia di Brera. *Aplar 6 - Applicazioni Laser Nel Restauro, Firenze, Auditorium Di Sant'Apollonia*.
- Ceroni, M., & Elia, G. (2008). *Diagnostica per i beni culturali: tecnologia e metodologia applicata alla diagnosi e studio delle opere d'arte*. ISBN-13: 978-8860553256
- Challinor, J. M. (1991). The scope of pyrolysis methylation reactions. *Journal of Analytical and Applied Pyrolysis*, 20, 15–24. [https://doi.org/10.1016/0165-2370\(91\)80059-H](https://doi.org/10.1016/0165-2370(91)80059-H)
- Challinor, J. M. (2001). The development and applications of thermally assisted hydrolysis and methylation reactions. *Journal of Analytical and Applied Pyrolysis*, 61(1–2), 3–34. [https://doi.org/10.1016/S0165-2370\(01\)00146-2](https://doi.org/10.1016/S0165-2370(01)00146-2)
- Chaney, C. (1973). *Plaster mold and model making*. New York, London : Von Nostrand Reinhold.
- Charr, M. (2019). *Legal Case Concerning a 3D Scan of a Museum Artefact May Impact on All Institutions*. <https://www.museumnext.com/article/legal-case-concerning-a-3d-scan-of-a-museum-artefact-may-impact-on-all-institutions/> (last accessed 27/03/2021)
- Chiavari, G., Fabbri, D., & Prati, S. (2005). Effect of pigments on the analysis of fatty acids in siccative oils by pyrolysis methylation and silylation. *Journal of Analytical and Applied Pyrolysis*, 74(1), 39–44. <https://doi.org/https://doi.org/10.1016/j.jaap.2004.11.013>
- Chiriu, D., Ricci, P. C., Cappellini, G., Salis, M., Loddo, G., & Carbonaro, C. M. (2018). Ageing of ancient paper: A kinetic model of cellulose degradation from Raman spectra. *Journal of Raman Spectroscopy*, 49(11), 1802–1811. <https://doi.org/10.1002/jrs.5462>
- Cipriani, A., & Fodaro, D. (2015). 1790, Vincenzo Pacetti e il busto di Pio VI per la nuova galleria dell'Accademia di San Luca. In Parlato, E. (ed.), *Curiosa itinera. Scritti per Daniela Gallavotti Cavallero*. Ginevra Bentivoglio, 487–495.
- Čížová, K., Vizárová, K., Ház, A., Vykydalová, A., Cibulková, Z., & Šimon, P. (2019). Study of the degradation of beeswax taken from a real artefact. *Journal of Cultural Heritage*, 37, 103–112. <https://doi.org/https://doi.org/10.1016/j.culher.2018.04.020>

- Clarke, M., Townsend, J. H., & Stijnman, A. (2005). *Art of the past: sources and reconstructions: proceedings of the first symposium of the Art Technological Source Research study group*. London: Archetype Publications
- Clenshaw, C. W., & Curtis, A. R. (1960). A method for numerical integration on an automatic computer. *Numerische Mathematik*, 2(1), 197–205.
https://doi.org/10.1007/BF01386223
- Clérin, P. (1988). *La sculpture: toutes les techniques*. Lethielleux: Dessain et Tolra. ISBN 13: 9782249277597
- Cléry, A. (1896). *A preservative composition, applicable also for the manufacture of artificial stone, statuary and the like*, Patent No. 16840.
- Clifford, T. (1992). The plaster shops of the rococo and neo-classical era in Britain. *Journal of the History of Collections*, 4(1), 39–65. https://doi.org/10.1093/jhc/4-1-39
- Cocks, A. S., Clucas, P., Smart, T., & Gibbon, D. (1980). *The Victoria and Albert Museum: the making of the collection*. London: Windward.
- Coelho, C., Nanabala, R., Ménager, M., Commereuc, S., & Verney, V. (2012). Molecular changes during natural biopolymer ageing—The case of shellac. *Polymer Degradation and Stability*, 97(6), 936–940.
https://doi.org/10.1016/j.polymdegradstab.2012.03.024
- Colombini, M. P., Bonaduce, I., & Gautier, G. (2003). Molecular Pattern Recognition of Fresh and Aged Shellac. *Chromatographia*, 58(5), 357–364.
https://doi.org/10.1365/s10337-003-0037-3
- Colombini, M. P., & Modugno, F. (2009). *Organic mass spectrometry in art and archaeology*. John Wiley & Sons. ISBN:9780470741917
- Coon, C. (2009). *An investigation into cleaning techniques for an untreated 19th-century plaster cast in the Victoria and Albert collection*. City and Guilds of London Art School. Unpublished thesis.
- Cox, K. G., Price, N. B., & Harte, B. (1974). *An introduction to the practical study of crystals, minerals, and rocks*. London: Halsted Press.
- Craddock, P. (2009). *Scientific investigation of copies, fakes and forgeries*. London: Routledge. ISBN: 9780367606275
- Creagh, D. C., & Bradley, D. A. (2000). *Radiation in Art and Archeometry*. Elsevier. ISBN: 9780080540191
- Cremonesi, P. (1999). *L'uso degli enzimi nella pulitura di opere policrome*. Padova: Il prato.
- Cremonesi, P. (2004). *L'uso dei solventi organici nella pulitura di opere policrome*. Padova: Il prato. ISBN-13: 978-8887243857
- Cremonesi, P. (2013). *Rigid gels and enzyme cleaning*. In Mecklenburg, M. F., Charola, A. E., & Koestler, R. J. (eds), *New Insights into the Cleaning of Paintings: Proceedings from the Cleaning 2010 International Conference, Universidad Politecnica de Valencia and Museum Conservation Institute*. 179–183. Smithsonian Contributions to Museum Conservation. Washington, DC: Smithsonian Institution.

- Cremonesi, P., & Casoli, A. (2017). Thermo-reversible rigid agar hydrogels: their properties and action in cleaning. *Gels in the Conservation of Art*. Archetype Publications Ltd, 19–27.
- da Silveira Paulo, M., do Rosário Veiga, M., & de Brito, J. (2007). Gypsum coatings in ancient buildings. *Construction and Building Materials*, 21(1), 126–131. <https://doi.org/10.1057/palgrave.jba.2950075>
- Dailey, M. C., & Duffy, E. W. (1948). *Gypsum product*. Patent No. 446844.
- Dajnowski, A., Jenkins, A., & Lins, A. (2009). The use of lasers for cleaning large architectural structures. *APT Bulletin*, 40(1), 13–23.
- Danford, R. (2016). *Manipulating Matter: Figural Stucco Sculpture in the Early Middle Ages*. Johns Hopkins University. Thesis. <https://jscholarship.library.jhu.edu/bitstream/handle/1774.2/60649/DANFORD-DISSERTATION-2016.pdf?sequence=1>
- Davies, G. (1991). The Albacini cast collection: character and significance. *Journal of the History of Collections*, 3(2), 145–165. <https://doi.org/10.1093/jhc/3.2.145>
- de Bas, W. J. (1920). *Improvement in plastic composition*. Patent No. 143768.
- de Jonge, L. (1985). *The art of doing: plaster techniques*. Amsterdam: van Dobbenburgh. ISBN 13: 9789065770332
- De Viguierie, L., Payard, P. A., Portero, E., Walter, P., & Cotte, M. (2016). The drying of linseed oil investigated by Fourier transform infrared spectroscopy: Historical recipes and influence of lead compounds. *Progress in Organic Coatings*, 93, 46–60. <https://doi.org/10.1016/j.porgcoat.2015.12.010>
- Delegou, E. T., Ntoutsis, I., Kiranoudis, C. T., Sayas, J., & Moropoulou, A. (2018). Advanced and novel methodology for scientific support on decision-making for stone cleaning. *Advanced Materials for the Conservation of Stone*. Springer. 299–324. ISBN: 978-3-319-72259-7
- Derrick, M. R., Stulik, D., & Landry, J. M. (2000). *Infrared spectroscopy in conservation science*. Los Angeles: Getty Publications. http://hdl.handle.net/10020/gci_pubs/infrared_spectroscopy
- Dini, R. (2018). *An analysis of Walter Benjamin's The work of art in the age of mechanical reproduction*. London: Taylor & Francis. <https://doi.org/10.4324/9781912284894>
- Disalvo, L. (2012). Plaster Cast Collections from the 1904 Louisiana Purchase Exposition in Context: Examining Culturally Determined Significance through Environment and Time. *Material Culture Review*, 74, 131–148. https://id.erudit.org/iderudit/mcr74_75art09
- Dlugogorski, B. Z., Kennedy, E. M., & Mackie, J. C. (2012). Low temperature oxidation of linseed oil: a review. *Fire Science Reviews*, 1(1), 3. <https://doi.org/10.1186/2193-0414-1-3>
- Doménech-Carbó, M. T., Yusá-Marco, D. J., Bitossi, G., Silva, M. F., Mas-Barberá, X., & Osete-Cortina, L. (2008). Study of ageing of ketone resins used as picture varnishes by FT-IR spectroscopy, UV-Vis spectrophotometry, atomic force microscopy and scanning electron microscopy X-ray microanalysis. *Analytical and Bioanalytical Chemistry*, 391(4), 1351–1359. <https://doi.org/10.1007/s00216-008-1864-8>

- Domingues, J. A. L., Bonelli, N., Giorgi, R., Fratini, E., Gorel, F., & Baglioni, P. (2013). Innovative hydrogels based on semi-interpenetrating p (HEMA)/PVP networks for the cleaning of water-sensitive cultural heritage artifacts. *Langmuir*, 29(8), 2746–2755. <https://doi.org/10.1021/la3048664>
- Domínguez, M. M. B. (2013). Cleaning plaster surfaces with agar-agar gels: evaluation of the technique. *Ge-Conservación/Conservação*, 4, 111–126. <https://doi.org/10.37558/gec.v4i0.153>
- Dorsett, C., & Stewart, M. (2012). Cast Contemporaries: artists respond to the completion of the Cast Collection Project at Edinburgh College of Art. <http://castcontemporaries.weebly.com/index.html>
- ECOSURF™ LF Specialty Surfactants*. (2012). Dow. <https://www.dow.com/content/dam/dcc/documents/en-us/mark-prod-info/119/119-02272-01-ecosurf-lf-specialty-surfactants-overview.pdf?iframe=true> (last accessed 27/03/2021)
- El Hazzat, M., Sifou, A., Aarsalane, S., & El Hamidi, A. (2019). Novel approach to thermal degradation kinetics of gypsum: application of peak deconvolution and Model-Free isoconversional method. *Journal of Thermal Analysis and Calorimetry*, 1–15. <https://doi.org/10.1007/s10973-019-08885-3>
- Emerick, K. (2014). *Conserving and managing ancient monuments: Heritage, democracy, and inclusion* (Vol. 14). Suffolk, GBR: Boydell & Brewer Ltd.
- Erhardt, D., & Mecklenburg, M. F. (1995). Accelerated vs natural ageing: Effect of ageing conditions on the ageing process of cellulose. *MRS Online Proceedings Library Archive*, 352. <https://doi.org/10.1557/PROC-352-247>
- Fabian, H. & Mantele, W. (2002). *Infrared Spectroscopy of Proteins*. In Chalmers, J. M., & Griffiths, P.R. (eds.), *Handbook of Vibrational Spectroscopy*. Chichester: Wiley, 3399–3425.
- Farag, Y., & Leopold, C. S. (2009). Physicochemical properties of various shellac types. *Dissolution Technologies*, 16, 33–39. <https://doi.org/10.14227/DT160209P33>
- Fash, B. W. (2004). Cast Aside: Revisiting the Plaster Cast Collections from Mesoamerica. *Visual Resources*, 20(1), 3–17. <https://doi.org/10.1080/0197376042000191541>
- Fehlmann, M. (2007). As Greek as it gets: British attempts to recreate the Parthenon. *Rethinking History*, 11(3), 353–377. <https://doi.org/10.1080/13642520701353256>
- Felice, A. (2018). Felice Calchi. <http://www.felicecalchi.com/> (last accessed 27/03/2021)
- Feller, R. L. (1976). The relative solvent power needed to remove various aged solvent-type coatings. *Congress of the International Institute for the Conservation of Historic and Artistic Works. Session on Solvents and Solvent Action*.
- Feller, R. L. (1994). *Accelerating ageing—photochemical and thermal aspects*. The Getty Conservation Institute. Los Angeles: Getty Publications.
- Florio, P. A., & Mersereau, E. P. (1955). Control of appearance changes due to soiling: The mechanism, measurement, and reduction of soiling changes in carpet during use. *Textile Research Journal*, 25(7), 641–649. <https://doi.org/10.1177%2F004051755502500711>

- Flour, I. (2008). On the Formation of a National Museum of Architecture: the Architectural Museum versus the South Kensington Museum. *Architectural History*, 51, 211–238. <https://doi.org/10.1017/S0066622X00003087>
- Fodaro, D., Pelosi, C., & Sforzini, L. (2014). La pulitura di sculture in gesso. Alcuni casi studio di laser cleaning. *Progetto Restauro*, 18(68), 8–16.
- Forsyth, K. (1995). *The inscriptions on the Dupplin Cross*. In Bourke, C. (ed.), *From the Isles of the North: Early Medieval Art in Ireland and Britain*, Belfast. Belfast: HMSO, 237-244. ISBN: 9780337112010
- Foster, S. M., (2015). Circulating agency: the V&A, Scotland and the multiplication of plaster casts of 'Celtic crosses', *Journal of the History of Collections*, 27(1), 73–96, <https://doi.org/10.1093/jhc/fhu008>
- Foster, S. M., & Curtis, N. G. W. (2016). The Thing about Replicas—Why Historic Replicas Matter. *European Journal of Archaeology*, 19(1), 122–148. <https://doi.org/10.1179/1461957115Y.0000000011>
- Foster, S. M. and Jones, S. J. (2020a). *My Life as a Replica: St John's Cross, Iona*. Oxford: Windgather. ISBN: 9781911188605
- Foster, S., & Jones, S. (2020b). *New Futures for Replicas: Principles and Guidance for Museums and Heritage*. University of Stirling. <https://replicas.stir.ac.uk/principles-and-guidance/>
- Fratelli, M., & Signorini, E. (2008). *Problemi conservativi dei manufatti dell'Ottocento: i dipinti, la carta, i gessi; atti, problemi di restauro, giornate di studio*, Milano, 2-8-15-23-30 maggio 2006, Spazio Oberdan. Il Prato. http://www.gam-milano.com/fileadmin/user_upload/_imported/fileadmin/sito/experience/vita_in_mu seo/ProblemiConservativi_low.pdf
- Frederick, F. F. (1899). *Plaster casts and how they are made*. New York: Comstock.
- Frederiksen, Rune, & Marchand, E. (2010). *Plaster casts: making, collecting and displaying from classical antiquity to the present* (Vol. 18). Berlin: de Gruyter.
- Freese, S., Diraoui, S., Mateescu, A., Frank, P., Theodorakopoulos, C., & Jonas, U. (2020). Polyolefin-Supported Hydrogels for Selective Cleaning Treatments of Paintings. *Gels*, 6(1), 1. <https://doi.org/10.3390/gels6010001>
- Freire-Lista, D. M., Greif, V., de Buergo, M. Á., & Fort, R. (2015). Gypsum decay simulation: Risco de las Cuevas case study, Madrid, Spain. *Engineering Geology for Society and Territory*-Volume 8, Springer. 491–494. <https://doi.org/10.1007/978-3-319-09408-3>
- Freire, M. T., Santos Silva, A., Veiga, M. do R., Dias, C. B., & Manhita, A. (2020). Stucco Marble in the Portuguese Architecture: Multi-analytical Characterisation. *International Journal of Architectural Heritage*, 1–17. <https://doi.org/10.1080/15583058.2020.1765051>
- Freire, M. T., Santos Silva, A., do Rosário Veiga, M., & de Brito, J. (2015). The history of Portuguese interior plaster coatings: A mineralogical survey using XRD. *Archaeometry*, 57(S1), 147–165. <https://doi.org/10.1111/arcm.12130>
- Fritz, C. (1999). Towards the reconstruction of Magdalenian artistic techniques: the contribution of microscopic analysis of mobiliary art. *Cambridge Archaeological Journal*, 9(2), 189–208. <https://doi.org/10.1017/S0959774300015377>

- Gamer, M. (2019). The Smugglerius, re-viewed. *The Sculpture Journal*, 28(3), 331–419.
- Gapper, C. (1999). What is 'Stucco'? English Interpretations of an Italian Term. *Architectural History*, 42, 333–343. <https://doi.org/10.2307/1568718>
- Galatis, P., Boyatzis, S., & Theodorakopoulos, C. (2012). Removal of a synthetic soiling mixture on mastic, shellac & Laropal® K80 coatings using two hydrogels. *E-Preservation Science*, 9, 72–83. <http://www.morana-rtd.com/e-preservationscience/TOC.html>
- Gariani, G., Lehuédé, P., Leroux, L., Wallez, G., Goubard, F., Bouquillon, A., & Bormand, M. (2018). First insights on the mineral composition of “stucco” devotional reliefs from Italian Renaissance Masters: investigating technological practices and raw material sourcing. *Journal of Cultural Heritage*, 34, 23–32. <https://doi.org/10.1016/j.culher.2018.05.003>
- Getchell, N. F. (1955). Cotton Quality Study: III: Resistance To Soiling. *Textile Research Journal*, 25(2), 150–194.
- Gianasso, E. (2014). Stucchi e gessi. In Marchis, V. (ed.), *Storie Di Cose*. Citta Di Torino: Archivio Storico, 38–46.
- Gipsformerei*. (2018). <https://www.smb.museum/en/museums-institutions/gipsformerei/home.html> (last accessed 27/03/2021)
- Gipsoteca Mondazzi*. (2018). <http://www.gipsoteca.it/> (last accessed 27/03/2021)
- Gold, R. (1994). Reconstruction and analysis of bismuth painting. Painted Wood: History and Conservation, *Proceedings of a Symposium Organized by the Wooden Artifacts Group of the American Institute for Conservation of Historic and Artistic Works*, 166–178.
- Graepler, D., & Ruppel, J. (2019). *Wei wie Gips?: Die Behandlung der Oberflchen von Gipsabgssen*. *Wissenschaftliche Fachtagung Archologisches Institut Und Sammlung Der Gipsabgsse*, Gttingen, 13-15 Oktober 2016: VML Verlag Marie Leidorf.
- Gramtorp, D., Botfeldt, K., Glastrup, J., & Simonsen, K. P. (2015). Investigation and conservation of Anne Marie Carl-Nielsen’s wax models. *Studies in Conservation*, 60(2), 97–106. <https://doi.org/10.1179/2047058413Y.0000000111>
- Grau-Bov, J., & Strli, M. (2013). Fine particulate matter in indoor cultural heritage: a literature review. *Heritage Science*, 1(1), 8. <https://doi.org/10.1186/2050-7445-1-8>
- Graulis, S., Chateigner, D., Downs, R. T., Yokochi, A. F. T., Quirs, M., Lutterotti, L., Manakova, E., Butkus, J., Moeck, P., & Le Bail, A. (2009). Crystallography Open Database—an open-access collection of crystal structures. *Journal of Applied Crystallography*, 42(4), 726–729. <https://doi.org/10.1107/s0021889809016690>
- Grehk, T. M., Berger, R., & Bexell, U. (2008). Investigation of the drying process of linseed oil using FTIR and ToF-SIMS. *Journal of Physics: Conference Series*, 100(1), 12019.
- Guderzo, M., & Lochman, T. (2017). *Il valore del gesso come modello, calco, copia per la realizzazione della scultura*, 2-3 ottobre 2015. Quarto Convegno Internazionale Sulle Gipsoteche, Possagno.

- Guillén, M. D., Ruiz, A., Cabo, N., Chirinos, R., & Pascual, G. (2003). Characterization of sachá inchi (*Plukenetia volubilis* L.) Oil by FTIR spectroscopy and ¹H NMR. Comparison with linseed oil. *Journal of the American Oil Chemists' Society*, 80(8), 755–762. <https://doi.org/10.1007/s11746-003-0768-z>
- Gulotta, D., Saviello, D., Gherardi, F., Toniolo, L., Anzani, M., Rabbolini, A., & Goidanich, S. (2014). Setup of a sustainable indoor cleaning methodology for the sculpted stone surfaces of the Duomo of Milan. *Heritage Science*, 2(1), 6. <https://doi.org/10.1186/2050-7445-2-6>
- Gunstone, F. D. (2011). *Production and trade of vegetable oils. Vegetable Oils in Food Technology: Composition, Properties and Uses*, 1. <https://doi.org/10.1002/9781444339925.ch1>
- Gupta, A., Singh, P., & Shivakumara, C. (2010). Synthesis of BaSO₄ nanoparticles by precipitation method using sodium hexa metaphosphate as a stabilizer. *Solid State Communications*, 150(9–10), 386–388. <https://doi.org/10.1016/j.ssc.2009.11.039>
- Gypsum - properties, definitions and uses. Vol. 108.* (1921). United States Bureau of Standards.
- Hackney, S. (1984). The distribution of gaseous air pollution within museums. *Studies in Conservation*, 29(3), 105–116. <https://doi.org/10.2307/1506012>
- Hajji, S., Turki, T., Boubakri, A., Ben Amor, M., & Mzoughi, N. (2017). Desalination and Water Treatment Study of cadmium adsorption onto calcite using full factorial experiment design. *Desalination and Water Treatment*, 83, 222–233. <https://doi.org/10.5004/dwt.2017.21079>
- Halpine, S. M. (1992). Amino acid analysis of proteinaceous media from Cosimo Tura's 'The Annunciation with Saint Francis and Saint Louis of Toulouse.' *Studies in Conservation*, 37(1), 22–38.
- Hanor, J. S. (2000). Barite–Celestine Geochemistry and Environments of Formation. *Reviews in Mineralogy and Geochemistry*, 40(1), 193–275. <https://doi.org/10.2138/rmg.2000.40.4>
- Harrison, L. S. (1961). Evaluation of Spectral Radiation Hazards in Window-Lighted Galleries. *Studies in Conservation*, 6(sup1), 1–6.
- Haskell, F., & Penny, N. (1981). *Taste and the antique: The lure of classical sculpture, 1500-1900*. London: Yale University Press. ISBN-13: 978-0300029130
- Holtorf, C. (2002). Notes on the life history of a pot sherd. *Journal of Material Culture*, 7(1), 49–71.
- Hofmeister, A. M., & Bowey, J. E. (2006). Quantitative infrared spectra of hydrosilicates and related minerals. *Monthly Notices of the Royal Astronomical Society*, 367(2), 577–591. <https://doi.org/10.1111/j.1365-2966.2006.09894.x>
- Horie, C. V. (2010). *Materials for conservation: organic consolidants, adhesives and coatings*. Routledge. ISBN-13: 978-0750669054
- Hubbard, C. (2015). Conservation of the Weston Cast Court at the V&A. <https://www.pmsa.org.uk/news/2019/5/2/conservation-of-the-weston-cast-court-at-the-vampa>

- Hubbard, C., & Pretzel, B. (2016). *Report on a study of the use of latex cleaning product on historic plaster casts*. Unpublished report. Retrieved from Collection Management System.
- Hudson-Lamb, D. L., Strydom, C. A., & Potgieter, J. H. (1996). The thermal dehydration of natural gypsum and pure calcium sulphate dihydrate (gypsum). *Thermochimica Acta*, 282, 483–492. [https://doi.org/10.1016/0040-6031\(95\)02819-6](https://doi.org/10.1016/0040-6031(95)02819-6)
- Huertos, E. G., & León, M. I. C. (1994). Metodología para valorar la eficacia de los tratamientos de conservación de la piedra. Aplicación a la caliza de la torre de la Catedral de Málaga. *Boletín de La Sociedad Española de Mineralogía*, 17, 179–192.
- Hughes, J., Jones, S., & Yarrow, T. (2014). Materiality, authenticity and value in the historic environment: a study of the effects of material transformation and scientific intervention. In *Sustaining the Impact of UK Science and Heritage Research. AHRC/EPSRC Science and Heritage Programme*, 27-28. University College London.
- Hughes, A., & Sullivan, M. (2016). Targeted cleaning of works on paper: rigid polysaccharide gels and conductivity in aqueous solutions. *The Book and Paper Group Annual*, 25, 30-41.
- Hunter, F., & Sheridan, A. (2016). *Ancient lives: object, people and place in early Scotland. Essays for David V. Clarke on his 70th birthday*. Leiden: Sidestone Press. ISBN: 978-90-8890-376-2
- Ioannides, M., Fink, E., Brumana, R., Patias, P., Doulamis, A., Martins, J., & Wallace, M. (2018). *Digital Heritage. Progress in Cultural Heritage: Documentation, Preservation, and Protection: 7th International Conference, EuroMed 2018, Nicosia, Cyprus, October 29–November 3, 2018, Proceedings* (Vol. 11196). Springer.
- Isella, E., Bonelli, D., Cerea, S., Mancini, F., Ruppen, V., Botteon, A., & Sansonetti, A. (2017). Experiences at the Academy of Fine Arts of Brera in Milan, Italy: the application of laser-technology on three case studies of the historical heritage. In Targowsk, P. (ed.), *Lasers in the Conservation of Artworks XI, Proceedings of LACONA XI*. NCU Press. <https://doi.org/10.12775/3875-4.16>
- Inspiring Beautiful Free shoot*. (2014). <http://www.vam.ac.uk/blog/network/inspiring-beautiful-free-shoot> (last accessed 27/03/2021)
- Izzo, F. C., van den Berg, K. J., van Keulen, H., Ferriani, B., & Zendri, E. (2014). Modern oil paints—formulations, organic additives and degradation: some case studies. In *Issues in contemporary oil paint*, 75-104. Springer, Cham.
- Janssens, K. (2004). X-ray based methods of analysis. *Comprehensive Analytical Chemistry* (Vol. 42), 129-226. Amsterdam: Elsevier BV. [https://doi.org/10.1016/S0166-526X\(04\)80008-4](https://doi.org/10.1016/S0166-526X(04)80008-4)
- Jelle, B. P. (2012). Accelerated climate ageing of building materials, components and structures in the laboratory. *Journal of Materials Science*, 47(18), 6475–6496. <https://dx.doi.org/10.1007/s10853-012-6349-7>
- Jones, B. (2011). *Analyses of cleaning treatments on plaster casts with organic coatings*. City and Guilds of London Art School. Unpublished thesis.

- Jones, S. (2010). Negotiating authentic objects and authentic selves: Beyond the deconstruction of authenticity. *Journal of Material Culture*, 15(2), 181–203. <https://doi.org/10.1177%2F1359183510364074>
- Jørgensen, K. D., & Posneb, A. S. (1959). Study of the setting of plaster. *Journal of Dental Research*, 38(3), 491–499. <https://doi.org/10.1177%2F00220345590380030901>
- Kanngießler, B., Malzer, W., Mantouvalou, I., Sokaras, D., & Karydas, A. G. (2012). A deep view in cultural heritage—confocal micro X-ray spectroscopy for depth resolved elemental analysis. *Applied Physics A*, 106(2), 325–338. <http://dx.doi.org/10.1007/s00339-011-6698-0>
- Kemp, W. (1912). *The Practical Plasterer. A compendium of Plain and Ornamental Plaster Work*. (Fourth ed.). London: Capio Lumen.
- Kenndler, E., Schmidt-Beiwel, K., Mairinger, F., & Pöhm, M. (1992). Identification of proteinaceous binding media of easel paintings by gas chromatography of the amino acid derivatives after catalytic hydrolysis by a protonated cation exchanger. *Fresenius' Journal of Analytical Chemistry*, 342(1–2), 135–141. <https://doi.org/10.1007/BF00321708>
- Keppie, L. J. F. (1998). *Roman inscribed and sculptured stones in the Hunterian Museum, University of Glasgow*. London: Society for the Promotion of Roman Studies. ISBN: 0907764223
- Khoshhesab, Z. M. (2012). Reflectance IR spectroscopy. *Infrared Spectroscopy, Materials Science, Engineering and Technology*, 11, 233–244. <https://doi.org/10.5772/37180>
- Klimchouk, A. (1996). The dissolution and conversion of gypsum and anhydrite. *International Journal of Speleology*, 25(3), 2. <http://dx.doi.org/10.5038/1827-806X.25.3.2>
- Kling, R., & Schiffer, J. (1969). The potential environment about the water molecule in gypsum. *Chemical Physics Letters*, 3(2), 64–66. [https://doi.org/10.1016/0009-2614\(69\)80048-5](https://doi.org/10.1016/0009-2614(69)80048-5)
- Klosowska, A., & Obarzanowski, M. (2010). Plaster casts in the collection of the National Museum in Krakow. Conservation issues. *Plaster casts of the works of art. History of collection, Conservation, Exhibition practice*. Krakow: Muzeum Narodowe w Krakow ie. ISBN: 9788375810592
- Koblitz, F. F. (1977). *Modified gypsum composition*. Patent No. 1 461 812.
- Kotwaliwale, N., Bakane, P., & Verma, A. (2007). Changes in textural and optical properties of oyster mushroom during hot air drying. *Journal of Food Engineering*, 78(4), 1207–1211. <https://doi.org/10.1016/j.jfoodeng.2005.12.033>
- Kupiec, C. (2019). Copies and connoisseurship: Luca della Robbia's Visitation in America, 1888–1909. *The Sculpture Journal*, 28(3), 381–419.
- Kumar, R. S., & Rajkumar, P. (2014). Characterization of minerals in air dust particles in the state of Tamilnadu, India through FTIR, XRD and SEM analyses. *Infrared Physics & Technology*, 67, 30–41.
- Kumarathanan, R., Rajkumar, A. B., Hunter, N. R., & Gesser, H. D. (1992). Autoxidation and yellowing of methyl linolenate. *Progress in lipid research*, 31(2), 109-126. [https://doi.org/10.1016/0163-7827\(92\)90005-4](https://doi.org/10.1016/0163-7827(92)90005-4)

- Lafuente, B., Downs, R. T., Yang, H., & Stone, N. (2016). The power of databases: the RRUFF project. *Highlights in mineralogical crystallography*, 1–29. Berlin: de Gruyter. <https://doi.org/10.1515/9783110417104-003>
- Laxton, E. T. (1887). *Process of hardening and preserving plaster-of-Paris casts and molds and making them impervious to water, &c.* Patent No. 371550.
- Lazzari, M., & Chiantore, O. (1999). Drying and oxidative degradation of linseed oil. *Polymer Degradation and Stability*, 65(2), 303–313. [https://doi.org/10.1016/S0141-3910\(99\)00020-8](https://doi.org/10.1016/S0141-3910(99)00020-8)
- Lebedev, S. A. (2016). Methodology of science and general-scientific methods of research. *European Researcher. Series A*, 4, 196–207. <https://doi.org/10.13187/er.2016.105.196>
- Legodi, M. A., De Waal, D., Potgieter, J. H., & Potgieter, S. S. (2001). Rapid determination of CaCO₃ in mixtures utilising FT-IR spectroscopy. *Minerals Engineering*, 14(9), 1107–1111. [https://doi.org/10.1016/S0892-6875\(01\)00116-9](https://doi.org/10.1016/S0892-6875(01)00116-9)
- Lending, M. (2017). *Plaster monuments: architecture and the power of reproduction*. Princeton: Princeton University Press. ISBN: 9780691177144
- Lewry, A. J., & Williamson, J. (1994). The setting of gypsum plaster. *Journal of Materials Science*, 29(23), 6085–6090. <https://doi.org/10.1007/BF00354546>
- Li, D. H. W. (2010). A review of daylight illuminance determinations and energy implications. *Applied Energy*, 87(7), 2109–2118. <https://doi.org/10.1016/J.APENERGY.2010.03.004>
- Littlefair, P. J. (1985). The luminous efficacy of daylight: a review. *Lighting Research & Technology*, 17(4), 162–182. <https://doi.org/10.1177/0144771535850170040401>
- Liu, X. Y., Timar, M. C., & Varodi, A. M. (2019). A comparative study on the artificial UV and natural ageing of beeswax and Chinese wax and influence of wax finishing on the ageing of Chinese Ash (*Fraxinus mandshurica*) wood surfaces. *Journal of Photochemistry and Photobiology B: Biology*, 201, 111607. <https://doi.org/https://doi.org/10.1016/j.jphotobiol.2019.111607>
- Lorenzi Moulage d'Art*. (2018). <http://www.lorenzi.fr/> (last accessed 28/03/2021)
- Lowenthal, D. (1999). Authenticity: rock of faith or quicksand quagmire? Conservation: *The Getty Conservation Institute Newsletter*, 14(3), 5–8.
- Luxán, M. P., Dorrego, F., & Laborde, A. (1995). Ancient gypsum mortars from St. Engracia (Zaragoza, Spain): Characterization. Identification of additives and treatments. *Cement and Concrete Research*, 25(8), 1755–1765. [https://doi.org/10.1016/0008-8846\(95\)00171-9](https://doi.org/10.1016/0008-8846(95)00171-9)
- Luxford, N., & Thickett, D. (2011). Designing accelerated ageing experiments to study silk deterioration in historic houses. *Journal of the Institute of Conservation*, 34(1), 115–127. <http://dx.doi.org/10.1080/19455224.2011.581118>
- Madonia, G., & Forti, P. (2003). *Le aree carsiche gessose d'Italia*. Bologna: Istituto italiano di speleologia.
- MacDonald, J., Thomson, B., & Tongue, K. (1992). *Chemical cleaning of sandstone: Comparative laboratory studies*. Stone Cleaning and the Nature, Soiling and Decay Mechanisms of Stone: Proceedings of the International Conference Held in Edinburgh, UK, 14-16 April 1992, 217–226.

- Maguregui, M., Sarmiento, A., Escribano, R., Martinez-Arkarazo, I., Castro, K., & Madariaga, J. M. (2009). Raman spectroscopy after accelerated ageing tests to assess the origin of some decayed products found in real historical bricks affected by urban polluted atmospheres. *Analytical and Bioanalytical Chemistry*, 395(7), 2119–2129. <https://doi.org/10.1007/s00216-009-3153-6>
- Mahmoud, H. M., Kantiranis, N., & Stratis, J. (2012). A technical characterization of Roman plasters, Luxor temple, Upper Egypt. *Mediterranean Archaeology and Archaeometry*, 12(2), 81–93.
- Mallégol, J., Gardette, J.-L., & Lemaire, J. (1999). Long-term behavior of oil-based varnishes and paints I. Spectroscopic analysis of curing drying oils. *Journal of the American Oil Chemists' Society*, 76(8), 967–976. <https://doi.org/10.1007/s11746-999-0114-3>
- Mallégol, J., Lemaire, J., & Gardette, J.-L. (2000). Drier influence on the curing of linseed oil. *Progress in Organic Coatings*, 39(2), 107–113. [https://doi.org/https://doi.org/10.1016/S0300-9440\(00\)00126-0](https://doi.org/https://doi.org/10.1016/S0300-9440(00)00126-0)
- Manfredi, M., Barberis, E., Rava, A., Robotti, E., Gosetti, F., & Marengo, E. (2015). Portable diffuse reflectance infrared Fourier transform (DRIFT) technique for the non-invasive identification of canvas ground: IR spectra reference collection. *Analytical Methods*, 7(6), 2313–2322. <https://doi.org/10.1039/C4AY02006E>
- Marcinkowski, W., & Zaucha, T. (2010). *Kraków na wyciągnięcie ręki. Rzeźba architektoniczna ze zbiorów Muzeum Narodowego w Krakowie/Krakow within your reach. Architectural sculpture in the collection of the National Museum in Krakow*. Krakow: MNK.
- Marinescu, M., Emandi, A., Dului, O. G., Stanculescu, I., Bercu, V., & Emandi, I. (2014). FT-IR, EPR and SEM–EDAX investigation of some accelerated aged painting binders. *Vibrational Spectroscopy*, 73, 37–44. <https://doi.org/https://doi.org/10.1016/j.vibspec.2014.04.006>
- Martin de Fonjaudran, C., Nevin, A., Piqué, F. & Cather, S. (2008). Stratigraphic analysis of organic materials in wall painting samples using micro-FTIR attenuated total reflectance and a novel sample preparation technique. *Analytical and Bioanalytical Chemistry* 392, 77–86.
- Massa, V., & Scicolone, G. C. (1991). *Le vernici per il restauro: i leganti*. Firenze: Nardini Editore. ISBN-13: 978-8840440156
- Masschelein-Kleiner, L. (1985). *Ancient binding media, varnishes and adhesives*. Roma: ICCROM. ISBN: 92-9077-119-4
- Mateescu, A., Freese, S., Frank, P., Jonas, U., & Theodorakopoulos, C. (2017). Novel surface-attached gels from photo-crosslinkable polyacrylamides for the cleaning of works of art. *Gels in the Conservation of Art*, 237–244. <https://doi.org/10.3390/gels6010001>
- Mazzeo, R., Joseph, E., Prati, S. & Millemaggi, A. (2007). Attenuated Total Reflection-Fourier transform infrared microspectroscopic mapping for the characterisation of paint cross-sections. *Analytica Chimica Acta* 599, 107–117.
- Maxwell, I. (1992). *Stone cleaning: For better or worse? An overview*. Stone Cleaning and the Nature, Soiling and Decay Mechanisms of Stone: Proceedings of the International Conference Held in Edinburgh, UK, 14-16 April 1992, 3–49.

- McGlinchey, C. (1994). Color and light in the museum environment. *The Metropolitan Museum of Art Bulletin*, 51(3), 44–52.
- McKeen, L. W. (2015). *Fluorinated coatings and finishes handbook: The definitive user's guide*. William Andrew. ISBN: 9780815517245
- Megens, L., Joosten, I., Tagle, A. D., & Dooijes, R. (2011). *The composition of plaster casts*. <http://www.kennisvoorcollecties.nl/en/projects/objects-in-context/conservation-of-plaster-collections/>
- Meilach, D. Z. (1966). *Creating with plaster*. London: Blandford Press.
- Melita, L., Węglowska, K., & Tamburini, D. (2020). Investigating the Potential of the Er:YAG Laser for the Removal of Cemented Dust from Limestone and Painted Plaster. *Coatings*, 10, 1099. <https://doi.org/10.3390/coatings10111099>
- Mendoza Cuevas, A., Bernardini, F., Gianoncelli, A., & Tuniz, C. (2015). Energy dispersive X-ray diffraction and fluorescence portable system for cultural heritage applications. *X-Ray Spectrometry*, 44(3), 105–115. <https://doi.org/10.1002/xrs.2585>
- Meneghetti, S. M. P., de Souza, R. F., Monteiro, A. L., & de Souza, M. O. (1998). Substitution of lead catalysts by zirconium in the oxidative polymerization of linseed oil. *Progress in Organic Coatings*, 33(3–4), 219–224.
- Merrifield, M. P. (1846). *The Art of Fresco Painting: As Practised by the Old Italian and Spanish Masters, with a Preliminary Inquiry Into the Nature of the Colours Used in Fresco Painting, with Observation and Notes*. London: C. Gilpin.
- Miliani, C., Rosi, F., Daveri, A., & Brunetti, B. G. (2012). Reflection infrared spectroscopy for the non-invasive in situ study of artists' pigments. *Applied Physics A*, 106(2), 295–307. <https://doi.org/10.1007/s00339-011-6708-2>
- Millar, W. (1899). *Plastering, plain & decorative. A practical treatise on the art & craft of plastering and modelling, including full description of the various tools, materials, processes and appliances employed*. (Batsford, B. T. ed.) Dorset: Donhead Publishing Ltd. ISBN-13: 978-1873394878
- Miller, S. G. (2005). *Plaster Casts at Berkeley. Collections of the Hearst Museum of Anthropology & Department of Classics at UC Berkeley. An Exhibition of Rare Plaster Casts of Ancient Greek and Roman Sculpture*. pp. vi+ 76+ ii.
- Mills, J. S. (1966). The Gas Chromatographic Examination of Paint Media. Part 1. Fatty Acid Composition and Identification of Dried Oil Films. *Studies in Conservation*, 11(2), 92–107. <https://doi.org/10.2307/1505447>
- Mills, J., & White, R. (2012). *Organic chemistry of museum objects*. Oxford: Routledge. ISBN: 9780750646932
- Miramón, J. G. (2019). *Conservación y restauración de esculturas en yeso en la Real Academia de Bellas Artes de San Fernando*. Universidad Complutense de Madrid. Thesis.
- Moropoulou, A., Bakolas, A., & Bisbikou, K. (1995). Characterization of ancient, byzantine and later historic mortars by thermal and X-ray diffraction techniques. *Thermochimica Acta*, 269, 779–795. [https://doi.org/10.1016/0040-6031\(95\)02571-5](https://doi.org/10.1016/0040-6031(95)02571-5)

- Moropoulou, A., Zendri, E., Ortiz, P., Delegou, E. T., Ntoutsis, I., Balliana, E., Becerra, J., & Ortiz, R. (2019). Scanning Microscopy Techniques as an Assessment Tool of Materials and Interventions for the Protection of Built Cultural Heritage. *Scanning*, 2019. <https://doi.org/10.1155/2019/5376214>
- Morris, R. J. (1963). Infrared spectrophotometric analysis of calcium sulfate hydrates using internally standardized mineral oil mulls. *Analytical Chemistry*, 35(10), 1489–1492. <https://doi.org/10.1021/ac60203a019>
- Müller, M., Wienold, J., Walker, W. D., & Reindl, L. M. (2009). Characterization of indoor photovoltaic devices and light. *2009 34th IEEE Photovoltaic Specialists Conference (PVSC)*, 738–743. <https://doi.org/10.1002/ese3.110>
- Nardelli, F., Martini, F., Lee, J. *et al.* (2021). The stability of paintings and the molecular structure of the oil paint polymeric network. *Scientific Reports* 11(1), 1-13. <https://doi.org/10.1038/s41598-021-93268-8>
- Nel, P., Lynch, P. A., Laird, J. S., Casey, H. M., Goodall, L. J., Ryan, C. G., & Sloggett, R. J. (2010). Elemental and mineralogical study of earth-based pigments using particle-induced X-ray emission and X-ray diffraction. *Nuclear Instruments and Methods in Physics Research Section A: Accelerators, Spectrometers, Detectors and Associated Equipment*, 619(1–3), 306–310. <https://doi.org/10.1016/j.nima.2009.12.003>
- Nenci, C. (2006). *Gli stucchi italiani. Nuove ricerche su alcune opere in stucco dell'Abruzzo*. Stucs et Décors de La Fin de l'Antiquité Au Moyen Âge (Ve-XIIe Siècle) Actes Du Colloque International Tenu à Poitiers Du 16 Au 19 Septembre 2004, 269–283. <https://doi.org/10.1484/M.BAT-EB.3.149>
- Neven, S. (2009). Comparative analysis of painting recipes: a new contribution to the study of the texts of the Strasbourg family. *Sources and Serendipity. Testimonies of Artists' Practice*, 65–71. <http://hdl.handle.net/2268/150332>
- Nowik, W. (1995). Acides amines et acides gras sur un même chromatogramme—un autre regard sur l'analyse des liants en peinture. *Studies in Conservation*, 40(2), 120–126. <https://doi.org/10.1179/sic.1995.40.2.120>
- Oleari, C. (1998). *Misurare il colore: spettrofotometria, fotometria e colorimetria: fisiologia e percezione*. Milano: Hoepli Editore. ISBN: 9788820341268
- Ordonez, E., & Twilley, J. (1997). Clarifying the haze: efflorescence on works of art. *Analytical Chemistry*, 69(13), 416A-422A.
- O'Toole, K. (2007). The Hellenic Gallery at the Museum of Perth-Is it a Story of Contested, or of Complementary, Heritage? *The Rag*, 2(4). http://www.humanities.uwa.edu.au/__data/assets/pdf_file/0004/1267348/RAG_vol_2_issue_4.pdf
- Oyman, Z. O., Ming, W., & Van der Linde, R. (2005). Oxidation of drying oils containing non-conjugated and conjugated double bonds catalyzed by a cobalt catalyst. *Progress in Organic Coatings*, 54(3), 198–204. <https://doi.org/10.1016/j.porgcoat.2005.06.004>
- Palache, C., Berman, H., & Frondel, C. (1951). *Dana's system of mineralogy*. (7th edn), vol II. New York: Wiley, 1124, 555–565.
- Pande, S. B., Raghorte, V. R., & Sisyawar, A. C. (2012). *Study of luminescent materials and its scientific application*. Mumbai: Bionano Frontier, 5.

- Pasquini, L. (2002). *La decorazione a stucco in Italia fra Tardo Antico e Alto Medioevo* (Longo Ed.). Ravenna: Le Tessere.
- Pastorova, I., Van der Berg, K. J., Boon, J. J., & Verhoeven, J. W. (1997). Analysis of oxidised diterpenoid acids using thermally assisted methylation with TMAH. *Journal of Analytical and Applied Pyrolysis*, 43(1), 41–57. [https://doi.org/10.1016/S0165-2370\(97\)00058-2](https://doi.org/10.1016/S0165-2370(97)00058-2)
- Patterson, A., & Trusted, M. (2018). *The Cast Courts*. London: V&A publishing. ISBN-13: 978-1851779796
- Payne, E. M. (2015). *Digital comparison of 19th-century plaster casts and original classic sculptures*. Digital Classicist London & Institute of Classical Studies seminar, London. <https://www.digitalclassicist.org/wip/wip2015-03ep.html>
- Payne, E. M. (2019a). Casting a new canon: Collecting and treating casts of Greek and Roman Sculpture, 1850–1939. *The Cambridge Classical Journal*, 65, 113–149. <https://doi.org/10.1017/S1750270519000034>
- Payne, E. M. (2019b). 3D imaging of the Parthenon sculptures: an assessment of the archaeological value of nineteenth-century plaster casts. *Antiquity*, 93(372), 1625–1642. <https://doi.org/10.15184/aqy.2019.179>
- Payne, E. M. (2020). The conservation of plaster casts in the nineteenth century. *Studies in Conservation*, 65(1), 37–58. <https://doi.org/10.1080/00393630.2019.1610845>
- Pearce, S. (2013). *On collecting: An investigation into collecting in the European tradition*. London: Routledge. ISBN: 9780415075619
- Pelosi, C., Fodaro, D., Sforzini, L., Rubino, A. R., & Falqui, A. (2013). Study of the laser cleaning on plaster sculptures. The effect of laser irradiation on the surfaces. *Optics and Spectroscopy*, 114(6), 917–928. <https://doi.org/10.1134/S0030400X13060118>
- Pentzien, S., Conradi, A., & Krüger, J. (2011). The influence of paper type and state of degradation on laser cleaning of artificially soiled paper. *Lasers in the Conservation of Artworks VIII*, 59–65. London: Taylor & Francis Group. ISBN: 9780429212963
- Perusini, T., Zendri, E., Crescenzo, M. M. D., & Iseppi, D. (2009). *La pulitura di sculture in gesso del novecento mediante applicazione di gel*. Paper Presented at the VII Congresso Internazionale IGIC - Lo Stato Dell'Arte 7, Castel Dell'Ovo, Napoli.
- Piva, G. (2010). *Manuale pratico di tecnica pittorica* (Quinta ed.). Milano: Ulrico Hoepli. ISBN: 9788820304591
- Plaster & plaster casts: materiality and practice*. (2010). Conference report. <http://www.vam.ac.uk/content/articles/p/plaster-and-plaster-casts-materiality-and-practice-conference-report/>
- Pollio, V. (1914). *The Ten Books on Architecture* (Translated). Cambridge: Harvard University Press. ISBN: 9780674992771
- Poli, T., Piccirillo, A., Zoccali, A., Conti, C., Nervo, M., & Chiantore, O. (2014). The role of zinc white pigment on the degradation of shellac resin in artworks. *Polymer Degradation and Stability*, 102, 138–144. <https://doi.org/10.1016/J.POLYMDEGRADSTAB.2014.01.026>

- Popescu, C.-M., Lisa, G., Manoliu, A., Gradinariu, P., & Vasile, C. (2010). Thermogravimetric analysis of fungus-degraded lime wood. *Carbohydrate Polymers*, 80(1), 78–83. <https://doi.org/10.1016/j.carbpol.2009.10.058>
- Prati, S., Joseph, E., Sciutto, G., & Mazzeo, R. (2010). New advances in the application of FTIR microscopy and spectroscopy for the characterization of artistic materials. *Accounts of Chemical Research*, 43(6), 792–801. <https://doi.org/10.1021/ar900274f>
- Prati, S., Rosi, F., Sciutto, G., Mazzeo, R., Magrini, D., Sotiropoulou, S. & Van Bos, M. (2012). Evaluation of the effect of six different paint cross section preparation methods on the performances of Fourier Transformed Infrared microscopy in attenuated total reflection mode. *Microchemical Journal* 103, 79–89.
- Prati, S., Sciutto, G., Catelli, E., Ashashina, A. & Mazzeo, R. (2013). Development of innovative embedding procedures for the analyses of paint cross sections in ATR FITR microscopy. *Analytical and Bioanalytical Chemistry* 405, 895–905.
- Price, B. A., Pretzel, B., & Lomax, S. Q. (2009). *Infrared and Raman Users Group Spectral Database*. (2007 ed). Philadelphia: IRUG. www.irug.org
- Price, C. A., & Doehne, E. (2011). *Stone conservation: an overview of current research*. Los Angeles: Getty publications. ISBN: 978-1-60606-046-9
- Pritchard, D. C. (1995). *Lighting* (Fifth ed.). Singapore: Longman publishers. ISBN: 9780582357990
- Procter, P. (2000). *Cambridge international dictionary of English* (E. fakulteta Univerza Mariboru Ed.). Cambridge University Press.
- Quill, J., Fedor, G., Brennan, P., & Everett, E. (2004). *Quantifying the indoor light environment: testing for light stability in retail and residential environments*. NIP & Digital Fabrication Conference, 2004(2), 689–698.
- Rathgen, F. (2013). *The preservation of antiquities: a handbook for curators*. Cambridge University Press. ISBN: 9781107635258
- Regert, M., Colinart, S., Degrand, L., & Decavallas, O. (2001). Chemical alteration and use of beeswax through time: accelerated ageing tests and analysis of archaeological samples from various environmental contexts. *Archaeometry*, 43(4), 549–569. <https://doi.org/10.1111/1475-4754.00036>
- Reynolds-Kaye, J. (2019). Circulating casts of the Coatlicue: Mariana Castillo Deball's unearthing of the Aztec earth goddess's history of reproduction and display. *Sculpture Journal*, 28(3), 365–380.
- RHOPOINT Instruments Manual*. (2020). Rhopoint. <https://www.rhopointinstruments.com/downloads/manuals/> (last accessed 28/03/2021)
- Ribechini, E., Modugno, F., Colombini, M. P., & Evershed, R. P. (2008). Gas chromatographic and mass spectrometric investigations of organic residues from Roman glass unguentaria. *Journal of Chromatography A*, 1183(1–2), 158–169. <https://doi.org/10.1016/j.chroma.2007.12.090>
- Rieppel, L. (2015). Plaster cast publishing in nineteenth-century palaeontology. *History of Science*, 53(4), 456–491. <https://doi.org/10.1177%2F0073275315580954>

- Risdonne, V., Ellis, A., Alexander, C., & Clough, K. (2018a). *Lasting Impressions 2018: the roles of reproductions in the museum*. Newcastle upon Tyne.
- Risdonne, V., Ellis, A., Alexander, C., & Clough, K. (2018b). Lasting Impressions 2018 blog. <https://lastingimpressions.mystrikingly.com/> (last accessed 28/03/2021)
- Risdonne, V., Hubbard, C., Borges, V. H. L., & Theodorakopoulos, C. (2021). Materials and Techniques for the Coating of Nineteenth-Century Plaster Casts: A Review of Historical Sources. *Studies in Conservation*. <https://doi.org/10.1080/00393630.2020.1864896>
- Risdonne, V., & Theodorakopoulos, C. (2021). *Database of results. Materials and techniques for coating of the nineteenth-century plaster casts. A scientific and archival investigation of the Victoria & Albert Museum cast collection*. Northumbria University. <https://doi.org/https://doi.org/10.25398/rd.northumbria.14053985>
- Rizzutto, M. A., Curado, J. F., Bernardes, S., Campos, P., Kajiya, E. A. M., Silva, T. F., Rodrigues, C. L., Moro, M., Tabacniks, M., & Added, N. (2015). *Analytical techniques applied to study cultural heritage objects*. 2015 International Nuclear Atlantic Conference - INAC 2015. São Paulo, Brazil. ISBN: 978- 85- 99141- 06-9
- Roberts, A. G. (1968). *Organic coatings; properties, selection, and use* (Vol. 7). US Department of Commerce, National Bureau of Standards.
- Rodrigues, J. D., & Grossi, A. (2007). Indicators and ratings for the compatibility assessment of conservation actions. *Journal of Cultural Heritage*, 8(1), 32–43. <http://dx.doi.org/10.1016%2Fj.culher.2006.04.007>
- Roduit, B., & Odlyha, M. (2006). Prediction of thermal stability of fresh and aged parchment. *Journal of thermal analysis and calorimetry*, 85(1), 157-164. <https://doi.org/10.1007/s10973-005-7410-4>
- Rosi, F., Cartechini, L., Sali, D. & Miliani, C. (2019). Recent trends in the application of fourier transform infrared (FT-IR) spectroscopy in Heritage Science: From micro: From non-invasive FT-IR. *Physical Sciences Reviews* 4, 1–19.
- Ross, S. D., & Farmer, V. C. (1974). Sulphates and other oxy-anions of Group VI. *The Infrared Spectra of Minerals*, 4, 423–444.
- Rotili, V. (2009). *La fortuna della copia in gesso: teoria e prassi tra Sette e Ottocento*. Università degli studi Roma Tre. PhD Thesis.
- Sackler, A. M. (2005). *Scientific examination of art: Modern techniques in conservation and analysis*. Washington, DC: The National Academies Press. <https://doi.org/10.17226/11413>
- Salavessa, E., Jalali, S., Sousa, L. M. O., Fernandes, L., & Duarte, A. M. (2013). Historical plasterwork techniques inspire new formulations. *Construction and Building Materials*, 48, 858–867. <https://dx.doi.org/10.1016/j.conbuildmat.2013.07.064>
- Salomone, G. (1947). *Guida pratica per la preparazione dei prodotti chimici: Prodotti minerali*. Torino: Lavagnolo editore.
- Sansonetti, A., Casati, M., Striova, J., Canevali, C., Anzani, M., & Rabbolini, A. (2012). *A cleaning method based on the use of agar gels: New tests and perspectives*. 12th International Congress on the Deterioration and Conservation of Stone. Columbia University, New York.

- Samain, L., Silversmit, G., Sanyova, J., Vekemans, B., Salomon, H., Gilbert, B., Grandjean, F., Long, G. J., Hermann, R. P., Vincze, L., & Strivay, D. (2011). Fading of modern Prussian blue pigments in linseed oil medium. *Journal of Analytical Atomic Spectrometry*, 26(5), 930–941. <https://doi.org/10.1039/C0JA00234H>
- Sandu, I. C. A., Joosten, I., & Leal, N. (2015). Optical imaging applications for the study of cultural heritage artifacts. *Advances in Laser and Optics Research*, 1–45. New York: Nova Science Publishers. ISBN: 978-1-63463-494-6
- Sano, N., Cumpson, P. J., Cwiertnia, E., Perry, J. J., & Singer, B. W. (2014). Multivariate analysis studies of the ageing effect for artist's oil paints containing modern organic pigments. *Surface and Interface Analysis*, 46(10–11), 786–790. <https://doi.org/10.1002/sia.5467>
- Sapin, C. (2004). *Stucs et décors de la fin de l'Antiquité au Moyen Âge (du Ve au XIIe siècle)*. Bulletin Du Centre d'études Médiévales d'Auxerre| BUCEMA, 8.
- Sarkar, P. C., & Kumar, K. K. (2001). An investigation into the different forms of lac resin using FT-IR and diffuse reflectance spectroscopy. *Pigment & Resin Technology*, 30(1), 25–34. <https://doi.org/10.1108/03699420110364138>
- Schulman, Y. (2020). *Advanced Thermal Analysis of Phase Change Materials - Three Organic Waxes using Modulated TGA and Modulated DSC*. <https://www.tainstruments.com/pdf/literature/TA406.pdf> (last accessed 28/03/2021)
- Saumarez-Smith, M. W. (1991). *Introducing the Victoria and Albert Museum*. London: The Victoria and Albert Museum. ISBN-13: 978-1851771066
- Scala (Ed.). (1991). *The Victoria and Albert Museum*. ISBN-13: 978-0863503344
- Scalarone, D., van der Horst, J., Boon, J. J., & Chiantore, O. (2003). Direct-temperature mass spectrometric detection of volatile terpenoids and natural terpenoid polymers in fresh and artificially aged resins. *Journal of Mass Spectrometry*, 38(6), 607–617. <https://doi.org/10.1002/jms.470>
- Schilling, M. R., & Khanjian, H. P. (1996). Gas chromatographic analysis of amino acids as ethyl chloroformate derivatives. Part 2, effects of pigments and accelerated ageing on the identification of proteinaceous binding media. *Journal of the American Institute for Conservation*, 35(2), 123–144.
- Seidl, V., Knop, O., & Falk, M. (1969). Infrared studies of water in crystalline hydrates: gypsum, CaSO₄·2H₂O. *Canadian Journal of Chemistry*, 47(8), 1361–1368. <https://doi.org/10.1139/v69-223>
- Serafima, S., Dului, O. G., Manea, M. M., & Niculescu, G. (2016). FTIR, XRF and optical microscopy analysis of the painting layer of an early 19th-century icon. *Romanian Reports in Physics*, 68(1), 191–202.
- Sharma, S. K., Shukla, S. K., & Vaid, D. N. (1983). Shellac-structure, characteristics & modification. *Defence Science Journal*, 33(3), 261–271. <https://doi.org/10.14429/dsj.33.6181>
- Sharpe, E. (2014). *V&A casts new light on plaster casts*. *Conservation*. Issue 263. <http://ec2-79-125-124-178.eu-west-1.compute.amazonaws.com/articles/VA-casts-new-light-on-plaster-casts/36358>

- Shreve, O. Do, Heether, M. R., Knight, H. B., & Swern, D. (1950). Infrared absorption spectra. Some long-chain fatty acids, esters, and alcohols. *Analytical Chemistry*, 22(12), 1498–1501.
- Sifontes, A., Cañizales, E., Toro-Mendoza, J., Ávila, E., Hernández, P., Delgado, B., Gutiérrez, B., Díaz, Y., & Cruz-Barrios, E. (2015). Obtaining Highly Crystalline Barium Sulphate Nanoparticles via Chemical Precipitation and Quenching in Absence of Polymer Stabilizers. *Journal of Nanomaterials*, 2015. <https://doi.org/10.1155/2015/510376>
- Šimek, P., Heydová, A., & Jegorov, A. (1994). High-resolution capillary gas chromatography and gas chromatography-mass spectrometry of protein and non-protein amino acids, amino alcohols, and hydroxycarboxylic acids as their tert-butyltrimethylsilyl derivatives. *Journal of High-Resolution Chromatography*, 17(3), 145–152. <https://doi.org/10.1002/jhrc.1240170305>
- Simon, J. (2011). *Plaster figure makers: a short history*. <https://www.npg.org.uk/research/programmes/plaster-figure-makers-history> (last accessed 28/03/2021)
- Simpson-Grant, M. (2000). The use of ultraviolet-induced visible-fluorescence in the examination of museum objects, part 2. *Conserve O Gram*, 1(10).
- Sinclair, R. G., McKay, A. F., Myers, G. S., & Jones, R. N. (1952). The Infrared Absorption Spectra of Unsaturated Fatty Acids and Esters. *Journal of the American Chemical Society*, 74(10), 2578–2585.
- Singer, B., & McGuigan, R. (2007). The simultaneous analysis of proteins, lipids, and diterpenoid resins found in cultural objects. *Journal of Analytical, Environmental and Cultural Heritage Chemistry*, 97(7), 405–417. <https://doi.org/10.1002/adic.200790044>
- Singh, K. (2019). Sanchi, in and out of the museum. *Sculpture Journal*, 28(3), 345–364.
- Smith, G. (1810). *The Laboratory or School of Arts*. London: Law and Gilbert.
- Smith, B. J., Gomez-Heras, M., & McCabe, S. (2008). Understanding the decay of stone-built cultural heritage. *Progress in Physical Geography*, 32(4), 439–461. <https://doi.org/10.1177/0309133308098119>
- Sotiropoulou, S., Sciutto, G., Tenorio, A. L., Mazurek, J., Bonaduce, I., Prati, S., Mazzeo, R., Schilling, M., & Colombini, M. P. (2018). Advanced analytical investigation on degradation markers in wall paintings. *Microchemical Journal*, 139, 278–294. <https://doi.org/https://doi.org/10.1016/j.microc.2018.03.007>
- Steven, H. (2005). White gold alloys: Colour measurement and grading. *Gold Bulletin*, 38(2), 55–67.
- Stevenson, A., & Waite, M. (2011). *Concise Oxford English dictionary* (Luxury ed.). Oxford University Press.
- Stroobant, E., & De Hoffmann, V. (2001). *Mass Spectrometry: Principles and Applications*, (Third ed.). John Wiley & Sons. ISBN: 978-0-470-03310-4
- Stuart, B. H. (2007). *Analytical techniques in materials conservation*. John Wiley & Sons. ISBN: 978-0-470-01280-2

- Sullivan, M. G. (2019). Plaster of Paris is [...] a production of Derbyshire': practical geology and the plaster revolution in British sculptors' workshops, 1745–1845. *The Sculpture Journal*, 28(3)(419), 299–314.
- Svečnjak, L., Baranović, G., Vinceković, M., Prđun, S., Bubalo, D., & Gajger, I. T. (2015). An approach for routine analytical detection of beeswax adulteration using FT-IR-ATR spectroscopy. *Journal of Apicultural Science*, 59(2), 37–49.
- Symoniuk, E., Ratusz, K., & Krygier, K. (2016). Comparison of the oxidative stability of linseed (*Linum usitatissimum* L.) oil by pressure differential scanning calorimetry and Rancimat measurements. *Journal of Food Science and Technology*, 53(11), 3986–3995. <https://doi.org/10.1007/s13197-016-2398-2>
- Tamburini, D., Dyer, J., & Bonaduce, I. (2017). The characterisation of shellac resin by flow injection and liquid chromatography coupled with electrospray ionisation and mass spectrometry. *Scientific Reports*, 7(1), 1–15. <https://doi.org/10.1038/s41598-017-14907-7>
- Tatzber, M., Stemmer, M., Spiegel, H., Katzlberger, C., Haberhauer, G., & Gerzabek, M. H. (2007). An alternative method to measure carbonate in soils by FT-IR spectroscopy. *Environmental Chemistry Letters*, 5(1), 9–12. <https://doi.org/10.1007/s10311-006-0079-5>
- The Architectural Courts, South Kensington Museum. The Trajan Column and the Portico de la Gloria, Santiago de Compostella. (1873, October 4). *The Builder*, 789.
- The Glasgow School of Art. Archives and Collection*. (2020). <https://gsaarchives.net/collections/index.php/informationobject/browse?sort=lastUpdated> (last accessed 28/03/2021)
- The New Court, South Kensington. (1873, April 25). *The Building News*.
- The New Court at South Kensington. (1873, October 31). *The Building News*.
- The South Kensington Museum. (1882, September 20). *The Times*.
- Theodorakopoulos, C., & Hubbard, C. (2017). CfS VA-UNN CDP_2017_Casts. Unpublished project proposal.
- Theodorakopoulos, C., Zafiropoulos, V., Boon, J. J., & Boyatzis, S. C. (2007). Spectroscopic investigations on the depth-dependent degradation gradients of aged triterpenoid varnishes. *Applied spectroscopy*, 61(10), 1045-1051. <https://doi.org/10.1366/2F000370207782217833>
- Theodorakopoulos, C., & Zafiropoulos, V. (2009). Depth-profile investigations of triterpenoid varnishes by KrF excimer laser ablation and laser-induced breakdown spectroscopy. *Applied surface science*, 255(20), 8520-8526. <https://doi.org/10.1016/j.apsusc.2009.06.012>
- Thomson, G. (2013). *The museum environment*. Amsterdam: Elsevier. ISBN: 9781483102719
- Tietze, A. (1998). Classical casts and colonial galleries: the life and afterlife of the 1908 Beit Gift to the National Gallery of Cape Town. *South African Historical Journal*, 39(1), 70–90. <https://doi.org/10.1080/02582479808671330>
- Toniolo, L., Zerbi, C. M., & Bugini, R. (2009). Black layers on historical architecture. *Environmental Science and Pollution Research*, 16(2), 218–226. <https://doi.org/10.1007/s11356-008-0046-8>

- Trickey, J. H. (1884). *Art or process of and composition for making artificial stone*. Patent No. 308111.
- Trusted, H. (2017). *Displaying Plaster Casts at the Museum; South Kensington and the Reproduction of Sculpture*. Unpublished report.
- Turco, A. (1990). *Il Gesso. Lavorazione, trasformazione, impieghi*. Milano: Hoepli. ISBN: 9788820317065
- Uhlenhuth, E. (1879). *Vollständige Anleitung zum Formen und Gießen oder genaue Beschreibung aller in den Künsten und Gewerben dafür angewandten Materialien: als: Gips, Wachs, Schwefel, Leim, Harz, Guttapercha, Thon, Lehm, Sand und deren Behandlung behufs Darstellung von Gypsfig*. Hartleben.
- Vahur, S., Teearu, A., Peets, P., Joosu, L., & Leito, I. (2016). ATR-FT-IR spectral collection of conservation materials in the extended region of 4000-80 cm⁻¹. *Analytical and Bioanalytical Chemistry*, 408(13), 3373–3379. <https://doi.org/10.1007/s00216-016-9411-5>
- Van der Doelen, G. A. (1999). Molecular studies of fresh and aged triterpenoid varnishes. University of Amsterdam, PhD thesis. <https://hdl.handle.net/11245/1.180090>
- Van der Weerd, J., Brammer, H., Boon, J. J., & Heeren, R. M. A. (2002). Fourier transform infrared microscopic imaging of an embedded paint cross-section. *Applied Spectroscopy*, 56(3), 275–283. <https://doi.org/10.1366%2F0003702021954683>
- van Loon, A., & Boon, J. J. (2004). Characterization of the deterioration of bone black in the 17th century Oranjezaal paintings using electron-microscopic and micro-spectroscopic imaging techniques. *Spectrochimica Acta Part B: Atomic Spectroscopy*, 59(10–11), 1601–1609. <https://doi.org/10.1016/j.sab.2004.03.021>
- Vandevoorde, D., Cnudde, V., Dewanckele, J., Boone, M., de Bouw, M., Meynen, V., Lehmann, E., & Verhaeven, E. (2012). *Comparison of non-destructive techniques for analysis of the water-absorbing behaviour of stone*. 12th International Congress on the Deterioration and Conservation of Stone.
- Vandevoorde, D., Cnudde, V., Dewanckele, J., Brabant, L., de Bouw, M., Meynen, V., & Verhaeven, E. (2013). Validation of in situ applicable measuring techniques for analysis of the water adsorption by stone. *Procedia Chemistry*, 8(1), 317–327. <https://doi.org/10.1016/j.proche.2013.03.039>
- Vanni, F. (2019). Aspetti meno noti della scultura mediobizantina: la decorazione a stucco. Dialoghi Con Bisanzio. *Spazi Di Discussione, Percorsi Di Ricerca Atti Dell'VIII Congresso Dell'Associazione Italiana Di Studi Bizantini*, 1119–1140.
- V&A website - Search the Collections. (2020). <https://collections.vam.ac.uk/> (last accessed 28/03/2021)
- Veasey, N. (2019). *Revealing hidden structures through X-rays*. <https://www.vam.ac.uk/articles/revealing-hidden-structures-x-rays> (last accessed 28/03/2021)
- Ventolà, L., Vendrell, M., Giraldez, P., & Merino, L. (2011). Traditional organic additives improve lime mortars: New old materials for restoration and building natural stone fabrics. *Construction and Building Materials*, 25(8), 3313–3318. <https://doi.org/https://doi.org/10.1016/j.conbuildmat.2011.03.020>

- Vergès-Belmin, V. (1996). Towards a definition of common evaluation criteria for the cleaning of porous building materials: a review. *Science and Technology for Cultural Heritage*, 5(1), 69–83.
- Victoria and Albert Museum Annual Report and Accounts 2017-2018*. (2018). <https://vanda-production-assets.s3.amazonaws.com/2018/07/18/10/54/31/2e78a797-70aa-4a6d-a6c4-db71a4ffa8b0/VAAR%20-%20final%20web%20version%2018%2007%202018.pdf> (last accessed 28/03/2021)
- Vulliamy, E. (2016). Artists “steal” Queen Nefertiti bust by secretly scanning and releasing 3D printing data online. <https://www.independent.co.uk/arts-entertainment/art/news/artists-secretly-scan-queen-nefertiti-bust-and-release-3d-printing-data-online-a6895061.html> (last accessed 28/03/2021)
- Wachowiak, M. J., Karas, B. V., & Baltrusch, R. E. (2009). *Reconstruction of a nineteenth-century plaster piece mold and recreation of a casting*. Computer Applications to Archaeology 2009, Williamsburg, Virginia, USA, March 22-26, 2009.
- Wade, R. (2014). The production and display of Domenico Brucciani’s plaster cast of Hubert Le Sueur’s equestrian statue of Charles I. *The Sculpture Journal*, 23(2), 250.
- Wade, R., 2019. *Domenico Brucciani and the Formatori of 19th-century Britain*. London: Bloomsbury Visual Arts. ISBN: 9781501332197
- Wager, V. H. (1963). *Plaster casting for the student sculptor*. London: Alec Tiranti.
- Wainwright, C., & Gere, C. (2002). The making of the South Kensington Museum I: The Government Schools of Design and founding collection, 1837–51. *Journal of the History of Collections*, 14(1), 3–23. <https://doi.org/10.1093/jhc/14.1.3>
- Waldstein, C. (1889). *Catalogue of casts in the Museum of Classical Archaeology*. London: Macmillan and Company.
- Wei, S., Pintus, V., & Schreiner, M. (2013). A comparison study of alkyd resin used in artworks by Py-GC/MS and GC/MS: the influence of ageing. *Journal of Analytical and Applied Pyrolysis*, 104, 441–447. <http://dx.doi.org/10.1016/j.jaap.2013.05.028>
- Werner, N., & Schmitz, W. (1973). *Giessener Beiträge zur Kunstgeschichte*, Vol. 4.
- Westwood, J. O. (1876). *A descriptive catalogue of the fictile ivories in the South Kensington Museum: with an account of the continental collections of classical and mediaeval ivories*. London: Chapman & Hall.
- White, R. (1984). The characterization of proteinaceous binders in art objects. *National Gallery Technical Bulletin*, 8, 5–14. <http://www.nationalgallery.org.uk/technical-bulletin/white1984>
- Whitehead, C. (2005). Henry Cole’s European Travels and the Building of the South Kensington Museum in the 1850s. *Architectural History*, 207–234. <http://dx.doi.org/10.1017/S0066622X00003786>
- Williamson, P. (1996). *European sculpture at the Victoria and Albert Museum*. London: Victoria and Albert Museum Publishing. ISBN-13: 978-1851771738
- Willneff, E. A., Schroeder, S. L. M., & Ormsby, B. A. (2014). Spectroscopic techniques and the conservation of artists’ acrylic emulsion paints. *Heritage Science*, 2(1), 25. <https://doi.org/10.1186/s40494-014-0025-y>

- Wolbers, R. C. (1992). *The use of a synthetic soiling mixture as a means for evaluating the efficacy of aqueous cleaning materials on painted surfaces*. Conservation, Restauration Des Biens Culturels: Revue de l'ARAAFU, 4, 22–29.
- Wolbers, R. C. (2000). *Cleaning painted surfaces: aqueous methods*. London: Archetype Publications Ltd. ISBN-13: 978-1873132364
- Wolbers, R. C., & Little, M. A. (2007). The surface revealed: cleaning of two painted plaster sculptures. *Objects Specialty Group Postprints* Volume 11 2004, 154–171.
- Wolf, A. (1901). *Improvement in composition for coating surfaces*. Patent No. 15204.
- Young, M., & Urquhart, D. (1992). *Abrasive cleaning of sandstone buildings and monuments: an experimental investigation*. Stone Cleaning and the Nature, Soiling and Decay Mechanisms of Stone: Proceedings of the International Conference Held in Edinburgh, UK, 14-16 April 1992, 128–140.
- Zolnay, G. J. (1910). *Process of making art models, &c*. Patent No. 968505.

ABOUT THE AUTHOR

Valentina Risdonne was born in 1988 in L'Aquila, Italy. In 2010, she obtained her B.Sc. degree in Technologies for the conservation of Cultural Heritage at the University of Perugia (1st class Hons) and, in 2016, her M.Sc. degree in Sciences for the conservation of Cultural Heritage at the University of Parma (1st class Hons). She was professionally trained as a plasterer and decorator of historical buildings in Italy from 2013 to 2014. From 2015 to 2017 she collaborated with the Science Section at the Victoria and Albert Museum in several research projects. In 2019 she worked with Historic Royal Palaces to the documentation of the Rubens ceiling painting at Banqueting House in London, UK. Her PhD research, focused on the materials for coating the nineteenth-century plaster casts, was initiated in 2017 and funded by the Art and Humanities Research Council. The project is based on a Collaborative Doctoral Partnership between Northumbria University and Victoria and Albert Museum. ORCID: [0000-0002-0063-4156](https://orcid.org/0000-0002-0063-4156)

